Petrogenesis of alkaline rocks- isotopic and geochemical constraints

David R. Nelson

Thesis submitted for the degree of
DOCTOR OF PHILOSOPHY

THE AUSTRALIAN NATIONAL UNIVERSITY,
CANBERRA.
November, 1987

Statement

The new oxygen and carbon isotope data for carbonatites given in this thesis were obtained by Dr A.R. Chivas and co-workers of the Environmental Geochemistry Group, Research School of Earth Sciences. Dr B.W. Chappell and the staff of the X-Ray/INAA Laboratory, Department of Geology, The Australian National University, produced some of the major- and trace-element data given in this thesis on geological materials which I prepared for this purpose. The remaining original analytical data and all interpretations and conclusions presented in this thesis are my own unless otherwise acknowledged.

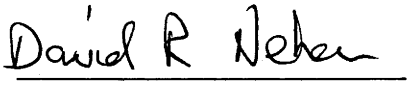

David R. Nelson

I call on those that call me son,
Grandson, or great-grandson,
Our uncles, aunts, great-uncles or great-aunts,
To judge what I have done.
Have I, that put it into words,
Spoilt what old loins have sent?
Eyes spiritualised by death can judge,
I cannot, but I am not content.

W.B. Yeats

Acknowledgements- This thesis owes its existence to the companionship, support and scientific collaboration of many people. I would especially like to acknowledge the invaluable contribution of Janet Callaghan throughout the long years of its duration. Without her encouragement and support during some difficult times, this thesis would not have been completed. Discussions with my supervisor, Malcolm McCulloch, Professor A.E. Ringwood and fellow student Bill McDonough have played a major part in shaping many of the ideas and interpretations presented in this thesis. Dr Shen-Su Sun, Robin Maier, Dr John Foster and Dr John Richards offered valuable advice about the black magic of Pb isotopes. I am also particularly grateful to both Dr Allan Chivas and Dr Bruce Chappell for generously providing stable isotope and major- and trace-element data respectively. This thesis has benefitted from my discussions with Keith Bell (Carleton Univ., Ottawa), John Bristow (De Beers Consolidated Mines Ltd.), Bill Compston (R.S.E.S.), Gareth Davies (Univ. of Leeds, U.K.), Geoff Davies (R.S.E.S.), Steve Foley (M.P.I., Mainz), Hans Hensel (R.S.E.S. and Dept. of Geology, A.N.U.), Robert Hill (R.S.E.S.), Lynton Jaques (B.M.R.), Sue Kesson (R.S.E.S.), Hugh O'Niell (R.S.E.S.), John Sheraton (B.M.R.), Shen-Su Sun (B.M.R.), Roald Vollmer (formerly of Univ. of Leeds, U.K.) and Ian Williams (R.S.E.S.) and from technical advice or assistance given by Mike Bower (B.M.R.), Dieter Burmann (R.S.E.S), Joe Cali (R.S.E.S.), Joan Cowley (R.S.E.S.), Hans Hensel (R.S.E.S. and Dept. of Geology, A.N.U.), Bill Hibberson (R.S.E.S.), Les Kinsley (R.S.E.S.), Elmer Kiss (R.S.E.S.), Robin Maier (R.S.E.S.), Derek Millar (R.S.E.S.), Norm Schram (R.S.E.S.), Nick Ware (R.S.E.S.) and Liz Webber (Dept. of Geology, A.N.U.). Geological samples were generously provided by P. Aspen (Dept. of Geology, Univ. of Edinburgh), S. Bergman (ARCO Resources, Texas), L.P. Black (B.M.R.), A.R. Chivas (R.S.E.S), K.D. Collerson (formerly of R.S.E.S.), A.J. Crawford (Dept. of Geology, Univ. of Tasmania), A. Cundari (Dept. of Earth Sciences, Univ. of Melbourne), R.K. Duncan (C.S.B.P. and Farmers Ltd.), J. Ferguson (Greater Pacific Investments), H. Hensel (R.S.E.S. and Dept. of Geology, A.N.U.), A.L. Jaques (B.M.R.), A. Langworthy (formerly of B.M.R.), J.D. Lewis (Geol. Surv. W. Aust.), M.T. McCulloch (R.S.E.S.), I. McDougall (R.S.E.S.), E. Nakamura (I.P.G., Paris), J. Sheraton (B.M.R.), L. Sutherland (Aust. Museum) and S.R. Taylor (R.S.E.S.). Finally, thanks are due to my fellow students and friends at the R.S.E.S. for making my time at the School so enjoyable and satisfying.

Abstract

Geochemical and isotopic (Pb, Nd, Sr, Ca, O and C) data are presented for a wide variety of potassic, kimberlitic and carbonatitic rocks. On the basis of differences in major- and trace-element geochemistry, isotopic characteristics and tectonic setting, the potassic rock suite has been divided into two sub-groups. These sub-groups are also considered to reflect important petrogenetic differences. Representatives of the "anorogenic" potassic sub-group are confined to stabilised Archaean or Early Proterozoic crustal blocks and adjacent mobile belts and are characterised by high K_2O/Na_2O ratios (molar K_2O/Na_2O > ~3), high TiO_2 (> ~2 wt%), K_2O, P_2O_5 and incompatible trace-element abundances (e.g. Ba, Rb, Th, Sr, Zr, and the light rare-earth elements) and low Al_2O_3, CaO and Na_2O abundances, generally radiogenic $^{87}Sr/^{86}Sr$ and unradiogenic $^{143}Nd/^{144}Nd$ and $^{206}Pb/^{204}Pb$. Examples of anorogenic sub-group potassic magmas include the lamproites from the West Kimberley region of northwestern Australia and from the Holsteinsborg region of central west Greenland, Gaussberg leucitites, the Priestley Peak melasyenite from east Antarctica, and the madupites, orendites and wyomingites from Leucite Hills, Wyoming. Representatives of the "orogenic" potassic sub-group are largely confined to Phanerozoic tectonic settings and have generally lower TiO_2 (< ~2 wt%), Nb, Ta and Zr, less radiogenic $^{87}Sr/^{86}Sr$ and more radiogenic $^{143}Nd/^{144}Nd$ and $^{206}Pb/^{204}Pb$ than representatives of the "anorogenic" sub-group. Orogenic potassic magmas also typically have lower abundances of the light rare-earth elements, and some representatives possess negative Eu anomalies. Examples of this sub-group include potassic lavas from Italy and from oceanic regions such as the Sunda and Banda sectors of the Indonesian arc and Ullung-do Island. A few potassic occurrences from orogenic tectonic settings have characteristics which are transitional between the two sub-groups (i.e. the southeastern Australian leucitites, which have higher TiO_2, and the Spanish lamproites, which have higher K_2O/Na_2O, lower CaO and Na_2O, more radiogenic $^{87}Sr/^{86}Sr$ and unradiogenic $^{143}Nd/^{144}Nd$, compared to other representatives of the orogenic sub-group). Both sub-groups possess trace-element and isotopic features which are consistent with the contamination of their magma sources by incompatible-element-rich and isotopically-evolved "metasomatic" components. It is proposed that these metasomatic components are principally derived from subducted sedimentary material. In the case of the anorogenic sub-group, the subducted sediments (or metasomatic components derived from them) have been stored for long periods within the subcontinental lithosphere. The increase in U/Pb of MORB and ocean-island reservoirs with time, as indicated by their position to the right of the geochron on the $^{206}Pb/^{204}Pb$-$^{207}Pb/^{204}Pb$ diagram, can be accounted for by the existence of substantial reservoirs of low-U/Pb, sediment-derived components within the subcontinental lithosphere.

Geochemical data obtained for 13 carbonatites from Africa, Australia, Brazil, Europe and the United States indicate that they possess generally high Ba, Th, LREE, Sr and low Cs, Rb, K and HREE abundances. Some examples have low Ti, Nb, Ta, P, Zr, Hf and U concentrations which are consistent with variable fractionation of sphene, apatite, perovskite, monazite or zircon. The carbonatite samples examined range in age from Proterozoic to Tertiary and possess a range in initial $^{87}Sr/^{86}Sr$ of 0.7020 to 0.7054, initial ε_{Nd} values of -0.4 to +3.8 and (with the exception of the Brazilian Jacupiranga carbonatite) generally radiogenic initial Pb isotopic compositions. $\delta^{18}O_{SMOW}$ of the intrusive carbonatites range from +5.5 to +12.4 ‰. Higher $\delta^{18}O_{SMOW}$ values of +14 and +17 ‰ are found in the volcanically-emplaced Proterozoic Goudini complex of South Africa, suggesting the involvement of secondary

alteration processes. $\delta^{13}C_{PDB}$ ranges from -0.5 to -6.6 ‰ with samples having near-primary $\delta^{18}O_{SMOW}$ (between +5.5 and +8 ‰) possessing $\delta^{13}C_{PDB}$ between -2.9 and -6.6 ‰. On the initial Sr-Nd isotope diagram, most carbonatites plot below the mantle array and below or within the field characteristic of many ocean-island basalts. The Pb isotopic compositions of carbonatites generally lie along the array defined by oceanic basalts. The isotopic similarities between ocean-island basalts and carbonatites from a number of continents favour an asthenospheric mantle "plume" origin for carbonatites. This conclusion suggests that some ocean-island alkali basalts may have been derived from trace-element-depleted mantle sources which have been re-fertilised by low-viscosity, trace-element-rich carbonatitic melts. The common close spatial and temporal association and the overlap in trace-element geochemistry and isotopic characteristics of Group 1 (basaltic) kimberlites and carbonatites argues strongly for a genetic relationship. Although secondary differentiation processes such as late-stage melt/vapour fractionation may play some role, the extreme LREE-enrichment typical of carbonatites requires their derivation by small degrees of melting (<≈1%) from a garnet-rich eclogitic source. This source may originally have been CO_2- and volatile-rich subducted oceanic lithosphere.

Calcium isotopic data are presented for oceanic basalts, potassic igneous rocks, carbonatites, a marine carbonate, a trough sediment, and chemical and clastic sediments from Archaean and Proterozoic terrains. An overall external precision of ±0.018% (95% confidence) was obtained for $^{40}Ca/^{42}Ca$ measurements. By comparison with the mid-ocean ridge basalt, no resolvable enrichments in ^{40}Ca from radiogenic decay of ^{40}K were detected in the Hawaiian ocean-island or Banda and Aleutian island-arc samples, the marine carbonate, the trough sediment or in the carbonatite samples. Potassic rocks from the West Kimberley region, Gaussberg and southeastern Spain also possess $^{40}Ca/^{42}Ca$ ratios which are analytically indistinguishable from the value found in oceanic basalts and carbonatites, suggesting that; a). the increase in K/Ca of the sources of these potassic magmas occurred some time after the trace-element- and LREE-enrichment, b). the K/Ca ratio of the magmas has been increased substantially during partial melting or melt extraction, and/or c). the calcium in the magmas has been diluted by mixing with unradiogenic calcium derived from other sources. In contrast, enrichments in ^{40}Ca were detected in genetically-unrelated kimberlitic and potassic intrusions from the Holsteinsborg region of central west Greenland. The excess ^{40}Ca in the Greenland kimberlites is unsupported, indicating that the K/Ca ratio has been reduced, probably during extraction of the kimberlite magmas from CO_3^{2-}-rich sources. The radiogenic $^{40}Ca/^{42}Ca$ of the Greenland kimberlites is not accompanied by radiogenic $^{87}Sr/^{86}Sr$, suggesting that the kimberlite major- and trace-element components have been decoupled, possibly with much of the major elements derived from the subcontinental lithosphere and the trace elements largely derived from sources located within the asthenosphere. The radiogenic $^{40}Ca/^{42}Ca$ of the Greenland lamproites is consistent with their derivation from subcontinental lithospheric sources which have been enriched in K for >1 Ga prior to their emplacement. Gypsum samples and pelitic clastic sediments from Archaean and Early Proterozoic terrains possess substantial enrichments in ^{40}Ca relative to oceanic basalts. Application of the ^{40}K-^{40}Ca decay scheme using presently available technology can provide useful petrogenetic and chronological information which complements that provided by other techniques.

Table of Contents

page

Table of Contents (continued)

Table of Contents (continued)

page

Table of Contents (continued)

page

Table of Contents (continued)

page

List of Tables

page

Text

Appendices

List of Figures

page

Text

List of Figures (continued)

Appendices

1. BACKGROUND TO AND AIMS OF THIS RESEARCH

1.1 Introduction

The recent identification in olivine- and leucite-lamproites from the Kimberley region, Western Australia, of Sr and Nd isotopic compositions indicating derivation from ancient (>1 Ga) "enriched" (radiogenic $^{87}Sr/^{86}Sr$, unradiogenic $^{143}Nd/^{144}Nd$) mantle sources (McCulloch *et al.* 1983) has led to speculation that much of the isotopic diversity displayed by mantle-derived magmas may be the result of mixing between such enriched mantle reservoirs and mantle possessing more typical isotopic compositions. Although similar unusual Sr and Nd isotopic compositions have also been found in some continental tholeiitic suites (for example, in continental tholeiitic suites from South Africa, Antarctica, India, North America and Tasmania), it has not been possible to discount the influence of crustal contamination on the isotopic compositions of the magmas during their ascent and emplacement in these cases. McCulloch *et al.* (1983) argued that the Sr and Nd isotopic compositions of the Western Australian lamproites are unlikely to be the result of crustal contamination processes as the lamproites possess extreme enrichment in the light rare-earth elements and Sr, making their isotopic compositions insensitive to contamination processes and requiring the assimilation of large amounts of crustal material. There is no evidence of such extensive contamination in the major- and trace-element geochemistry of the lamproites. Further examples of magmas believed to be derived from so-called "enriched mantle" sources have also recently been recognised (e.g. Smith 1983, Vollmer and Norry 1983a, Vollmer *et al.* 1984, Fraser *et al.* 1985, Nelson *et al.* 1986a and this thesis), suggesting that such isotopically unusual components may play a significant role in the Earth's geochemical and isotopic evolution.

This research was initiated in an attempt to characterise these isotopically anomalous mantle components, to assess their global significance and to investigate their possible modes of origin. It is the purpose of this introductory chapter to familiarise the reader with the basic principles of the investigative methods used and provide a general overview of the problems examined during this research. The use of radiogenic isotopes as mantle tracers will be briefly outlined, followed by a general discussion of some relevant aspects of mantle evolution and possible implications for the origins of isotopically-anomalous mantle components. Since this study began, the emphasis of research has expanded and diversified considerably- from initially concentrating primarily on an examination of one particular group of magmas, the ultrapotassic suite, into the consideration of a wide range of broadly-related geological problems such as the origins of kimberlites, carbonatites and ocean-island magmas, the mode of growth of the continental crust and evolution of the subcontinental lithosphere, the chemistry of marine sediments and the global implications of mantle recycling of crustal material via subduction. This chapter will also attempt to clarify how consideration of these diverse areas of research may contribute to an investigation of the origins of isotopically anomalous mantle components.

1.2 Application of isotopes as tracers

Apart from their geochronological applications, radiogenic isotopes can also provide information about incompatible-element enrichment and depletion events within magma source regions. The use of isotopes as mantle tracers has expanded considerably since the development and application in the 1970's of the ^{147}Sm-^{143}Nd isotope system, which provided a means of determining the time-integrated history

of light rare-earth element enrichment of magma source regions. When used in conjunction with ^{87}Rb-^{87}Sr, ^{232}Th-$^{235, 238}U$-$^{208, 207, 206}Pb$ and other radiogenic decay systems, a powerful tool for the investigation of the Earth's differentiation history became available. Early isotope tracer studies (such as those cited in DePaolo 1979) found that the $^{87}Sr/^{87}Sr$ and $^{143}Nd/^{144}Nd$ characteristics of a wide range of mantle-derived magmas show a strong negative correlation. This is believed to reflect the similar behavior of Rb/Sr and Nd/Sm ratios during partial melting and magmatic differentiation processes. However, the ratios Th/Pb and U/Pb do not appear to have behaved in a simple manner throughout the Earth's differentiation history and mantle-derived magmas display a wide range of Pb isotopic characteristics which are not simply correlated with the other isotope systems. It is for this reason that this study has a strong reliance on the U-Pb isotope system (despite analytical difficulties which limit its potential usefulness) used in conjunction with Rb-Sr and Sm-Nd.

Most radiogenic isotope tracer schemes in common use (such as those outlined above) are based on elements which occur in only trace amounts in most mantle-derived rocks. There is, however, accumulating evidence that the major-element and trace-element components of some mantle-derived magmas have undergone divergent evolutionary histories, and that trace-element components have in some instances been introduced to the source regions of some magmas from other sources. The term "metasomatism" is sometimes applied to describe this process of the decoupling of major and trace elements. (Unfortunately this term is currently used rather loosely and there is no consensus as to its meaning. In this thesis, the term "metasomatism" will be applied in a very general sense, to denote the process or processes responsible for the introduction of foreign components, via melts or fluids, to regions of the mantle). One decay scheme, based on the decay of the radiogenic isotope ^{40}K to ^{40}Ca ($t_{1/2}$ = 1.47 Ga), potentially enables investigation of the evolutionary histories of the major-element components of rocks. Until recently, application of the ^{40}K-^{40}Ca decay scheme was severely limited by a number of analytical difficulties. However, re-assessment of these difficulties undertaken as part of this research has suggested that an important new mantle tracer, based on the major element calcium, can be usefully applied to a wide number of geological problems. Further discussion of this investigation of the ^{40}K-^{40}Ca radiogenic decay scheme is given in Section C of this thesis.

1.3 Enriched mantle components and isotope systematics

In its current usage, the term "enriched mantle" refers to those mantle components having initial $^{87}Sr/^{87}Sr$ and $^{143}Nd/^{144}Nd$ compositions lying within the lower right-hand quadrant of the Sr-Nd isotope diagram (see, for example, Fig. 2.4), in response to a time-integrated history of high Rb/Sr and Nd/Sm compared to Bulk Earth estimates. Such components are also typically enriched in incompatible elements such as K, Cs, Ba, Th, U, Pb and the light rare-earth elements compared to "depleted" mantle components such as those from which mid-ocean ridge basalts are derived. As the upper continental crust generally also plots within the enriched quadrant, it is necessary to evaluate the possible influence of crustal contamination processes on magmas having enriched mantle isotopic signatures. The isotopic characteristics of magmas derived from enriched sources can potentially offer some constraints on the timing of the enrichment events, providing that mixing with other components, such as the continental crust and more typical mantle, can be discounted. The Sm-Nd isotope system is the most useful in this respect, as the similar chemistries of Sm and Nd allow the Nd isotopic evolution trajectories of the source

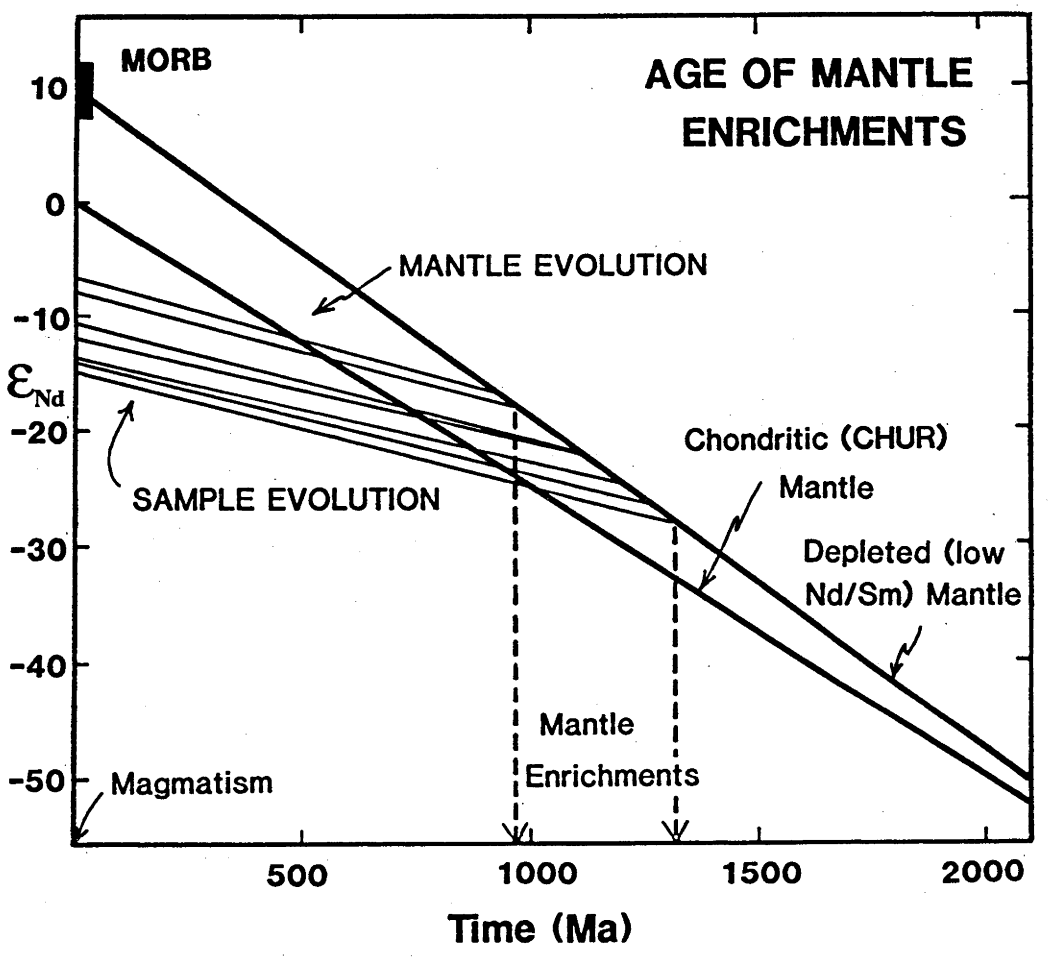

Fig. 1.1 Evolution of Nd in enriched mantle sources (in this case, the W.A. lamproites) with time. The slopes of the sample evolution trajectories are determined from the measured $^{147}Sm/^{144}Nd$ and provide minimum estimates ("model ages") of the time elapsed since the Sm/Nd ratios diverged from that of the mantle (locus of model depleted and chondritic mantle evolution shown).

regions to be approximated by the Sm/Nd ratio measured in the extracted magma (see Fig. 1.1). Because the Sm/Nd ratio of the melt is likely to be lower than that of the source and the initial isotopic composition of the source is unknown, Sm-Nd model ages are usually interpreted as minimum estimates of the time elapsed since the Nd/Sm ratio and Nd isotopic composition diverged from model mantle values. Pb-Pb "mantle isochrons" have also been used to date mantle enrichment events (e.g. Vollmer and Norry 1983a, 1983b) but in many cases these Pb-Pb isotope arrays are mixing lines and have no age significance.

Although enriched mantle components are primarily identified on the basis of their Sr and Nd isotopic characteristics (in conjunction with other aspects of major- and trace-element geochemistry), application of the Pb isotope system has provided some interesting insights into the evolution of these components. In contrast to the Rb-Sr and Sm-Nd isotope systems, which apart from indicating a time-averaged history of high Rb/Sr and Sm/Nd, cannot provide any information about the time-dependent variation of these ratios, the coupled decay of ^{235}U to ^{207}Pb and ^{238}U to ^{206}Pb enables constraints to be placed on the time-dependent variation of U/Pb within enriched mantle sources. This is illustrated in Fig. 1.2. The geochron is the isochron on which all present-day terrestrial (~4.5 Ga old) single-stage (constant U/Pb) Pb compositions should lie if their initial Pb isotopic composition were that of primodial Pb (approximated by the most unradiogenic Pb known, that of Canyon Diablo troilite). As the

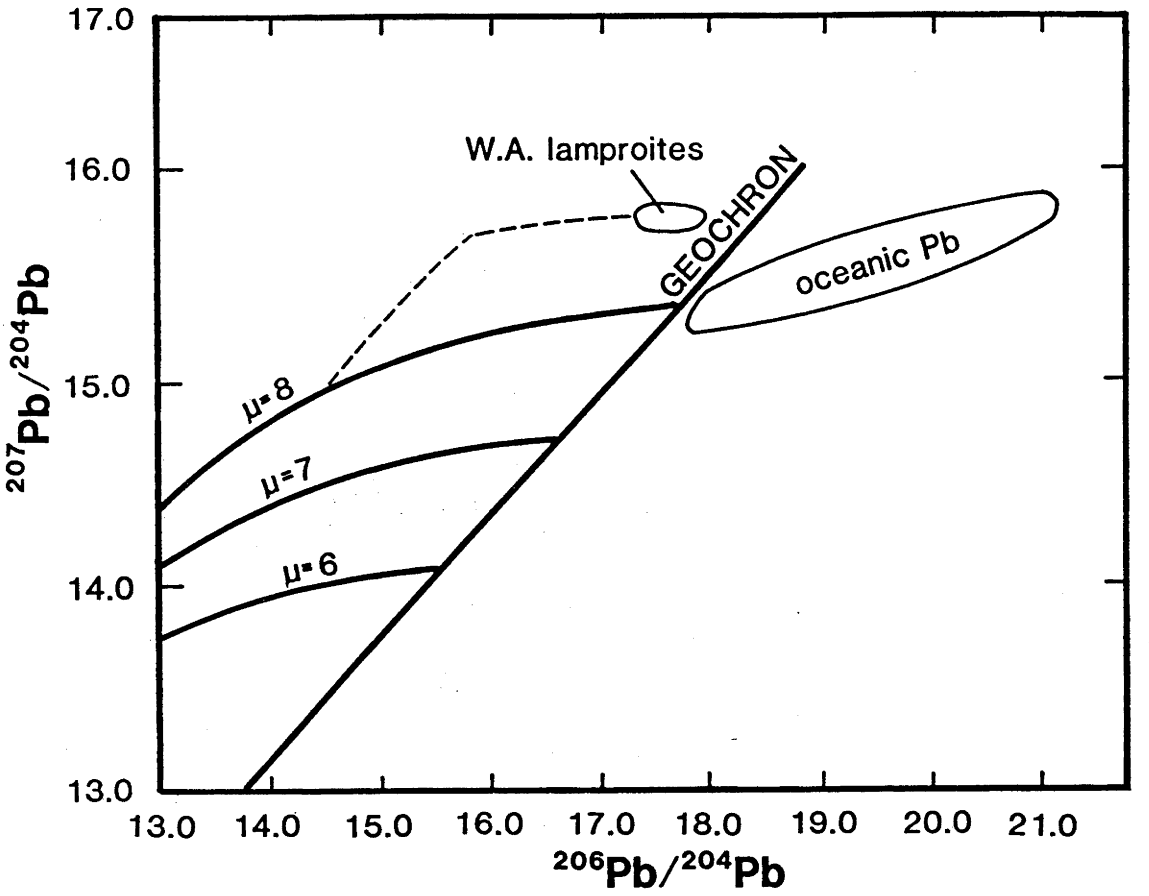

Fig. 1.2 Growth curves for $^{238}U/^{204}Pb$ = 6, 7 and 8 for terrestrial Pb, displayed on a $^{207}Pb/^{204}Pb$-$^{206}Pb/^{204}Pb$ diagram. Most oceanic Pb, including that of mid-oceanic ridge and ocean-island basalts, plots to the right of the present-day geochron, indicating derivation of oceanic basalts from sources which have undergone a recent increase in U/Pb. Western Australian lamproites have Pb isotopic compositions lying to the left of the geochron and have more radiogenic $^{207}Pb/^{204}Pb$ (see Chapter 3 of this thesis), indicating a complex multistage history of U/Pb variation.

half-life of the decay of ^{235}U to ^{207}Pb ($t_{1/2}$ = 713 Ma) is substantially shorter than the half-life of ^{238}U to ^{206}Pb ($t_{1/2}$ = 4.51 Ga), most of the ^{235}U has decayed since the Earth's formation and the $^{207}Pb/^{204}Pb$ ratio is therefore more sensitive to variation in the U/Pb ratio in the early stages of the Earth's history. Most young mid-ocean ridge and ocean-island basalts have Pb isotopic compositions which lie to the right of the geochron, indicating that the U/Pb ratios of their sources have not remained constant but have increased with time. This has been variously attributed to the preferential loss of Pb relative to U from the Earth's mantle to the core (*cf.* Vollmer 1977a, Allègre *et al.* 1982), the storage of Pb in the lower crust (O'Nions *et al.* 1979) or the recycling of U-rich sediments into the deep mantle (Hofmann and White 1980). However, as will be shown later in this thesis, lamproites from the West Kimberley region of Western Australia possess Pb isotopic compositions which lie to the left of the geochron and have considerably more radiogenic $^{207}Pb/^{204}Pb$ than most oceanic Pb (Fig. 1.2). This indicates a multistage history of U/Pb variation, involving an earlier period of high U/Pb in order to increase the $^{207}Pb/^{204}Pb$ ratio, followed by a more recent period of low U/Pb to retard the evolution of the $^{206}Pb/^{204}Pb$ ratio. One of the most intriguing findings of this research is that similar Pb isotopic compositions, requiring the same unusual history of U/Pb variation, are also found in many other examples of potassic magmatism derived from enriched mantle sources. Possible reasons for this are discussed in some detail in Chapter 7 of this thesis.

1.4 Mantle components and potassic, kimberlitic and carbonatitic magmatism

Earlier Sr isotopic studies, such as those of Hoefs and Wedepohl (1968), Bell and Powell (e.g. Bell and Powell 1969, Powell and Bell 1970) and Vollmer (1976), found that highly potassic magmas commonly possessed radiogenic initial $^{87}Sr/^{86}Sr$. (Throughout this thesis, the term "potassic" is applied to rocks having molar K_2O/Na_2O considerably greater than unity and the term "ultrapotassic" used to refer to rocks having molar K_2O/Na_2O greater than 3). It was generally widely accepted that this was due to extensive interaction of the magmas with the intruded continental crust. However, a few more recently published Nd isotopic studies (e.g. McCulloch *et al.* 1983, Collerson and McCulloch 1983) have argued that, at least in a few specific cases, this explanation is not tenable. As no satisfactory mechanism had been advanced to explain the unusual chemical characteristics (such as the high K/Na ratios) of potassic magmas, this research initially concentrated on the isotopic and geochemical characterisation of potassic magmatism, in order to determine whether the unusual geochemical and isotopic properties of these magmas were the result of extensive interaction with continental crust or the result of their derivation from geochemically- and isotopically-anomalous mantle sources.

The common close spatial association of potassic, kimberlitic and carbonatitic magmatism and their supposed close geochemical affinities led some earlier workers (e.g. Holmes 1932, Wade and Prider 1940, Borley 1967, Cundari 1973) to suggest that a genetic connection exists between these magmas. The existence of a possible genetic relationship is testable using isotopic tracers, so examples of carbonatitic and kimberlitic magmas were also examined during the course of this research. Although suggesting a genetic link between carbonatites and Group 1 (basaltic) kimberlites, the results of this investigation rule out the possibility of a genetic link between the potassic igneous suite and carbonatitic magmas. The long-term evolutionary histories of the sources of Group 1 kimberlitic and carbonatitic magmas, as indicated by their Sr, Nd and Pb isotopic compositions, are generally similar to those inferred for the sources of alkali basalts from some ocean islands, implying that similar processes may have been involved in the generation of these groups. There are, however, many examples of continental provinces (for example, South Africa, central west Greenland, the Kimberley region of Western Australia and the Arunta region of Central Australia) in which potassic magmas apparently derived from enriched mantle sources occur in close proximity to kimberlitic and/or carbonatitic magmatism. It is also notable that volcanics of the Italian and Spanish potassic provinces have isotopic characteristics extending from one end-member isotopically resembling some ocean islands (i.e. the Pietre Nere volcano, which isotopically resembles the St Helena type of ocean island) to another end-member having enriched mantle isotopic characteristics (Vulsini, Sabatini, Vico and Spanish lamproites; see Fig. 2.9, p26). Possible relationships between kimberlitic, carbonatitic and ocean-island magmatism and of these magma types and potassic magmatism are discussed in later sections of this thesis.

1.5 Possible mechanisms for the generation of mantle isotopic heterogeneities

It is now generally accepted that the Earth's upper mantle and the overlying lithosphere are geochemically and isotopically heterogeneous and must somehow be segregated into a number of globally extensive but not necessarily continuous reservoirs, each having their own distinctive isotopic characteristics. For example, the isotopic evidence indicates that the source regions of many ocean-island alkali basalts and of tholeiitic basalts erupted at oceanic spreading centres have undergone divergent

evolutionary histories for at least 1 Ga. There is presently no consensus about the overall configuration of long-lived global heterogeneities within the Earth or the processes causing them. It is, however, worth emphasising that while the existence of similar isotopic characteristics in a particular group of mantle-derived magmas may suggest that they have been derived from a common reservoir (e.g. a primitive, undifferentiated mantle reservoir or an incompatible-element-depleted mantle reservoir), it may also simply indicate the involvement of a common process in the generation of members of each group, possibly during many independent and unrelated events, so producing a similar geochemical (and consequently, isotopic) result. Any consideration of the origins of enriched or other components within the mantle should therefore entail consideration of the processes by which such components are generated. Although this may seem an obvious point, there has been a tendency in the geological literature to blandly attribute any variety of unusual geochemical and isotopic properties to "the subcontinental lithosphere" or to "heterogeneities within the mantle" without any real regard to their cause. The primary emphasis of this research is to elucidate the mechanisms by which these mantle heterogeneities may arise.

The diverse isotopic features of some continental provinces have been interpreted as evidence for the existence of long-lived isotopic heterogeneities within the subcontinental lithosphere (*cf.* Allègre *et al.* 1982). The advent of models advocating an important role for the subcontinental lithosphere in generating isotopic heterogeneity within the convecting mantle (for example, McKenzie and O'Nions 1983) has further emphasised the need for isotopic characterisation of the subcontinental lithosphere. Such isotopic characterisation also has important implications for the Earth's thermal and isotopic evolutionary history and in the assessment of models of crustal growth, such as lateral accretion versus underplating models. The recent discovery of Sr and Nd isotopic compositions indicating ancient enrichment in sub-calcic garnet inclusions within diamonds from African kimberlites (Richardson *et al.* 1984) has been interpreted as indicating that the subcontinental lithosphere beneath the South African continent has been stabilized to depths extending to the diamond stability field since the Archaean. As many occurrences of alkaline magmatism possessing isotopically-evolved features are found in old stable cratonic regions, the subcontinental lithosphere may be the site of storage of these enriched mantle components. The mechanisms producing incompatible-element enrichment at these great depths remain unknown but may involve processes such as the incorporation within the base of the subcontinental lithosphere of low-velocity-zone melts, the underplating of hotspot plume melts, as has been suggested by Brooks *et al.* (1976), or by subcretion processes during subduction beneath the continental margin.

It has long been realised that vast quantities of oceanic lithosphere must have been subducted into the mantle during the Earth's recent history, but it is only relatively recently that any consideration has been given to the fate of this subducted material. Several authors (e.g. Chase 1981, Hofmann and White 1982, Ringwood 1982) have proposed that the isotopic signatures of some ocean-island basalts are consistent with their derivation from basaltic oceanic crust which has been subducted into the mantle. This proposal stimulated much interest and led to a rapid expansion of the geochemical and isotopic database on ocean-island magmas. From these studies, it is now evident that ocean-island basalts possess a wide range of isotopic characteristics, some of which could be interpreted as indicating their derivation from subducted oceanic crust. In the case of a few ocean islands (e.g. Kerguelen, Gough, Tristan da Cunha and Society Islands), which have comparatively higher $^{207}Pb/^{204}Pb$ and $^{87}Sr/^{86}Sr$ and lower $^{143}Nd/^{144}Nd$, it has also been suggested that their isotopic characteristics are consistent with the involvement of subducted

sedimentary components. The possibility that a link exists between the subduction and mantle recycling of oceanic crust and sediments and the generation of potassic, kimberlitic and carbonatitic magmatism will also be explored in detail later this thesis.

SECTION A. POTASSIC MAGMATISM

The following section, consisting of 6 chapters, presents the results of geochemical and isotopic investigations of potassic rocks from different tectonic settings. Representatives of the potassic rock suite examined in this study have been separated into two main sub-groups; those which occur in late Proterozoic or Palaeozoic Fold Belts or intra-oceanic environments, termed the "orogenic" sub-group (the subject of Chapter 2), and those which are confined to stable cratonic tectonic environments, termed the "anorogenic" sub-group (dealt with in Chapter 3). Because the interpretation of field relationships and isotopic data from geologically older rocks requires special treatment, some Palaeozoic and Proterozoic occurrences of potassic and kimberlitic rocks from central Australia, east Antarctica and west Greenland, are dealt with separately in Chapters 4, 5 and 6. It will be argued in the last chapter of this section (Chapter 7) that the division between orogenic and anorogenic potassic igneous suites separates two petrogenetically-related groups which differ only in the extent of involvement of the subcontinental lithosphere as a site of temporary storage of their magma sources.

2. Orogenic potassic igneous provinces

2.1 Introduction

Although many highly-potassic igneous rocks possess geochemical features (such as high Mg-numbers and Ni and Cr contents) consistent with a mantle origin, the high K/Na ratios of these magmas suggest that they are unlikely to be derived from unmodified or "primitive" mantle sources. Experimental work (e.g. Eggler 1978, Wendlandt 1984) has demonstrated that melts of peridotite formed in the presence of CO_2 at pressures of ~27 kbar would be carbonatitic, whereas the presence of H_2O or F may enhance the stability of phlogopite (Foley *et al.* 1986). These studies suggest that small degrees of partial melting of phlogopite-bearing peridotite at depths below the level of amphibole stability and in the presence of CO_2 might produce a high-K_2O liquid with high Mg/Ca. The prerequisite modification (i.e. by the addition of volatiles) of the mantle sources of ultrapotassic rocks has commonly been attributed to metasomatic processes, often considered to be associated with either subduction or intraplate rifting (e.g. Cundari 1979, Edgar 1980).

That the generation of potassic magmas may be related to the operation of subduction processes is suggested by the occurrence of volcanoes erupting potassic lavas in several island arcs (e.g. Batu Tara and Muriah volcanoes of the Indonesian arc). Based on geochemical similarities with modern-day arc lavas, other recent studies (e.g. Thompson 1977, Holm and Munksgaard 1982, Peccerillo *et al.* 1984, Venturelli *et al.* 1984, Peccerillo 1985, Rogers *et al.* 1985) have also suggested that subduction-related processes are involved in the genesis of the potassic lavas of Italy and Spain. Ninkovich and Hays (1972) and Hatherton and Dickinson (1968, 1969) noted that a positive correlation exists between K_2O content and depth of earthquake epicentre for island-arc volcanics of the Pacific, Indonesian and Atlantic oceans. Ninkovich and Hays (1972) attributed this relationship to the involvement of fluids, derived from the subducted slab, which have scavenged potassium from the overlying mantle. Alternatively, the higher pressure-temperature stability field of phlogopite compared to other hydrous mantle phases may allow it to remain stable to greater depths within the subducting slab. Melts rich in potassium may therefore conceivably be derived by the eventual breakdown of phlogopite within the subducted slab, below the stability field of amphibole (*cf.* Fyfe and McBirney 1975).

Some earlier isotopic studies of potassic rocks from tectonically active regions (e.g. Whitford 1978, Whitford *et al.* 1978, Hawkesworth and Vollmer 1979, Nixon *et al.* 1984) have found that they commonly possess radiogenic initial Sr and unradiogenic initial Nd isotopic compositions compared to typical mantle values. Although these characteristics may have been acquired by crustal contamination, in a few instances the potassic suites are found intruding crustal terrains which may be too young to have evolved the radiogenic Sr and unradiogenic Nd isotopic compositions required. Several authors (Chase 1981, Hofmann and White 1982, Ringwood 1982) have suggested that ancient mantle isotopic heterogeneities such as those identified by isotopic studies of some ocean-island basalts may be the result of the recycling of oceanic crust and sediments into the mantle via subduction. For example, Ringwood (1982) envisaged that partial melts enriched in incompatible elements may rise as magma diapirs from the subducted "megalith" as it attains thermal equilibrium with the surrounding mantle. Such plumes could also conceivably be the sources of orogenic potassic magmas, providing an explanation for their evolved

isotopic character.

In this chapter, radiogenic isotopes are applied as tracers in an attempt to investigate the processes involved in the generation of potassic magmas located within young orogenic tectonic environments.

2.2 Samples

2.2.1 Southeast Australian leucitites

The southeast Australian olivine leucitites occur as minor flow remnants along a north-south trending line extending from central New South Wales to Cosgrove in Victoria (Fig. 2.1). The geochemistry and mineralogy of the New South Wales occurrences have been described by Cundari (1973) and the Cosgrove occurrence by Birch (1978). Representative geochemical analyses of the lavas are given in Table 2.1. The leucitites are characterised by generally high TiO_2 (3.8 to 7.9 wt%), MgO (4.5 to 15.2 wt%), K_2O (3.7 to 7.3 wt%), P_2O_5 (0.8 to 2.9 wt%), H_2O^+, Cr, Ni, Zr, Ba and Sr, and low SiO_2 (41.8 to 46.9 wt%), Al_2O_3 (7.5 to 12.1 wt%) and Na_2O (0.7 to 3.3 wt%; Cundari 1973). They are located within the Lachlan Fold Belt, which consists of Palaeozoic geosynclinal sediments and granites but which is possibly underlain by Precambrian basement. Leucitite outcrop distribution was noted by Cundari (1973) to conform to regional north-south structural trends, characterised by block-faulting and regional uplift. Potassic volcanism is temporally and spatially closely associated with alkali basalts, which several studies (e.g. Wass and Rogers 1980, O'Reilly and Griffin 1984) have shown to have been derived from metasomatised mantle. Wellman and McDougall (1974) demonstrated a prominent southward temporal migration of Cainozoic igneous activity, a feature also displayed by the leucitites, and attributed it to the northward migration of the eastern part of the Australian continent over several hotspots. Sutherland (1983) proposed that the southerly migration of volcanism may have been related to movement of the continent over former sites of sea-floor spreading.

A vitrophyric analcimite occurrence at Inglewood in southeastern Queensland (see Fig. 2.1) was described by Wilkinson (1977), who considered the analcime to be an alteration product of leucite. The analcimite is believed to be of Cainozoic age (probably Late Oligocene-Early Miocene) and is possibly related to the extensive Cainozoic alkali basaltic volcanism of southeastern Queensland.

The Harden olivine analcimite, located ~200 km southeast of the New South Wales leucitite occurrences (see Fig. 2.1), is of Early Jurassic age (Wellman *et al.* 1970). Major- and trace-element analyses reported by Cundari (1973; see Table 2.1) suggest affinities with mid-Mesozoic nepheline-bearing intrusions and minor flows which occur throughout the southeastern highlands region of New South Wales.

2.2.2 Spanish lamproites

The location, geochemistry and mineralogy of the ultrapotassic rocks from southeastern Spain is given in Venturelli *et al.* (1984). Representative geochemical analyses of the Spanish lamproites are given in Table 2.1. The lamproites have generally variable SiO_2 (53.4 to 68.5 wt%) and MgO (1.7 to 16.6 wt%), high K_2O (3.7 to 8.8 wt%), P_2O_5 (0.5 to 2.1 wt%) Ni, Cr, Zr, Ba, Th and the light rare-earth elements, and low TiO_2 (1.0 to 1.9 wt%) CaO (2.2 to 9.9 wt%), total Fe (calculated as Fe_2O_3,

Table 2.1 Major- and trace- element analyses of some representative orogenic potassic rocks examined in this study.

Analysis	1.	2.	3.	4.	5.	6.	7.	8.	9.
Sample	GA-3479	E7980	70-139	SP-039	SP-077	VEN-1	CUP-10	ULL-1	AJCF2
Location	El Capitan	Cosgrove	Harden	Zeneta	Calasparra	San Venanzo	Cupaello	Ullung-do	Fiji
Rock-type	leucitite	leucitite	analcimite	lamproite	lamproite	melilitite	melilitite	leucitite	ankaramite
SiO_2	44.97	42.57	40.51	68.0	54.6	42.0	43.8		44.95
TiO_2	4.68	4.49	4.10	1.03	1.75	0.77	1.2		0.89
Al_2O_3	8.60	9.75	10.38	12.6	9.52	10.5	7.4		12.08
Fe_2O_3	3.02	3.51	4.36	1.92	5.66	2.3	4.7		11.42
FeO[a]	6.67	8.61	8.43	-	-	4.70	2.45		-
MnO	0.12	0.18	0.19	0.01	0.07	0.13	0.12		0.18
MgO	13.64	9.98	12.83	2.01	13.3	13.0	11.3		5.84
CaO	7.89	11.38	10.46	2.42	2.87	15.8	15.4		11.67
Na_2O	0.88	2.88	3.50	1.99	0.69	1.00	0.27		2.70
K_2O	7.09	2.96	1.49	7.06	8.86	8.3	4.4		1.44
P_2O_5	0.87	1.22	0.79	0.89	0.95	0.42	1.28		0.89
H_2O^+	0.86	-	2.34	-	-	0.20	5.90		-
SO_2	-	-	-	-	-	0.11	0.41		-
CO_2	-	-	1.22	-	-	0.36	0.40		-
LOI	0.44	1.6	0.35	1.96	1.60	0.52	1.22		-
SUM	99.73	99.13	100.95	99.89	99.87	100.11	100.25		
Cr	330	462	265	432	638	923	85	6.5	18
V	-	-	-	86	91	-	-	-	-
Sc	-	-	-	16	14	-	-	4.9	36.4
Ni	437	131	349	173	657	104	57	-	17
Co	42	43	43	16	31	31	28	9.7	38
Cu	-	70	-	37	75	-	-	-	38
Zn	-	114	-	38	60	-	-	-	87
Li	-	-	-	33	38	-	-	-	-
Cs	-	-	-	-	-	-	-	1.47	4.0
Ba	1100	1022	1140	2040	2050	-	-	901	510
Rb	218	82	79	259	541	444	456	155	68
Sr	940	1269	780	568	526	1709	4749	573	870
Pb	-	-	-	-	-	-	-	-	5
Y	-	33	-	25	24	-	-	-	28
Th	-	-	-	85	112	-	-	19.4	1.8
U	-	-	-	-	-	-	-	2.1	0.6
Zr	515	367	230	350	680	335	761	391	144
Hf	-	-	-	-	-	-	-	12	4.06
Nb	-	-	-	27	32	-	-	-	1.5
Ta	-	-	-	-	-	-	-	6.6	0.3
Mo	-	-	-	-	-	-	-	7	6
Sb	-	-	-	-	-	-	-	0.16	-
La	-	-	-	-	-	-	-	81	21.3
Ce	-	-	-	122	274	-	-	142	49.9
Nd	-	-	-	-	-	-	-	44	36.8
Sm	-	-	-	-	-	-	-	6.1	10.2
Eu	-	-	-	-	-	-	-	2.27	2.77
Gd	-	-	-	-	-	-	-	5.2	7.1
Tb	-	-	-	-	-	-	-	0.83	0.99
Ho	-	-	-	-	-	-	-	0.67	1.14
Yb	-	-	-	-	-	-	-	2.29	2.85
Lu	-	-	-	-	-	-	-	0.321	0.422

[a] Where FeO is not given, all Fe has been determined as Fe_2O_3.

1. New South Wales leucitite analysis from Cundari (1973; his analysis CPT-11-II)
2. Harden analcimite analysis from Cundari (1973; his analysis HAR-II).
3. Cosgrove leucitite analysis (E7980) from Birch (1978).
4 - 5. Spanish lamproite analyses (SP-039 and SP-077) from Venturelli *et al.* (1984).
6 - 7. Italian melilitite analyses by A. Cundari (personal communication).
8 - 9. Ullung-do Island leucitite and Fiji ankaramite analyses from this study.

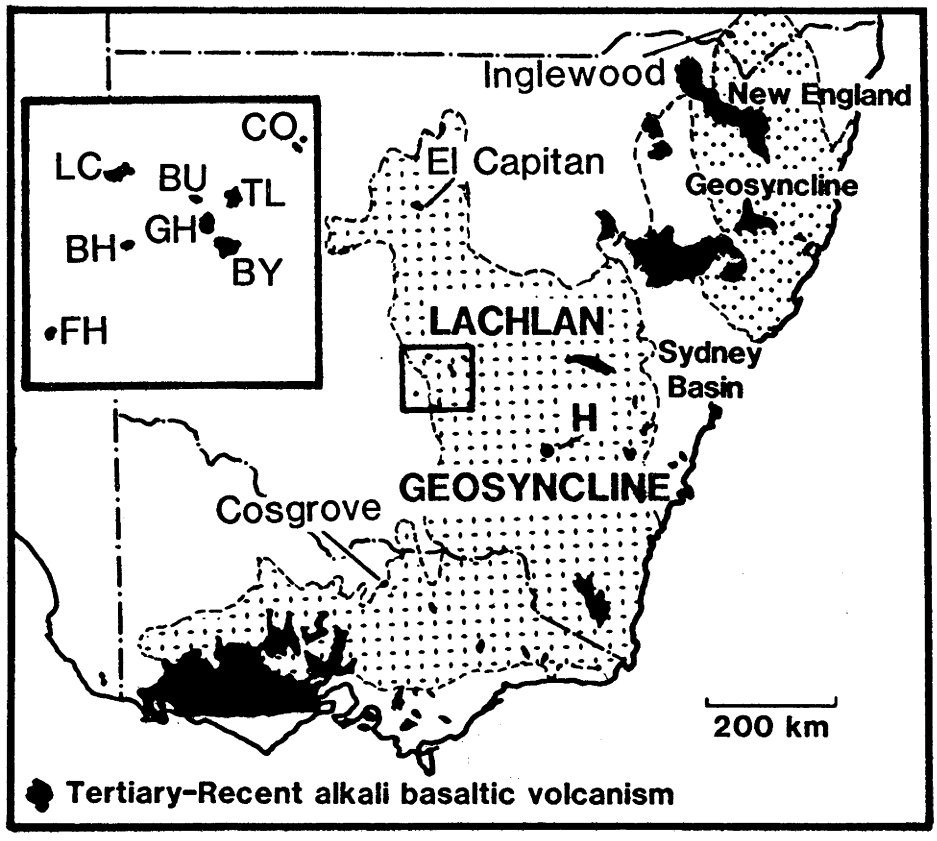

Fig. 2.1 Localities and regional geology of leucitites from southeastern Australia. H- Harden analcimite (early Jurassic age). Inset: BH- Begargo Hill, BU- Burgooney, BY- Bygalore, CO- Condobolin, FH- Flagstaff Hill, GH- Gorman Hill, LC- Lake Cargellico, TL- Tullibigeal.

from 1.9 to 9.9 wt%) and Na_2O (0.6 to 3.3 wt%) contents (Venturelli *et al.* 1984). The tectonic evolution of the region is controversial, but most models invoke recent subduction processes. Arana and Vegas (1974) proposed that the increasing K_2O content of calc-alkaline volcanism from south to north indicates that a northward-dipping subduction zone was active during the Lower Miocene. The ultrapotassic intrusives were regarded as the most northerly and therefore deepest expression of arc volcanism resulting from the subduction of the African plate under the Iberian plate. A possible association between potassic volcanism and post-Nappe block-faulting during the Pliocene has been suggested by Nixon *et al.* (1984).

2.2.3 Italian leucite melilitites

The Plio- to Pleistocene age San Venanzo and Cupaello volcanoes are located within the northeastern part of the "Roman Co-magmatic Region", central Italy. The bedrock of this region consists of Mesozoic and Cainozoic clastic and carbonate sediments, possibly underlain by Palaeozoic metamorphic basement (Ferrara *et al.* 1985 and references cited therein). The petrology and geochemistry of lavas from these two volcanoes was examined by Mittempergher (1965). Major- and trace-element analyses of the San Venanzo and Cupaello lavas examined here are given in Table 2.1. San Venanzo lavas are predominantly kalsilite-bearing leucite olivine melilitites and those from Cupaello kalsilite diopside melilitites. The lavas possess generally low SiO_2 (41 to 44 wt%) TiO_2 (0.7 to 1.2 wt%) and Na_2O (0.3 to 1 wt%) and high MgO (11 to 13 wt%) CaO (15.5 to 16 wt%) and K_2O (4 to 8 wt%) contents. $^{18}O/^{16}O$ compositions obtained on alteration-free samples (Holm and Munksgaard 1982, Taylor *et al.* 1984, Ferrara

et al. 1985) indicate strong enrichments in ^{18}O ($\delta^{18}O_{SMOW}$ values of +12 to +14 ‰ were found). Vollmer (1976) reported an $^{87}Sr/^{86}Sr$ value of 0.71037 for a San Venanzo sample and Holm and Munksgaard (1982) obtained an $^{87}Sr/^{86}Sr$ value of 0.71120 for a sample from Cupaello. On the basis of the extreme $^{18}O/^{16}O$ and $^{87}Sr/^{86}Sr$ compositions of the San Venanzo and Cupaello lavas compared to other lavas from the Roman region, Holm and Munksgaard (1982) argued that the lavas were derived from "metasomatised" mantle sources which represented the extreme (high $^{87}Sr/^{86}Sr$ and $^{18}O/^{16}O$) mantle end-member of the Roman province. This was disputed by Taylor *et al.* (1984) and Ferrara *et al.* (1985) who argued that the extreme features of the San Venanzo and Cupaello lavas were at least partly the result of extensive crustal contamination.

The tectonic setting of the Italian region has been the subject of much debate. Ninkovich and Hays (1972) argued that the potassic magmatism was related to northward-dipping subduction under the Calabrian arc. However, Barbieri *et al.* (1973) and Cundari (1980) have emphasised that the depth of earthquake foci increases westward (i.e. away from the Roman region) and have argued for an intraplate rift setting, analogous to the Rhine and East African alkaline provinces. There is, however, general agreement that the calc-alkaline and leucite-tephritic volcanism of the Aeolian arc, located to the south of Italy, is related to subduction processes.

2.2.4 Ullung-do Island leucitite

Ullung-do (Utsuryoto) Island is located in the western part of the Sea of Japan, 130 km from the eastern coast of Korea. Petrological studies by Tsuboi (1920) recognised several stages of volcanism, commencing with predominantly basaltic volcanism followed by trachytic and phonolitic flows and pyroclastics. Leucite-bearing lavas were described from an intra-caldera dome (Arpong Hill), and were interpreted by Tsuboi (1920) to be the products of the final stage of volcanism on the island.

2.2.5 Fiji leucite-bearing ankaramite

The Fijian islands are located within a tectonically complex region adjacent to the convergent boundaries of the Pacific and Indian plates. The tectonic evolution of the region and its influence on the geochemistry of magmatism on the islands has been examined by Gill (1984) and Gill *et al.* (1984). According to these authors, prior to ~8 Ma ago, tholeiitic and andesitic volcanism with arc-like trace-element characteristics predominate, whereas from ~ 5 to 3 Ma ago, during which the arc was disrupted and the Lau and North Fiji Basins formed, alkali olivine basalts considered by Gill (1984) to have trace-element and isotopic affinities with ocean-island basalts were erupted.

Geochemical and isotopic analyses were obtained on a leucite-bearing ankaramite from Fiji as part of a reconnaissance study. The sample examined consisted of phenocrysts of leucite, phillipsite psuedomorphing leucite (see Table 2.2), clinopyroxene and opaques set in a glassy groundmass. Major-element analysis (Table 2.1) indicates that the flow from which the sample was taken is differentiated and has low SiO_2 and TiO_2 contents accompanied by relatively high Al_2O_3 and CaO.

Table 2.2 Some representative microprobe analyses of phenocryst phases in the Fiji ankaramite.

Analysis	1.	2.	3.	4.	5.
SiO_2	48.18	50.96	47.84	45.60	49.73
TiO_2	<0.10	0.21	0.13	-	0.39
Al_2O_3	22.95	20.24	23.33	22.54	2.73
Cr_2O_3	<0.10	<0.10	<0.10	-	<0.11
Fe_2O_3	-	-	-	0.02	-
FeO	0.18	0.15	0.33		7.36
BaO	-	-	-	0.22	-
MnO	<0.09	<0.09	<0.09	-	0.15
MgO	<0.09	<0.09	<0.09	-	13.43
CaO	8.08	6.37	8.29	7.72	23.50
Na_2O	<0.11	0.22	<0.11	1.50	<0.13
K_2O	5.60	8.01	5.70	5.63	<0.06
H_2O	-	-	-	16.58	-
Total	84.99	86.16	85.61	99.81	97.30
Number of ions on the basis of 32 (phillipsite) and 6 (clinopyroxene) oxygens.					
Si	10.32	10.85	10.21	10.10	1.91
Ti		0.03	0.02		0.01
Al	5.80	5.08	5.87	5.89	0.12
Fe	0.03	0.03	0.06		0.24
Mg					0.77
Ca	1.85	1.45	1.90	1.84	0.97
Na		0.09		0.64	
K	1.53	2.17	1.55	1.59	
Ca					49.0
Mg					39.0
Fe					12.0

1 - 3. Phillipsite psuedomorphing leucite phenocrysts, Fiji ankaramite.
4. Phillipsite, occurring as amygdale in Tertiary basalt, Glenariff, Co. Antrim, Northern Ireland. (from Walker 1983).
5. Clinopyroxene phenocryst, Fiji ankaramite.

2.3 Analytical Procedures

Samples were supplied either as small hand-specimens (Italian, Ullung-do Island and Fiji samples), rock chips (New South Wales leucitites) or rock powders which had been prepared using a tunsten carbide swing mill (Spanish lamproites). For geochemical analysis, the sample was crushed using a tungsten carbide swing mill. Major-element analyses were obtained by XRF spectrometry on fused glass discs using an automated Siemens SRS300 spectrometer (located within the Department of Geology, A.N.U.), following the procedure of Norrish and Hutton (1969). Abundances of the elements Ni, Cu, Rb, Sr, Y, Zr, Nb, and Pb were determined by XRF on pressed powder pellets using a Phillips PW1400 spectrometer and using the method of Norrish and Chappell (1977). The other trace elements were obtained by instrumental neutron activation analysis on ~300 mg of powdered sample. For isotopic analysis, hand-specimens were sawn into ~3 cm^3 cubes which were then thoroughly washed in demineralised H_2O. The cubes were coarsely crushed in a stainless steel mortar and small (~15 mg) rock chips with fresh fracture surfaces were carefully hand-picked for analysis. About 250 to 500 mg of hand-picked chips were dissolved in teflon pressure vessels in HF-$HClO_4$ at 200 °C for at least 48 hours, the solution then

evaporated and re-dissolved in 6 N HCl in the teflon pressure vessel at 200 °C for at least 24 hours. The resulting solution was evaporated, re-dissolved in 1 N HCl and split into 2 aliquots, one of which was spiked with mixed ^{85}Rb-^{84}Sr and ^{147}Sm-^{150}Nd spikes and processed for Sr and Nd isotopic analysis and the second used for Pb isotopic composition. Where correction to the Pb isotopic composition for radiogenic decay of U was thought necessary, a third split was mixed with ^{235}U-^{208}Pb spike for U and Pb concentration analysis. The remaining details of the analytical techniques are described in Appendix 1.

2.4 Results

The results of Rb-Sr, Sm-Nd and U-Pb concentration and isotopic analysis are presented in Tables 2.3 and 2.4 and compared with other relevant data in Figs. 2.4 to 2.9.

2.4.1 Southeast Australian leucitites

K-Ar dating has given ages ranging from 10 to 16 Ma for the New South Wales leucitites and 6 Ma for the Cosgrove occurrence (Wellman *et al.* 1970, Wellman 1974, Sutherland 1983). (Where necessary, quoted ages have been re-calculated using the constants of Steiger and Jäger 1977). The correction for radiogenic decay since emplacement is within or just outside the analytical uncertainty for Rb/Sr and Sm/Nd isotope systems and for most of the Pb analyses. Nd/Sm ranges from 5.4 to 7.1 (chondritic ≈ 3), indicating that the leucitites are highly LREE-enriched. Nd and Sr isotopic compositions lie within the mantle array (Fig. 2.4), extending from the "depleted" quadrant for the most southerly occurrence, the Cosgrove leucitite (ε_{Nd} = +1.5, $^{87}Sr/^{86}Sr$ = 0.7042), into the "enriched" quadrant for the most northerly New South Wales occurrence at El Capitan (ε_{Nd} = -4.1, $^{87}Sr/^{86}Sr$ = 0.7057). As Th concentrations were not determined for the southeast Australian rocks, the small age corrections to $^{208}Pb/^{204}Pb$ were made assuming Th/U = 4. The Condobolin leucitite (GA-3476) has high U/Pb and the age correction to $^{206}Pb/^{204}Pb$ and $^{208}Pb/^{204}Pb$ is significant compared to the analytical error. Age-corrected Pb isotopic compositions show little variation, with the exception of the Cosgrove sample which has significantly lower $^{207}Pb/^{204}Pb$ than the other members of the suite, and the El Capitan leucitite which has slightly lower $^{206}Pb/^{204}Pb$. The Pb isotopic compositions of the New South Wales leucitites are characterised by relatively high $^{207}Pb/^{204}Pb$ and $^{208}Pb/^{204}Pb$ compared to those of MORB but are similar to those determined by Cooper and Green (1969) for contemporaneous Tertiary-Recent continental alkali basalts from western Victoria.

The Cosgrove leucitite is chemically and petrographically distinct from the New South Wales leucitites, being poorer in olivine and leucite and richer in clinopyroxene (Birch 1978), reflected in its lower MgO, K_2O, Rb, Ni, and higher in CaO, total Fe, Na_2O, and possibly TiO_2 contents and lower LREE/HREE (see Tables 2.1 and 2.3). These features imply derivation of the Cosgrove leucitite from a more depleted source than the New South Wales leucitites, consistent with the isotopic data (i.e. the lower $^{207}Pb/^{204}Pb$ and $^{87}Sr/^{86}Sr$ and higher $^{143}Nd/^{144}Nd$ of the Cosgrove leucitite). The Cosgrove leucitite has Pb, Sr and Nd isotopic compositions within the range determined for the southeast Australian Tertiary-Recent Newer alkali basalts (Cooper and Green 1969, McDonough *et al.* 1985).

Although the exact age of emplacement of the Inglewood analcimite is not known, an age of 22 Ma has been assumed, based on K-Ar studies of nearby volcanism with which the Inglewood leucitite is

Table 2.3 Strontium and neodymium isotopic data for orogenic potassic suites.

Sample	Rb	Sr	Sm	Nd	$^{87}Rb/^{86}Sr$	$^{87}Sr/^{86}Sr$[a] meas	$^{87}Sr/^{86}Sr$[a] initial	$^{147}Sm/^{144}Nd$	$^{143}Nd/^{144}Nd$[b]	ε_{Nd}
	---- ppm ----									
New South Wales leucitites										
GA-3470 Begargo Hill	179	2065	14.5	88.9	0.250	0.70562 ±4	0.70557	0.0989	0.51182 ±2	-0.3
GA-3471 Begargo Hill	78.9	1251	14.1	86.6	0.182	0.70514 ±3	0.70511	0.0983	0.51180 ±1	-0.7
GA-3472 Bygalore	159	1779	24.6	159	0.258	0.70523 ±6	0.70519	0.0938	0.51177 ±2	-1.3
GA-3473 Bygalore	128	1577	20.0	124.9	0.234	0.70522 ±4	0.70518	0.0973	0.51181 ±3	-0.6
GA-3474 Gorman Hills	147	1396	20.7	135.1	0.305	0.70502 ±4	0.70496	0.0937	0.51181 ±2	-0.4
GA-3475 Tullibigeal	173	1353	18.9	119.1	0.369	0.70554 ±5	0.70548	0.0962	0.51178 ±3	-1.1
GA-3476 Condobolin	135	1494	14.9	93.0	0.260	0.70506 ±6	0.70501	0.0967	0.51185 ±3	+0.3
GA-3478 L. Cargellico	143	1670	17.3	107.1	0.248	0.70525 ±4	0.70520	0.0979	0.51181 ±2	-0.5
GA-3480 Burgooney	105	1323	14.6	88.6	0.229	0.70513 ±4	0.70508	0.0998	0.51184 ±1	+0.1
GA-3481 Flagstaff	185	1265	15.1	92.7	0.423	0.70522 ±4	0.70515	0.0986	0.51178 ±2	-1.2
GA-3479 El Capitan	265	972	16.7	118.3	0.596	0.70572 ±4	0.70561	0.0851	0.51163 ±2	-4.1
Victorian leucitite										
E7980 Cosgrove	76	1230	13.9	75.2	0.179	0.70422 ±3	0.70420	0.112	0.51192 ±2	+1.5
Queensland analcimite										
HH-321 Inglewood	56.1	1492	15.9	90.9	0.109	0.70518 ±5	0.70515	0.106	0.51177 ±2	-1.2
New South Wales Jurassic analcimite										
70-139 Harden	96	816	9.27	49.3	0.423	0.70522 ±4	0.70405	0.114	0.51185 ±2	+0.3
Italian leucite melilitites										
Ven-1 San Venanzo	185	1774	13.9	75.7	0.300	0.71058 ±4	0.71058	0.111	0.51125 ±2	-11.4
Cup-10 Cupaello	276	5761	34.3	187.8	0.139	0.71118 ±5	0.71118	0.110	0.51129 ±2	-10.6
Spanish lamproites										
SP-034 Aljorra	176	547	19.1	100.7	0.931	0.72083 ±6	0.72073	0.115	0.51126 ±2	-11.2
SP-039 Zeneta	173	555	18.7	90.0	0.903	0.72069 ±4	0.72060	0.126	0.51119 ±2	-12.6
SP-044 Fortuna	29.9	558	21.7	108.1	0.155	0.71798 ±3	0.71796	0.121	0.51125 ±2	-11.4
SP-049 Fortuna	306	539	23.4	120.5	1.647	0.71809 ±3	0.71792	0.118	0.51126 ±2	-11.2
SP-055 Jumilla	232	816	28.0	148.1	0.822	0.71688 ±5	0.71680	0.114	0.51122 ±2	-12.1
SP-067 Cancarix	241	902	30.2	160.4	0.774	0.71750 ±5	0.71742	0.114	0.51125 ±2	-11.5
SP-077 Calasparra	266	584	30.7	161.3	1.317	0.72074 ±6	0.72061	0.115	0.51124 ±3	-11.7
SP-081 Puebla de Mula	413	991	22.8	107.7	1.205	0.71745 ±5	0.71733	0.128	0.51124 ±2	-11.6
Ullung-do Island leucitite										
Ull-1 5th stage	-	444	-	-	-	0.70449 ±3	0.70449	-	0.51179 ±3[c]	-0.9
Fiji ankaramite										
AJCF2	-	-	-	39.6	-	0.70404 ±4	0.70404	-	0.51217 ±3	+6.5

[a] Errors given refer to within-run precision at the $2\sigma_{mean}$ level. Uncertainty in $^{87}Rb/^{86}Sr$ is 0.5% (2σ). $^{87}Sr/^{86}Sr$ normalised using $^{86}Sr/^{88}Sr = 0.1194$. Initial $^{87}Sr/^{86}Sr$ calculated using the (re-calculated) K-Ar ages of Wellman *et al.* (1970), Wellman (1974) and Sutherland (1983) for southeast Australian samples, 22 Ma for the Inglewood analcimite and 7 Ma for the Spanish lamproites. NBS-987 standard value is 0.71022 ±4. E & A standard carbonate value is 0.70800 ±3.

[b] Uncertainty in $^{147}Sm/^{144}Nd$ is 0.1% (2σ). Nd isotopic ratios normalised using $^{146}Nd/^{142}Nd = 0.636151$. Age corrections to Nd isotopic compositions are within analytical error for all samples except Harden (see text). The value obtained for BCR-1 standard is 0.511833 ±20. $\varepsilon_{Nd} = (^{143}Nd/^{144}Nd_{meas}/^{143}Nd/^{144}Nd_{CHUR} - 1) \times 10^4$ where $^{143}Nd/^{144}Nd_{CHUR} = 0.511836$.

[c] Analyst: E. Nakamura.

Table 2.4 Uranium, thorium, lead concentration and lead isotopic data for orogenic potassic suites.

Sample	U[a]	Th	Pb	$^{238}U/^{204}Pb$	$^{206}Pb/^{204}Pb$[b]		$^{207}Pb/^{204}Pb$	$^{208}Pb/^{204}Pb$	
	ppm				meas	initial	meas	meas	initial
New South Wales leucitites									
GA-3470 Begargo Hill	-	-	-	-	18.235		15.595	38.644	
GA-3471 Begargo Hill	-	-	-	-	18.217		15.621	38.333	
GA-3472 Bygalore	2.43	-	9.64	18.4	18.223	(18.19)[c]	15.618	38.202	(38.16)[c,d]
GA-3473 Bygalore	2.42	-	11.33	15.4	18.245	(18.21)	15.603	38.135	(38.09)
GA-3474 Gorman Hills	2.43	-	11.05	15.7	18.121	(18.09)	15.606	38.346	(38.30)
GA-3475 Tullibigeal	2.46	-	12.33	14.4	18.074	(18.05)	15.623	38.295	(38.27)
GA-3476 Condobolin	2.72	-	2.2	89.9	18.430	(18.25)	15.593	38.532	(38.30)
GA-3478 L. Cargellico	-	-	-	21.5	18.308	(18.27)	15.617	38.270	
GA-3480 Burgooney	-	-	-	-	18.236		15.584	38.408	
GA-3481 Flagstaff	-	-	-	-	18.172		15.595	38.193	
GA-3479 El Capitan	2.14	-	9.32	16.6	17.877	(17.84)	15.593	38.125	(38.07)
Victorian leucitite									
E7980 Cosgrove	-	-	-	-	18.350		15.553	38.345	
Queensland analcimite									
HH-321 Inglewood	3.19	-	6.92	34.5	19.156	(19.04)	15.637	39.522	(39.37)
New South Wales Jurassic analcimite									
70-139 Harden	-	-	-	-	19.075		15.579	38.445	
Spanish lamproites									
SP-034 Aljorra	-	-	89.4	-	18.659		15.675	39.025	
SP-039 Zeneta	-	(85)	-	-	18.755		15.706	39.064	
SP-044 Fortuna	21.9	-	105	15.4	18.793	(18.78)	15.739	39.198	(39.18)
SP-049 Fortuna	20.3	(89)	64.4	23.4	18.759	(18.73)	15.688	39.067	(39.03)
SP-055 Jumilla	15.4	(105)	67.0	17.1	18.802	(18.78)	15.718	39.146	(39.10)
SP-067 Cancarix	15.9	(128)	117	10.0	18.788	(18.78)	15.702	39.084	(39.05)
SP-077 Calasparra	-	(112)	-	-	18.815		15.712	39.066	
SP-081 Puebla de Mula	29.0	(123)	74.8	28.7	18.809	(18.78)	15.715	39.065	(39.02)
Ullung-do Island leucitite									
Ull-1 5th stage	-	-	-	-	18.005		15.505	38.654	

[a] U and Pb concentrations determined by isotope dilution mass spectrometry; values in brackets determined by XRF analysis; Th concentrations for Spanish lavas from Venturelli *et al.* (1984).

[b] Errors (based on two-way analysis of variance of duplicate analyses) at the 1σ level; $^{206}Pb/^{204}Pb$ ±0.011, $^{207}Pb/^{204}Pb$ ±0.014, $^{208}Pb/^{204}Pb$ ±0.033. The values obtained for NBS-981 during this study (average of 7 analyses) are; $^{206}Pb/^{204}Pb$ = 16.927 ±0.009, $^{207}Pb/^{204}Pb$ = 15.486 ±0.013, $^{208}Pb/^{204}Pb$ = 36.668 ±0.044.

[c] Corrected for ^{238}U and ^{232}Th decay since emplacement, using ages from references cited in Table 2.3. The age correction to $^{207}Pb/^{204}Pb$ is insignificant compared to the analytical error for all samples except the Harden analcimite.

[d] Where Th data is not available, the age-correction is made assuming Th/U = 4.

associated (Wellman and McDougall 1974). Despite some uncertainty in the exact age of volcanism, the age corrections to the measured Nd, Sr and Pb isotopic ratios are within or close to the analytical error. Initial Sr and Nd isotope ratios overlap with those of the New South Wales olivine leucitites, but the analcimite has slightly higher initial $^{207}Pb/^{204}Pb$ and substantially higher initial $^{206}Pb/^{204}Pb$. The combined isotope data therefore indicate that the Inglewood analcimite and the New South Wales suite were derived from isotopically similar sources, but with the Inglewood analcimite source having higher recent U/Pb.

After correction for age of emplacement (determined by Wellman *et al.* 1970, as 198 ±3 Ma), the Nd and Sr isotopic data indicate that the Harden analcimite was derived from a depleted source with ε_{Nd} = +2.4 and initial $^{87}Sr/^{86}Sr = 0.7042$. U and Th abundances have not been determined so it is not possible to correct precisely for their radioactive decay since emplacement. Assuming reasonable values for μ ($^{238}U/^{204}Pb$) of 20 and Th/U of 4 results in age-corrected $^{206}Pb/^{204}Pb$ of 18.45, $^{207}Pb/^{204}Pb$ of 15.55 and $^{208}Pb/^{204}Pb$ of 37.65. Although $^{206}Pb/^{204}Pb$ and $^{208}Pb/^{204}Pb$ estimated in this way is subject to considerable uncertainty, the correction to $^{207}Pb/^{204}Pb$ is small (i.e. ~ -0.03). The Pb isotopic data therefore indicate that the source of the Harden analcimite had $^{207}Pb/^{204}Pb$ lower than that of the New South Wales olivine leucitite suite but comparable to that of the Cosgrove olivine leucitite.

2.4.2 Spanish lamproites

Whole-rock and mineral K-Ar data on several of the Spanish lamproites indicates ages of ~ 6 to 8 Ma (Bellon and Letousey 1977, Nobel *et al.* 1981). The high Rb/Sr ratios (Table 2.3) require small but significant age corrections to be applied to the Sr isotopic data. Initial Sr isotopic compositions show a wide range and are highly radiogenic (0.717 to 0.720), similar to the values reported by Powell and Bell (1970) for samples from Jumilla. Nd/Sm varies from 4.8 to 5.2, suggesting moderate LREE-enrichment. Nd isotopic compositions are unradiogenic and fall within the narrow range of ε_{Nd} of from -11.2 to -12.6, indicating that the sources of these rocks have had long-term LREE-enrichment (>1 Ga). These isotopic features are like those of the Western Australian lamproites (McCulloch *et al.* 1983) and the micaceous South African kimberlites (Smith 1983, see Fig. 3.3). The measured Pb isotopic compositions are within the range $^{206}Pb/^{204}Pb$ of 18.66 to 18.81, $^{207}Pb/^{204}Pb$ of 15.67 to 15.74 and $^{208}Pb/^{204}Pb$ of 39.0 to 39.2. Of present-day reservoirs, the Pb isotopic compositions of the Spanish ultrapotassic rocks most closely resembles that of pelagic oceanic sediments (e.g. Sun 1980).

2.4.3 Italian leucitite melilitites

Both Italian samples analysed possess high concentrations of Sr and the light rare-earth elements (see Table 2.3). Their highly radiogenic $^{87}Sr/^{86}Sr$ ratios are similar to the values previously reported for lavas from these volcanoes (Vollmer 1976, Holm and Munksgaard 1982). On the initial Sr-Nd isotope diagram (Fig. 2.4), the San Venanzo and Cupaello lavas lie along the array previously defined for Italian potassic lavas, but extend the array towards more radiogenic Sr and unradiogenic Nd values. The Nd isotopic compositions of the Italian melilitites are within the narrow range determined for the Spanish lamproites, although the Italian lavas possess less radiogenic Sr isotopic compositions.

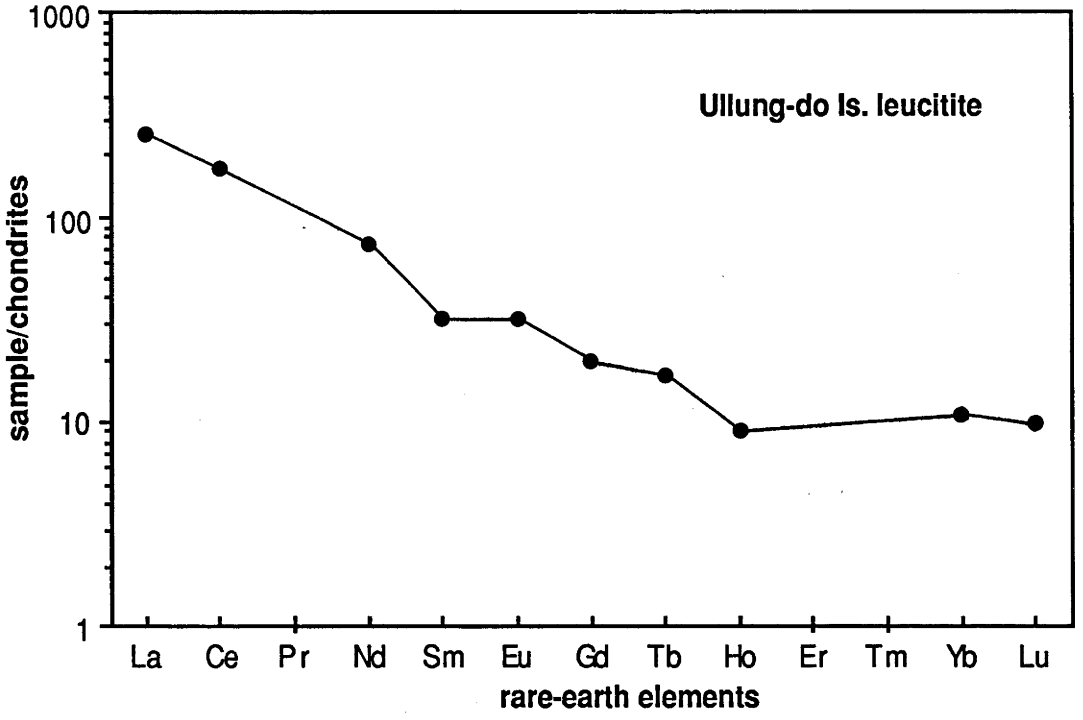

Fig. 2.2 Chondrite-normalised rare-earth element abundance pattern for the leucitite from Ullung-do Island. The chondrite abundances used are those of Taylor and Gordon (1977).

2.4.4 Ullung-do Island leucitite

Rare-earth element analytical results for the Ullung-do Island leucitite are given in Table 2.1 and shown normalised to chondritic abundances in Fig. 2.2. Notable features of the rare-earth element pattern are the relatively steep negative normalised light rare-earth element gradient, almost flat normalised heavy rare-earth elements and the small positive Eu anomaly (Eu/Eu^{*} = 1.19). The Ullung-do Island leucitite also possesses relatively low transition-element contents (suggesting significant crystal fractionation has occurred) accompanied by high Ba and Th contents and high Th/U (7.75).

Compared to most oceanic magmatism, the Ullung-do Island leucitite has relatively radiogenic $^{87}Sr/^{86}Sr$ and significantly unradiogenic $^{143}Nd/^{144}Nd$ (Table 2.3; see Fig. 2.4). The $^{206}Pb/^{204}Pb$ ratio (Table 2.5) lies within the range observed for mid-ocean ridge basalts (Fig. 2.5), but the leucitite has slightly higher $^{207}Pb/^{204}Pb$ and significantly higher $^{208}Pb/^{204}Pb$ (see Fig. 2.6) than is found in MORB, plotting within the Kerguelen field. The radiogenic $^{208}Pb/^{204}Pb$ and $^{87}Sr/^{86}Sr$ and unradiogenic $^{143}Nd/^{144}Nd$ suggests a mantle source resembling that of many ocean-island basalts rather than that of mid-ocean ridge basalts. Several other Pb isotopic studies of alkali basalts from the southwestern Japan region (Kurasawa 1968, Tatsumoto and Knight 1969, Allègre *et al.* 1979) have found Pb isotopic compositions comparable to some ocean islands. The relatively unradiogenic $^{207}Pb/^{204}Pb$ of the leucitite implies that its source was not substantially contaminated by Pb derived from subducted sediments.

2.4.5 Fiji leucite-bearing ankaramite

The results of major- and trace- element analysis of the Fiji ankaramite are given in Table 2.1 and the chondrite-normalised rare-earth element pattern given in Fig. 2.3. The rare-earth element pattern is unusual in having virtually flat chondrite-normalised abundances of the light (between La and Nd) and

heavy (between Ho and Lu) rare-earth elements but a steep negative gradient for the middle (between Nd and Ho) rare-earth elements. A negative Ce anomaly is evident in the pattern, suggesting that the rare-earth abundances have been modified by secondary (perhaps late-stage hydrothermal) processes. Further supporting evidence of this is provided by the low major-element sum (totalling 92.1 %; H_2O and other volatiles have not been determined), which suggests that the glassy groundmass of the sample is extensively hydrated, and the phillipsite psuedomorphs of leucite.

The Sr and Nd isotopic compositions of the Fiji ankaramite ($^{87}Sr/^{86}Sr$ and ε_{Nd} values of 0.7040 and +6.5 respectively, see Table 2.3) are similar to those found by Gill (1984) and most closely resemble the values characteristic of island-arc and ocean-island magmas (Fig. 2.4).

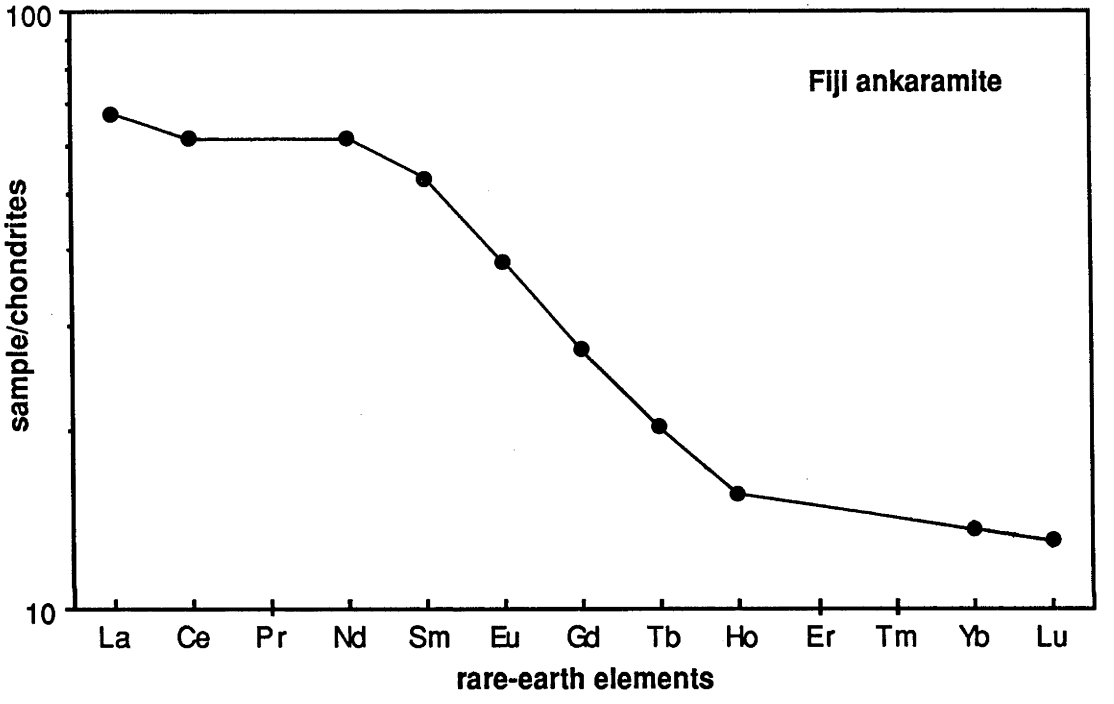

Fig. 2.3 Chondrite-normalised rare-earth element abundance pattern for the ankaramite from Fiji. The chondrite abundances used are those of Taylor and Gordon (1977).

2.5 Discussion

2.5.1 Southeast Australian leucitites

Although the evolved isotopic characteristics of the New South Wales leucitites may be attributed to contamination by continental crust, there is no compelling evidence for the assimilation of crustal material in the major- and trace-element characteristics of the lavas. The suite has high Ni (average ~375 ppm), Cr (~400 ppm), MgO (12.4 wt%), $Mg/(Mg + Fe^{2+})$ (excluding some of the fractionated Begargo Hill samples, averaging ~0.71 recalculated assuming $Fe^{3+}/(Fe^{2+}+Fe^{3+}) = 0.15$), combined with low SiO_2 (44.3 wt%) and Al_2O_3 (8.7 wt%) (Cundari 1973), consistent with their derivation from the mantle. In addition, while the El Capitan leucitite (GA-3479) has the most radiogenic Sr and least radiogenic Nd and is therefore the most likely candidate to have been contaminated by continental crust, there is no evidence of this in its major- and trace-element chemistry. Taylor *et al.* (1984) analysed the same samples used in this study for $^{18}O/^{16}O$, and found that the whole-rock and leucite phases are enriched in ^{18}O but that the clinopyroxenes have $\delta^{18}O_{SMOW}$ of ~ +6.5 ‰, considered to represent primary magmatic values.

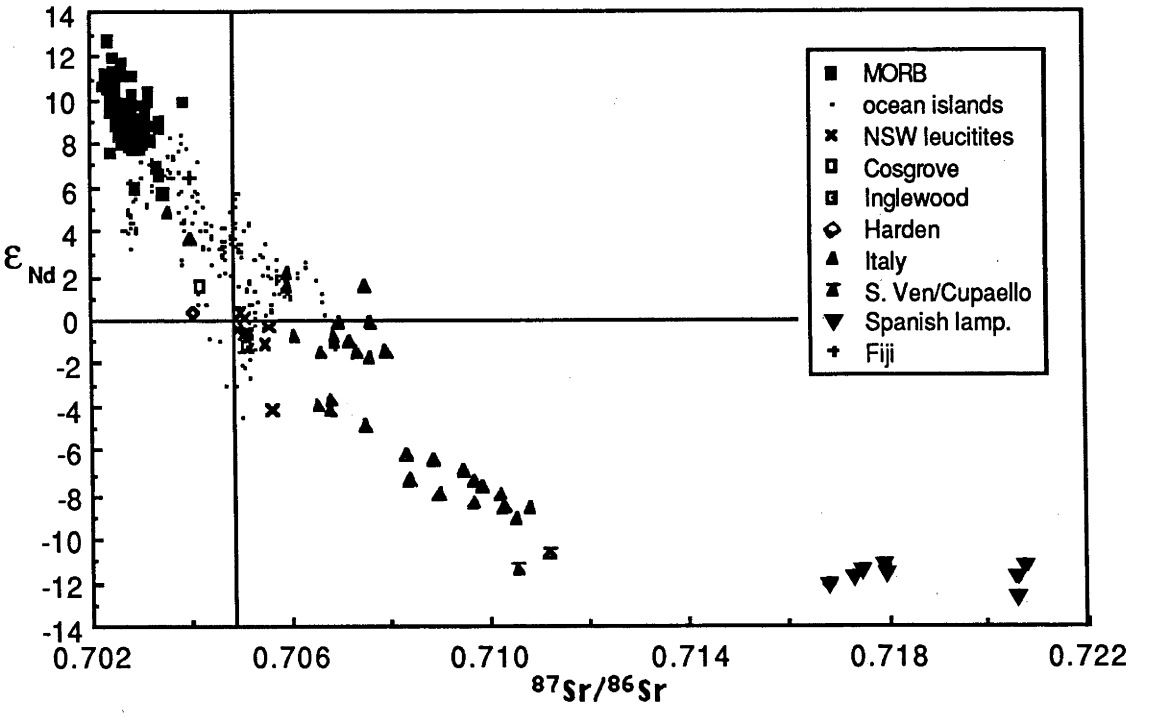

Fig. 2.4 Nd-Sr isotope initial ratio correlations for orogenic potassic samples compared to the fields for mid-ocean ridge and ocean-island basalts. The negative correlation between Sr and Nd isotopic compositions for potassic rocks is consistent with mixing between two isotopically distinct components. Additional data sources- MORB: Cohen and O'Nions (1982a), White and Hofmann (1982), Ito *et al.* (1987). Ocean islands: Cohen and O'Nions (1982b), Richardson *et al.* (1982), Vidal *et al.* (1984), Palacz and Saunders (1986), Wright and White (1986), Dupuy *et al.* (1987). Potassic suites: Hawkesworth and Vollmer (1979) and this study.

They attributed the high ^{18}O of the leucites to interaction with late-stage K-rich magmatic fluid with high $\delta^{18}O$ (~ +8 ‰), although they did not discount the possibility of the involvement of small amounts of meteoric water which had isotopically equilibrated with magmatic fluid. The primary $\delta^{18}O$ values estimated from the clinopyroxenes are similar to the values of alkali basalts and argue against the assimilation of upper crustal material. It is unlikely that the possible involvement of small amounts of meteoric water could have significantly effected the Sr, Nd and Pb isotopic compositions.

The variation in isotopic characteristics of the New South Wales leucitites may therefore be the result of either: a) contamination of their sources by a component having radiogenic $^{87}Sr/^{86}Sr$, unradiogenic ε_{Nd} and $^{207}Pb/^{204}Pb \geq 15.6$; or b) derivation from variably enriched mantle sources which have evolved the observed isotopic compositions since the enrichment events. The latter alternative is considered less likely as a period of at least ~300 Ma is required to produce the observed range in Nd isotopic compositions of 4 ε-units from closed system decay within source regions which have undergone varying degrees of incompatible-element enrichment (i.e. increase in Nd/Sm and Rb/Sr accompanied by a decrease in U/Pb), assuming a source Sm/Nd like that of the leucitites themselves. As the source Sm/Nd is likely to be considerably higher than that of the leucitite melt, this time estimate is probably greatly underestimated. The El Capitan leucitite has the highest measured K_2O/Na_2O, Rb/Sr and Nd/Sm ratios and significantly more radiogenic Sr and less radiogenic Nd compared to the other New South Wales leucitites, (see Figs. 2.7 and 2.8), consistent with greater contribution of an incompatible-element- and K-enriched, high $^{87}Sr/^{86}Sr$, low ε_{Nd} component to its source, but also has identical $^{207}Pb/^{204}Pb$ to the

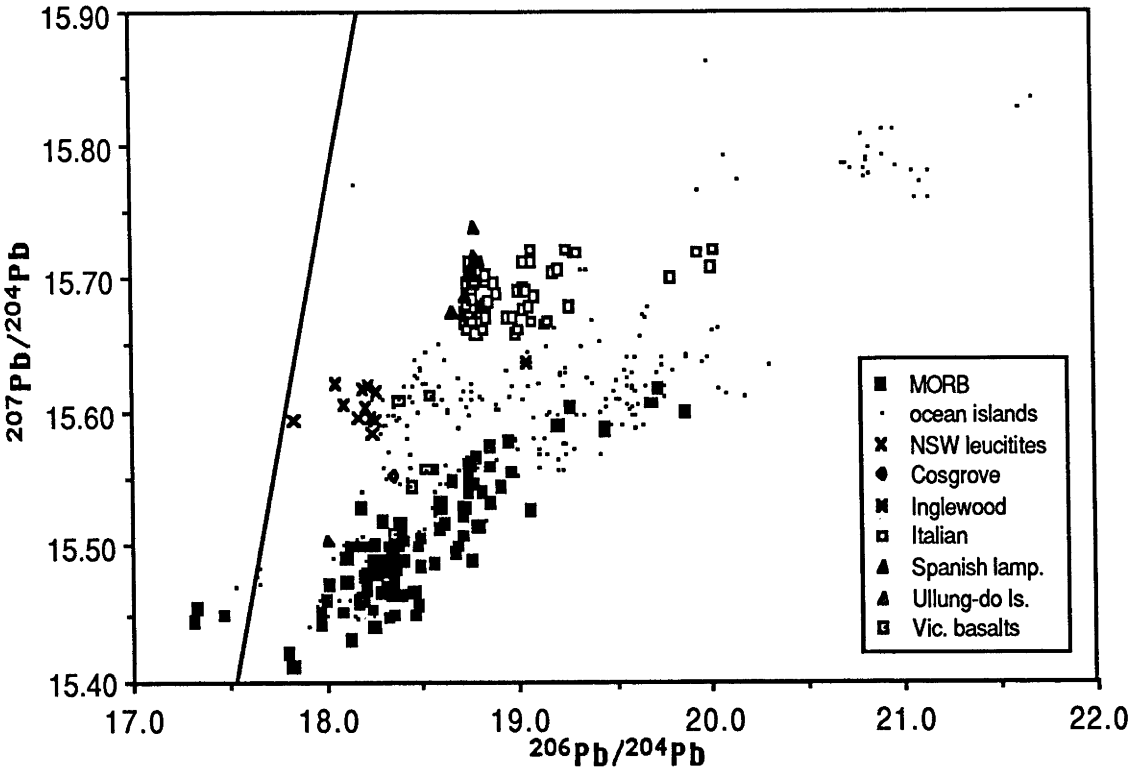

Fig. 2.5 $^{206}Pb/^{204}Pb$-$^{207}Pb/^{204}Pb$ variation in orogenic potassic rocks, compared to the fields for mid-ocean ridge and ocean-island basalts. Additional data sources- MORB: as in Fig. 2.4 and Dupré and Allègre (1980), Sun (1980). Ocean islands: as in Fig. 2.4 and Sun (1980). Victorian Newer basalts (Cooper and Green 1969, McDonough *et al.* 1985). Potassic rocks: Vollmer (1976, 1977b), Vollmer and Hawkesworth (1980) and this study.

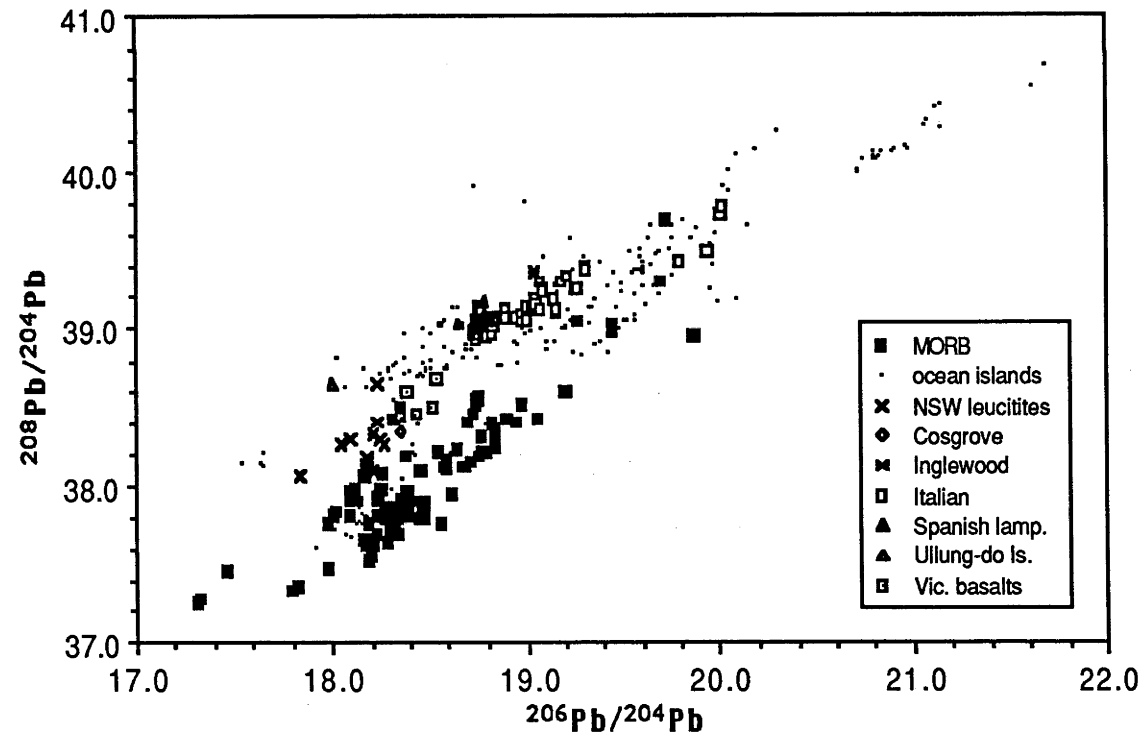

Fig. 2.6 $^{206}Pb/^{204}Pb$-$^{208}Pb/^{204}Pb$ variation in orogenic potassic rocks, compared to the fields for mid-ocean ridge and ocean-island basalts. Additional data sources- MORB: as in Fig. 2.4 and Dupré and Allègre (1980), Sun (1980). Ocean islands: as in Fig. 2.4 and Sun (1980). Victorian Newer basalts (Cooper and Green 1969, McDonough *et al.* 1985). Potassic rocks: Vollmer (1976, 1977b), Vollmer and Hawkesworth (1980) and this study.

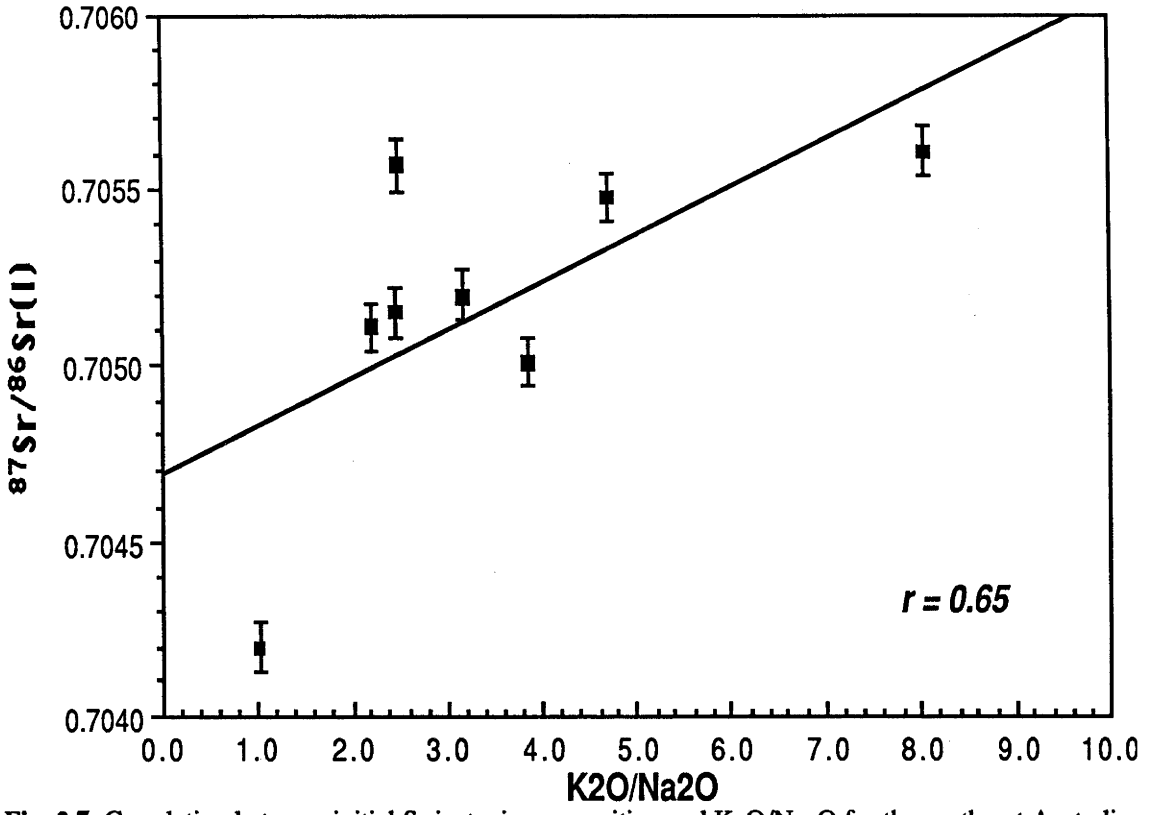

Fig. 2.7 Correlation between initial Sr isotopic composition and K_2O/Na_2O for the southeast Australian leucitites. There is a weak positive correlation, suggesting that the sources of the leucitites may have been contaminated by a high K_2O/Na_2O, radiogenic Sr component. Data sources: Cundari (1973), Birch (1978) and this study.

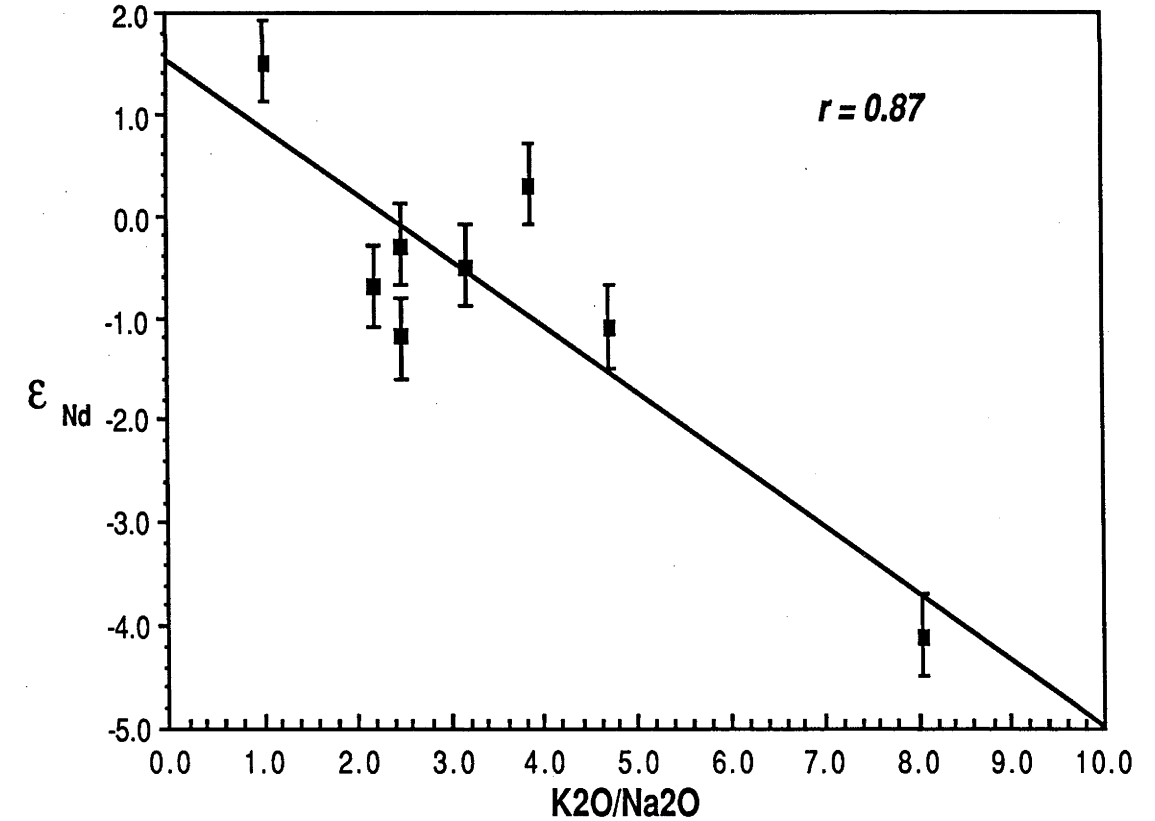

Fig. 2.8 Correlation between initial Nd isotopic composition and K_2O/Na_2O for the southeast Australian leucitites. There is a weak negative correlation, consistent with the involvement of a contaminating component with high K_2O/Na_2O and unradiogenic Nd. Data sources as in Fig. 2.7.

other New South Wales leucitite occurrences. This suggests that either the Pb isotopic compositions of the leucitites are dominated by that of the added component, or that the added component and the invaded mantle had similar $^{207}Pb/^{204}Pb$. The less radiogenic $^{206}Pb/^{204}Pb$ of the El Capitan leucitite compared to the other New South Wales occurrences may be due to some variation in the timing or degree of enrichment in the leucitite sources, or may indicate differences in the $^{206}Pb/^{204}Pb$ of the added components involved at El Capitan and the other occurrences.

The geochemical and isotopic data are therefore consistent with the derivation of the New South Wales leucitites from mantle which has been contaminated by a component with $^{87}Sr/^{86}Sr \geq 0.7057$, $\varepsilon_{Nd} \leq -4$ and $^{207}Pb/^{204}Pb \approx 15.6$. Compared to the Tertiary-Recent Victorian Newer alkali basalts (McDonough *et al.* 1985), the Cosgrove leucitite has similar Sr, Nd and Pb isotopic compositions whereas the New South Wales leucitites have higher $^{87}Sr/^{86}Sr$ and lower $^{143}Nd/^{144}Nd$, forming an extension of the array displayed by the Newer basalts into the enriched quadrant on the $^{87}Sr/^{86}Sr$-$^{143}Nd/^{144}Nd$ diagram. The New South Wales leucitites have similar $^{207}Pb/^{204}Pb$ and $^{208}Pb/^{204}Pb$ but have lower $^{206}Pb/^{204}Pb$ than the Newer basalts (Cooper and Green 1969; see Figs. 2.5 & 2.6). Although these features may simply reflect regional isotopic heterogeneity within the subcontinental lithosphere beneath southeastern Australia, they may also be interpreted as mixing trends, with the addition of a component having isotopic characteristics like those of the New South Wales leucitites to the sources of the Newer basalts responsible for their isotopic variation. Wellman and McDougall (1974) and Sutherland (1983) showed that the locations and eruption ages of the southeast Australian leucitites and Newer basalts are consistent with the initiation of volcanism by the passage of the Australian continent over a hotspot. As the isotope variation found in the Newer basalts was attributed by McDonough *et al.* (1985) to mixing between a component derived from the hotspot plume and the subcontinental lithosphere, it is conceivable that the hotspot plume represents the enriched, low $^{206}Pb/^{204}Pb$ end-member component. Further Pb isotope analyses of the Newer basalts are required in order to assess this possibility.

A number of studies of Cainozoic alkali basaltic volcanism and incorporated xenoliths from the eastern margin of New South Wales (e.g. Kesson 1973, Wass and Rogers 1980, O'Reilly and Griffin 1984) have argued that the mantle from which the products of volcanism were derived was chemically and isotopically heterogeneous. The widespread occurrence of amphibole ±mica ±apatite-bearing mantle xenoliths has been interpreted as evidence for the operation of metasomatic processes in the source regions of the host lavas. O'Reilly and Griffin (1984) found a range of Sr isotope compositions of from 0.7031 to 0.7054 for New South Wales alkali basalts, and attributed the isotope variation to the metasomatic addition of varying amounts of radiogenic Sr to their sources. Much of the New South Wales alkali basaltic volcanism considered by O'Reilly and Griffin (1984) and others to be derived from metasomatised subcontinental lithosphere predates, and is therefore unrelated to the passage of the hotspot responsible for the leucitite volcanism. Although leucitite volcanism was probably activated by the hotspot, metasomatism of the leucitite sources may have been related to that of the sources of the New South Wales alkali basalts and may have occurred prior to the passage of the hotspot.

2.5.2 Spanish lamproites

The isotopic characteristics of the Spanish lamproites may be attributed to assimilation of crustal material during emplacement of the magmas. The lamproites are characterised by comparatively high Nd concentrations (90 to 160 ppm), requiring the assimilation of substantial amounts of crustal material to produce the observed unradiogenic Nd isotopic compositions. If assimilation of large amounts of upper crust has occurred, it might be anticipated that the isotopic characteristics of those intrusions having lower trace-element contents might display more evidence of this contamination. There is, however, no correlation between Nd content and ε_{Nd} or between SiO_2 content and other geochemical or isotopic parameters which might reflect bulk assimilation of crustal material. Generation of the unradiogenic Nd isotopic compositions of the Spanish lamproites by crustal assimilation also requires the involvement of relatively old crustal material with an average crustal residence time of at least ~1.4 Ga. The lamproites intrude relatively young Proterozoic basement which may not have had sufficient prior history to have evolved the isotopic characteristics required. Furthermore, many of the intrusions which have "crustal" isotopic characteristics also have high MgO, Ni and Cr contents accompanied by generally low Al_2O_3, CaO and Na_2O contents. These features are inconsistent with the generation of the enriched mantle isotopic character by bulk assimilation of substantial amounts of upper crustal material.

2.5.3 Italian leucite melilitites

A number of previous stable and radiogenic isotopic studies of the Italian potassic lavas (e.g. Taylor and Turi 1976, Turi and Taylor 1976, Vollmer 1977b, Taylor *et al.* 1984, Ferrara *et al.* 1985) have argued for the extensive assimilation of crustal material within high-level magma chambers to explain their anomalously high $^{18}O/^{16}O$ and radiogenic Sr and Pb isotopic compositions. Although not fully discounting the possibility of crustal contamination in the more evolved lavas, other studies (e.g. Hawkesworth and Vollmer 1979, Vollmer and Hawkesworth 1980, Holm and Munksgaard 1982, Rogers *et al.* 1985) have argued that these unusual isotopic properties are at least in part due to their derivation from so-called "enriched" mantle sources. Chemical analysis of the San Venanzo and Cupaello melilitites (Table 2.1) indicate that they possess relatively low SiO_2 (42 to 44 wt%) and Na_2O (1.0 to 0.27 wt%) and high MgO (13 to 11 wt%), Ni and Cr contents, consistent with a mantle derivation and indicating that they have undergone relatively little differentiation. In addition, the very high concentrations of Sr and Nd of these lavas (Table 2.3) make their Sr and Nd isotopic compositions insensitive to assimilation of crustal material. Consideration of these aspects of the major- and trace-element characteristics of lavas from San Venanzo and Cupaello suggest that the radiogenic Sr and unradiogenic Nd of these lavas are unlikely to be entirely the result of bulk upper crustal assimilation processes. Nevertheless, the high

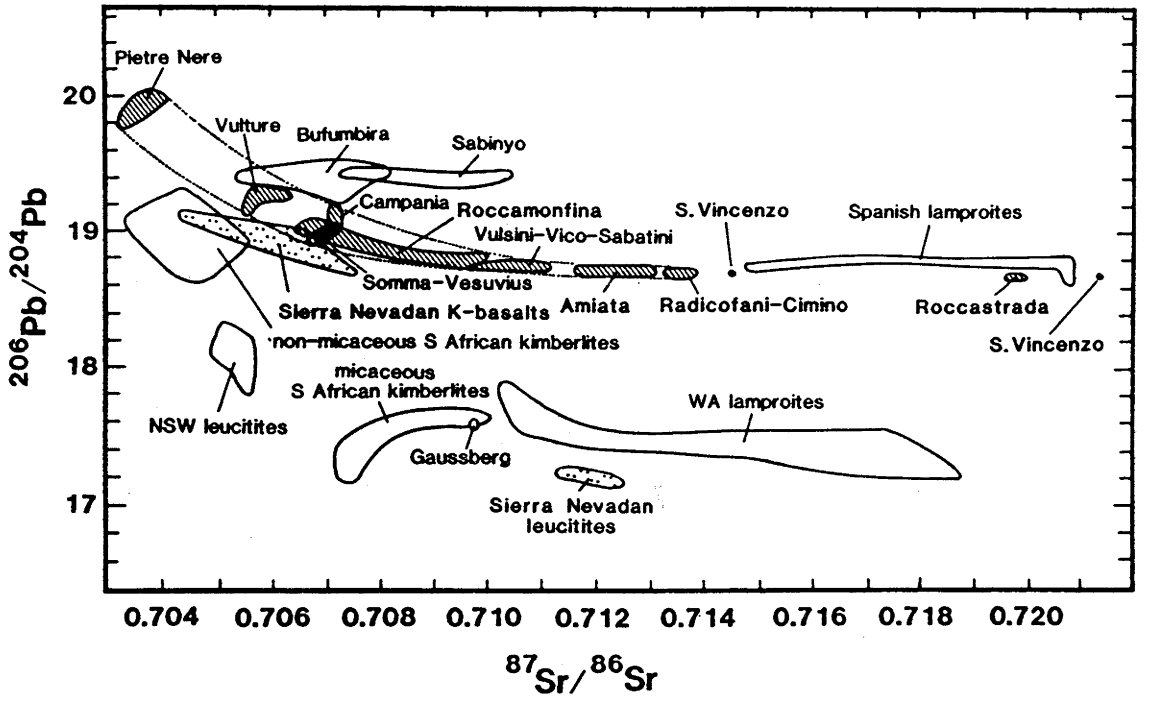

Fig. 2.9 Fields of initial isotopic compositions of $^{206}Pb/^{204}Pb$ against $^{87}Sr/^{86}Sr$ for ultrapotassic suites and some kimberlites. In many cases the range of $^{87}Sr/^{86}Sr$ is large while $^{206}Pb/^{204}Pb$ variation is limited, suggesting that one component has dominated the Pb isotope character. As the field for the Italian lavas extends towards that of the Spanish lamproites (also the case for $^{207}Pb/^{204}Pb$ and $^{208}Pb/^{204}Pb$ vs $^{87}Sr/^{86}Sr$), the "metasomatic" components in both cases may be the same. Additional data sources: Vollmer (1976, 1977b), Vollmer and Hawkesworth (1980), Van Kooten (1981), Collerson and McCulloch (1983), McCulloch *et al.* (1983), Smith (1983).

$^{18}O/^{16}O$ of these lavas provides strong evidence for the involvement of crustal contaminants. It is unlikely that these high $^{18}O/^{16}O$ values are entirely attributable to Rayleigh fractionation during the operation of metasomatic processes within the mantle, as was suggested by Hawkesworth and Vollmer (1979). A possible alternative explanation which is at least qualitatively consistent with both the stable and radiogenic isotopic data is that the mantle sources of these lavas have been contaminated by components derived from the upper continental crust. This alternative will be examined in more detail later (see also Chapter 7).

Comparison between Pb and Sr isotopes of potassic rocks from this and other studies are displayed in Fig. 2.9. Lavas from Italy and Spain resemble those of Western Australia and from the Virungan volcanic field in possessing large ranges in their Sr isotopic compositions but limited variation in Pb compositions, particularly $^{206}Pb/^{204}Pb$, and very high $^{207}Pb/^{204}Pb$. An interesting aspect of the Italian isotopic data is that they lie on a extension of the correlations displayed by the lamproites from Spain on the Sr-Pb isotope diagram (Fig. 2.9). The Pb isotopic compositions of the Spanish lavas are similar to those of the Roman region, which have among the most radiogenic Sr and unradiogenic Nd of the Italian lavas (i.e. most like the Spanish lamproites). This may indicate that the contaminating component invoked to explain the isotopic correlations of lavas from Italy is similar to that identified in the Spanish lamproites. This component has the Sr, Nd and Pb isotopic characteristics of continental crust or sediments derived from continental crust.

2.5.4 Ullung-do Island leucitite

Nakamura *et al.* (1985) found that the island-arc character, indicated by enrichment in K, Ba, Sr and Rb and depletion of TiO_2 and Ta, of alkali basalts across the Japanese island arc to Korea and Eastern China becomes progressively weaker, and that the trace-element patterns of islands from the Sea of Japan show little or no evidence of the influence of subduction processes. In support of this, Peng *et al.* (1986) found that although the Cainozoic basalts of eastern China isotopically resemble those of some ocean islands and island arcs, they have geochemical affinities with continental basalts. The Sr and Nd isotopic compositions of the Ullung-do Island leucitite are also similar to those of some ocean-island and island-arc lavas and indicate that the leucitite was not derived from a mantle source resembling that from which mid-ocean ridge basalts are derived. The relatively unradiogenic $^{207}Pb/^{204}Pb$ limits the possible involvement of subducted oceanic crust and sediments as a source of its high K_2O, as has been proposed to explain the well-documented relationship between potassium and depth of Benioff zone evident in some island arcs (*cf.* Dickinson and Hatherton 1967). The radiogenic $^{208}Pb/^{204}Pb$ suggests affinities with ocean-island rather than island-arc lavas.

2.5.5 Fiji leucite-bearing ankaramite

Gill (1984) argued that the trace-element and isotopic ratios of calc-alkaline and shoshonitic Fijian lavas suggested a contribution from ocean-island-type sources rather than from sources directly arising from the operation of subduction zone processes. However, as with the Ullung-do Island leucitite, the geochemical and isotopic results for the Fiji ankaramite demonstrate the difficulties which are often encountered in distinguishing between island-arc and ocean-island magmas. In an attempt to explain the similarities between island-arc and ocean-island magmas, Morris and Hart (1983) proposed a model in which island-arc magmatism sometimes taps ocean-island-like blobs which are imbedded within a MORB-like matrix distributed throughout the Earth's upper mantle. This model was strongly contested by Perfit and Kay (1986) who argued that the geochemical and isotopic characteristics of island-arc magmas mostly result from mixing between depleted mantle and subducted oceanic crust and sediments. Although the meagre data obtained on Fijian lavas during this reconnaissance study cannot contribute substantially to this discussion, it is worth emphasising that while subduction-related processes may be implicated in the generation of the Italian and Spanish high-K suites, the Italian isotopic data also require the involvement of ocean-island-like sources. This is evident from Fig. 2.9, where the isotopic array for the Italian province extends from one end-member (represented by the Pietre Nere volcano, which has $^{87}Sr/^{86}Sr$ of 0.7033, ε_{Nd} of +4.5 and radiogenic Pb, with the very radiogenic $^{208}Pb/^{204}Pb$ characteristic of ocean islands) which isotopically resembles the St Helena type of ocean island, to another end-member isotopically resembling modern oceanic sediments. This observation supports the model of Morris and Hart (1983) that ocean-island sources are widely distributed throughout the Earth's upper mantle and may be tapped by subduction zone magmatism. Further discussion of the origin and significance of ocean-island isotopic signatures can be found in Section B of this thesis.

2.5.6 Implications for the genesis of potassic magmas from orogenic settings

From the results obtained in this and other studies, it is evident that many orogenic potassic suites possess geochemical and isotopic characteristics consistent with their derivation from geochemically and isotopically anomalous "enriched" mantle sources. An inverse correlation between initial $^{87}Sr/^{86}Sr$ and initial $^{143}Nd/^{144}Nd$ is displayed by many orogenic potassic suites (see Fig. 2.4). This correlation is indicative of mixing between isotopically "enriched" components and mantle sources possessing the isotopic characteristics of either mid-ocean ridge or (at least in the case of the Italian potassic suite) ocean-island basalts. Whitford (1975), Whitford *et al.* (1978) and Varne (1985) demonstrated that the K_2O contents of east Sunda arc volcanics correlate positively with $^{87}Sr/^{86}Sr$ and negatively with $^{143}Nd/^{144}Nd$, also consistent with mixing between two components, one isotopically "enriched" and also rich in K_2O. That most orogenic potassic suites examined so far lie along or plot close to a single curvi-linear array on the initial Sr-Nd isotope diagram (Fig. 2.4) suggests that a common process involving isotopically similar end-members is responsible for the generation of most orogenic potassic magma suites.

In contrast with most continental potassic magmas, K-rich lavas from island arcs and subduction-related settings commonly have low TiO_2, Ta, Nb and Zr, characteristics they share with most arc magmatism. Several studies (e.g. Nicholls and Whitford 1978, Foden and Varne 1980) favour the derivation of high-K arc lavas from mantle which has been modified by the addition of a LIL-rich component to their source regions, although the source of the excess K_2O in high-K island-arc volcanism is controversial. Geochemical and isotopic studies of lavas from the west Sunda arc, Indonesia, (Whitford 1975, Whitford *et al.* 1981) demonstrated that although tholeiitic and calc-alkaline lavas display evidence consistent with contamination by a component derived from subducted lithosphere, the leucite-bearing lavas of Mt. Muriah, situated ~300 km above the Benioff zone, manifest least evidence of such contamination. However, leucite-normative lavas from the east Sunda arc region have radiogenic Sr compared to calc-alkaline lavas from the same region (Whitford *et al.* 1978), suggesting that they may have been more strongly contaminated by a sedimentary component derived from the subducted slab. White *et al.* (1983) has also argued for the involvement of subducted sediments in the genesis of lavas from the Sunda arc to account for their Sr and Pb isotopic characteristics. It seems likely that melts or fluids derived from the subducted slab are involved, but that in a few cases (such as Mt Muriah) these may not be isotopically distinguishable from the invaded mantle.

A number of other recent studies (e.g. Thompson 1977, Edgar 1980, Civetta *et al.* 1981, Venturelli *et al.* 1984, Peccerillo *et al.* 1984, Peccerillo 1985, Rogers *et al.* 1985, Nelson *et al.* 1986a) have also argued, on the basis of geochemical similarities with modern arc lavas, for the involvement of subduction processes in the genesis of potassic volcanism of Italy and southeastern Spain. Trace-element characteristics of the Spanish lavas, such as their high Ba concentrations, low K/Rb, high Ba/La and rare-earth-element patterns with negative Eu-anomalies (Venturelli *et al.* 1984, Nixon *et al.* 1984) are consistent with contamination of their mantle source by a component resembling modern oceanic sediments. The Spanish lavas possess Sr, Nd and Pb isotopic compositions similar to those of modern sediments and, although possibly complicated by extensive high-level crustal contamination in the more differentiated magmas (e.g. Turi and Taylor 1976), the involvement of a similar crustal component can

also account for the isotopic and trace-element features of the Italian potassic suite. Several geochemical studies of Italian potassic lavas (e.g. Hawkesworth and Vollmer 1979, Civetta *et al.* 1981, Peccerillo *et al.* 1984) have also found that their rare-earth-element patterns typically possess pronounced negative Eu anomalies. None of the liquidus mineral phases in the lavas are capable of producing these Eu anomalies. Hawkesworth and Vollmer (1979) proposed that either a residual Ca^{2+}- and Eu-rich phase was retained in the mantle sources of the lavas or that the "metasomatising" fluids involved possessed these anomalies. As the rare-earth-element patterns of upper crust and sediments typically possess negative Eu anomalies, this feature is also consistent with the involvement of a crustal contaminant within the magma sources. The radiogenic and oxygen isotope characteristics of even the most primitive of the Italian potassic lavas also strongly suggest the involvement of a crustal contaminant.

Although there is convincing tectonic and geochemical evidence for the operation of subduction during and after the Cambrian period within the Lachlan Fold Belt (see for example, Crook 1980 or Nelson *et al.* 1984), there is no clear evidence of an association of the southeast Australian leucitites with subduction processes. On the contrary, it is clear from Table 2.1 that the southeast Australian leucitites possess relatively high TiO_2 contents and have chemical affinities with anorogenic province potassic magmas rather than with arc magmas. The Ullung-do Island and southeast Australian leucitites isotopically resemble the lavas of some ocean islands, such as those of Kerguelen and Society Islands (see Figs. 2.4, 2.5 and 2.6), and may therefore have been derived from hotspot plumes. In support of this, the studies of Wellman and McDougall (1974) and Sutherland (1983) have convincingly demonstrated an association of the southeast Australian leucitites with hotspot activity. Alternatively, in the case of the southeast Australian leucitites, the hotspot may have been responsible for the re-activation of the leucitite magma sources located within pre-existing enriched subcontinental lithosphere beneath the Lachlan Fold Belt. The trace-element enrichment of these subcontinental lithospheric sources may have been associated with subduction during the Cambrian.

2.6 Summary

The results of this and other studies indicate that many examples of potassic magmas from orogenic settings are derived from trace-element- and isotopically-enriched mantle sources. Two separate mechanisms by which this mantle enrichment may be generated have been identified:

1. *Processes directly related to the operation of subduction* - Mantle trace-element and isotopic enrichments are in this case due to "metasomatic" components (fluids or melts) derived from subducted lithosphere. Of potassic suites representing this group, two sub-groups are recognisable, based principally on isotopic differences. One sub-group, consisting of the Spanish lamproites, Italian potassic lavas such as those of San Venanzo and Cupaello, and the K-rich lavas from within the eastern Sunda and Banda arcs (Whitford *et al.* 1981, Varne 1985), display geochemical and isotopic evidence consistent with the involvement of crustal contaminants within their mantle sources. These magmas were probably derived from a subduction zone mantle wedge which has been contaminated by subducted sediments. The second sub-group, represented by Mt Muriah from the west Sunda arc, lacks any direct isotopic evidence of the involvement of crustal components. It is possible that melts or fluids derived from the subducted slab are also involved in this case, but that they have not imparted a

distinctive isotopic character to the lavas.

2. *Processes related to hotspot activity* - Some oceanic island lavas believed to be the products of hotspot activity, such as those of Kerguelen, Tristan da Cunha, Gough and Society Islands, have isotopic characteristics indicating derivation from enriched mantle sources (see, for example, White 1985 and references cited therein). The Ullung-do Island leucitite isotopically closely resembles some of these ocean islands (see Figs. 2.4, 2.5 and 2.6), although the possibility that volcanism on the island is associated with subduction along the Japan arc cannot be confidently ruled out. Weaver *et al.* (1986) argued that the geochemical and isotopic characteristics of ocean-island magmas from enriched mantle sources (such as those of Kerguelen, Tristan da Cunha, Gough and Society Islands) are due to the involvement of a small amount of subducted sediment within their mantle sources. If this is the case, the distinction between hotspot-related and subduction-related mechanisms for the generation of isotopically anomalous mantle emphasised here becomes less obvious. Southeast Australian leucitite volcanism is clearly related to hotspot activity but it is unclear whether the hotspot plume is simply the trigger for volcanism from enriched sources within the subcontinental lithosphere or provides the source of the magmas themselves.

It is noteworthy that leucite-bearing rocks with moderate to high K_2O/Na_2O have also been reported from a number of ocean islands, such as Kerguelen and Tristan da Cunha (see Barker *et al.* 1964). Bishop and Woolley (1973) recognised two separate petrogenetic lineages, one sodic and one potassic, on the Marquesas Island of Ua Pu, whereas Duncan *et al.* (1986) demonstrated that the lavas of the island possess isotopic variations indicating derivation from isotopically heterogeneous mantle sources. Mildly potassic lavas (with K_2O contents similar to or higher than Na_2O) have also been reported from Gough (Le Maitre 1962), Cape Verde, St Helena and St Paul Islands (see discussion in Gupta and Yagi 1980). It is also curious that mildly potassic lavas are generally confined to those ocean islands (such as Kerguelen, Tristan da Cunha and Gough) which possess relatively radiogenic $^{207}Pb/^{204}Pb$ values compared to the MORB-OIB Pb-Pb isotope array, as this feature has been attributed to the involvement of recycled sedimentary components (see, for example, Weaver *et al.* 1986). Differences in the K_2O/Na_2O ratios of ocean-island lavas are usually attributed to differentiation processes, but it is possible that they are the result of partial melting of mantle sources which have undergone varying degrees of "metasomatic" trace-element enrichment. Further detailed geochemical and isotopic studies of these ocean-island lavas are required to evaluate this suggestion.

3. Anorogenic potassic igneous provinces

3.1 Introduction

Many occurrences of potassic magmatism possessing enriched mantle isotopic characteristics intrude stabilised cratons (for example, the Western Australian lamproites, Group 2 South African kimberlites and Leucite Hills potassic lavas), suggesting that enriched mantle components may exist within the subcontinental lithosphere of these regions. In support of this, Richardson *et al.* (1984) found Sr and Nd isotopic compositions indicating ancient enrichment in sub-calcic garnet inclusions in diamonds from African kimberlites and argued that a harzburgitic subcontinental lithosphere, stabilized to depths within the diamond stability field since the Archaean, is the source of diamonds and by implication, diamond-bearing kimberlites and lamproites themselves. The mechanisms responsible for the generation of this enriched subcontinental lithosphere are presently unknown but have been the subject of much speculation. The low-velocity zone, defined by the attenuation of s-wave velocity and where the geothermal gradient approaches or intersects the melting curve, may contain small amounts of melt which are likely to be highly enriched in incompatible elements (*cf.* Green 1976). Cooling of the lithosphere may result in the incorporation of such incompatible-element-enriched material within the base of the subcontinental lithosphere, allowing its long term storage and eventually producing isotopically evolved, "enriched" mantle. Alternatively, as it is likely that most (if not all) cratonic blocks have at some stage in their evolutionary histories been rimmed by active continental margins, trace-element and isotopic enrichment of the subcontinental lithosphere by subduction-related processes is also conceivable.

This and the following three chapters present the results of Sr, Nd and Pb isotopic investigation of some representatives of potassic igneous rocks which have intruded stabilised cratons (termed "anorogenic" potassic rocks). The implications of the results of this study for the mechanisms responsible for generation of enriched subcontinental lithosphere will be discussed more fully in Chapter 7.

3.2 Samples

3.2.1 Western Australian lamproites

The early Miocene Western Australian lamproites consist of some ~100 bodies intruding the Precambrian to Mesozoic basement rocks of the King Leopold Mobile Zone, the Lennard Shelf and the Fitzroy Trough, immediately south of the southwestern margin of the Precambrian Kimberley Block (Atkinson *et al.* 1984, see Fig. 3.1). Many of the intrusions are localised along deep west northwest-trending tensional faults and fractures with long histories of activity. Details of the geochemistry and mineralogy of the lamproites can be found in Jaques *et al.* (1984a) and Jaques *et al.* (1986a). The samples analysed for Pb isotopic composition in this study are the same as those analysed by McCulloch *et al.* (1983) for Nd and Sr isotopic composition. Some representative geochemical analyses of the Western Australian lamproites are given in Table 3.1.

Table 3.1 Representative major- and trace- element analyses of some relevant potassic rocks from anorogenic settings.

Analysis	1.	2.	3.	4.	5.	6.
location	Ellendale	Noonkanbah	Gaussberg	Leucite Hills	Leucite Hills	Priestley Peak
rock-type	lamproite	lamproite	leucitite	wyomingite	madupite	melasyenite
SiO_2	41.5	53.2	50.9	52.4	45.5	49.6
TiO_2	3.62	5.84	3.42	2.5	2.4	3.27
Al_2O_3	3.64	8.34	9.86	9.7	8.4	9.10
Fe_2O_3	-	-	2.46	4.7	6.3	2.45
FeO	8.10	6.60	3.78	-	-	4.06
MnO	0.13	0.08	0.09	0.06	0.11	0.08
MgO	25.00	7.80	7.95	7.2	9.7	8.77
CaO	4.99	3.22	4.63	4.6	10.1	5.32
Na_2O	0.46	0.57	1.65	1.5	0.9	0.89
K_2O	4.12	9.89	11.61	10.2	6.9	9.83
P_2O_5	1.68	0.98	1.48	1.7	2.4	3.38
H_2O	6.36	2.98	1.22	-	-	0.90
SO_3	-	-	0.11	-	-	0.53
CO_2	0.45	0.50	0.05	-	-	0.02
F	-	-	0.33	-	-	1.03
SUM	100.23	100.00	99.54			100.80
Cr	1006	348	306	350	511	348
V	85	210	106	86	110	143
Sc	21	14	-	12	20	-
Ni	1004	346	233	256	192	298
Co	70	33	-	20	28	-
Cu	56	66	29	-	-	80
Zn	71	77	79	-	-	86
Li	9	10	-	-	-	-
Cs	-	-	-	2.0	3.0	-
Ba	10334	9871	5550	5730	7350	9700
Rb	479	275	315	279	210	314
Sr	1312	1184	1808	2500	5100	2590
Pb	50	52	40	27	57	58
Y	16	20	18	-	-	36
Th	60	23	30	-	-	48
U	2	3	2.5	-	-	6
Zr	1133	1144	1270	1210	1004	1420
Nb	184	123	90	50	116	43
Mo	3	4	-	-	-	-
Sn	9	13	2	-	-	-
Ga	4	17	18	-	-	15
As	-	-	3.0	-	-	-
La	421	292	210	157	402	138
Ce	734	435	337	354	850	268
Nd	-	-	-	131	292	-
Sm	-	-	-	17.4	39	-
Eu	-	-	-	4.2	8.0	-
Tb	-	-	-	1.8	3.5	-
Yb	-	-	-	1.3	1.6	-

1 - 2. Ellendale (average of 89 olivine lamproite analyses) and Noonkanbah leucite lamproite (average of 100 analyses) from Jaques *et al.* (1986a).

3. Gaussberg leucitite (average of 11 analyses) from Sheraton and Cundari (1980).

4 - 5. Leucite Hills wyomingite (major elements average of 23 analyses, trace elements are average values for wyomingites and orendites) and madupite (major elements average of 12 analyses) from Kuehner *et al.* (1981) and Vollmer *et al.* (1984).

6. Priestley Peak analysis from Sheraton and England (1980).

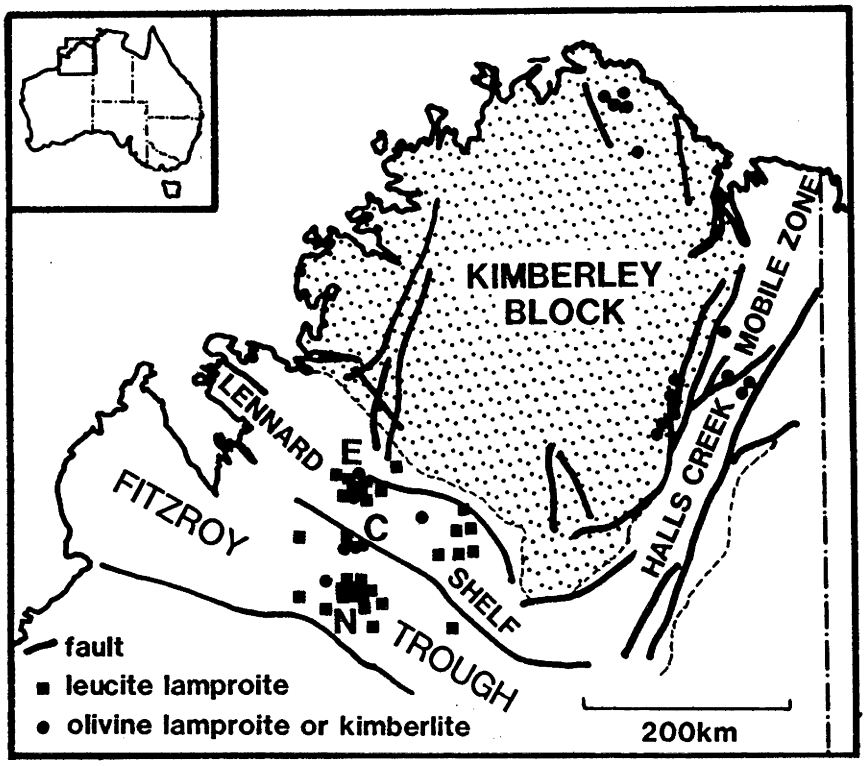

Fig. 3.1 Generalised geology of the Kimberley region, northwest Australia, showing localities of the Ellendale (E), Calwynyardah (C) and Noonkanbah (N) lamproite fields.

3.2.2 Gaussberg leucitites

Gaussberg is an isolated volcano located on the eastern margin of the Antarctic continent (see Fig. 5.1). Attempts have been made to relate Gaussberg volcanism to hotspot activity (Duncan 1981) but, as emphasised by Sheraton and Cundari (1980), there is no evidence relating the volcanism to any other area of Cainozoic volcanic activity. Isotopic analyses of granitic crustal xenoliths indicates their derivation from early Proterozoic or late Archaean crust (Collerson and McCulloch 1983), suggesting that Gaussberg is sited on stable continental basement. Collerson and McCulloch (1983) have also presented Sr and Nd isotopic and some geochemical analyses of the Gaussberg samples analysed here for Pb isotopic composition. Gaussberg leucitites are characterised by extreme K_2O (up to 12 wt%) and incompatible-element contents, high TiO_2 (averaging 3.4 wt%) and Mg/(Mg+Fe) values of ~0.70 (Sheraton and Cundari 1980). An average geochemical analysis is given in Table 3.1.

3.2.3 Leucite Hills potassic lavas

The Leucite Hills potassic volcanic field, Wyoming, consists of some 22 separate occurrences of probable Pleistocene age, which are believed to have intruded the Archaean Wyoming craton. The lavas are chemically remarkably similar to the Western Australian lamproites (see Table 3.1 and Fig. 3.2). Vollmer *et al.* (1984) determined $^{87}Sr/^{86}Sr$ values of between 0.7053 to 0.7061 and ε_{Nd} of -10.5 to -17.0 (see Fig. 3.3) and argued that the Leucite Hills lavas were derived from enriched mantle sources. After the isotopic results of Leucite Hills lavas presented here were obtained, Salters and Barton (1985) published a short abstract presenting new isotopic data which they had obtained for Leucite Hills lavas, including a range of Pb isotopic compositions. Their results indicated that Leucite Hills lavas possess low $^{206}Pb/^{204}Pb$ of 17.23 to 17.59 and $^{207}Pb/^{204}Pb$ of 15.46 to 15.49, with madupites having generally

higher $^{206}Pb/^{204}Pb$ and $^{208}Pb/^{204}Pb$ ratios than orendites and wyomingites.

Two hand-specimens of Leucite Hills lavas were obtained for analysis. In thin section, the samples consist of phenocrysts of phlogopite in a fine glassy groundmass and are therefore classified, following Kuehner *et al.* (1981), as wyomingites. Sample LH-4 is vesicular and LH-7 flow-textured.

The trace-element geochemistry of samples examined here is compared in Fig. 3.2, in which trace-element abundances have been normalised to estimated primitive mantle abundances. Noteworthy is the remarkable similarity in the trace-element characteristics of the Western Australian lamproites, leucitites from Gaussberg and potassic magmas from Leucite Hills and from east Antarctica (the latter are the subject of Chapter 5). The patterns show extremely high abundances of all trace elements and pronounced positive Ba spikes, with some patterns displaying prominent negative Nb anomalies.

3.3 Analytical Procedure

Western Australian and Gaussberg whole rock samples were provided as powders which had been crushed in a tungsten carbide swing mill. Mineral seperates (phlogopite and clinopyroxene from Western Australian lamproite samples) were leached in 6 N HCl for ~10 minutes to remove surface contamination. About 250 to 500 mg of sample powder was dissolved in teflon pressure capsules in HF and $HClO_4$ at 200 °C for at least 48 hours, the solution then evaporated and re-dissolved in 6 N HCl in teflon pressure capsules at 200 °C for a further 24 hours. The resulting solution was then re-dissolved in 1 N HCl and split into aliquots, one of which was spiked with mixed ^{85}Rb-^{84}Sr and ^{147}Sm-^{150}Nd spikes and the other aliquot used for Pb isotopic analysis. Where correction to the Pb isotopic composition for radiogenic decay of U was thought necessary, a third aliquot was mixed with mixed ^{235}U-^{208}Pb spike for U and Pb concentration analysis. The Leucite Hills hand-specimens were coarsely crushed in a stainless steel mortar and small (~15 mg) rock chips with fresh fracture surfaces were carefully selected for isotopic analysis. About 250 mg of hand-picked chips were leached in warm 1 N HCl for ~15 minutes to remove surface contamination and dissolved in teflon beakers using HF-$HClO_4$ and 6 N HCl. The resulting solution was then processed for Pb isotopic analysis. Rb-Sr and Sm-Nd analysis was undertaken on unleached and leached hand-picked chips which were spiked with mixed ^{85}Rb-^{84}Sr and ^{147}Sm-^{150}Nd spikes and dissolved in teflon pressure capsules. Analytical techniques are described more fully in Appendix 1.

3.4 Results

Isotopic results are given in Tables 3.2 and 3.3 and presented diagrammatically in Figs. 3.3 to 3.5.

3.4.1 Western Australian lamproites

Correction for radiogenic decay of U since emplacement of the Fitzroy lamproites during the Early Miocene (Wellman 1973, Jaques *et al.* 1984b) is small for $^{206}Pb/^{204}Pb$ (~ -0.04 for the highest U/Pb sample analysed, WAK-6L) and is insignificant for the other Pb isotope ratios. The lamproites have relatively low $^{206}Pb/^{204}Pb$ of from 17.24 to 17.88, extremely high and variable $^{207}Pb/^{204}Pb$ values ranging from 15.69 to15.80 and $^{208}Pb/^{204}Pb$ of 37.80 to 38.59. Acid-washed clinopyroxene separated from the "P" Hill lamproitic intrusion (WAK-13L) has Pb isotopic composition within the range

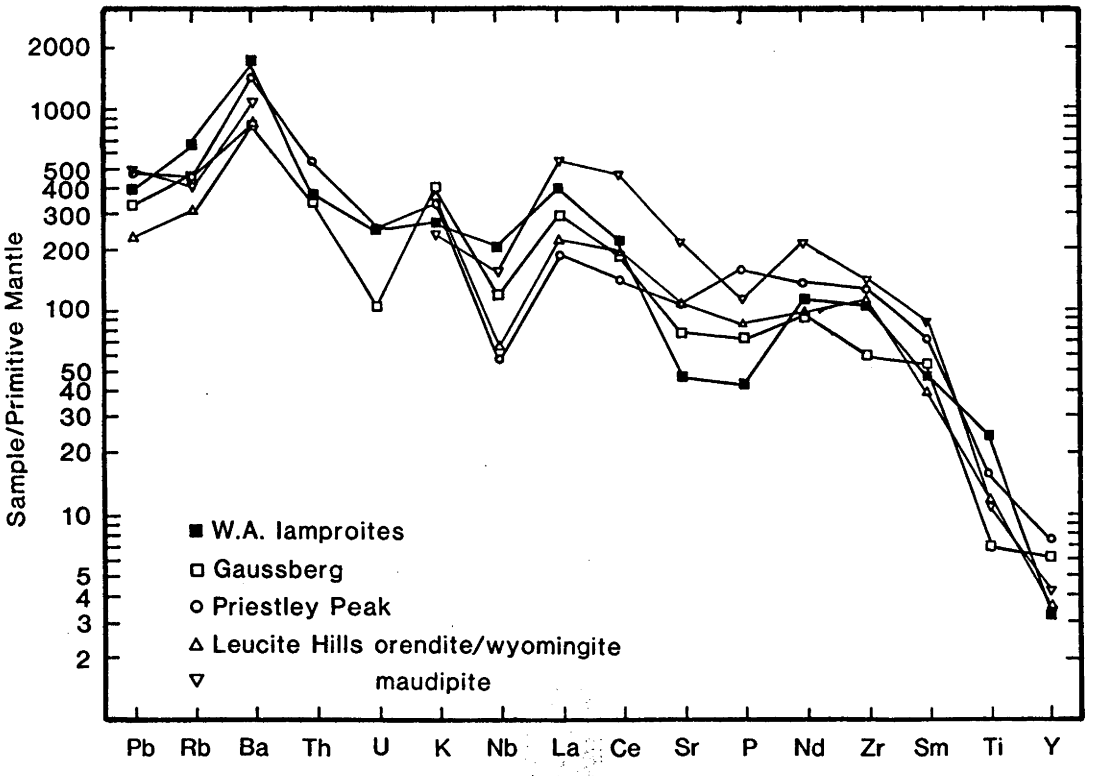

Fig. 3.2 Averaged trace-element abundances in lamproites from Western Australia, leucitites from Gaussberg and the Priestley Peak melasyenite dyke and Leucite Hills potassic lavas, normalised to estimated primitive mantle abundances (taken from McDonough *et al.* 1985 and Nelson *et al.* 1986a). These anorogenic potassic suites display similar trace-element patterns, with positive Ba concentration anomalies and small negative Nb anomalies. Data sources; Western Australian lamproites, Jaques *et al.* (1984a), McCulloch *et al.* (1983), this study; Gaussberg leucitites, Sheraton and Cundari (1980), Collerson and McCulloch (1983); Priestley Peak melasyenite, Sheraton and England (1980) and Leucite Hills lavas, Kuehner *et al.* (1981), Vollmer *et al.* (1984).

displayed by the Western Australian lamproitic suite. In addition, acid-washed phlogopite separated from the Mt Percy lamproite (WAK-10L) has Pb isotopic composition within analytical error of the host lava. These mineral isotope data indicate that the unusual Pb isotopic compositions of the Western Australian lamproites represent magmatic compositions and are unlikely to have been significantly affected by post-emplacement alteration. A distinctive feature of the Pb compositions is their unusual position to the left of the geochron (Fig. 3.4).

3.4.2 Gaussberg leucitites

Fission track, geomorphological and K-Ar studies suggest that Gaussberg volcanism is of Late Pleistocene-Recent age (Sheraton and Cundari 1980, Tingey *et al.* 1983) so corrections to the Pb isotopic data for age of emplacement are unnecessary. Leucitites from Gaussberg have similar Pb isotopic signatures to those displayed by the Western Australian lamproites, but with slightly lower $^{207}Pb/^{204}Pb$ (Fig. 3.4). Nd and Sr isotopic characteristics (Collerson and McCulloch 1983) of Gaussberg leucitites are also similar to those of the Western Australian suite except for the slightly lower $^{87}Sr/^{86}Sr$ (0.7097, compared with 0.710 to 0.720; McCulloch *et al.* 1983). A crustal xenolith (82-24) has Pb isotopic composition distinct from the host leucitite, with significantly higher $^{208}Pb/^{204}Pb$. The very high $^{208}Pb/^{204}Pb$ of the xenolith indicates that it is unlikely that the Pb isotopic compositions of the leucitites have been substantially modified by assimilation of crustal material like that of the xenolith.

Table 3.2 Strontium and neodymium isotopic analyses of Leucite Hills potassic lavas.

Sample	Rb	Sr	Sm	Nd	$^{87}Rb/^{86}Sr$	$^{87}Sr/^{86}Sr$[a]	$^{147}Sm/^{144}Nd$	$^{143}Nd/^{144}Nd$[b]	ε_{Nd}
		------ppm------							
Leucite Hills, Wyoming									
LH-4	263	2137	15.79	124.0	0.3557	0.70593 ±4	0.0770	0.51107 ±2	-14.9
LH-7	296	3022	20.69	157.1	0.2833	0.70564 ±5	0.0796	0.51103 ±2	-15.8
LH-7 leached						0.70558 ±5			

[a] Errors refer to within run precision at the $2\sigma_{mean}$ level. Uncertainty in $^{87}Rb/^{86}Sr$ is 0.5% (2σ). $^{87}Sr/^{86}Sr$ normalised using $^{86}Sr/^{88}Sr = 0.1194$. NBS-987 standard value is 0.71022 ±4. E & A standard carbonate value is 0.70800 ±3.

[b] Uncertainty in $^{147}Sm/^{144}Nd$ is 0.1% (2σ). Nd isotopic ratios normalised using $^{146}Nd/^{142}Nd = 0.636151$. The value obtained for BCR-1 standard is 0.511833 ±20. $\varepsilon_{Nd} = [(^{143}Nd/^{144}Nd_{meas} / ^{143}Nd/^{144}Nd_{CHUR}) -1] \times 10^4$ where $^{143}Nd/^{144}Nd_{CHUR} = 0.511836$.

3.4.3 Leucite Hills potassic lavas

Both Leucite Hills samples examined have high concentrations of Sr, Sm and Nd and high Nd/Sm ratios (and by implication, LREE/HREE). Sr and Nd isotopic compositions of the Leucite Hills wyomingites (Table 3.2) plot within the fields previously determined for wyomingites by Vollmer *et al.* (1984; see Fig. 3.3). U and Pb concentrations have not been determined, but average values for Pb of 27 ppm were reported for orendite/wyomingites by Kuehner *et al.* (1981). The Pb isotope compositions of Leucite Hills wyomingites (Table 3.3) are slightly more radiogenic than those reported for wyomingites by Salters and Barton (1985) but are comparable to their results for madupites. The wyomingites have unradiogenic $^{206}Pb/^{204}Pb$ (Fig. 3.4) and plot to the left of the geochron. Their $^{208}Pb/^{204}Pb$ is particularly low compared to the other examples of potassic magmatism examined here (Fig. 3.5) and indicate a long time-integrated history of low Th/U. The isotopic characteristics of Leucite Hills potassic volcanics indicate a generally similar long-term history of Sm/Nd and U/Pb but generally lower Rb/Sr compared to other examples of potassic magmatism from Western Australia and Gaussberg.

3.5 Discussion

3.5.1 Isotopic characteristics of anorogenic potassic magmas

The results of this and other isotopic studies indicate that anorogenic potassic igneous suites are characterised by generally unradiogenic $^{143}Nd/^{144}Nd$ and $^{206}Pb/^{204}Pb$ and radiogenic $^{87}Sr/^{86}Sr$ and $^{207}Pb/^{204}Pb$. In contrast to potassic suites from young orogenic settings (see Fig. 2.4), anorogenic potassic suites as a group possess a range of initial $^{87}Sr/^{86}Sr$ ratios which are not simply correlated with initial $^{143}Nd/^{144}Nd$ compositions (see Fig. 3.3). Furthermore, potassic magmas from anorogenic tectonic settings commonly possess considerably less radiogenic $^{206}Pb/^{204}Pb$ compositions than those from young orogenic tectonic settings (contrast the $^{206}Pb/^{204}Pb$ and $^{207}Pb/^{204}Pb$ isotopic results for orogenic suites given in Fig. 2.5 with those for anorogenic suites in Fig. 3.4).

Table 3.3 Uranium, thorium, lead concentration and lead isotopic data for anorogenic potassic suites.

Sample		U[a]	Th	Pb	$^{238}U/^{204}Pb$	$^{206}Pb/^{204}Pb$[b]		$^{207}Pb/^{204}Pb$	$^{208}Pb/^{204}Pb$	
		----- ppm -----				meas	initial	meas	meas	initial
Western Australian lamproites										
WAK-2L	Mt North	(7)	(54)	64.6	(7.8)	17.440	(17.42)[c]	15.773	38.414	(38.35)[c]
WAK-6L	Oscar Plug	(8)	(21)	(46)	(12.5)	17.538	(17.50)	15.687	38.043	(38.01)
WAK-10L	Mt Percy	(8)	(68)	104	(5.5)	17.324	(17.31)	15.733	38.194	(38.15)
	phlogopite[d]	-	-	-	-	17.342		15.736	38.167	
WAK-11L	Noonkanbah	-	-	(37)	-	17.448		15.724	38.079	
WAK-13L	'P' Hill cpx[d]	-	-	-	-	17.352		15.729	37.919	
WAK-14L	Fishery Hill	(1)	(21)	(51)	(1.4)	17.239	(17.23)	15.716	37.797	(37.77)
WAK-25L	Walgidee Hill	(3)	(25)	(46)	(4.7)	17.414	(17.40)	15.729	38.096	(38.06)
WAK-30L	Walgidee Hill	(2)	(30)	(23)	(6.2)	17.485	(17.46)	15.694	38.046	(37.95)
WAK-15K	Ellendale	(<1)	(59)	(32)	(<2.2)	17.594	(17.59)	15.764	38.466	(38.33)
WAK-16K	Ellendale	3.23	(18)	(22)	(6.6)	17.882	(17.86)	15.741	38.593	(38.53)
WAK-17L	Ellendale	2.10	(14)	(50)	(7.2)	17.287	(17.26)	15.758	38.140	(38.12)
WAK-20K	Ellendale	(4)	(60)	(47)	(6.1)	17.454	(17.43)	15.705	38.300	(38.21)
WAK-21K	Ellendale	(2)	(63)	(53)	(2.7)	17.473	(17.46)	15.730	38.369	(38.28)
WAK-27L	Ellendale	(2)	(31)	41.3	(3.5)	17.508	(17.50)	15.796	38.572	(38.52)
Gaussberg										
82-24	crustal xenolith	-	-	-	-	18.083		15.721	41.384	
82-27	leucitite	-	-	-	-	17.602		15.674	38.478	
82-30	leucitite	-	-	-	-	17.588		15.649	38.402	
Leucite Hills										
LH-4	wyomingite[d]	-	-	-	-	17.596		15.535	37.441	
LH-7	wyomingite	-	-	-	-	17.494		15.556	37.500	
LH-7	wyomingite[d]	-	-	-	-	17.47		15.56	37.46	

[a] U, Th and Pb concentrations in brackets determined by XRF analysis (from A.L. Jaques, personal commmunication). Other concentration values determined by isotope dilution mass spectrometry.

[b] Errors (based on two way analysis of variance of duplicate analyses) at the 1σ level; $^{206}Pb/^{204}Pb$ ±0.011, $^{207}Pb/^{204}Pb$ ±0.014, $^{208}Pb/^{204}Pb$ ±0.033. The values obtained for NBS-981 during this study (average of 7 analyses) are; $^{206}Pb/^{204}Pb$ = 16.927 ±0.009, $^{207}Pb/^{204}Pb$ = 15.486 ±0.013, $^{208}Pb/^{204}Pb$ = 36.668 ±0.044.

[c] Corrected for ^{238}U and ^{232}Th decay since emplacement, using 20 Ma for Western Australian lamproites. The age correction to $^{207}Pb/^{204}Pb$ is insignificant compared to the analytical error for all samples.

[d] Pb isotopic analysis undertaken on acid-leached samples.

$^{87}Sr/^{86}Sr$ and $^{143}Nd/^{144}Nd$ values for the Western Australian lamproites (from McCulloch *et al.* 1983 and Fraser *et al.* 1985) display a weak negative correlation (see Fig 3.6). The incompatible-element characteristics, radiogenic $^{87}Sr/^{86}Sr$ and $^{207}Pb/^{204}Pb$ and unradiogenic $^{143}Nd/^{144}Nd$ of the Western Australian lamproites and other examples of anorogenic potassic magmatism may be attributed to the involvement of crustal contaminants. However, these magmas are insensitive to crustal contamination processes because of their extremely high concentrations of trace elements, including Sr, Pb and the rare-earth elements. Geochemical considerations exclude their contamination by bulk assimilation

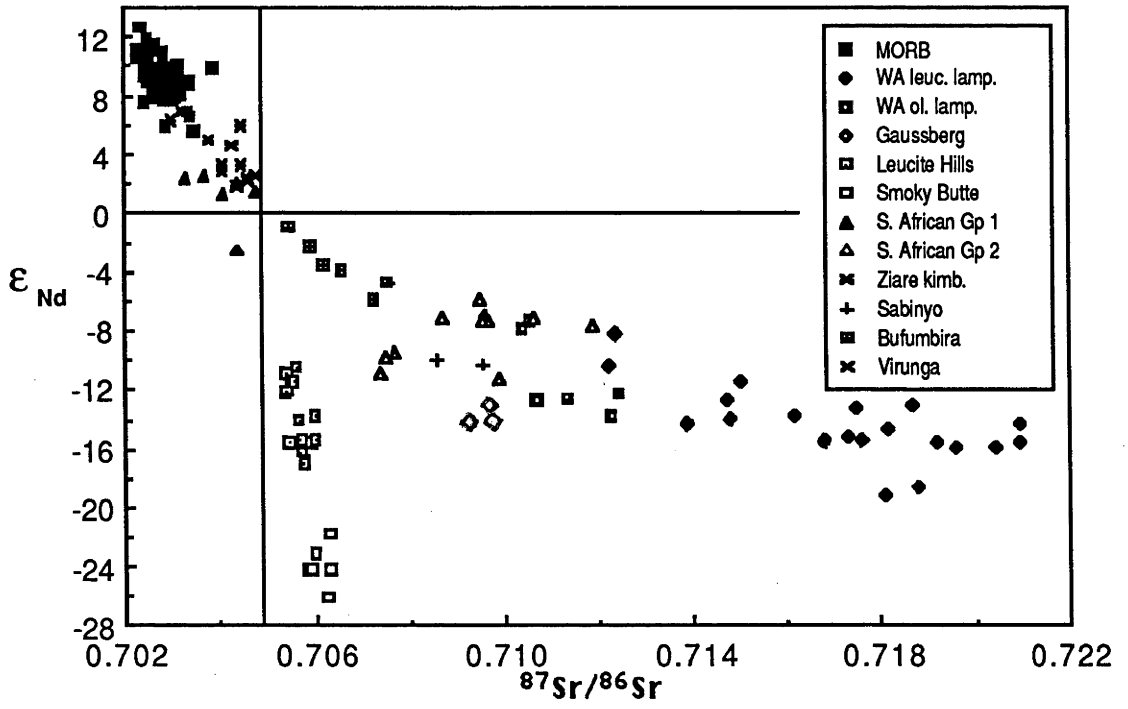

Fig. 3.3 Initial Sr-Nd isotope correlation for anorogenic potassic and selected kimberlitic rocks, compared to the field for mid-ocean ridge basalts. Data sources- MORB: as in Fig. 2.4. Potassic rocks: Collerson and McCulloch (1983), McCulloch *et al.* (1983), Smith (1983), Vollmer and Norry (1983a), Vollmer *et al.* (1984), Fraser *et al.* (1985), Weis and Demaiffe (1985) and this study.

processes because of the substantial amounts of crustal material required to modify their isotopic compositions. For example, because of the extreme degree of LREE-enrichment of these magmas, bulk assimilation of felsic granulite within the lower continental crust will effectively dilute their incompatible-element contents and should therefore produce a positive correlation between Nd concentration and ε_{Nd}. In the case of the Western Australian lamproites, a correlation in the opposite sense is observed (Fig. 3.7). Although selective contamination processes (for example, by highly LREE-enriched phases such as monazite or allanite) could account for this correlation, there is no evidence in the trace-element patterns (i.e. large positive Th or P_2O_5 spikes) of the assimilation of such phases, nor can this process explain the Sr or Pb isotopic characteristics of these magmas. Crustal contamination via specialised mechanisms, such as volatile transfer or zone refining, is unable to account for the high Mg-numbers and Ni and Cr contents or the presence of mantle xenoliths (and in one case, diamonds).

An alternative interpretation which may account for the unusual geochemical and isotopic properties of these magmas, such as their generally high MgO, Ni, Cr and low Al_2O_3, CaO and Na_2O, is that they were derived from relatively depleted (lherzolitic or harzburgitic) mantle sources which have been contaminated by "metasomatic" components possessing enriched mantle isotopic characteristics. Weak correlations are evident between K_2O/Na_2O and Sr and Nd isotopic compositions in the Western Australian lamproites (see Fig. 3.8 and Fig. 3.9), consistent with this interpretation. The very high abundances of incompatible trace elements and the steep LREE-enriched rare-earth element patterns characteristic of these magmas also suggest that the sources of these magmas have undergone re-fertilisation with incompatible trace elements. Otherwise, unrealistically small degrees of partial melting (substantially less than 1%) would be required to generate such trace-element enrichment by derivation of the magmas from primitive or trace-element depleted mantle sources.

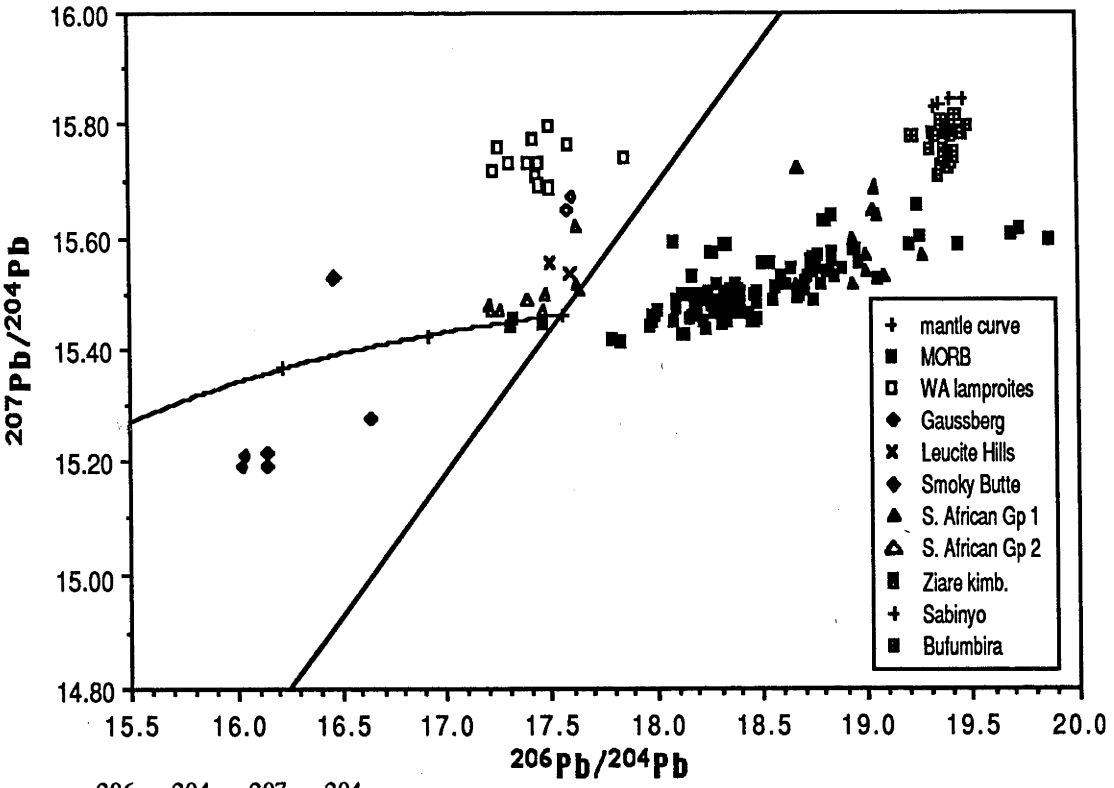

Fig. 3.4 $^{206}Pb/^{204}Pb$-$^{207}Pb/^{204}Pb$ variation in anorogenic potassic rocks, compared to the fields for mid-ocean ridge basalts. Additional data sources- MORB: as in Fig. 2.5. Potassic rocks: as in Fig. 3.3.

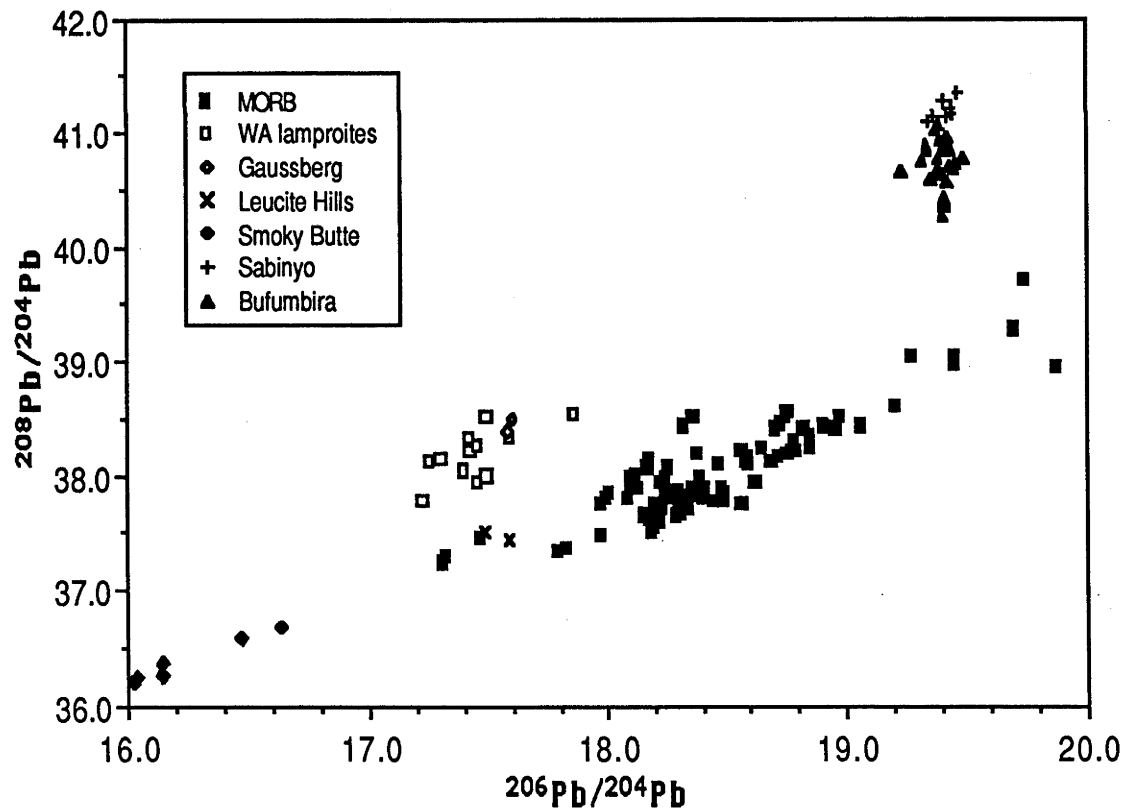

Fig. 3.5 $^{206}Pb/^{204}Pb$-$^{208}Pb/^{204}Pb$ variation in anorogenic potassic rocks, compared to the fields for mid-ocean ridge basalts. Additional data sources- MORB: as in Fig. 2.5. Potassic rocks: as in Fig. 3.3.

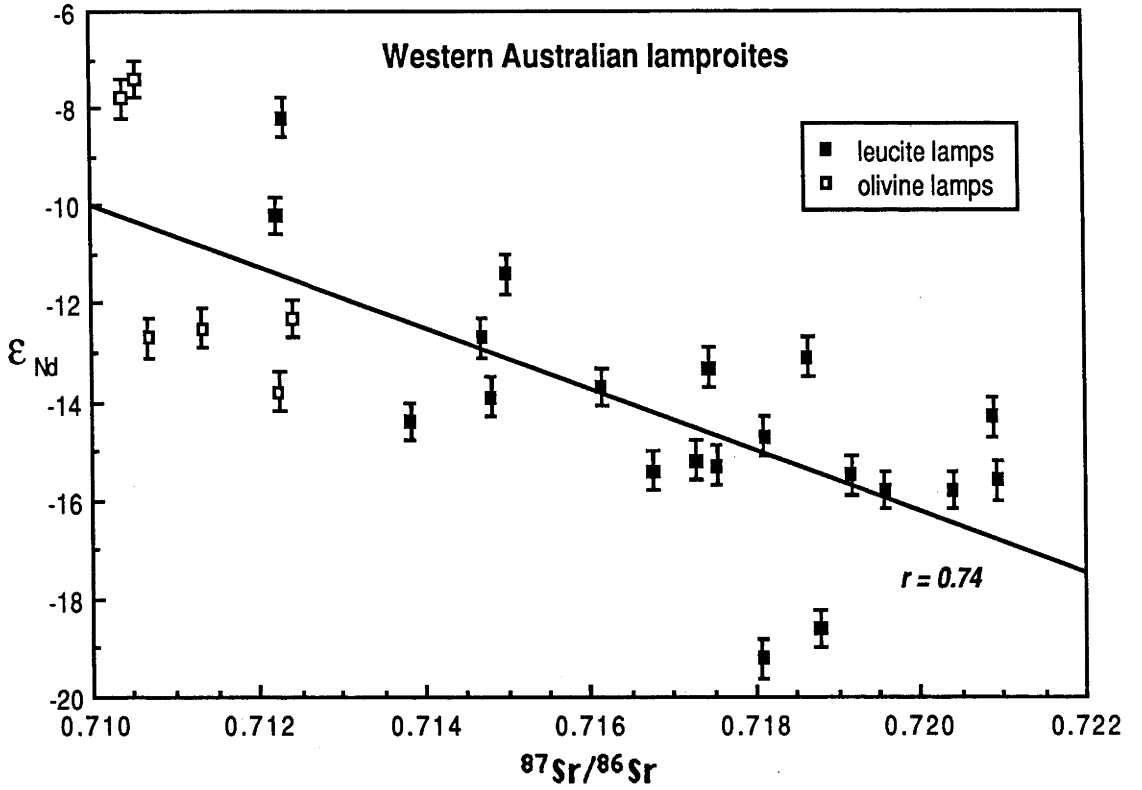

Fig. 3.6 Initial Sr-Nd isotope correlation for the Western Australian lamproites. A weak negative correlation is evident. Data from McCulloch *et al.* (1983) and Fraser *et al.* (1985).

Compared to other examples of continental potassic magmatism considered to be derived from enriched mantle sources, Leucite Hills and Smoky Butte potassic lavas have similar or less radiogenic $^{143}Nd/^{144}Nd$ and have significantly less radiogenic $^{87}Sr/^{86}Sr$ (Fig. 3.3). The isotopic differences displayed by these potassic suites may be due to differences in the isotopic compositions of the"metasomatic" contaminants involved, to the existence of different long-term Rb/Sr and Sm/Nd ratios within the "metasomatised" source regions of the magmas and/or to differences in the time elapsed between enrichment and magma generation events. Alternatively, the trend may be the result of mixing of two components (for example, the MORB source and an enriched mantle source having Sr and Nd isotopic characteristics like the Spanish or Western Australian lamproites) as was suggested by McCulloch *et al.* (1983). If mixing between enriched and depleted mantle components is involved, the Leucite Hills Sr and Nd isotopic characteristics, for example, may indicate that the depleted mantle end-member is more strongly influencing the Sr isotopic composition of the mix (i.e. the ratio $[Sr/Nd]_D/[Sr/Nd]_E$ is larger) than is the case in the Western Australian and other examples.

The distinctive Pb isotopic signatures of the Western Australian lamproites, Gaussberg leucitites and Leucite Hills lavas is indicative of ancient sources which have had high U/Pb early in their histories, followed by more recent low U/Pb, relative to the array displayed by mid-ocean ridge and ocean-island basalts. In contrast, the sources of most mid-ocean ridge and many ocean-island basalts have undergone an increase (either progressively or episodically) in their U/Pb ratios. The Western Australian lamproites display little variation in $^{206}Pb/^{204}Pb$ for the correspondingly large variation in $^{207}Pb/^{204}Pb$. McCulloch *et al.* (1983) modelled the correlation between Nd and Sr isotopes displayed by the Western Australian lamproites by mixing of enriched and depleted components. This is consistent with the Pb

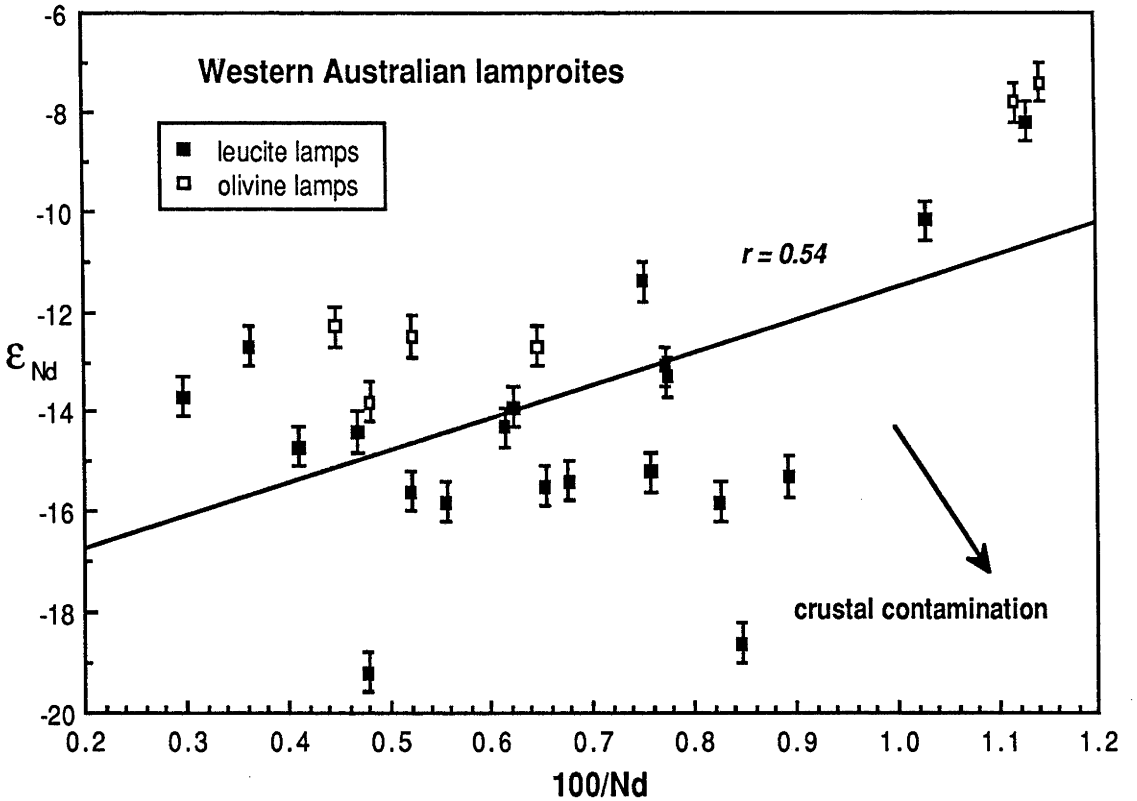

Fig. 3.7 Nd isotopic composition versus 100 times the reciprocal of the Nd concentration for the Western Australian lamproites. Custal contamination by bulk assimilation processes should result in a negative correlation on this diagram. However, a weak positive correlation evident, suggesting that the unradiogenic Nd isotopic compositions are not due to bulk assimilation of continental crustal material. Data from McCulloch *et al.* (1983) and Fraser *et al.* (1985).

isotope variation, which is most readily explained by mixing. However, rather than trending towards the present-day MORB field on the $^{206}Pb/^{204}Pb$ - $^{207}Pb/^{204}Pb$ diagram (Fig. 3.4), the Western Australian lamproite array (excluding WAK-16L) appears to extend to more primitive $^{206}Pb/^{204}Pb$ values. The array may result from the mixing, at some time in the past, of a high $^{207}Pb/^{204}Pb$ component with a MORB component (i.e. when the MORB reservoir had $^{207}Pb/^{204}Pb \approx 15.5$ like the present-day value, but had $^{206}Pb/^{204}Pb$ less than ~ 17.0). A primitive or (more probably) depleted mantle component which dominates the major elements can account for the high MgO, Ni, Cr and low Al_2O_3, CaO and Na_2O contents of Western Australian, Gaussberg and Leucite Hills potassic magmas, whereas a "metasomatic" component enriched in incompatible elements and which dominates the isotopic characteristics can account for their trace-element contents. If produced at depth, these metasomatic components may pass through isotopically different regions of the mantle and subcontinental lithosphere, resulting in the observed isotopic correlations.

3.5.2 Significance of the high $^{207}Pb/^{204}Pb$, low $^{206}Pb/^{204}Pb$ components

That ultrapotassic rocks from Gaussberg, Western Australia and Leucite Hills possess similar unusual isotopic compositions is strong evidence for their generation by a common process. Although their $^{87}Sr/^{86}Sr$, $^{143}Nd/^{144}Nd$ and $^{207}Pb/^{204}Pb$ isotopic characteristics are more like those of the upper continental crust, many aspects of their major- and trace-element characteristics, such as their high Mg/(Mg+Fe) and Ni and Cr contents and the presence of mantle xenocrysts (and in the case of the Western

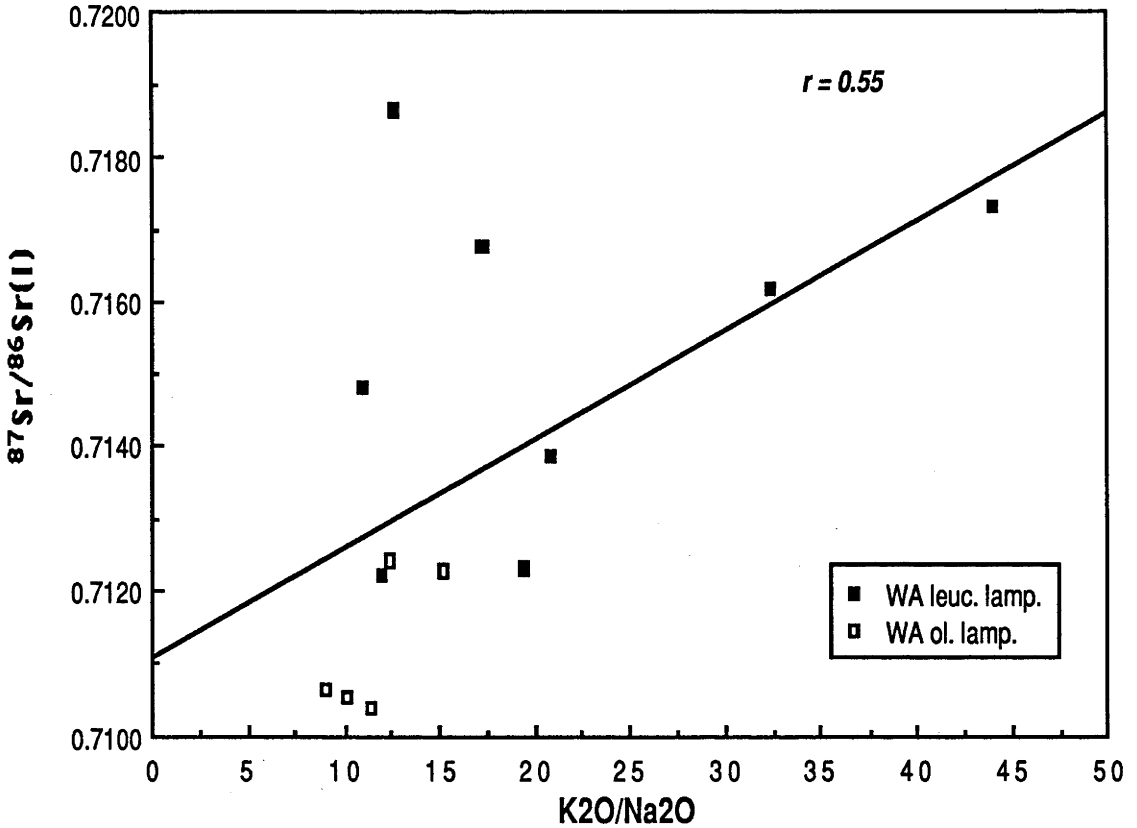

Fig. 3.8 Correlation between initial Sr isotopic composition and K_2O/Na_2O for the Western Australian lamproites. A very weak positive correlation is evident, consistent with the contamination of the sources of the lamproites by a high K_2O/Na_2O, radiogenic Sr component. Data from McCulloch *et al.* (1983) and Jaques *et al.* (1986a).

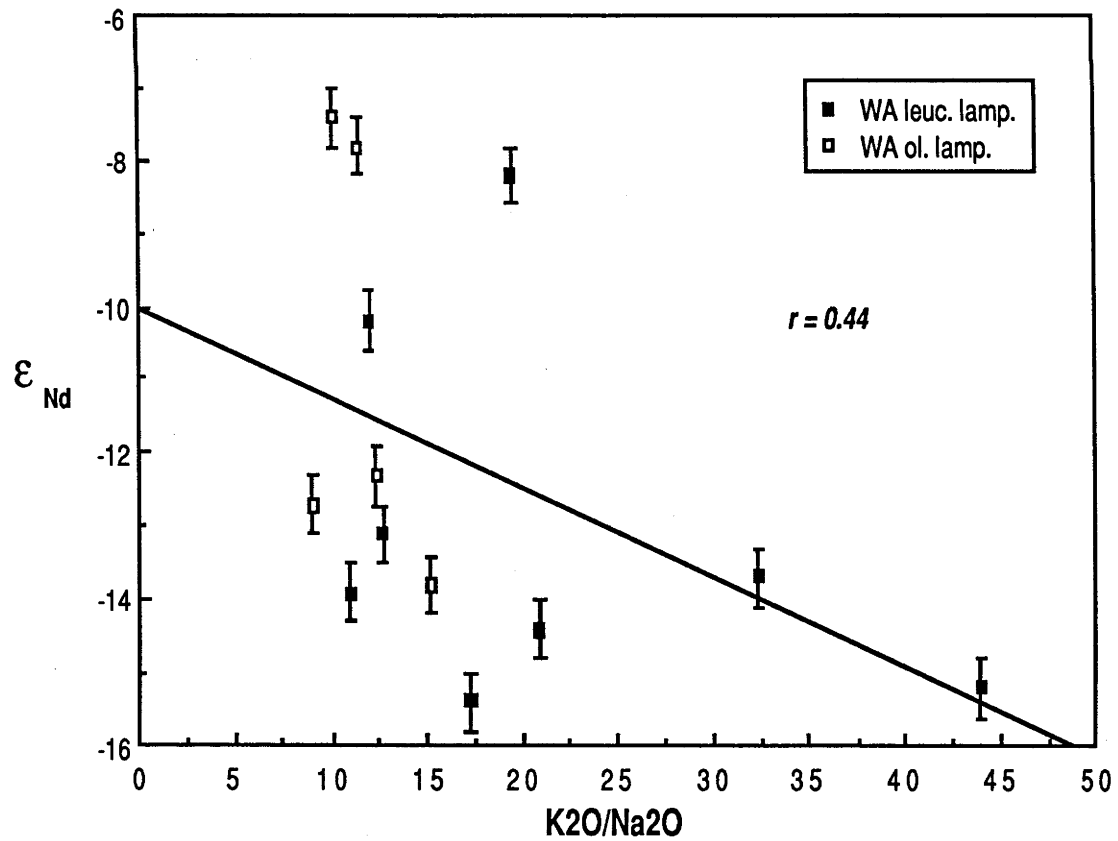

Fig. 3.9 Correlation between initial Nd isotopic composition and K_2O/Na_2O for the Western Australian lamproites. Data sources given in Fig. 3.8.

Australian lamproites, diamonds) are more consistent with a mantle origin. In the following modelling of the isotope data, some general inferences about the long term histories of the sources of the Western Australian lavas are made.

The unusual Pb isotopic compositions of these suites require an evolution involving at least two stages. A general model of the evolution of their Pb is shown in Fig. 3.10. Modelling of the high $^{207}Pb/^{204}Pb$, low $^{206}Pb/^{204}Pb$ component recognised in the Western Australian lamproites (see Appendix A2.1 for a listing of the computer program used for this modelling) allows the ranges of possible values of μ_1 and μ_2 and minimum age for t_1, the time of differentiation of the component from the mantle, to be determined. Figure 3.10 shows, for selected values of t_1, the range of possible values for μ_1 and μ_2 plotted against t_2, the time at which the U/Pb ratio was lowered. The modelling uses the Pb composition of the Western Australian lamproite having the highest $^{207}Pb/^{204}Pb$ and relatively low $^{206}Pb/^{204}Pb$ (WAK-27L), regarded as the least contaminated by Pb from other sources. In the case of an evolution involving two stages (where $t_1 = t_0$), the range of possible values for μ_1 and μ_2 is given by the $t_1 = 4.5$ Ga curves. For decreasing values of t_2, μ_1 approaches 8.6 while μ_2 approaches zero, until at t_2 ~500 Ma, μ_2 becomes negative and it is not possible to generate the measured Pb composition of WAK-27L. Because a two stage model requires the existence of an extremely ancient, moderately high U/Pb reservoir, perhaps the only instance where a two-stage model could be applied is when the first stage reservoir is known to be very ancient sialic crust.

A more general and geologically more plausible three-stage model differs from the two stage case in having an earlier period prior to the high U/Pb stage during which the Pb evolves in the 'normal' mantle reservoir with μ_0 ~8.0. It can be seen from Fig. 3.10 that younger values of t_1 require higher μ_1 and lower μ_2, until at t_1 ~2.1 Ga $\mu_2 < 0$ and it becomes impossible to produce the Pb isotopic composition of WAK-27L. A first-stage $\mu_0 = 8.0$ has been used, based on ore Pb isotope data from Archaean greenstone belts (e.g. Tilton 1983, Roddick 1984, Dupré *et al.* 1984) although the three-stage modelling is not particularly sensitive to the value of μ_0. For example, no solutions are possible for $t_1 < 2.1$ Ga using the Cumming and Richards (1975) Model 3 growth curve based on conformable ores, which is considered to provide a reasonable upper limit of the value of time integrated μ_0 evolution for the mantle (as ores are likely to contain some Pb derived from the crust), while using values of $\mu_0 < 8.0$ will tend to increase the minimum allowable values of t_1.

The three-stage modelling establishes that the Pb component identified in the Western Australian lamproites cannot have differentiated from primitive mantle at times less than 2.1 Ga ago. From Fig. 3.10 it is apparent that for older values of t_1, lower and more geologically reasonable values of μ_1 are possible. Younger values of t_1 require higher values for μ_1 or longer periods between the events t_1 and t_2.

Additional information about the source history of the Western Australian lamproites is provided by their Sm-Nd isotopic systematics. For example, Zindler *et al.* (1984) estimated that during low degrees of modal melting (~ <1%) of a garnet lherzolite source, the Sm/Nd ratio of the melt will be at least one half that of the source. The measured Sm/Nd values of the Western Australian lamproites are relatively constant at ~0.11 (McCulloch *et al.* 1983), implying a source Sm/Nd of at least 0.22. A minimum period of 2.1 Ga is required for a source with Sm/Nd ratio equal to or greater than this value to evolve the

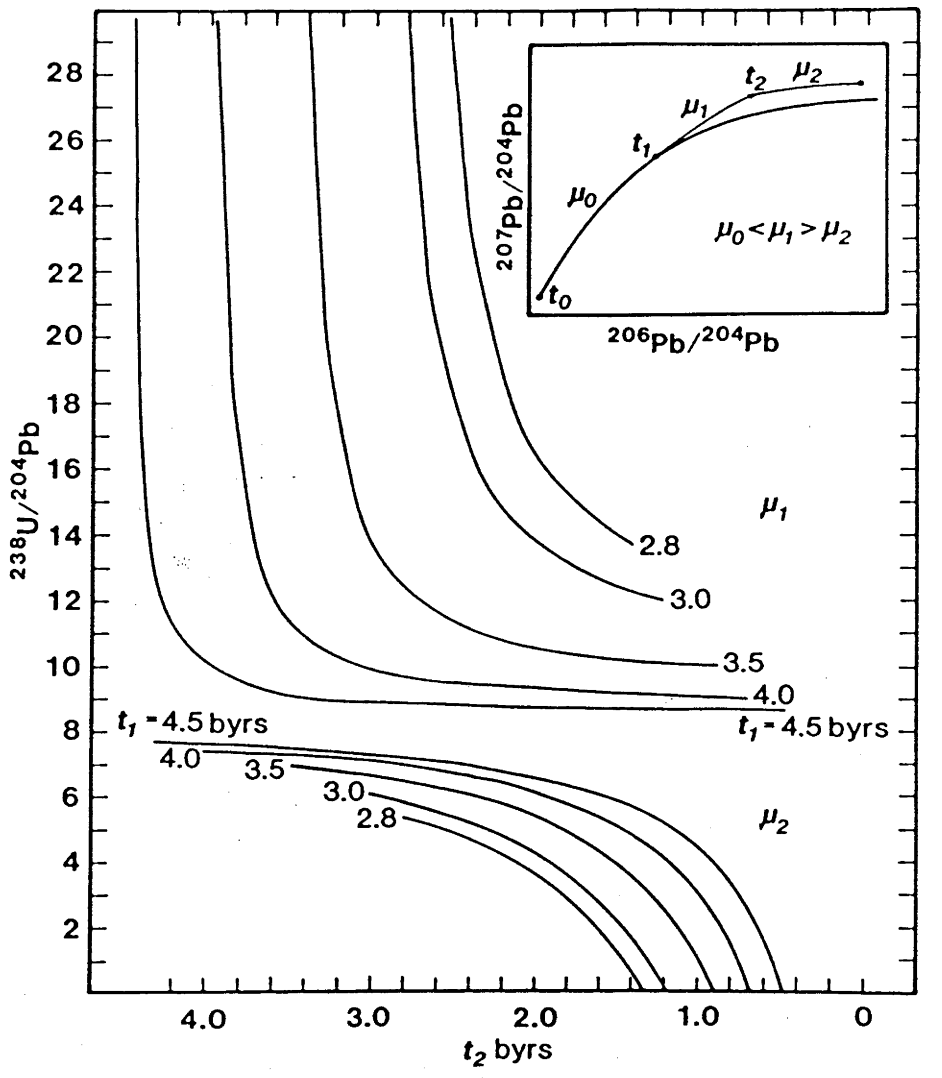

Fig. 3.10 Three-stage evolution of the sources of Pb in the Western Australian lamproites. At time t_1, the components differentiate from the mantle reservoir with higher $^{238}U/^{204}Pb$ (μ_1) and at time t_2 an event lowers the U/Pb (μ_2) of the components. The initial Pb compositions at t_0 are those of Canyon Diablo troilite (Tatsumoto 1973). A mantle reservoir μ_0 of 8.0 and the end Pb isotopic composition of WAK-27L have been used. Solutions are given for μ_1 (upper curves) and μ_2 (lower curves) for selected values of t_1 (in Ga), plotted against t_2 on the lower axis, for two- and three-stage models. The t_1 = 4.5 Ga curves give the range of possible values of μ_1 and μ_2 for a model involving only two stages. For a three stage model, younger values of t_1 require higher values of μ_1 and lower values of μ_2 until at t_1 ~2.1 Ga, values of μ_2 become negative.

Nd isotopic compositions observed in the Western Australian lamproites from an initially depleted mantle source. As the Pb isotope data indicates a more complex history, probably involving at least two stages, the calculated Nd depleted mantle model source ages should be regarded as an estimate of the minimum age of first differentiation of the lamproite sources from primitive mantle (*cf.* McCulloch *et al.* 1983). The minimum estimate of ~2.1 Ga for the differentiation event is in accord with the value determined from the Pb isotopic systematics.

3.5.3 Implications for the genesis of anorogenic potassic magmas

The available geochemical and isotopic data taken from this and other earlier studies favour the generation of many examples of continental potassic volcanism by the invasion of regions of the subcontinental mantle by isotopically foreign, incompatible-element-enriched "metasomatic" components. In many cases these components possess radiogenic $^{87}Sr/^{86}Sr$ and $^{207}Pb/^{204}Pb$ combined with unradiogenic $^{206}Pb/^{204}Pb$ and $^{143}Nd/^{144}Nd$ relative to modern mid-ocean ridge basalts, indicating that the sources of these components have had long and complex histories. The trace-element and isotopic identity of the resulting melts is strongly influenced by that of the added component and may result in isotope/isotope and isotope/abundance relations indicative of mixing. In addition to Western Australian, Gaussberg and Leucite Hills lavas examined here, the isotopic characteristics of potassic lavas from Virunga (Vollmer and Norry 1983a) are also consistent with the addition to their sources of a similar radiogenic $^{207}Pb/^{204}Pb$ and $^{87}Sr/^{86}Sr$, unradiogenic $^{143}Nd/^{144}Nd$ component, but the sources of the Virungan lavas may have evolved variable $^{87}Sr/^{86}Sr$ since the mixing event.

That most examples of potassic magmatism possessing highly evolved, enriched mantle isotopic characteristics intrude stabilised Precambrian cratons is strong indirect evidence that the subcontinental lithosphere acts as a storage site for these enriched mantle components. Their unusual Sr and Nd isotopic compositions may therefore have evolved during this period of storage within the subcontinental lithosphere. However, the Pb isotopic compositions of these potassic magmas indicate that although their sources possessed generally low U/Pb ratios during their more recent history (i.e. probably during the time of their storage within the subcontinental lithosphere), these components possessed substantially higher U/Pb ratios (i.e. $\mu > 8$) earlier in their history. The most reasonable interpretation of these distinctive Pb isotopic compositions is that these components possessed generally radiogenic $^{207}Pb/^{204}Pb$ values prior to their incorporation within the lithosphere. This constrains the sources of these components, prior to their incorporation into the subcontinental lithosphere, to a few geological reservoirs;

1. *Subducted sediments* - the findings of this study are consistent with the recent proposal of Thompson *et al.* (1984) that potassic magmas may be derived from subducted sedimentary components. As sediments derived from old continental provenances typically possess radiogenic $^{87}Sr/^{86}Sr$ and unradiogenic $^{143}Nd/^{144}Nd$, the enriched mantle Sr and Nd isotopic characteristics of anorogenic potassic magmas may be inherited from the sediments themselves. Alternatively, the enriched mantle Sr and Nd isotopic character may be the result of the isotopic evolution of portions of the subcontinental lithosphere which have become enriched in incompatible elements by subduction-related processes. Although Western Australian, Gaussberg, Leucite Hills and Virungan ultrapotassic magmas cannot be obviously related to any modern subduction zone, the antiquity of the source enrichments indicated by the isotopic data suggest that subduction processes cannot be discounted. These subducted sedimentary components may become incorporated within the subcontinental lithosphere during periods of active subduction along the cratonic margins.

2. *Ocean-island "plume" melts* - radiogenic $^{207}Pb/^{204}Pb$ values are also found in the alkali basalts of some ocean islands. These ocean-island Pb isotopic signatures have been interpreted as indicating derivation from high U/Pb subducted oceanic lithosphere having mantle residence times of at least ~1

Ga (Chase 1981, Hofmann and White 1982). Partial melting of subducted "megaliths" may cause incompatable-element-enriched diapirs to rise upward, contaminating the overlying regions of the mantle and manifesting as hotspots in oceanic regions (and possibly also in regions of relatively thin subcontinental lithosphere). In regions of thick lithosphere, these "plumes" may underplate the subcontinental lithosphere. After a considerable period of storage within the lithosphere, this underplated material may be re-activated, manifesting as highly potassic igneous activity. The enriched mantle Sr and Nd isotopic characteristics may have evolved during the period of storage within the subcontinental lithosphere.

3.6 Summary

Important geochemical and isotopic differences justify the distinction between potassic magmatism occurring within stable Archaean cratonic environments (i.e. so-called "anorogenic" settings) and that found within tectonically younger environments (termed "orogenic" environments in this thesis). It is apparent that representatives of the anorogenic potassic suite possess the most evolved isotopic characteristics so far identified for mantle-derived magmas. Several examples from unrelated continental regions possess generally similar unusual isotopic features (i.e. moderately to highly radiogenic $^{87}Sr/^{86}Sr$ and $^{207}Pb/^{204}Pb$, and highly unradiogenic $^{143}Nd/^{144}Nd$ and $^{206}Pb/^{204}Pb$) requiring derivation from sources which have undergone similar complex, multistage evolutionary histories and suggesting their generation by a common mechanism. There is strong circumstantial evidence that some aspects of these isotopically unusual characteristics have evolved during a long period of storage within the subcontinental lithosphere. However, the multistage evolutionary histories of U/Pb variation indicate that these unusual components probably possessed radiogenic $^{207}Pb/^{204}Pb$ relative to that of the Earth's mantle prior to their incorporation within the subcontinental lithosphere, suggesting that they were originally derived from either upper continental crustal or from ocean-island-like sources.

Further detailed discussion and assessment of these results can be found in Chapter 7.

4. The Mordor Complex

4.1 Introduction

Well-preserved examples of potassic magmatism older than Phanerozoic age are particularly rare in the geological record. This apparent scarcity of Archaean or Proterozoic examples of potassic magmatism might suggest that the prevailing conditions did not favour the generation of these chemically unusual magmas during the earlier part of the Earth's history, perhaps as a result of the generally higher heatflow or the operation of a different tectonic regime. As many Phanerozoic occurrences of potassic magmatism are now known to possess isotopic characteristics indicating derivation from enriched mantle sources, it is of particular interest to establish whether this is also the case for older examples, particularly if models for the generation of potassic magmatism involving recycling processes (discussed in Chapter 7) have validity.

The Mordor Complex, located ~50 km east-northeast of Alice Springs in central Australia (see Fig. 4.1), consists of well-preserved, highly differentiated alkaline magmas ranging in composition from phlogopite-bearing werhlites and lherzolites to consanguinous monzonites and syenites (Langworthy and Black 1978). Foley *et al.* (1987) have recently pointed out that the few Proterozoic occurrences of potassic magmatism known are predominantly lamproites (members of their Group 1) which are distinguished by their low contents of Al_2O_3, CaO and Na_2O and high K_2O/Al_2O_3. However, in contrast to lamproites, the Mordor magmas are only mildly peraluminous and are potassic to ultrapotassic, with atomic K_2O/Na_2O between 2 and 5. The Mudtank carbonatite (examined in Section B of this thesis) is situated 50 km to the north-northwest of the Mordor Complex, providing further evidence of a possible relationship (if not a genetic link, then perhaps a tectonic one) between potassic/kimberlitic and carbonatitic magmatism. Langworthy and Black (1978) have shown that samples of the Mordor Complex display a continuous smooth variation in chemical features which can be accounted for entirely by differentiation and fractionation processes and also argued that contamination of the magmas by the Precambrian leucocratic gneiss and amphibolite country-rock was inconsistent with geochemical and Sr isotopic systematics. Rb-Sr whole-rock data obtained by these authors indicated an age of ~1100 Ma with an initial $^{87}Sr/^{86}Sr$ ratio of 0.7106 ±0.0006. The high initial $^{87}Sr/^{86}Sr$ ratio, confirmed by two internal (mineral) isochrons, is of particular interest, and was interpreted by Langworthy and Black (1978) as a primary feature of the source magma from which the complex differentiated. The extensive differentiation of the Mordor Complex has resulted in a wide range in the Sm/Nd ratio and the complex is therefore suitable for analysis using the Sm-Nd technique, enabling the precise determination of both the age and the $^{143}Nd/^{144}Nd$ initial ratio. An important advantage of the Sm-Nd isotopic system over the Rb-Sr system is the greater immobility of the rare-earth elements compared to Rb and Sr during metamorphism, so the possible effects of metamorphic resetting of the Rb-Sr isotopic system can also be evaluated.

This study was undertaken in order to evaluate the assertion of Langworthy and Black (1978) that the radiogenic initial $^{87}Sr/^{86}Sr$ and the variability of the initial Sr isotopic composition of the complex are primary features, and to determine the initial Nd isotopic composition of the complex. An unradiogenic initial $^{143}Nd/^{144}Nd$ ratio accompanying the radiogenic initial $^{87}Sr/^{86}Sr$ of the complex will suggest that

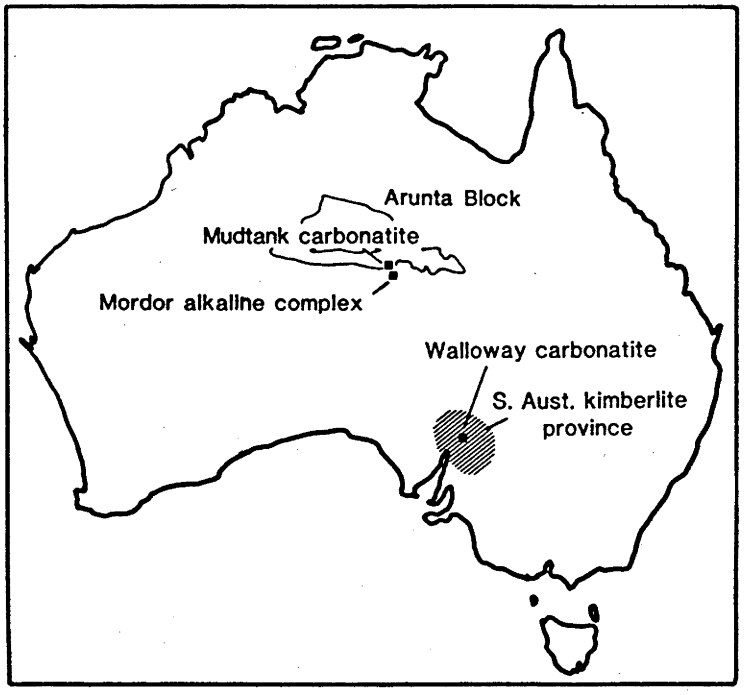

Fig. 4.1 Location of the Mordor Complex, Arunta Block. Locations of the Mudtank carbonatite and the South Australian kimberlite/carbonatite province are also shown.

Proterozoic potassic magmas are also derived from so-called "enriched mantle" sources, as has been found for younger (mostly Phanerozoic) examples. The samples used in this study are those used in the study of Langworthy and Black (1978) and because they are petrographically and geochemically fresh, selected whole-rock samples were also analysed for U and Pb concentrations and Pb isotopic compositions, in an attempt to determine the initial Pb isotopic characteristics of the complex.

4.2 Analytical Procedure

Samples were supplied as powders which had been crushed in an agate Siebtechnik mill. About 500 mg of sample powder was dissolved in conc. HF-$HClO_4$ in teflon pressure capsules at 200 °C for at least 48 hours, the resulting solution evaporated and the sample re-dissolved in 6 N HCl in teflon pressure capsules for a further 24 hours. The sample was then re-dissolved in 1 N HCl and split into 3 aliquots, 2 of which were mixed with ^{147}Sm-^{150}Nd (for Sm-Nd concentration and Nd isotopic composition analysis) and ^{235}U-^{208}Pb (for U and Pb concentration analysis) spikes respectively and the third used for Pb isotopic composition analysis, following procedures which are described more fully in Appendix 1.

4.3 Results

4.3.1 Sm-Nd isotopic analysis

The results of Sm-Nd analysis are presented in Table 4.1. Measured Nd/Sm ratios range from 4.7 to 6.2, indicating that the magmas are moderately LREE-enriched, and the measured $^{143}Nd/^{144}Nd$ ratios range from $\varepsilon_{Nd}(0)$ of -19.9 to -24.3. The results define a poorly-constrained Sm-Nd isochron (Fig. 4.2) indicating an age of 1100 ±280 Ma (MSWD = 0.53; all quoted errors are at the 95% confidence level) and with an initial ε_{Nd} of -10.3 ±3.1. The large error in the age and initial ratio of the Sm-Nd isochron is

Table 4.1 Samarium-neodymium isotopic data for the Mordor Complex.

Sample		Sm	Nd	$^{147}Sm/^{144}Nd$[a]	$^{143}Nd/^{144}Nd$[b]	$\varepsilon_{Nd}(0)$	ε_{Nd}[c]
		----ppm----					
3434	phlog. lherzolite	3.248	16.82	0.1167	0.51073 ±2	-21.7	-10.2
3435	phlog. lherzolite	11.88	56.02	0.1283	0.51074 ±2	-21.4	-11.6
3438	phlog. hy. shonkinite	6.132	78.04	0.1070	0.51066 ±3	-23.1	-10.2
3441	phlog. lherzolite	12.15	63.45	0.1158	0.51073 ±3	-21.5	-9.9
3446	phlog. shonkinite	16.73	95.73	0.1057	0.51068 ±2	-22.5	-9.5
3450	phlog. wehrlite	8.32	40.31	0.1248	0.51082 ±2	-19.9	-9.6
3452	phlog. wehrlite	12.45	72.22	0.1259	0.51079 ±3	-20.4	-10.2
4142	syenite	9.73	60.39	0.0975	0.51060 ±3	-24.1	-9.9
4202	melamonzonite	21.92	128.07	0.1035	0.51064 ±2	-23.3	-9.9
4213	monzonite	28.24	170.43	0.1002	0.51063 ±2	-23.5	-9.7
4578	shonkinite	11.42	68.40	0.1010	0.51059 ±2	-24.3	-10.6

[a] Uncertainty in $^{147}Sm/^{144}Nd$ is 0.1% (2σ).

[b] Nd isotopic ratios normalised using $^{146}Nd/^{142}Nd = 0.636151$. The value obtained for BCR-1 standard is 0.511833 ±20. $\varepsilon_{Nd}(0) = (^{143}Nd/^{144}Nd_{meas}/^{143}Nd/^{144}Nd_{CHUR} - 1) \times 10^4$ where $^{143}Nd/^{144}Nd_{CHUR} = 0.511836$.

[c] ε_{Nd} calculated at 1.12 Ga using $^{147}Sm/^{144}Nd_{CHUR} = 0.1967$.

mainly due to the limited spread in the measured $^{147}Sm/^{144}Nd$ and $^{143}Nd/^{144}Nd$ ratios. The low MSWD indicates that the points fit the isochron within their assigned analytical error. One sample (#3435) with higher $^{147}Sm/^{144}Nd$ is not within experimental error of the line defined by the other points and has been omitted from the regression. The Sm-Nd isochron age is in general agreement with the age of 1120 ±90 Ma determined from whole-rock and mineral Rb-Sr isochrons (re-calculated from Langworthy and Black 1978, using the revised decay constants recommended by Steiger and Jäger 1977). The negative initial ε_{Nd} suggests that the magmas comprising the complex were derived from a source which was LREE-enriched for probably at least ~600 Ma prior to their emplacement, consistent with the assertion of long-term high Rb/Sr in the source made by Langworthy and Black (1978) from consideration of the Rb-Sr isotopic systematics.

4.3.2 U-Pb isotopic analysis

The U and Pb concentration and Pb isotopic results are given in Table 4.2. Measured U/Pb ratios are generally low (< 6.45), apparently a common feature of many potassic magmas (for example, low U/Pb ratios are also found in the Western Australian lamproites, see Chapter 3). On a Pb-Pb isotope diagram (Fig. 4.3) the measured Pb isotopic compositions form an approximately linear array with a slope (0.130) corresponding to an age of ~2100 Ma, which is ~1000 Ma older than the emplacement age of the Mordor Complex indicated by the Rb-Sr and Sm-Nd isochrons. The degree of variation of the Pb-Pb correlation from a linear array is greater than can be accounted for by experimental error alone. Regression of $^{238}U/^{204}Pb$ against $^{206}Pb/^{204}Pb$ (Fig. 4.4) gives a Model 3 age of 1000 ±240 Ma, in agreement with the ages obtained by Rb-Sr and Sm-Nd methods, with a poorly defined initial ratio of 16.52 ±0.19. The

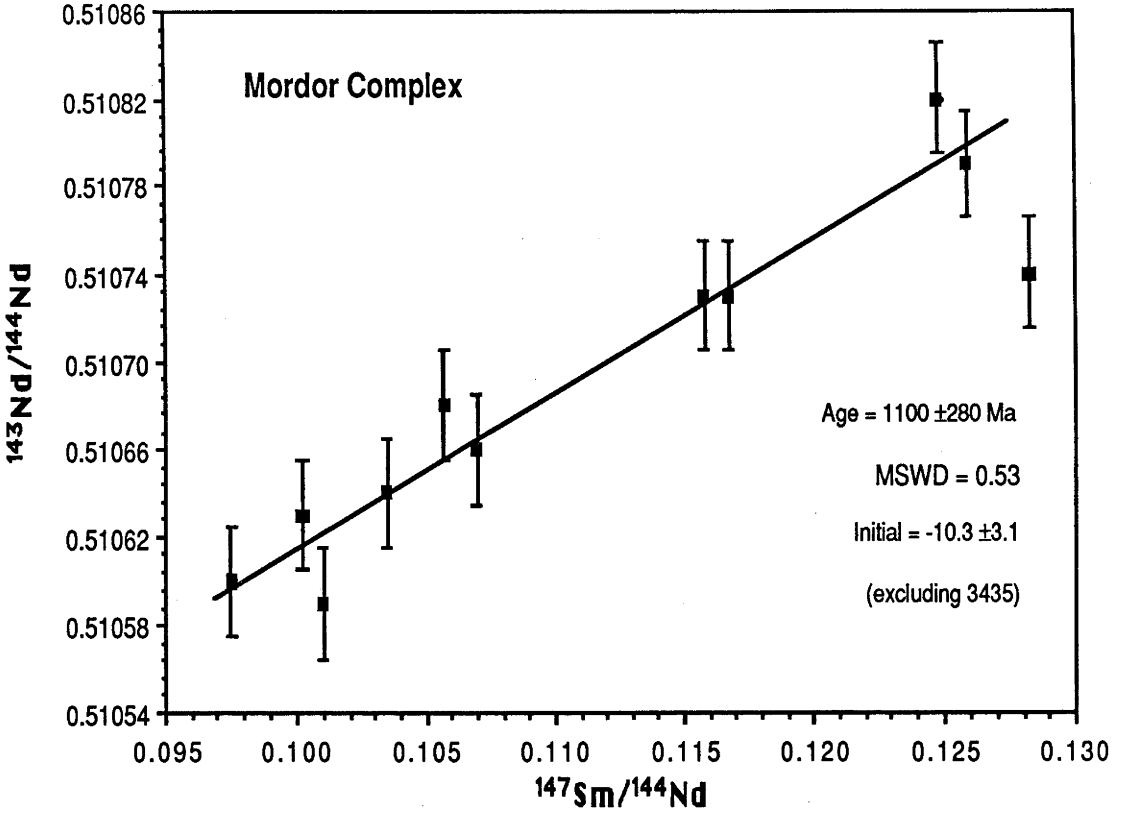

Fig. 4.2 $^{147}Sm/^{144}Nd$ -$^{143}Nd/^{144}Nd$ isochron diagram for the Mordor Complex.

Model 3 fit indicates that the error in the regression is independent of the U/Pb ratio and is therefore more likely to be due to variability in the initial ratio rather than post-emplacement mobility of U or Pb. Langworthy and Black (1978) have also argued that the complex may have possessed some variation in the initial Sr isotopic composition. Sample #3441, which has considerably higher $^{207}Pb/^{204}Pb$ than the other samples, does not lie on the ^{238}U-^{206}Pb isochron. The disparity between the ^{238}U-^{206}Pb and Pb-Pb isochron ages is due at least in part to the omission of sample #3441 and the absence of 3 data points (samples #3446, #3450 and #4142), for which U concentrations have not been determined, from the ^{238}U-^{206}Pb regression. As the ^{238}U-^{206}Pb system has (at least partly) recognised the 1.12 Ga emplacement event, it is unlikely that the 2.1 Ga age indicated by the Pb-Pb correlation has any direct chronological meaning. Instead, the Pb-Pb array probably reflects variation in the initial Pb isotopic compositions, particularly the initial $^{207}Pb/^{204}Pb$, during the emplacement event at 1.12 Ga (for further discussion, see below).

The initial $^{206}Pb/^{204}Pb$ and $^{207}Pb/^{204}Pb$ ratios calculated using the measured $^{238}U/^{204}Pb$ ratios and an age of 1.12 Ga are given in Table 4.2. Apart from sample #3441, the calculated initial ratios lie within a relatively narrow range of from 16.35 to 16.58 for $^{206}Pb/^{204}Pb$ and from 15.45 to 15.54 for $^{207}Pb/^{204}Pb$. This initial Pb isotopic composition estimated for the Mordor Complex is considerably more radiogenic than the values estimated for the MORB mantle reservoir (which can be approximated by a single stage curve with $\mu \approx 8$; see discussion in Chapter 3) at 1.1 Ga and comparable to those of the Cumming and Richards (1975) Model 3 Pb ore growth curve at this time.

Table 4.2 Uranium-lead isotopic data for the Mordor Complex.

Sample	U[a]	Pb	$^{238}U/^{204}Pb$	$^{206}Pb/^{204}Pb$[b]		$^{207}Pb/^{204}Pb$		$^{208}Pb/^{204}Pb$
	----ppm----			meas	initial	meas	initial	meas
3434 phlog. lherzolite	0.251	5.693	3.13	16.942	(16.35)[c]	15.517	(15.47)	38.162
3435 phlog. lherzolite	0.919	21.14	3.10	16.963	(16.37)	15.537	(15.49)	38.237
3438 phlog. hy. shonk.	1.127	24.19	3.32	17.088	(16.46)	15.551	(15.50)	38.198
3441 phlog. lherzolite	0.978	25.17	2.79	17.397	(16.87)	15.601	(15.56)	38.293
3446 phlog. shonkinite		12.04		16.979		15.498		37.715
3450 phlog. wehrlite		3.439		16.902		15.491		37.289
3452 phlog. wehrlite	0.064	3.341	1.13	16.666	(16.41)	15.480	(15.46)	37.233
4142 syenite		35.48		16.639		15.457		36.826
4202 melamonzonite	1.190	36.03	2.34	17.027	(16.58)	15.523	(15.49)	37.713
4213 monzonite	0.223	9.83	1.60	16.882	(16.58)	15.560	(15.54)	37.509
4578 shonkinite	3.219	36.58	6.45	17.645	(16.42)	15.587	(15.49)	39.669

[a] U and Pb concentrations determined by isotope dilution mass spectrometry. Uncertainty in $^{238}U/^{204}Pb$ is estimated at <0.5% (2σ).

[b] All Pb isotopic analyses performed in duplicate. Errors (based on two-way analysis of variance of duplicate analyses) at the 1σ level; $^{206}Pb/^{204}Pb$ ±0.011, $^{207}Pb/^{204}Pb$ ±0.014, $^{208}Pb/^{204}Pb$ ±0.033. The values obtained for NBS-981 during this study are; $^{206}Pb/^{204}Pb$ = 16.927 ±0.009, $^{207}Pb/^{204}Pb$ = 15.486 ±0.013, $^{208}Pb/^{204}Pb$ = 36.668 ±0.044.

[c] Age corrections to Pb isotopic ratios (in brackets) calculated using an age of 1.12 Ga.

4.4 Discussion

4.4.1 Analysis of the excess scatter in the isochrons of the Mordor Complex

All three geochronological systems applied to the Mordor Complex display evidence of scatter in excess of that which is attributable to experimental error. This "geological error" probably reflects either variation in the initial isotopic characteristics of the complex or is due to the partial resetting of the isotope systems following its emplacement. If not interpreted correctly, this geological error can cause substantial shifts in the slopes of isochrons and consequently, incorrect ages. The following discussion presents the results of a mathematical analysis of the geological error in the isochrons of the Mordor Complex.

If the geological error is due to variation in the initial ratio of the complex, it might be anticipated that variation in the initial $^{87}Sr/^{86}Sr$ is somehow correlated with variation in the initial $^{143}Nd/^{144}Nd$. This possibility has been examined as a function of age using two independent parameters. The MSWD (mean square of weighted deviates) is commonly used as a measure of the scatter of points about a line. Normally, points are weighted inversely as the square of their analytical error. However, because the internal (or within-run) analytical error of all isotopic analyses examined here is similar to or less than the external error (based on the analytical reproducibility of the analyses), all points have been weighted equally in the calculation of an analogous parameter, the "mean square of unweighted deviates" (or MSUD). As with the MSWD, this parameter cannot distinguish between scatter about a line and scatter around a point. Consequently, a second parameter, the correlation co-efficient (or *r*), has also been used as

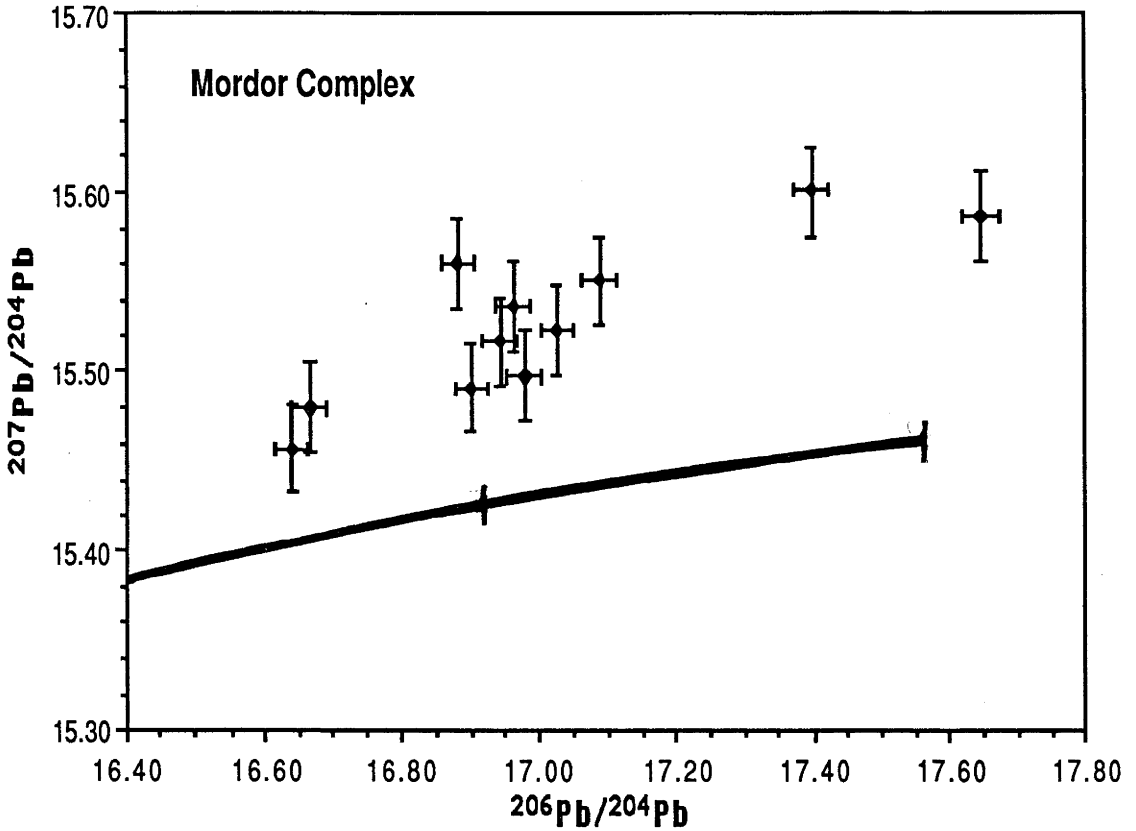

Fig. 4.3 $^{207}Pb/^{204}Pb$- $^{206}Pb/^{204}Pb$ isotope diagram for the Mordor Complex. The single-stage growth curve with $\mu = 8$ (which approximates the Pb isotopic evolution of the mantle) is shown for comparison.

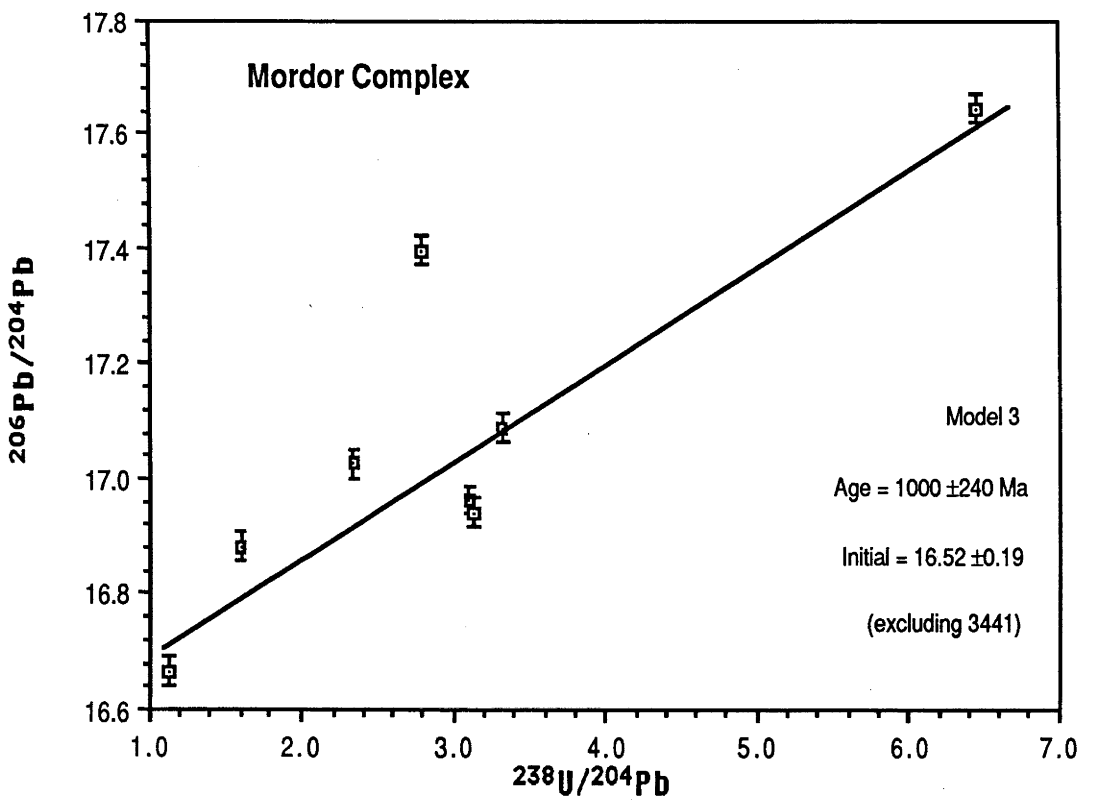

Fig. 4.4 $^{238}U/^{204}Pb$-$^{206}Pb/^{204}Pb$ isochron diagram for the Mordor Complex.

a measure of the degree of linearity of the age-corrected data array. Because different geological processes may be responsible for causing scatter in whole-rock and mineral data (for example, crustal assimilation by a magma operates on a whole-rock scale, whereas scatter on a mineral scale is generally due to post-emplacement processes), only whole-rock analyses have been used in the following analysis. Error in $^{87}Rb/^{86}Sr$ and $^{147}Sm/^{144}Nd$ have not been taken into account in the calculations. Although the uncertainty in the initial $^{87}Sr/^{86}Sr$ and $^{143}Nd/^{144}Nd$ due to error in these ratios will increase with emplacement age, this is not likely to significantly affect the results of the analysis over the narrow age range examined.

The results of the analysis of co-variation between initial $^{87}Sr/^{86}Sr$ (data taken from Langworthy and Black 1978) and initial $^{143}Nd/^{144}Nd$ with age are presented in Figs. 4.5 and 4.6. The computer program used for this analysis is listed in Apendix A2.2. It is apparent from these two figures that the age-corrected $^{87}Sr/^{86}Sr$ and $^{143}Nd/^{144}Nd$ are most strongly correlated at ~1200 Ma. This age is within error of the Rb-Sr and Sm-Nd isochron ages. These results imply that the Mordor Complex possessed a range of initial $^{87}Sr/^{86}Sr$ and initial $^{143}Nd/^{144}Nd$ compositions which were negatively correlated. The age-corrected $^{87}Sr/^{86}Sr$ and $^{143}Nd/^{144}Nd$ array at 1180 Ma is plotted in Fig. 4.7. Although in general, mixing processes will generate curved rather than linear arrays on an $^{87}Sr/^{86}Sr$-$^{143}Nd/^{144}Nd$ diagram, it is evident from Fig. 4.7 that, because of the limited range in initial $^{87}Sr/^{86}Sr$ and initial $^{143}Nd/^{144}Nd$ values compared to the analytical error, the age-corrected array can be regarded as linear.

A similar analysis can be performed on the U-Pb data (see Appendix A2.3 for computer program listing). If the scatter in the $^{207}Pb/^{204}Pb$- $^{206}Pb/^{204}Pb$ array (Fig. 4.3) is due to re-distribution of U and Pb during an event occurring after emplacement of the complex, this excess scatter in the age-corrected array should dissappear at the time of this re-distribution event. However, throughout the age range 1550 Ma to 0 Ma examined, both the MSUD and the correlation co-efficient ***r*** remain virtually constant. The total variation in ***r*** is from 0.865 at 1500 Ma to a minimum of 0.829 at 1200 Ma, with the present-day (i.e. 0 Ma) value being 0.846. The scatter is therefore virtually independent of the present-day U/Pb ratio of the rocks, suggesting that it is due to variation in their initial Pb isotopic compositions or that a re-distribution event disturbed the U-Pb systematics of the complex very recently.

The slope on the $^{207}Pb/^{204}Pb$- $^{206}Pb/^{204}Pb$ array at the emplacement age of ~1180 Ma is 0.1565, which corresponds to a Pb-Pb age of ~2420 Ma. The slope of the array is, however, relatively sensitive to the assumed emplacement age. For example, an error of ±100 Ma in the emplacement age translates to an error of ±0.0147 in the slope of the array or ±160 Ma in the corresponding Pb-Pb age. Uncertainty in the slope of the age-corrected array due to propagation of analytical error is also likely to be substantial. As the correlation in the age-corrected $^{87}Sr/^{86}Sr$-$^{143}Nd/^{144}Nd$ array is probably due to mixing, it is likely that the $^{207}Pb/^{204}Pb$-$^{206}Pb/^{204}Pb$ array is also the result of mixing and has no age significance.

4.4.2 Initial isotopic characteristics of the Mordor Complex

The isotopic data indicate that the parent magmas of the Mordor Complex had the following isotopic characteristics during its emplacement ~1.18 Ga ago; initial $^{87}Sr/^{86}Sr \approx 0.710$ to 0.711, $\varepsilon_{Nd} \approx -10.3$ ±3.1, initial $^{206}Pb/^{204}Pb \approx 16.52$ and initial $^{207}Pb/^{204}Pb \approx 15.50$. There is also evidence from all of these isotope systems that the complex possessed some variability in its initial isotopic compositions.

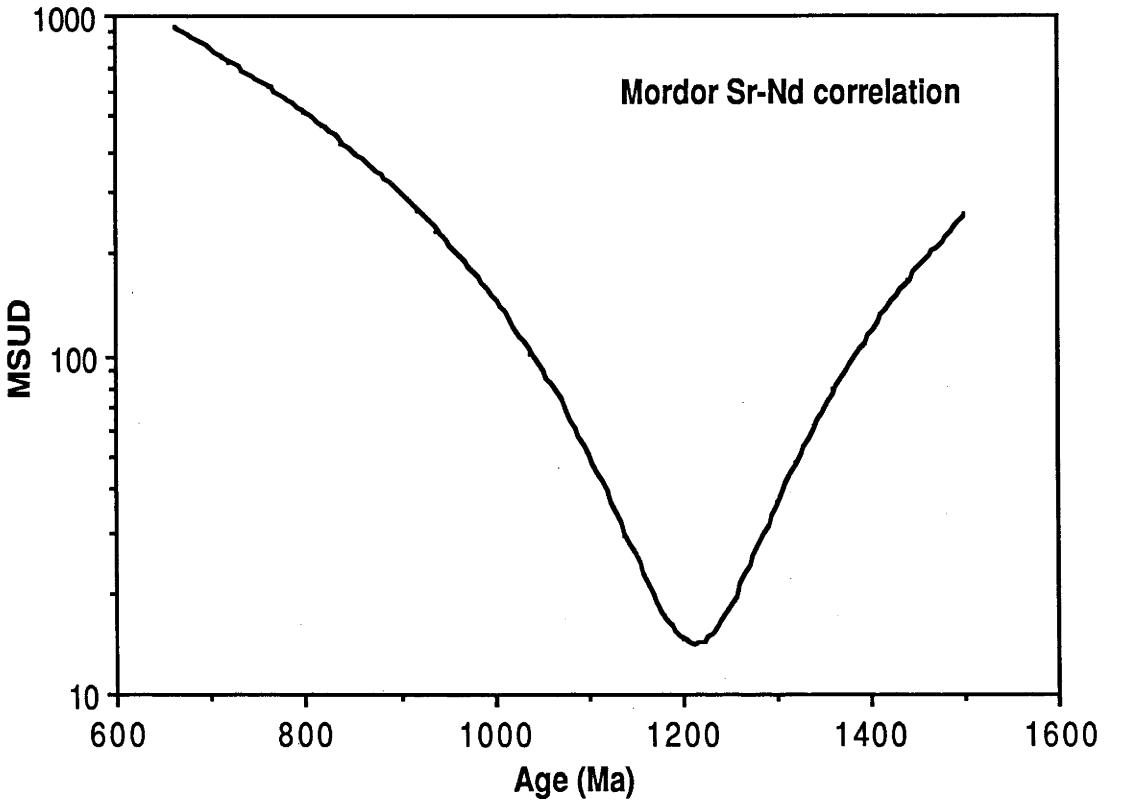

Fig. 4.5 Correlation between age-corrected values of $^{87}Sr/^{86}Sr$ versus $^{143}Nd/^{144}Nd$ plotted against age. The mean square of unweighted deviates (MSUD) is used here as a measure of the deviation of the age-corrected values from a single line or point (note log scale). The diagram demonstrates that the age-corrected array clusters or is most linear at ~1200 Ma.

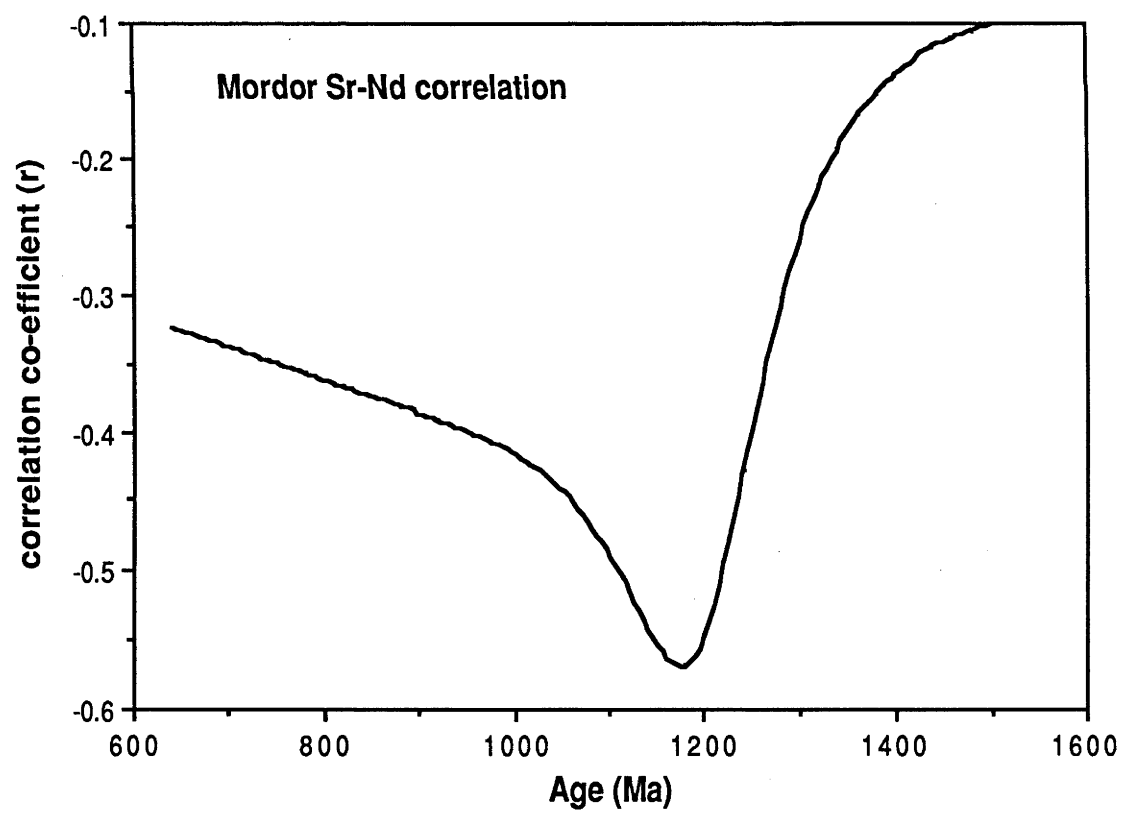

Fig. 4.6 Correlation between age-corrected values of $^{87}Sr/^{86}Sr$ versus $^{143}Nd/^{144}Nd$ plotted against age. The correlation co-efficient (r) is used here as a measure of the linearity of the age-corrected values. The age-corrected array is most linear at ~1180 Ma.

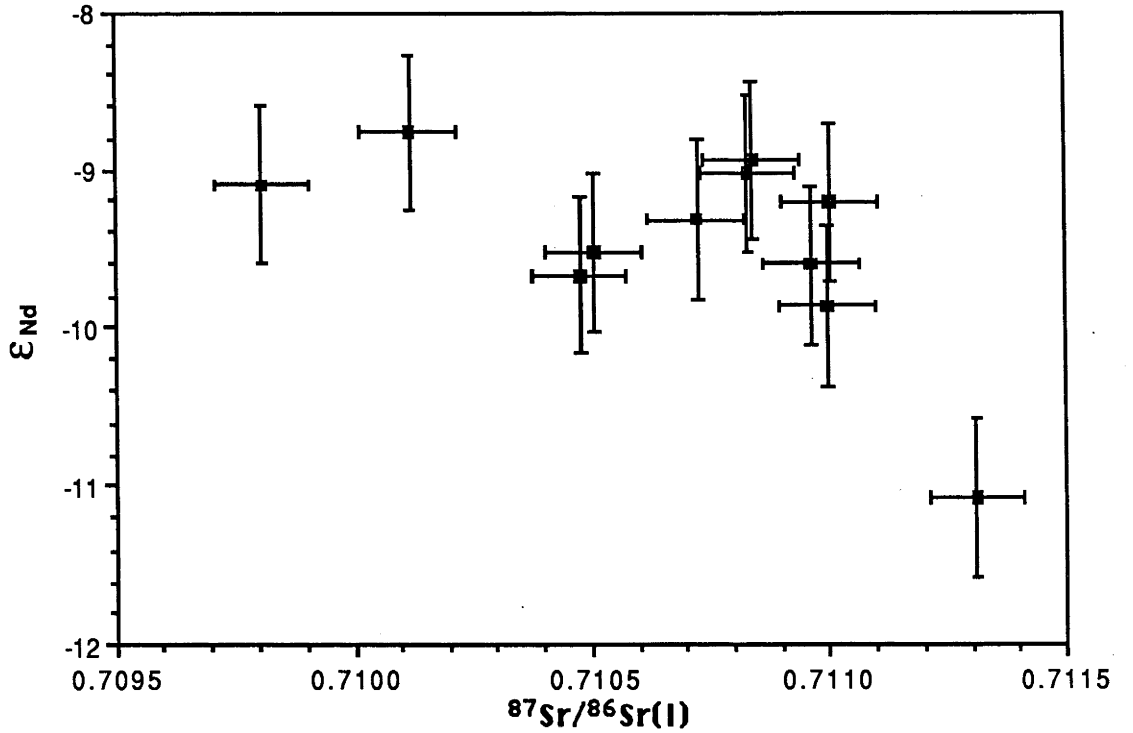

Fig. 4.7 Age-corrected (1180 Ma) array of $^{87}Sr/^{86}Sr$ versus $^{143}Nd/^{144}Nd$ for the Mordor Complex. Error-bars are 2σ analytical uncertainty limits- no account has been made of error introduced by the age correction.

The Mordor Complex lies within the enriched quadrant on an initial Sr-Nd isotope diagram and within the array defined by most other (Phanerozoic) examples of potassic magmatism. The initial Sr and Nd isotopic compositions are similar to those of potassic lavas from Sabinyo (Vollmer and Norry 1983a) and the Roman province (Hawkesworth and Vollmer 1979; see Fig. 2.4 and Fig. 3.3). The evolved Sr and Nd initial isotopic compositions indicate that the Mordor magma sources have been enriched in both Rb/Sr and the light rare-earth elements for at least ~600 Ma prior to emplacement of the complex.

4.4.3 The tectonic setting and origin of the Mordor Complex

The Mordor Complex is situated within the Arunta Inlier, an early Proterozoic ensialic mobile belt composed principally of medium- to high-grade metamorphic sediments, mafic rocks and granites. The tectonic evolution of the Arunta Inlier has been summarised by Black *et al.* (1983), Stewart *et al.* (1984), Shaw *et al.* (1984) and Windrim and McCulloch (1987). According to Shaw *et al.* (1984), it commenced with mafic and felsic magmatism and deposition of shale and limestone within an east-west-trending rift basin, followed by rapid deformation and regional metamorphism during the Strangways Event, aproximately 1800 to 1750 Ma ago. Windrim and McCulloch (1987) obtained a regional Sm-Nd isochron of 2070 ±125 Ma for both felsic and mafic granulites and interpreted this as the formation age (i.e. the mantle extraction age) of Arunta Block crust. The initial ε_{Nd} of ~ +1.5, also obtained for both felsic and mafic rock populations regressed separately, was interpreted as indicating little crustal prehistory for the felsic rocks and led Windrim and McCulloch (1987) to speculate that the protoliths of the felsic rocks were melts of a young mafic protocrust generated during a rifting and attenuation event. Shaw *et al.* (1984) proposed that limited subduction and crustal overthrusting during the Strangways Event caused

crustal thickening and the insertion of an elongate subcrustal wedge of asthenosphere within the thickened subcontinental lithosphere. A similar scenario involving continental collision and underthrusting of the Arunta block was favoured by Windrim and McCulloch (1987). An ensialic setting for the underthrusting event was inferred from the absence of ophiolite complexes and andesitic rocks from the central Australian mobile belts, noted by Shaw *et al.* (1979). A further 4 stages of deformation, metamorphism and granitic intrusion have also been recognised. The Inlier is cut by several major north-west-trending gravity lineaments which are believed to represent deep crustal fractures. The Mordor Complex and the Mudtank carbonatite lie near the Woolanga Gravity Lineament, a major structural gravity and magnetic lineament which can been traced for several hundred kilometres and which marks the eastern margin of the occurrence of older (Division 1) mafic granulite.

The initial ε_{Nd} of -10 for the complex requires at least ~600 Ma of prehistory for the sources of the complex prior to its emplacement at ~1200 Ma. As the formation age of the Arunta Inlier determined by Windrim and McCulloch (1987) is ~2070 Ma, this suggests that the heterogeneity producing the LREE-enrichment within the sources of the Mordor Complex originated shortly after (i.e. within ~400 Ma of) the initial formation of Arunta Inlier crust. If the Sm/Nd ratios of the Mordor magmas were not substantially modified by crystal fractionation, a better estimate of the minimum period of prehistory can be obtained by assuming a Mordor source Sm/Nd ratio equivalent to that of the highest Sm/Nd ratio displayed by the Mordor magmas, as magma extraction is likely to result in a decrease in the Sm/Nd ratio and the highest Sm/Nd ratio of the magmas therefore provides a minimum estimate of the source Sm/Nd. Assuming that the Mordor source had a minimum $^{147}Sm/^{144}Nd$ ratio of 0.126 (as indicated by sample #3452; the higher ratio of #3435 is not used as this sample does not lie on the Sm-Nd isochron and may have had a substantially different initial ratio compared to the rest of the suite), an ε_{Nd} of -10 would require a time period of at least ~1100 Ma to evolve from an initially chrondritic source. If the Mordor Complex magma sources were derived from Arunta block crust with ε_{Nd} of +1.5 at 2070 Ma, a minimum $^{147}Sm/^{144}Nd$ ratio of 0.0928 is required to evolve an ε_{Nd} of -10.3 at 1200 Ma. This $^{147}Sm/^{144}Nd$ ratio is lower than the values typical of upper crustal rocks (which commonly possess $^{147}Sm/^{144}Nd$ ratios between 0.10 and 0.13) and is substantially lower than the values found in the Mordor magmas. The Mordor Sm-Nd isotopic systematics therefore suggest that crust older than that recognised by Windrim and McCulloch (1987) exists within the Arunta Block.

The Mordor Complex therefore represents a further example of potassic magmatism from an intra-cratonic setting which has been derived from an enriched mantle source, and provides convincing evidence that the processes generating enriched mantle sources such as those from which many Phanerozoic examples of alkaline magmatism are derived have operated at least since the mid-Proterozoic.

5. Potassic mafic dykes from Antarctica

5.1 Introduction

Throughout the early to middle Proterozoic, the eastern part of the Antarctic continent was extensively intruded by continental tholeiitic and high-Mg mafic dykes, whereas during the late Proterozoic (< ~1 Ga ago), magmatism with alkaline affinities, ranging from alkali olivine basalt to alkali melasyenite and alnölite, predominates (Sheraton 1983). Two episodes of dyke emplacement during the early Proterozoic in the Enderby Land region have been recognised (Sheraton and Black 1981); an earlier predominantly tholeiitic and high-Mg intrusion event at 2350 ±48 Ma, shortly after the last major metamorphism-deformation event (dated from the Napier Complex by U/Pb zircon by Black and James 1979, at ~2480 Ma), followed by intrusion of the Amundsen continental tholeiitic dykes at 1190 ±200 Ma. Based on trace-element and Sr isotopic evidence, Sheraton and Black (1981) argued that the early Proterozoic dykes were generated from depleted ($^{87}Sr/^{86}Sr = 0.7020 \pm 0.0008$, low TiO_2, P_2O_5 and Y) source regions which were enriched in highly incompatible elements (particularly K, Rb, Th, U, Pb and As) shortly before the emplacement event. The low initial $^{87}Sr/^{86}Sr$ and consistency of trace-element abundance patterns was regarded as evidence that crustal contamination processes were not responsible for the incompatible-element enrichment of the high-Mg suite but that these features were inherited from the magma source region. The late Proterozoic Amundsen dykes were divided into two groups, one of which (Group 1) was considered to be derived from a chemically homogeneous mantle source with high $^{87}Sr/^{86}Sr$ of 0.7041 ±0.0005. Group 2 Amundsen dykes were believed to be derived from chemically and isotopically heterogeneous mantle sources which Sheraton and Black (*op. cit.*) suggested may have been metasomatised contemporaneously with the sources of the Early Proterozoic high-Mg suite. Evidence for the operation of metasomatic enrichment processes of the subcontinental lithosphere beneath east Antarctica therefore extends to the beginning of the Proterozoic, whereas the low initial $^{87}Sr/^{86}Sr$ ratio of early Proterozoic dykes suggests that prior to this time the subcontinental mantle was not particularly anomalous.

Fractionated, highly alkaline dykes of probable Cambrian to Eocene age have been described from the high-grade gneiss terrains of the Prince Charles Mountains, Mac Robertson Land, and from Priestley Peak in Enderby Land, east Antarctica (Sheraton and England 1980, Sheraton 1983; see Fig. 5.1). These melasyenite dykes are characterised by high TiO_2, K_2O, P_2O_5, F, Rb, Sr, Zr, Nb, Ba, La, Ce, Pb, Th, U but relatively low Al_2O_3, CaO and Na_2O and are therefore chemically similar to lamproites from the West Kimberley region (Jaques *et al.* 1984a) and to leucitites from Gaussberg (Sheraton and Cundari 1980). As there are several other lines of evidence which suggest that the mantle beneath the east Antarctic region has experienced at least one enrichment episode since the early Proterozoic, a reconnaissance isotopic study of a few well-preserved alkaline dykes was undertaken. The findings of this study have implications for interpretation of the isotopic characteristics of the major Gondwanaland continental tholeiite provinces of Tasmania, South Africa and Antarctica. In addition, a relatively continuous record of mantle-derived magmatism since the beginning of the Proterozoic is represented on the Antarctic continent and may allow investigation of the isotopic evolution of the Antarctic subcontinental lithosphere over this time.

5.2 Samples and Analytical Procedure

Two samples from the northern Prince Charles Mountains region (see Fig. 5.1), an alkali olivine basalt from Fox Ridge (#6928-0225) and a leucite tristanite from Manning Massif (#7328-1594), and one sample from Mt Bayliss (#7328-1545) in the southern Prince Charles Mountains, have been included in this study. The northern Prince Charles mountains region consists mostly of Late Proterozoic (~1000 Ma) gneiss, whereas the Mt Bayliss dyke intrudes Archaean (~2.8 Ga) basement gneiss. Details of the ages, geochemistry and petrography of these samples can be found in Sheraton and England (1980) and Sheraton (1983). The low Mg-numbers and Ni and Cr contents of the Fox Ridge, Manning Massif and Mt Bayliss samples (atomic Mg/[Mg+total Fe] of 0.50, 0.58 and 0.58 respectively) suggests that they have undergone considerable crystal fractionation. These samples are highly enriched in incompatible elements and lack significant Nb anomalies. The Priestley Peak alkali melasyenite dyke (#7728-3439D) is the youngest intrusion recognised from the Archaean Napier Complex, Enderby Land. Its geochemistry and petrography was described by Sheraton and England (1980). The high Mg-number of 0.71 and high Ni (298 ppm) and Cr (348 ppm) contents suggest that the Priestley Peak dyke may represent a near-primary magma. A Rb-Sr combined mineral and whole-rock isochron obtained by Black and James (1983) indicated a Silurian age of 482 ±3 Ma with high initial $^{87}Sr/^{86}Sr$ ratio of 0.70852 ±0.00007. The trachybasalt dyke from Bunger Hills (#7728-4730), Queen Mary Land, has an Mg-number of 0.50 and is geochemically similar to the Prince Charles Mountains and Priestley Peak samples in having high K_2O contents and K_2O/Na_2O ratios. Both the Priestley Peak and Bunger Hills samples have highly incompatible-element-enriched trace-element patterns with positive Ba and negative Nb anomalies, although in the case of the Bunger Hills sample, these anomalies may be the result of late stage crystal fractionation.

Approximately 500 mg of sample powder was dissolved in teflon pressure capsules in concentrated HF-$HClO_4$ at 200 °C for at least 48 hours, the resulting solution evaporated and the sample re-dissolved in 6 N HCl in teflon pressure capsules at 200 °C for a further 24 hours. The solution was then re-dissolved in 1 N HCl and split into 3 aliquots, two of which were spiked with mixed ^{147}Sm-^{150}Nd (for Sm-Nd concentration and Nd isotopic analysis) and ^{235}U-^{208}Pb (for U-Pb concentration analysis) spikes and the third used for Pb isotopic analysis. Further details of the analytical techniques can be found in Appendix 1.

5.3 Results

5.3.1 Prince Charles Mountains region

The results of Nd isotopic analysis and the calculated initial Nd isotopic compositions using determined ages are given in Table 5.1. All samples have high Nd/Sm ratios indicating strong light rare-earth-element enrichment. The age correction to the Nd isotopic composition of the leucitite tristanite lava from Manning Massif (7328-1594) is less than 1 ε-unit, giving an initial ε_{Nd} of -9.3. The negative initial ε_{Nd} indicates derivation of the leucite tristanite from a source region having time-integrated light rare-earth-element enrichment. As the measured Sm/Nd ratio of the tristanite lava is

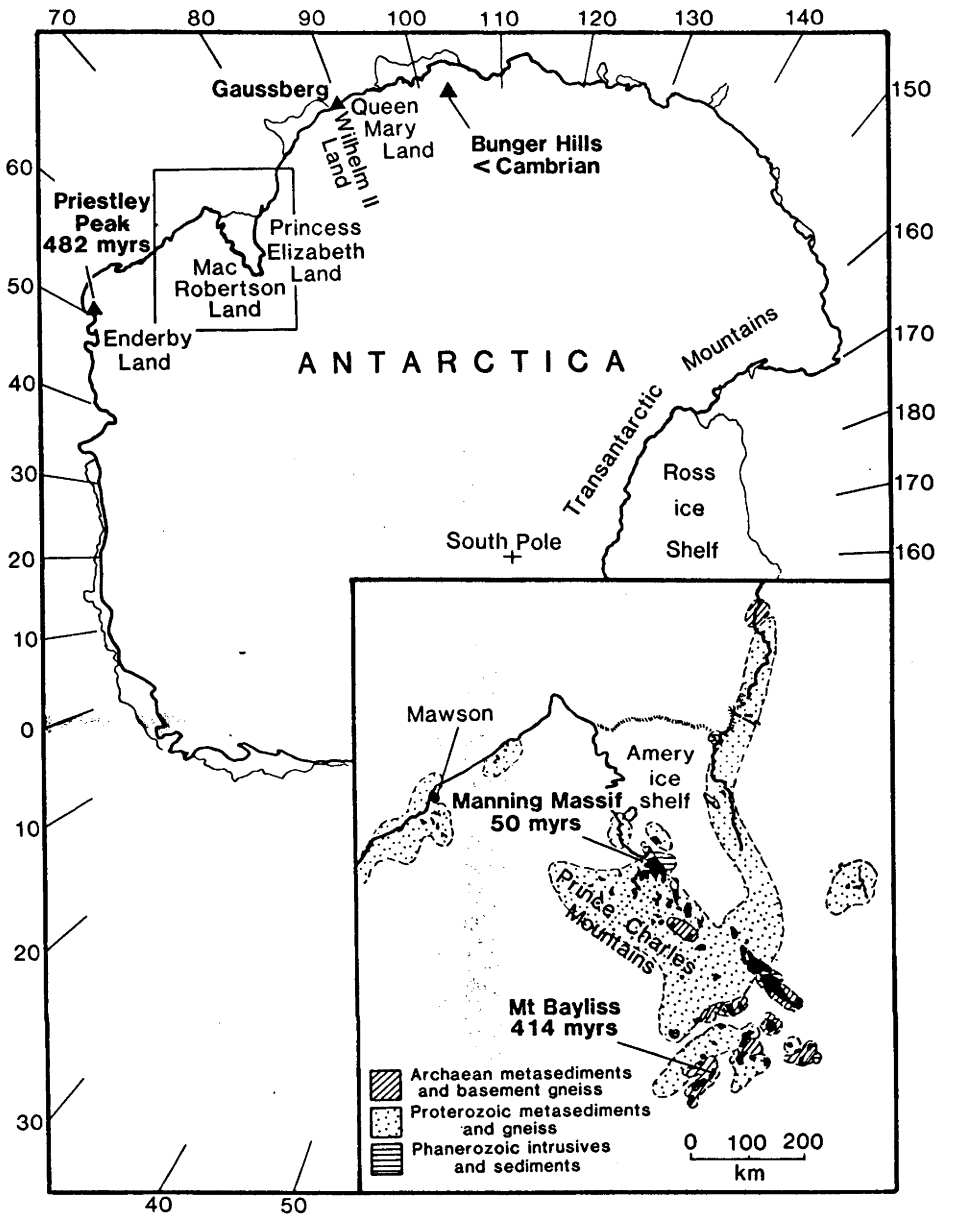

Fig. 5.1 Locality map of Antarctic samples analysed and other localities referred to in this study.

likely to represent a lower limit of the source Sm/Nd ratio (because Nd is generally more incompatible than Sm in the magma source and the Sm/Nd ratio in the melt is therefore likely to be less than that of the source following partial melting), the source of the tristanite must have been LREE-enriched for a minimum period of ~700 Ma in order to evolve an initial ε_{Nd} of -9.3 from an initially LREE-depleted or chondritic mantle source. However, the Fox Ridge alkali olivine basalt (6928-0225), emplaced within ~20 km of and ~450 Ma before the Manning Massif leucite tristanite, has a positive initial ε_{Nd} of +1.2, indicating derivation from a time-integrated LREE-depleted source. The Mt Bayliss alkali melasyenite (#7328-1545), situated ~400 km south of the Manning Massif and Fox Ridge sample localities and emplaced ~20 Ma after the Fox Ridge alkali basalt, has a negative initial ε_{Nd} of -12. The initial $^{143}Nd/^{144}Nd$ ratios therefore indicate that although the source LREE-enrichment and generation events of the Fox Ridge alkali basalt may have been nearly synchronous, this is clearly not the case for the Manning Massif and Mt Bayliss lavas.

Table 5.1 Age and samarium-neodymium isotopic data for east Antarctic alkaline dykes.

Sample	Age (Ma)	Sm	Nd	$^{147}Sm/^{144}Nd$[a]	$^{143}Nd/^{144}Nd$[b]	$\varepsilon_{Nd}(0)$	ε_{Nd}
		-----ppm-----					
Northern Prince Charles Mountains, MacRobertson Land							
7328-1594	50 ±2						
Manning Massif	(K-Ar)	9.347	64.28	0.0879	0.51132 ±1	-10.0	-9.3
6928-0225	504 ±20						
Fox Ridge	(K-Ar)	8.082	46.01	0.1062	0.51159 ±2	-4.7	+1.2
Southern Prince Charles Mountains, MacRobertson Land							
7328-1545	414±10						
Mt Bayliss	(K-Ar)	2.932	20.94	0.0847	0.51092 ±2	-18.0	-12.1
Enderby Land							
7728-3439D	482 ±3						
Priestley Peak	(Rb-Sr)	32.45	189.4	0.1036	0.51081 ±3	-20.0	-14.3
					$^{87}Sr/^{86}Sr(I) = 0.70852 \pm 7$[c]		
Queen Mary Land							
7728-4730	probably Cambrian or younger						
Bunger Hills		20.03	131.5	0.0921	0.51062 ±2	-23.7	< -16.3

[a] Uncertainty in $^{147}Sm/^{144}Nd$ is 0.1% (2σ).

[b] Nd isotopic ratios normalised to $^{146}Nd/^{142}Nd = 0.636151$. All errors quoted refer to within-run precision at the $2\sigma_{mean}$ level. BCR-1 standard gives 0.511833 ±20. ε_{Nd} calculated using $^{143}Nd/^{144}Nd_{CHUR} = 0.511836$ and $^{147}Sm/^{144}Nd_{CHUR} = 0.1967$.

[c] from Black and James (1983).

The Pb isotopic data are given in Table 5.2 and presented graphically on a Pb-Pb isotope diagram in Fig. 5.2. There is generally excellent agreement between the X-ray fluorescence U and Pb concentration determinations of Sheraton and England (1980) and Sheraton (1983) and the isotope-dilution determinations of this study. All samples have high concentrations of both U and Pb and, with the exception of the Fox Ridge alkali basalt and Mt Bayliss dyke, have U/Pb ratios close to those estimated for the depleted mantle from Pb isotopic studies of MORB. Corrections to $^{206}Pb/^{204}Pb$ for decay since emplacement are small for the 50 Ma old Manning Massif tristanite and, because of the lower U/Pb, to the Mt Bayliss dyke, but are considerably larger for the Fox Ridge alkali basalt. The age correction to the measured $^{207}Pb/^{204}Pb$ ratios are within analytical error for the Manning Massif and Mt Bayliss lavas. Both the Manning Massif and Mt Bayliss samples have unusually high initial $^{207}Pb/^{204}Pb$ ratios combined with relatively low initial $^{206}Pb/^{204}Pb$ (see Fig. 5.2). These unusual Pb isotopic characteristics, the general features of which are independent of any uncertainty introduced by the age corrections, and the unradiogenic Nd isotopic compositions of the Manning Massif and Mt Bayliss high-K magmas are similar to those of lamproites from Western Australia and leucites from Gaussberg (see Chapter 3).

Table 5.2 Uranium and lead concentration and lead isotopic data for east Antarctic alkaline dykes.

Sample	U[a]	Pb	$^{238}U/^{204}Pb$	$^{206}Pb/^{204}Pb$[b]		$^{207}Pb/^{204}Pb$		$^{208}Pb/^{204}Pb$	
	----ppm----			meas	initial	meas	initial	meas	initial
Northern Prince Charles Mountains, MacRobertson Land									
Manning Massif	4.14	36.4	8.20	17.749	(17.68)[c]	15.729	(15.72)	38.296	(38.21)[c]
7328-1594	[4.0]	[36]							
Fox Ridge	1.57			18.440	(16.10)	15.581	(15.45)	39.034	(36.10)
6928-0225	[1.5]	[4]	28.8						
Southern Prince Charles Mountains, MacRobertson Land									
Mt Bayliss	1.89	28.4	4.88	17.904	(17.58)	15.799	(15.78)	39.016	(38.61)
7328-1545	[2.0]	[28]							
Enderby Land									
Priestley Peak	7.90	61.6	9.32	17.646	(16.92)	15.742	(15.70)	38.909	(38.00)
7728-3439D	[6]	[58]							
Queen Mary Land									
Bunger Hills	11.3	101.2	8.22	17.904		15.689		39.276	
7728-4730	[11]	[104]							

[a] U and Pb concentrations determined by isotope dilution mass spectrometry; values in brackets determined by XRF (from Sheraton and England 1980 and Sheraton 1983).

[b] All Pb isotopic analyses obtained in duplicate. Errors (based on two way analysis of variance of duplicate analyses) at the 1σ level; $^{206}Pb/^{204}Pb$ ±0.011, $^{207}Pb/^{204}Pb$ ±0.014, $^{208}Pb/^{204}Pb$ ±0.033. The values obtained for NBS-981 during this study are; $^{206}Pb/^{204}Pb$ = 16.927 ±0.009, $^{207}Pb/^{204}Pb$ = 15.486 ±0.013, $^{208}Pb/^{204}Pb$ = 36.668 ±0.044.

[c] Corrected for ^{238}U and ^{232}Th decay since emplacement, using ages cited in Table 5.1. Corrections to $^{208}Pb/^{204}Pb$ made assuming Th/U = 4.

Because of the age and high U/Pb ratio of the Fox Ridge alkali basalt, a large age correction to the $^{206}Pb/^{204}Pb$ is necessary and the uncertainty in the initial $^{206}Pb/^{204}Pb$ is consequently greater. However, the Fox Ridge sample has substantially lower measured $^{207}Pb/^{204}Pb$ than the Mt Bayliss and Manning Massif samples. The calculated initial $^{206}Pb/^{204}Pb$ and $^{207}Pb/^{204}Pb$ ratios are similar to those estimated for the MORB source region at ~500 Ma ago, although the initial Nd isotopic composition of the Fox Ridge alkali basalt is too low ($\varepsilon_{Nd} \approx +1.2$) to be consistent with derivation from a MORB source.

5.3.2 Priestley Peak, Enderby Land

The measured $\varepsilon_{Nd}(0)$ of -20.0 of the Priestley Peak alkali melasyenite corrects to an initial ε_{Nd} of -14.3 at the emplacement age of 482 Ma. An initial $^{87}Sr/^{86}Sr$ of 0.70852 ±7 was obtained from a mineral Rb-Sr isochron by Black and James (1983). These initial Sr and Nd isotopic characteristics are similar to those of leucitites from Gaussberg (Collerson and McCulloch 1983; see Fig. 5.3), situated ~1500 km southeast of Priestley Peak and believed to be of late Pleistocene age. Age corrections to the

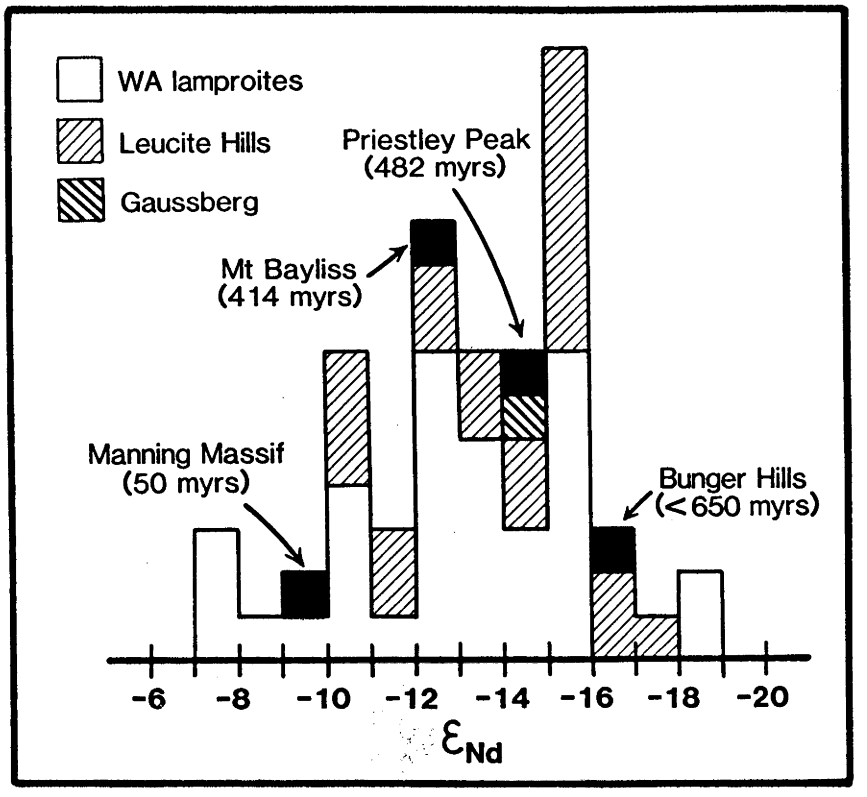

Fig. 5.2 Histogram of Nd isotopic compositions of Antarctic alkaline dykes compared to potassic magmas from other localities (from Collerson and McCulloch 1983, McCulloch *et al.* 1983, Vollmer *et al.* 1984 and Fraser *et al.* 1985).

Pb isotopic compositions are relatively large but, as with the Manning Massif and Mt Bayliss samples and lamproites from the West Kimberley, the Priestley Peak melasyenite also has unusually high $^{207}Pb/^{204}Pb$ and low $^{206}Pb/^{204}Pb$, irrespective of possible errors introduced by the age correction. This unusual Pb isotopic composition indicates derivation from an ancient source having high U/Pb early in its history, followed by a period of low U/Pb. The multi-stage history of U/Pb variation indicated by the Priestley Peak Pb isotopic composition cannot be related to fractionation of the U/Pb ratio during the emplacement event or during post-emplacement alteration. For example, assuming the most extreme case, where $^{235}U/^{204}Pb = 0$ for the 482 Ma following emplacement, the Pb isotopic composition of the Priestley Peak melasyenite still lies considerably above the mantle Pb growth curve and still requires a similar multistage history of U/Pb variation. As with the initial Sr and Nd isotopic compositions, the calculated initial Pb isotopic composition of the Priestley Peak melasyenite is also similar to that of Gaussberg leucitites (see Fig. 5.3).

5.3.3 Bunger Hills, Queen Mary Land

The exact age of emplacement of the Bunger Hills trachybasalt is presently unknown, but is believed to be younger than Cambrian. Assuming an emplacement age less than 600 Ma, the measured $\varepsilon_{Nd}(0)$ of the trachybasalt of -23.7 (Table 5.1) corrects to an initial ε_{Nd} of less than -16.3 (i.e. the initial ε_{Nd} lies between -23.7 and -16.7), similar to that of Gaussberg and Priestley Peak. The trace-element characteristics of the Bunger Hills trachybasalt are also remarkably similar to those of the Priestley Peak

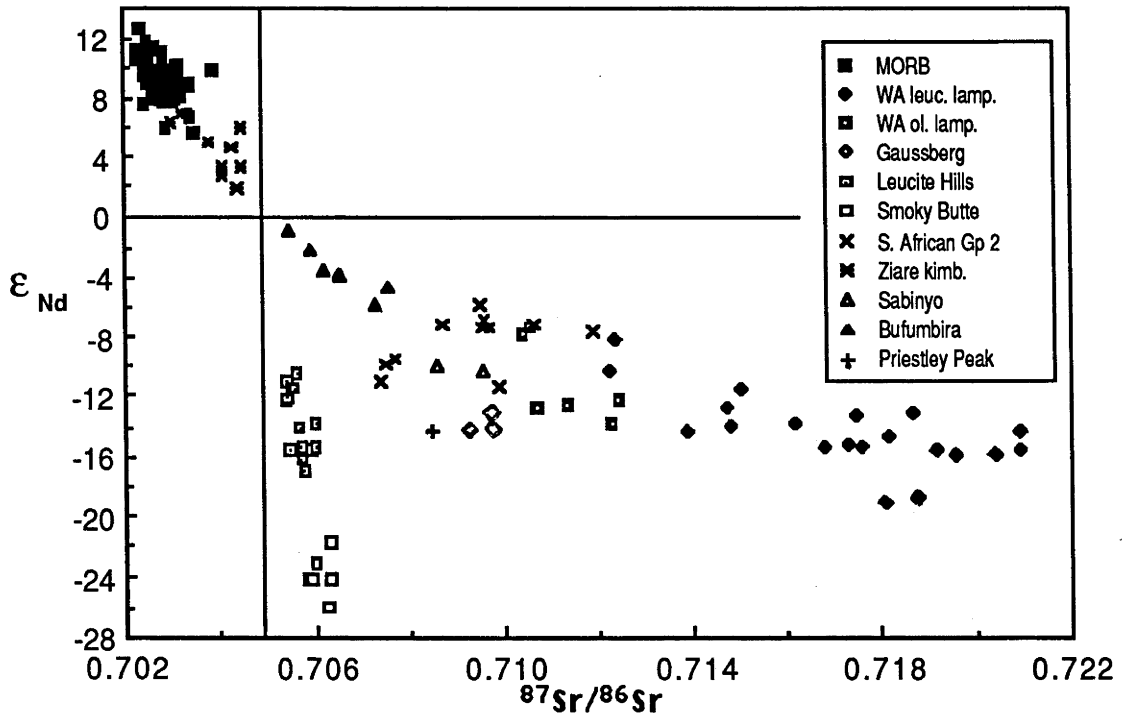

Fig. 5.3 Initial Sr-Nd isotope diagram showing the Priestley Peak melasyenite at its emplacement age of 482 Ma, compared to the fields of mid-ocean ridge basalts and other potassic suites (see caption to Fig. 3.3 for additional data sources).

melasyenite (see Fig. 4 of Sheraton 1980) and Gaussberg leucitites (Sheraton and Cundari 1980). The Bunger Hills trachybasalt has a high Pb content and, as with the Gaussberg and Priestley Peak samples, has high measured $^{207}Pb/^{204}Pb$ and low $^{206}Pb/^{204}Pb$ (Table 5.2). Because the measured (post-emplacement) $^{238}U/^{204}Pb$ of 8.22 is too high to cause the low measured $^{206}Pb/^{204}Pb$, and as the high $^{207}Pb/^{204}Pb$ requires a long history (>1 Ga) of high U/Pb, the high $^{207}Pb/^{204}Pb$ and low $^{206}Pb/^{204}Pb$ of the Bunger Hills dyke is a feature that probably existed prior to its emplacement and may therefore have been inherited from its source.

5.4 Discussion

The long history of emplacement of isotopically-evolved and chemically-similar magmatism in the Prince Charles Mountains region (as exemplified by the Silurian Mt Bayliss dyke and Tertiary Manning Massif lavas) may be interpreted as circumstantial evidence that the isotopically-evolved mantle sources from which these magmas were derived are located within the subcontinental lithosphere. If this is the case, the contrasting geochemical and isotopic characteristics of the Fox Ridge alkali basalt and Manning Massif leucite tristanite suggest that the subcontinental lithosphere beneath the Prince Charles Mountains region is isotopically heterogeneous (either laterally or vertically) on a scale of ~10 kms.

In addition to this small scale heterogeneity, the general similarity of unusual chemical and Nd and Pb isotopic compositions of magmas from Priestley Peak, Enderby Land, Mt Bayliss and Manning Massif in Mac Robertson Land, Bunger Hills, Queen Mary Land, and Gaussberg in Wilhelm II Land (Sheraton and Cundari 1980, Collerson and McCulloch 1984, Nelson *et al.* 1986a and Chapter 3 of this thesis), extending almost 2000 km across the eastern margin of the east Antarctic shield, suggests the

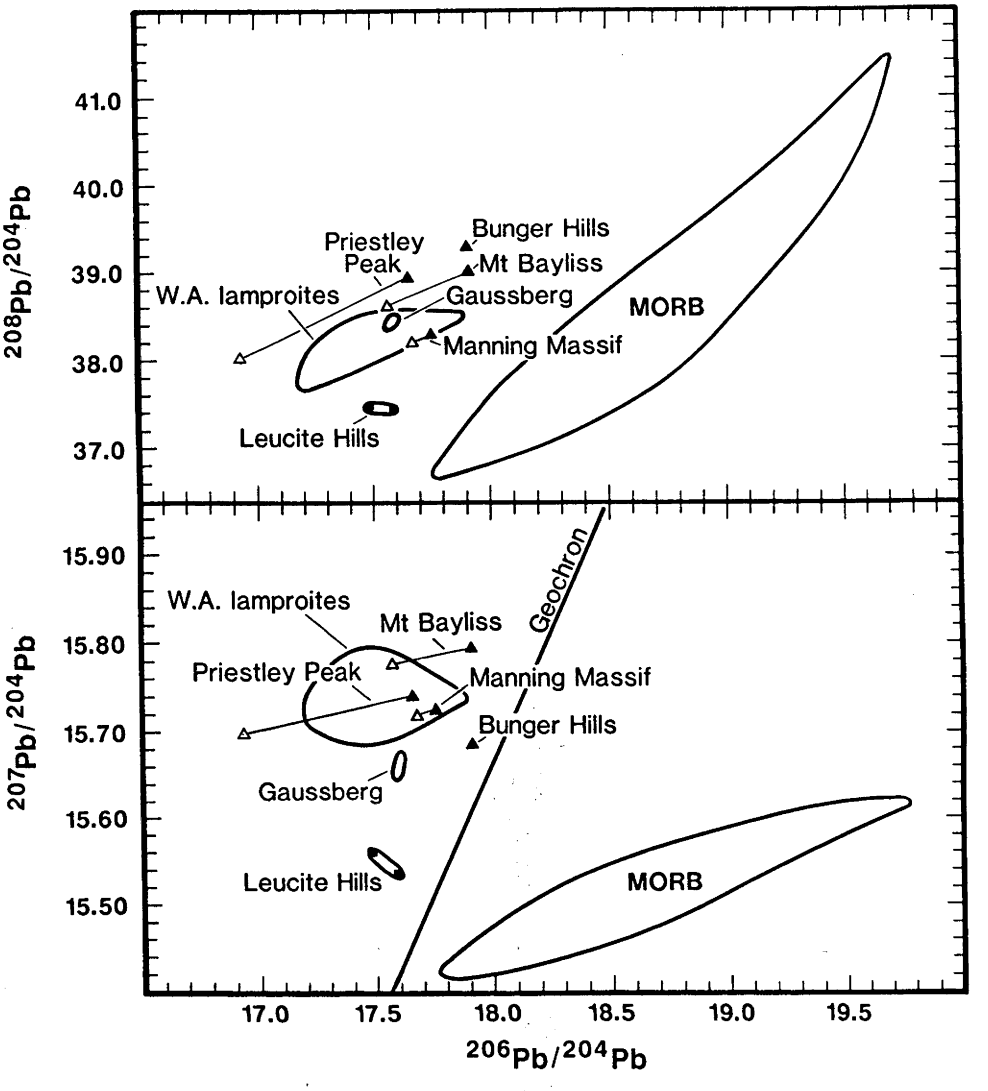

Fig. 5.4 Pb-Pb isotope compositions of Antarctic dykes (Δ = measured, ▲ = age-corrected compositions). Also shown for comparison are the fields for Western Australian lamproites, Leucite Hills high-K lavas, Gaussberg leucitites (data from Chapter 3 of this thesis) and mid-ocean ridge basalts (from Dupré and Allègre 1980, Cohen and O'Nions 1982a).

operation of large-scale mantle enrichment processes. Lamprophyre dykes in the central Transantarctic Mountains of similar age to those of the Fox Ridge and Priestley Peak intrusions have also been reported (James and Tingey 1983) but as yet little is known of their geochemistry. Furthermore, the similarity of isotopic characteristics of the Antarctic potassic mafic magmas with potassic mafic intrusions from Leucite Hills, Wyoming and of lamproites from Western Australia implies that the sources of these chemically-related and globally-distributed magmas have had similar long-term (i.e. >2 Ga) histories. In particular, the distinctive Pb isotopic compositions of all of these magmas indicate a similar history of U/Pb variation involving an earlier high U/Pb stage followed by a more recent low U/Pb stage. These chemical and isotopic similarities provide strong evidence that a common mechanism, operating over a timescale of ~1 Ga, is responsible for the generation of all of these examples of potassic magmatism.

The widespread Jurassic continental tholeiites of the Ferrar Supergroup, extending along the Transantarctic Mountains for 3000 km across the Antarctic continent, also have anomalously high initial $^{87}Sr/^{86}Sr$ (Kyle *et al.* 1983 and references therein). Although this has been attributed to crustal

contamination, Hoefs *et al.* (1980) demonstrated that a correlation exists between initial $^{87}Sr/^{86}Sr$ and $\delta^{18}O$ in the Kirkpatrick Dolerite and suggested that the high initial $^{87}Sr/^{86}Sr$ may not be entirely due to crustal contamination but may have been inherited from the source region. In addition, reconstructions of Gondwanaland prior to its break-up during the Triassic (e.g. Craddock 1975) place the eastern part of the Antarctic continent adjacent to the Jurassic-early Cretaceous Karoo tholeiitic and Cretaceous kimberlite provinces of South Africa. Geochemical and isotopic studies of South African micaceous kimberlites (e.g. Smith 1983, Fraser *et al.* 1985) and Karoo continental tholeiites (e.g. Hawkesworth *et al.* 1983) have argued that enriched mantle exists within the subcontinental lithosphere beneath the region. If garnet inclusions in South African diamonds are samples of the subcontinental lithosphere, the Sr and Nd isotopic results of Richardson *et al.* (1984) indicate that parts of the South African subcontinental lithosphere may have been enriched in the light rare-earth elements and Rb/Sr for at least ~3 Ga.

The relationship between the causes of enrichment within the subcontinental lithosphere of the Gondwanaland continents and their tectonic evolutionary history is difficult to assess. As the Pacific margin of Gondwanaland, including the western margin of the South American continent, the west Antarctic margin and the eastern margin of the Australian continent, was an active continental margin during the late Precambrian to middle Palaeozoic, it is possible that subduction processes were at least partly responsible for these enrichments. The increase in alkaline magmatism in east Antarctica from the late Proterozoic onward, for example, may relate to the commencement and operation of subduction. However, as outlined above, mafic magmatism displaying evidence of source enrichments are known from the early Proterozoic of Antarctica. The timing of Ferrar, Karoo and Tasmanian Dolerite magmatism coincides with the initial stages of rifting and the break-up of Gondwanaland.

Further discussion of the implications of the isotopic results obtained on Antarctic alkaline dykes can be found in Chapter 7 of this thesis.

6. Lamproites and kimberlites from central west Greenland.

6.1 Introduction

The Precambrian basement rocks of the Holsteinsborg region of west Greenland are intruded by numerous small dykes of kimberlitic, carbonatitic and lamproitic affinities. The kimberlites have been petrographically and geochemically compared to the micaceous kimberlite varieties of South Africa (Andrews and Emeleus 1976) and contain abundant xenoliths of olivine-rich peridotite and less commonly, garnet xenocrysts. Microdiamonds have also been recovered from four kimberlite samples (Prast 1973). In recent petrological and geochemical studies of the lamproitic intrusions, Scott (1979, 1981) demonstrated that they are highly potassic, containing up to 10 wt% K_2O, and geochemically resemble lamproites from the Kimberley region of Western Australia (Jaques *et al.* 1984a) and from Leucite Hills, Wyoming (Carmichael 1967, Kuehner *et al.* 1981). As with the continental provinces of South Africa and the West Kimberley in Western Australia, this region of west Greenland therefore provides a further example of the close spatial (if not temporal) association of kimberlitic, carbonatitic and potassic magmatism. In her earlier study, Scott (1979) suggested that the kimberlites and lamproites were genetically related, with the lamproites derived from an originally kimberlitic parent magma following extensive fractionation. However, mica Rb-Sr age-dating of some of the intrusions (Smith 1979, Scott 1981) suggested that the lamproites were emplaced about 600 Ma earlier than the kimberlites, indicating that derivation of the lamproites from a magma parental to the kimberlites is highly unlikely.

The following study was undertaken in order to isotopically characterise the kimberlites and lamproites of the region, to investigate the nature of their magma sources and to investigate possible reasons for the association of kimberlitic and potassic magmatism.

6.2 Geological Setting

The geology of the region in which the kimberlite and lamproite dykes occur has been described in earlier studies by Watterson (1974), Bak *et al.* (1975), Andrews and Emeleus (1976) and Scott (1981). The dykes are confined to the early Proterozoic Nagssugtoqidian mobile zone, which forms the northern margin of a pre-Nagssugtoqidian (Archaean) crustal block. They occur as thin sheets a few centimeters to several meters thick, often extending laterally for several kilometers, and bounded by sharp contacts. There is little evidence of post-emplacement deformation.

At least five separate episodes of alkaline dyke emplacement have been recognised in central west and southwest Greenland (Larsen *et al.* 1983). The earliest episode is represented by the Tupertalik carbonatite, which intruded the Archaean crustal block south of the Nagssugtoqidian mobile zone at ~2650 Ma. Lamprophyric dykes were emplaced during two separate episodes at ~1800 Ma and ~1200 Ma. Kimberlitic and carbonatitic dykes (including the Sarfartôq carbonatite) were intruded at ~600 Ma in the Holsteinsborg region. During the latest episode at 225 - 115 Ma, numerous kimberlite, carbonatite and lamprophyre dykes were emplaced, mostly in southwestern Greenland.

This study focusses on lamproites emplaced during the ~1200 Ma event and kimberlites dating from the ~600 Ma emplacement event.

6.3 Samples and Analytical Procedure

For this investigation, petrographically fresh hand-specimens of 5 kimberlite, 4 lamproite and one anomolous lamprophyre were analysed. These samples were selected from those examined by Scott (1979) to include both representative and geochemically anomalous compositions. Major- and trace-element analyses of these samples (from Scott 1979) are given in Table 6.1. Further details of their petrography and chemistry can be found in Scott (1979, 1981).

Sawn rock-slabs were scrubbed thoroughly with a clean plastic brush in demineralised water and repeatedly ultrasonically cleaned in a water bath to remove loose material. The cleaned rock-slabs were then coarsely crushed in a stainless steel mortar and small (~15 mg) rock chips with fresh fracture surfaces were hand-selected for isotopic analysis. For Rb-Sr and Sm-Nd analysis, about 70 to 90 mg of rock chips were totally spiked with ^{85}Rb-^{84}Sr and ^{147}Sm-^{150}Nd spikes and decomposed in teflon pressure vessels in HF-$HClO_4$ at 200 °C for at least 48 hours, the resulting solution evaporated and re-dissolved in 6 N HCl in the teflon pressure vessel at 200 °C for a further 24 hours. For U-Pb isotopic analysis, about 700 mg to 1 g of rock chips were decomposed in teflon pressure vessels as outlined above. The solution was then evaporated, re-dissolved in 1 N HCl and split into 2 unequal aliquots, the smallest of which (~1/3 of total volume) was spiked with ^{253}U-^{208}Pb spike and the largest aliquot used for Pb isotopic composition. Further details of the analytical procedure can be found in Appendix 1.

6.4 Results

6.4.1 Rb-Sr and Sm-Nd isotopic analysis

The results of Rb-Sr, Sm-Nd and U-Pb concentration analysis are tabulated in Tables 6.2 and 6.3 and presented diagrammatically in Figs. 6.1 and 6.2. The measured isotopic compositions have been age-corrected to the time of emplacement using the ages determined by Smith (1979) and Scott (1981). These kimberlite and lamproite ages were obtained by combining Rb-Sr mineral data from several separate intrusions to define the isochrons. The ages are consistent with other age determinations for kimberlites and lamproites from the region (see compilation by Larsen *et al.* 1983) although considerably younger (176 Ma) and older (1780 to 1970 Ma) emplacement ages were found for "lamprophyre" dykes from the Qaqarssuk and Sarfartôq regions (see Larsen *et al.* 1983). Because of their relatively young emplacement age and generally low Rb/Sr ratios (with the exception of sample #5508), the age-corrected $^{87}Sr/^{86}Sr$ ratios of the kimberlites are insensitive to possible error in the emplacement ages. For example, an error of ±100 Ma in the emplacement age of kimberlite sample #5508, which has the highest $^{87}Rb/^{86}Sr$ (0.449), corresponds to an error in the age-corrected $^{87}Sr/^{86}Sr$ of ±0.00064. For the lamproite having the highest $^{87}Rb/^{86}Sr$ (sample #5611), an error of ±100 Ma in the emplacement age results in a corresponding uncertainty in the initial $^{87}Sr/^{86}Sr$ of ±0.00045. In the case of the Sm-Nd data, an error of ±100 Ma in the emplacement age results in a maximum error in the age-corrected ε_{Nd} of ±1.6 ε-units for lamproite sample #5622, which has the lowest $^{147}Sm/^{144}Nd$.

There is generally good agreement between the XRF-determined Rb and Sr concentrations of Scott (1979; see Table 6.1) and those determined during this study by isotope dilution (Table 6.2), even though the isotopic results were obtained on coarse rock-chips which may not necessarily be representative of the

Table 6.1 Major- and trace- element analyses (from Scott 1979) of central west Greenland kimberlites and lamproites examined in this study.

Analysis	1.	2.	3.	4.	5.	6.	7.	8.	9.	10.
Sample	5508	5903	5907	5932	5973	5611	5622	5634	5652	5672
SiO_2	31.18	30.45	16.40	30.30	32.98	38.28	39.21	41.92	49.60	40.45
TiO_2	2.57	2.12	1.94	3.36	4.07	2.24	2.24	3.15	4.15	2.38
Al_2O_3	3.38	0.44	1.28	1.72	3.50	5.60	5.01	7.01	8.64	6.43
Fe_2O_3	3.71	3.95	3.49	4.26	5.42	2.33	1.49	2.46	2.21	2.72
FeO[a]	7.69	9.23	5.45	8.44	8.42	4.83	6.14	5.27	4.75	9.76
MnO	0.18	0.23	0.19	0.27	0.20	0.09	0.10	0.10	0.07	0.19
MgO	26.00	35.75	17.24	30.84	23.24	15.30	21.61	11.17	6.32	15.84
CaO	9.78	6.50	24.81	9.49	12.02	8.99	5.02	6.65	4.32	13.66
Na_2O	0.28	0.05	0.14	0.11	0.17	1.60	1.13	1.95	1.60	0.84
K_2O	2.84	0.29	0.99	1.40	2.27	6.27	6.25	7.54	10.03	1.14
P_2O_5	0.44	0.40	1.80	0.32	0.91	0.76	0.94	1.31	1.26	0.33
H_2O^+	3.59	2.91	3.16	3.82	3.86	3.30	3.36	2.43	1.12	3.65
CO_2	8.29	6.71	23.39	6.67	2.72	9.00	5.94	6.68	2.93	0.77
SUM	99.93	99.03	100.78	101.00	99.78	98.59	98.44	97.64	97.00	98.16
V	271	269	247	372	518	219	236	318	359	437
Cr	1357	1756	816	1840	1172	755	744	393	164	1797
Ni	770	1275	329	994	652	557	782	291	54	306
Cu	102	34	91	78	157	30	28	53	26	159
Zn	69	80	60	82	82	75	81	99	111	82
Rb	107	9	53	43	75	144	162	159	216	30
Sr	793	749	2524	744	908	1385	2549	2174	2365	409
Y	18	13	25	17	18	17	19	25	19	18
Zr	209	90	412	101	535	557	505	844	1648	142
Ba	1298	688	2210	932	766	1730	2838	3149	2590	990
La	276	443	582	238	82	221	322	351	344	42
Ce	291	604	687	313	173	284	384	441	423	103
U[a]	4.64		13.04		3.56	1.58	1.26	2.30		

[a] Uranium analyses (by isotope dilution) from this study.

1. kimberlite, Umanarssuk region.
2-4. kimberlite, Sarfartûp nunâ region.
5. kimberlite, Manitsorssuaq region.
6-7. lamproite, Sagdlerssuaq region.
8. lamproite, Kingap timerdlia region.
9. lamproite, Sagdlerssuaq region.
10. anomalous lamprophyre, Sagdlerssuaq region.

sample. Calculated initial $^{87}Sr/^{86}Sr$ values for the kimberlites display a relatively limited range of from 0.7027 to 0.7033, whereas the lamproites have considerably more radiogenic initial $^{87}Sr/^{86}Sr$ values of from 0.7045 to 0.7060. The kimberlites and lamproites have generally similar Nd and Sm concentrations, and possess Nd/Sm ratios indicating steep light-rare-earth-element enrichment. Initial ε_{Nd} values range from +1.3 to +3.9 for the kimberlites, indicating derivation from sources having a time-integrated history of light rare-earth element depletion compared to bulk earth evolution. By contrast, the lamproites possess initial ε_{Nd} values of from -10 to -13.

Compared to both the kimberlites and lamproites, the "anomalous" lamprophyre (sample #5672) has considerably lower Nd and Sm concentrations and only moderate light rare-earth element enrichment. The Nd isotopic results suggest that it is unlikely that the anomalous lamprophyre was emplaced during the

Table 6.2 Strontium and neodymium isotopic analyses of kimberlites and lamproites from central west Greenland.

	Rb	Sr	Sm	Nd	$^{87}Rb/^{86}Sr$	$^{87}Sr/^{86}Sr$[a] meas	$^{87}Sr/^{86}Sr$[a] initial	$^{147}Sm/^{144}Nd$	$^{143}Nd/^{144}Nd$[b]	$\varepsilon_{Nd}(0)$	ε_{Nd}
	-----ppm-----										
kimberlites (Age 587 ±24 myrs; Smith 1979, Scott 1981)											
Sarfartûp nunâ											
5903	11.42	682.1	16.82	135.6	0.0483	0.70342 ±3	0.70302	0.0750	0.51152 ±2	-6.2	+2.9
5907	54.91	2799	24.38	195.8	0.0566	0.70377 ±4	0.70330	0.0753	0.51150 ±2	-6.6	+2.4
5932	56.64	723.8	16.34	117.7	0.2259	0.70464 ±4	0.70275	0.0840	0.51155 ±2	-5.6	+2.9
Umanarssuk											
5508	125.1	804.9	10.28	77.74	0.4488	0.70658 ±8	0.70282	0.0799	0.51145 ±2	-7.5	+1.3
Manitsorssuaq											
5973	81.2	854.1	9.038	146.3	0.2745	0.70525 ±4	0.70295	0.0841	0.51160 ±2	-4.6	+3.9
lamproites (Age 1227 ±12 myrs; Smith 1979, Scott 1981)											
Sagdlerssuaq											
5611	153.7	1437	12.88	100.5	0.3088	0.71050 ±4	0.70507	0.0775	0.51037 ±2	-28.6	-9.9
5652	198.1	2455	15.69	132.8	0.2330	0.70860 ±8	0.70450	0.0714	0.51016 ±2	-32.7	-13.0
5622	178.5	2952	11.70	103.0	0.1746	0.70912 ±5	0.70605	0.0687	0.51023 ±2	-31.5	-11.4
Kingap timerdlia											
5634	163.9	2228	18.05	142.7	0.2124	0.70846 ±6	0.70473	0.0765	0.51035 ±2	-29.1	-10.2
anomalous lamprophyre											
Sagdlerssuaq											
5672	37.74	682.2	9.831	57.31	0.1597	0.70551 ±4		0.1037	0.51148 ±3	-7.0	

[a] Errors refer to within run precision at the $2\sigma_{mean}$ level. Uncertainty in $^{87}Rb/^{86}Sr$ is 0.5% (2σ). Sr isotope ratios normalised using $^{86}Sr/^{88}Sr = 0.1194$. NBS-987 standard value is 0.71022 ±4. E & A standard carbonate value is 0.70800 ±3.

[b] Error in $^{147}Sm/^{144}Nd$ is 0.1% (2σ). Nd isotopic ratios normalised using $^{146}Nd/^{142}Nd = 0.636151$. The value obtained for BCR-1 standard is 0.511833 ±20. $\varepsilon_{Nd} = (^{143}Nd/^{144}Nd_{meas}/ ^{143}Nd/^{144}Nd_{CHUR} -1) \times 10^4$ where $^{143}Nd/^{144}Nd_{CHUR} = 0.511836$.

same episode as the lamproites (i.e. ~1227 Ma ago), as this age requires that the intrusion possess an initial ε_{Nd} of +7.7, an unreasonably high value for mantle-derived magmas at this time. By this reasoning, it is unlikely that the anomalous lamprophyre is older than ~1000 Ma. An emplacement age contemporaneous with that of the Holsteinsborg kimberlites (i.e. ~590 Ma) corresponds to a more reasonable initial ε_{Nd} of -0.05. At this emplacement age, the initial $^{87}Sr/^{86}Sr$ of the lamprophyre is 0.7042, whereas at 1227 Ma the initial $^{87}Sr/^{86}Sr$ is 0.7027. Assuming a Mesozoic emplacement age, the initial $^{87}Sr/^{86}Sr$ of the anomalous lamprophyre would lie within the range of values of from 0.7029 to 0.7058 determined by Hansen (1981) for Mesozoic lamprophyres from southern west Greenland.

6.4.2 U-Pb isotopic analysis

U-Pb isotopic results obtained for 3 lamproite samples are given in Table 6.3 and plotted along with the locus of the Pb mantle growth curve (i.e. with $\mu \approx 8$, based on a single-stage evolution of the least radiogenic Pb isotopic compositions of mid-ocean ridge basalts) in Fig. 6.2. The lamproites possess generally high Pb concentrations and low U/Pb ratios, and the age corrections to the measured

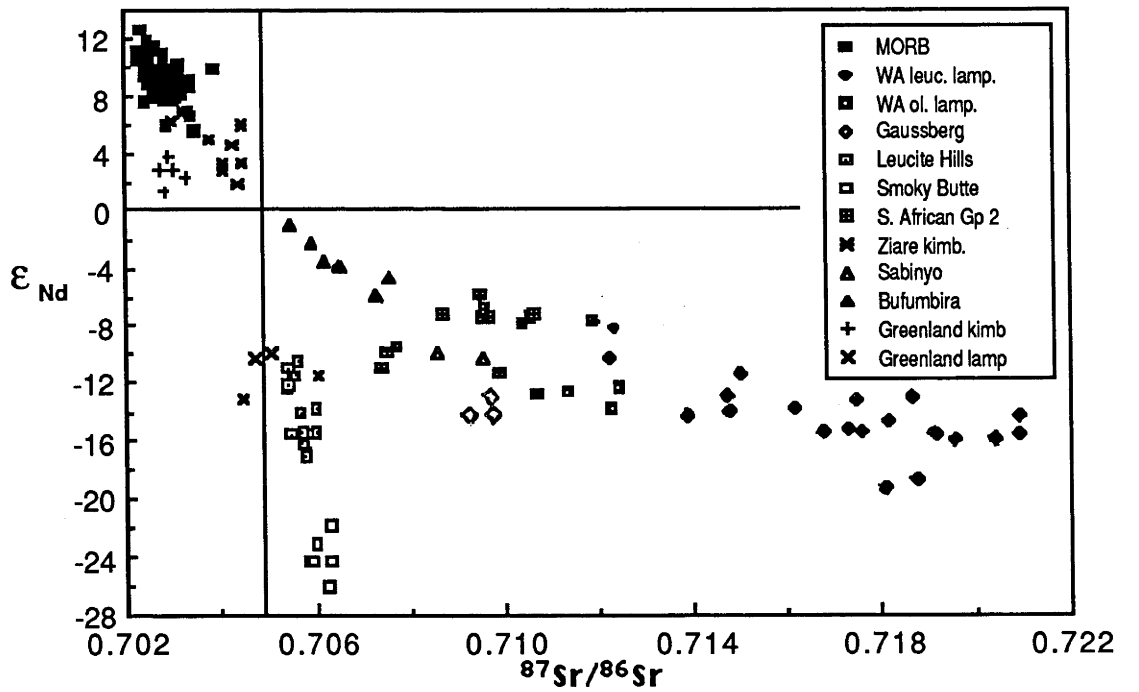

Fig. 6.1 Initial Sr-Nd isotope diagram showing the fields for kimberlites and lamproites from central west Greenland, compared to fields of mid-ocean ridge basalts and other examples of anorogenic potassic magmas. Data sources as in Fig. 3.3.

$^{207}Pb/^{204}Pb$ ratios for ^{235}U decay since their emplacement ~1227 Ma ago are relatively small (i.e. < ~0.09). However, corrections to the measured $^{206}Pb/^{204}Pb$ ratios are substantial (i.e. < ~1.1) and the initial Pb isotopic compositions of the lamproites must therefore be interpreted with some caution. Despite the uncertainty the age correction introduces, both the measured and age-corrected Pb isotopic compositions of the lamproites are considerably less radiogenic than the model mantle reservoir at the time of their emplacement (see Fig. 6.2). As their measured (uncorrected) Pb isotopic compositions are also less radiogenic than the mantle reservoir at 1227 Ma, it is probable that the lamproites would still

Table 6.3 Uranium and lead isotopic data for lamproites from central west Greenland.

Sample		U[a]	Pb	$^{238}U/^{204}Pb$	$^{206}Pb/^{204}Pb$[b]		$^{207}Pb/^{204}Pb$		$^{208}Pb/^{204}Pb$	
		---ppm---			meas	initial[c]	meas	initial[c]	meas	initial[c]
5611	Sagdlerssuaq	1.58	20.34	5.18	15.315	(14.23)	15.044	(14.96)	35.904	(34.60)
5622	Sagdlerssuaq	1.26	25.31	3.34	15.117	(14.42)	15.122	(15.06)	36.464	(35.62)
5634	Kingap tim.	2.30	47.44	3.23	15.313	(14.64)	15.014	(14.96)	35.843	(35.03)

[a] U and Pb concentrations determined by isotope dilution mass spectrometry.

[b] Data obtained on the RSES Finnigan-MAT multi-collector mass spectrometer. Ratios have been corrected for mass fractionation using 0.11 %/m.u. based on multiple analyses of the NBS-981 common Pb standard. The analytical uncertainty is <0.1% (1σ).

[c] Corrected for ^{238}U and ^{232}Th decay since emplacement, using an age of 1227 Ma. Age corrections to $^{208}Pb/^{204}Pb$ are made assuming Th/U = 4.

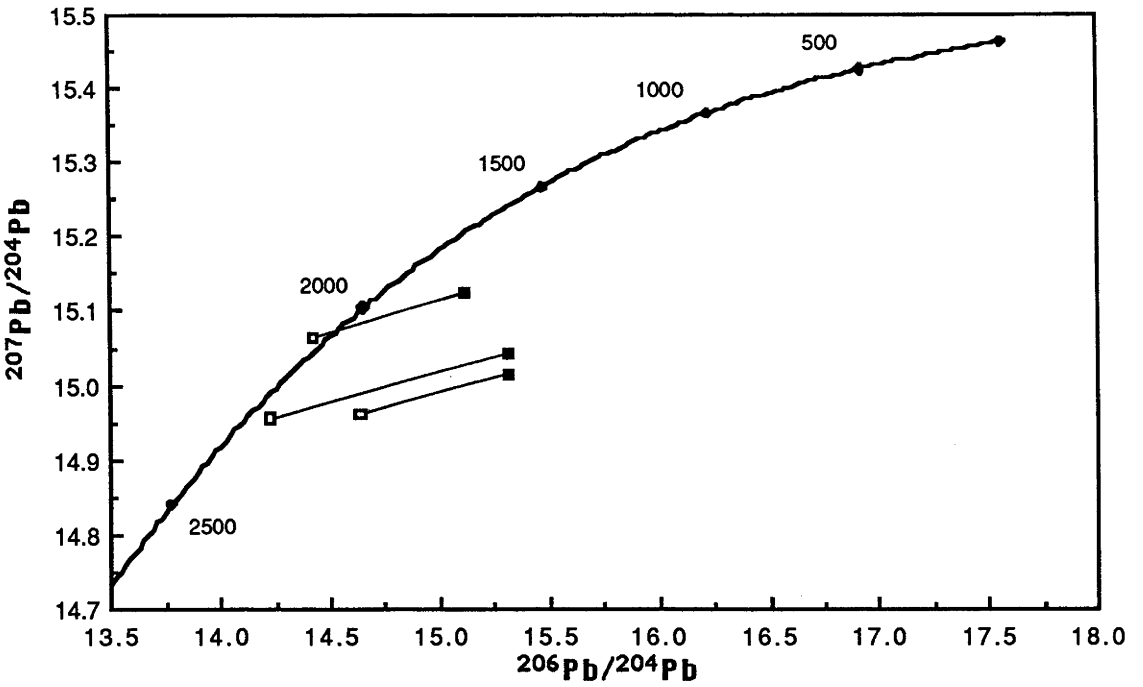

Fig. 6.2 Measured (■) and age-corrected (□) Pb-Pb isotope compositions for lamproites from central west Greenland. Also shown for comparison is the mantle model growth curve (with $\mu = 8.0$). Both measured and age-corrected Pb isotopic compositions are considerably less radiogenic than anticipated mantle values (given by the $\mu = 8$ curve) at the time of emplacement of the lamproites.

have possessed unradiogenic initial Pb isotopic compositions even if they had been effected by post-emplacement alteration of the U/Pb ratio by mobility of uranium.

6.5 Discussion

The isotopic results indicate that the kimberlites of central western Greenland were derived from time-integrated light rare-earth depleted mantle sources, similar to that from which the South African Group 1 (so-called "basaltic") kimberlites were derived (Smith 1983). Compared to the kimberlites, the Greenland lamproites possess considerably more radiogenic initial $^{87}Sr/^{86}Sr$ and unradiogenic initial $^{143}Nd/^{144}Nd$. Although these isotopic features may have been acquired by crustal interaction, the lamproites are characterised by high concentrations of Sr (1437 to 2952 ppm) and Nd (100 to 143 ppm), requiring the assimilation of substantial amounts of crustal material to modify their Sr and Nd isotopic compositions. For example, assuming contamination by bulk assimilation processess of typical continental crustal material possessing 50 ppm Nd and ε_{Nd} of -25, a mantle-derived magma with 100 ppm Nd and ε_{Nd} of +5 would need to assimulate 2 times its original mass of crustal material to acquire an ε_{Nd} of -10. However, the lamproites possess high Mg-numbers (atomic Mg/[Mg + total Fe] values are generally greater than 0.85) and transition-element concentrations (>290 ppm Ni and >390 ppm Cr, except for #5652 which has considerably lower Ni and Cr contents; see Table 6.1) combined with low SiO_2 (<42 wt%, except for #5652 which has ~50 wt%) Al_2O_3 (<8.6 wt%) and Na_2O (<2 wt%) contents. These features are not consistent with the assimilation of such substantial amounts of crustal material. The lamproites were therefore probably derived from so-called enriched mantle sources, as has been argued for anorogenic lamproitic rocks from other localities (see Chapter 3 of this thesis). The isotopic results clearly do not support a direct genetic connection between the lamproites and kimberlites of central

western Greenland.

In Fig. 6.1, the initial Sr and Nd isotopic results obtained for the central west Greenland kimberlites and lamproites are compared to data from other localities. A notable feature is the similarity of the Sr and Nd isotopic results for the central western Greenland kimberlites with those of Group 1 kimberlites from South Africa, whereas the Greenland lamproites bear some isotopic resemblance to the Group 2 (micaceous) kimberlites and to Leucite Hills madupites. This isotopic bi-modality appears to be a common feature of anorogenic alkaline magmatism (i.e. that occuring within old, stabilised crustal blocks). For example, in addition to central west Greenland and South Africa, such isotopic bi-modality is also found in the Kimberley Block of Western Australia, where it is represented by the Cummin Range carbonatite and the Western Australian lamproites, and the Arunta Block of central Australia, where it is represented by the Mudtank carbonatite and the Mordor Complex.

Assuming that Pb evolution within the Earth's mantle can be approximated by a single-stage history with $\mu \approx 8$, the unradiogenic Pb isotopic compositions of the lamproites indicates that their sources must have evolved in isolation in a low-μ environment following extraction from the mantle reservoir. Although the Pb isotopic compositions of the lamproites plot near the $\mu = 8$ growth curve and their $^{207}Pb/^{204}Pb$ ratios were comparable to that of the Earth's mantle at the time of their emplacement, their $^{206}Pb/^{204}Pb$ ratios were considerably less radiogenic than that of contemporaneous Pb within the Earth's mantle (Fig. 6.2). Their Pb isotopic compositions therefore require a history of μ variation involving a period of high μ, to elevate their $^{207}Pb/^{204}Pb$ ratios, followed by a period of low μ during which evolution of both $^{206}Pb/^{204}Pb$ and $^{207}Pb/^{204}Pb$ ratios was retarded. This evolutionary history is similar to that indicated by the Pb isotopic compositions of other examples of anorogenic potassic magmatism, such as the Western Australian lamproites and lamproites from Smoky Butte, Montana.

The implications of the isotopic results obtained on central west Greenland lamproites for the petrogenesis of potassic igneous rocks are discussed in Chapter 7. Further discussion of the isotopic characteristics of kimberlites and implications for kimberlite petrogenesis can be found in Section B of this thesis.

7. SYNTHESIS- Petrogenesis of potassic magmas as inferred from geochemical and isotopic evidence

7.1 Introduction

Despite a long history of investigation (see Gupta and Yagi 1980, for a review), the petrogenesis of the ultrapotassic suite has remained enigmatic. A number of recent isotopic studies (for example, McCulloch *et al.* 1983, Collerson and McCulloch 1983, Vollmer and Norry 1983a, Vollmer *et al.* 1984, Fraser *et al.* 1985, Nelson *et al.* 1986a, b, and this thesis) have found that, in contrast to other mantle-derived magmas, many examples of potassic magmatism possess highly radiogenic Sr and unradiogenic Nd isotopic compositions (see Figs. 2.4 and 3.3). Although these isotope characteristics may have been acquired by extensive assimilation of continental crust, these studies have generally argued against the operation of crustal contamination processes in favour of an "enriched mantle" origin. The high Mg-numbers and Ni and Cr contents of these magmas and the presence of mantle xenoliths (and in one case, diamonds) are cited in support of this. Furthermore, the extremely high contents of most trace elements (including Sr and the rare-earth elements) of these magmas make them insensitive to bulk contamination processes, requiring the assimilation of substantial amounts of crustal material to modify their Sr and Nd isotopic characteristics. As geochemical and isotope correlations indicative of mixing are evident in many potassic suites (for example, in the Italian, Spanish and Western Australian examples), most recently advanced petrogenetic models (e.g. McCulloch *et al.* 1983, Jaques *et al.* 1984a, Vollmer *et al.* 1984) invoke partial melting of a lherzolitic or harzburgitic mantle source which has been variably contaminated by an incompatible-element-rich "metasomatic" component. However, the question of the ultimate sources of these "metasomatic" components, which presumably confer the enriched mantle isotopic character to the sources of potassic magmas, is rarely addressed and remains problematic.

In this chapter, a model is proposed in which the mantle sources of at least some examples of both orogenic and anorogenic potassic magmas have been contaminated by crustal components. In the case of orogenic potassic suites, it will be argued that their geochemical and Sr, Nd and Pb isotopic characteristics are consistent with contamination of their mantle sources by components derived from recently-subducted sediments. For potassic suites located within anorogenic tectonic settings, it will be argued here that the crustal contaminants involved were also derived from subducted marine sediments, but that in these cases the "enriched mantle" sources from which anorogenic potassic magmas are derived have been stored for long time periods within the subcontinental lithosphere. These interpretations reconcile the mantle characteristics of many examples of potassic magmatism (for example, their high Mg-numbers and transition-element concentrations) with apparent crustal features such as their incompatible-element patterns and Sr, Nd and Pb isotope characteristics. Furthermore, the complex multistage U/Pb fractionation histories indicated by the unusual Pb isotopic compositions of anorogenic potassic magmas are not readily explained by models advocating their generation entirely within the upper mantle or subcontinental lithosphere, but are consistent with this interpretation.

Discussion of the Ca isotopic results and their implications for the petrogenesis of ultrapotassic rocks can be found in Chapter 9 of this thesis.

7.2 Can sediments be subducted?

The relative importance of mantle recycling, via subduction, of continent-derived sedimentary material has been a contentious issue in the long-standing debate about the rate of differentiation of the continental crust throughout geological time. A number of authors (e.g. Moorbath 1978, O'Nions *et al.* 1979, Jacobsen and Wasserburg 1979, Allègre and Jaupart 1985) have argued that the mass of the continents has grown steadily throughout the Earth's history by the progressive and irreversible addition of new mantle-derived material to the continental crust. Proponents of this view stress the difficulties associated with the destruction, by subduction into the mantle, of continental crust or sediments, due to their buoyancy and low melting temperatures, and regard the mantle-like initial isotopic compositions of some Archaean and Proterozoic granite terrains as evidence of crustal growth during rapid (100 to 300 Ma duration) "accretion/differentiation super-events" (Moorbath 1975, 1978). However, this view has been strongly contested by Armstrong (1968, 1981) and others who advocate the continuous recycling into the mantle since the early Archaean of continental material at a steadily decreasing rate. In this model, magmatic addition of new material from the mantle to the crust is balanced by the destruction of a small proportion of continental mass by the subduction and mixing of sediments into the mantle.

In an attempt to resolve this controversy, one approach has been the use of the sedimentary mass flux of modern subduction zones as a means of estimating the mass of missing sedimentary material which may have been subducted into the mantle. Using present-day observed sediment thicknesses and subduction rates, these studies (e.g. Hussong and Uyeda 1981, Karig and Kay 1981, Kay 1984, Hole *et al.* 1984) indicate that the total input of pelagic sediment entering some trenches, such as the Mariana trench, is far greater than the estimated sediment contribution to the total arc volcanic and plutonic output. The generally higher concentrations of ^{10}Be in island-arc lavas (Brown *et al.* 1982) provide evidence of some contribution of subducted sediment to island-arc magmatism, although Sr and Pb isotope (Meijer 1976, Cohen and O'Nions 1982b) and trace-element studies (Morris and Hart 1980, Kay 1980, McLennan and Taylor 1981, McCulloch and Perfit 1981, Kay *et al.* 1981, Karig and Kay 1981, Kay 1984, Hole *et al.* 1984) suggest that the overall contribution of subducted sedimentary material to island-arc magmatism is generally small, accounting for probably less than a few percent of the total mass of island-arc magmatism. A further consideration is the extent of re-working of sediments within the ocean basins by turbidity currents, which may transport sedimentary mass away from trenches. However, a significant proportion of continent-derived sedimentary material is probably entering the trenches of at least some modern subduction zones and is either being "subcreted" beneath the fore-arc region (Karig and Kay 1981) or recycled into the deeper mantle (Hole *et al.* 1984).

The difficulties involved in the subduction of sediments, because of their low densities and melting temperatures, requires that either they are physically trapped within cooler parts of the subducting slab (for example, within grabens) or that they are carried down by convection of the mantle directly overlying and perhaps frozen onto the slab. While these difficulties suggest that sedimentary material which may be carried down with the slab will eventually enter the overlying mantle, the absence of a pronounced sedimentary signature in many island-arc volcanics so far examined implies that, for a substantial proportion of subducted sediment, this may occur at depths greater than the depth of generation of island-arc volcanism.

7.3 Sediment subduction and orogenic potassic magmatism

Available geochemical studies (e.g. Nicholls and Whitford 1978, Foden and Varne 1980) of the few known occurrences of potassic lavas from presently active subduction zones, such as the leucite-normative lavas from the Sunda arc, Indonesia, indicate that apart from their high K_2O content and K_2O/Na_2O, they possess many features in common with more typical island-arc magmatism. Whitford (1978), Whitford *et al.* (1978) and Varne (1985) demonstrated that K_2O contents of east Sunda arc volcanics correlated positively with $^{87}Sr/^{86}Sr$ and negatively with $^{143}Nd/^{144}Nd$, consistent with mixing between two components, one isotopically "enriched" and also rich in K_2O. Based on geochemical and Sr and Nd isotopic similarities between the Kimberley lamproites and orogenic lavas of the Sunda and Banda arcs to the north of the Kimberley craton, Varne (1985) proposed that arc volcanoes which have erupted K-rich lavas were tapping subcontinental mantle similar to that from which the Kimberley lamproites were derived. However, differences between the Pb isotopic compositions of the arc rocks (White *et al.* 1983) and the lamproites (Fraser *et al.* 1985, Nelson *et al.* 1986a and this thesis) are not consistent with the direct involvement of the Kimberley lamproite source in the generation of the arc lavas. An alternative explanation, advanced by Whitford *et al.* (1978), Whitford *et al.* (1981) and White *et al.* (1983) and which is consistent with the Pb isotopic results obtained by White *et al.* (1983), is that recently subducted sediments were involved in the genesis of the Sunda arc lavas. A similar explanation was proposed by Whitford and Jezek (1982) to account for the generally similar geochemical and isotopic characteristics of high-K calc-alkaline lavas from the Banda arc. It will be argued here that the geochemical and isotopic similarities of the Western Australian lamproites and the high-K arc lavas noted by Varne (1985) *do* provide support for the derivation of these magmas by a common petrogenetic process, with the Pb isotopic differences due to the involvement of comparatively younger, recently subducted sediments in the case of the arc lavas and, in the case of the lamproites, to the involvement of ancient subducted sedimentary components which have been stored for long periods within the subcontinental lithosphere of the Kimberley craton.

A number of other recent studies (e.g. Thompson 1977, Edgar 1980, Civetta *et al.* 1981, Venturelli *et al.* 1984, Peccerillo *et al.* 1984, Peccerillo 1985, Rogers *et al.* 1985, Nelson *et al.* 1986a) have also argued, on the basis of geochemical similarities with modern arc lavas, for the involvement of subduction processes in the genesis of other examples of "orogenic" potassic volcanism, such as those of Italy and southeastern Spain. Trace-element characteristics of the Spanish lavas, such as their high Ba concentrations, low K/Rb, high Ba/La and rare-earth element patterns with negative Eu anomalies (Venturelli *et al.* 1984, Nixon *et al.* 1984) are also consistent with contamination of their mantle sources by a component resembling modern sediments. Isotopic analysis (see Chapter 2) indicates that the Spanish lavas possess Sr, Nd and Pb isotope ratios similar to those of modern sediments and, although possibly complicated by extensive high-level crustal contamination in the more differentiated magmas (e.g. Turi and Taylor 1976), the involvement of a similar crustal component can also account for the isotopic and trace-element features of the Italian potassic suite.

There are significant geochemical and isotopic differences between potassic magmas occurring within active (or "orogenic") tectonic settings and those from tectonically stable ("anorogenic") continental settings. As with most arc lavas, K-rich magmas found within active subduction zones commonly have low TiO_2, Ta, Nb and Zr contents, and although they may be characterised by generally more extreme (i.e.

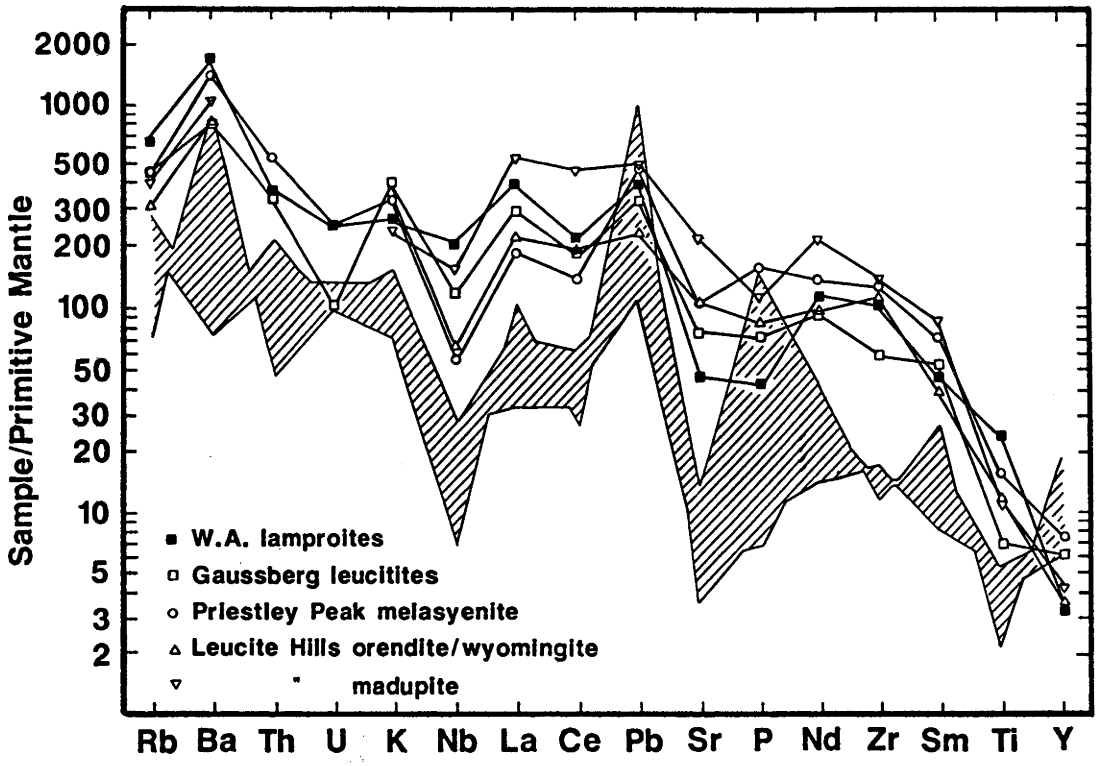

Fig. 7.1 Trace-element abundances (in order of increasing compatibility in garnet peridotite) normalised to the abundances estimated for primitive mantle (from McDonough *et al.* 1985 and Nelson *et al.* 1986a) of potassic magmas from Western Australia (McCulloch *et al.* 1983; Jaques *et al.* 1984a; Nixon *et al.* 1984; Nelson *et al.* 1986a), Antarctica (Sheraton and England 1980; Sheraton and Cundari 1980; Sheraton 1983; Collerson and McCulloch 1983) and Leucite Hills (Kuehner *et al.* 1981; Vollmer *et al.* 1984). Th and U abundances for Leucite Hills examples not available. The field of normalised trace-elements (hatched) for 4 sediments (3 slates and 1 pelagic mud composite) from Thompson *et al.* (1984) also shown for comparison.

more radiogenic $^{87}Sr/^{86}Sr$ and unradiogenic $^{143}Nd/^{144}Nd$) isotopic character, they are nevertheless demonstrably geochemically and isotopically related to the arc lavas with which they occur. Although potassic magmas from anorogenic tectonic environments possess generally similar radiogenic $^{87}Sr/^{86}Sr$ and unradiogenic $^{143}Nd/^{144}Nd$ compositions by comparison with orogenic high-K lavas, the findings of this study (Chapter 3) indicate that they commonly possess unusual Pb isotopic compositions, with highly unradiogenic $^{206}Pb/^{204}Pb$, which are unique to potassic magmas from anorogenic settings. The remaining discussion in this chapter focusses principally on the interpretation of these unusual geochemical and isotopic characteristics.

7.4 Chemical and isotopic characteristics of anorogenic potassic magmatism

Averaged element abundance patterns for potassic magmas from 4 separate localities, normalised to estimated primitive mantle abundances (from McDonough *et al.* 1985 and Nelson *et al.* 1986a), are shown in Fig. 7.1. Diamond-bearing lamproites from Western Australia, leucitites from Gaussberg, high-K alkaline dykes from MacRobertson Land, Enderby Land and Queen Mary Land regions of east Antarctica and madupites, wyomingites and orendites from Leucite Hills, Wyoming, have remarkably similar geochemical characteristics. All are characterised by high Mg-numbers (each locality averaging Mg/(Mg+total Fe) > 0.65 with the exception of Manning Massif, Mt Bayliss and Bunger Hills samples,

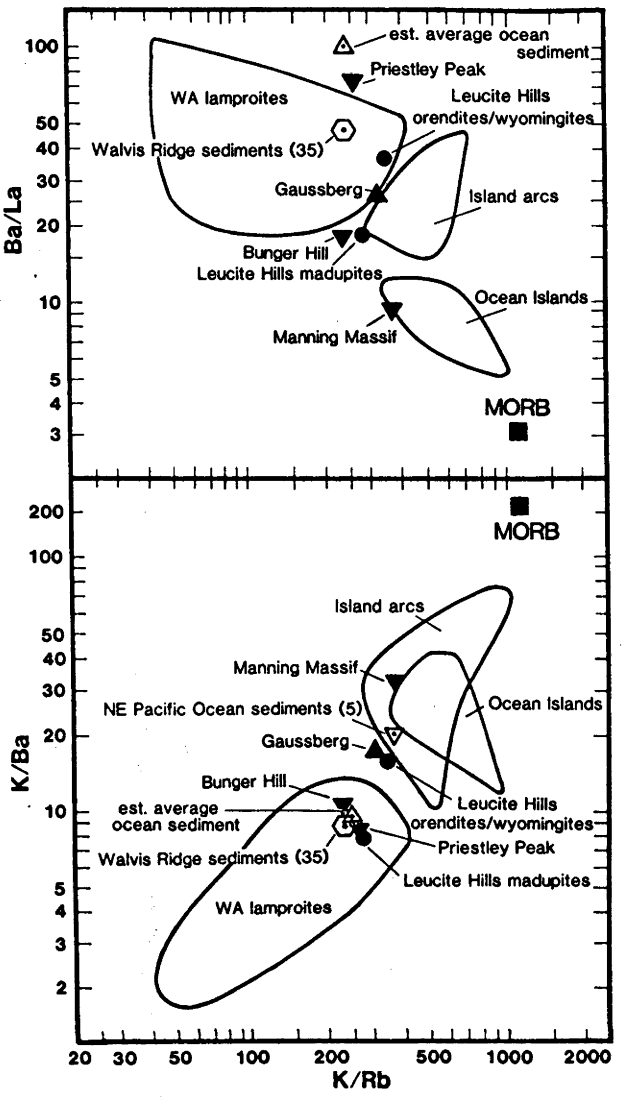

Fig. 7.2 Incompatible-element ratios K/Ba, Ba/La and K/Rb for a variety of rock-types. Modern oceanic sediments and many examples of potassic magmatism have generally low K/Rb, variable but low K/Ba and high Ba/La compared to mid-ocean ridge basalts. Ocean-island and island-arc basalts have intermediate values. Data sources; Jakes and White (1972), Church (1973), Erlank and Kable (1976), White and Bryan (1977), Kay (1980), Sheraton and Cundari (1980), Morris and Hart (1983), Jaques *et al.* (1984a), Liu and Schmitt (1984), Venturelli *et al.* (1984).

which have Mg-numbers of 0.58, 0.58 and 0.50 respectively) and high Ni and Cr contents, as well as high to extreme abundances of K_2O, TiO_2, P_2O_5, SO_2, H_2O, F, Cl, Ba, LREE, high K_2O/Na_2O and Fe^{3+}/Fe^{2+}, and relatively low abundances of Al_2O_3, CaO and Na_2O. The ratios of highly incompatible elements of these magmas more closely resemble those of subduction-related magmas and pelagic sediments than those of other mantle-derived rocks. The arc-like Ba/La and Ba/Nb ratios of some examples of high-K magmas have been previously noted by Thompson *et al.* (1984) and Varne (1985). For example, the Western Australian lamproites possess high Th/U (averaging 5.8) and Ba/La ratios (36.6) and low K/Rb (146) and K/Ba ratios (6.07, average of 20 analyses by Jaques *et al.* 1984a, see Fig. 7.2). Although these ratios may be effected by extensive fractionation of some mineral phases, such as leucite and phlogopite, there is no correlation between Ba/La and K/Ba ratios and differentiation parameters such as wt% MgO (see Fig. 7.3). Th/U and K/Rb ratios are respectively positively and negatively correlated with wt% MgO (i.e. olivine lamproites have generally higher Th/U and lower K/Rb ratios than leucite lamproites) indicating

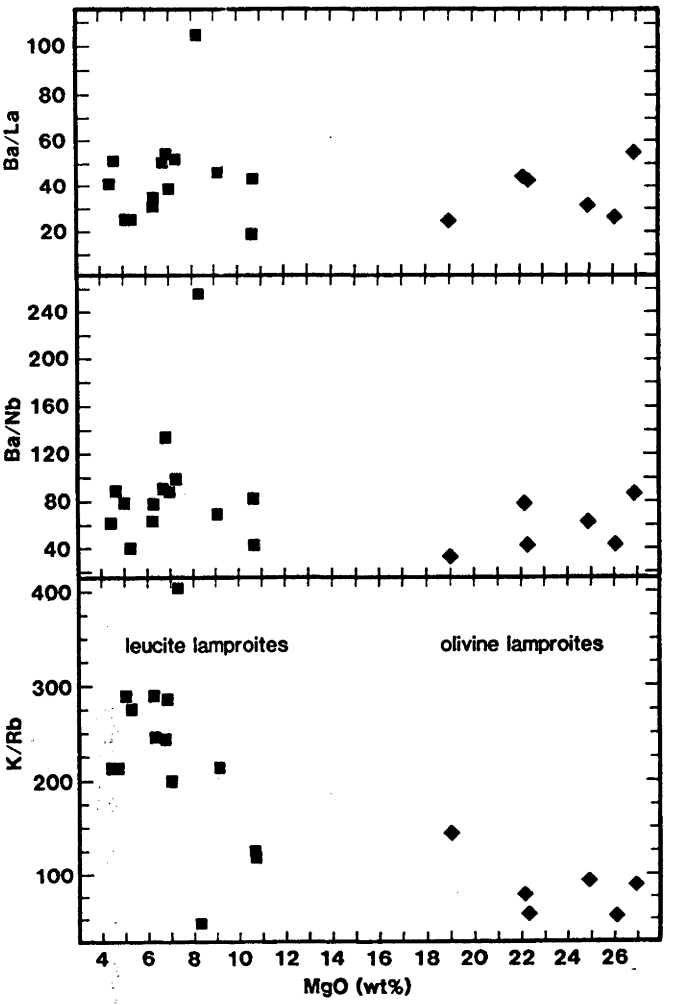

Fig. 7.3 Incompatible-element ratios Ba/La, Ba/Nb and K/Ba versus wt% MgO for the Western Australian lamproites. A weak negative correlation exists between K/Rb and wt% MgO, suggesting that differentiation processes have increased the K/Rb ratio. There is no correlation between Ba/La and Ba/Nb and wt% MgO. Data from Jaques *et al.* (1984a)

that although these ratios may have been influenced by differentiation processes, the high Th/U and low K/Rb are not due to crystal fractionation. The Western Australian lamproite values compare with ranges for pelagic sediments of 4.7 to 7.5 for Th/U (Elderfield *et al.* 1981, Thomson *et al.* 1984, White *et al.* 1985; considerably lower Th/U values, <0.1, may be typical of metalliferous sediments such as those examined by Veeh 1981), 7.2 to 47 for Ba/La (White *et al.* 1985, and average of 35 Walvis Ridge sediments analysed by Liu and Schmitt 1984), 240 for K/Rb (estimated by Kay 1980, and average value for 35 Walvis Ridge sediments from Liu and Schmitt 1984) and 8.6 to 9.9 for K/Ba (Kay 1980, Liu and Schmitt 1984). By contrast, ocean-island alkali basalts typically possess Th/U between 3.7 and 4.3 (compilation by Galer and O'Nions 1985), Ba/La of 5 to 13, K/Rb of 370 to 900 and K/Ba between 12 and 40 (from compilation by Morris and Hart 1983).

The isotopic characteristics of all anorogenic potassic suites so far examined indicate generally similar long-term histories of U/Pb and Sm/Nd (see, for example, Chapters 3, 5 and 6, and Figs. 3.3 and 3.4), although a considerable range in $^{87}Sr/^{86}Sr$ is evident. In particular, the Pb isotope compositions of these examples of potassic magmatism indicate a history of U/Pb variation involving at least two stages; an earlier high U/Pb stage is required to generate the high $^{207}Pb/^{204}Pb$ while there is still sufficient of the

parent ^{235}U, followed by a low U/Pb stage to retard the increase in $^{206}Pb/^{204}Pb$ by the decay of the parent ^{238}U. Long histories are required to generate these unusual Pb isotopic compositions. For example, modelling of the Pb isotopic compositions of the Western Australian lamproites (see Chapter 3 of this thesis) indicates that their Pb cannot have differentiated from the mantle later than ~2.1 Ga ago, and is probably much older. The Pb isotope ratios of these potassic magmas are unlike those of modern marine sediments, due to the histories of more recent low U/Pb. Because of the similar chemical behavior of uranium and lead during igneous processes, the dramatic fractionation events lowering the U/Pb ratios in the sources of these potassic magmas are considered unlikely to have been the result of magmatic fractionation/differentiation processes. However, an effective means of fractionating uranium from lead is by either weathering, sedimentation or hydrothermal processes at the Earth's surface, due to the greater insolubility of U^{4+} in aqueous systems under reducing conditions.

To investigate the possible involvement of sediments in the generation of potassic magmatism in more detail, further discussion of some aspects of the geochemical and isotopic properties of marine sediments is warranted.

7.5 The chemistry of marine sediments

The isotopic characteristics of modern marine sediments vary with provenance, with most of the observed variation attributable to mixing in varying proportions of material derived from the upper continental crust (a continental detrital component) with that derived from the mantle (consisting of a hydrothermal component principally derived from oceanic spreading centers and a terrigenous component derived from young arcs). The proportion of each component derived from these sources varies depending on the element, with a large proportion of the Sr and most of the Nd found in oceanic sediments and manganese nodules derived from continental sources (Dasch *et al.* 1971, Addy 1979, Elderfield *et al.* 1981, Goldstein and O'Nions 1981). Most studies of oceanic sedimentary Pb have found relatively uniform Pb isotopic compositions with high $^{207}Pb/^{204}Pb$ and moderate $^{206}Pb/^{204}Pb$ (Chow and Patterson 1962, Dasch *et al.* 1971, Reynolds and Dasch 1971, Church 1973, Meijer 1976, Unruh and Tatsumoto 1976, Sun 1980, White *et al.* 1985) consistent with a predominantly upper continental derivation, although a study of metalliferous sediments from the Nazca plate (Dasch 1981) found Pb isotopic compositions resembling those of mid-ocean ridge basalts, indicating that sediments located near oceanic spreading centers may contain a considerable proportion of mantle-derived Pb (see Fig. 7.4). The similar $^{206}Pb/^{204}Pb$ ratio of the MORB and continent-derived components results in relatively limited variation in the observed $^{206}Pb/^{204}Pb$ ratio of modern sediments, whereas considerable variation is observed in $^{207}Pb/^{204}Pb$ due to the much higher $^{207}Pb/^{204}Pb$ of continental detritus relative to MORB.

If time-scales of mantle recycling of $\sim 10^8$-10^9 years apply, possible differences in the geochemistry of Archaean and Proterozoic sediments compared to their modern counterparts and the effects of radiogenic decay during storage in the mantle must also be considered. As there are no modern equivalents to the extensive banded iron formations and chert sediments of the Archaean and early Proterozoic, sedimentation processes operating during the Archaean may have differed from those operating today. Geochemical (e.g. Taylor and McLennan 1981, McLennan 1982, McLennan and Taylor 1983, McLennan *et al.* 1984) and Nd isotopic studies (e.g. McCulloch and Wasserburg 1978, Hamilton *et al.* 1983, Miller and O'Nions 1985)

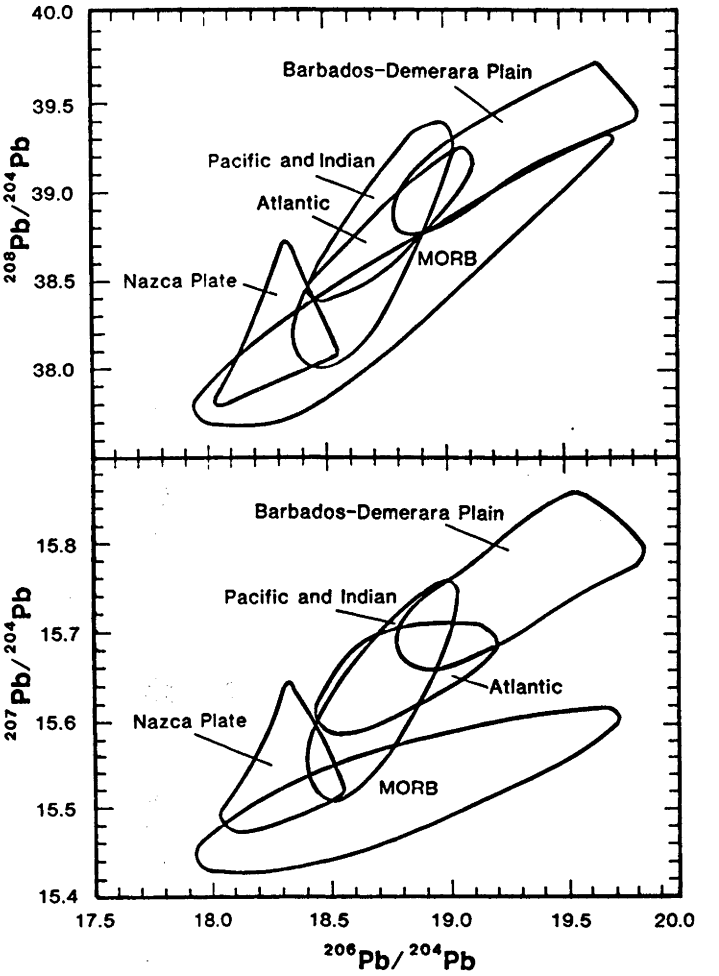

Fig. 7.4 Pb-Pb isotope ratios of modern marine sediments compared to those of mid-ocean ridge basalts. Data sources; Sediments- Chow and Patterson (1962), Reynolds and Dash (1971), Church (1973), Meijer (1976), Unruh and Tatsumoto (1976), Sun (1980), Dash (1981), White *et al.* (1985). Mid-ocean ridge basalts- Dupré and Allègre (1980), Cohen and O'Nions (1982a).

suggest that Archaean clastic and chemical sediments were typically less LREE-enriched and isotopically less-evolved than modern sediments. These features are believed to reflect the more mafic character of the Archaean continental crust from which the sediments were derived. Sr isotopic studies of chemical sediments (e.g. Veizer and Compston 1976) have found that many Archaean carbonates have $^{87}Sr/^{86}Sr$ values similar to that of the contemporaneous mantle, with a significant increase in $^{87}Sr/^{86}Sr$ occurring toward the end of the Archaean. The low $^{87}Sr/^{86}Sr$ of many Archaean carbonates was attributed by Veizer *et al.* (1982) to extensive interaction of Archaean seawater and ocean-floor basalts, possibly as a consequence of a higher Archaean geothermal gradient. It is likely that the Pb isotopic compositions of Archaean marine sediments were also influenced to some extent by this process. Continental crust was already well-differentiated by the late Archaean, however, and provided a source of radiogenic Sr and Pb to the marine environment. Oceanic sediments during the geologic past therefore probably possessed Pb isotopic compositions which varied with provenance from contemporaneous mantle to upper crustal values. The Sm/Nd ratio of modern oceanic pelagic sediments are generally similar to those estimated for the upper continental crust, implying that this ratio is not substantially fractionated by erosion and sedimentation processes. The Rb/Sr ratio is dependent on the clay/carbonate content and is more variable. However, the available data (Chow and Patterson 1962, Church 1973, Calvert 1976, Chester and Ashton 1976, Unruh

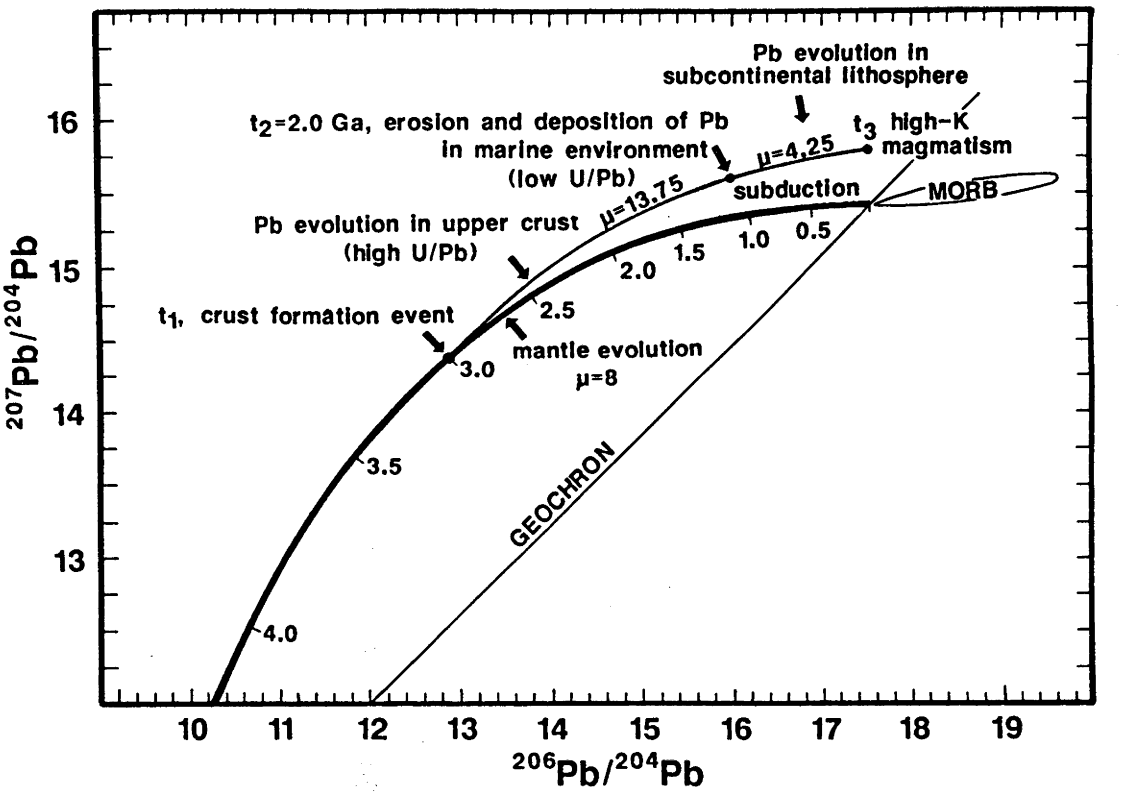

Fig. 7.5 Proposed mechanism to explain the Pb isotopic evolutionary history of this group of potassic magmas. As an example, a possible Pb evolution trajectory for Ellendale lamproite WAK-27L (analysis from Chapter 3 of this thesis) is shown. At time t_1 (for the example shown, 3.0 Ga ago), Pb is extracted from the mantle during a crust forming event and evolves for some period in the high U/Pb upper crust. For the example shown, μ ($^{238}U/^{204}Pb$) is 13.75 for 1.0 Ga. At t_2 (2.0 Ga ago), this upper crustal Pb is eroded from the continent and deposited in the low μ marine environment. These sediments are then subducted into the mantle and stored in the subcontinental lithosphere. For the example shown, μ is 4.25 during this ~2.0 Ga period.

and Tatsumoto 1976, White *et al.* 1985) suggests that the U/Pb ratio of modern pelagic oceanic sediments is extremely variable and is commonly low, and may have been generally lower during the Archaean when the lower degree of oxidation of the Earth's atmosphere would favour the less-soluble U^{4+} ion over U^{6+}. If sediment subduction has been an important process throughout the Earth's evolution, this has important implications for the global U/Pb and Th/U budget, as will be discussed later.

Since the late Archaean at least, the Nd isotopic composition and Sm/Nd ratio of oceanic sediments were therefore probably similar to those of the contemporaneous upper crust, whereas Sr and Pb isotopic compositions were influenced by a combination of contemporaneous mantle and upper crustal inputs. For oceanic sediments containing a significant proportion of continent-derived Pb, fractionation of the U/Pb ratio during sedimentation will retard further isotopic evolution of their already radiogenic upper crustal Pb (Fig. 7.5). Although processes acting during subduction (i.e. dehydration or partial melting) may modify the chemistry of subducted sediments, their effect on the Rb/Sr, Sm/Nd and U/Pb ratios of sediments is dependent on the element partitioning effects of the various mineral phases involved in the subduction zone and is largely unknown. If the extent of such modification is not too severe, the Nd isotopic characteristics of subducted oceanic sediments following their storage within the mantle will evolve roughly parallel to the upper continental crust (i.e. towards highly unradiogenic Nd), due to the similarity of the Sm/Nd ratio

of oceanic sediments and the upper continental crust. However, if extensive partial melting of the sediments occurs within the subduction zone, an increase in the Sm/Nd ratio of the residue is likely. The effect of this on the Nd isotopic evolution of the sediments is not quantifiable and depends on the extent of Sm/Nd fractionation. If the Sm/Nd ratio of the sediments following the extraction of a melt remains less than chondritic (i.e. they are still LREE-enriched) their Nd isotopic composition will remain unradiogenic, whereas if the sediments become LREE-depleted, they will evolve more radiogenic Nd during the period of their storage within the mantle or the subcontinental lithosphere. The subducted sediments, or possibly a melt derived from both subducted oceanic crust and sediments, may become incorporated into the subcontinental lithosphere during or after periods of active subduction along the cratonic margin. At some later stage this modified lithosphere is re-activated, generating potassic magmatism derived from so-called "enriched mantle" sources.

7.6 Sediment subduction and anorogenic potassic magmatism

Although the effects of partial melting and mixing with the mantle must be considered, many aspects of the geochemistry of these examples of continental potassic magmatism are consistent with the involvement of a sedimentary component. High Ba contents and Ba/La and low K/Rb are features which have been attributed to the involvement of sediment components in studies of island-arc lavas (e.g. Kay 1980, McCulloch and Perfit 1980). The generally high Th/U ratios may reflect the low U abundances in the sedimentary source or may have been compounded by preferential loss of U relative to Th from the subducted slab in exsolved fluids during dehydration (Newman *et al.* 1984). The highly variable oxidation state of this group of potassic magmas (Foley 1985), their high abundances of P_2O_5 (≤3.3 wt%) and of volatiles such as F (≤1.0 wt%), Cl (≤0.1 wt%) and H_2O (>6 wt%) (Sheraton and Cundari 1980, Sheraton and England 1980, Kuehner *et al.* 1981, Jaques *et al.* 1984a), their variable but generally radiogenic Sr and their unradiogenic Nd are all readily explained by the involvement of sedimentary components. As the isotopic evolution of Pb in sediments may be severely retarded following its erosion from the continents and deposition in the ocean basins, the unradiogenic $^{206}Pb/^{204}Pb$ of these magmas may be an indication of the time elapsed during sedimentation and storage within the convecting mantle or subcontinental lithosphere, whereas variation in the $^{207}Pb/^{204}Pb$ may reflect the nature and age of the continental provenance.

The presence of diamonds in the Western Australian lamproites provides further support for the involvement of recycling processes, as an extremely wide range of $\delta^{13}C$ values (including values as low as -34 ‰ vs PDB) have been documented by carbon isotopic studies of diamonds from kimberlites and lamproites (Sobolev *et al.* 1979, Milledge *et al.* 1983, Swart *et al.* 1983, Ozima *et al.* 1985, Jaques *et al.* 1986b) consistent with an origin of some diamonds from sedimentary sources of carbon. A wide range of $^3He/^4He$ ratios were also recently reported by Ozima *et al.* (1985) for diamonds. These authors interpreted the high $^3He/^4He$ ratios of some diamonds as indicating that they had remained closed systems for almost the age of the Earth. However, an alternative interpretation is offered by the recently confirmed high $^3He/^4He$ ratios of some ocean sediments (Ozima *et al.* 1984) and manganese nodules (Sano *et al.* 1985), believed to be carried by interplanetary dust particles (Amari and Ozima 1985). Furthermore, a common mineral assemblage of diamond inclusions, olivine + knorringite-rich garnet + enstatite, has been attributed

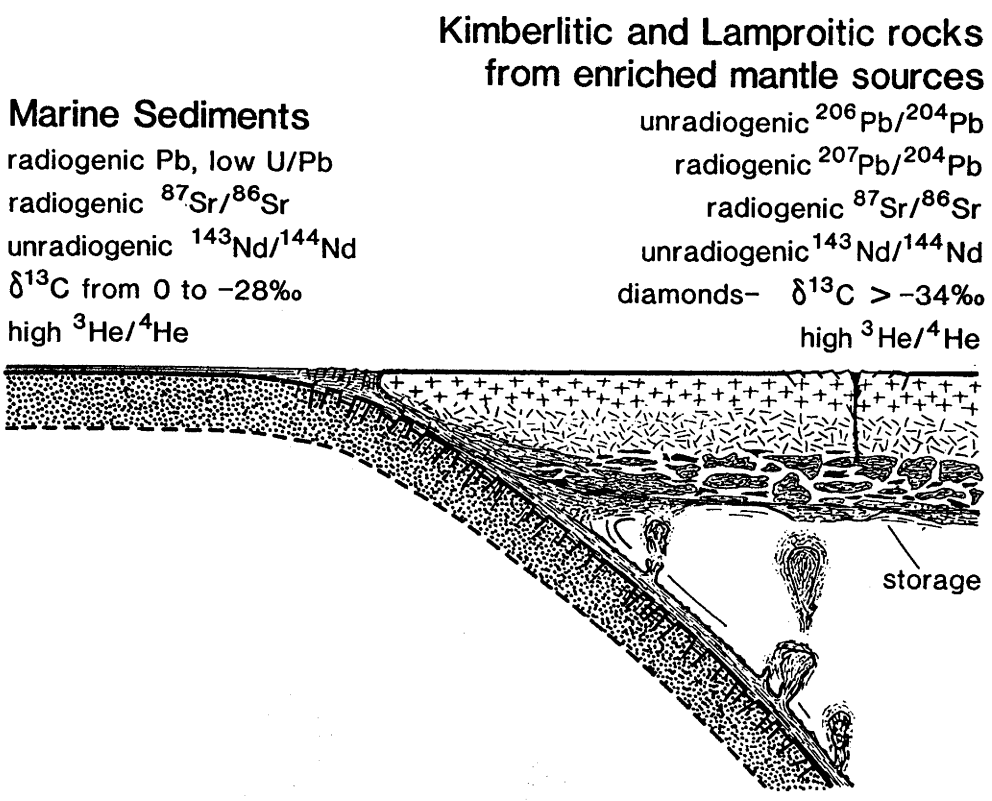

Fig. 7.6 Schematic representation of processess which may be responsible for the generation of enriched mantle sources from which anorogenic potassic magmatism is derived.

to recrystallisation of olivine + chrome spinel + enstatite cumulates within oceanic crust following its hydrothermal alteration and partial melting during subduction into the mantle (Ringwood 1977). These data argue for the involvement of components derived from both subducted sediments and oceanic crust in the formation of diamonds.

Although most examples of continental potassic magmatism are not obviously associated with any known modern or past subduction zones, their unusual multistage Pb isotopic compositions indicate that a significant time period has elapsed between the event lowering the U/Pb ratio (i.e. sediment formation) and subsequent potassic magmatism. It is therefore not surprising that they are commonly not associated with the operation of modern subduction processes. That most are found intruding Archaean or early Proterozoic cratons provides indirect evidence that the sources of these examples of continental potassic magmatism are stored within the subcontinental lithosphere. Evidence for the operation of subduction during the Proterozoic has been presented for Antarctica by Craddock (1975) and the western American continent by Lipman *et al.* (1972).

The mechanism by which the enriched mantle sources of continental potassic magmas are generated is represented schematically in Fig. 7.6.

7.7 Sediment recycling and mantle evolution

Unless subducted sedimentary components are well mixed with the mantle, the overall effect of the incorporation of high Th/U, low U/Pb sediments within the subcontinental lithosphere is a re-distribution of Th, U and Pb within the continental crust and subcontinental lithosphere and its direct effect on the

isotopic evolution of the Earth's mantle may not even be detectable. However, the position of MORB, ocean-island and upper continental crust Pb to the right of the geochron indicates that their sources have undergone either progressive or episodic enrichment in U relative to Pb, requiring the existence of a compensating reservoir from which U has been donated. This compensating reservoir should possess relatively unradiogenic Pb and lie to the left of the geochron. Although the Earth's core (Allègre *et al.* 1982) and the lower continental crust (O'Nions *et al.* 1979) have been advanced as possible reservoirs in which this missing unradiogenic Pb is stored, due to the operation of sediment subduction processes, the subcontinental lithosphere may also have acquired these characteristics. The existence of substantial reservoirs of low U/Pb, enriched mantle components within the subcontinental lithosphere can therefore compensate for the generally radiogenic Pb of the MORB and ocean-island source reservoirs.

SECTION B. CARBONATITIC AND KIMBERLITIC MAGMATISM

8.1 Introduction

Carbonatites are magmatic, carbonate-rich (>50 wt%) rocks characterised by high abundances of Sr, Ba, P and the light rare-earth elements. Examples have been reported from both continental settings, commonly associated with nephelinitic or kimberlitic igneous provinces, and more recently from oceanic settings, such as the Cape Verde and Canary Islands (Allègre *et al.* 1971, Silva *et al.* 1981, Barrera *et al.* 1981) and the Solomon Islands (Nixon and Boyd 1979). Despite the interest these unusual rocks have attracted, their origin still remains a perplexing petrogenetic problem. Earlier models favouring the syntexis of limestone are untenable in the light of subsequent isotopic studies. Other proposals have invoked such mechanisms as Na-rich carbonate/silicate liquid immiscibility (demonstrated experimentally by Hamilton *et al.* 1979), fractional crystallisation from an alkaline silicate parent magma or extreme alkali metasomatism of silicate rocks during the differentiation of an intrusive ultrabasic magma. More recently, experimental evidence favours a primary igneous origin for carbonatitic magmas, emphasising the important role of CO_2 in their genesis. CO_2 is a major component in volcanic glasses and is probably contained in minor carbonate phases such as dolomite or magnesite in the upper mantle (Brey *et al.* 1983). Experimental studies (e.g. Wyllie and Huang 1976, Wendlandt 1984) indicate that, due to a rapid increase in the solubility of CO_2 and a concomittant lowering of the solidus temperature at pressures ~25-30 kbar, partial melts of carbonate-bearing peridotite at these pressures will be carbonate-rich. Carbonatite magmas may therefore be produced by small degrees of partial melting of carbonated peridotite at depths greater than ~80 km, followed by the separation of a carbonatitic liquid by immiscibility processes.

Radiogenic isotope studies (e.g. Bell *et al.* 1973, Lancelot and Allègre 1974, Basu and Tatsumoto 1980, Bell *et al.* 1982, Barreiro 1983, Roden *et al.* 1985, Grünenfelder *et al.* 1986) indicate that most carbonatites studied so far have generally similar isotopic characteristics, with unradiogenic initial $^{87}Sr/^{86}Sr$ (~0.703), slightly positive ε_{Nd} and radiogenic initial Pb compared to those of MORB, and isotopically resemble alkali basalts from many ocean islands. As the isotopic characteristics of ocean-island basalts have been interpreted as evidence that they are derived from subducted oceanic lithosphere (Chase 1981, Hofmann and White 1982), a similar origin is also suggested for carbonatites. Alternatively, Bell *et al.* (1982) and Bell and Blenkinsop (1986, 1987a) have argued that Canadian carbonatites are derived from a depleted upper mantle reservoir which has remained coupled to the Canadian continental crust since the late Archaean. Barreiro (1983) also proposed a similar model for carbonatites from Westland, New Zealand, involving crystallisation at depth of a LREE- and carbonate-rich magma originally derived from the depleted mantle. At some later time, during which the evolution of its $^{143}Nd/^{144}Nd$ ratio had been retarded, this magma was re-activated, resulting in carbonatitic magmatism having only slightly positive ε_{Nd}. CO_2-dominated "metasomatic" processes have also been implicated in the generation of continental alkaline volcanism. For example, Norry *et al.* (1980) reported Sr-, Nd- and Pb- isotope compositions similar to those of carbonatites and ocean islands for alkali basalts, basanites, nephelinites and phonolites from the Kenya rift. These authors argued for the operation of CO_2-metasomatism of the sources of these magmas in order to account for their silica-undersaturation and

unusual trace-element chemistry. Information concerning the relative mobility of trace elements in carbonate fluids provided by the characterisation of the trace-element features of carbonatites may be of value in understanding these processes.

In this study, trace-element and isotopic data are reported for carbonatites and kimberlites of a variety of localities and ages. Although it is recognised that many carbonatite complexes have had complicated histories of differentiation and intrusion, the approach adopted here is to compare broad geochemical and isotopic features of many different complexes in order to identify possible common processes which may be responsible for the generation of carbonatite magmas. The data obtained are used to: a). characterise the sources of carbonatites; b). evaluate the hypotheses advanced for carbonatite origin; c). investigate possible relationships between carbonatite and kimberlite magmas, and; d). assess the importance of CO_2-rich "metasomatic" processes within the mantle.

8.2 Samples

Localities and emplacement ages of the carbonatite samples examined in this study are summarised in Fig. 8.1.

8.2.1 African carbonatites

Six African carbonatite localities, ranging in age from mid-Proterozoic to Tertiary, have been sampled. The youngest carbonatite locality examined, from the Napak alkaline complex in eastern Uganda, consists of both intrusive and extrusive alkaline rocks surrounding a central core of carbonatite (Lokupoi carbonatite) which have intruded Precambrian granitic gneiss. The petrology and geochemistry of the complex has been investigated by King (1965) and King and Sutherland (1966). The carbonatite sample obtained for this study (#6336) consists of a flow-banded fine-grained calcite-carbonatite (alvikite, following the terminology of Streckeisen 1979) containing rare phenocrysts of phlogopite, minor rutile and magnetite. A mid- to late-Tertiary emplacement age is indicated by lower Miocene mammalian fauna in sediments interbedded with the volcanics and from K-Ar studies (Baker *et al.* 1971). The Sukulu and nearby Tororo carbonatites, situated about 150 km south of Napak, are believed to be of similar age. Their petrology, geochemistry and field relationships have been summarised by King and Sutherland (1966) and Heinrich (1966). The Sukulu sample examined here (#6335) is a melanite-bearing calcite-dolomite carbonatite and the Tororo sample (#6330) is a scapolite-bearing alvikite containing minor melanite. Details of the geology and geochemistry of the Kangankunde carbonatite, Malawi, can be found in Garson (1966). An early Cretaceous K-Ar age of 126 Ma was reported for this carbonatite by Snelling (1965). The specimen from the Kangankunde complex used in this study (#3432) is a coarse monazite-scapolite dolomite carbonatite (beforsite). The Nachendazwaya carbonatite, located in Tanzania near the border with Malawi, is believed to be genetically related to the Ilomba Hill carbonatite complex (Gittins 1966), 2 km further south in Malawi, which has been dated by the U-Pb zircon method at 655 Ma (Snelling *et al.* 1964). A similar K-Ar age of 680 Ma has been reported for phlogopite from metasomatised country rock adjacent to the Nkombwa carbonatite ~75 km to the southwest in Zambia (Snelling 1965). The Nachendazwaya carbonatite specimen (#7122) is an apatite-biotite-magnetite sövite (coarse-grained calcite carbonatite) having rare phenocrysts of blue-green amphibole and trace amounts of

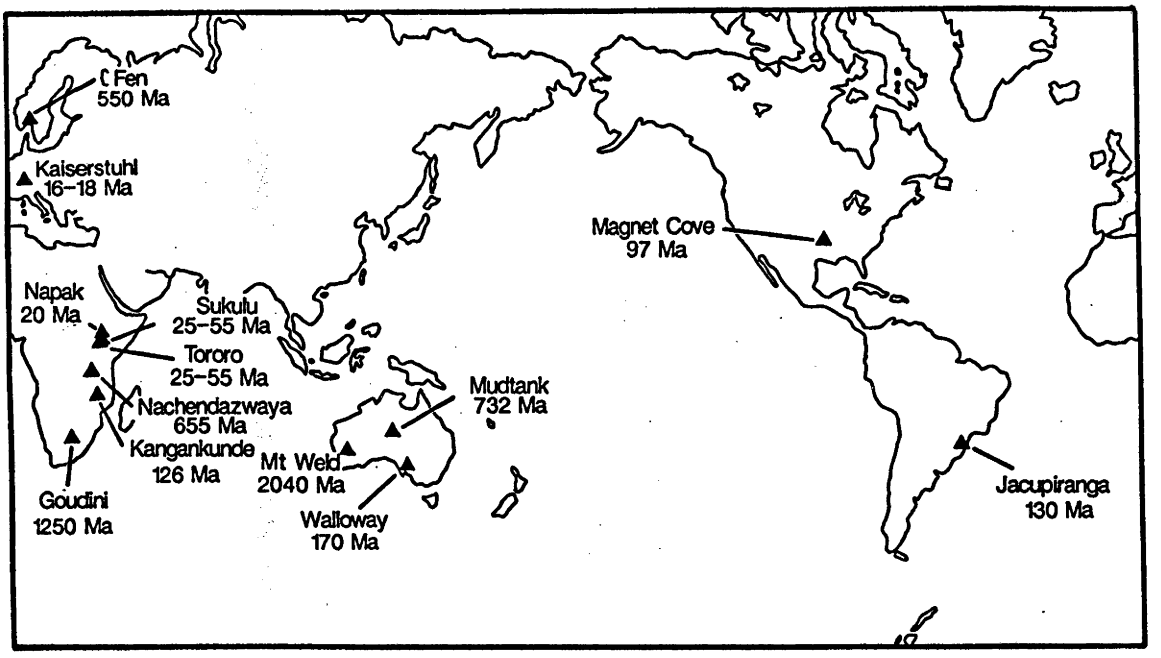

Fig. 8.1 Localities and emplacement ages of carbonatite complexes examined in this study.

rutile. The age of the Goudini carbonatite, South Africa, is uncertain, but has been tentatively correlated with magmatic activity associated with the Pienaars River Alkaline Complex which dates from 1430 to 1300 Ma ago (Harmer 1986). Goudini specimen #33174 consists of ocelli of coarse calcite up to several millimeters in diameter with radial aggregates of green amphibole (probably riebeckite), scapolite, magnetite, nepheline, goethite and opaques in a carbonate matrix and #33176 is a fine-grained apatite-bearing calcite-dolomite carbonatite with minor sodic amphibole (riebeckite), albitised plagioclaise, white mica (possibly fuchsite) and chlorite. The Zoutpan carbonatite, situated ~30 km north of Pretoria, is believed to be younger than Cretaceous (Verwoerd 1966). Zoutpan sample #33182 consists of calcite with minor chlorite, haematite, magnetite, quartz and sulphides (possibly chalcopyrite).

8.2.2 Australian carbonatites and kimberlites

The Jurassic Walloway carbonatite occurs as a ~10 km long, 100 to 800 m wide diapir associated with a suite of contemporaneous carbonate-rich ultrabasic lamprophyric and kimberlitic intrusions located in the Flinders Ranges region of South Australia (Tucker and Collerson 1972, Stracke *et al.* 1979). The mineralogy and chemistry of the Walloway and nearby kimberlitic intrusions at Terowie and Orroroo have been described by Ferguson and Sheraton (1979) and Scott-Smith *et al.* (1984). The Walloway carbonatite specimen examined here (#7821-0009) is a coarse-textured calcite carbonatite (sövite) containing minor phlogopite (commonly rimmed by sodic amphibole), nepheline, sodic amphibole and opaques. The Mudtank carbonatite complex, located on the deep-seated Woolanga Lineament 50 km east-northeast of Alice Springs in central Australia, consists of 4 separate lenses of crystalline, micaceous and feldspathic carbonate rocks and has been reliably dated by both U-Pb zircon and Rb-Sr whole-rock techniques at 732 ±5 Ma and 735 ±75 Ma respectively (Black and Gulson 1978). Further details of the geology and geochemistry can be found in Black and Gulson (1978) and references therein. Mudtank sample #7590-2015 is a coarse apatite-bearing dolomite carbonatite (beforsite). The Mt Weld carbonatite, located

within the Eastern Goldfields province of the Yilgarn Block, Western Australia, consists of a ~4 km diameter circular intrusion which has been dated by both K-Ar and Rb-Sr techniques at ~2040 Ma (reported in Willett *et al.* 1986). Its emplacement is believed to be tectonically related to the long-active deep-seated Laverton tectonic zone. Two samples of coarse calcite carbonatite (sövite) containing phenocrysts of apatite, magnetite and biotite (#MW-1 and #MW-2) were obtained for this study.

The field relationships, petrology and geochemistry of the kimberlitic intrusions of the Jugiong area, southeast New South Wales, have been described by Stracke *et al.* (1979), Ferguson *et al.* (1979) and Ferguson and Sheraton (1979). Although closely resembling kimberlite in their mode of emplacement, nodule-type and heavy-mineral contents, the intrusions differ from more typical kimberlite in their higher SiO_2, Al_2O_3 and Na_2O and lower MgO and incompatible-element contents, and have chemical affinities with olivine nephelinite or melilitite (Ferguson and Sheraton 1979).

8.2.3 Jacupiranga carbonatite

The Jacupiranga alkalic complex is an oval-shaped plug of ~65 km^2 area consisting of a central body of carbonatite surrounded by jacupirangites, pyroxenites, ijolites and syenites, that have intruded the Precambrian schists and granodiorite of southwest São Paulo, Brazil. The age of intrusion is well constrained by both K-Ar (Amaral 1978) and Rb-Sr (Roden *et al.* 1985) methods at 131 ±3 Ma, contemporaneous with both the flood basaltic volcanism of Paranà to the west and the opening of the South Atlantic Ocean. Roden *et al.* (1985) reported a range in initial $^{87}Sr/^{86}Sr$ and ε_{Nd} values of 0.7051 to 0.7053 and +0.1 to +1.6 respectively from the 5 distinct intrusions which comprise the central body of the Jacuparinga alkalic complex and attributed the range in initial isotopic compositions to crustal contamination. Both Jacupiranga samples examined here (#5961 and #5963) are magnetite- and phlogopite- bearing sövites.

8.2.4 Kaiserstuhl and Fen carbonatites

The Kaiserstuhl is situated in the Upper Rhine Graben ~15 km from Freiburg im Breisgau, Germany. Carbonatitic, phonolitic and other alkalic intrusives form the core of the complex, which is rimmed by pyroclastics. Kaiserstuhl carbonatite specimen #K-3 consists of coarse calcite with minor biotite, melanite and apatite. K-Ar dating indicates emplacement ages of 16-18 Ma (in Wimmenauer 1966). The Fen carbonatite, Norway, has been the subject of extensive study (e.g. Barth and Ramberg 1966, Mitchell and Crocket 1970, Griffin and Taylor 1975) and has been dated by several independent techniques at ~550 Ma old. Specimen #NBS-18 consists of carbonate from the Fen carbonatite prepared for use as a stable-isotope standard (Friedman *et al.* 1982).

8.2.5 Magnet Cove carbonatite

The Magnet Cove carbonatite complex, Arkansas, is a ~6 km^2 oval body that has intruded Palaeozoic shales and sandstones and consists of ijolite and carbonatite intrusions surrounded by ring dykes of phonolite, melteigite, jacupirangite and nepheline syenite (Erickson and Blade 1963). Zartman *et al.* (1967) obtained K-Ar and mica Rb-Sr ages of 97 Ma indicating emplacement of the complex during the late Cretaceous. Specimen #MC-1 consists of coarse (~1 cm^3) rhombs of transparent calcite.

8.3 Analytical procedures

Major-element analyses were obtained by X-ray fluorescence spectrometry on fused glass discs using an automated Siemens SRS300 spectrometer in the ANU Department of Geology, following the procedure of Norrish and Hutton (1969). Abundances of the trace elements Ni, Cu, Zn, Rb, Sr, Y, Zr, Nb and Pb were determined by X-ray fluorescence on pressed powder pellets using a Phillips PW1400 spectrometer and the method of Norrish and Chappell (1967). The other trace-element abundances were obtained on ~300 mg of powdered sample by instrumental neutron activation analysis using an internal synthetic kimberlite standard included in each batch. All geochemical analyses given here represent averages of at least two determinations.

Samples for isotopic analysis were sawn into ~3 cm^3 cubes, scrubbed thoroughly and then washed in an ultrasonic bath in ultrapure H_2O and acetone. The cubes were then coarsely crushed in a stainless steel percussion mortar and small rock chips with fresh fracture surfaces were hand-picked and used for isotopic analysis. About 1-3 g of carbonatite chips were initially treated with 6N HCl in teflon beakers until all carbonate was decomposed, the solution then evaporated and the residue dissolved using a mixture of HF-$HClO_4$. The resulting solution was then re-dissolved in 1N HCl and split into two aliquots, one of which was spiked with mixed ^{235}U-^{208}Pb spike and the other used for Pb isotopic composition. Rb-Sr and Sm-Nd concentration and isotopic analyses were undertaken on ~70 mg of sample chips using mixed ^{85}Rb-^{84}Sr and ^{147}Sm-^{150}Nd spikes. Samples were dissolved in HF-$HClO_4$ in teflon pressure capsules at 200 °C or in teflon beakers for at least 48 hrs. The remaining procedures for Rb-Sr, Sm-Nd and U-Pb concentration and isotopic analysis are described more fully in Appendix A1. All Pb isotopic composition analyses were performed in duplicate or triplicate and the analytical error, based on two-way analysis of variance of replicate analyses, is < ±0.1% at the 1σ level. The total procedural blanks were ~1 ng for Sr, <1 ng for Nd and <5 ng for Pb and were insignificant for all analyses.

Carbonates for $\delta^{13}C$ and $\delta^{18}O$ analysis were reacted in duplicate with 100% H_3PO_4 at 25 °C for 1 day (calcite samples) and 3 days (dolomitic/ankeritic samples) and analysed on a highly-modified MS-12 triple-collector mass spectrometer (overall precision ±0.1‰). $\delta^{18}O$ values were calculated using 1000lnα values for acid-liberated CO_2 of 10.20 for calcite and 11.03 for dolomite/ankerite. $\delta^{13}C$ and $\delta^{18}O$ values are expressed as per mil differences relative to the PDB and SMOW standards. $\delta^{18}O_{SMOW}$ and $\delta^{13}C_{PDB}$ (‰) values for NBS-18 and NBS-19 standards of +7.20, -5.00 and +28.65, +1.95, respectively, are obtained in this laboratory.

CO_2 contents (Table 8.1) of calcitic samples were measured by manometry of the CO_2 evolved at 25 °C. After collection of the CO_2 evolved at 25 °C from ankeritic samples, the phosphoric acid was boiled vigorously for ten minutes and the additional CO_2 released measured manometrically to provide a total CO_2 content. Due to the small sample weight (20 mg) and inhomogeneity of the samples, reproducibility of the manometric yields is ±3%, and is largely responsible for some of the poorer major-element sums (Table 8.1).

8.4 Results

8.4.1 Major- and trace-element analysis

Geochemical data are tabulated in Table 8.1 and presented diagrammatically in Figures 8.2 to 8.5. In Figures 8.2 and 8.4, the concentrations of trace elements have been normalised to estimated primitive mantle abundances (from McDonough *et al.* 1985 and Nelson *et al.* 1986) and plotted in order of increasing compatibility in peridotitic mantle of garnet lherzolite mineralogy. Also shown for comparison are trace-element patterns for ocean-island basalts (Chen and Frey 1983, Thompson *et al.* 1984, Palacz and Saunders 1986). General features of the geochemistry of carbonatites apparent from Table 8.1 and Fig. 8.2 are; a) the typically high abundances of Ba, Th, LREE, Sr, variable abundances of Rb, Nb, Ta, P and low Cs, K, Ti and HREE abundances of most examples; b) with the notable exception of Goudini and Walloway carbonatites, most examples possess large negative Zr and Hf concentration anomalies. These negative Zr and Hf anomalies are generally accompanied by large negative U anomalies and (with some exceptions) high Th/U ratios. The South African Goudini and South Australian Walloway carbonatites possess higher SiO_2, Sc, Cr, Sc, Ni, Co, Rb, Zr and Hf than the other low-SiO_2, U- and Zr- anomalous carbonatites.

Rare-earth element concentrations normalised to chondritic values are plotted in Fig. 8.3. The rare-earth element patterns for two secondary vein carbonates samples of sedimentary origin are also shown for comparison in Fig. 8.3 and also in Fig 8.5. All carbonatites have steep LREE-enriched patterns with low HREE abundances. Slight decoupling of the LREE from the HREE is apparent in a few of the patterns, especially those of Nachendazwaya, Mudtank and Jacupiranga (#5963) examples for which the patterns are steepest between Sm and Tb. The Goudini carbonatite #33176 pattern possesses a positive slope between Nd and Eu. Small positive Eu anomalies are evident in the Kaiserstuhl (#K-3) and Magnet Cove (#MC-1) carbonatite patterns and in the Terowie kimberlite (#0090) pattern.

Although the Zoutpan sample (#33182) possesses a major element composition similar to that of the other carbonatites examined, it has substantially lower abundances of Ba, Th, Sr and the rare-earth elements (Table 8.1 and Fig. 8.4). The Zoutpan rare-earth element pattern shows only slight LREE-enrichment and a prominent negative Eu anomaly is evident (Fig. 8.5). Compared to the Walloway sedimentary carbonate vein analyses given in Table 8.1, the Zoutpan sample has substantially higher abundances of Cr, Sc, Ni and Cu, Sr, Zr Nb and the rare-earth elements. Nevertheless, the Zoutpan sample lacks many of the trace-element features characteristic of carbonatites and may be of sedimentary origin.

8.4.2 Rb-Sr and Sm-Nd isotope analysis

Sr and Nd isotopic analyses for carbonatites are presented in Table 8.2 and are compared with available data for carbonatites from other studies and with the fields of modern ocean-island basalts, MORB and non-micaceous (Group 1) South African kimberlites on an initial Sr-Nd isotope diagram in Fig. 8.6. As most of the carbonatites have very low Rb contents and high abundances of Sr, correction of the measured $^{87}Sr/^{86}Sr$ for ^{87}Rb decay since emplacement is small and insensitive to possible errors in the emplacement ages. In order to minimise the possibility of contamination during rock crushing,

Table 8.1. Major- and trace- element analyses of carbonatites, associated alkaline igneous rocks and secondary (sedimentary) carbonate veins.

location	Lokupoi	Tororo	Sukulu	Kangankunde	Nachendaz.	Goudini	Goudini
sample	6336	6330	6335	3432	7122	33174	33176
rock-type	carbonatite	alvikite	carbonatite	carbonatite	sövite	carbonatite	carbonatite
main carbonate	calcite	calcite	dolomite	dolomite	calcite	ankeritic dolomite	ankeritic dolomite
SiO_2	0.82	1.06	0.02	1.17	1.27	25.12	15.90
TiO_2	0.08	-	-	-	0.50	4.36	3.49
Al_2O_3*	0.19	0.02	0.01	0.17	0.35	3.23	2.83
Fe_2O_3*	1.99	2.26	1.62	1.73	7.79	14.95	12.93
MnO	0.46	0.55	0.39	0.56	0.29	0.20	0.32
MgO	1.30	1.42	16.90	3.92	3.42	6.49	8.92
CaO	55.40	54.70	36.21	6.83	49.48	15.94	21.24
Na_2O	0.10	0.09	0.06	0.21	0.13	3.08	3.15
K_2O	0.13	0.01	0.01	-	0.02	2.83	0.14
P_2O_5	0.21	2.37	5.86	3.77	3.60	0.44	0.68
S	0.06	0.11	0.03	0.40	-	0.17	0.03
CO_2	43.9	39.4	34.8	21.9	36.9	19.1	30.2
SUM	104.64	101.97	95.91		103.75	95.91	99.83
Cr	-	-	-	-	2.7	665	364
Sc	19	0.26	5.7	1.86	5.44	38	19
Ni	2	<1	<1	16	<1	232	425
Co	6	-	3	-	11	30	848
Cu	<1	2	<1	148	1	134	82
Zn	20	31	15	159	25	163	137
Cs	-	-	-	-	-	-	-
Ba	2450	2970	56	18900	690	3140	1100
Rb	3	<0.5	<0.5	<0.5	1	26.5	1
Sr	1250	6930	2760	280000	4430	1490	4360
Pb	41	7	<1	99	9	11	37
Y	143	159	23	27	55	46	98
Th	126	35	4.8	164	4.7	57	93
U	-	-	-	-	42	1.4	3.6
Zr	<1	<1	<1	12930	2	459	715
Hf	-	0.16	0.14	1.0	0.36	16.8	25.4
Nb	1030	116	390	123	97	113	91
Ta	-	-	2.1	-	49.7	5.2	3.8
Mo	-	-	-	-	11	18	-
Sb	0.4	0.07	-	0.4	-	5.0	1.7
Au	-	-	-	-	0.01	-	-
La	1890	446	115	25700	162	174	121
Ce	3370	865	277	23000	365	416	233
Nd	1260	362	138	11000	178	217	118
Sm	205	69	25.7	1030	36.2	42.1	39.8
Eu	49	18.6	6.4	153	9.8	12.6	17.1
Gd	87	43.1	16.7	224	21.3	33	51
Tb	13.6	6.4	2.62		2.91	4.4	6.5
Ho	6.7	7.1	1.33		2.86	2.2	4.6
Yb	13.0	7.5	1.35		3.79	2.7	6.4
Lu	1.63	0.79	0.137	<1	0.373	0.38	0.79

* All Fe calculated as Fe_2O_3. (-) not detected, (nd) not determined.

Table 8.1 (continued)

location	Walloway	Walloway†	Terowie	Mt Weld	Mt Weld	Jacupiranga	Jacupiranga
sample	0009	0081	0090	MW-1	MW-2	5961	5963
rock-type	carbonatite	carb. kimb.	kimberlite	sövite	sövite	carbonatite	carbonatite
main carbonate	calcite	calcite		calcite	calcite	calcite	calcite
SiO_2	7.69	21.99	36.39	2.25	2.84	0.24	0.40
TiO_2	1.64	1.83	4.48	0.04	0.01	0.04	0.01
Al_2O_3	3.02	3.40	6.62	0.12	0.23	0.17	0.05
Fe_2O_3	7.49	10.39	14.45	9.20	2.51	2.38	0.98
MnO	0.13	0.22	0.17	0.22	0.16	0.08	0.11
MgO	4.97	22.23	17.16	2.30	2.21	1.95	4.39
CaO	41.88	17.03	2.52	45.86	50.37	52.26	50.64
Na_2O	0.12	0.03	0.49	0.47	0.51	0.27	0.21
K_2O	0.74	0.10	2.02	0.47	0.47	0.05	0.01
P_2O_5	0.85	1.72	1.26	2.43	4.18	7.16	0.17
S	0.02	-	0.20	0.20	0.26	0.16	0.41
CO_2	34.5	11.2	nd	32.2	36.4	34.5	41.9
SUM	99.28				95.75	100.15	99.28
Cr	810		1080	-	-	-	-
Sc	30	23	34	8.1	5.2	10.7	10.4
Ni	155	523	745	<1	3	2	1
Co	28		82	4.6	11	12	27
Cu	28	65	nd	nd	nd	5	7
Zn	35	100	107	25	20	7	2
Cs	0.31		7.1	0.69	0.4	-	-
Ba	2340	3000	3440	800	1100	820	720
Rb	28.5	5	126	28.0	20.5	1.0	<0.5
Sr	980	1700	225	5600	7010	5290	5880
Pb	7		63	106	110	4	4
Y	18	25	21	73	97	34	32
Th	39	54	23.6	60	56	2.3	0.25
U	6.5		3.4	10.5	76	-	-
Zr	244	430	330	227	184	<1	5
Hf	7.5		9.7	1.9	2.41	-	0.26
Nb	265	418	220	3140	398	7.5	1.5
Ta	12.8		11.8	66	86	1.7	0.17
Mo	-		-	-	18	-	-
Sb	0.6		-	0.12	-	-	-
Au	-		-	-	0.25	-	0.05
La	203	392	97	256	328	134	90
Ce	351	472	192	577	665	282	188
Nd	115		74	252	322	136	86
Sm	17.4		12.9	47	66	27.4	17
Eu	4.07		4.07	13.5	18.6	7.0	4.7
Gd	9.5		6.9	29	40	15.7	10.9
Tb	1.26		1.24	4.1	6.7	2.16	1.33
Ho	0.86		0.81	2.9	5.4	1.57	1.36
Yb	1.29		1.64	4.7	6.4	1.68	2.16
Lu	0.16		0.22	0.56	0.67	0.186	0.27

* All Fe calculated as Fe_2O_3. (-) not detected, (nd) not determined.

† Walloway carbonated kimberlite (#0081) analysis from Ferguson and Sheraton (1979).

Table 8.1 (continued)

location	Mudtank	Kaiserstuhl	Kaiserstuhl	Magnet Cove	Zoutpan	Walloway	Walloway
sample	2015	K-2	K-6	MC-1	33182	0007	0008
rock-type	sövite	carbonatite	phonolite	sövite	carbonate	carbonate	carbonate
main carbonate	dolomite	calcite		calcite	calcite		
SiO_2	0.85			0.23	6.82	4.95	
TiO_2	-			0.04	1.25	-	
Al_2O_3	0.25			0.05	1.13	0.17	
Fe_2O_3*	7.12			0.08	8.82	2.98	
MnO	0.33			0.11	0.91	0.18	
MgO	15.02			0.14	3.08	15.73	
CaO	33.37			56.38	44.72	34.28	
Na_2O	0.03			0.24	0.01	0.01	
K_2O	0.17			0.02	0.13	0.13	
P_2O_5	2.99			0.88	1.08	0.02	
S	-			0.02	0.11	-	
CO_2	40.6			nd	nd	nd	
SUM	100.72						
Cr	2.4	1.0	0.39	-	63	1.1	2.5
Sc	15.2	0.066	0.255	0.25	11.5	1.5	5.0
Ni	3	3	<1	<1	28	2	8
Co	18	12	8	0.10	23	3	5
Cu	2	56	7	nd	4	40	6
Zn	28	24	124	5	50	14	31
Cs	0.04	0.91	4.02	-	-	-	-
Ba	310	3360	1860	470	147	35	147
Rb	9.5	12.5	231	<0.5	1	1	2.5
Sr	2690	11580	1930	5290	340	121	124
Pb	3	3	29	70	9	2	<1
Y	18	20	22	25	4	8	
Th	2.7	3.80	49.8	1.4	0.62	0.80	
U	0.1	1.9	2.2	0.3	4.0	1.32	0.61
Zr	<1	<1	755	31	118	6	9
Hf	-	0.08	12.6	0.04	3.98	0.07	0.12
Nb	3.0	930	255	6.5	27	<0.5	0.5
Ta	-	1.43	6.2	-	3.0	-	-
Mo	-	-	-	-	-	0.5	-
Sb	0.2	0.05	0.55	0.04	0.4	0.10	0.11
Au	-	-	-	-	-	-	-
La	113	280	173	120	31.1	3.83	6.90
Ce	248	410	284	125	72.4	8.34	14.9
Nd	112	80	66	29	38.9	4.5	7.9
Sm	19.8	9.2	6.9	5.0	11.9	1.71	2.51
Eu	5.04	2.40	1.76	1.72	1.97	0.340	0.373
Gd	9.6	4.7	5.0	4.0	10.6	1.16	1.56
Tb	1.21	0.75	0.62	0.66	1.64	0.159	0.264
Ho	0.88	0.71	0.65	0.69	4.02	0.278	0.48
Yb	1.09	1.77	2.51	2.1	13.5	0.413	0.76
Lu	0.144	0.191	0.343	0.268	2.12	0.054	0.102

* All Fe calculated as Fe_2O_3. (-) not detected, (nd) not determined.

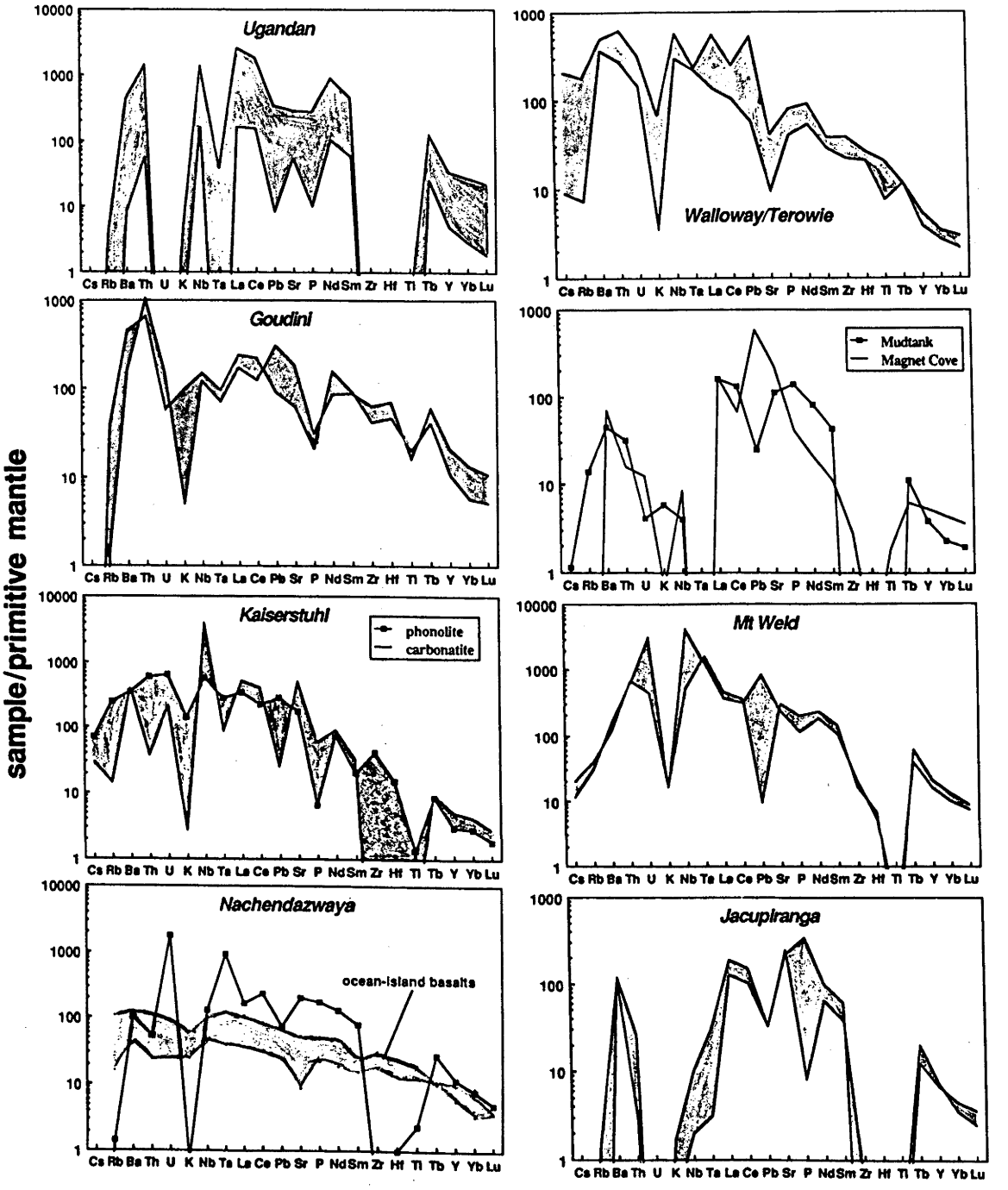

Fig. 8.2 Trace-element abundances normalised to estimated primitive mantle abundances (from McDonough *et al.* 1985 and Nelson *et al.* 1986) for carbonatites and a phonolite from Kaiserstuhl. Two groups are distinguishable; those possessing pronounced negative Zr and Hf anomalies typically accompanied by negative U anomalies and a second group (comprising the Walloway and Goudini carbonatites) which lack these features and generally possess relatively smooth trace-element patterns but with negative K anomalies. The latter group also have higher abundances of SiO_2 and the transition elements. Also shown for comparison is the field of trace-element patterns for some ocean-island basalts (from Chen and Frey 1983, Thompson *et al.* 1984 and Palacz and Saunders 1986). Ocean-island basalt patterns also commonly possess negative K anomalies which may be a characteristic of the OIB source.

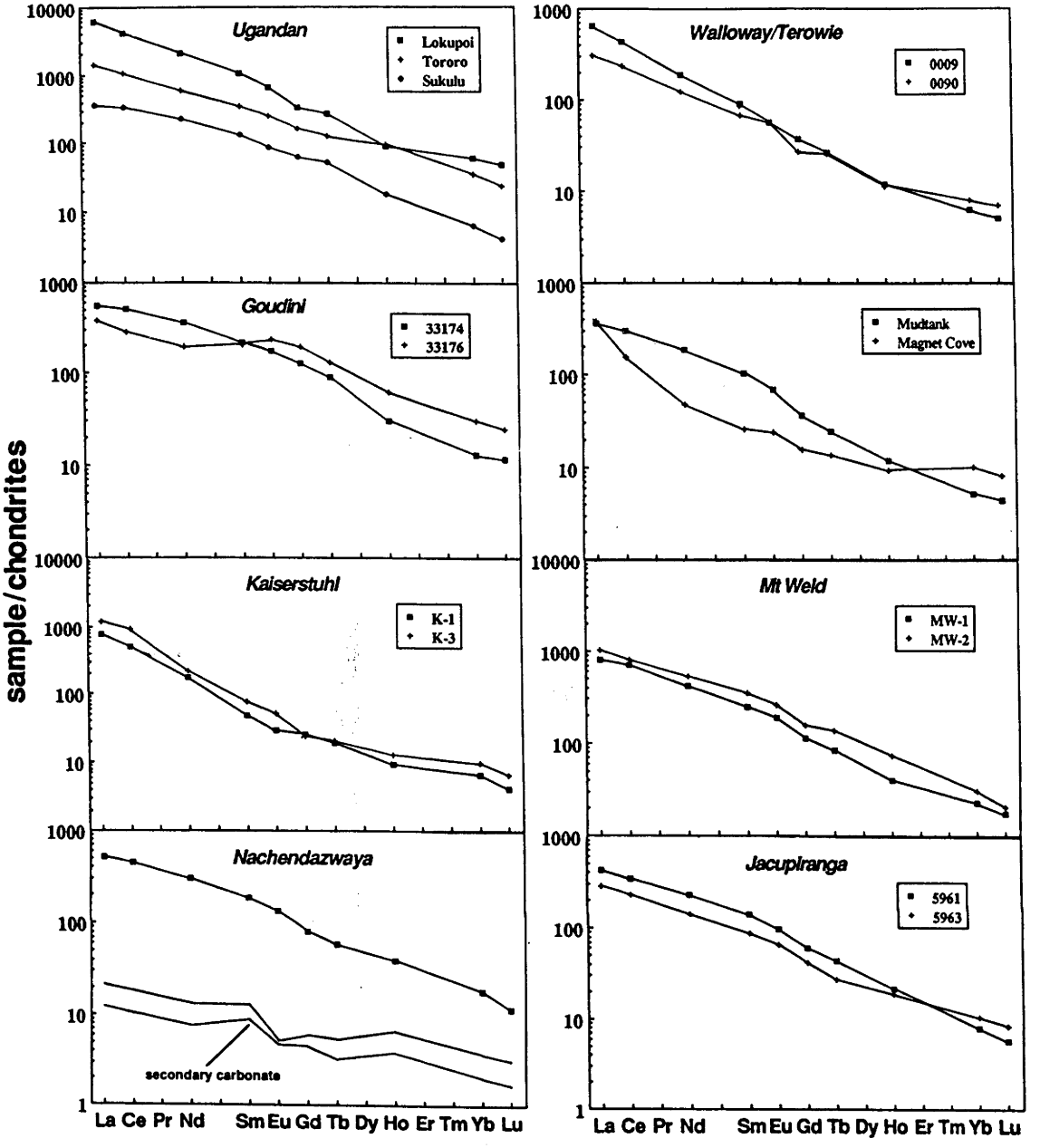

Fig. 8.3 Chondrite-normalised rare-earth element patterns for carbonatites and the Kaiserstuhl phonolite. Chondritic values are those of Taylor and Gorton (1977). The rare-earth patterns for two secondary (sedimentary origin) carbonate veins (from the Walloway region, South Australia) are also shown for comparison.

isotopic analysis was undertaken on small hand-picked chips, which are not likely to be geochemically representative of the larger hand-specimen. This has resulted in some discrepancies between the concentrations of Rb, Sr, Sm, Nd, U and Pb determined by isotope dilution and those determined by XRF/INAA. However, there is generally good agreement between the Rb/Sr, Sm/Nd and U/Pb ratios determined by these methods.

Sr and Nd isotopic compositions of Tororo, Sukulu, Kaiserstuhl, Fen, Magnet Cove and Jacupiranga carbonatites from this study generally agree within analytical error with the results obtained in previous studies of these complexes (e.g. Bell and Powell 1970, Mitchell and Crocket 1970, Roden *et al.* 1985, Bell and Blenkinsop 1987b, Tilton *et al.* 1987). Derry and Jacobsen (1986) reported a wide range of ε_{Nd} values of +3.1 to +7.7 for the intrusive rocks of the Fen Complex, indicating that some carbonatite

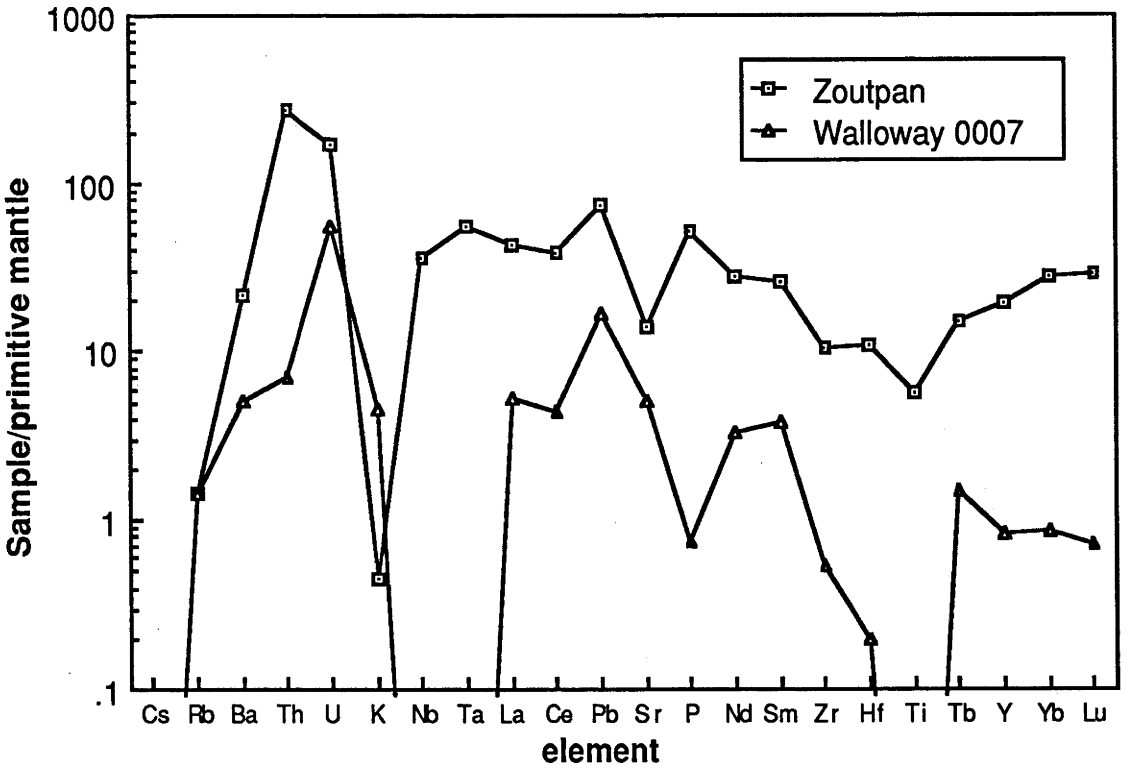

Fig. 8.4 Trace-element abundances normalised to estimated primitive mantle abundances (from McDonough *et al.* 1985 and Nelson *et al.* 1986) for sedimentary carbonate samples from Zoutpan, South Africa, and Walloway, South Australia.

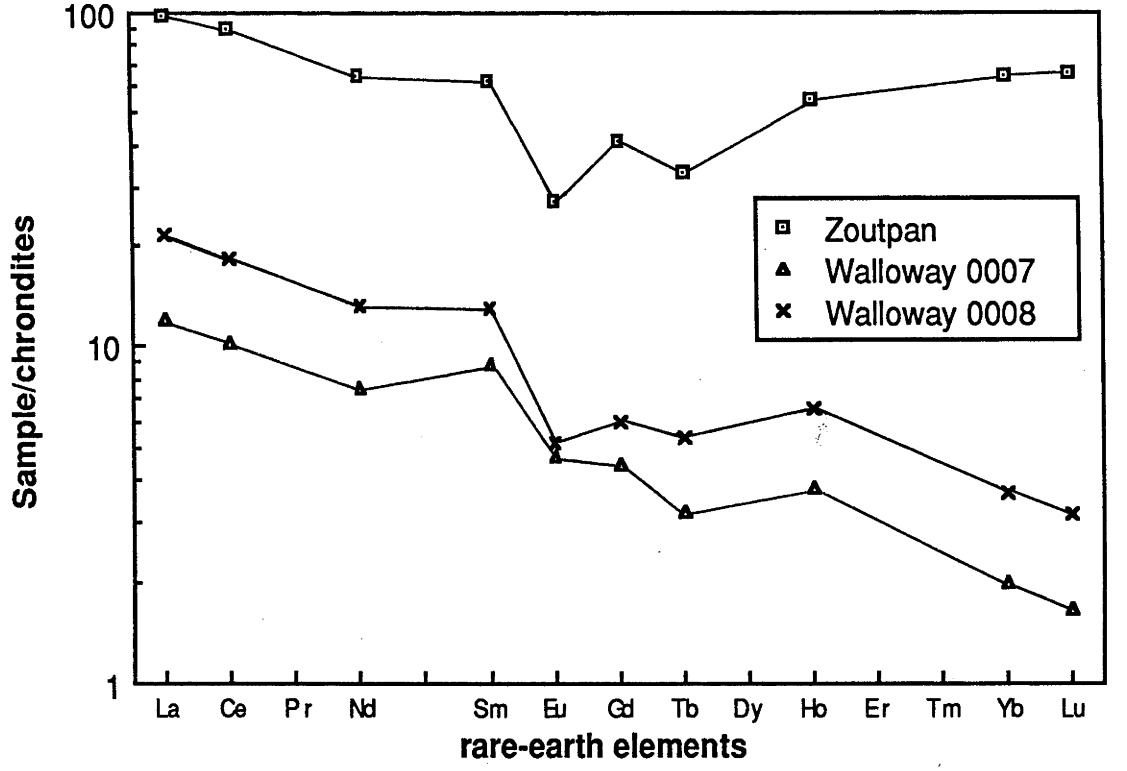

Fig. 8.5 Chondrite-normalised (from Taylor and Gorton 1977) rare-earth element abundance patterns for carbonates of sedimentary origin from Zoutpan and Walloway.

complexes display considerable isotopic heterogeneity, possibly as a result of late-stage hydrothermal processes. Nevertheless, it is apparent from Fig. 8.6 that most carbonatites fall within a restricted range of initial $^{87}Sr/^{86}Sr$ of between 0.7025 to 0.7036 and have initial ε_{Nd} between 0 and +4. The Walloway

Table 8.2 Sr and Nd isotopic results for carbonatites, associated alkaline igneous rocks and the Zoutpan sedimentary carbonate.

	Sample	Rb	Sr	Sm	Nd	$^{87}Rb/^{86}Sr$	$^{87}Sr/^{86}Sr$ meas	$^{87}Sr/^{86}Sr$ initial	$^{147}Sm/^{144}Nd$	$^{143}Nd/^{144}Nd$[a]	$\varepsilon_{Nd}(0)$[b]	ε_{Nd}
		ppm										
Australia												
Strangways Range, Northern Territory (732 ±5 Ma; Black and Gulson 1978)												
2015	Mudtank carb.	9.97	2731	18.23	116.3	0.0105	0.70329±5	0.7032	0.0948	0.51151±2	-6.5	+3.2
Walloway/Terowie, South Australia (160 - 180 Ma; Stracke *et al.*, 1979)												
0009	carbonatite	2.91	999.4	16.61	126.8	0.0084	0.70547±4	0.7054	0.0792	0.51175±2	-1.6	+0.9
0081	carb. kimb.	4.66	1463	17.54	129.2	0.0092	0.70490±4	0.7049	0.0821	0.51172±2	-2.3	+0.2
0090	kimberlite	130	461.6	9.54	58.32	0.8170	0.7085[c]		0.0989	0.51192±3	+1.7	+3.8
Mt Weld, Western Australia (2060 Ma; Willett *et al.*, 1986, this study)												
MW-1	carbonatite	23.2	6033	40.88	244.5	0.0111	0.70235±5	0.7020	0.1011	0.51057±2	-24.8	+0.3
MW-2	carbonatite	18.6	7410	50.61	297.7	0.0072	0.70220±6	0.7020	0.1028	0.51060±2	-24.2	+0.4
Magnet Cove, Arkansas (97 Ma; Zartman *et al.*, 1967)												
MC-1	carbonatite	5.38	5597	5.35	33.53	0.0028	0.70360±4	0.7036	0.0965	0.51197±2	+2.6	+3.8
Kaiserstuhl, Germany (16 - 18 Ma; Wimmenauer 1966)												
K-2	carbonatite	12.6	17989	11.63	108.5	0.0020	0.70362±4	0.7036	0.0648	0.51199±2	+3.0	+3.2
K-3	carbonatite	10.6	15012	14.07	131.5	0.0020	0.70368±4	0.7037	0.0647	0.51201±2	+3.4	+3.6
K-1	phonolite	157	4281	8.39	87.26	0.1057	0.70406±3	0.7040	0.0581	0.51196±2	+2.4	+2.7
K-6	phonolite	200	1435	6.75	60.74	0.2995	0.70423±3	0.7042	0.0673	0.51196±2	+2.3	+2.6
K-5	lava clast	165	991	8.56	49.01	0.4823	0.70434±6	0.7042	0.1056	0.51199±2	+2.9	+3.2
Fen, Norway (≈550 Ma; see Mitchell and Crocket 1970)												
NBS-18	carbonatite	0.26	6457	22.82	127.3	0.0001	0.70289±6	0.7029	0.1085	0.51167±2	-3.3	+3.0
Jacupiranga, Brazil (130 Ma; Amaral 1978, Roden *et al.*, 1985)												
5961	carbonatite	1.53	5370	26.30	152.5	0.0008	0.70507±6	0.7050	0.1043	0.51178±4	-1.1	+0.5
5963	carbonatite	0.27	6161	15.79	88.27	0.0001	0.70525±6	0.7052	0.1082	0.51174±4	-1.9	-0.4
Uganda (17 - 22 Ma; Baker *et al.*, 1971)												
6336	Napak carb.	0.930	1226	197.2	1453	0.0022	0.70325±3	0.7032	0.0821	0.51197±2	+2.7	+2.9
	(25 - 55 Ma; Baker *et al.*, 1971)											
6330	Tororo carb.	0.056	7100	60.31	354.2	-	0.70360±3	0.7036	0.1030	0.51187±2	+0.7	+1.1
6335	Sukulu carb.	0.063	2783	16.83	101.1	-	0.70311±4	0.7031	0.1007	0.51199±2	+3.1	+3.5
Kangankunde, Malawi (126 ±6 Ma; Snelling 1965)												
3432	carbonatite	0.013	>20000	720	8620	-	0.70313±4	0.7031	0.0505	0.51187±3	+0.8	+3.1
Nachendazwaya, Tanzania (≈655 Ma; Snelling *et al.*, 1964)												
7122	carbonatite	0.48	3754	24.03	130.0	0.0004	0.70251±4	0.7025	0.1118	0.51160±2	-4.6	+2.5
Goudini, South Africa (≈1.2 Ga; Verwoerd 1966, Harmer 1986, this study)												
33174	carbonatite	32.1	1637	34.98	187.4	0.0565	0.70389±4	0.7029	0.1129	0.51116±2	-13.2	+0.2
33176	carbonatite	1.18	3705	30.32	94.06	0.0009	0.70272±4	0.7027	0.1949	0.51180±2	-0.6	-0.4
Zoutpan, South Africa												
33182	carbonate	0.719	277.1	9.875	36.59	-	0.71853±5		0.1632	0.51116±2	-13.2	

[a] Nd isotopic ratios normalised using $^{146}Nd/^{142}Nd = 0.636151$. BCR-1 standard measured in this laboratory is 0.511833±20. NBS-987 $^{87}Sr/^{86}Sr$ is measured at 0.71022±4, E & A standard carbonate is 0.70800±3. All errors quoted refer to within-run precision at the 95% confidence level.

[b] Epsilon notation calculated using $^{143}Nd/^{144}Nd_{CHUR} = 0.511836$, $^{147}Sm/^{144}Nd_{CHUR} = 0.1967$. Decay constants used are those recommended by Steiger and Jäger (1977) and $\lambda_{Sm} = 6.54 \times 10^{-12}\ yr^{-1}$.

[c] Rb-Sr concentration and isotope data from Stracke *et al.* (1979).

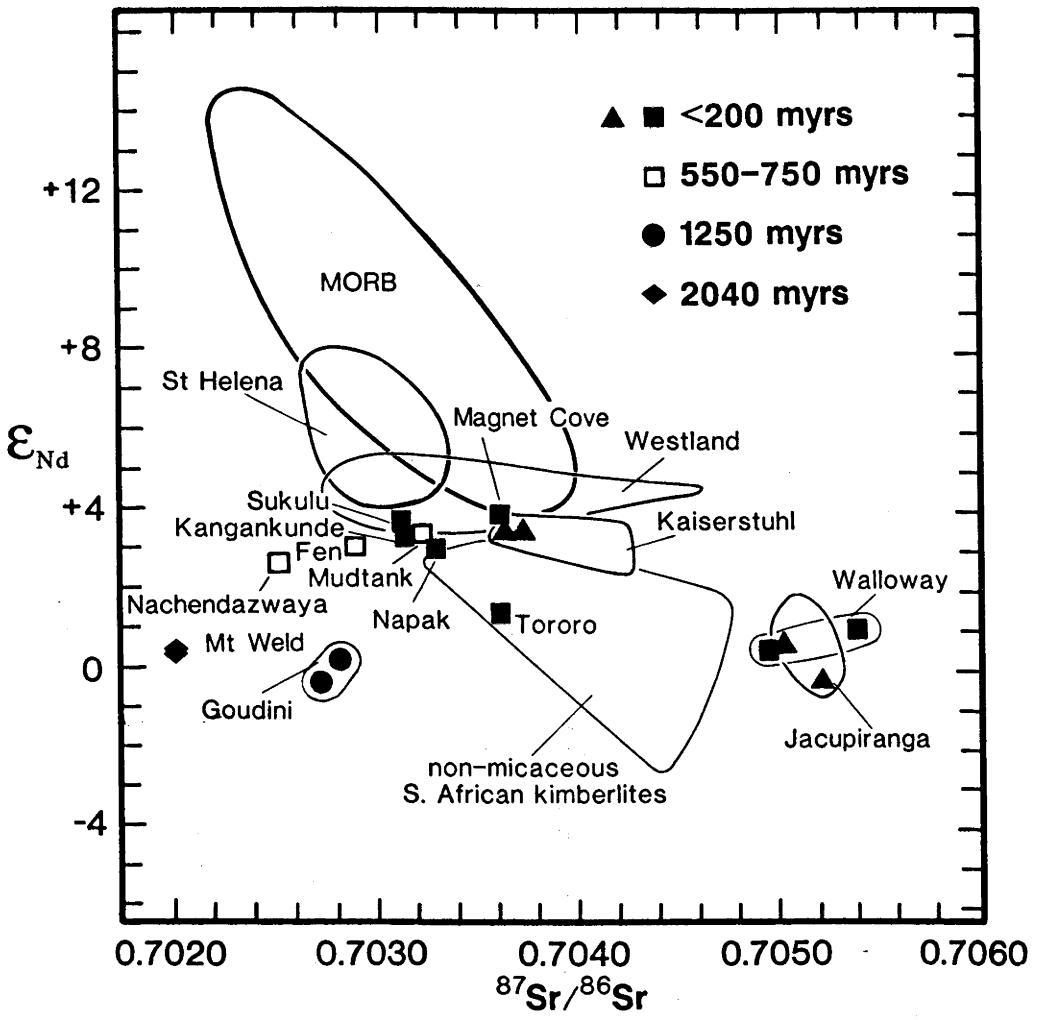

Fig. 8.6 Initial ε_{Nd} versus initial $^{87}Sr/^{86}Sr$ for carbonatites compared to the fields for MORB, Group 1 (basaltic) South African kimberlites and alkali basalts from the St Helena isotopic type of ocean islands (comprising St Helena, Ascension, Comoros and Austral ocean islands). The carbonatites have been separated into four age groups. Mixtures of a component isotopically resembling young carbonatite and the depleted MORB mantle reservoir could generate the Sr and Nd isotopic characteristics of some ocean-island basalts. Additional data sources; Roden *et al.* (1985), Barreiro (1983), Smith (1983), Vidal *et al.* (1984), White and Hofmann (1982), O'Nions *et al.* (1977), Dupré and Allègre (1980), Cohen and O'Nions (1982a, b).

carbonatite and the associated carbonated micaceous kimberlite have initial Nd isotopic compositions within this range but have more radiogenic initial $^{87}Sr/^{86}Sr$ of 0.7049 and 0.7054 respectively.

Although Stracke *et al.* (1979) obtained a phlogopite- whole-rock two-point Rb-Sr isochron for the Terowie kimberlitic intrusion, a sufficiently precise initial $^{87}Sr/^{86}Sr$ could not be determined. The Jacupiranga carbonatite also possesses significantly more radiogenic Sr than the other carbonatites despite having ε_{Nd} values (-0.4 and +0.5) which are only slightly lower than the range of isotopic compositions of most of the other examples. The younger African (i.e. Sukulu, Tororo, Lokupoi and Kangankunde) and Westland carbonatites fall below the mantle array and below the fields of St Helena, Austral, Comoros and Ascension ocean-island basalts on the initial Sr-Nd isotope diagram (Fig. 8.6). The older occurrences, such as the Proterozoic Mt Weld and Goudini carbonatites, the late Precambrian Mudtank and Nachendazwaya carbonatites and the Cambrian Fen carbonatite, have generally less radiogenic initial $^{87}Sr/^{86}Sr$ and similar ε_{Nd} values compared to those of younger carbonatites. Phonolites associated with

the Kaiserstuhl carbonatite occurrences have ε_{Nd} within analytical error of the carbonatites but have slightly more radiogenic initial $^{87}Sr/^{86}Sr$.

The age-corrected ε_{Nd} and initial $^{87}Sr/^{86}Sr$ values of ~ -10 and 0.7185 respectively for the Zoutpan sample (assuming a Cretaceous emplacement age) are also unlike those of the other examples and supports the earlier assertion that this sample is probably a carbonate of sedimentary origin.

As with many ocean-island and continental alkali basalts, the Nd isotopic characteristics of most of the carbonatites examined in this study indicate their derivation from sources with time-integrated near-chondritic LREE/HREE or slight LREE-depletion, despite the LREE-enrichment evident in the magmas themselves. The initial Sr and Nd isotopic characteristics of carbonatites of various ages from throughout the world therefore indicate derivation from sources which have had generally similar long-term evolutionary histories.

Sr and Nd isotopic data for the Jugiong kimberitic intrusions of southeast New South Wales are given in Table 8.3. The results indicate that the intrusions possess $^{87}Sr/^{86}Sr$ and ε_{Nd} values (0.7046 to 0.7056 and ~ 0 respectively) which overlap with those of Group 1 (basaltic) South African kimberlites. The Sr and Nd isotopic compositions of the Jugiong intrusions are also generally similar to those of some carbonatites (e.g. the Jacupiranga and Walloway carbonatites).

8.4.3 U-Pb isotope analysis

Whole-rock U and Pb concentration and Pb isotopic composition analyses are given in Table 8.4. The carbonatites possess an extremely wide range of U and Pb concentrations and U/Pb ratios. Corrections to the Pb isotope ratios for post-emplacement radiogenic decay of U and Th are significant for Mudtank, Walloway, Nachendazwaya and Goudini samples and the age-corrected Pb isotopic compositions will be reliable only if there has been no mobility of U, Th or Pb since their emplacement. Age corrections to the remaining examples are relatively small due to either the younger emplacement ages, lower U/Pb ratios or a combination of these factors. For example, the Cambrian Fen carbonatite requires a correction of -0.33 (or 1.6%) to the $^{206}Pb/^{204}Pb$ and the correction to $^{207}Pb/^{204}Pb$ is within the analytical uncertainty. Due to possible error in the Th/Pb correction assumptions (age corrections have been applied using thorium abundances calculated from the INAA-determined Th/U ratio and the isotope dilution uranium abundances), a much larger uncertainty applies to the calculated initial $^{208}Pb/^{204}Pb$ ratios. Despite the wide variation in U/Pb, most of the carbonatites have radiogenic Pb isotopic compositions (Fig. 8.7) and plot along the Pb-Pb array determined for mid-ocean ridge and ocean-island basalts. Kaiserstuhl samples overlap the field of the Society group of ocean islands, whereas the younger African carbonatites have considerably more radiogenic Pb which extends beyond the St Helena field. Similar radiogenic Pb compositions were found in Ugandan carbonatites (including samples from Napak, Sukulu and Tororo) by Lancelot and Allègre (1974). Radiogenic initial Pb compositions have also been reported by Grünenfelder *et al.* (1986) for the Cretaceous Oka carbonatite from Quebec and by Williams *et al.* (1986) for the Oldoinyo Lengai carbonatite. The Cambrian Fen carbonatite has an initial Pb isotopic composition similar to that of some Ugandan carbonatites.

The Jacupiranga carbonatite is exceptional in having unradiogenic initial Pb and lies to the unradiogenic side of the modern geochron, although it still plots along an extension of the Pb-Pb array of

Table 8.3 Strontium and neodymium isotopic analyses of Jugiong kimberlitic intrusions.

	Rb	Sr	Sm	Nd	$^{87}Rb/^{86}Sr$	$^{87}Sr/^{86}Sr$[a] meas	initial	$^{147}Sm/^{144}Nd$	$^{143}Nd/^{144}Nd$[b]	ε_{Nd}
	-----ppm-----									
Intrusion 1, kimberlite										
0041	26.2	794	8.02	43.68	0.0950	0.70501±5	0.7050	0.111	0.51183 ±2	-0.1
Intrusion 2, kimberlite lapillus										
0047	48.7	1289			0.1089	0.70465±8	0.7046			
Intrusion 4, kimberlite autolith										
0067A	45.5	779	7.73	41.20	0.1687	0.70560±5	0.7056	0.113	0.51184 ±3	+0.0
Intrusion 4, kimberlite autolith										
0067B	49.6	944	7.09	38.56	0.1517	0.70561±8	0.7056	0.111	0.51184 ±2	+0.1

[a] Errors refer to within run precision at the $2\sigma_{mean}$ level. Uncertainty in $^{87}Rb/^{86}Sr$ is 0.5% (2σ). Sr isotope ratios normalised using $^{86}Sr/^{88}Sr = 0.1194$. Initial Sr isotopic composition calculated using an emplacement age of 11 Ma (from Stracke *et al.* 1979). NBS-987 standard value is 0.71022 ±4, E & A standard carbonate gives 0.70800 ±3.

[b] Error in $^{147}Sm/^{144}Nd$ is 0.1% (2σ). Nd isotopic ratios normalised using $^{146}Nd/^{142}Nd = 0.636151$. Age corrections to Nd isotopic compositions are within the analytical error. The value obtained for BCR-1 standard is 0.511833 ±20. $\varepsilon_{Nd} = (^{143}Nd/^{144}Nd_{meas}/^{143}Nd/^{144}Nd_{CHUR} -1) \times 10^4$ where $^{143}Nd/^{144}Nd_{CHUR} = 0.511836$.

modern oceanic basalts. Roden *et al.* (1985) demonstrated that the Jacupiranga carbonatite is isotopically heterogeneous, with later intrusions possessing slightly more radiogenic initial Sr isotopic compositions, and argued that the Sr and Nd isotopic composition of the Jacupiranga carbonatite has been modified by crustal assimilation. If the Pb isotopic composition of the Jacupiranga intrusion has also been modified by crustal assimilation, its unradiogenic Pb isotopic compositions suggest that this assimilation probably occurred within the lower crust, as the lower crust is generally believed to be depleted in U and to possess unradiogenic Pb. The stable-isotope characteristics of the Jacupiranga carbonatite (see below) have apparently not been affected by assimilation of the extensive amounts of crustal material required to modify the Sr isotopic composition.

The large difference in both the Sm/Nd and U/Pb ratios of the two Goudini samples enables determination of the age of emplacement. Regression of the Goudini analyses gives an Sm-Nd age of 1190 ±80 Ma and a similar but imprecise Pb-Pb age of 1110 ±300 Ma (1σ errors given on ages). These emplacement ages are similar to those determined for a variety of alkaline rocks and kimberlites from the region (Harmer 1986). The two Mt Weld Pb analyses yield a Pb-Pb age of 2090 ±10 Ma, within error of the K-Ar age of 2064 ±40 Ma but statistically significantly older than the Rb-Sr age of 2020 ±17 Ma (Willett *et al.* 1986).

The Zoutpan carbonate sample #33182, although of probable sedimentary origin, also possesses high U abundance, high μ and radiogenic measured Pb isotopic compositions (Table 8.4). The Walloway limestones also have generally high inferred μ values. This observation suggests that uranium is preferentially enriched relative to Pb in sedimentary carbonates, either during deposition or by post-

Table 8.4 Lead, oxygen and carbon isotopic analyses of carbonatites, some associated alkaline igneous rocks and the Zoutpan sedimentary carbonate.

Sample		U	Pb	$^{238}U/^{204}Pb$	$^{206}Pb/^{204}Pb$[a]		$^{207}Pb/^{204}Pb$		$^{208}Pb/^{204}Pb$		$\delta^{18}O$	$\delta^{13}C$
		-ppm-			meas	initial	meas	initial	meas	initial[b]	SMOW	PDB
Australia												
Strangways Range, Northern Territory												
2015	Mudtank carb.	0.391	3.12	9.20	18.538	17.38	15.589	15.52	38.840	-	+7.5	-3.6
Walloway/Terowie, South Australia												
0009	carbonatite	7.08	5.81	98.4	21.743	19.11	15.784	15.65	42.814	-	+8.3	-1.8
0081	carb. kimb.	7.71									+12.2	-6.5
0090	kimberlite	4.42	12.17	27.5	19.547	18.84	15.642	15.61	40.008	-	-	-
Mt Weld, Western Australia												
MW-1	carbonatite	-	24.5	-	50.476	-	19.484	-	264.72	-	+8.9	-5.6
MW-2	carbonatite	-	25.6	-	244.09	-	44.56	-	71.20	-	+7.2	-5.4
Magnet Cove, Arkansas												
MC-1	carbonatite	-	0.815	-	18.95		15.50		38.58		+7.5	-5.4
Kaiserstuhl, Germany												
K-2	carbonatite	2.38	3.73	47.7	19.357	19.23	15.604	15.60	39.288	39.1	+7.8	-6.5
					19.334	19.21	15.626	15.62	39.351	39.2		
K-3	carbonatite	5.70	3.57	119	19.487	19.17	15.601	15.59	39.263	39.3	+7.8	-6.6
K-1	phonolite	19.07	35.05	40.9	19.490	19.38	15.673	15.67	39.493	39.4	-	-
K-6	phonolite	2.52	30.43	6.19	19.197	19.18	15.673	15.67	39.468	39.4	-	-
K-5	lava clast	2.26	3.91	43.3	19.573	19.46	15.646	15.64	39.357	39.2	-	-
Fen, Norway												
NBS-18	carbonatite	0.282	5.84	3.73	20.442	20.11	15.701	15.68	40.696	-	+7.2	-5.0
Jacupiranga, Brazil												
5961	carbonatite	0.013	4.58	0.20	17.273	17.27	15.457	15.45	37.970	37.9	+7.1	-6.1
5963	carbonatite	0.237	9.13	1.84	17.140	17.10	15.445	15.44	37.800	37.7	+7.3	-5.6
Uganda												
6336	Napak carb.	0.566	40.52	1.08	20.719	20.71	15.780	15.78	40.379	40.1	+12.4	-2.0
6330	Tororo carb.	0.350	6.34	4.33	21.068	21.04	15.865	15.86	41.112	40.5	+11.1	-2.1
6335	Sukulu carb.	0.027	1.06	1.97	21.154	21.14	15.781	15.78	40.646	40.6	+7.3	-2.9
Kangankunde, Malawi												
3432	carbonatite	0.077	89.3	0.065	20.115	20.11	15.772	15.77	39.660	-	+5.5	-3.0
Nachendazwaya, Tanzania												
7122	carbonatite	4.11	6.82	63.6	48.804	42.00	17.847	17.43	38.545	-	+9.6	-4.2
Goudini, South Africa												
33174	carbonatite	2.29	12.28	17.9	22.005	18.17	15.856	15.54	57.940	-	+17.4	-0.5
33176	carbonatite	2.03	36.7	4.43	18.409	17.46	15.580	15.50	45.681	-	+13.8	-2.4
Zoutpan, South Africa												
33182	carbonate	2.87	6.80	42.1	29.125		16.722		53.665		+12.9	-1.8

[a] Analyses of NBS-981 common-Pb standard gave $^{206}Pb/^{204}Pb$ =16.927 ±0.009, $^{207}Pb/^{204}Pb$ =15.486 ±0.013, $^{208}Pb/^{204}Pb$ = 36.668 ±0.044 (1σ errors).

[b] Corrections to $^{208}Pb/^{204}Pb$ made using Th/U ratio determined by INAA.

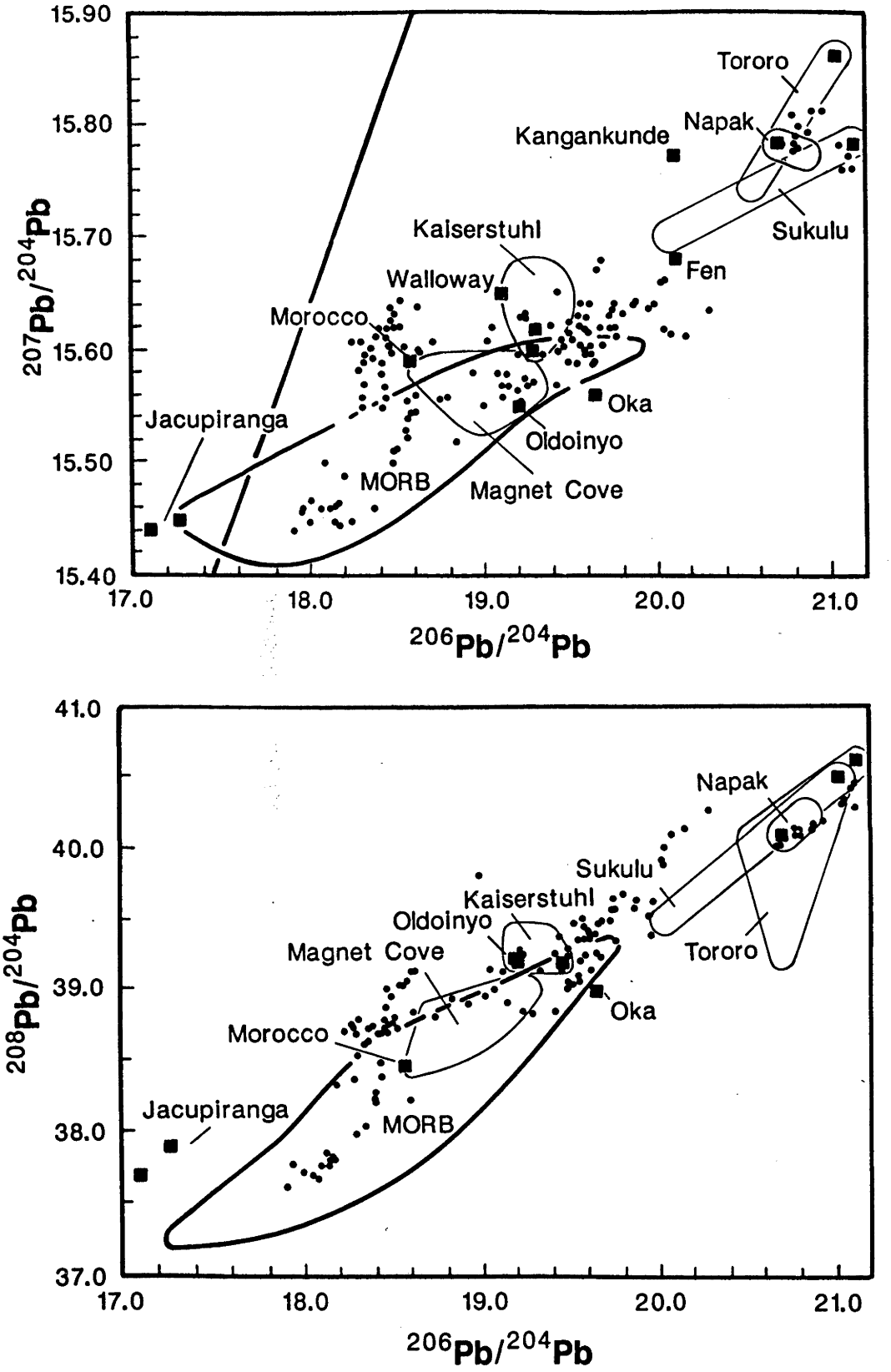

Fig. 8.7 a). $^{206}Pb/^{204}Pb$ versus $^{207}Pb/^{204}Pb$ and b). $^{206}Pb/^{204}Pb$ versus $^{208}Pb/^{204}Pb$ for carbonatites compared to the fields for MORB, and the St Helena isotopic type of ocean islands (individual data-points, taken from the literature, are shown). Some of the samples in Table 8.4 require relatively large age corrections, so only samples for which initial Pb compositions can be confidently determined are shown. In general, carbonatites have Pb isotopic compositions which fall along the array defined by oceanic (mid-ocean ridge and ocean-island) basalts. Data sources as in Fig. 8.4 and Lancelot and Allègre (1974), Sun (1980), Grünenfelder *et al.* (1986), Williams *et al.* (1986) and Tilton *et al.* (1987).

depositional processes.

8.4.4 O and C isotope analysis

$^{18}O/^{16}O$ and $^{13}C/^{12}C$ results are given in Table 8.4 and shown graphically in Fig. 8.8. The carbon and oxygen isotopic compositions of Kaiserstuhl, Tororo and Sukulu carbonatites from this study fall within the ranges determined for these localities by previous studies (Gonfiantini and Tongiorgi 1964, Deines and Gold 1973; see Fig. 8.8). The results of Pineau *et al.* (1973) and this study indicate similar carbon but slightly heavier oxygen isotopic compositions for the Lokupoi carbonatite compared to those of the other Ugandan carbonatites. The Cretaceous Kangankunde carbonatite has a carbon isotopic composition within the range of $\delta^{13}C$ obtained by Suwa *et al.* (1975) (averaging -3.4 ‰ using only those samples with $\delta^{18}O$ between +6 and +8 ‰) for the Mbeya carbonatite of similar age (Snelling 1965) located near the southwest border of Tanzania, whereas the late Precambrian Nachendazwaya example, situated near the Mbeya carbonatite, has slightly lighter carbon. These results support the assertion of Deines and Gold (1973) of regional variation in the carbon isotopic compositions of carbonatites from East Africa, with the inter-rift region surrounding Lakes Victoria, Malawi and Chilwa (where Tororo, Sukulu, Lokupoi, Kangankunde and Nachendazwaya carbonatites are located) characterised by higher ^{13}C contents (between -2.4 and -4.4 ‰) compared to their results for carbonatites located within the East and West African Rifts (-5.8 to -7.9 ‰).

The Goudini complex consists predominantly of ejected tuffaceous material and breccia (Verwoerd 1966). Deines and Gold (1973) have observed that volcanically emplaced carbonatites generally display greater carbon and (especially) oxygen isotopic variability than plutonic carbonatites and attributed this to the greater opportunities available for isotopic exchange during emplacement of the volcanic carbonatites. The heavy carbon and oxygen compositions of the Goudini samples compared with results obtained from other localities probably reflect greater loss of isotopically light carbon and oxygen during their emplacement and substantial post-emplacement isotopic exchange of these samples with their surroundings.

Carbon- and oxygen- isotope analyses for the Mudtank carbonatite from this study are significantly heavier than those reported by Wilson (1979). Correction of Wilson's (1979) results to account for recent re-calibration of the C.S.I.R.O. internal standard (for $\delta^{13}C_{PDB}$, from -12.8 to -13.3 ‰ and for $\delta^{18}O_{PDB}$, from -5.6 to -5.3 ‰) indicates $\delta^{13}C_{PDB}$ and $\delta^{18}O_{SMOW}$ values of -4.8 and +7.2 ‰ respectively, compared to our results of -3.6 and +7.5. The slight discrepancy between these two data sets may reflect some carbon- and oxygen- isotope heterogeneity in this intrusion.

Many of our carbonatite samples have oxygen- isotope compositions outside the range of +6 to +8 ‰ vs SMOW, considered by Deines and Gold (1973) to represent the range of values expected for primary carbonatites. However, there is compelling evidence from the large amount of ^{13}C data on carbonatites for the existence of considerable isotopic heterogeneity which is difficult to attribute entirely to secondary processes. Although the regional ^{13}C compositions displayed by the African rift carbonatites noted by Deines and Gold (1973) may be due to subtle regional differences, either in the style of emplacement or in the basement rocks through which the carbonatites intrude, these differences may also indicate that the sources of carbonatites are isotopically heterogeneous. If this is the case for ^{13}C, it is probable also for

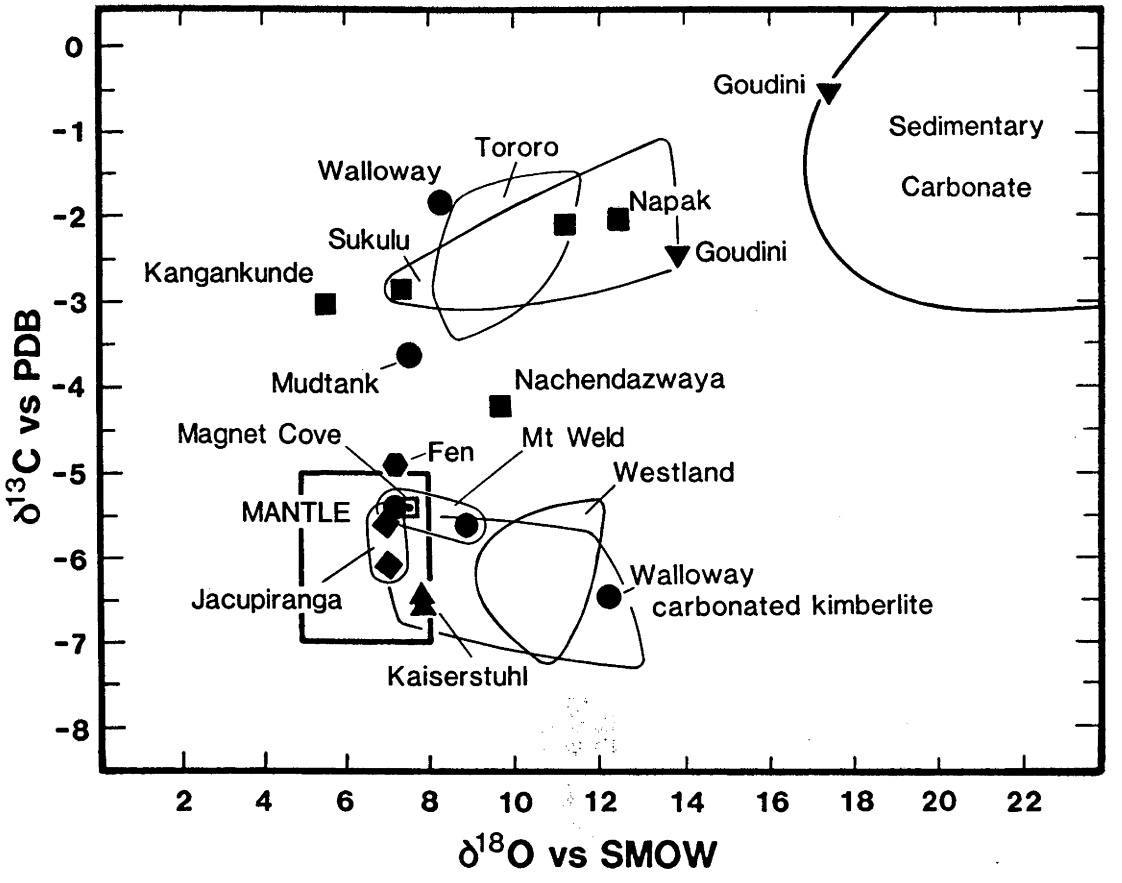

Fig. 8.8 Oxygen- and carbon- isotope compositions of carbonatites compared to the inferred mantle field (determined from isotopic studies of MORB, from Des Marais and Moore, 1984 and Kyser *et al.* 1982) and to the field of sedimentary carbonate. Additional data from Deines and Gold (1973) and Blattner and Cooper (1974). The isotopically heavy oxygen and carbon of the volcanically-emplaced Goudini carbonatite may result from greater degree of isotopic exchange during its emplacement compared to intrusively-emplaced carbonatites. The trend toward isotopically heavier carbon and oxygen compared to inferred mantle compositions may be attributable to crustal interaction during emplacement, Rayleigh fractionation processes (i.e. preferential loss of the lighter isotopes in volatile phases) or may reflect differences within the source regions of carbonatites.

^{18}O. Distinguishing between the effects of primary and secondary variation in oxygen (and to a lesser extent, carbon) isotopic compositions is, however, likely to prove difficult even with detailed sampling of each locality.

A recent study of carbon isotopic compositions in mid-ocean ridge basalts by Des Marais and Moore (1984) has also found $\delta^{13}C$ values between -5 and -7 ‰. Kyser *et al.* (1982) reported a range of $\delta^{18}O$ for mantle-derived basic lavas between +4.9 to +8.3 ‰, with most mid-ocean ridge and alkali basalts having values between +5.0 and +6.2 ‰. If these compositions are typical of mantle values, they indicate that most carbonatites have similar or slightly higher $\delta^{13}C$ and $\delta^{18}O$ values compared to mantle values. Two exceptions, both of which have considerably lighter $\delta^{13}C$ values, are the modern Oldoinyo Lengai carbonatite volcano (Suwa *et al.* 1975), whose lavas are deliquescent and readily exchange carbon and oxygen with the atmosphere, and the recently discovered carbonatites from the Murun alkalic block, Aldan (Plyusnin *et al.* 1984).

8.5 Discussion

8.5.1 Geochemical characteristics of carbonatites and associated magmatism

Although magmas parental to carbonatites are probably generated by extremely low degrees of partial melting of a peridotitic or eclogitic source and are therefore likely to have high abundances of incompatible trace elements, the trace-element characteristics of carbonatites are anticipated to be strongly influenced by the operation of complex secondary processes such as extensive differentiation, liquid immiscibility or volatile transport. The pronounced negative anomalies of U, Zr, Hf, Nb, Ta and Ti displayed by the carbonatites in Fig. 8.2 may be attributed entirely to late-stage fractional crystallisation processes, including removal of sphene, apatite, perovskite, monazite or zircon. However, abundances of Ba, P and Sr are in most cases not anomalous compared with the degree of enrichment displayed by the light and middle REE which have similar incompatibility. Apart from negative anomalies for K, the Goudini and Walloway carbonatites have relatively smooth trace-element abundance patterns (Fig. 8.2) suggesting that they have not undergone extensive modification by secondary processes. Negative K anomalies are also common in the trace-element patterns of ocean-island basalts (see Fig. 8.2) and may be characteristic of ocean-island sources. The Goudini and Walloway carbonatites have similar HREE abundances but have significantly higher SiO_2, Cr, Sc, Ni and Co concentrations compared to the other examples, consistent with the suggestion that they have undergone substantially less differentiation.

As the Nd isotopic compositions of carbonatites indicate that they are derived from sources having time-integrated near-chondritic LREE/HREE or slight LREE-depletions, generation of the extreme LREE/HREE of carbonatites requires either an unusual source mineralogy, specialised conditions during melt generation and extraction processes or the operation of suitable secondary differentiation processes. Wendlandt and Harrison (1979) demonstrated that the HREE are preferentially partitioned into the carbonate melt during carbonate/silicate immiscibility. Carbonatites typically have low abundances of the HREE, suggesting that immiscibility processes are not responsible for the REE fractionation. These authors have also shown that the LREE are fractionated into any CO_2-vapour phase present relative to silicate or carbonate melts, especially at low pressures. Transport of the LREE in a vapour phase may therefore contribute to the extreme LREE-enrichment of carbonatites. However, many carbonatites possess enrichments in the elements Ba, Sr and P similar to that of the REE (evident from the relatively flat normalised patterns of these elements in Fig. 8.2). This is unlikely to be due to melt/vapour enrichment processes but instead, suggests that the enrichment is due to partial melting processes. Modelling of La/Yb ratios indicates that modal, non-modal or fractional partial melting of garnet lherzolite or eclogite like those found as xenoliths in kimberlite pipes is incapable of producing the extreme La/Yb ratios found in some kimberlites and carbonatites (Fig. 8.9; see Appendix A2.4 for a listing of the computer program used). McKenzie (1985) has suggested that because of the extremely low viscosity of carbonate melts, segregation of very small melt fractions (as low as 0.1%) on geologically reasonable timescales may be possible. Extreme fractionation of La from Yb can occur in low melt fractions (<~1%) generated from eclogitic sources with relatively high modal abundances of garnet (i.e. Gnt_{80}:Cpx_{20}, see Fig. 8.9). Under these circumstances, the extreme LREE-enrichment and low HREE abundances of carbonatites may be a primary magmatic feature and may not require the operation of

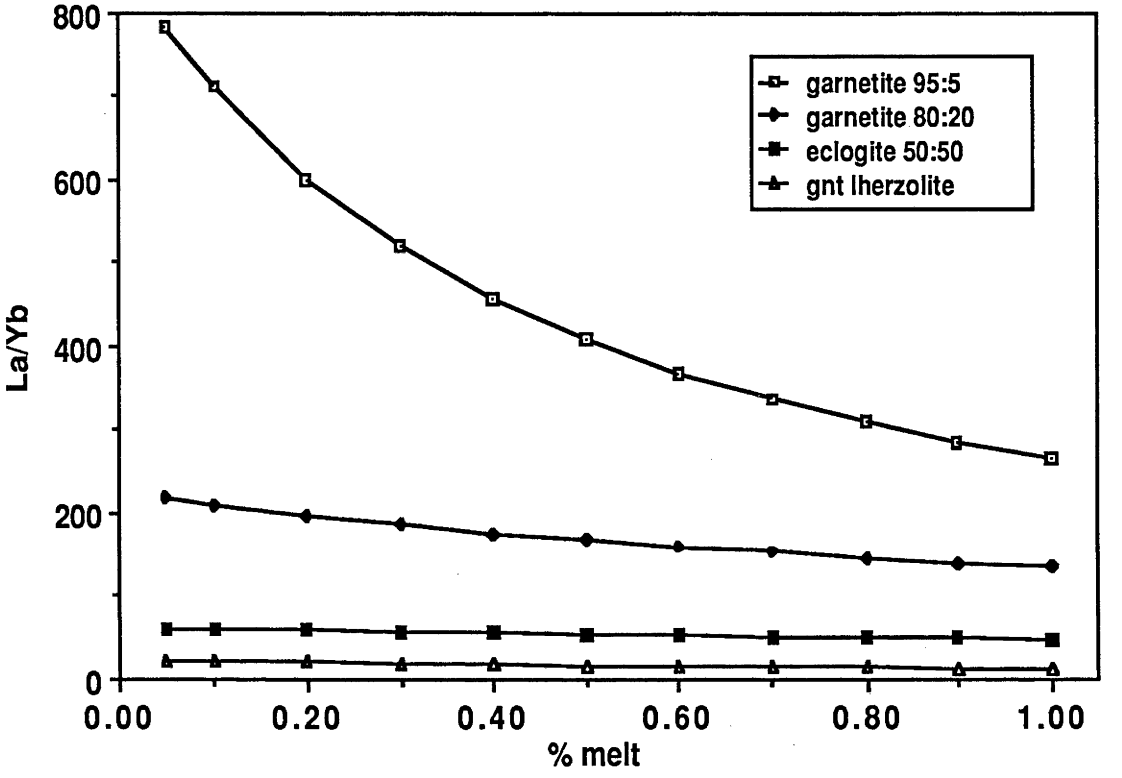

Fig. 8.9 Enrichment of La to Yb produced by different degrees of modal melting a of garnet lherzolite source (modal composition Ol_{70}:Opx_{20}:Cpx_5:Gnt_5) and for eclogitic sources with different modal proportions of garnet to clinopyroxene. The melting equations of Shaw (1970) and distribution co-efficients of Wood (1979) have been used. Non-modal or continuous fractional melting produce similar curves to those of modal melting for the conditions examined. Carbonatites and kimberlites typically have La/Yb ratios between 50 to 150.

secondary processes. This general conclusion is probably still valid for melts generated at high pressures even though it is possible that distribution co-efficients determined from rocks of low-pressure origin are not applicable at very high pressures or for highly volatile-rich melts. At depths greater than ~350 km, subducted basaltic oceanic crust is believed to transform to garnet-rich eclogitic assemblages (Ringwood 1982) and may therefore provide a suitable source material for carbonatite and kimberlite generation.

Small Ce- and Eu-anomalies have been observed in the rare-earth patterns of some carbonatites (e.g. Wimmenauer 1966, Loubet *et al.* 1972, Eby 1975, Möller *et al.* 1980). Eby (1975) demonstrated that many different mineral phases of the Oka carbonatite possess positive or negative Eu anomalies even though the whole rocks from which these phases were separated lack Eu anomalies. Both the Eu and Ce anomalies are therefore probably strongly influenced by competition for the REE between minerals and/or a volatile phase during late-stage crystallisation. Loubet *et al.* (1972) found a correlation between the magnitude of the negative Ce anomaly and $\delta^{18}O$ in Ugandan carbonatites and attributed this to increasing oxidation during carbonatite differentiation. This correlation might also be caused by melt/CO_2-rich vapour fractionation or by secondary alteration processes. The slight decoupling of LREE and HREE apparent in rare-earth element patterns of some differentiated carbonatites might reflect preferential substitution of the LREE and HREE into different mineral lattice sites during crystallisation (for example, the LREE in calcite Ca lattice sites or in monazite etc. and the HREE in zircon or in dolomite Mg and Fe sites) or may be due to vapour/melt fractionation processes.

8.5.2 Isotopic characteristics of carbonatites and associated magmatism

From the results of this and earlier studies, it is apparent that carbonatites comprise an isotopically relatively homogeneous group of magmas possessing a restricted range of radiogenic and (when the effects of secondary alteration processes are taken into account) stable-isotope characteristics. Most young carbonatites have initial $^{87}Sr/^{86}Sr$ ~0.703. Similar initial $^{87}Sr/^{86}Sr$ ratios have been reported by Bell and Powell (1970) and Bell *et al.* (1982) for Cambrian and mid- to late- Proterozoic examples from Ontario, Canada. However, a few carbonatites, such as the Na-rich carbonatite from the active Oldoinyo Lengai volcano in Tanzania (Bell *et al.* 1973) and carbonatites from India and Pakistan (Deans and Powell 1968) have considerably more radiogenic initial $^{87}Sr/^{86}Sr$ ratios. The Oldoinyo Lengai carbonatite has Nd (ε_{Nd} of ~0; DePaolo 1978, Bell and Blenkinsop 1987b) and Pb isotopic compositions ($^{206}Pb/^{204}Pb$ of 19.19, $^{207}Pb/^{204}Pb$ of 15.55 and $^{208}Pb/^{204}Pb$ of 39.14, given in Williams *et al.* 1986) similar to those of other carbonatites, although a wide range of $^{87}Sr/^{86}Sr$ ratios have been reported (Powell 1966, Bell *et al.* 1973, DePaolo 1978, Bell and Blenkinsop 1987b). Powell (1965) noted that vein carbonatites commonly possess more radiogenic Sr isotopic compositions than central intrusive complex examples. Because of their extreme concentrations of Sr, Powell (1965) argued against crustal contamination, but instead proposed that vein carbonatites were genetically unrelated to central intrusive complex carbonatites. The Walloway carbonatite is a vein carbonatite and although it possesses significantly more radiogenic Sr than the central intrusive complex carbonatites examined in this study, it has similar Nd and Pb isotopic compositions, suggesting that a genetic relationship does exist in this case. Involvement of late-stage fluids during emplacement of the Walloway carbonatite, suggested by petrographic features such as the rimming of mica phenocrysts by sodic amphibole, may have resulted in isotopic exchange of Sr with the country rock and may account for the more radiogenic Sr of this intrusion.

All Nd isotopic compositions so far reported for mid-Proterozoic to Recent carbonatites indicate time-integrated near-chondritic or depleted LREE/HREE histories, with most having ε_{Nd} values between 0 and +5. For example, Bell and Blenkinsop (1987a) reported initial ε_{Nd} values between 0 to +5 for twelve Canadian carbonatites ranging in age from 1900 to 110 Ma. Similar ε_{Nd} values to those reported by Bell and Blenkinsop (1987a) were presented by Kwon and Tilton (1986) for the early Proterozoic Cargill and Borden carbonatites from Ontario. Basu and Tatsumoto (1980) measured ε_{Nd} values of +3.3 and +5.3 (after correction for instrumental bias) for the Paleozoic McClure Mountains and Mesozoic Magnet Cove carbonatites respectively, whereas Sun *et al.* (1986) found an initial $^{87}Sr/^{86}Sr$ of 0.703 and ε_{Nd} of +2.0 ±0.4 for the late Proterozoic Cummins Range carbonatite of Western Australia. Midende *et al.* (1986) have reported similar initial $^{87}Sr/^{86}Sr$ and ε_{Nd} values for 3 carbonatites, of late Precambrian to Cretaceous age, from the western branch of the African rift. Cohen *et al.* (1984) also found similar isotopic characteristics ($^{87}Sr/^{86}Sr$ of 0.7035, ε_{Nd} of +1.8, $^{206}Pb/^{204}Pb$ of 20.60, $^{207}Pb/^{204}Pb$ of 15.77 and $^{208}Pb/^{204}Pb$ of 40.30) in an ankaramite from the Recent-age Lashaine carbonatite vent, Tanzania. An initial ε_{Nd} of between ~0 has also been determined for the late Archaean Siilinjarvi carbonatite, eastern Finland (A.R. Basu, personal communication). Furthermore, initial ε_{Nd} values of ~ +3.5 and $^{87}Sr/^{86}Sr$ of 0.7046 have been measured in alnoites from Malaita in the Solomon Islands (Basu and Tatsumoto 1980, Bielski-Zyskind *et al.* 1984). The Malaita alnöite was suggested by Allen and Deans (1965) to be genetically related to carbonatite, a suggestion later supported by Nixon *et al.* (1980).

However, the early Proterozoic Phalaborwa Complex, South Africa, is exceptional in having highly negative initial ε_{Nd} (Allsopp and Eriksson 1986). The Phalaborwa complex consists of a carbonatite core and closely associated alkali-rich dykes emplaced during many intrusive events and possesses considerable Sr and Nd isotopic diversity which is believed to be a primary feature of the magmatism (Allsopp and Eriksson 1986).

Bell and Blenkinsop (1986, 1987a) suggested that a correlation exists between the ages of Canadian carbonatites and their initial Sr and Nd isotopic compositions and argued that most Canadian carbonatites were derived from a common trace-element-depleted mantle source which had remained coupled to the Canadian Shield. However, this correlation is not confined only to carbonatites found within the Canadian shield but (when allowance is made for the influence of crustal contamination) is a global phenomenon (Fig. 8.10) and therefore does not provide support for a subcontinental lithospheric origin for carbonatites. Furthermore, this correlation does not necessarily require all carbonatites to be derived from a single common reservoir. As the correlation holds for carbonatites from a number of separate continents, it probably reflects ageing, at a similar rate, of a number of spatially discontinuous but isotopically similar reservoirs within the Earth. Moreover, the correlation strongly suggests that similar processes have been responsible for generating the sources of carbonatites worldwide. Barreiro (1983) proposed a two-stage mechanism involving freezing at depth and later re-activation of a carbonate-rich melt originally derived from depleted mantle to produce the Westland dyke swarm, New Zealand. However, as the Nd isotopic compositions of carbonatites produced by this mechanism are a function of the time elapsed between crystallisation and re-activation, the Nd isotopic consistency which is observed in carbonatites worldwide argues against the operation of this mechanism.

The possible role of CO_2 in the generation of highly alkaline continental magmatism is suggested by the close association between carbonatitic, nephelinitic and phonolitic magmatism in many alkaline complexes. Phonolites associated with the Kaiserstuhl carbonatite occurrences have ε_{Nd} values within analytical error of the carbonatites but have slightly higher initial $^{87}Sr/^{86}Sr$. Other studies (for example, Mitchell and Crocket 1970, Bell and Powell 1970, Bell *et al.* 1973, Barreiro 1983, Allsopp and Eriksson 1986) have also found a considerable range of Sr isotopic compositions for alkaline (potassic and nephelinitic) and carbonatite magmas from the same intrusive complex, with the alkaline silicate magmas commonly (but not universally) possessing the more radiogenic initial Sr isotopic compositions. In some cases, this isotopic variation may result from interaction of the alkaline silicate magmas with the wall rocks, as these magmas have considerably lower Sr contents compared to carbonatite magmas and are therefore more sensitive to contamination processes. Although carbonatites may have differentiated from an alkaline silicate parent, the lower $^{87}Sr/^{86}Sr$ of some carbonatites compared to the alkaline silicate magmas with which they are associated rules out the possibility that the carbonatite differentiated within a closed system from the alkaline silicate magmas in these complexes. Instead, the Sr isotopic variability suggests that in these complexes, the associated silicic magmas may not be directly genetically related to the carbonatites, but may have been generated during the passage of a CO_2-rich magma through the upper mantle and crust, as this is likely to induce melting in the surrounding mantle and crust wall-rocks.

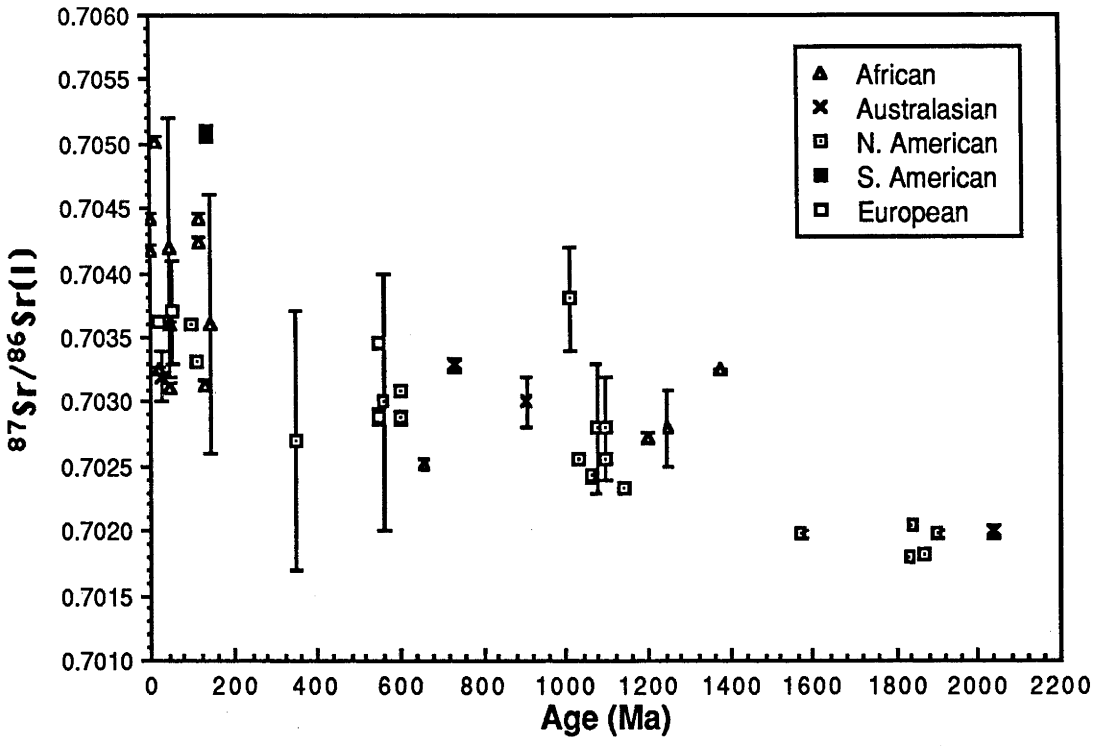

a).

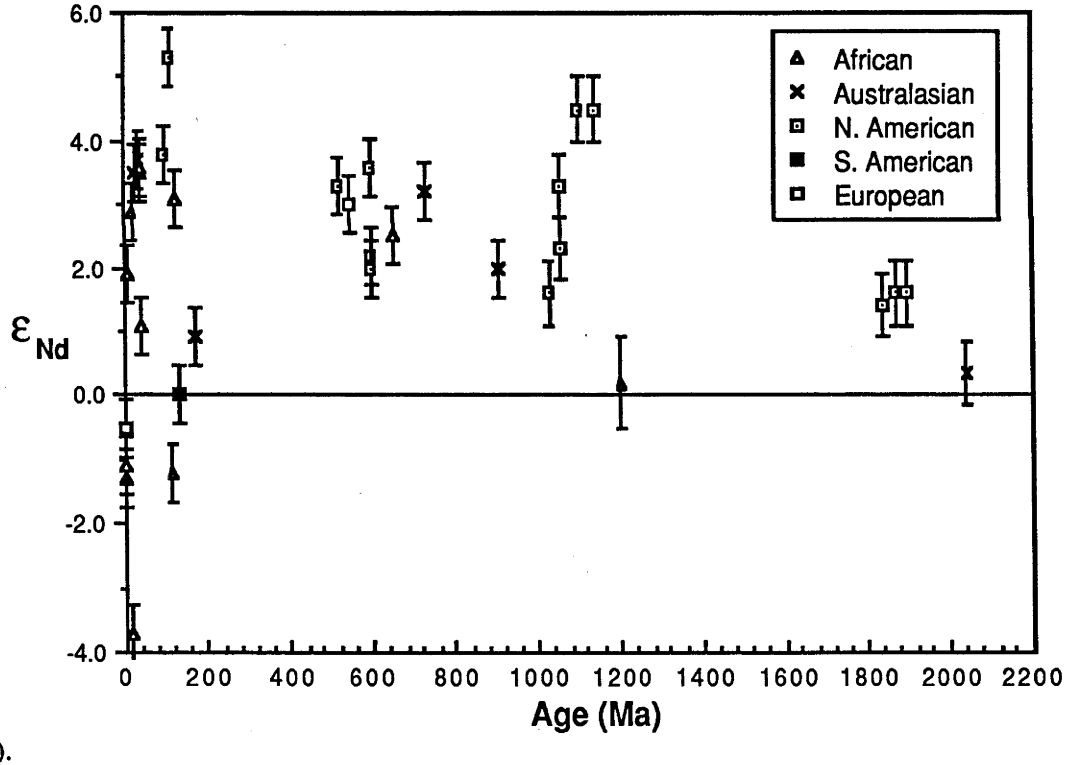

b).

Fig 8.10 a). Initial Sr, and b). Initial Nd isotopic composition versus age of emplacement for carbonatites from throughout the world. When the possible effects of crustal contamination are considered, there is a general trend to higher initial $^{87}Sr/^{86}Sr$ and ε_{Nd} for younger carbonatites. Analytical error limits are shown; no account has been made for error in the age determinations. Although this trend is relatively well-defined for the well-characterised Canadian carbonatites (see Bell and Blenkinsop 1987a), it is not confined to any one continent but is a global feature. Additional data sources; Bell and Powell (1970), Welke *et al.* (1974), Black and Gulson (1978), Stracke *et al.* (1979), Basu and Tatsumoto (1980), Barreiro (1983), Neilsen and Buchardt (1985), Grünenfelder *et al.* (1986), Bell and Blenkinsop (1987a, b).

8.5.3 Possible relationships between carbonatites, kimberlites and ocean islands

The similar Sr, Nd and Pb isotopic characteristics of most carbonatites and some ocean-island basalts suggest a common origin for these otherwise apparently unrelated magma groups. As carbonatites have extreme abundances of incompatible elements, it is conceivable that the basalts of some ocean islands represent mixtures between a carbonatitic component and (for example) a component derived from a depleted mantle reservoir. On the initial Sr-Nd isotope diagram (Fig. 8.6), many young carbonatites lie below the mantle array with the fields for many ocean-island basalts positioned between the field of young carbonatites and that of mid-ocean ridge basalts, consistent with this suggestion. The same applies for the Pb isotope characteristics (Fig. 8.7); many young carbonatites possess initial Pb isotopic compositions which lie along the array of ocean-island basalts. The isotopic similarities between ocean-island basalts and carbonatites raises the possibility that the sources of some ocean-island basalts consist of trace-element-depleted mantle, such as that from which mid-ocean ridge basalts are derived, which has been re-fertilised by incompatible-element-rich, low-viscosity carbonate melts. Alternatively, the isotopic similarities may indicate that carbonatites and ocean-island basalts are derived from sources which have had similar long-term isotopic histories but with the obvious chemical differences controlled by differences in other variables, such as degree of partial melting, depth of generation or CO_2 content in the sources. Although melts generated from peridotite following addition of a component with trace-element characteristics like that of carbonatite would be expected to inherit the large anomalies evident in the trace-element patterns of some carbonatites, as discussed earlier, these anomalies are probably due to high-level, late-stage differentiation processes. If carbonatitic magmas have relatively smooth normalised trace-element patterns prior to the extensive operation of differentiation processes (as is suggested by the trace-element patterns of the Walloway and Goudini carbonatites), evidence of fertilisation of the sources of ocean-island alkali basalts by these carbonatitic components would not be readily detectable. Such trace-element fertilisation of the source regions of alkali basalts alleviates the need for the low degrees of partial melting which the high abundances of incompatible trace elements of alkali basalts were thought to require.

If CO_2-rich components are involved in the generation of the alkali basalts of ocean islands, it might be anticipated that carbonatites would be common on ocean islands. As pointed out by Silva *et al.* (1981) and Le Bas (1984), when only plutonic rocks are considered, rocks belonging to the carbonatite-ijolite association are volumetrically relatively abundant on ocean islands. Moreover, the plutonic basement rocks of ocean islands are rarely exposed unless the island is subjected to uplift and extensive erosion, as in the case of the Cape Verde Islands. In addition, CO_2-rich magmas intruding continental regions must pass through a considerable thickness of crust, during which the magma can unmix into carbonate and silicic components. By contrast, introduction of a CO_2-rich component to mantle peridotite in the hotter oceanic environment (and probably also in regions of thin, young continental crust) is likely to cause large-scale melting at shallow depths. Under these conditions, segregation of carbonatitic magma may be more difficult and alkali basaltic volcanism would be expected to predominate. Furthermore, experimental studies (*cf.* Wendlandt 1984 and references therein) have shown that the major-element characteristics of any partial melt generated from carbonated peridotite depends strongly on the solubility of CO_2 in the melt which in turn varies with depth of melt generation. At pressures less than ~25 kbar, the solubility

of CO_2 in the melt is generally low and the melt becomes progressively less silica-undersaturated with decreasing pressure (Wyllie and Huang 1975). Partial melting of carbonated peridotite at depths less than ~70 km may produce a melt resembling the alkali basalts of some ocean islands. At pressures approaching 25 kbar, the melts may resemble kimberlite magmas. At pressures greater than 25 kbar, partial melting of peridotite in the presence of CO_2 will produce carbonate-rich magmas (Wyllie and Huang 1975, Holloway *et al.* 1977). Depth of magma generation therefore strongly influences the major-element chemistry of magmas derived from peridotite in the presence of CO_2. As the depth of magma generation is likely to be influenced by both geothermal gradient and crustal thickness, kimberlitic and carbonatitic rocks are likely to be more common in stabilised, thickened cratons and might be expected to be less common in the oceanic environment. It is noteworthy that the oceanic island of Malaita, Solomon Islands, from which alnöites have been reported (Nixon and Boyd 1979), lies along the southern margin of the Ontong Java Plateau, which consists of thickened (up to 40 km) crust (Kroenke 1972).

The importance of CO_2 in the generation of kimberlites is well established (e.g. Spera and Bergman 1980). For example, Bailey (1984) demonstrated a correlation between CaO and CO_2 in kimberlites and suggested that a $CaCO_3$ component is involved in their generation. The "alleged" close association between kimberlitic and carbonatitic magmatism is controversial (see Gaspar and Wyllie 1984) but the recent recognition of two genetically distinct groups of kimberlites (Smith 1983) may help to clarify possible relationships between kimberlites and carbonatites. South African Group 1 (non-micaceous) kimberlites have Sr, Nd, Pb and $\delta^{13}C$ isotopic compositions closely resembling those of carbonatites. Smith (1983) has also noted the isotopic similarities between Group 1 kimberlites and ocean islands. A close spatial and temporal relationship exists between kimberlitic and carbonatitic rocks at both the Walloway/Terowie region, South Australia and in Pretoria, South Africa. Although many of the kimberlitic intrusives at Walloway are evolved and contain generally lower trace-element contents than typical kimberlite (Ferguson and Sheraton 1979), diamond-bearing intrusions of the same age have been identified in the Walloway region and one has been classified as hypabyssal, calcite-phlogopite-kimberlite (Scott-Smith *et al.* 1984). The Walloway carbonated kimberlite and Terowie kimberlitic intrusion have similar slightly positive ε_{Nd}, like that of the Walloway carbonatite, suggesting a genetic relationship. The emplacement age of the Goudini carbonatite is within error of that of the Premier kimberlite pipe, and "carbonatites" at Premier have initial $^{87}Sr/^{86}Sr$ of 0.7028 (Powell 1966, Welke *et al.* 1974) and ε_{Nd} values (Basu and Tatsumoto 1980) identical to that of the Goudini carbonatite. Although the Goudini and Walloway carbonatites are isotopically similar to other carbonatites, these two carbonatites lack the distinctive negative U and Hf anomalies found in all of the other carbonatites examined. As discussed earlier, these anomalies are probably due to crystallisation of phases such as monazite or zircon. The high SiO_2 contents and lower degree of trace-element enrichment of the Walloway and Goudini carbonatites compared to the other carbonatites indicates incomplete segregation of carbonate and silicate phases. If, as the evidence presented here suggests, kimberlites and carbonatites are genetically related, these two carbonatites may be transitional between kimberlite and more differentiated carbonatite.

8.5.4 Evolution of the sources of carbonatites

Many carbonatites possess isotopic characteristics indicating that their sources have long histories of high U/Pb, low Rb/Sr and LREE-depletion. Hofmann and White (1982) have attributed similar isotopic characteristics found in ocean-island basalts to subducted oceanic lithosphere which has been enriched in uranium during hydrothermal circulation or low-temperature alteration and stored in the mantle for ~1-2 Ga. Subducted altered basaltic crust is also likely to be CO_2- and volatile-rich, offering an excellent source material for carbonatite generation. At depth, subducted basalt converts to eclogite, which Treiman and Essene (1983) have advanced as a possible source for Na-rich carbonatites (with the jadeitic pyroxene component of eclogite providing a source of Na). Derivation from a garnet-rich eclogitic source can also explain the extreme LREE-enrichment typical of carbonatites. The relatively unradiogenic initial Sr and slightly radiogenic initial Nd of carbonatites is also compatible in general terms with an origin from ancient low Rb/Sr, slightly LREE-depleted, altered basaltic crust. If this is the case, the difference in the Pb isotopic characteristics of young carbonatites and the MORB depleted mantle reservoir from which their subducted basaltic sources may have been derived indicates a recycling rate similar to that inferred for ocean-island sources (Chase 1981) of the order of ~1.5 Ga. Although the correlations between initial $^{87}Sr/^{86}Sr$, ε_{Nd} and emplacement age of Fig. 8.10 require a relatively rapid and steady recycling rate, a rate of this order is probably rapid enough to generate such a trend.

A number of $\delta^{13}C$ and $\delta^{18}O$ studies of carbonatites have been undertaken in an attempt to determine values characteristic of the mantle. These studies found a considerable range of $\delta^{13}C$ and $\delta^{18}O$ compositions which overlap with those more recently determined for mid-ocean ridge basalts. Although these $\delta^{13}C$ and $\delta^{18}O$ compositions have been interpreted as representing primitive mantle values, the radiogenic Pb isotope characteristics of carbonatites are not compatible with a primitive mantle origin. Furthermore, if carbonatites are derived from subducted lithosphere which has been subjected to degassing, low-temperature alteration and/or hydrothermal processes, significant shifts in $\delta^{13}C$ and $\delta^{18}O$ from mantle values are probable. Because of the low concentrations of magmatic carbon in tholeiitic basalt, the $\delta^{13}C$ composition of altered MORB will be strongly influenced by that of the contaminants. Phanerozoic pelagic carbonates and secondary carbonates in weathered and hydrothermally altered basalt generally have $\delta^{13}C_{PDB}$ values of ~ 0 to +2 ‰ (Degens 1969, Anderson and Lawrence 1976, McKenzie 1980). Measurements of the oxygen isotopic compositions of altered oceanic tholeiites (for example, Gregory and Taylor 1981) have generally found both ^{18}O enrichments, attributed to low-temperature hydrothermal exchange, and depletions, probably due to high-temperature exchange, with $\delta^{18}O_{SMOW}$ values typically ranging from +4 to +12 ‰. The $\delta^{13}C$ and $\delta^{18}O$ values of carbonatites fall within the range of altered and unaltered sea-floor tholeiite and it is therefore conceivable that the shifts towards higher $\delta^{13}C$ and $\delta^{18}O$ values, relative to those of MORB, found in many carbonatites is due to exchange of carbon and oxygen of the oceanic lithospheric sources of carbonatites with seawater, prior to their subduction. Because of the generally low Rb, Sr and REE concentrations of secondary carbonate compared to oceanic tholeiites (*cf.* McCulloch *et al.* 1981), the Sr and Nd isotopic evolution of oceanic crust may not be significantly affected by the addition of secondary carbonate during low-temperature alteration processes, although some shifts towards more radiogenic $^{87}Sr/^{86}Sr$ might be anticipated due to Sr exchange with seawater. The generally radiogenic Pb isotopic compositions of many carbonatites may

be attributable to uptake of uranium from seawater by basalt during low-temperature alteration, as was advanced by Hofmann and White (1982).

The geochemical and stable and radiogenic isotopic characteristics of carbonatites are therefore consistent with their generation from subducted oceanic lithospheric sources. That similar isotopic features are found in some late Archaean alkaline and carbonatite complexes, such as the Siilinjarvi Carbonatite Complex of eastern Finland and in the Poohbah Lake complex from the Superior Province of the Canadian Shield, suggests that subduction and recycling processes have operated since at least the late Archaean. Future detailed studies of carbonatite complexes of different ages may enable the geochemical and isotopic evolution of ocean-island sources throughout the Earth's differentiation history to be determined.

SECTION C. THE ^{40}K-^{40}Ca RADIOGENIC DECAY SCHEME- a reconnaissance study

9.1 Introduction

Although the minor branch of decay of ^{40}K (mostly by neutron capture) to ^{40}Ar has been extensively applied in geochronological studies, the major branch of ^{40}K decay to ^{40}Ca ($t_{1/2}$ = 1.47 Ga; see Fig 9.1), has received little attention. There are two main reasons for this;

1. The much greater abundance of the daughter, ^{40}Ca, relative to the parent, ^{40}K, in most geological materials, results in only small increments of ^{40}Ca due to radiogenic decay of ^{40}K over time. For example, the increase in the $^{40}Ca/^{42}Ca$ ratio due to radiogenic decay of ^{40}K of the Earth's mantle during its 4.5 Ga history is only ~0.0027 or 0.0018%.
2. The daughter isotope, ^{40}Ca, comprises almost 97% of naturally-occurring calcium, with the next most abundant isotope, ^{44}Ca, comprising only ~2% (see Fig. 9.1). Measurement of the small increments in the abundance of ^{40}Ca due to ^{40}K decay requires the simultaneous measurement of at least two ratios with approximately equal precision, the first to measure the increment due to radiogenic decay of the parent isotope and the second to correct for fractionation effects induced prior to or during isotopic analysis. Until recently, it has not been possible to measure the two Ca isotopic ratios required with the precision necessary to make the ^{40}K-^{40}Ca decay scheme widely applicable to geological problems.

These difficulties have limited the range of possible applications of the ^{40}K-^{40}Ca radiogenic decay scheme to the investigation of very high K/Ca rocks and minerals (e.g. Coleman 1971). Furthermore, most previous ^{40}K-^{40}Ca isotopic studies (for example, Marshall and DePaolo 1982, and references given therein) have been restricted to geochronological investigations, for which other techniques, such as ^{87}Rb-^{87}Sr, offer considerable advantages over the ^{40}K-^{40}Ca method. However, recent advances in mass spectrometry technology have considerably improved the level of analytical precision attainable and as a consequence, the range of possible applications of the ^{40}K-^{40}Ca decay scheme has been broadened.

The following study was undertaken principally to investigate the potential usefulness of the ^{40}K-^{40}Ca method as a petrogenetic tracer. In Fig. 9.2, the relationship between the K/Ca ratio (expressed as wt% K_2O/CaO), duration (in Ga) and the consequent increase in ^{40}Ca abundance (represented by the loci of increments, in parts of 10^4, in the $^{40}Ca/^{42}Ca$ ratio) is shown. Although the attainable analytical precision still limits application of the technique to the examination of samples having geologically long histories of high K/Ca, the ^{40}K-^{40}Ca method can potentially provide useful petrogenetic information which would be unavailable by other means. For example, the Sr, Nd and Pb isotopic characteristics of some ultrapotassic rock suites suggest that their source regions may have possessed high K/Ca ratios (i.e. wt% K_2O/CaO >1) for periods of at least ~2 Ga (see discussion in Chapter 7). If this has been the case, increases in the abundance of ^{40}Ca should be resolvable at the measurement precision presently attainable. It has also been suggested (see Chapter 7) that the major-element and trace-element components of at least some ultrapotassic rock suites have been derived from entirely different sources. This hypothesis may be examined by comparison of the isotopic characteristics of trace elements (such as Sr, Nd and Pb) with that of the major element calcium.

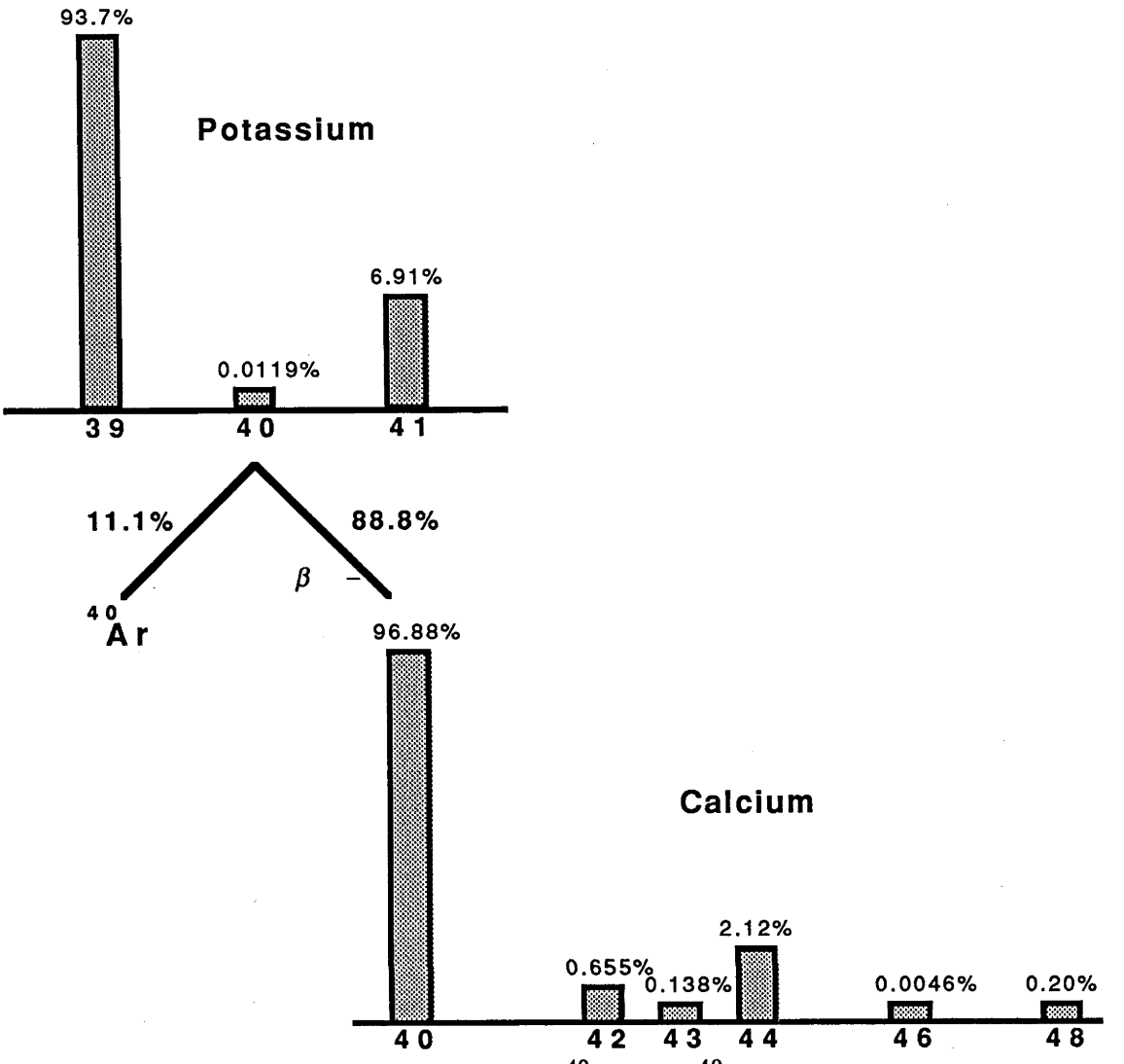

Fig. 9.1 Decay scheme showing branched decay of ^{40}K to both ^{40}Ar (mostly by electron capture) and to ^{40}Ca by β-decay.

In addition to its petrogenetic applications, the ^{40}K- ^{40}Ca decay scheme can also contribute to our understanding of intra- and infra-crustal recycling processes. This is because weathering processes commonly stabilise alkali-rich clay minerals in mature sediments, resulting in an increase in the K/Ca ratio and consequently, measurable increases in the abundance of ^{40}Ca in old (i.e. > ~2 Ga) sediments.

In this study, the results of a calcium isotopic investigation of a variety of igneous and sedimentary rock-types are presented. This research was primarily directed towards the assessment of perceived analytical difficulties associated with the technique and the investigation of some useful geological applications.

9.2 Analytical Procedures

Details of the analytical procedures used in this study and a discussion of the sources of analytical error in Ca isotopic analyses can be found in Appendix 1.4. The results obtained for 12 analyses of the Tridacna Ca isotope standard obtained throughout the 5 month period of this study indicate an external precision of 0.018% (i.e. ±0.028) at the 95% confidence level for measurements of the $^{40}Ca/^{42}Ca$ ratio.

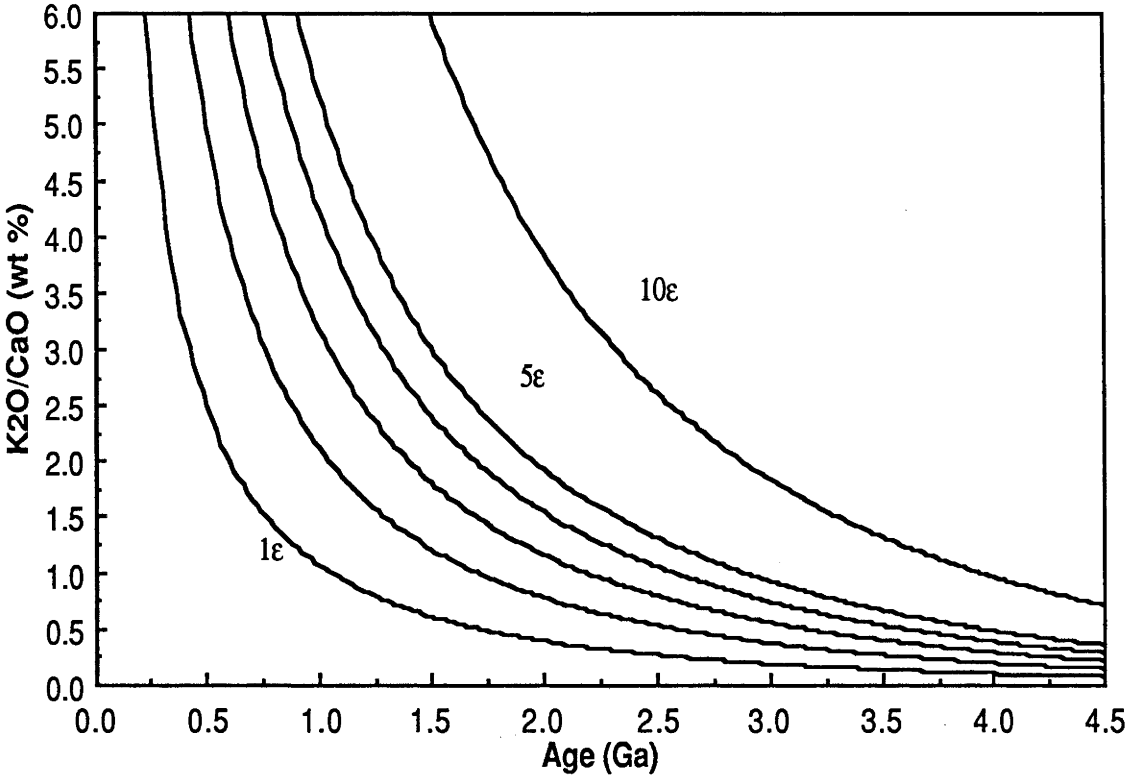

Fig. 9.2 Wt% K_2O/CaO versus age (in Ga), showing the increase in ^{40}Ca abundance resulting from the radiogenic decay of ^{40}K. The curves represent the loci of increments in the $^{40}Ca/^{42}Ca$ ratio in parts in 10^4. The analytical precision obtained during this study is ±1.9 ε-units (95% confidence). Resolvable differences are limited by this analytical precision to samples having high K/Ca ratios for long time periods (e.g. wt% K_2O/CaO > 0.20 for 4.0 Ga or wt% K_2O/CaO > 0.38 for at least 3.0 Ga. For comparison, most primitive basalts have wt% K_2O/CaO substantially less than 0.08).

This is in general agreement with the external precision error estimate of 0.022% (or ±0.034 for the $^{40}Ca/^{42}Ca$ ratio) at the 95% confidence level indicated by a 2-way analysis of variance of duplicate Ca isotopic analyses for 30 of the samples given in this study.

9.3 Results

9.3.1 Oceanic and island-arc lavas

Ca and Sr isotopic data obtained for mid-ocean ridge, ocean-island and island-arc lavas are given in Table 9.1. The basalt sample #529-4, from the Famous area of the mid-Atlantic ridge, was selected for analysis because it is chemically well-catagorised (see Langmuir *et al.* 1977) and possesses major- and trace-element characteristics typical of primitive mid-ocean ridge basalts. For the purposes of this study, this basalt has been adopted as a Ca isotopic reference. Results obtained for other rock samples are expressed using the epsilon notation as follows;

$$\varepsilon_{Ca} = [(^{40}Ca/^{42}Ca_{sample} - {}^{40}Ca/^{42}Ca_{basalt})/ {}^{40}Ca/^{42}Ca_{basalt}] \times 10^4 \qquad (1)$$

where, from Table 9.1, $^{40}Ca/^{42}Ca_{basalt} = 151.078$.

The results are therefore expressed as differences, in parts of 10^4, from the $^{40}Ca/^{42}Ca$ value of Earth's mantle. Because of the low K/Ca ratio of the Earth's mantle (i.e. ~0.01), the mantle $^{40}Ca/^{42}Ca$ value should represent the least radiogenic terrestrial $^{40}Ca/^{42}Ca$ value. No $^{40}Ca/^{42}Ca$ ratio obtained for other

Table 9.1 Calcium and strontium isotopic data for basalts, island-arc lavas and a trough sediment.

Sample		$^{87}Sr/^{86}Sr$[a]	$^{43}Ca/^{44}Ca$[b]	$^{40}Ca/^{42}Ca$[b]	blocks	ε_{Ca}[c]
MORB						
529-4	Famous area	0.7029	0.064877 ±9	151.078 ±8	(27)	0
			0.064853 ±4	151.064 ±39	(11)	-0.93 ±2.6
			0.064847 ±10	151.067 ±11	(12)	-0.73
Ocean-island basalts						
BHVO-1	Hawaii	0.70345 ±3	0.064849 ±14	151.106 ±13	(8)	+1.85
			0.064862 ±10	151.113 ±10	(13)	+2.32
			0.064854 ±6	151.085 ±8	(15)	+0.46
			0.064862 ±9	151.102 ±9	(10)	+1.59
Island-arc volcanics and trough sediments						
MK-17	Unalaska basalt, Aleutian arc	0.70311 ±4	0.064861 ±5	151.129 ±16	(10)	+3.38
			0.064850 ±8	151.074 ±9	(4)	-0.26
AK4-33	Akutan basalt, Aleutian arc	0.70308 ±5	0.064856 ±8	151.076 ±7	(17)	-0.13
			0.064834 ±9	151.095 ±16	(14)	+1.13
MK-3A	Unalaska andesite, Aleutian arc	0.70291 ±4	0.064865 ±24	151.101 ±22	(9)	+1.52
			0.064867 ±12	151.089 ±19	(9)	+0.73
B5328	Wetar basalt, Banda arc	0.70446 ±5	0.064858 ±6	151.129 ±9	(13)	+3.38
			0.064857 ±3	151.118 ±5	(24)	+2.65
B5561	Wetar dacite, Banda arc	0.70827 ±5	0.064869 ±15	151.108 ±12	(12)	+1.99
B5128	Wetar rhyolite, Banda arc	0.72030 ±5	0.064814 ±21	151.113 ±18	(11)	+2.32
			0.064833 ±29	151.074 ±20	(15)	-0.26
SS4	Timor Trough, shale	0.74105 ±5	0.064855 ±7	151.113 ±14	(24)	+2.32

[a] $^{87}Sr/^{86}Sr$ isotopic data for Famous area basalts from White and Bryan (1977), for Aleutian arc lavas from McCulloch and Perfit (1981) and for Banda arc lavas and sediments from M. Abbott (unpublished data).

[b] Ratios normalised to $^{42}Ca/^{44}Ca = 0.31221$. Based on multiple analyses of the Tridacna calcium standard, the external precision is ±0.028 or ±1.9 ε_{Ca} units (95% confidence) for $^{40}Ca/^{42}Ca$. Individual analyses represent separate mass spectrometry runs of new loads. Within-run precision (at 95% confidence) shown as an indication of run quality.

[c] $\varepsilon_{Ca} = [(^{40}Ca/^{42}Ca_{sample} - 151.078)/151.078] \times 10^4$.

rock samples should therefore be statistically significantly less than this value.

It is noteworthy that the Tridacna calcium standard possesses a $^{40}Ca/^{42}Ca$ value (ε_{Ca} = -0.07 ±1.9, from Table A1.8) which is indistinguishable from the value obtained for the mid-ocean ridge basalt sample. This result indicates that the $^{40}Ca/^{42}Ca$ ratio of modern seawater is identical, within the analytical uncertainty, to that of the Earth's mantle. This is in contrast to the case for strontium, in

Table 9.2 Major- element analyses[a] of some igneous and sedimentary rocks examined in this study.

Sample	B5328	B5128	AK4-33	SS4	AUS-52	AUS-75	AUS-81
Location	Wetar	Wetar	Aleutian	Timor	Narryer	Narryer	Narryer
Rock-type	basalt	rhyolite	basalt	shale	pelite	pelite	calc-silic
SiO_2	51.91	76.84	49.32	61.31	51.68	53.56	56.27
TiO_2	0.56	0.20	1.34	0.77	0.50	0.48	0.74
Al_2O_3	16.72	13.36	18.41	25.00	26.32	18.00	10.79
Cr_2O_3	0.07	0.07	0.06	0.05	0.07	0.05	0.07
FeO	9.19	2.20	11.81	5.12	10.72	10.28	10.15
MnO	0.06	0.05	0.09	0.05	0.08	0.13	0.09
MgO	6.19	0.06	4.76	1.32	4.99	5.61	4.62
CaO	13.48	1.84	10.43	0.61	1.92	8.93	16.41
Na_2O	1.32	2.82	3.08	0.87	0.23	1.73	0.81
K_2O	0.59	2.72	0.79	5.00	3.58	1.30	0.14

[a] Sample powders were fused, in duplicate, on Mo strips under an Ar atmosphere and the resultant glasses analysed using an energy-dispersive electron microprobe. Analyses given represent averages of at least 10 microprobe determinations. Oxide totals have been summed to 100%.

which a substantial proportion of marine Sr has been derived from the upper continental crust and is considerably more radiogenic than the mantle value. Either the Ca derived from the Earth's continental crust is insufficiently radiogenic, or the Ca flux to the oceans from mantle sources (e.g. hydrothermal input from ridge crests) outweighs that derived from the upper continental crust.

The ε_{Ca} of +1.56 ±0.68 (average and $2\sigma_{mean}$ error of the 4 analyses given Table 9.1) for the ocean-island alkali basalt BHVO-1, from the Kilauea caldera, Hawaii, is within the 2σ external precision limit of the value obtained for the Famous area mid-Atlantic ridge basalt.

Also given in Table 9.1 are Ca isotopic data obtained on lavas from the Aleutian and Banda island arcs and a sediment from the Timor Trough. Major-element data for some of the island-arc samples given in Table 9.1 are listed in Table 9.2. The Banda island-arc volcanics possess a wide range of $^{87}Sr/^{86}Sr$ (i.e. 0.7044 to 0.7223), $^{143}Nd/^{144}Nd$ (ε_{Nd} of +3.4 to -11.0) and $\delta^{18}O$ (+9.8 to +13.7 ‰ vs SMOW) values (McCulloch *et al.* 1982), indicating the assimilation of substantial amounts of crustal material. The $^{40}Ca/^{42}Ca$ ratios of both Banda and Aleutian arc lavas are within error of the value obtained for the mid-ocean ridge basalt. The Timor Trough sediment also possesses a $^{40}Ca/^{42}Ca$ ratio which is within error of the mid-ocean ridge basalt, despite its high K_2O/CaO ratio (see Table 9.1) and very radiogenic $^{87}Sr/^{86}Sr$ ratio of 0.7410.

9.3.2 Carbonatites

Ca isotopic results obtained for carbonatites from a variety of localities are listed in Table 9.3. Although the intrusion ages range from Early Proterozoic (for the Mt Weld carbonatite) to Tertiary (for the Ugandan examples), corrections to the measured $^{40}Ca/^{42}Ca$ ratio for β-decay of ^{40}K since emplacement are unnecessary, due to the low K/Ca ratios. With the exception of the Sukulu carbonatite, all other carbonatite samples examined possess $^{40}Ca/^{42}Ca$ values within the analytical uncertainty of the

Table 9.3 Calcium isotopic data for carbonatites.

Sample	Emplacement age[a] (Ma)	$^{43}Ca/^{44}Ca$[b]	$^{40}Ca/^{42}Ca$[b]	blocks	ε_{Ca}[c]
Mudtank, Northern Territory	732	0.064849 ±13	151.100 ±10	(22)	+1.46
#7590-2015		0.064853 ±15	151.093 ±13	(14)	+0.99
Mt Weld, Western Australia	2040	0.064866 ±13	151.097 ±10	(15)	+1.26
#MW-2		0.064839 ±13	151.083 ±15	(15)	+0.33
Kaiserstuhl, West Germany	17	0.064842 ±8	151.101 ±10	(10)	+1.52
#K-3					
Jacupiranga, Brazil	130	0.064852 ±5	151.073 ±6	(15)	-0.33
#5963					
Magnet Cove, Arkansas	97	0.064809 ±30	151.117 ±19	(12)	+2.58
#MC-1					
Lokupoi, Uganda	19	0.064864 ±20	151.102 ±19	(24)	+1.59
#6336					
Tororo, Uganda	40	0.064825 ±11	151.099 ±11	(25)	+1.39
#6330		0.064852 ±5	151.123 ±8	(12)	+2.98
Sukulu, Uganda	40	0.064852 ±11	151.114 ±11	(15)	+2.38
#6335		0.064827 ±19	151.162 ±19	(13)	+5.56
Kangankunde, Malawi	126	0.064913 ±51	151.062 ±45	(7)	-1.06
#3432					
Nachendazwaya, Tanzania	655	0.064800 ±26	151.082 ±17	(4)	+0.26
#7122					

[a] Sources of emplacement age data are given in Chapter 8 of this thesis.

[b] Ratios normalised to $^{42}Ca/^{44}Ca = 0.31221$. Based on multiple analyses of the Tridacna calcium standard, the external precision is ±0.028 or ±1.9 ε_{Ca} units (95% confidence) for $^{40}Ca/^{42}Ca$. Individual analyses represent separate mass spectrometry runs of new loads. Within-run precision shown as an indication of run quality.

[c] $\varepsilon_{Ca} = [(^{40}Ca/^{42}Ca_{sample} - 151.078)/151.078] \times 10^4$.

mantle value, given by the value obtained for the mid-ocean ridge basalt. Although the average of the two Sukulu analyses give an ε_{Ca} of +3.97, which is statistically outside the mantle value, one of the two Sukulu Ca runs statistically overlaps with the mantle value. The Tororo and Lokupoi carbonatites are spatially closely associated with the Sukulu carbonatite but both have ε_{Ca} values (+1.59 and +1.59 respectively) which are within the upper uncertainty limit of the mantle value. The Ugandan carbonatites possess unusually radiogenic Pb isotopic compositions, consistent with their sources having evolved in isolation from the Earth's convecting mantle for at least 1.5 Ga (see Section B). It is therefore

conceivable that they may have evolved radiogenic Ca compared to more typical mantle values during this time. However, without further supporting evidence (i.e. further duplicate analyses or improvement in the external precision), the significance of the Sukulu Ca data should be interpreted cautiously.

9.3.3 Potassic igneous rocks

Ca isotopic results obtained for some selected potassic igneous rocks are tabulated in Table 9.4. Age corrections to the measured $^{40}Ca/^{42}Ca$ ratios are unnecessary for the Western Australian and Spanish lamproites and Gaussberg leucitites, due to their young emplacement ages. For the central west Greenland kimberlites and lamproites, small corrections to the measured $^{40}Ca/^{42}Ca$ ratios for in-situ decay of ^{40}K have been applied, but these corrections are within the analytical error of the measurements (i.e. the maximum correction applied is -0.023, to Greenland lamproite #5622). The results in Table 9.4 indicate that the Western Australian, Spanish and Gaussberg samples possess $^{40}Ca/^{42}Ca$ ratios which are within error of the value obtained for the mid-Atlantic ridge basalt (and are therefore indistinguishable from the mantle value). However, the average ε_{Ca} value of the 4 analyses obtained for the Greenland kimberlites is +2.68 ±0.46, statistically significantly higher than the mantle value. Furthermore, both age-corrected $^{40}Ca/^{42}Ca$ ratios for the two central west Greenland lamproites analysed (ε_{Ca} of +3.36 and +4.90) are statistically significantly more radiogenic than the mantle value.

9.3.4 Chemical and clastic sediments from ancient terrains

Ca isotopic results obtained for gypsum samples from selected Australian Proterozoic and Archaean terrains are given in Table 9.5. The gypsum samples possess radiogenic $^{87}Sr/^{86}Sr$ values (i.e. from 0.7104 to 0.7461; see Table 9.5), suggesting that most of their Sr is derived from the surrounding continental crust. Apart from the sample from Lake Frome, which is located in terrain predominantly of Proterozoic age or younger, the $^{40}Ca/^{42}Ca$ ratios of the gypsum samples are significantly more radiogenic than the mantle value. Furthermore, a positive correlation exists between $^{87}Sr/^{86}Sr$ and the mean $^{40}Ca/^{42}Ca$ values obtained for the gypsum samples (Fig. 9.3).

In Table 9.6, Ca isotopic data for clastic sediments from the Archaean Mt Narryer region of Western Australia are given. The pelite sample AUS-52 has a high K_2O/CaO ratio (see Table 9.2), accompanied by a highly radiogenic $^{40}Ca/^{42}Ca$ ratio (i.e. $\varepsilon_{Ca}(0) \approx +25$). Pelite sample AUS-75 possesses an $\varepsilon_{Ca}(0)$ of +2.9, which is within error of the mid-oceanic ridge basalt sample. The $\varepsilon_{Ca}(0)$ value of +3.9 for the calc-silicate sample AUS-81 is resolvably more radiogenic than the mid-oceanic ridge basalt sample at the 2σ level. The sediment K-Ca isotopic data define a K-Ca isochron (Fig. 9.4) indicating an age of 4.17 ±0.38 Ga, with the pelite sample AUS-52 largely controlling the age.

Table 9.4 Calcium isotopic data for potassic and kimberlitic rocks.

Sample	K	Ca[a]	$^{40}K/^{42}Ca$	$^{43}Ca/^{44}Ca$	$^{40}Ca/^{42}Ca$[b]	blocks	$\varepsilon_{Ca}(0)$[c]	ε_{Ca}[d]
	------ ppm ------							
Western Australian lamproites (20 Ma)								
WAL-10	77600	27020	0.0535	0.064844±15	151.095±16	(13)	+1.13	+1.09
WAL-14	75100	22500	0.0622	0.064873±15	151.070±14	(18)	-0.53	+1.12
				0.064840±25	151.121±19	(25)	+2.85	
WAL-15	33400	35100	0.0177	0.064860 ±5	151.069 ±5	(22)	-0.60	-0.43
				0.064865 ±4	151.074 ±4	(23)	-0.26	
WAL-20	35100	32200	0.0203	0.064851 ±5	151.072±25	(35)	-0.40	-0.27
				0.064879±11	151.076 ±9	(10)	-0.13	
WAL-25	72460	41300	0.0327	0.064857 ±5	151.093 ±6	(15)	+0.99	+1.57
				0.064859 ±7	151.111±27	(3)	+2.18	
Gaussberg leucitites (0 Ma)								
82-27				0.064852 ±5	151.087 ±6	(19)	+0.60	-0.13
				0.064843 ±8	151.065±12	(7)	-0.86	
82-30				0.064857±11	151.097±14	(8)	+1.26	+1.26
Spanish lamproites (8 Ma)								
SP-034				0.064854 ±5	151.078±10	(9)	0	+0.13
				0.064854 ±9	151.082±12	(10)	+0.26	
SP-049	56800	20500	0.0516	0.064861 ±3	151.078 ±4	(25)	0	-0.01
Central west Greenland kimberlites (587 Ma)								
5508	23600	69900	0.00628	0.064857 ±5	151.108±17	(7)	+1.98	+2.66
				0.064841 ±7	151.126 ±9	(20)	+3.18	
5973	18800	85900	0.00409	0.064843±13	151.124±13	(15)	+3.04	+2.91
				0.064854 ±7	151.116 ±9	(15)	+2.52	
Central west Greenland lamproites (1227 Ma)								
5611	52000	64200	0.0151	0.064846 ±9	151.150±14	(13)	+4.76	+4.90
				0.064851 ±7	151.163 ±9	(15)	+5.63	
5622	51900	35900	0.0269	0.064858±20	151.124±16	(15)	+3.04	+3.36
				0.064849 ±5	151.163±10	(5)	+5.63	

[a] K and Ca concentration data from Jaques *et al.* (1986), Venturelli *et al.* (1984) and Scott (1979).

[b] Ratios normalised to $^{42}Ca/^{44}Ca = 0.31221$. Based on multiple analyses of the Tridacna calcium standard, the external precision is ±0.028 or ±1.9 ε_{Ca} units (95% confidence) for $^{40}Ca/^{42}Ca$. Individual analyses represent separate mass spectrometry runs of new loads. Within-run precision (at 95% confidence) shown as an indication of run quality.

[c] $\varepsilon_{Ca}(0) = [(^{40}Ca/^{42}Ca_{sample} - 151.078)/151.078] \times 10^4$.

[d] ε_{Ca} calculated using the average value of dupicated $^{40}Ca/^{42}Ca$ ratios, the ages indicated and the following additional parameters; $\lambda_K = 0.5543 \times 10^{-9}$ yr^{-1}, $\lambda_{\beta^-}/\lambda_K = 0.8952$, mantle K/Ca (atomic) = 0.01 and present-day mantle $^{40}Ca/^{42}Ca = 151.078$.

Table 9.5 Strontium and calcium isotopic data for gypsum samples.

Sample	$^{87}Sr/^{86}Sr$[a]	$^{43}Ca/^{44}Ca$	$^{40}Ca/^{42}Ca$[b]	blocks	$\varepsilon_{Ca}(0)$[c]
Lake Frome, South Australia (Proterozoic basement)					
#LF 82/3	0.710388	0.064832 ±20	151.112 ±22	(25)	+2.25
		0.064829 ±32	151.123 ±32	(20)	+2.98
		0.064857 ±3	151.130 ±9	(17)	+3.44
Lake Gilmor (south side), Western Australia (Archaean granitic basement)					
#GY-207	0.718751	0.064880 ±12	151.143 ±12	(8)	+4.30
		0.064853 ±5	151.137 ±9	(14)	+3.91
Lake Yarra Yarra, Western Australia (Archaean granitic basement)					
#GY-185	0.725995	0.064854 ±9	151.142 ±19	(5)	+4.24
		0.064849 ±5	151.156 ±12	(10)	+5.16
Lake Moore (north side), Western Australia (Archaean granitic basement)					
#GY-165	0.730424	0.064855 ±4	151.148 ±6	(14)	+4.63
		0.064856 ±13	151.153 ±17	(9)	+4.96
Lake Brown, Western Australia (Archaean granitic basement)					
#GY-127	0.746118	0.064843 ±9	151.162 ±8	(20)	+5.56
		0.064850 ±7	151.173 ±10	(13)	+6.29

[a] Sr isotope data from M.T. McCulloch and A.R. Chivas (unpublished data). Analytical error for $^{87}Sr/^{86}Sr$ is $<\pm 0.00003$ (95% confidence).

[b] Ratios normalised to $^{42}Ca/^{44}Ca = 0.31221$. Based on multiple analyses of the Ca Tridacna standard, the external precision is ±0.028 or ±1.9 ε_{Ca} units (95% confidence) for $^{40}Ca/^{42}Ca$. Individual analyses represent separate mass spectrometry runs of new loads. Within-run precision (at 95% confidence) shown as an indication of run quality.

[c] $\varepsilon_{Ca}(0) = [(^{40}Ca/^{42}Ca_{sample} - 151.078)/151.078] \times 10^4$.

9.4 Discussion

9.4.1 Ocean-island and island-arc lavas

Resolvable enrichments in ^{40}Ca, compared to the mantle $^{40}Ca/^{42}Ca$ value, were not detected in either the ocean-island or island-arc lavas examined in this study. This result is perhaps not surprising for the Hawaiian alkali basalt. However, the $^{87}Sr/^{86}Sr$, $^{143}Nd/^{144}Nd$ and $^{18}O/^{16}O$ isotopic characteristics of the Banda arc lavas (McCulloch *et al.* 1982) provide convincing evidence for the involvement of substantial amounts of crustal material in their generation. The very radiogenic $^{87}Sr/^{86}Sr$ value obtained for the highly-contaminated Wetar rhyolite (i.e. $^{87}Sr/^{86}Sr = 0.7203$) and the Timor Trough sediment ($^{87}Sr/^{86}Sr = 0.7410$; from Table 9.1) suggests the involvement of sedimentary detritus predominantly derived from an old continental platform (probably northwest Australia). As the Ca isotopic results obtained for gypsum samples (Table 9.5) and sediments derived from Archaean terrains (Table 9.6) indicate

Table 9.6 Calcium isotopic data for clastic sediments from the Mt Narryer region, Western Australia.

Sample	K[a]	Ca[a]	$^{40}K/^{42}Ca$	$^{43}Ca/^{44}Ca$	$^{40}Ca/^{42}Ca$[b]	blocks	$\varepsilon_{Ca}(0)$[c]	T_{Ca}[d] (Ga)
	ppm							
pelites								
AUS-52	29700	13700	0.0403	0.064866 ±14	151.427 ±14	(7)	+23.10	4.39
				0.064856 ±15	151.475 ±15	(5)	+26.28	
AUS-75	10800	63800	0.00315	0.064858 ±4	151.124 ±4	(19)	+3.04	5.21
				0.064857 ±2	151.120 ±5	(11)	+2.78	
calc-silicates								
AUS-81	1160	117300	0.00018	0.064857 ±5	151.142 ±8	(9)	+4.24	-
				0.064846 ±10	151.132 ±10	(5)	+3.57	

[a] K and Ca concentration data from Table 9.2.

[b] Ratios normalised to $^{42}Ca/^{44}Ca = 0.31221$. Based on multiple analyses of the Tridacna calcium standard, the external precision is ±0.028 or ±1.9 ε_{Ca} units (95% confidence) for $^{40}Ca/^{42}Ca$. Individual analyses represent separate mass spectrometry runs of new loads. Within-run precision (at 95% confidence) shown as an indication of run quality.

[c] $\varepsilon_{Ca}(0) = [(^{40}Ca/^{42}Ca_{sample} - 151.078)/151.078] \times 10^4$.

[d] T_{Ca} calculated using the average value of duplicated $^{40}Ca/^{42}Ca$ ratios and the following additional parameters; $\lambda_K = 0.5543 \times 10^{-9}$ yr^{-1}, $\lambda_\beta / \lambda_K = 0.8952$, mantle K/Ca (atomic) = 0.01 and present-day mantle $^{40}Ca/^{42}Ca = 151.078$.

that sedimentary material derived from old terrains may possess radiogenic $^{40}Ca/^{42}Ca$, radiogenic $^{40}Ca/^{42}Ca$ values might be anticipated in the Timor Trough sediment (and perhaps also in the Wetar rhyolite). The trough sediment, however, possesses a $^{40}Ca/^{42}Ca$ ratio which is within error of the mantle value. A possible explanation for the unradiogenic $^{40}Ca/^{42}Ca$ ratio of the trough sediment is that its calcium may have been largely derived from seawater, or may have exchanged with seawater calcium, as the Tridacna calcium standard $^{40}Ca/^{42}Ca$ results suggest that seawater calcium is isotopically indistinguishable from mantle calcium. If this is the case, the radiogenic $^{87}Sr/^{86}Sr$ value of the sediment compared to the seawater value indicates that this process has not substantially influenced the strontium isotope systematics of the sediment.

9.4.2 Carbonatites

The Ca isotopic results given in Table 9.3 indicate that, with the possible exception of the Ugandan Sukulu example, carbonatites generally possess Ca isotopic compositions which are indistinguishable from that of the Earth's mantle. This conclusion supports the findings of the study by Marshall and DePaolo (1982), in which Ca isotopic data for a single carbonatite (from Mountain Pass, California) was obtained. In Section B of this thesis, a model was presented advocating the derivation of carbonatites by small degrees of partial melting (i.e. < ~1%) of subducted, altered oceanic crust, which had in many cases

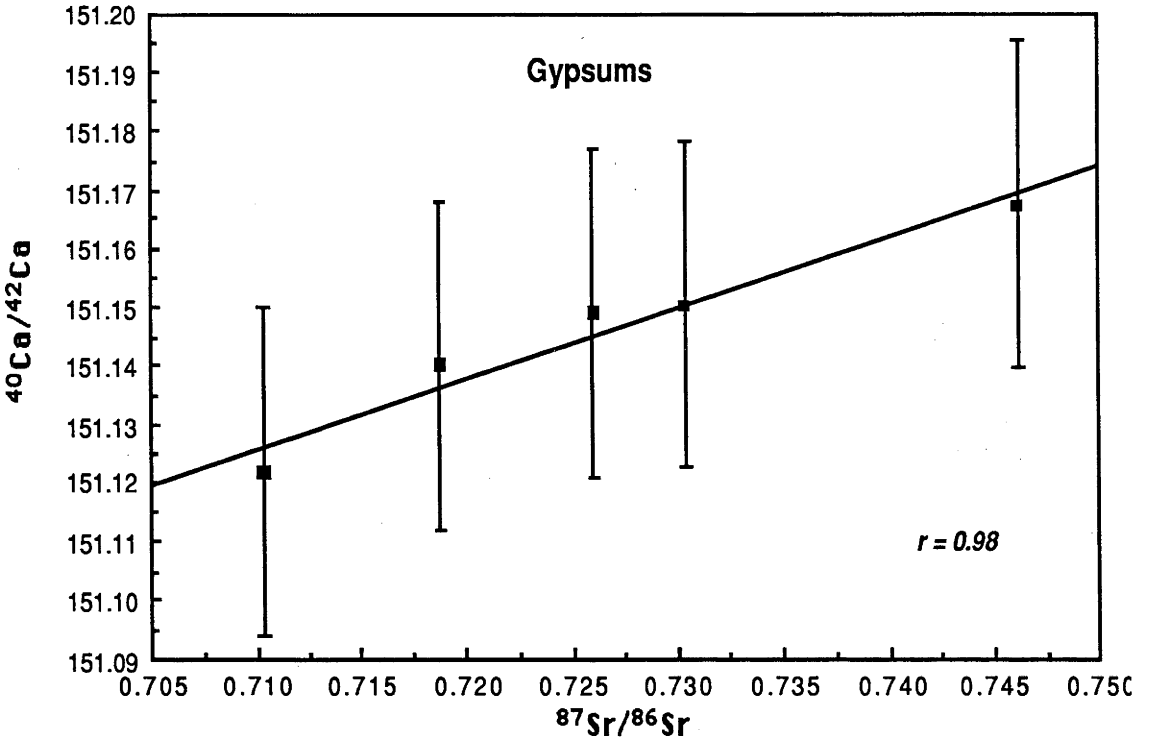

Fig. 9.3 $^{40}Ca/^{42}Ca$ versus $^{87}Sr/^{86}Sr$ for gypsum samples. Error-bars on $^{40}Ca/^{42}Ca$ are ±0.028 or 95% confidence external precision limits based on multiple analyses of the Tridacna calcium standard. The Tridacna analyses were obtained over a 5 month period and probably over-estimate the analytical error appropriate for a comparison of the gypsum $^{40}Ca/^{42}Ca$ results (obtained over a period of a few days). For example, all duplicated analyses of the 5 gypsum samples agree within their within-run 2σ precision, which averages ±0.014.

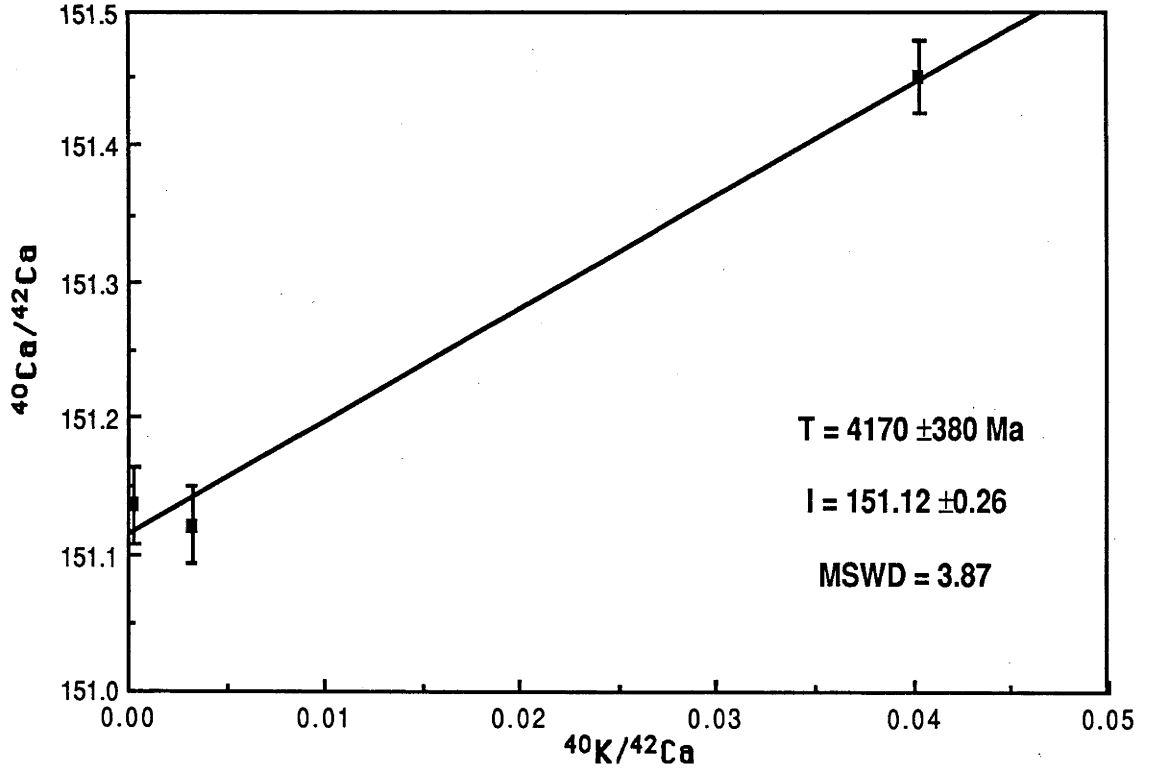

Fig. 9.4 $^{40}K/^{42}Ca$ - $^{40}Ca/^{42}Ca$ isochron diagram for sediments from the Mt Narryer region of Western Australia. $^{40}K/^{42}Ca$ ratios have been calculated from the concentration data given in Table 9.2. Based on duplicate microprobe analyses, the error in $^{40}K/^{42}Ca$ is estimated to be <10% (2σ).

been stored within the Earth's mantle for at least 1 Ga. Based on differences between the $\delta^{13}C$ and $\delta^{18}O$ values of carbonatites and those characteristic of the Earth's mantle, it was also suggested that some proportion of the carbonate was of secondary origin, resulting from low-temperature interaction of the oceanic crust with seawater. However, the Ca isotopic results obtained for the Tridacna standard (see Table A1.8) indicate that the $^{40}Ca/^{42}Ca$ value of modern seawater is identical within error to the value determined for the Earth's mantle (based on the analysis of the mid-Atlantic ridge basalt sample). Therefore, the presence of secondary Ca derived from seawater cannot be confirmed by Ca isotopic analysis.

The significance of the radiogenic $^{40}Ca/^{42}Ca$ value obtained for the Sukulu carbonatite is difficult to assess. As with other carbonatites, the Sukulu carbonatite possesses an extremely low K/Ca ratio (i.e. atomic K/Ca ≈ 0.0003, from Table 8.1) so if the radiogenic Ca is a source characteristic, a mechanism is required (silicate/carbonate segregation?) to lower the K_2O/CaO ratio from a relatively high value of at least 1, necessary to evolve the measured ε_{Ca} of ~4 within a realistic time period (see Fig. 9.2), to this very low value. The Sr, Nd and Pb isotopic characteristics of the Sukulu carbonatite rule out the possibility that the radiogenic Ca reflects extensive interaction of the carbonatite with the surrounding continental crust.

9.4.3 Potassic igneous rocks

For a sample having wt% K_2O/CaO of 3, a time period of at least 1.24 Ga is required in order for it to evolve a $^{40}Ca/^{42}Ca$ ratio which is statistically significantly different from the mantle value (i.e. with an ε_{Ca} of at least +3.8, to be outside the 95% confidence precision level of both measurements). For a wt% K_2O/CaO of 1, at least 2.5 Ga is required. Assuming that their sources possessed K/Ca ratios similar to those of the magmas themselves (i.e. wt% $K_2O/CaO \approx 1$ to 3), the Ca isotopic results obtained for the Western Australian lamproites and Gausberg leucitites indicate that their sources cannot be older than ~2.5 Ga. Because potassium is likely to be more incompatible than calcium in most mantle mineralogies and crystal fractionation may increase the K/Ca ratio, the K/Ca ratio of the magmas probably provide a maximum estimate of that of their sources. However, for at least the more primitive Western Australian representatives (such as the Ellendale samples), the K/Ca ratios of the magmas are probably close to the values of their sources. Using the XRF-determined wt% K_2O and CaO values and maximum possible $^{40}Ca/^{42}Ca$ ratios (i.e. the upper limit of the 95% confidence error) for Ellendale olivine lamproites WAL-15 and WAL-20 indicates maximum possible model ^{40}K-^{40}Ca ages of ~1.55 Ga. As the Nd and Pb isotopic compositions of the Western Australian lamproites require source ages of at least 2.1 Ga (but probably much older; see Chapter 3), the Ca isotopic data suggest that either the K enrichment (i.e. increase in the K/Ca ratio) of the lamproite sources occurred some time after the trace element enrichment (i.e. the increase in Rb/Sr and Nd/Sm), or that most of the calcium in the lamproites has been derived from a different source to that from which the potassium and the trace elements Pb and Nd was derived. It is likely that the enrichment in K and the incompatible trace elements occurred synchronously, but that the radiogenic calcium generated has been diluted by mixing with unradiogenic mantle-derived calcium or calcium from other sources.

The radiogenic $^{87}Sr/^{86}Sr$ values of the lamproites from southeastern Spain (i.e. from 0.717 to 0.721; see Table 2.3) indicate derivation from sources having long histories of high Rb/Sr and, because of the similar geochemical behavior of K/Ca and Rb/Sr ratios, presumably also high K/Ca. However, as with the Western Australian and Gaussberg potassic lavas, the Spanish lamproites also possess Ca isotopic compositions which are indistinguishable from the mantle value. In Section A of this thesis, it was argued that a component derived from subducted sediments may be involved in the genesis of potassic igneous rocks. In contrast with the Western Australian and Gaussberg examples, for which it was argued that their sources were stored and evolved largely within the subcontinental lithosphere, the Sr, Nd and Pb isotopic characteristics of the Spanish lamproites suggest the involvement of recently-subducted sedimentary material. Although sediments derived from old cratons may be expected to possess measurably radiogenic calcium, as discussed earlier (see Section 9.4.1), when radiogenic calcium from these sources enters the marine environment, it is likely to be diluted by mixing with unradiogenic marine calcium. Furthermore, mixing within the mantle with unradiogenic mantle calcium is also likely to occur. These processes may account for the unradiogenic $^{40}Ca/^{42}Ca$ ratios of the Spanish lamproites.

The Ca isotopic data obtained for central west Greenland kimberlites and lamproites (Table 9.4) indicate that these samples possess $^{40}Ca/^{42}Ca$ ratios which are significantly more radiogenic than the mantle value. Using the mean wt% K_2O/CaO value for the kimberlites from Scott (1979) (i.e. 0.104, from the 5 kimberlite analyses given in Table 6.2) and the mean $^{40}Ca/^{42}Ca$ ratio age-corrected using the emplacement ages of Smith (1979) (i.e. ε_{Ca} = +2.63 ±0.46), the Greenland kimberlites have ^{40}K-^{40}Ca model ages of 5670 ±300 Ma (errors on model ages are calculated using the 95% confidence uncertainty limits on the $^{40}Ca/^{42}Ca$ measurement. Error in the model age is insensitive to analytical error in the K_2O/CaO ratio and has been ignored in the error calculation. For example, an error of ±0.1% in the wt% K_2O/CaO ratio propagates to an error of only ±3 Ma in the ^{40}K-^{40}Ca model age for wt% K_2O/CaO ratios ≤ 1 and for model ages < 2.0 Ga). If the measured K_2O/CaO ratios represent maximum estimates for the source regions of the kimberlitic and lamproitic magmas (due to the greater incompatibility of potassium relative to calcium), these model ages represent the minimum time required for the radiogenic Ca to evolve *prior to emplacement of the intrusions* (i.e. add emplacement ages to model ages to give the time from the present). The Greenland kimberlite ^{40}K-^{40}Ca model ages are older than the age of the Earth, indicating that some proportion of the radiogenic Ca is unsupported. The K/Ca ratios of the kimberlites or their sources must therefore have been lowered at some time during their history. It is likely that the calcium contents (and K/Ca ratios) of the kimberlites have been increased by magmatic processes during their generation, possibly due to the greater solubility of CO_3^{2-} in silicate melts at depths of ~25 kbar. U-Pb ion microprobe zircon ages of up to 3820 Ma have been reported from a tonalitic Amîtsoq gneiss from the nearby Godthåb region of southern west Greenland (Kinny 1986). Assuming that the kimberlite sources are this age or younger, a K_2O/CaO ratio of at least 0.298 ±0.049 is required for the measured $^{40}Ca/^{42}Ca$ ratio found in the kimberlites (ε_{Ca} of +2.68 ±0.46) to have evolved within this time. This is almost 3 times higher than the average wt% K_2O/CaO ratio of 0.104 presently found in the kimberlites.

A further surprising feature of the Ca isotopic results obtained for the Greenland kimberlites is that their radiogenic Ca is not accompanied by radiogenic Sr isotopic compositions (see Table 6.1) as might be anticipated from consideration of the similar geochemical behavior of K and Rb and of Ca and Sr. Although the radiogenic Ca may be due to interaction of the kimberlitic magma with the upper continental crust, either during or following emplacement, the unradiogenic Sr isotopic compositions of the kimberlites are not consistent with this proposal. The kimberlites also possess relatively radiogenic Nd isotopic compositions (with ε_{Nd} of between +1.3 and +3.9; see Table 6.2) and isotopically resemble carbonatites and some ocean-island basalts (see discussion in Chapter 8, especially 8.5.3). One plausible explanation for the puzzling Ca isotopic compositions of the kimberlites is that the Ca (and presumably other more compatible major elements) has been decoupled from, and has undergone entirely different histories to, the trace elements (such as Sr and Nd). The major elements may have been derived from ancient sources with relatively high K/Ca but low abundances of trace elements such as Sr and Nd, possibly located within the subcontinental lithosphere, whereas the trace elements may have been introduced from another source.

Model ^{40}K-^{40}Ca ages for the Greenland lamproites #5611 and #5622 are 3400 $^{+700}/_{-500}$ Ma and 2060 $^{+570}/_{-860}$ Ma respectively. Using the average lamproite wt% K_2O/CaO ratio of 1.35 (the mean of 4 lamproite analyses given in Table 6.1) and the mean measured lamproite $^{40}Ca/^{42}Ca$ ratio (ε_{Ca} = +4.77 ±1.05), the ^{40}K-^{40}Ca model age is 2400 $^{+270}/_{-320}$ Ma. This model age is ~1200 Ma older than the emplacement age of the lamproites. If the greater incompatibility of potassium relative to calcium caused an increase in the K/Ca ratio during generation of the lamproite magmas, this model age will under-estimate the time required to generate the observed radiogenic $^{40}Ca/^{42}Ca$ ratios. The lamproite ^{40}K-^{40}Ca model ages are in general accord with model ages inferred from their ^{147}Sm-^{143}Nd isotopic systematics. The ^{40}K-^{40}Ca isotopic systematics of the Greenland lamproites therefore do not require the derivation of their major- and trace-element components from sources which have undergone different evolutionary histories.

9.4.4 Chemical and clastic sediments from old terrains

The Ca isotopic results obtained on gypsum samples provides unequivocal evidence that most of the calcium within the gypsums has not been derived directly from the oceans. Sulphur isotopic analysis of the gypsum samples indicates that they possess $\delta^{34}S$ values of between +16 and +20 ‰ (A.R. Chivas and B. Lyons, personal communication). By contrast, Donnelly *et al.* (1977) analysed sulphides in 52 sedimentary rock samples from the Archaean Yilgarn Block for their sulphur isotopic compositions and found that the sediments possessed $\delta^{34}S$ values between -7.6 and +5.2 ‰. These authors argued that the sulphide within the sediments was predominantly of magmatic origin and was probably precipitated from hydrothermal solutions. The bulk of the sulphate in the gypsum samples therefore could not be derived from the surrounding continental crust, but may have been derived from the oceans and carried inland, in rainwater or as aerosol, possibly in the form of dilute sulphuric acid. Alternatively, the gypsums could have formed by the evaporation of brines trapped within inland lakes if the sulphate concentration in the brines was substantially higher than the calcium concentration. Most of the calcium could then have been

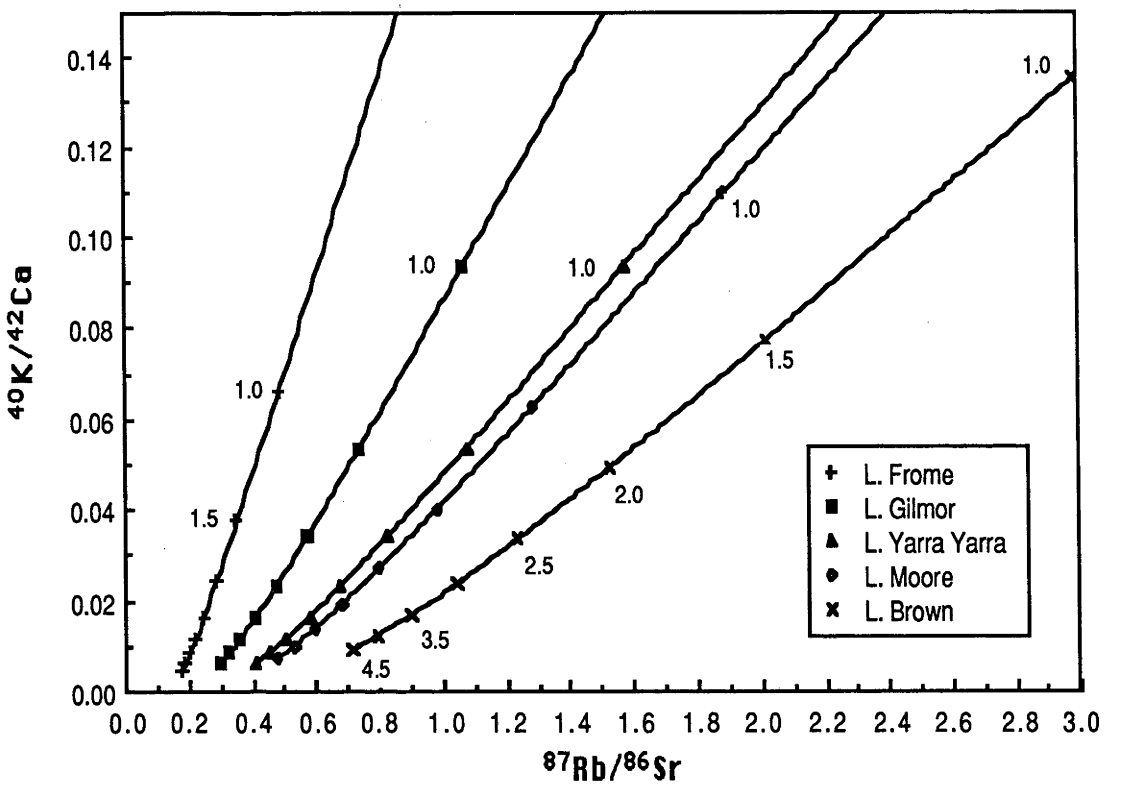

Fig. 9.5 Curves of possible $^{87}Rb/^{86}Sr$ and $^{40}K/^{42}Ca$ values for the crustal catchment $^{87}Sr/^{86}Sr$ and $^{40}Ca/^{42}Ca$ ratios represented by the gypsum samples. The curves have been calculated assuming that the continental crust differentiated from a mantle with $^{87}Rb/^{86}Sr$ =0.090, $^{40}K/^{42}Ca$ = 0.00018, present-day $^{87}Sr/^{86}Sr$ = 0.70478 and present-day $^{40}Ca/^{42}Ca$ = 151.078. The ticks on the curves are crustal residence times corresponding to the $^{87}Rb/^{86}Sr$ and $^{40}K/^{42}Ca$ ratios. The curves for the 5 gypsum samples do not intersect, indicating that the crustal catchments have had unique histories of [K/Ca]/[Rb/Sr].

derived by interaction with the surrounding upper crust.

Assuming that most of the Sr and Ca within the gypsum samples has been derived from the surrounding crustal catchment and that the Sr and Ca isotopic characteristics of the gypsums represent average values for the region, the relationship between the average K/Ca and Rb/Sr ratios of the crustal catchment can be determined. This relationship is shown in Fig. 9.5, in which the curves represent the loci of $^{87}Rb/^{86}Sr$ and $^{40}K/^{42}Ca$ ratios required in order to evolve the observed $^{87}Sr/^{86}Sr$ and $^{40}Ca/^{42}Ca$ values. These ratios are also dependent on the regional mean crustal residence time, or the time at which the crust differentiated from the Earth's mantle. The curves have been calculated assuming that the continental crust was extracted, during single short-lived differentiation events, from a mantle having a constant $^{87}Rb/^{86}Sr$ of 0.090 and present-day $^{87}Sr/^{86}Sr$ of 0.70478 (corresponding to an $^{87}Sr/^{86}Sr$ of 0.6988 at 4.55 Ga). For reasonable crustal residence times of between 1.5 and 4.0 Ga, the gypsum samples require $^{40}K/^{42}Ca$ and $^{87}Rb/^{86}Sr$ ratios of 0.01 to 0.08 and 0.2 to 2.0 respectively, corresponding to K_2O/CaO and Rb/Sr ratios of 0.46 to 3.70 and 0.07 to 0.70. These K_2O/CaO and Rb/Sr ratios are respectively ~5.5 to 44 and ~2 to 22 times the corresponding values of the Earth's mantle (i.e. mantle $K_2O/CaO \approx 0.08$ and $Rb/Sr \approx 0.031$). A narrower range of $^{40}K/^{42}Ca$ and $^{87}Rb/^{86}Sr$ values for each gypsum catchment can also be determined from Fig. 9.5 if the crustal residence time is assumed from the regional field geology. As mixing with mantle- or seawater-derived Sr and Ca will reduce the

observed $^{40}Ca/^{42}Ca$ and $^{87}Sr/^{86}Sr$ values of the gypsums, the calculated K_2O/CaO and Rb/Sr ratios probably represent minimum estimates of the values required to evolve the Ca and Sr isotopic characteristics of the surrounding crust. The curves for the gypsum samples do not intersect, indicating that the crustal regions sampled by the gypsums have undergone unique histories of [K/Ca]/[Rb/Sr]. A minimum range of 0.2 to 0.7 for $^{87}Rb/^{86}Sr$ is indicated for the 5 continental crustal regions examined.

The calcium isotopic results obtained for the Mt Narryer clastic sediments (see Table 9.6) demonstrate that substantial radiogenic enrichments in ^{40}Ca may occur in pelitic sediments from ancient terrains. However, the results also suggest that the K-Ca isotope system has not remained closed. Although Froude *et al.* (1983) reported ion microprobe U-Pb zircon ages of 4.1 to 4.2 Ga from the Mt Narryer region, these authors argued that the sediments hosting these old zircons are unlikely to be older than ~3.5 Ma. The 3-point K-Ca isochron age of 4.17 ±0.38 Ga defined by the Mt Narryer sediments (Fig. 9.4) is therefore unlikely to represent the depositional age of the sediments. The slope of this isochron is largely controlled by pelite sample AUS-52, which has an unrealistically old ^{40}K-^{40}Ca model age of 4.39 Ga (Table 9.6). Furthermore, the other Mt Narryer sediments analysed have either unrealistically old (i.e. AUS-75; the error on this ^{40}K-^{40}Ca model age is large because of the low K/Ca ratio) or undefined (i.e. AUS-81) ^{40}K-^{40}Ca model ages, indicating that there has been some re-mobilisation of K and/or Ca.

The results obtained for the Mt Narryer sediments suggest that although substantial enrichments in ^{40}Ca may be generated in sufficiently ancient pelitic sediments, the mobility of K and/or Ca may limit the potential usefulness of the K-Ca decay scheme as a means of dating sediments by either of the K-Ca isochron and model age methods.

Summary

This study has demonstrated that, using relatively simple chemical and mass spectrometry procedures, the K-Ca method can be successfully applied to a variety of petrogenetic and geochronological problems. In the case of its application to igneous rocks, it has been shown that the K-Ca isotope system can provide valuable petrogenetic information which cannot be obtained by other techniques.

The $^{40}Ca/^{42}Ca$ results obtained for all rock-types examined in this study are summarised in Fig. 9.6. The main conclusions which can be drawn from the results of this study are;

1. The $^{40}Ca/^{42}Ca$ ratio of the calcium isotopic standard prepared from the *Tridacna Gigas* shell is indistinguishable from the value measured in oceanic basalts. This implies that the $^{40}Ca/^{42}Ca$ ratio of modern seawater is identical, within the levels of precision presently attainable, to that of the Earth's mantle.
2. Relative to the Famous area mid-ocean ridge basalts, no measurable enrichments in ^{40}Ca were detected in either Hawaiian ocean-island basalts, Banda and Aleutian island-arc calc-alkaline lavas or a Banda arc trough sediment. Application of the ^{40}K-^{40}Ca decay scheme to the identification of recycled crustal material in island-arc and ocean-island lavas is likely to be hindered by the buffering of any radiogenic Ca derived from the upper contental crust by unradiogenic marine- and/or mantle-derived Ca.

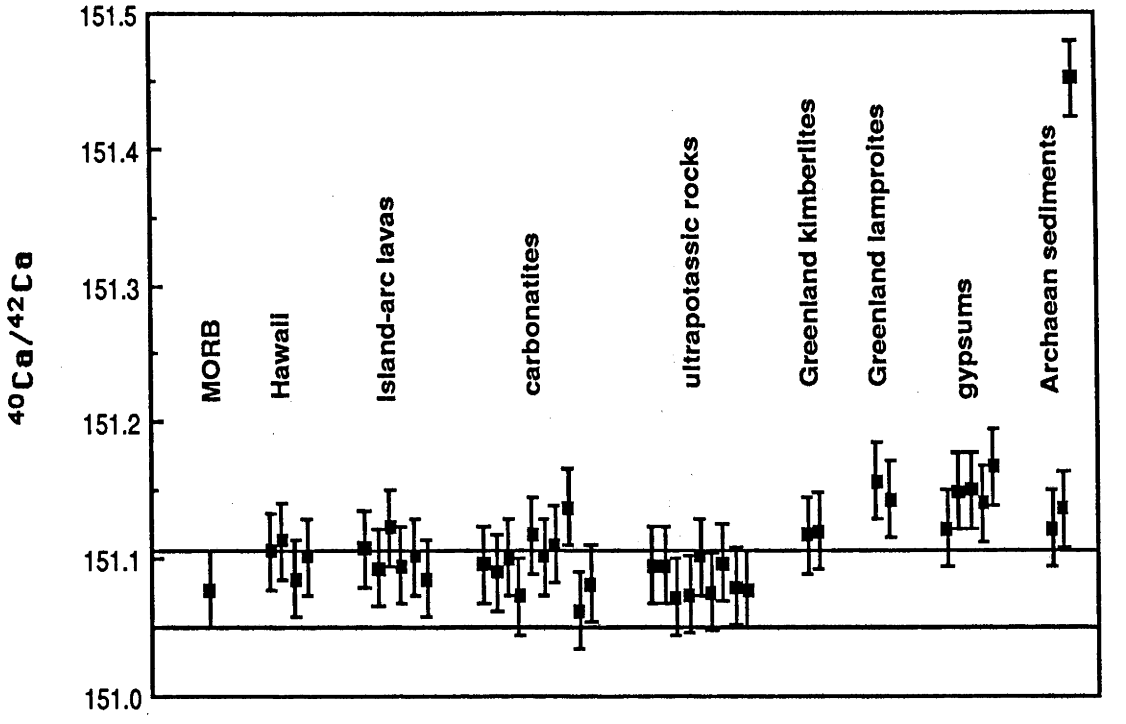

Fig. 9.6 Summary of $^{40}Ca/^{42}Ca$ results for various rock-types examined during this study. The horizontal lines delimit the 2σ boundaries of the mantle value (as given by the mid-ocean ridge basalt analysis). Error-bars are ±0.028 or 2σ limits for an individual analysis. In some instances (for example, the central west Greenland kimberlites), the results of a number of runs have been pooled and the analytical error for these pooled groups is less than that which applies for a single analysis.

3. Carbonatite samples from 9 carbonatite complexes possess $^{40}Ca/^{42}Ca$ ratios which are statistically indistinguishable from those of oceanic basalts. The results obtained for one carbonatite sample, from the Ugandan Sukulu complex, suggest that the carbonatite may possess a small enrichment in ^{40}Ca.
4. Relatively undifferentiated lavas from the Western Australian, Gaussberg and Spanish potassic suites possess $^{40}Ca/^{42}Ca$ ratios which are analytically indistinguishable from the value found in oceanic basalts and carbonatites. This suggests that; a). the increase in K/Ca of the sources of these potassic magmas has not occurred synchronously with the trace-element enrichment (in particular, the enrichment in the light rare-earth elements) but at some later time; b). the K/Ca ratio of the magmas has been increased substantially during partial melting, melt extraction and/or differentiation, or c). the calcium in the magmas has been diluted by mixing with calcium derived from other sources.
5. Resolvable enrichments in ^{40}Ca abundance are present in kimberlitic and potassic dykes from central west Greenland. In the case of the Greenland kimberlites, the radiogenic $^{40}Ca/^{42}Ca$ is unsupported, with the K_2O/CaO ratio of the kimberlites being ~1/3 of the value required to generate the ^{40}Ca enrichment. As the radiogenic $^{40}Ca/^{42}Ca$ is not accompanied by radiogenic $^{87}Sr/^{86}Sr$ or unradiogenic $^{143}Nd/^{144}Nd$, it is likely that the kimberlite major- and trace-element components have been decoupled, with much of the major elements possibly derived from the subcontinental lithosphere of the Greenland region and the trace elements derived from some other

source (possibly located in the asthenosphere; see discussion in Chapter 8). The radiogenic $^{40}Ca/^{42}Ca$ ratio found in the central west Greenland lamproites is consistent with their derivation from subcontinental lithospheric sources which have undergone enrichment in K and the incompatible trace elements at least ~2 Ga ago and at least 1 Ga prior to their emplacement.

6. Chemical and pelitic clastic sediments from ancient (Archaean and early Proterozoic) terrains possess substantial enrichments in ^{40}Ca relative to oceanic basalts. Calcium extracted from gypsum samples from Western Australian evaporite deposits has largely been derived from the surrounding crustal basement. The results obtained for the pelitic sediments indicate that the ^{40}K-^{40}Ca isotope system has not remained closed.

Apart from the insights offered by its application as a petrogenetic tracer to the genesis of highly potassic igneous rocks, perhaps the most promising future application of the ^{40}K-^{40}Ca isotope system is suggested by the results obtained for crustal rocks from ancient terrains. In particular, when applied in conjunction with other stable and radiogenic isotope schemes, the ^{40}K-^{40}Ca system may prove useful in the examination of intra-crustal weathering processes and recycling rates.

REFERENCES

Introduction and Section A.

Addy S.K. (1979) Rare earth element patterns in manganese nodules and micronodules from northwest Atlantic. *Geochim. Cosmochim. Acta* **43**, 1105-1115.

Allègre C.J., Ben Othman D., Polve M. and Richard P. (1979) The Nd-Sr isotopic correlation in mantle materials and geodynamic consequences. *Phys. Earth Planet. Interiors* **19**, 293-306.

Allègre C.J., Richard P., Treuil M. and Joron J.L. (1979) Neodymium-strontium-lead isotopes and magmatophile elements (Zr, Hf, Ta, Th, U, Ba, Cs, Rb) in east-west Japan traverse. Consequences for island arc magmatism. (abstr.) *Eos Trans. Amer. Geophys. Union* **60**, 413-414.

Allègre C.J., Dupré B. and Brevart O. (1982) Chemical aspects of the formation of the core. *Phil. Trans. Roy. Soc. London* **A 306**, 49-59.

Allègre C.J., Dupré B., Richard P. and Rousseau D. (1982) Subcontinental versus oceanic mantle, II. Nd-Sr-Pb isotopic comparison of continental tholeiites with mid-ocean ridge tholeiites, and the structure of the continental lithosphere. *Earth Planet. Sci. Lett.* **57**, 25-34.

Allègre C.J. and Jupart C. (1985) Continental tectonics and continental kinetics. *Earth Planet. Sci. Lett.* **74**, 171-186.

Amari S. and Ozima M. (1985) Search for the origin of exotic Helium in deep-sea sediments. *Nature* **317**, 520-522.

Arana V. and Vegas R. (1974) Plate tectonics and volcanism in the Gibraltar arc. *Tectonophys.* **24**, 197-212.

Andrews J.R. and Emeleus C.H. (1976) Kimberlites of West Greenland. In *Geology of Greenland* (eds. A. Escher and W.S. Watt). Grønlands Geologiske Undersøgelse, Copenhagen. pp. 575-581.

Armstrong R.L. (1968) A model for Sr and Pb isotope evolution in a dynamic earth. *Rev. Geophys.* **6**, 175-199.

Armstrong R.L. (1981) Radiogenic isotopes: the case for crustal recycling on a near-steady-state no-continental-growth Earth. *Phil. Trans. Roy. Soc. London* **A 301**, 443-472.

Atkinson W.J., Hughes F.E. and Smith C.B. (1984) A review of the kimberlitic rocks of Western Australia. In *Kimberlites I: Kimberlites and Related Rocks.* (ed. J. Kornprobst). Elsevier, Amsterdam. pp. 195-224.

Bak J., Sørensen K., Grocott J., Korstgård J.A., Nash D. and Watterson J. (1975) Tectonic implications of Precambrian shear belts in western Greenland. *Nature* **254**, 566-569.

Barbieri F., Gasparini P., Innocenti F. and Villari L. (1973) Volcanism of the southern Tyrrhenian Sea and its geodynamic implications. *J. Geophys. Res.* **78**, 5221-5232.

Bell K. and Powell J.L. (1970) Strontium isotopic studies of alkalic rocks: the alkalic complexes of eastern Uganda. *Geol. Soc. Amer. Bull.* **81**, 3481-3490.

Bellon H. and Letousey J. (1977) Volcanism related to plate-tectonics in the western and eastern Mediterranean Basins. Technip., Paris. pp. 165-184.

Birch W.D. (1978) Mineralogy and geochemistry of the leucitite at Cosgrove, Victoria. *J. Geol. Soc. Aust.* **25**, 369-385.

Bishop A.C. and Woolley A.R. (1973) A basalt-trachyte-phonolite series from Ua-Pu, Marquesas Islands, Pacific Ocean. *Contrib. Mineral. Petrol.* **39**, 309-326.

Black L.P. and James P.R. (1983) Geological history of the Archaean Napier Complex of Enderby Land. In *Proceedings of the 4th International Symposium of Antarctic Earth Science.* (eds. R.L. Oliver, P.R. James and J.B. Jago). Australian Academy of Science, Canberra. pp. 11-15.

Black L.P., Shaw R.D. and Stewart A.J. (1983) Rb-Sr geochronology of Proterozoic events in the Arunta Inlier, Central Australia. *B.M.R. J. Aust. Geol. Geophys.* **8**, 129-137.

Borley G.D. (1967) Potassium-rich volcanic rocks from southeastern Spain. *Mineral. Mag.* **36**, 364-379.

Brooks C., James D.E. and Hart S.R. (1976) Ancient lithosphere: its role in young continental volcanism. *Science* **193**, 1086-1094.

Brown L., Klein J., Middleton R., Sacks I.S. and Tera F. (1982) ^{10}Be in island arc volcanoes and implications for subduction. *Nature* **299**, 718-720.

Calvert S.E. (1976) The mineralogy and geochemistry of near-shore sediments. In *Chemical Oceanography.* (eds. J.P. Riley and R. Chester). Vol. 6, 2nd edition. Academic Press, London. pp. 187-280.

Carmichael I.S.E. (1967) The mineralogy and petrology of the volcanic from the Leucite Hills, Wyoming. *Contrib. Mineral. Petrol.* **15**, 24-66.

Catanzaro E.J., Murphy T.J., Shields W.R. and Garner E.L. (1968) Absolute isotopic abundance ratios of common, equal atom, and radiogenic lead isotopic standards. *J. Res. Nat. Bureau Stand. (U.S.)* **72A**, 261-267.

Chase C.G. (1981) Oceanic island Pb: Two stage histories and mantle evolution. *Earth Planet. Sci. Lett.* **52**, 277-284.

Chester R. and Aston S.R. (1976) The geochemistry of deep sea sediments. In *Chemical Oceanography.* (eds. J.P. Riley and R. Chester). Vol. 6, 2nd edition. Academic Press, London. pp. 281-390.

Civetta L., Innocenti F., Manetti P., Peccerillo A. and Poli G. (1981) Geochemical characteristics of potassic volcanics from Mts Ernici (southern Latium, Italy). *Contrib. Mineral. Petrol.* **78**, 37-47.

Chow T.J. and Patterson C.C. (1962) The occurrence and significance of Pb isotopes in pelagic sediments. *Geochim. Cosmochim. Acta* **26**, 263-308.

Church S.E. (1973) Limits of sediment involvement in the genesis of orogenic volcanic rocks. *Contrib. Mineral. Petrol.* **39**, 17-32.

Cohen R.S. and O'Nions R.K. (1982a) The lead, neodymium and strontium isotopic structure of ocean ridge basalts. *J. Petrol.* **23**, 299-324.

Cohen R.S. and O'Nions R.K. (1982b) Identification of recycled continental material from Sr, Nd and Pb isotope investigations. *Earth Planet. Sci. Lett.* **61**, 73-84.

Collerson K.D. and McCulloch M.T. (1983) Nd and Sr isotope geochemistry of leucite-bearing lavas from Gaussberg, East Antarctica. In *Proceedings of the 4th International Symposium of Antarctic Earth Science.* (eds. R.L. Oliver, P.R. James and J.B. Jago). Australian Academy of Science, Canberra. pp. 676-680.

Cooper J.A. and Green D.H. (1969) Lead isotope measurements on lherzolite inclusions and host basanites from western Victoria, Australia. *Earth Planet. Sci. Lett.* **6**, 69-76.

Craddock C. (1975) Tectonic evolution of the Pacific margin of Gondwanaland. In *Gondwana Geology.* (ed. K.S.W. Campbell). Australian National University Press, Canberra. pp. 609-618.

Crook K.A.W. (1980) Fore-arc evolution in the Tasman Geosyncline: the origin of the southeast Australian continental crust. *J. Geol. Soc. Aust.* **27**, 215-232.

Cumming G.L. and Richards J.R. (1975) Ore lead isotope ratios in a continuously changing Earth. *Earth Planet. Sci. Lett.* **28**, 155-171.

Cundari A. (1973) Petrology of the leucite-bearing lavas in New South Wales. *J. Geol. Soc. Aust.* **20**, 465-492.

Cundari A. (1979) Petrogenesis of leucite-bearing lavas in the Roman volcanic region, Italy. The Sabatini lavas. *Contrib. Mineral. Petrol.* **70**, 9-21.

Cundari A. (1980) Role of subduction in the genesis of leucite-bearing rocks: facts or fashion? *Contrib. Mineral. Petrol.* **73**, 432-434.

Dasch E.J., Dymond J. and Heath G.R. (1971) Isotopic analysis of metalliferous sediments from the East Pacific Rise. *Earth Planet. Sci. Lett.* **13**, 175-180.

Dasch E.J. (1981) Lead isotopic composition of metalliferous sediments from the Nazca plate. *Geol. Soc. Amer. Memoir* **154**, 199-209.

DePaolo D.J. (1979) Implications of correlated Nd and Sr isotopic variations for the chemical evolution of the crust and mantle. *Earth Planet. Sci. Lett.* **43**, 201-211.

Dickinson W.R. and Hatherton T. (1967) Andesitic volcanism and seismicity around the Pacific. *Science* **157**, 801-803.

Dosso L, Vidal P., Cantagrel J.M., Lameyre J. and Marot S.Z. (1979) "Kerguelen: continental fragment or ocean island?":petrology and isotopic geochemistry evidence. *Earth Planet. Sci. Lett.* **43**, 44-60.

Duncan R.A. (1981) Hotspots in the southern oceans- an absolute frame of reference for motion of the Gondwana continents. *Tectonophys.* **74**, 29-42.

Duncan R.A., McCulloch M.T., Barscus H.G. and Nelson D.R. (1986) Plume versus lithospheric sources for melts at Ua Pu, Marquesas Islands. *Nature* **322**, 534-538.

Dupré B. and Allègre C.J. (1980) Pb-Sr-Nd isotopic correlation and chemistry of North Atlantic mantle. *Nature* **286**, 17-22.

Dupré B., Chauvel C. and Arndt N.T. (1984) Pb and Nd isotopic study of two Archean komatiitic flows from Alexo, Ontario. *Geochim. Cosmochim. Acta* **48**, 1965-1972.

Dupuy C, Vidal P., Barscus H.G. and Chauvel C. (1987) Origin of basalts from the Marquesas Archipelago (south central Pacific Ocean): isotope and trace element constraints. *Earth Planet. Sci. Lett.* **82**, 145-152.

Edgar A.D. (1980) Role of subduction in the genesis of leucite-bearing rocks: discussion. *Contrib. Mineral. Petrol.* **73**, 429-431.

Eggler D.H. (1978) The effect of CO_2 upon partial melting of peridotite in the system Na_2O-CaO-Al_2O_3-MgO-$Si0_2$-CO_2 to 34 Kb, with an analysis of melting in a peridotite-H_2O-CO_2 system. *Amer. J. Sci.* **278**, 305-343.

Elderfield H., Hawkesworth C.J., Greaves M.J. and Calvert S.E. (1981) Rare earth element geochemistry of oceanic ferromanganese nodules and associated sediments. *Geochim. Cosmochim. Acta* **45**, 513-528.

Erlank A.J. and Kable E.D.J. (1976) The significance of incompatible elements in Mid-Atlantic Ridge basalts from 45° N with particular reference to Zr/Nb. *Contrib. Mineral. Petrol.* **54**, 281-291.

Ferrara G., Laurenzi M.A., Taylor H.P., Tonarini S. and Turi B. (1985) Oxygen and strontium isotope studies of K-rich volcanic rocks from the Alban Hills, Italy. *Earth Planet. Sci. Lett.* **75**, 13-28.

Foden J.D. and Varne R. (1980) The petrology and tectonic setting of Quarternary-Recent volcanic centres of Lombok and Sumbawa, Sunda arc. *Chem. Geol.* **30**, 201-226.

Foley S.F. (1985) The oxidation state of lamproitic magmas. *Tschermaks Mineral. Petrog. Mitt.* **34**, 217-238.

Foley S.F., Taylor W.R. and Green D.H. (1986) The effects of flourine on phase relationships in the system $KAlSiO_4$-$MgSiO_4$-SiO_2 with application to the genesis of ultrapotassic rocks. *Contrib. Mineral. Petrol.* **94**, 183-192.

Foley S.F., Venturelli G., Green D.H. and Toscani L. (1987) The ultrapotassic rocks: characteristics, classification, and constraints for petrogenetic models. *Earth Sci. Rev.* **24**, 81-134.

Fraser K.J., Hawkesworth C.J., Erlank A.J., Mitchell R.H. and Scott-Smith B.H. (1985) Sr, Nd and Pb isotope and minor element geochemistry of lamproites and kimberlites. *Earth Planet. Sci. Lett.* **76**, 57-70.

Fyfe W.S. and McBirney A.R. (1975) Subduction and structure of andesitic volcanic belts. *Amer. J. Sci.* **275A**, 285-297.

Galer S.J.G. and O'Nions R.K. (1985) Residence time of thorium, uranium and lead in the mantle with implications for mantle convection. *Nature* **316**, 778-782.

Gill J.B. (1984) Sr-Pb-Nd isotopic evidence that both MORB and OIB sources contribute to ocean island arc magmas in Fiji. *Earth Planet. Sci. Lett.* **68**, 443-458.

Gill J.B., Stork A.L. and Whelan P.M. (1984) Volcanism accompanying back-arc basin development in the southwest Pacific. *Tectonophys.* **102**, 207-224.

Goldstein S.L. and O'Nions R.K. (1981) Nd and Sr isotopic relationships in pelagic clays and ferromanganese deposits. *Nature* **292**, 324-327.

Green D.H. (1976) Experimental petrology in Australia- a review. *Earth Sci. Rev.* **12**, 99-138.

Gupta A.K. and Yagi K. (1980) *Petrology and Genesis of the Leucite-bearing Rocks.* Springer-Verlag, Berlin. 252p.

Hamilton P.J., O'Nions R.K., Bridgewater D. and Nutman A. (1983) Sm-Nd studies of Archaean metasediments and metavolcanics from West Greenland and their implications for the Earth's early history. *Earth Planet. Sci. Lett.* **62**, 263-272.

Hansen K. (1981) Systematic Sr-isotopic variation in alkaline rocks from West Greenland. *Lithos* **14**, 183-188.

Hart S.R. (1971) K, Rb, Cs, Sr and Ba contents and Sr isotope ratios of ocean floor basalts. *Phil. Trans. Roy. Soc. London* **A 268**, 573-587.

Hatherton T. and Dickinson W.R. (1968) Andesite volcanism and seismicity in New Zealand. *J. Geophys. Res.* **73**, 4615-4619.

Hatherton T. and Dickinson W.R. (1969) The relationship between andesitic volcanism and seismicity in Indonesia, the Lesser Antilles and other island arcs. *J. Geophys. Res.* **74**, 5301-5310.

Hawkesworth C.J. and Vollmer R. (1979) Crustal contamination versus enriched mantle: $^{143}Nd/^{144}Nd$ and $^{87}Sr/^{86}Sr$ evidence from the Italian volcanics. *Contrib. Mineral. Petrol.* **69**, 151-165.

Hawkesworth C.J., Erlank A.J., Marsh J.S., Menzies M.A. and van Calsteren P. (1983) Evolution of the continental lithosphere: evidence from volcanics and xenoliths in southern Africa. In *Continental Basalts and Mantle Xenoliths.* (eds. C.J. Hawkesworth and M.J. Norry). Shiva Ltd., London. pp. 111-138.

Hoefs J. and Wedepohl K.H. (1968) Strontium isotope studies on young volcanic rocks from Germany and Italy. *Contrib. Mineral. Petrol.* **19**, 328-338.

Hoefs J., Faure G. and Elliot D.H. (1980) Correlation of $\delta^{18}O$ and initial $^{87}Sr/^{86}Sr$ ratios in Kirkpatrick basalt on Mt. Falla, Transantarctic Mountains. *Contrib. Mineral. Petrol.* **75**, 199-203.

Hofmann A.W. and White W.M. (1980) The role of subducted oceanic crust in mantle evolution. *Carnegie Inst. Wash. Yearb.* **79**, 477-483.

Hofmann A.W. and White W.M. (1982) Mantle plumes from ancient oceanic crust. *Earth Planet. Sci. Lett.* **57**, 421-436.

Hole M.J., Saunders A.D., Marriner G.F. and Tarney J. (1984) Subduction of pelagic sediments: implications for the origin of Ce-anomalous basalts from the Marinas Islands. *J. Geol. Soc. London* **141**, 453-472.

Holm P.M. and Munksgaard N.C. (1982) Evidence for mantle metasomatism: an oxygen and strontium isotope study of the Vulsinian District, Central Italy. *Earth Planet. Sci. Lett.* **60**, 376-388.

Hussong D.M., and Uyeda S. (1981) Tectonic processes and the history of the Mariana arc: a synthesis of the results of Deep Sea Drilling Project Leg 60. In *Initial Reports of the Deep Sea Drilling Project* **60**, 909-929. U.S. Government Printing Office, Washington.

Ito E., White W.M. and Gopel C. (1987) The O, Sr, Nd and Pb isotope geochemistry of MORB. *Chem. Geol.* **62**, 157-176.

Jacobsen S.B. and Wasserburg G.J. (1979) The mean age of mantle and crustal reservoirs. *J. Geophys. Res.* **84**, 7411-7427.

Jakes P. and White A.J.R. (1972) Major and trace element abundances in volcanic rocks of orogenic areas. *Geol. Soc. Amer. Bull.* **83**, 29-40.

James P.R. and Tingey R.J. (1983) The Precambrian geological evolution of the east Antarctic metamorphic shield: a review. In *Proceedings of the 4th International Symposium of Antarctic Earth Science*. (eds. R.L. Oliver, P.R. James and J.B. Jago). Australian Academy of Science, Canberra. pp. 5-10.

Jaques A.L., Lewis J.D., Smith C.B., Gregory G.P., Ferguson J., Chappell B.W., and McCulloch M.T. (1984a) The diamond-bearing ultrapotassic (lamproitic) rocks of the West Kimberley region, Western Australia. In *Kimberlites I: Kimberlites and Related Rocks* (ed. J. Kornprobst). Elsevier, Amsterdam. pp. 225-254.

Jaques A.L., Webb A.W., Fanning C.M., Black L.P., Pidgeon R.T., Ferguson J., Smith C.B. and Gregory G.P. (1984b) The age of the diamond-bearing pipes and associated leucite lamproites of the West Kimberley region, Western Australia. *B.M.R. J. Aust. Geol. Geophys.* **9**, 1-7.

Jaques A.L., Lewis J.D. and Smith C.B. (1986a) The kimberlites and lamproites of Western Australia. *Geol. Surv. West. Aust. Bull.* **132**.

Jaques A.L., Sheraton J.W., Hall A.E., Smith C.B., Sun S.-S., Drew R. and Foudoulis C. (1986b) Composition of crystalline inclusions and C-isotopic composition of Argyle and Ellendale diamonds. (extended abstr.) 4th Int. Kimberlite Conf., Perth. *Geol. Soc. Aust. Abstr. Ser.* **16**, 426-430.

Karig D.E. and Kay R.W. (1981) Fate of sediments on the decending plate at convergent margins. *Phil. Trans. Roy. Soc. London* **A 301**, 233-251.

Kay R.W. (1980) Volcanic arc magmas: implication of a melting-mixing model for element recycling in the crust-upper mantle. *J. Geol.* **88**, 497-522.

Kay R.W. (1984) Elemental abundances relevant to identification of magma sources. *Phil. Trans. Roy. Soc. London* **A 310**, 535-547.

Kesson S.E. (1973) The primary geochemistry of the Monaro alkaline volcanics, southeastern Australia-evidence for upper mantle heterogeneity. *Contrib. Mineral. Petrol.* **42**, 93-108.

Kuehner S.M., Edgar A.D. and Arima M. (1981) Petrogenesis of the ultrapotassic rocks from the Leucite Hills, Wyoming. *Amer. Mineral.* **66**, 663-677.

Kurasawa H. (1968) Isotopic composition of lead and concentrations of uranium, thorium, and lead in volcanic rocks from Dogo and the Oki Islands, Japan. *Geochem. J.* **2**, 11-28.

Kyle P.R., Pankhurst R.J. and Bowman J.R. (1983) Isotopic and chemical variations in Kirkpatrick Basalt Group rocks from southern Victoria Land. In *Proceedings of the 4th International Symposium of Antarctic Earth Science.* (eds. R.L. Oliver, P.R. James and J.B. Jago). Australian Academy of Science, Canberra. pp. 234-237.

Langworthy A.P. and Black L.P. (1978) The potassic Mordor Complex, Central Australia. *Contrib. Mineral. Petrol.* **67**, 51-62.

Larsen L.M., Rex D.C. and Secher K. (1983) The age of carbonatites, kimberlites and lamprophyres from southern West Greenland: recurrent alkaline magmatism during 2500 million years. *Lithos* **16**, 215-221.

Le Maitre R.W. (1962) Petrology of volcanic rocks, Gough Island, South Atlantic. *Geol. Soc. Amer. Bull.* **73**, 1309-1340.

Lipman P.W., Protska H.J. and Christiansen R.L. (1972) Cenozoic volcanism and plate tectonic evolution of the western United States. *Phil. Trans. Roy. Soc. London* **A 271**, 217-248.

Liu Y.-G. and Schmitt R.A. (1984) Chemical profiles in sediment and basalt samples from Deep Sea Drilling Project Leg 74, Hole 525A, Walvis Ridge. In *Initial Reports of the Deep Sea Drilling Project* **74**, 713-730. U.S. Government Printing Office, Washington.

McCulloch M.T. and Perfit M.R. (1980) $^{143}Nd/^{144}Nd$, $^{87}Sr/^{86}Sr$ and trace element constraints on the petrogenesis of Aleutian island arc magmas. *Earth Planet. Sci. Lett.* **56**, 167-179.

McCulloch M.T. and Wasserburg G.J. (1981) Sm-Nd and Rb-Sr chronology of continental crust formation. *Science* **200**, 1003-1011.

McCulloch M.T. and Chappell B.W. (1982) Nd isotopic characteristics of S- and I- type granites. *Earth Planet. Sci. Lett.* **58**, 51-64.

McCulloch M.T., Jaques A.L., Nelson D.R. and Lewis J.D. (1983) Nd and Sr isotopes in kimberlites and lamproites from Western Australia: an enriched mantle origin. *Nature* **302**, 400-403.

McDonough W.F., McCulloch M.T. and Sun S-S. (1985) Isotopic and geochemical systematics in Tertiary-Recent basalts from southeastern Australia and implications for the evolution of the subcontinental lithosphere. *Geochim. Cosmochim. Acta* **49**, 2051-2068.

McKenzie D. (1985) The extraction of magma from the crust and mantle. *Earth Planet. Sci. Lett.* **74**, 81-91.

McKenzie D. and O'Nions R.K. (1983) Mantle reservoirs and ocean island basalts. *Nature* **301**, 229-231.

McLennan S.M. and Taylor S.R. (1981) Role of subducted sediments in island-arc magmatism: constraints from REE patterns. *Earth Planet. Sci. Lett.* **54**, 423-430.

McLennan S.M. (1982) On the geochemical evolution of sedimentary rocks. *Chem. Geol.* **37**, 335-350.

McLennan S.M. and Taylor S.R. (1983) Geochemical evolution of Archean shales from South Africa. 1. The Swaziland and Pongola Supergroups. *Precamb. Res.* **22**, 93-124.

McLennan S.M., Taylor S.R. and McGregor V.R. (1984) Geochemistry of Archean rocks from West Greenland. *Geochim. Cosmochim. Acta* **48**, 1-13.

Meijer A. (1976) Pb and Sr isotopic data bearing on the origin of volcanic rocks from the Marianas island arc system. *Geol. Soc. Amer. Bull.* **87**, 1358-1369.

Menzies M. A. and Murthy R. (1980) Enriched mantle: Nd and Sr isotopes in diopsides from kimberlite nodules. *Nature* **283**, 634-636.

Milledge H.J., Mendelssohn M.J., Seal M., Rouse J.E., Swart P.K. and Pillinger C.T. (1983) Carbon isotopic variations in spectral type 2 diamonds. *Nature* **303**, 791-792.

Miller R.G. and O'Nions R.K. (1985) Source of Precambrian chemical and clastic sediments. *Nature* **314**, 325-330.

Mittempergher M. (1965) Volcanism and petrogenesis in the S. Venanzo area, Italy. *Bull. Volcanol.* **28**, 85-94.

Moorbath S. (1975) Evolution of Precambrian crust from strontium isotopic evidence. *Nature* **254**, 395-398.

Moorbath S. (1978) Age and isotope evidence for the evolution of continental crust. *Phil. Trans. Roy. Soc. London* **A 288**, 401-413.

Morris J.D. and Hart S.R. (1980) Lead isotope geochemistry of the Banda arc. *Eos Trans. Amer. Geophys. Union* **61**, 1157.

Morris J.D. and Hart S.R. (1983) Isotopic and incompatible element constraints on the genesis of island arc volcanics from Cold Bay and Amak Island, Aleutians, and implications for mantle structure. *Geochim. Cosmochim. Acta* **47**, 2015-2030.

Nakamura E., Campbell I.H. and Sun S-S. (1985) The influence of subduction processes on the geochemistry of Japanese alkaline basalts. *Nature* **316**, 55-58.

Nelson D.R., Crawford A.J. and McCulloch M.T. (1984) Nd-Sr isotopic and geochemical systematics in Cambrian boninites and tholeiites from Victoria, Australia. *Contrib. Mineral. Petrol.* **88**, 164-172.

Nelson D.R., McCulloch M.T. and Sun S.-S. (1986a) The origins of ultrapotassic rocks as inferred from Sr, Nd and Pb isotopes. *Geochim. Cosmochim. Acta* **50**, 231-245.

Nelson D.R., McCulloch M.T. and Ringwood A.E. (1986b) Ultrapotassic magmas: end-products of subduction and mantle recycling of sediments? (extended abstr.) 4th Int. Kimberlite Conf., Perth. *Geol. Soc. Aust. Abst. Ser.* **16**, 196-198.

Newman S., MacDougall J.D. and Finkel R.C. (1984) ^{230}Th-^{232}U disequilibrium in island arcs: evidence from the Aleutians and the Marianas. *Nature* **308**, 268-270.

Nicholls I.A. and Whitford D.J. (1978) Geochemical zonation in the Sunda volcanic arc, and the origin of K-rich lavas. *Bull. Aust. Soc. Explor. Geophys.* **9**, 93-98.

Ninkovich D. and Hays J.D. (1972) Mediterranean island arcs and origin of potash volcanoes. *Earth Planet. Sci. Lett.* **16**, 331-345.

Nixon P.H., Thirwall M.F., Buckley F. and Davies C.J. (1984) Spanish and Western Australian lamproites: aspects of whole rock geochemistry. In *Kimberlites I: Kimberlites and Related Rocks.* (ed. J. Kornprobst). Elsevier, Amsterdam. pp. 285-296.

Nobel F.A., Andriessen P.A.M., Hebeda E.H., Priem H.N.A. and Rondeel H.E. (1981) Isotopic dating of the post-alpine neogene volcanism in the Betic Cordilleras, southern Spain. *Geol. Mijnb.* **60**, 209-214.

Norrish K. and Chappell B.W. (1967) X-ray fluorescence spectrography. In *Physical Methods in Determinative Mineralogy.* (ed. J. Zussman). Academic Press, Oxford. pp. 161-214.

Norrish K. and Hutton J.T. (1969) An accurate X-ray spectrographic method for the analysis of a wide range of geological samples. *Geochim. Cosmochim. Acta* **33**, 431-453.

O'Nions R.K., Evensen N.M. and Hamilton P.J. (1979) Geochemical modelling of mantle differentiation and crustal growth. *J. Geophys. Res.* **84**, 6091-6101.

O'Reilly S.Y. and Griffin W.L. (1984) Sr isotopic heterogeneity in primitive basaltic rocks, southeastern Australia: correlation with mantle metasomatism. *Contrib. Mineral. Petrol.* **87**, 220-230.

Ozima M., Takayanagi, M., Zashu S. and Amari S. (1984) High $^{3}He/^{4}He$ ratio in ocean sediments. *Nature* **311**, 448-450.

Ozima M., Zashu S., Mattey D.P. and Pillinger C.T. (1985) Helium, argon and carbon isotopic compositions in diamonds and their implications in mantle evolution. *Geochem. J.* **19**, 127-134.

Palacz Z.A. and Saunders A.D. (1986) Coupled trace element and isotope enrichment in the Cook-Austral- Samoa islands, southwest Pacific. *Earth Planet. Sci. Lett.* **79**, 270-280.

Peccerillo A., Poli G. and Tolomeo L. (1984) Genesis, evolution and tectonic significance of K-rich volcanics from the Alban Hills (Roman comagmatic region) as inferred from trace element chemistry. *Contrib. Mineral. Petrol.* **86**, 230-240.

Peccerillo A. (1985) Roman comagmatic province (central Italy): evidence for subduction-related magma genesis. *Geology* **13**, 103-106.

Peng Z.C., Zartman R.E., Futa K. and Chen D.G. (1986) Pb-, Sr- and Nd-isotopic systematics and chemical characteristics of Cenozoic basalts, eastern China. *Chem. Geol. (Isotope Geosci.)* **59**, 3-33.

Perfit M. R. and Kay R.W. (1986) Comment on "Isotopic and incompatible element constraints on the genesis of island arc volcanics from Cold Bay and Amak Island, Aleutians, and implications for mantle structure" by J.D. Morris and S.R. Hart. *Geochim. Cosmochim. Acta* **50**, 477-481.

Powell J.L. and Bell K. (1970) Strontium isotopic studies of alkalic rocks. Localities from Australia, Spain, and the western United States. *Contrib. Mineral. Petrol.* **27**, 1-10.

Reynolds P.H. and Dash E.J. (1971) Lead isotopes in marine manganese nodules and the ore-growth curve. *J. Geophys. Res.* **76**, 5124-5129.

Richardson S.H., Erlank A.L., Duncan A.R. and Reid D.L. (1982) Correlated Nd, Sr and Pb isotope variation in Walvis Ridge basalts and implications for the evolution of their mantle source. *Earth Planet. Sci. Lett.* **59**, 327-342.

Richardson S.H., Gurney J.J. Erlank A.L. and Harris J.W. (1984) Origin of diamonds in old enriched mantle. *Nature* **310**, 198-202.

Ringwood A.E. (1977) Synthesis of pyrope-knorringite solid solution series. *Earth Planet. Sci. Lett.* **36**, 443-448.

Ringwood A.E. (1982) Phase transformations and differentiation in subducted lithosphere: implications for mantle dynamics, basalt petrogenesis and crustal evolution. *J. Geol.* **90**, 611-643.

Roddick J.C. (1984) Emplacement and metamorphism of Archaean mafic volcanics at Kambalda, Western Australia- geochemical and isotopic constraints. *Geochim. Cosmochim. Acta* **48**, 1305-1318.

Rogers N.W., Hawkesworth C.J., Parker R.J. and Marsh J.S. (1985) The geochemistry of potassic lavas from Vulsini, central Italy and implications for mantle enrichment processes beneath the Roman region. *Contrib. Mineral. Petrol.* **90**, 244-257.

Salters V.J.M. and Barton M. (1985) The geochemistry of ultrapotassic lavas from the Leucite Hills, Wyoming. (abstr.) *Eos Trans. Amer. Geophys. Union* **66**, 1109.

Sano Y., Toyoda K. and Wakita H. (1985) $^{3}He/^{4}He$ ratios of modern marine ferromanganese nodules. *Nature* **317**, 518-520.

Scott B.H. (1979) Petrogenesis of kimberlites and associated potassic lamprophyres from central west Greenland. In *Kimberlites, Diatremes and Diamonds: their Geology, Petrology, and Geochemistry.* (eds. F.R. Boyd and H.O.A. Meyer). American Geophysical Union, Washington. pp. 190-205.

Scott B.H. (1981) Kimberlite and lamproite dykes from Holsteinsborg, West Greenland. *Meddr. Grønland Geosci.* **4**, 24p.

Scott-Smith B.H., Danchin R.V., Harris J.W. and Stracke K.J. (1984) Kimberlites near Orroroo, South Australia. In *Kimberlites I: Kimberlites and Related Rocks.* (ed. J. Kornprobst). Elsevier, Amsterdam. pp. 121-142.

Shaw R.D., Langworthy A.P., Offe L.A., Stewart A.J., Allen A.R., Senior B.R. and Clarke D.B. (1979) Geological report on 1:100,000 scale mapping of the southeastern Arunta Block, Northern Territory. *B.M.R. Aust. Rec.* **1979/47**: Microform MF 133.

Shaw R.D., Stewart A.J. and Black L.P. (1984) The Arunta Inlier: a complex ensialic mobile belt in central Australia. Part 2: tectonic history. *Aust. J. Earth Sci.* **31**, 457-484.

Sheraton J.W. and Cundari A. (1980) Leucitites from Gaussberg, Antarctica. *Contrib. Mineral. Petrol.* **71**, 417-427.

Sheraton J.W. and England R.N. (1980) Highly potassic mafic dykes from Antarctica. *J. Geol. Soc. Aust.* **27**, 1-18.

Sheraton J.W. and Black L.P. (1981) Geochemistry and geochronology of Proterozoic tholeiitic dykes of East Antarctica: evidence for mantle metasomatism. *Contrib. Mineral. Petrol.* **78**, 305-317.

Sheraton J.W. (1983) Geochemistry of mafic igneous rocks of the northern Prince Charles Mountains, Antarctica. *J. Geol. Soc. Aust.* **30**, 295-304.

Smith C.B. (1979) Rb-Sr mica ages of various kimberlites. In *Chairmans Summaries and Poster Session Abstracts.* Kimberlite Symposium II. Cambridge, July 1979. pp. 61-66.

Smith C.B. (1983) Pb, Sr and Nd isotopic evidence for sources of southern African Cretaceous kimberlites. *Nature* **304**, 51-54.

Sobolev N.V., Galimov E.M., Ivanovskaya N.N. and Yefimova E.S. (1979) The carbon isotopic composition of diamonds containing crystalline inclusions. *Dokl. Akad. Nauk. S.S.R.* **249**, 1217-1220.

Steiger R.H. and Jäger E. (1977) Subcommision on geochronology: convention on the use of decay constants in geo- and cosmochronology. *Earth Planet. Sci. Lett.* **36**, 359-362.

Stewart A.J., Shaw R.D. and Black L.P. (1984) The Arunta Inlier: a complex ensialic mobile belt in central Australia. Part 1. stratigraphy, correlations and origin. *Aust. J. Earth Sci.* **31**, 445-455.

Stracke K.J., Ferguson J. and Black L.P. (1979) Structural setting of kimberlites in south-eastern Australia. In *Kimberlites, Diatremes and Diamonds: their Geology, Petrology, and Geochemistry.* (eds. F.R. Boyd and H.O.A. Meyer). American Geophysical Union, Washington. pp. 71-91.

Sun S-S. (1980) Lead isotopic study of young volcanics from mid-ocean ridges, ocean islands and island arcs. *Phil. Trans. Roy. Soc. London* **A 297**, 409-445.

Sutherland F.L. (1983) Timing, trace and origin of basaltic migration in eastern Australia. *Nature* **305**, 123-126.

Swart P.K., Pillinger C.T., Milledge H.J. and Seal M. (1983) Carbon isotopic variation within individual diamonds. *Nature* **303**, 793-795.

Tatsumoto M. and Knight R.J. (1969) Isotopic composition of lead in volcanic rocks from central Honshu- with regard to basalt petrogenesis. *Geochem. J.* **3**, 53-86.

Tatsumoto M. (1973) Time differences in the formation of meteorites as determined from the ratio of lead-207 to lead-206. *Science* **180**, 1279-1283.

Taylor H.P. and Turi B. (1976) High ^{18}O igneous rocks from the Tuscan magmatic Province, Italy. *Contrib. Mineral. Petrol.* **55**, 33-54.

Taylor H.P., Turi B. and Cundari A. (1984) $^{18}O/^{16}O$ and chemical relationships in K-rich volcanic rocks from Australia, East Africa, Antarctica, and San Venanzo-Cupaello, Italy. *Earth Planet. Sci. Lett.* **69**, 263-276.

Taylor S.R. and Gorton M.P. (1977) Geochemical application of Spark Source Mass Spectrometry - III. Element sensitivity, precision, accuracy. *Geochim. Cosmochim. Acta* **41**, 491-510.

Taylor S.R. and McLennan S.M. (1981) The composition and evolution of the continental crust: rare earth element evidence from sedimentary rocks. *Phil. Trans. Roy. Soc. London* **A 301**, 381-399.

Thompson R.N. (1977) Primary basalts and magma genesis. *Contrib. Mineral. Petrol.* **60**, 91-108.

Thompson R.N., Morrison M.A., Hendry G.L. and Parry S.J. (1984) An assessment of the relative roles of crust and mantle in magma genesis: an elemental approach. *Phil. Trans. Roy. Soc. London* **A 310**, 549-590.

Thompson J., Carpenter M.S.N., Colley S., Wilson T.R.S., Elderfield H. and Kennedy H. (1984) Metal accumulation rates in northwest Atlantic pelagic sediments. *Geochim. Cosmochim. Acta* **48**, 1935-1948.

Tilton G.R. (1983) Evolution of depleted mantle: the lead perspective. *Geochim. Cosmochim. Acta* **47**, 1191-1197.

Tingey R.J., McDougall I. and Gleadow A.J.W. (1983) The age and mode of formation of Gaussberg, Antarctica. *J. Geol. Soc. Aust.* **30**, 241-24.

Tsuboi S. (1920) On a leucite rock vulsinite vicoite from Utsuryoto Island in the sea of Japan. *Geol. Soc. Japan* **27**, 91-103.

Turi B. and Taylor H.P. (1976) Oxygen isotope studies of potassic volcanic rocks of the Roman Province, Central Italy. *Contrib. Mineral. Petrol.* **55**, 1-31.

Unruh D.M. and Tatsumoto M. (1976) Lead isotopic compositions and uranium, thorium and lead concentrations in sediments and basalts from the Nazca Plate. In *Initial Reports of the Deep Sea Drilling Project* **34**, 341-347. U.S. Government Printing Office, Washington.

Van Kooten G.K. (1981) Pb and Sr systematics of ultrapotassic and basaltic rocks from central Sierra Nevada, California. *Contrib. Mineral. Petrol.* **76**, 378-385.

Varne R. (1985) Ancient subcontinental mantle: a source for K-rich orogenic volcanics. *Geology* **13**, 405-408.

Veeh H.H. (1981) Uranium and thorium isotopic investigations in metalliferous sediments of the northwest Nazca plate. In *Nazca Plate: Crustal Formation and Andean Convergence*. (ed. L.D. Kulm). *Geol. Soc. Amer. Memoir* **154**, 251-267.

Veizer J. and Compston W. (1976) $^{87}Sr/^{86}Sr$ in Precambrian carbonates as an index of crustal evolution. *Geochim. Cosmochim. Acta* **40**, 905-914.

Veizer J., Compston W., Hoefs J. and Nielsen H. (1982) Mantle buffering of the early oceans. *Naturwissenschaften* **69**, 173-180.

Venturelli G., Capedri S., Di Battistini G., Crawford A., Kogarko L.N. and Celestini S. (1984) The ultrapotassic rocks of southeastern Spain. *Lithos* **7**, 37-54.

Vidal P., Chauvel C. and Brousse R. (1984) Large mantle heterogeneity beneath French Polynesia. *Nature* **307**, 536-538.

Vollmer R. (1976) Rb-Sr and U-Th-Pb systematics of alkaline rocks: the alkaline rocks of Italy. *Geochim. Cosmochim. Acta* **40**, 283-295.

Vollmer R. (1977a) Terrestrial lead isotope evolution and the formation time of the Earth's core. *Nature* **270**, 144-147.

Vollmer R. (1977b) Isotopic evidence for genetic relations between acid and alkaline rocks in Italy. *Contrib. Mineral. Petrol.* **60**, 109-118.

Vollmer R. and Hawkesworth C.J. (1980) Lead isotopic composition of the potassic rocks from Roccamonfina (South Italy). *Earth Planet. Sci. Lett.* **47**, 91-101.

Vollmer R. and Norry M.T. (1983a) Possible origin of K-rich volcanic rocks from Virunga, East Africa, by metasomatism of continental crustal material: Pb, Nd and Sr isotopic evidence. *Earth Planet. Sci. Lett.* **64**, 374-386.

Vollmer R. and Norry M.T. (1983b) Unusual isotopic variations in Nyiragongo nephelinites. *Nature* **301**, 141-143.

Vollmer R., Ogden P., Schilling J.-G., Kingsley R.H. and Waggoner D.G. (1984) Nd and Sr isotopes in ultrapotassic volcanic rocks from the Leucite Hills, Wyoming. *Contrib. Mineral. Petrol.* **87**, 359-368.

Wade A. and Prider R.T. (1940) The leucite-bearing rocks in the West Kimberley area, Western Australia. *Geol. Soc. London Q. J.* **96**, 39-98.

Walker G.P.L. (1962) Garronite, a new zeolite from Ireland and Iceland. *Mineral. Mag.* **33**, 173-186.

Wass S.Y. and Rogers N.W. (1980) Mantle metasomatism- precursor to continental alkaline volcanism. *Geochim. Cosmochim. Acta* **44**, 1811-1823.

Watterson J. (1974) Investigations on the Nagssugtoqidian boundary in the Holsteinsborg district, central west Greenland. *Grønlands Geol. Unders. Rapp.* **65**, 33-37.

Weaver B.L., Wood D.A., Tarney J. and Joron J.L. (1986) Role of subducted sediment in the genesis of ocean-island basalts: geochemical evidence from South Atlantic Ocean islands. *Geology* **14**, 275-278.

Wedepohl K.H. and Muramatsu Y. (1979) The chemical composition of kimberlites compared with the average composition of three basaltic magma types. In *Kimberlites, Diatremes and Diamonds: their Geology, Petrology and Geochemistry.* (eds. F.R. Boyd and H.O.A. Meyer). American Geophysical Union, Washington. pp. 300-312.

Weiss D. and DeMaiffe D. (1985) A depleted mantle source for kimberlites from Zaire: Nd, Sr and Pb isotopic evidence. *Earth Planet. Sci. Lett.* **73**, 269-277.

Wellman P., Cundari A. and McDougall I. (1970) Potassium-argon ages for leucite-bearing rocks from New South Wales, Australia. *J. Proc. Roy. Soc. N.S.W.* **103**, 103-107.

Wellman P. (1973) Early Miocene potassium-argon age for the Fitzroy Lamproites of Western Australia. *J. Geol. Soc. Aust.* **19**, 471-474.

Wellman P. (1974) Potassium-argon ages on the Cainozoic volcanic rocks of Eastern Victoria. *J. Geol. Soc. Aust.* **21**, 359-376.

Wellman P. and McDougall I. (1974) Cainozoic igneous activity in eastern Australia. *Tectonophys.* **23**, 49-65.

Wendlandt R.F. (1984) An experimental and theoretical analysis of partial melting in the system $KAlSiO_4$-CaO-MgO-SiO_2-CO_2 and applications to the genesis of potassic magmas, carbonatites and kimberlites. In *Kimberlites I: Kimberlites and Related Rocks.* (ed. J. Kornprobst). Elsevier, Amsterdam. pp. 359-369.

White W.M. and Bryan W.B. (1977) Sr-isotope, K, Rb, Cs, Sr, Ba, and rare earth geochemistry of basalts from the FAMOUS area. *Geol. Soc. Amer. Bull.* **88**, 571-576.

White W.M. and Hoffman A.W (1982) Sr and Nd isotope geochemistry of oceanic basalts and mantle evolution. *Nature* **296**, 821-825.

White W.M., Jenner G., Dupré B., Foden J. and Varne R. (1983) Pb isotope geochemistry of the Lesser Antilles and Sunda (Indonesia) island arcs. (abstr.) *Eos Trans. Amer. Geophys. Union* **64**, 333-334.

White W.M. (1985) Sources of oceanic basalts: radiogenic isotopic evidence. *Geology* **13**, 115-118.

White W.M., Dupré B. and Vidal P. (1985) Isotope and trace element chemistry of sediments from the Barbados Ridge-Demerara Plain region, Atlantic Ocean. *Geochim. Cosmochim. Acta* **49**, 1875-1886.

Whitford D.J. (1975) Strontium isotopic studies of the volcanic rocks of the Sunda arc, Indonesia, and their petrogenetic implications. *Geochim. Cosmochim. Acta* **39**, 1287-1302.

Whitford, D.J., Foden J.D. and Varne R. (1978) Sr isotope geochemistry of calc-alkaline and alkaline lavas from the Sunda arc in Lombok and Sumbawa, Indonesia. *Carnegie Inst. Wash. Yearb.* **77**, 613-620.

Whitford D.J., White W.M. and Jezek P.A. (1981) Neodymium isotopic composition of Quarternary island arc lavas from Indonesia. *Geochim. Cosmochim. Acta* **45**, 989-995.

Whitford D.J. and Jezek P.A. (1982) Isotopic constraints on the role of subducted sailic material in Indonesian island-arc magmatism. *Geol. Soc. Amer. Bull.* **93**, 504-513.

Wilkinson J.F.K. (1977) Analcime phenocrysts in a vitrophyric analcimite- primary or secondary? *Contrib. Mineral. Petrol.* **64**, 1-10.

Windrim D.P. and McCulloch M.T. (1987) Nd and Sr isotopic systematics of central Australian granulites: chronology of the evolution of the lower crust. *Contrib. Mineral. Petrol.* **94**, 289-303.

Wright E. and White W.M. (1986) The origin of Samoa: new evidence from Sr, Nd and Pb isotopes. *Earth Planet. Sci. Lett.* **81**, 151-162.

Zindler A., Jagoutz E. and Goldstein S. (1982) Nd, Sr and Pb isotopic systematics in a three- component mantle: a new perspective. *Nature* **298**, 519-523.

Zindler A., Staudigel H. and Batiza R. (1984) Isotope and trace element geochemistry of young Pacific seamounts: implications for scale of upper mantle heterogeneity. *Earth Planet. Sci. Lett.* **70**, 175-195.

Allègre C.J., Pineau F., Bernat M. and Javoy M. (1971) Geochemical evidence for the occurrence of carbonatites on the Cape Verde and Canary Islands. *Nature* **233**, 103.

Allen J.B. and Deans T. (1965) Ultrabasic eruptives with alnöitic-kimberlitic affinities from Malaita, Solomon Islands. *Mineral. Mag.* **34**, 16-34.

Allsopp H.L. and Eriksson S.C. (1986) The Phalaborwa complex; isotopic evidence for ancient lithospheric enrichment. (abstr.) Joint Ann. Meeting, G.A.C.-M.A.C., Carleton University, Ottawa, 40.

Amaral G. (1978) Potassium-argon studies on the Jacupiranga alkaline district, state of São Paulo, Brazil. In *Proceedings of the First International Symposium on Carbonatites*. Brasilia, Departmento Nacional da Producao Mineral. pp. 297-302.

Anderson T.F. and Lawrence J.R. (1976) Stable isotope investigations of sediments, basalts and authigenic phases from Leg 35 cores. In *Initial Reports of the Deep Sea Drilling Project* **35**, 497-505. U.S. Government Printing Office, Washington.

Baker B.H., Williams L.A.J., Miller J.A. and Fitch F.J. (1971) Sequence and geochronology of the Kenya rift volcanics. *Tectonophys.* **11**, 191-215.

Bailey D.K. (1984) Kimberlite: the mantle sample formed by ultrametasomatism. In *Kimberlites I: Kimberlites and Related Rocks.* (ed. J. Kornprobst). Elsevier, Amsterdam. pp. 323-357.

Barreiro B. (1983) An isotopic study of the Westland dyke swarm, South Island, New Zealand. *Carnegie Inst. Wash. Yearb.* **82**, 471-475.

Barrera J.L., Fernandez Santin S., Fuster J.M. and Ibarrola E. (1981) Ijolitas-sienitas-carbonatitas de los macizos del norte del complejo plutonico basal de Fuerteventura (Islas Canarias). *Bol. Geol. Mineral.* (Madrid) **92**, 309-321.

Barth T.F.W. and Ramberg I. (1966) The Fen complex. In *Carbonatites.* (eds. O.F. Tuttle and J. Gittins). Interscience, New York. pp. 225-257.

Basu A.R. and Tatsumoto M. (1980) Nd-isotopes in selected mantle-derived rocks and minerals and their implications for mantle evolution. *Contrib. Mineral. Petrol.* **75**, 43-54.

Bell K. and Powell J.L. (1970) Strontium isotopic studies of alkalic rocks: the alkalic complexes of eastern Uganda. *Geol. Soc. Amer. Bull.* **81**, 3481-3490.

Bell K., Dawson J.B. and Farquar R.M. (1973) Strontium isotope studies of alkalic rocks: the active carbonatite volcano Oldoinyo Lengai, Tanzania. *Geol. Soc. Amer. Bull.* **84**, 1019-1030.

Bell K., Blenkinsop J., Cole T.J.S. and Menagh D.P. (1982) Evidence from Sr isotopes for long-lived heterogeneities in the upper mantle. *Nature* **298**, 251-253.

Bell K. and Blenkinsop J. (1986) Carbonatites and the subcontinental mantle. (abstr.) Joint Ann. Meeting, G.A.C.-M.A.C., Carleton University, Ottawa. pp. 44.

Bell K. and Blenkinsop J. (1987a) Archean depleted mantle- evidence from Nd and Sr initial isotopic ratios of carbonatites. *Geochim. Cosmochim. Acta* **51**, 291-298.

Bell K. and Blenkinsop J. (1987b) Nd and Sr isotopic compositions of East African carbonatites: implications for mantle heterogeneity. *Geology* **15**, 99-102.

Bielski-Zyskind M., Wasserburg G.J. and Nixon P.J. (1984) Sm-Nd and Rb-Sr systematics in volcanics and ultramafic xenoliths from Malaita, Solomon Islands, and the nature of the Ontong Java Plateau. *J. Geophys. Res.* **89**, 2415-2424.

Black L.P. and Gulson B.L. (1978) The age of the Mud Tank carbonatite, Strangways Range, Northern Territory. *B.M.R. J. Aust. Geol. Geophys.* **3**, 227-232.

Blattner P. and Cooper A.F. (1974) Carbon and oxygen isotopic composition of carbonatite dikes and metamorphic country rock of the Haast Schist terrain, New Zealand. *Contrib. Mineral. Petrol.* **4**, 17-27.

Brey G., Brice W.R., Ellis D.J., Green D.H., Harris K.L. and Ryabchikov I.D. (1983) Pyroxene-carbonate reactions in the upper mantle. *Earth Planet. Sci. Lett.* **62**, 63-74.

Chase C.G. (1981) Oceanic island Pb: Two stage histories and mantle evolution. *Earth Planet. Sci. Lett.* **52**, 277-284.

Chen C.-Y. and Frey F.A. (1983) Origin of Hawaiian tholeite and alkali basalt. *Nature* **302**, 785-789.

Cohen R.S. and O'Nions R.K. (1982a) The lead, neodymium and strontium isotopic structure of ocean ridge basalts. *J. Petrol.* **23**, 299-324.

Cohen R.S. and O'Nions R.K. (1982b) Identification of recycled continental material in the mantle from Sr, Nd and Pb isotope investigations. *Earth Planet. Sci. Lett.* **61**, 73-84.

Cohen R.S., O'Nions R.K. and Dawson J.B. (1984) Isotope geochemistry of xenoliths from East Africa: implications for development of mantle reservoirs and their interaction. *Earth Planet. Sci. Lett.* **68**, 209-220.

Deans T. and Powell J.L. (1968) Trace elements and strontium isotopes in carbonatites, fluorites and limestones from India and Pakistan. *Nature* **218**, 750-752.

Degens E.T. (1969) Biogeochemistry of stable isotopes. In *Organic Geochemistry.* (eds. G. Eglinton and M.T.J. Murphy). Springer Verlag, New York. pp. 304-329.

Deines P. and Gold D.P. (1973) The isotopic composition of carbonatite and kimberlite carbonates and their bearing on the isotopic composition of deep-seated carbon. *Geochim. Cosmochim. Acta* **37**, 1709-1733.

DePaolo D.J. (1978) Nd and Sr isotope systematics of young continental igneous rocks. 4th Int. Isotope Conf., Geochronology, Cosmochronology, Isotope Geology. *U.S. Geol. Surv. Open-File Rep.* **78-701**, 91-93.

Derry L.A. and Jacobsen S.B. (1986) Nd and Sr isotopic measurements from the Fen Complex, south Norway. (abstr.) *Eos Trans. Amer. Geophys. Union* **67**, 1265.

Des Marais D.J. and Moore J.G. (1984) Carbon and its isotopes in mid-oceanic basaltic glasses. *Earth Planet. Sci. Lett.* **69**, 43-57.

Dupré B. and Allègre C.J. (1980) Pb-Sr-Nd isotopic correlation and chemistry of North Atlantic mantle. *Nature* **286**, 17-22.

Eby G.N. (1975) Abundance and distribution of the rare earth elements and yttrium in the rocks and minerals of the Oka carbonatite complex, Quebec. *Geochim. Cosmochim. Acta* **39**, 597-620.

Erickson R.L. and Blade L.V. (1963) Geochemistry and petrology of the alkalic igneous complex at Magnet Cove, Arkansas. *U.S. Geol. Surv. Prof. Paper* **425**.

Ferguson J. and Sheraton J.W. (1979) Petrogenesis of kimberlitic rocks and associated xenoliths of southeastern Australia. In *Kimberlites, diatremes and diamonds; their geology, petrology, and geochemistry.* (eds. F.R. Boyd and H.O.A. Meyer). American Geophysical Union, Washington. pp. 140-161.

Ferguson J., Arculus R.J. and Joyce J. (1979) Kimberlite and kimberlitic intrusives of southeastern Australia: a review. *B.M.R. J. Aust. Geol. Geophys.* **4**, 227-241.

Friedman I., O'Neil J. and Cebula G. (1982) Two new carbonate stable-isotope standards. *Geostandards Newsletter* **6**, 11-12.

Garson M.S. (1966) Carbonatites in southern Malawi. In *Carbonatites*. (eds. O.F. Tuttle and J. Gittins). Interscience, New York. pp. 33-71.

Gaspar J.C. and Wyllie P.J. (1984) The alleged kimberlite-carbonatite relationship: evidence from illmenite and spinel from Premier and Wesselton Mines and the Benfontein Sill, South Africa. *Contrib. Mineral. Petrol.* **85**, 133-140.

Gittins J. (1966) Summaries and biblographies of carbonatite complexes. In *Carbonatites*. (eds. O.F. Tuttle and J. Gittins). Interscience, New York. pp. 417-540.

Gonfiantini R. and Tongiorgi E. (1964) La composition isotopique des carbonatites du Kaiserstuhl. In *Report E.U.R. 1827 d.e.f. of the European Atomic Energy Commission.* (ed. L.V. Wambecke). pp. 193-199.

Gregory R.T. and Taylor H.P. Jr. (1981) An oxygen profile in a section of Cretaceous oceanic crust, Samail Ophiolite, Oman: evidence for $\delta^{18}O$ buffering of the oceans by deep (>5 km) seawater-hydrothermal circulation at mid-ocean ridges. *J. Geophys. Res.* **86**, 2737-2755.

Griffin W.L. and Taylor P.N. (1975) The Fen damkjernite: petrology of a "central complex kimberlite" In *Physics and Chemistry of the Earth.* (eds. L.H. Ahrens, F. Press, S.K. Runcorn and H.C. Urey) **9**, 163-177.

Grünenfelder M.H., Tilton G.R., Bell K. and Blenkinsop J. (1986) Lead and strontium isotope relationships in the Oka carbonatite complex, Quebec. *Geochim. Cosmochim. Acta* **50**, 461-468.

Hamilton D.L., Freestone I.C., Dawson J.B. and Donaldson C.H. (1979) Origin of carbonatites by liquid immiscibility. *Nature* **279**, 52-54.

Harmer R.E. (1986) Rb-Sr isotopic study of units of the Pienaars River Alkaline Complex, north of Pretoria, South Africa. *Trans. Geol. Soc. S. Africa* **88(2)**, 215-223.

Heinrich E.W. (1966) *The Geology of Carbonatites.* Rand McNally, Chicago. 555p.

Hofmann A.W. and White W.M. (1982) Mantle plumes from ancient oceanic crust. *Earth Planet. Sci. Lett.* **57**, 421-436.

Holloway J.R., Mysen B.O. and Eggler D.H. (1977) The solubility of CO_2 in liquids on the join $CaO\text{-}MgO\text{-}SiO_2\text{-}CO_2$. *Carnegie Inst. Wash. Yearb.* **75**, 626-631.

King B.C. (1965) Petrogenesis of the alkaline igneous rock suites of the volcanic and intrusive centres of eastern Uganda. *J. Petrol.* **6**, 67-100.

King B.C. and Sutherland D.S. (1966) The carbonatite complexes of eastern Uganda. In *Carbonatites*. (eds. O.F. Tuttle and J. Gittins). Interscience, New York. pp. 73-126.

Kroenke L.W. (1972) Geology of the Ontong Java Plateau. *Hawaiian Institute of Geophysics Report* **72-5**, Univ. of Hawaii. 19p.

Kwon S.T. and Tilton G.R. (1986) Comparative isotopic studies of Cargill and Borden carbonatite complexes from the Kapuskasing gravity high zone, Ontario. (abstr.) Joint Ann. Meeting, G.A.C.-M.A.C. Carleton University, Ottawa. pp. 92.

Kyser T.K., O'Neil J.R. and Carmichael I.S.E. (1982) Genetic relations among basic lavas and ultramafic nodules: evidence from oxygen isotope compositions. *Contrib. Mineral. Petrol.* **81**, 88-102.

Lancelot J.R. and Allègre C.J. (1974) Origin of carbonatitic magma in the light of the Pb-U-Th isotope system. *Earth Planet. Sci. Lett.* **22**, 233-238.

Le Bas M.J. (1984) Oceanic Carbonatites. In *Kimberlites I: Kimberlites and Related Rocks.* (ed. J. Kornprobst). Elsevier, Amsterdam. pp. 169-178.

Loubet M., Bernat M., Javoy M. and Allègre C.J. (1972) Rare earth contents in carbonatites. *Earth Planet. Sci. Lett.* **14**, 226-232.

McCulloch M.T. and Chappell B.W. (1982) Nd isotopic characteristics of S- and I- type granites. *Earth Planet. Sci. Lett.* **58**, 51-64.

McCulloch M.T., Gregory R.T., Wasserburg G.J. and Taylor H.P. Jr. (1981) Sm-Nd, Rb-Sr, and $^{18}O/^{16}O$ systematics in an oceanic crustal section: evidence from the Samail Ophiolite. *J. Geophys. Res.* **86**, 2721-2735.

McDonough W.F., McCulloch M.T. and Sun S.-S. (1985) Isotopic and geochemical systematics in Tertiary-Recent basalts from southeastern Australia and implications for the evolution of the sub-continental lithosphere. *Geochim. Cosmochim. Acta* **49**, 2051-2067.

McKenzie J. (1980) Stable isotope study of carbonate minerals from the basalt flows on Suiko Seamount: D.S.D.P. Leg 55 Hole 433C. In *Initial Reports of the Deep Sea Drilling Project* **55**, 653-657. U.S. Government Printing Office, Washington.

McKenzie D. (1985) The extraction of magma from the crust and mantle. *Earth Planet. Sci. Lett.* **74**, 81-91.

Midende G., Demaiffe D., Weis D. and Mennessier J.P. (1986) Sr, Nd and Pb isotope evidence for the origin of carbonatites from the western branch of the African Rift. (abstr.) *Eos Trans. Amer. Geophys. Union* **67**, 1267.

Mitchell R.H. and Crocket J.H. (1970) Isotopic composition of strontium in rocks of the Fen Alkaline Complex, south Norway. *J. Petrol.* **13**, 83-97.

Möller P., Morteani G. and Schley F. (1980) Discussion of REE distribution of carbonatites and alkalic rocks. *Lithos* **13**, 171-179.

Nelson D.R., McCulloch M.T. and Sun S.-S. (1986) The origins of ultrapotassic rocks as inferred from Sr, Nd and Pb isotopes. *Geochim. Cosmochim. Acta* **50**, 231-245.

Neilsen T.F.D. and Buchart B. (1985) Sr-C-O isotopes in nephelinitic rocks and carbonatites, Gardiner Complex, Tertiary of east Greenland. *Chem. Geol.* **53**, 207-217.

Nixon P.H. and Boyd F.R. (1979) Garnet-bearing lherzolites and discrete nodule suites from the Malaita alnöite, Solomon Islands, SW Pacific, and their bearing on oceanic mantle composition and geotherm. In *The Mantle Sample.* (eds. F.R. Boyd and H.O.A. Meyer). American Geophysical Union, Washington. pp. 400-423.

Nixon P.H., Mitchell R.H. and Rogers N.W. (1980) Petrogenesis of alnöitic rocks from Malaita, Solomon Islands, Melanesia. *Mineral. Mag.* **43**, 587-596.

Norrish K. and Chappell B.W. (1967) X-ray fluorescence spectrography. In *Physical Methods in Determinative Mineralogy.* (ed. J. Zussman). Academic Press, Oxford. pp. 161-214.

Norrish K. and Hutton J.T. (1969) An accurate X-ray spectrographic method for the analysis of a wide range of geological samples. *Geochim. Cosmochim. Acta* **33**, 6091-6101.

Norry M.J., Truckle P.H., Lippard S.J., Hawkesworth C.J., Weaver S.D. and Marriner G.F. (1980) Isotopic and trace element evidence from lavas, bearing on mantle heterogeneity beneath Kenya. *Phil. Trans. Roy. Soc. London* A **297**, 259-271.

O'Nions R.K., Hamilton P.J. and Evensen N.M. (1977) Variations in $^{143}Nd/^{144}Nd$ and $^{87}Sr/^{86}Sr$ ratios in oceanic basalts. *Earth Planet. Sci. Lett.* **34**, 13-22.

Palacz Z.A. and Saunders A.D. (1986) Coupled trace element and isotope enrichment in the Cook-Austral-Samoa islands, southwest Pacific. *Earth Planet. Sci. Lett.* **79**, 270-280.

Pineau F., Javoy M. and Allègre C.J. (1973) Etude systematique des isotopes de l'oxygene, du carbone et du strontium dans les carbonatites. *Geochim. Cosmochim. Acta* **37**, 2363-2377.

Plyusnin G.S., Vorob'yev I. and Perminov A.V. (1984) Isotopic composition ($\delta^{18}O$, $\delta^{13}C$) of carbonatites in the Murun alkalic rock block. *Dokl. Acad. Nauk. S.S.R.* **275**, 999-1003.

Powell J.L. (1965) Low abundance of Sr^{87} in Ontario carbonatites. *Amer. Mineral.* **50**, 1075-1079.

Powell J.L. (1966) Isotopic composition of strontium in carbonatites and kimberlites. *Mineral. Soc. India, IMA volume*, 58-66.

Ringwood A.E. (1982) Phase transformations and differentiation in subducted lithosphere: implications for mantle dynamics, basalt petrogenesis, and crustal evolution. *J. Geol.* **90**, 611-643.

Roden M.F., Murthy R.V. and Gaspar J.C. (1985) Sr and Nd isotopic composition of the Jacupiranga carbonatite. *J. Geol.* **93**, 212-220.

Scott-Smith B.H., Danchin R.V., Harris J.W. and Stracke K.J. (1984) Kimberlites near Orroroo, South Australia. In *Kimberlites I: Kimberlites and Related Rocks.* (ed. J. Kornprobst). Elsevier, Amsterdam. pp. 121-142.

Shaw D.M. (1970) Trace element fractionation during anatexis. *Geochim. Cosmochim. Acta* **34**, 237-243.

Silva L.C., Le Bas M.J. and Robertson A.H.F. (1981) An oceanic carbonatite volcano on Santiago, Cape Verde Islands. *Nature* **294**, 644-645.

Smith C.B. (1983) Pb, Sr and Nd isotopic evidence for sources of southern African Cretaceous kimberlite. *Nature* **304**, 51-54.

Snelling N.J., Hamilton E.I., Drysall A.R. and Stillman C.J. (1964) A review of age determinations from northern Rhodesia. *Econ. Geol.* **59**, 961-981.

Snelling N.J. (1965) Age determinations on three African carbonatites. *Nature* **205**, 491.

Spera F.J. and Bergman S.C. (1980) Carbon dioxide in igneous petrogenesis: 1. Aspects of the dissolution of CO_2 in silicate liquids. *Contrib. Mineral. Petrol.* **74**, 55-66.

Steiger R.H. and Jäger E. (1977) Subcommission on geochronology: convention on the use of decay constants in geo- and cosmochronology. *Earth Planet. Sci. Lett.* **36**, 359-362.

Stracke K.J., Ferguson J. and Black L.P. (1979) Structural setting of kimberlites in south-eastern Australia. In *Kimberlites, Diatremes and Diamonds: their Geology, Petrology, and Geochemistry.* (eds. F.R. Boyd and H.O.A. Meyer). American Geophysical Union, Washington. pp. 71-91.

Streckeisen A. (1979) Classification and nomenclature of volcanic rocks, lamprophyres, carbonatites, and melilitic rocks: recommendations and suggestions of the IUGS subcommission on the systematics of igneous rocks. *Geology* **7**, 331-335.

Sun S.-S. (1980) Lead isotopic study of young volcanics from mid-ocean ridges, ocean islands and island arcs. *Phil. Trans. Roy. Soc. London* **A 297**, 409-445.

Sun S.-S., Jaques A.L. and McCulloch M.T. (1986) Isotopic evolution of the Kimberley Block, Western Australia. (extended abstr.) 4th Int. Kimberlite Conf., Perth. *Geol. Soc. Aust. Abstr. Series* **16**, 346-348.

Suwa K., Oana S., Wada H. and Susumu O. (1975) Isotope geochemistry and petrology of African carbonatites. In *Physics and Chemistry of the Earth.* (eds. L.H. Ahrens, F. Press, S.K. Runcorn and H.C. Urey) **9**, 735-745.

Taylor S.R. and Gorton M.P. (1977) Geochemical application of Spark Source Mass Spectrometry - III. Element sensitivity, precision, accuracy. *Geochim. Cosmochim. Acta* **41**, 491-510.

Thompson R.N., Morrison M.A., Hendry G.L., and Parry S.J. (1984) An assessment of the relative roles of crust and mantle in magma genesis: an elemental approach. *Phil. Trans. Roy. Soc. London* A **310**, 549-590.

Tilton G.R., Kwon S.T. and Frost D.M. (1987) Isotopic relationships in Arkansas Cretaceous alkalic complexes. *Geol. Soc. Amer. Spec. Paper* **215.**

Treiman A.H. and Essene E.J. (1983) Mantle eclogite and carbonate as sources of sodic carbonatites and alkalic magmas. *Nature* **302**, 700-703.

Tucker D.H. and Collerson K.D. (1972) Lamprophyric intrusions of probable carbonatitic affinity from South Australia. *J. Geol. Soc. Aust.* **19**, 387-391.

Verwoerd W.J. (1966) South African carbonatites and their probable mode of origin. *Annale, Univ. Stellenbosch* **41** (serie A), number 2.

Vidal P., Chauvel C. and Brousse R. (1984) Large mantle heterogeneity beneath French Polynesia. *Nature* **307**, 536-538.

Welke H.J., Allsopp H.L. and Harris J.W. (1974) Measurements of K, Rb, U, Sr and Pb in diamonds containing inclusions. *Nature* **252**, 35-37.

Wendlandt R.F. (1984) An experimental and theoretical analysis of partial melting in the system $KAlSiO_4$-CaO-MgO-SiO_2-CO_2 and applications to the genesis of potassic magmas, carbonatites and kimberlites. In *Kimberlites I: Kimberlites and Related Rocks.* (ed. J. Kornprobst). Elsevier, Amsterdam. pp. 359-369.

Wendlandt R.F. and Harrison W.J. (1979) Rare earth partitioning between immiscible carbonate and silicate liquids and CO_2 vapour: results and implications for the formation of light rare earth-enriched rocks. *Contrib. Mineral. Petrol.* **69**, 409-419.

White W.M. and Hofmann A.W. (1982) Sr and Nd isotope geochemistry of oceanic basalts and mantle evolution. *Nature* **296**, 821-825.

Willett G.C., Duncan R.K. and Rankin R.A. (1986) Geology and economic evaluation of the Mt Weld carbonatite, Laverton, Western Australia. (extended abstr.) 4th Int. Kimberlite Conf., Perth. *Geol. Soc. Aust. Abstr. Series* **16**, 97-99.

Williams R.W., Gill J.B. and Bruland K.W. (1986) Ra-Th disequilibria systematics: timescale of carbonatite magma formation at Oldoinyo Lengai volcano, Tanzania. *Geochim. Cosmochim. Acta* **50**, 1249-1259.

Wilson A.F. (1979) Contrast in the isotopic composition of oxygen and carbon between the Mud Tank Carbonatite and the marbles in the granulite terrane of the Strangways Range, central Australia. *J. Geol. Soc. Aust.* **26**, 39-44.

Wimmenauer W. (1966) The eruptive rocks and carbonatites of the Kaiserstuhl, Germany. In *Carbonatites.* (eds. O.F. Tuttle and J. Gittins). Interscience, New York. pp. 183-204.

Wood D.A. (1979) Dynamic partial melting: its application to the petrogenesis of basalts erupted in Iceland, the Faeroe Islands, the Isle of Skye (Scotland) and the Troodos Massif (Cyprus). *Geochim. Cosmochim. Acta* **43**, 1031-1046.

Wyllie P.J. and Huang W.-L. (1975) Peridotite, kimberlite, and carbonatite explained in the system CaO-MgO-SiO_2-CO_2. *Geology* **3**, 621-624.

Wyllie P.J. and Huang W.-L. (1976) Influence of mantle CO_2 in the generation of carbonatites and kimberlites. *Nature* **257**, 297-299.

Zartman R.E., Brock M.R., Heyl A.V. and Thomas H.H. (1967) K-Ar and Rb-Sr ages from some alkalic intrusive rocks from central and eastern United States. *Amer. J. Sci.* **265**, 848-870.

Coleman M.L. (1971) Potassium-calcium dates from pegmatitic micas. *Earth Planet. Sci. Lett.* **12**, 399-405.

Donnelly T.H., Lambert I.B., Oehler D.Z., Hallberg J.A., Hudson D.R., Smith J.W., Bavington O.A. and Golding L. (1977) A reconnaissance study of stable isotope ratios in Archaean rocks from the Yilgarn Block, Western Australia. *J. Geol. Soc. Aust.* **24**, 409-420.

Esat M.T. (1984) A 61 cm radius multi-detector mass spectrometer at The Australian National University. *Nucl. Instr. Meth. Phys. Res.* **B5**, 545-553.

Froude D.O., Ireland T.R., Kinny P.D., Williams I.S., Compston W., Williams I.R. and Myers J.S. (1983) Ion microprobe identification of 4100-4200 myr-old terrestrial zircons. *Nature* **304**, 616-618.

Jaques A.L., Lewis J.D. and Smith C.B. (1986) The kimberlites and lamproites of Western Australia. *Geol. Surv. West. Aust. Bull.* **132.**

Kinny P.D. (1986) 3820 Ma zircons from a tonalitic Amîtsoq gneiss in the Godthåb district of southern West Greenland. *Earth Planet. Sci. Lett.* **79**, 337-347.

Langmuir C.H., Bender J.F., Bence A.E., Hanson G.H. and Taylor S.R. (1977) Petrogenesis of basalts from the Famous area: mid-Atlantic ridge. *Earth Planet. Sci. Lett.* **36**, 133-156.

Marshall B.D. and DePaolo D.J. (1982) Precise age determinations and petrogenetic studies using the K-Ca method. *Geochim. Cosmochim. Acta* **46**, 2537-2545.

McCulloch M.T. and Perfit M.R. (1981) $^{143}Nd/^{144}Nd$, $^{87}Sr/^{86}Sr$ and trace element constraints on the petrogenesis of Aleutian island arc magmas. *Earth Planet. Sci. Lett.* **56**, 167-179.

McCulloch M.T., Compston W., Abbott M., Chivas A.R., Foster J.J. and Nelson D.R. (1982) Neodymium, strontium, lead and oxygen isotopic and trace element constraints on magma genesis in the Banda island-arc, Wetar. *Res. School Earth Sci. Ann. Rep. 1982*, 236-238.

Russell W.A., Papanastassiou D.A. and Tombrello T.A. (1978) Ca isotope fractionation on the Earth and other solar system materials. *Geochim. Cosmochim. Acta* **42**, 1075-1090.

Scott B.H. (1979) Petrogenesis of kimberlites and associated potassic lamprophyres from central west Greenland. In *Kimberlites, Diatremes and Diamonds: their Geology, Petrology, and Geochemistry.* (eds. F.R. Boyd and H.O.A. Meyer). American Geophysical Union, Washington. 190-205.

Smith C.B. (1979) Rb-Sr mica ages of various kimberlites. In *Chairmans Summaries and Poster Session Abstracts.* Kimberlite Symposium II. Cambridge, July 1979. pp. 61-66.

Venturelli G., Capedri S., Di Battistini G., Crawford A., Kogarko L.N. and Celestini S. (1984) The ultrapotassic rocks of southeastern Spain. *Lithos* **7**, 37-54.

White W.M. and Bryan W.B. (1977) Sr-isotope, K, Rb, Cs, Sr, Ba, and rare-earth geochemistry of basalts from the Famous area. *Geol. Soc. Amer. Bull.* **88**, 571-576.

APPENDIX 1. Analytical Techniques

A1.1 Whole-rock Rb-Sr analytical procedure

For Sr isotopic analysis, a conventional cation exchange procedure using HCl as the elutriant has been used. This procedure is summarised in Table A1.1. Depending on the sample mineralogy and the type of information sought, samples were dissolved either in open teflon beakers or in high-pressure teflon capsules. In some cases (specified in the text of this thesis), samples were split into 3 aliquots (for Rb-Sr and Sm-Nd, U-Pb, and Pb isotopic analysis) following dissolution. The U-Pb concentration or Pb isotopic composition aliquots were not combined with the Rb-Sr and Sm-Nd -spiked aliquot because of an unacceptably high Pb blank in the mixed Rb-Sr and Sm-Nd spikes. If U-Pb isotopic data was not required, the samples were totally spiked before dissolution with ^{85}Rb-^{84}Sr and ^{147}Sm-^{150}Nd mixed spikes. Prior to the ion exchange chemistry, the samples were re-dissolved in 2 ml of 1 N HCl and centrifuged in pre-cleaned 2.5 ml capacity polyethylene centrifuge tubes. Purified Rb and Sr aliquots were loaded in HCl onto triple Re filaments and analysed on the single collector 60° MS-Z mass spectrometer, using a fully computer-controlled, pair-switching acquisition procedure. Sr runs were normalised to $^{86}Sr/^{88}Sr = 0.1194$. Total processing blanks were monitored periodically and were generally <5 ng for both Sr and Rb. Apart from the carbonatite samples, which generally contained very low Rb contents, most of the samples examined during this study contained very high Rb and Sr abundances and blank corrections were unnecessary.

Table A1.1 Details of ion exchange procedure used for routine whole-rock rubidium-strontium analysis.

first pass- 5g of Bio-Rad AG 50W-X8 (200-400 mesh)

	load	wash	wash	elute Rb	wash	elute Sr	wash	elute REE
normality	1 N	1 N	2.5 N	2.5 N	2.5 N	2.5 N	6 N	6 N
volume	2 ml	2 ml	15 ml	5 ml	6 ml	10 ml	4 ml	20 ml

Sr second pass- 2g of Bio-Rad AG 50W-X8 (200-400 mesh)

	load	wash	wash	wash	elute Sr
normality	1 N	1 N	1 N	2.5 N	2.5 N
volume	1 ml	1 ml	22 ml	8 ml	5 ml

Rb second pass- 1g of Bio-Rad AG 50W-X8 (200-400 mesh)

	load	wash	wash	elute Rb
normality	1 N	1 N	1 N	1 N
volume	1 ml	1 ml	7 ml	4 ml

A1.2 Whole-rock Sm-Nd analytical procedure

The procedure for routine Sm-Nd isotopic analysis used in the R.S.E.S. isotope laboratory has been described previously (e.g. McCulloch and Perfit 1981, McCulloch and Chappell 1982). Following separation of Rb and Sr from most of the major elements on the 5 g column, the rare-earth elements were eluted in 20 ml of 6 N NCl (see Table A.1.1). A second column, fitted with drop-counters, was used to

separate Sm and Nd from the other rare-earth elements. A ~3 mm diameter, 310 mm length bed of pre-cleaned Bio-Rad AG 50W-X4 (-400 mesh) cation exchange resin was used and the elutriant was 0.2 M 2-methyl lactic acid (D-propanoic acid, 2 hydroxy) with pH adjusted to 4.6 using conc. NH_4OH (aq.). Both Sm and Nd were loaded in 1 N HCl onto degassed triple Re filaments and analysed as the metal species using the MS-Z mass spectrometer. Following Wasserburg *et al.* (1981), measured Sm and Nd ratios were normalised assuming $^{148}Sm/^{152}Sm = 0.42045$ and $^{146}Nd/^{142}Nd = 0.636151$ respectively. The non-radiogenic ratio $^{142}Nd/^{144}Nd$ was routinely measured throughout Nd runs in order to monitor isobaric interference from ^{142}Ce and ^{144}Sm. In practice, isobaric interference by Ce or Sm was rarely encountered and no corrections were required to any of the Nd isotopic results reported in this thesis.

A1.3 Whole-rock U-Pb chemistry procedure

The following procedures for Pb isotopic analysis were developed as part of this research and comprised an important component of this thesis work. As whole-rock Pb isotopic analysis was not routinely undertaken at the RSES prior to this research, it was necessary to re-establish suitable chemical procedures and the means for preparing high-purity reagents. It was recognised that Pb background levels in the chemical reagents would be unavoidably high during the early stages of this work but would be reduced progressively as the distillation equipment and storage bottles became cleaner with continued use.

Where this was realistically possible, all of the chemical procedures outlined below were undertaken in Class-100 clean-air laminar or downdraft flowhoods.

A1.3.1 Sample preparation and dissolution

Hand-specimens were sawn into ~5 cm^3 cubes, scrubbed with a clean plastic scrubbing brush using de-mineralised H_2O and in some cases ultrasonically cleaned in ultrapure H_2O. The cleaned rock cubes were dried and then crushed in a pre-cleaned stainless steel percussion mill and small rock fragments from the centre of the crushed cube were carefully hand-picked, using stainless steel tweezers, for isotopic analysis. In a few cases, it was necessary to analyse rock powders as hand-specimens were not available. Because of the risk of contamination during crushing in these cases, only samples which had been prepared using suitable low-contamination methods were considered for isotopic analysis.

The hand-picked chips or rock powders were dissolved using 1 ml 70% HF and 100 µl conc. $HClO_4$ in either teflon pressure capsules or open beakers (depending on the mineralogy, age and whether concentration data was required) for 24 to 48 hours, then evaporated to dryness in a Class-100 downdraft exhausting hood.

If U and Pb concentrations were required, the sample was re-dissolved in 1.2 N HCl and split unequally, the splits weighed and the smaller aliquot (typically < 1/3 of the total solution) spiked with a mixed ^{208}Pb-^{235}U spike. The splits were then evaporated to dryness.

A1.3.2 Pb ion-exchange column chemistry

Where there was no restriction on the amount of sample available, the Pb was isolated from up to 3 g of sample using columns fabricated of quartz glass, ~8 mm internal diameter and containing 2 g (dry weight) of Dowex 1 X 8 (200-400 mesh) anion exchange resin which was re-cleaned and re-used after each

Table A1.2 Reagent lead blanks (as at 26/9/86)

Reagent	Preparation Method	Pb conc. 10^{-12} g/g
$HClO_4$ (conc.)	Pyrex distilled	600
HF (conc.)	2-bottle teflon distilled	20
1.2 N HBr	"	20
1.2 N HCl	2-bottle teflon distilled	17
6 N HCl	"	17
ultrapure H_2O	millipore, teflon distilled	7

sample. Routine total processing blanks of ~2 ng Pb for 3 g samples were possible using these columns (see Tables A1.1 & A1.2), enabling the processing of samples with < 0.4 ppm Pb without the need for blank corrections. Pb yields for these columns were determined periodically during the course of their use and were consistently better than 98%. Sample/processing blank ratios were typically substantially better than 10^4.

The ion exchange columns were cleaned using 6 N HCl, H_2O, 6 N HCl, H_2O and then conditioned with ~6 ml of 1.2 N HBr prior to use. 5 ml of 1.2 N HBr was added to the samples which were then centrifuged in pre-cleaned 7 ml capacity centrifuge tubes and loaded onto the columns. The columns were washed with 1 ml of 1.2 N HBr, then 8 ml of 1.2 N HBr, followed by 8 ml of 1.2 N HCl. After equilibrating the column with 1 ml of 6 N HCl, the Pb was eluted with a further 5 ml of 6 N HCl. For spiked samples, the initial load volume and the washes were collected for uranium extraction and analysis by the isotope dilution method.

Table A1.3 Lead chemistry processing blanks.

Date	Details	Pb Blank (10^{-9} g/)
6/4/84	total processing blank (dissolution in pressure capsules)	7.6
6/4/84	column processing blank (2 passes)	4.5
6/4/84	"	9
6/4/84	"	1.5
21/6/84	total processing blank (dissolution in pressure capsules)	12
17/1/85	"	34
4/4/85	"	12
8/5/85	loading blank (degassed rhenium)	0.019
22/6/85	total processing blank (dissolution in pressure capsules)	2
1/7/85	"	1.5
12/8/85	"	2.8
23/9/85	total processing blank (dissolution in open beakers)	2.7
24/9/85	column processing blank (2 passes)	0.75
1/10/85	loading blank (undegassed rhenium)	0.087
12/2/86	total processing blank (dissolution in open beakers)	5.7
12/2/86	column processing blank (2 passes)	1.3
28/3/86	"	0.56
28/3/86	"	0.84
28/3/86	total processing blank (dissolution in pressure capsules)	1.5
4/7/86	total processing blank (dissolution in open beakers)	8.4

Table A1.4 Microcolumn chemistry processing blank breakdown (as at 26/9/86).

Reagent	Volume used (µl)	Pb contribution (10^{-12} g)
$HClO_4$ (conc.)	30	18
HF (conc.)	500	10
0.6 N HBr	5500	110
0.6 N HCl	1500	26
6 N HCl	1500	26
loading blank		19
total processing blank		219

A single pass was usually sufficient for spiked Pb samples, but for unspiked Pb samples a second pass produced cleaner Pb separations and was found to result in better mass spectrometry runs. For the second pass, the sample was loaded onto the pre-cleaned, pre-conditioned 2 g columns in ~1 ml of warmed 1.2 N HCl, washed with 1 ml of 1.2 N HCl, then 10 ml of 1.2 N HCl and, after equilibration of the column with ~2 ml of 6 N HCl, the Pb eluted with 8 ml of 6 N HCl. One drop (~25 µl) of conc. $HClO_4$ was added to the Pb solution to destroy any resin present. One drop of 0.3 M H_3PO_4 was then added and the sample evaporated to dryness.

A1.3.3 Pb microcolumn chemistry

In cases where the sample size was limited (for example, mineral seperates), microcolumns of about 2 ml capacity, 4 mm internal diameter, constructed of heat-shrink teflon were used. After treatment with HF and $HClO_4$ or HNO_3 (and splitting and spiking if necessary), the samples were loaded in 1 ml of 0.6 N HBr directly onto the columns which contained about 1 cm height of pre-washed (6 N HCl, H_2O, 6 N HCl, H_2O), pre-conditioned (using 1.5 ml of 0.6 N HBr) Dowex 1 X 8 (200-400 mesh) anion exchange resin. The columns were then washed 2 or 3 times with 1.5 ml of 0.6 N HBr, then 1.5 ml of 0.6 N HCl and the Pb eluted with 1.5 ml of 6 N HCl. A second pass using zircon chemistry (sample loaded and washed with 3 N HCl and Pb eluted with 6 N HCl) was necessary for some samples. Pb yields for this technique were measured at better than 98%. The total processing Pb blank was typically ~250 pg, with the column chemistry contributing ~120 pg to the total blank (see Table A1.4).

A1.3.4 U chemistry

Heat-shrink teflon microcolumns of about 3 ml capacity were used for uranium purification. After evaporation to dryness, the samples were re-dissolved in 0.5 ml of 10 N HCl and loaded onto columns containing 0.5 ml of pre-washed and pre-conditioned Dowex 1 X 8 (200-400 mesh) anion exchange resin. Fe was removed using a minimum of 2 washes (~2.5 ml) of 0.25 N $(NH_4)_2SO_4$ and this reagent was removed using at least 4 washes of 10 N HCl. Uranium was eluted in 2.5 ml of H_2O. The uranium was loaded in 0.3 M H_3PO_4 onto a thin layer of tantalum oxide (Ta_2O_5 powder in aqueous solution) on an outgassed single Re filament and the uranium analysed as the oxide species.

A1.3.5 Pb mass spectrometry

Most laboratories which undertake whole-rock Pb analysis base their analytical uncertainty on multiple analyses of a Pb standard, such as NBS-981 common Pb. However, it is likely that this procedure considerably under-estimates the analytical uncertainty, as Pb purified from rock samples rarely emits as well and the mass fractionation corrections are commonly not as reproducible as those achievable for the very clean Pb loaded from a standard solution. For example, it was noticed during this work that analyses of Pb purified from carbonatite samples were not as reproducible as analyses of Pb extracted from silicate samples, suggesting that impurities (presumably determined by the type of rock matrix) somehow influenced the mass fractionation. In order to obtain an accurate measure of the analytical uncertainty for whole-rock samples, all samples were analysed in duplicate (and in many cases, triplicate) during the course of this research. The analytical uncertainty estimate is based on a two-way analysis of variance of replicate mass spectrometry runs for each sample. For silicate samples this analytical uncertainty at the 1σ level is; $^{206}Pb/^{204}Pb$ ±011, $^{207}Pb/^{204}Pb$ ±0.013 and $^{208}Pb/^{204}Pb$ ±0.033.

The silica gel used in this study was prepared by adding Merck silica gel powder to high-purity H_2O, ultrasoning the suspension and allowing several days for the coarser gel particles to settle. An aliquot of the suspension was decanted for use. About 15 µl of recently ultrasoned silica gel solution was added to the sample and <1/2 of the mixture loaded onto an outgassed single Re filament. The load was then evaporated at ~1 ampere for a few minutes. The filament current was then slowly increased until the phosphoric acid fumed off (generally at about 2.0 amperes) and the filament heated further until dull red heat was just perceptible. Typically, about 0.5 to 5 µg of Pb was analysed per run.

The quality of the mass spectrometry run was found to depend critically on the sample loading procedure adopted and the quality of the silica gel, although other factors, such as incorrectly degassed rhenium filaments and the purity of the Pb, also dramatically effected the beam intensity and stability. In order to monitor the quality of the mass spectrometry, ~100 ng to 1 µg loads of NBS-981 common Pb or NBS-982 equal-atom Pb standards were analysed prior to each mass spectrometry session. Samples were not analysed until the following criteria for runs of these standards were met;

1. intensity of ^{208}Pb signal >1 volt ($5x10^{-10}$ Ω resistor);
2. beam stability was satisfactory;
3. mass fractionation correction was within ±0.025 % $m.u.^{-1}$ of an accepted value (determined to be 0.15 % $m.u.^{-1}$).

A compilation of the results obtained for the NBS standards during the course of this research is given in Tables A1.5 & A1.6 and the results obtained for NBS-981 common Pb standard are plotted in Figs. A1.1 and A1.2. It should be emphasised, however, that many of the analyses given in Tables A1.4 and A1.5 were not complete mass spectrometry runs but consisted of only about 5 minutes of data collection (i.e. measurement of the baselines and the ratios $^{206}Pb/^{204}Pb$, $^{207}Pb/^{204}Pb$ and $^{208}Pb/^{204}Pb$ for one set each only). During analysis of a sample, ratios were collected, by pair switching, in the following repeated sequence; baseline, $^{208}Pb/^{206}Pb$, $^{207}Pb/^{206}Pb$, baseline, $^{204}Pb/^{206}Pb$, $^{208}Pb/^{206}Pb$. This data collection procedure results in errors on calculated $^{208}Pb/^{204}Pb$, $^{207}Pb/^{204}Pb$ and $^{206}Pb/^{204}Pb$ ratios which are strongly correlated. During the earlier part of this work, data was collected by direct measurement of the ratios $^{208}Pb/^{204}Pb$, $^{207}Pb/^{204}Pb$ and $^{206}Pb/^{204}Pb$. Errors in these ratios using

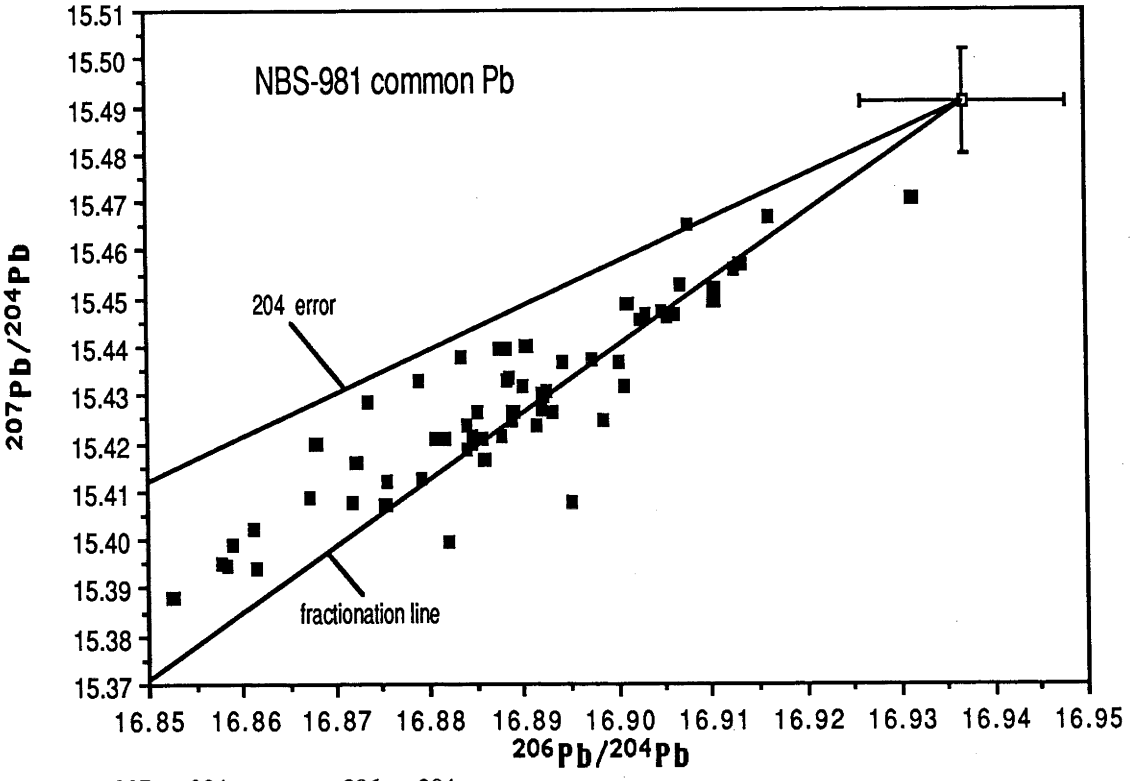

Fig. A1.1 $^{207}Pb/^{204}Pb$ versus $^{206}Pb/^{204}Pb$ results for the NBS-981 common-lead standard obtained during the course of this research.

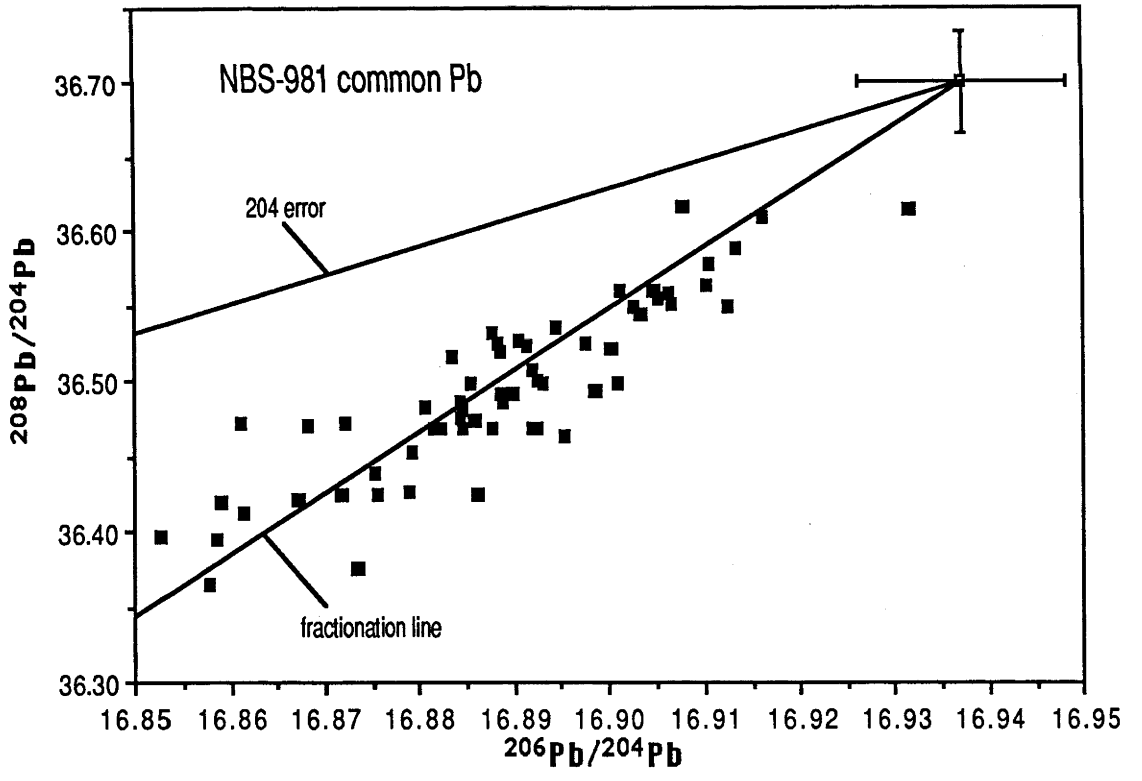

Fig. A1.2 $^{208}Pb/^{204}Pb$ versus $^{206}Pb/^{204}Pb$ results for the NBS-981 common-lead standard obtained during the course of this research.

Table A1.5 Compilation of analyses of NBS-981 common lead standard (uncorrected for mass fractionation) performed during the course of this research.

Date	$^{206}Pb/^{204}Pb$	$^{207}Pb/^{204}Pb$	$^{208}Pb/^{204}Pb$
14/6/84	16.8841	15.4235	36.4866
11/8/84	16.8905	15.4401	36.5260
13/8/84	16.8836	15.4377	36.5156
12/9/84	16.8718	15.4078	36.4248
17/9/84	16.8861	15.4165	36.4246
17/9/84	16.8579	15.3953	36.3655
17/9/84	16.8585	15.3947	36.3957
9/10/84	16.8858	15.4211	36.4748
25/10/84	16.9315	15.4706	36.6141
1/11/84	16.8823	15.3996	36.4680
14/1/85	16.8919	15.4267	36.4684
6/2/85	16.8681	15.4199	36.4710
6/2/85	16.8986	15.4249	36.4930
20/2/85	16.8756	15.4121	36.4256
28/2/85	16.8616	15.3943	36.4123
20/3/85	16.8953	15.4080	36.4631
18/4/85	16.9068	15.4527	36.5511
23/4/85	16.8847	15.4198	36.4689
9/5/85	16.8883	15.4394	36.5249
22/5/85	16.9079	15.4654	36.6160
29/5/85	16.8853	15.4263	36.4987
20/6/85	16.8734	15.4283	36.3759
20/6/85	16.8816	15.4207	36.4692
20/6/85	16.8673	15.4087	36.4209
22/6/85	16.9104	15.4520	36.5635
23/6/85	16.8900	15.4318	36.4919
23/6/85	16.8924	15.4295	36.4690
24/6/85	16.8877	15.4395	36.5317
24/6/85	16.8790	15.4327	36.4270
1/7/85	16.8886	15.4336	36.4917
1/7/85	16.9125	15.4558	36.5497
1/7/85	16.8878	15.4214	36.4689
2/7/85	16.8915	15.4234	36.5224
2/7/85	16.9162	15.4670	36.6100
2/7/85	16.9009	15.4319	36.4980
3/7/85	16.8975	15.4370	36.5253
10/7/85	16.9105	15.4492	36.5776
10/7/85	16.8723	15.4162	36.4715
18/7/85	16.8754	15.4074	36.4386
24/7/85	16.9013	15.4488	36.5598
6/9/85	16.8848	15.4212	36.4805
6/9/85	16.8806	15.4209	36.4824
23/9/85	16.8884	15.4330	36.5193
26/9/85	16.8792	15.4127	36.4536
30/9/85	16.8613	15.4024	36.4725
1/10/85	16.9003	15.4368	36.5217
7/10/85	16.9053	15.4459	36.5544
28/3/86	16.9048	15.4472	36.5603
4/4/86	16.8919	15.4304	36.5072
30/4/86	16.9063	15.4465	36.5590
13/5/86	16.8592	15.3990	36.4189
13/5/86	16.8926	15.4305	36.4999
21/5/86	16.8944	15.4365	36.5360
23/5/86	16.9026	15.4452	36.5488
25/5/86	16.9033	15.4463	36.5435
28/5/86	16.8841	15.4189	36.4753
18/11/86	16.9134	15.4572	36.5888
18/11/86	16.8892	15.4266	36.4921
17/12/86	16.8888	15.4249	36.4857
17/12/87	16.8931	15.4262	36.4979
9/1/87	16.8526	15.3878	36.3968
mean (n = 61)	16.8886	15.4283	36.4942
$\pm 2\sigma_{mean}$	±0.0041	±0.0047	±0.0146
fractionation (% $m.u.^{-1}$)	0.143	0.133	0.155
corrected (0.140 % $m.u.^{-1}$)	16.9359	15.4931	36.6985
certified values[a]	16.937	15.490	36.721

[a] from Catanzaro *et al.* (1968).

Table A1.6 Compilation of analyses of NBS-982 equal-atom lead standard (uncorrected for mass fractionation) obtained during the course of this research.

Date	$^{206}Pb/^{204}Pb$	$^{207}Pb/^{204}Pb$	$^{208}Pb/^{204}Pb$
16/5/84	36.5786	17.0467	36.4268
25/5/84	36.6035	17.0625	36.4683
25/5/84	36.6072	17.0629	36.4812
25/5/84	36.6034	17.0714	36.5010
2/6/84	36.6541	17.0929	36.5469
2/6/84	36.6932	17.1217	36.6345
2/6/84	36.6743	17.1069	36.5996
7/6/84	36.6487	17.0886	36.5421
7/6/84	36.6569	17.0961	36.5512
4/7/84	36.5488	17.1045	36.5187
4/7/84	36.6305	17.0894	36.5262
18/7/84	36.6904	17.1179	36.5972
25/7/84	36.6769	17.1067	36.5629
3/8/84	36.6121	17.0754	36.4891
17/8/84	36.6735	17.0869	36.5935
mean (n = 15)	36.6368	17.0887	36.5359
$\pm 2\sigma_{mean}$	±0.0208	±0.0104	±0.0274
fractionation (% m.u.$^{-1}$)	0.139	0.138	0.143
corrected (0.140 % m.u.$^{-1}$)	36.739	17.160	36.741
certified values[a]	36.739	17.160	36.745

[a] from Catanzaro *et al.* (1968).

this data aquisition sequence are not strongly correlated. To monitor possible problems caused by charged silica phosphate species, the mass spectrum was scanned and the baseline was measured at several mass positions (202.5 and 209.5) prior to and following data collection.

A1.4 Whole-rock Ca analytical procedure

1.4.1 Chemical separation

For silicate samples, approximately 2 to 5 mg of sample was dissolved using conc. HF and $HClO_4$ in teflon beakers for at least 24 hours. The resulting solution was then evaporated and re-dissolved in 6 N HCl. Where necessary, this procedure was repeated several times until a completely clear solution was obtained. Carbonate samples were pre-treated with 1 N HCl to destroy all carbonate prior to the HF-$HClO_4$ treatment. Gypsum samples (~3 mg) were dissolved in 3 N HCl. The solutions were then evaporated, re-dissolved in 1N HCl and loaded onto a bed of 2 g of pre-cleaned 200 mesh, Bio-Rad AG 50W-X8 (200-400 mesh) cation exchange resin in quartz glass columns. The potassium and most of the other major elements were removed using a 20 ml wash of 1 N HCl, followed by a 3.5 ml wash of 2.5 N HCl, and the calcium eluted in 4 ml of 2.5 N HCl. Calcium recovery using this procedure was found to be consistently better than 98%. All reagents used were distilled in sub-boiling two-bottle teflon stills. The total procedural Ca blank (determined by isotope dilution using a ^{43}Ca-enriched spike; see Appendix

A2.5 for further details) was < 60 ng, with the column chemistry and loading blank contributing ~15 ng to the total Ca blank.

1.4.2 Ca mass spectrometry

Between 5 and 25 μg of Ca was loaded in ~2 μl of 0.3 M H_3PO_4 onto an outgassed single tantalum filament and evaporated to dryness. The filament current was then increased until dull red heat was just perceptible and the tantalum filament had oxidised. The calcium was analysed using the R.S.E.S. Finnigan-MAT 261 mass spectrometer, which is fitted with a 7-faraday-cup collector. As the mass dispersion for the isotopes of interest (^{40}Ca to ^{44}Ca) was too large for simultaneous collection in static mode, a double-jump measurement procedure was adopted, with the isotopes ^{40}Ca, ^{41}K and ^{42}Ca collected simultaneously, followed by a second jump measuring ^{42}Ca, ^{43}Ca and ^{44}Ca for the mass fractionation correction using a second set of 3 faraday cups which were offset 0.25 mass units from the first set. The baselines for all cups were measured simultaneously at an offset of a further 0.25 mass units. Because of the greater abundance of ^{40}Ca, this isotope was measured using a 10^{10} Ω resistor and the other isotopes measured using 10^{11} Ω resistors. Typically, stable beams of ~5 volts of ^{40}Ca (10^{10} Ω) for several hours duration were readily obtainable. Isobaric interference at ^{40}Ca by ^{40}K was monitored by measurement of the abundance of ^{41}K, but the correction to the $^{40}Ca/^{42}Ca$ ratio for ^{40}K interference was always less than -0.0005 (or <0.0003% of the $^{42}Ca/^{44}Ca$ ratio) and was therefore insignificant in all mass spectrometry runs.

1.4.3 Mass fractionation correction

Russell *et al.* (1978) argued that a residual drift remained in the fractionation-corrected $^{40}Ca/^{42}Ca$ ratios of their data when corrected using the linear fractionation law. These authors found that the Rayleigh and exponential laws removed this drift and appeared to provide a better fit. Esat (1983) showed that commonly-used mass fractionation laws, such as the Rayleigh, exponential and power laws, have the general form:

$$R_{ik} = N\,[R_{jk}]^{\gamma} \qquad (1)$$

where N is a constant (different for each law),

$$R_{ik} = [\text{ion current of mass } i]/[\text{ion current of mass } k] \qquad (2)$$

and

$$\text{mass}_i > \text{mass}_j > \text{mass}_k \qquad (3)$$

The value of γ in equation (1) is a function of the mass of the ion species being measured and influences the degree of curvature of R_{ik} with variation in R_{jk} (see Fig. A1.3). The applicability of each of the mass fractionation laws (i.e. the value of γ) has been assessed in two ways;

1. by analysis of "equal-atom" Ca solutions, prepared by mixing common (^{40}Ca-enriched) calcium with ^{42}Ca-, ^{43}Ca- and ^{44}Ca-enriched spikes. Two solutions were prepared and analysed; solution #1 has approximately equal abundances of ^{40}Ca, ^{42}Ca and ^{44}Ca, and solution #2 has approximately equal abundances of ^{40}Ca, ^{42}Ca, ^{43}Ca and ^{44}Ca. Because errors due to resistor and amplifier non-linearity and to baseline corrections are minimised, error due to deviations from the mass fractionation laws should be more readily detectable in the analysis of these "equal-atom" solutions.

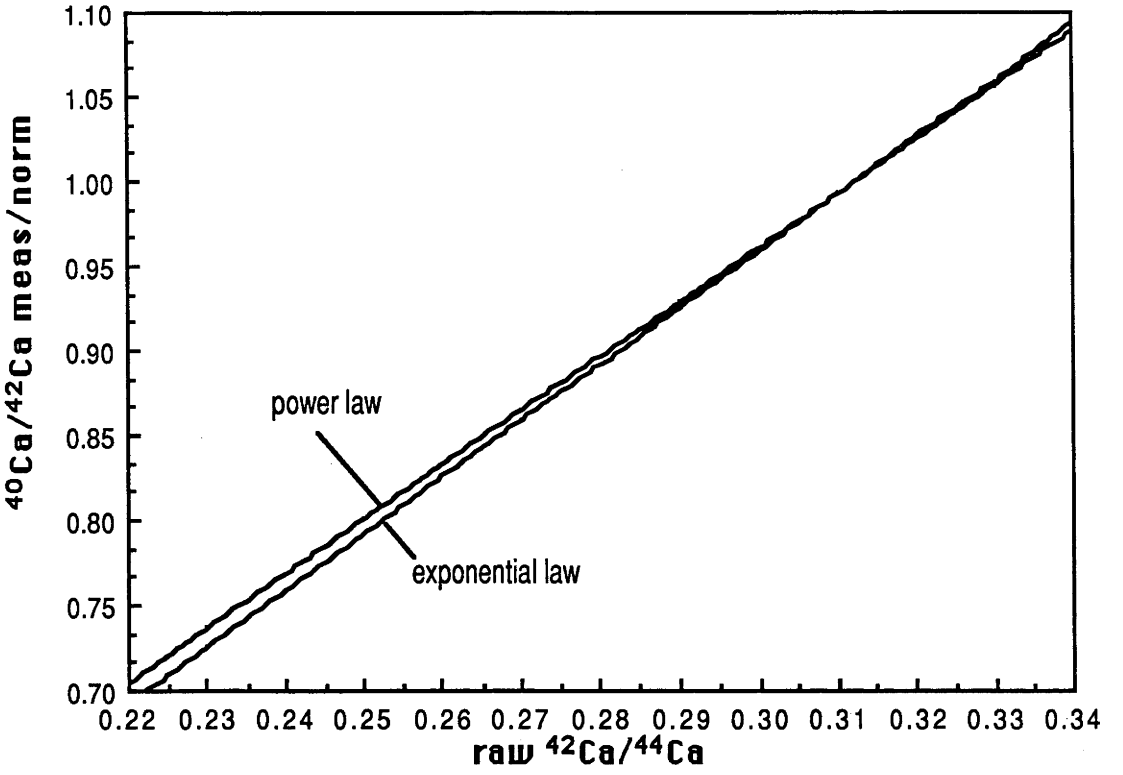

Fig. A1.3 Curves of measured/normalised $^{40}Ca/^{42}Ca$ versus raw $^{42}Ca/^{44}Ca$ values for various fractionation laws. The normalising $^{42}Ca/^{44}Ca$ value assumed is 0.31221. As the linear law is an approximation of the power law, the curves of these laws are almost identical at this scale. The empirical law curve (with an exponent of 1.054242) is very similar to the exponential law curve. For the majority of runs, 0.304 < raw $^{42}Ca/^{44}Ca$ < 0.311.

2. by comparison of the external precision (i.e. reproducibility) of $^{40}Ca/^{42}Ca$ analyses acquired for a Ca isotopic standard analysed repeatedly throughout the course of this study and corrected using different mass fractionation laws.

The results obtained for the "equal-atom" Ca solutions are summarised in Figs. A1.4 and A1.5. In Fig. A1.4, an analysis of solution #1 (~20 µg load) is shown. The $^{40}Ca/^{42}Ca$ ratios have been corrected by normalisation of the $^{42}Ca/^{44}Ca$ ratio to an arbitrary value ($^{42}Ca/^{44}Ca_{norm}$ = 0.83). The Finnigan-MAT data aquisition software uses a linear mass fractionation law where, for each $^{42}Ca/^{44}Ca$ scan, a factor ϕ was determined from the measured $^{42}Ca/^{44}Ca$ value:

$$\phi = (^{42}Ca/^{44}Ca_{meas})/(^{42}Ca/^{44}Ca_{norm}) \quad (4)$$

The $^{40}Ca/^{42}Ca$ ratio measured during the previous scan is corrected for mass fractionation as follows:

$$^{40}Ca/^{42}Ca_{corr} = (^{40}Ca/^{42}Ca_{meas})/\phi \quad (5)$$

This correction procedure to the $^{40}Ca/^{42}Ca$ ratio assumes that, at any time during the run, the ratio of the measured/"true" $^{40}Ca/^{42}Ca$ ratio, which differs from unity due to mass fractionation effects, is equivalent to the ratio of the measured/"true" $^{42}Ca/^{44}Ca$ ratio. For the analysis of solution #1, a within-run precision of 0.0012% (95% confidence) was obtained for the $^{40}Ca/^{42}Ca$ ratio, with the gain calibrations, performed every 5 blocks, clearly limiting any further improvement in the precision. No drifts which could be attributable to deviations from the mass fractionation law were observed in the fractionation-corrected $^{40}Ca/^{42}Ca$ ratio (Fig. 1.4b).

The results obtained for the ^{43}Ca-enriched solution #2 (~2 µg load) are shown in Fig. A1.5. During the early stages of this run, the raw $^{42}Ca/^{44}Ca$ ratio increased rapidly (Fig. A1.5a) until, at about block

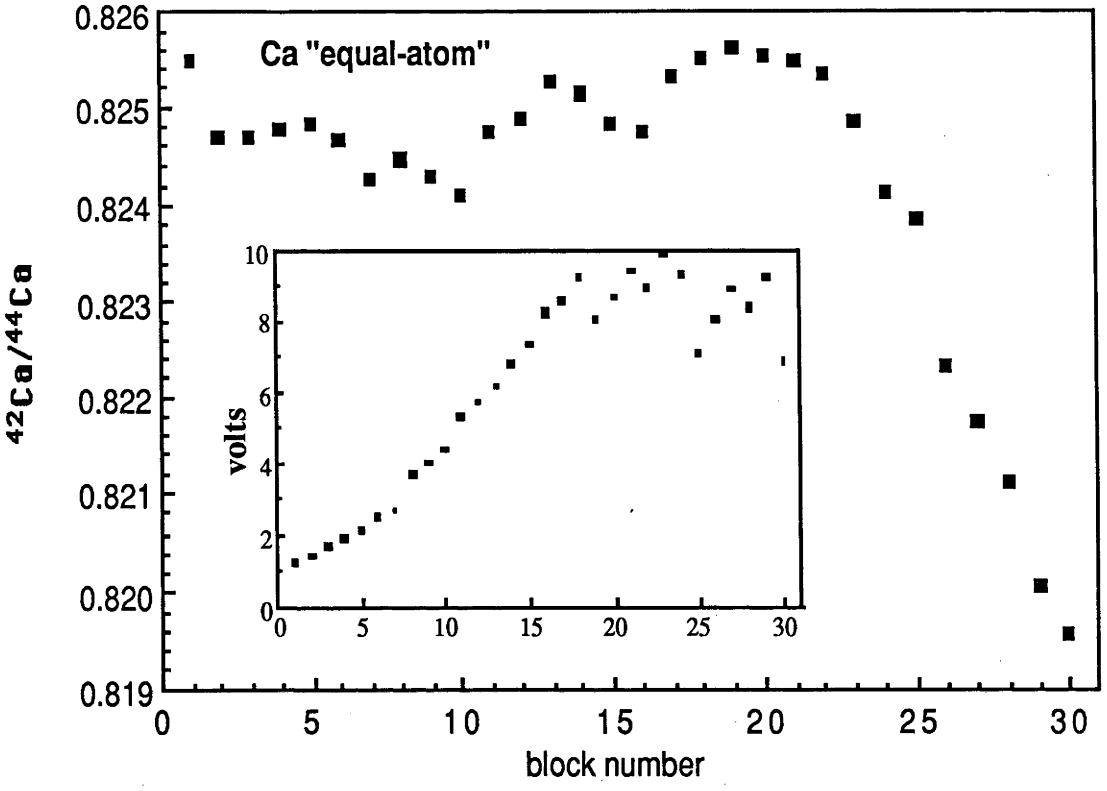

a).

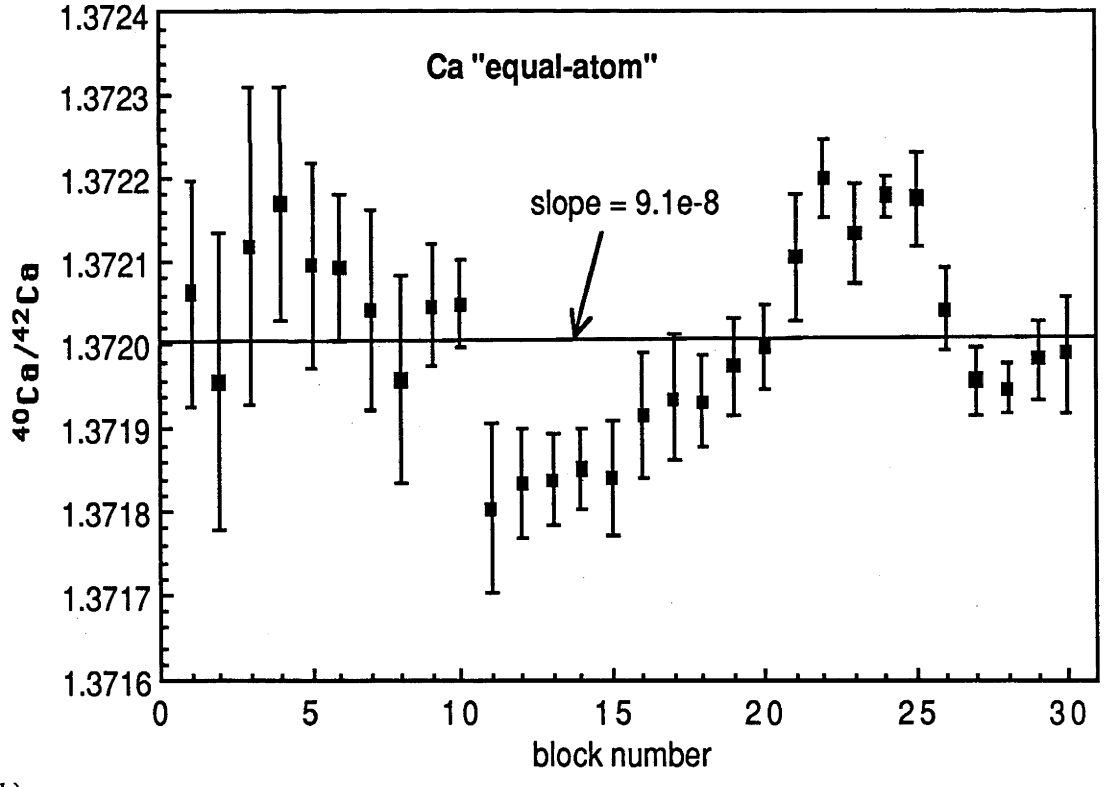

b).

Fig. A1.4 a). Variation in the raw $^{42}Ca/^{44}Ca$ ratio measured during run 1 of solution #1 "equal-atom" Ca. Each point represents the mean value, excluding 2σ outliers, of 10 scans. The inset shows the intensity (in volts, corrected to 10^{11} Ω resistor) of ^{40}Ca. b). Fractionation-corrected (linear law) $^{40}Ca/^{42}Ca$ for each block of 10 scans (with 1σ error-bars) of run 1, solution #1. An internal precision of 0.0012% (95% confidence) was obtained for the $^{40}Ca/^{42}Ca$ ratio. Gain calibrations have been performed every 5 blocks, and account for much of the scatter in the fractionation-corrected $^{40}Ca/^{42}Ca$ ratio.

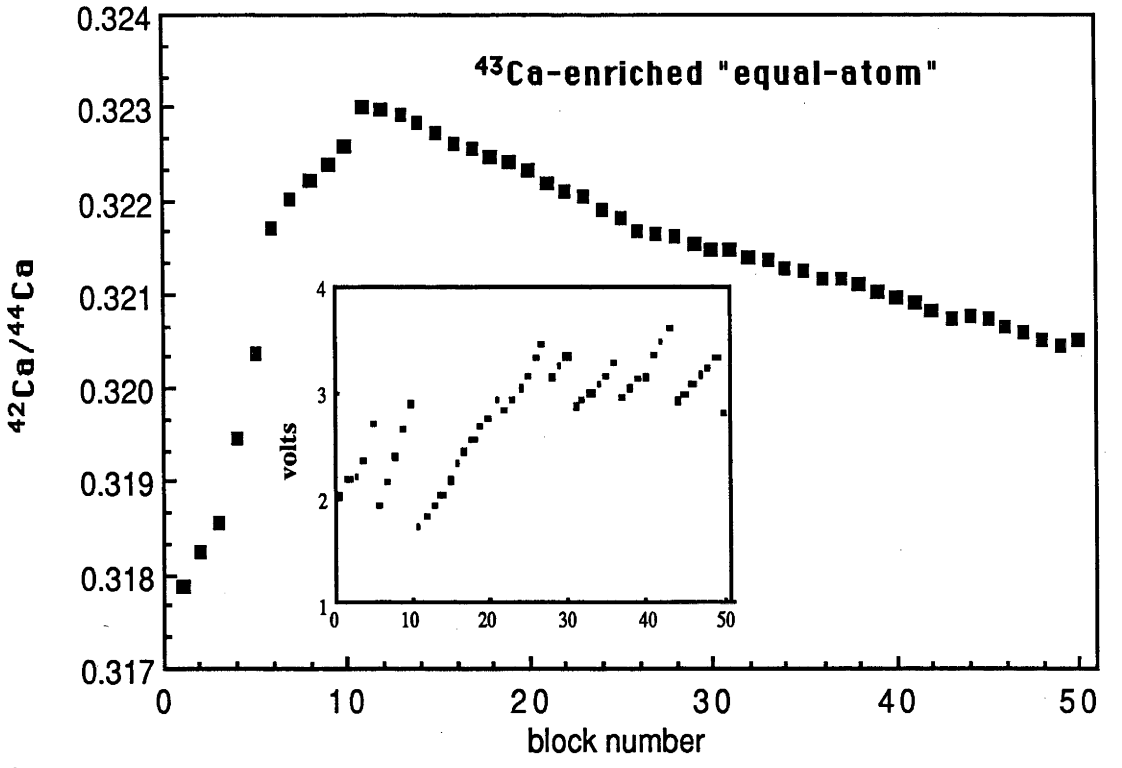

a).

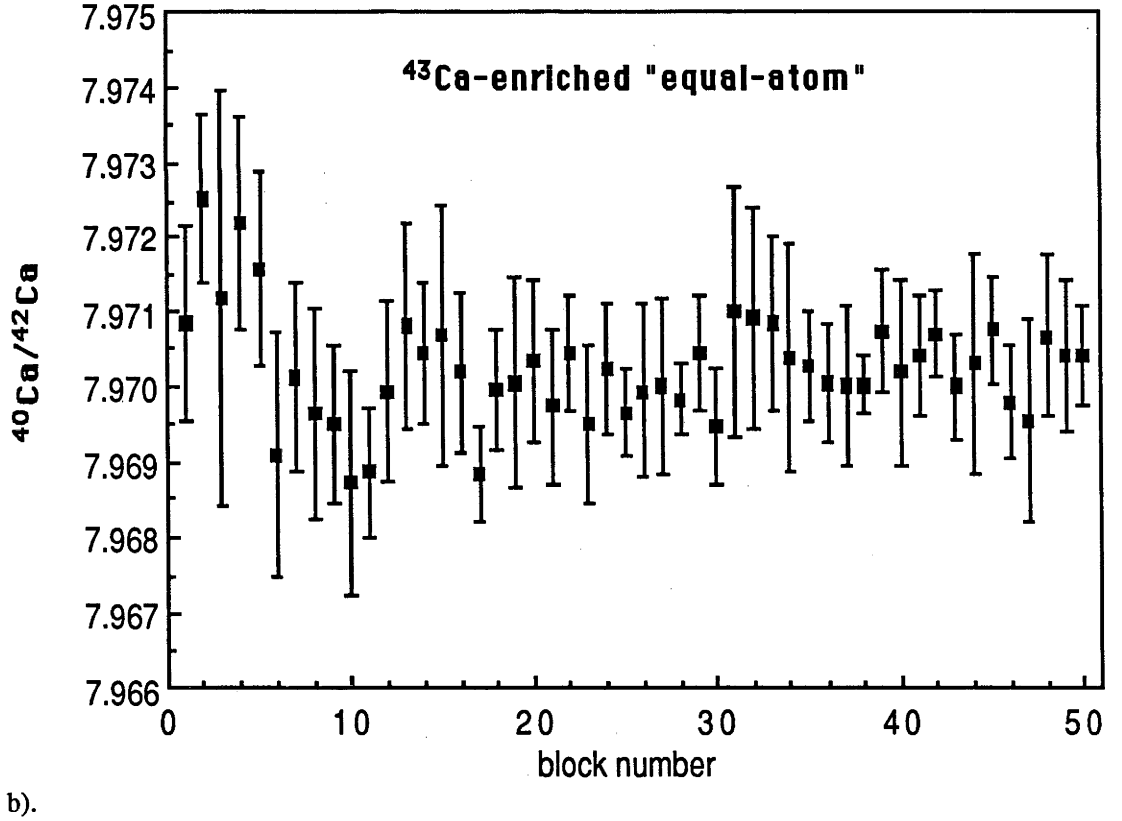

b).

Fig. A1.5 a). Variation in the raw $^{42}Ca/^{44}Ca$ ratio measured during run 1 of solution #2 "^{43}Ca-enriched equal-atom" Ca. Each point represents the mean value of 10 scans. The inset shows the intensity (in volts, corrected to 10^{11} Ω resistor) of ^{40}Ca. b). Fractionation-corrected (linear law) $^{40}Ca/^{42}Ca$ for each block of 10 scans (error-bars are 1σ) of run 1, solution #2. The linear law has removed all significant time-dependent drift in the $^{40}Ca/^{42}Ca$ ratio.

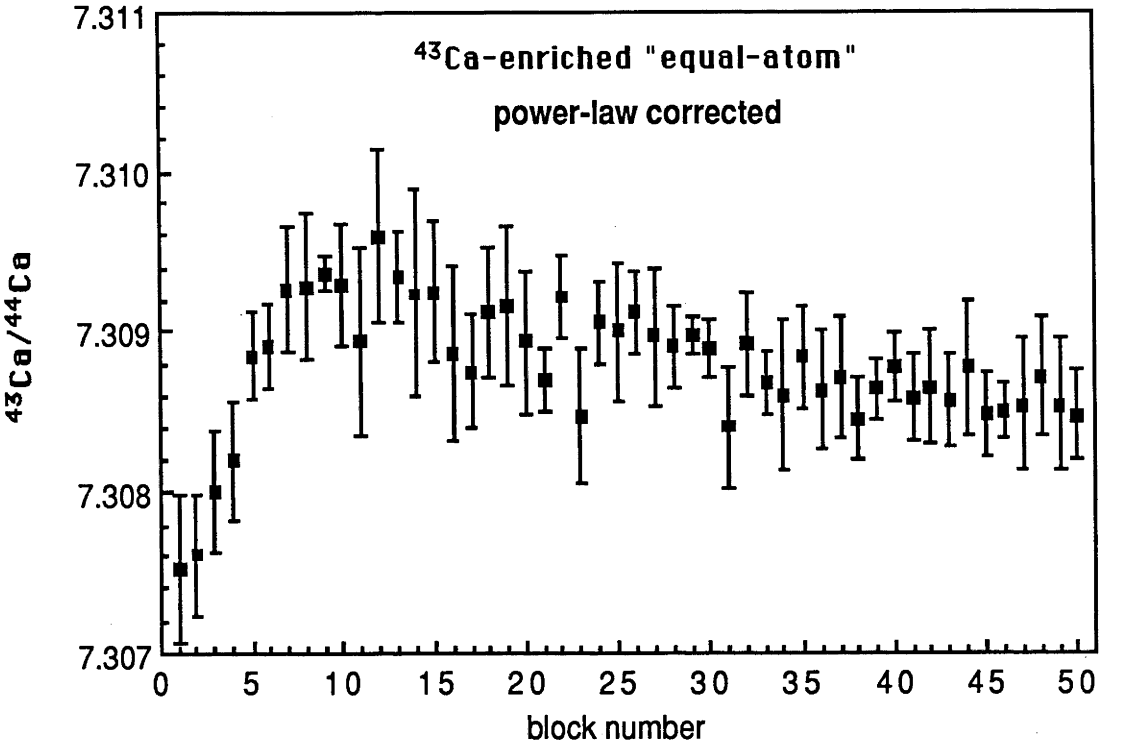

c).

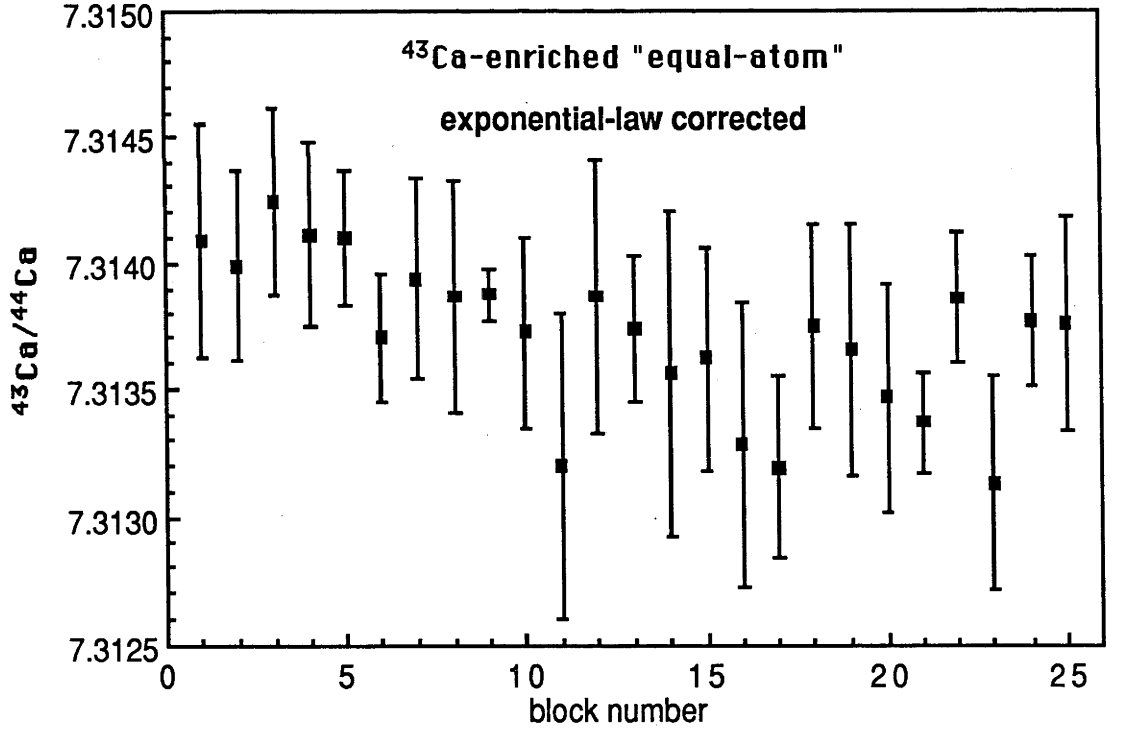

d).

Fig. A1.5 c). Variation in the power-law corrected $^{43}Ca/^{44}Ca$ ratio measured during run 1 of solution #2, "^{43}Ca-enriched equal-atom" Ca. Each point represents the mean value of 10 scans (Error-bars are 1σ). The linear law has failed to remove the time-dependent drift in the corrected $^{43}Ca/^{44}Ca$ ratio during the early stages of this run. d). Fractionation-corrected (exponental law) $^{43}Ca/^{44}Ca$ for each block of 10 scans (error-bars are 1σ and are approximate only) for the first 25 blocks of same run (run 1, solution #2) as is shown in Fig. A1.5c. The exponential law has removed all significant time-dependent drift in the $^{43}Ca/^{44}Ca$ ratio.

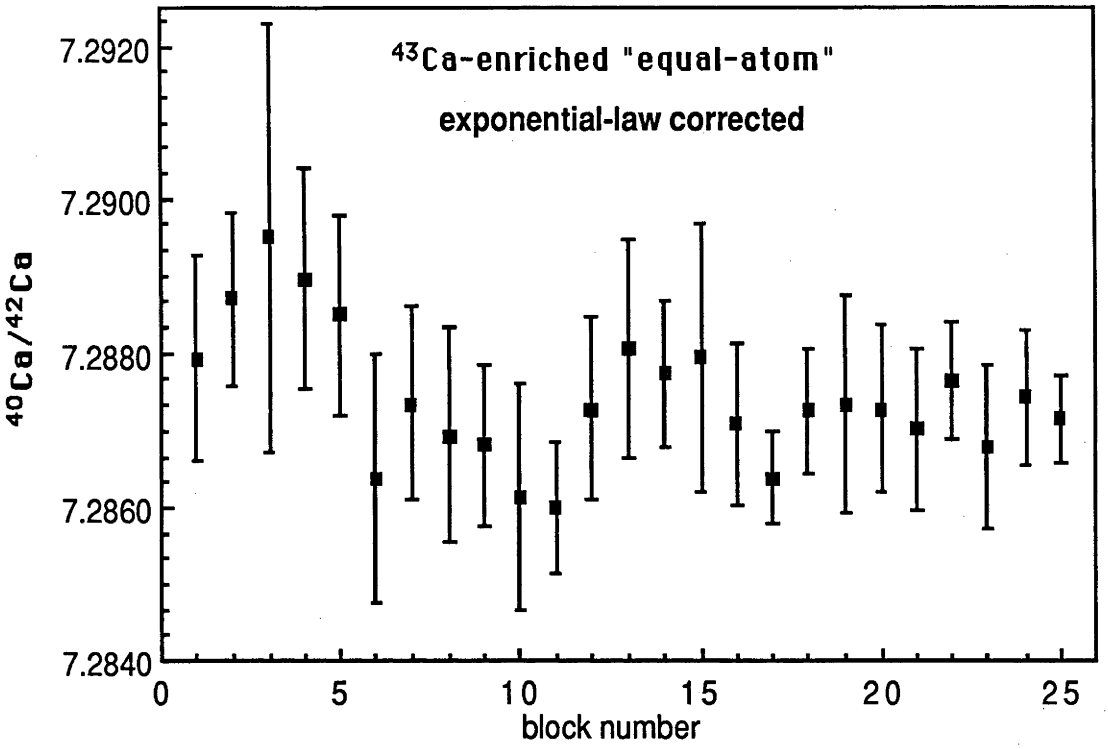

Fig. A1.5 e). Fractionation-corrected (exponental law) $^{40}Ca/^{42}Ca$ for each block of 10 scans for the first 25 blocks of same run (run 1, solution #2) as is shown in Fig. A1.5c. Application of the exponential law does not result in any significant time-dependent drift in the $^{40}Ca/^{42}Ca$ ratio. (Error-bars are 1σ and are approximate only).

10 (~70 minutes after commencement of the run and after operator intervention), the fractionation trend reversed and the raw $^{42}Ca/^{44}Ca$ ratio decreased steadily. The $^{40}Ca/^{42}Ca$ and $^{43}Ca/^{44}Ca$ ratios have been corrected, using the linear fractionation law, by normalisation of the $^{42}Ca/^{44}Ca$ ratio to an arbitrarily-selected value of 0.34. The $^{43}Ca/^{44}Ca$ ratio is measured synchronously with the $^{42}Ca/^{44}Ca$ ratio and the precision is consequently slightly greater than that attainable for the $^{40}Ca/^{42}Ca$ ratio. Although there is no significant drift in the linear-law-corrected $^{40}Ca/^{42}Ca$ ratio (Fig. A1.5b), the linear-law-corrected $^{43}Ca/^{44}Ca$ ratio increases with the raw $^{42}Ca/^{44}Ca$ ratio during the first 10 blocks and then levels off or decreases slightly (Fig. A1.5c). Re-calculation of the data obtained for this run using the exponential law removes this drift in the corrected $^{43}Ca/^{44}Ca$ ratio (Fig. A1.5d) without introducing any significant drift in the corrected $^{40}Ca/^{42}Ca$ ratio (Fig. A1.5e). These results confirm the findings of Russell *et al.* (1980) that, under some circumstances, small deviations from the linear mass fractionation laws may occur, and that the exponential mass fractionation law may more accurately describes the isotopic fractionation occurring on the filament, at least during the early stages of a Ca analysis. The magnitude of the deviations from the linear fractionation law observed for the $^{43}Ca/^{44}Ca$ ratio during this study were ~0.013% (from Fig. A1.5c). However, the deviations from the linear law are only observable where the mass differences between the normalising and normalised ratios are different. No significant deviation is evident in the linear-law-corrected $^{40}Ca/^{42}Ca$ ratio (Fig. A1.5b), and the exponential law applied to the same data does not result in any significant improvement (Fig. A1.5e). The difference between masses of the isotopes of the normalising ratio (mass difference ^{44}Ca - ^{42}Ca is 1.99686) and the ratio of interest to which the fractionation correction is applied (mass difference ^{42}Ca - ^{40}Ca is 1.99618) is similar in this study, so the linear, power and exponential laws are expected to produce quite similar results for the total

Table A1.7 $^{40}Ca/^{42}Ca$ isotopic results for the Tridacna calcium isotopic standard (obtained over the 5 month period of this study) re-calculated using various mass fractionation laws.

Run No.	exponential[a]	power	empirical	linear
1.	151.062 ±5	150.964 ±11	151.073 ±5	151.068 ±7
2.	151.077 ±7	150.949 ±10	151.092 ±7	151.077 ±9
3.	151.092 ±3	150.995 ±4	151.104 ±2	151.099 ±3
4.	151.082 ±3	150.963 ±5	151.097 ±3	151.088 ±5
5.	151.057 ±3	150.993 ±3	151.065 ±3	151.058 ±5
6.	151.074 ±4	150.958 ±3	151.088 ±4	151.079 ±6
7.	151.050 ±20	150.846 ±26	151.073 ±20	151.092 ±9
8.	151.063 ±3	150.870 ±12	151.087 ±4	151.074 ±8
9.	151.056 ±3	150.874 ±5	151.078 ±3	151.064 ±5
12.	151.096 ±10	150.980 ±27	151.110 ±8	151.103 ±6
means and external precision[b] (2σ);				
	151.071 ±30	150.939±104	151.087 ±27	151.080 ±28

[a] Ratios normalised to $^{42}Ca/^{44}Ca = 0.31221$. Errors quoted refer to within-run precision (at the 95% confidence level) calculated on the means of blocks of 10 scans, except for the linear law result which is calculated on individual scans.
exponential law: $^{40}Ca/^{42}Ca = {}^{40}Ca/^{42}Ca_{meas} \times (M42/M40)^{\gamma}$ where Mx = atomic mass of isotope *x*, and $\gamma = \ln(^{42}Ca/^{44}Ca_{meas}/0.31221)/\ln(M44/M42)$
power law: $^{40}Ca/^{42}Ca = {}^{40}Ca/^{42}Ca_{meas} / [(^{42}Ca/^{44}Ca_{meas}/0.31221)^{\alpha}]^{\gamma}$ where $\alpha = 1/(M42 - M44)$ and $\gamma = (M40 - M42)$.
empirical law: $^{40}Ca/^{42}Ca = {}^{40}Ca/^{42}Ca_{meas} \times (M42/M40)^{\alpha}$ where $\alpha = 1/(M42-M44)$ and $\gamma = 1.054242$.
linear law: $^{40}Ca/^{42}Ca = {}^{40}Ca/^{42}Ca_{meas}/(^{42}Ca/^{44}Ca_{meas} / 0.31221)$.

[b] All analyses have been weighted equally.

range of mass fractionation observed. Therefore, it is anticipated that no law is preferable over any other.

For the analysis of standards and samples, the measured Ca isotopic ratios were normalised to a value of $^{42}Ca/^{44}Ca = 0.31221$ to correct for the effects of mass fractionation, following Marshall and DePaolo (1982). The $^{43}Ca/^{44}Ca$ data obtained for samples and standards has also been corrected using the linear law:

$$^{43}Ca/^{44}Ca_{corr} = {}^{43}Ca/^{44}Ca_{meas}[1 + 0.5\phi] \qquad (6)$$

No major deviations from the average $^{43}Ca/^{44}Ca$ value (from Table A1.8, average $^{43}Ca/^{44}Ca$ = 0.064853 ±17) were observed in data obtained for any of the samples or standards analysed during this study.

A $CaCO_3$ solution prepared from the shell of *Tridacna Gigas* (Giant Clam) has been adopted as a Ca isotopic standard. The standard solution has an $^{87}Sr/^{86}Sr$ value of 0.70921 ±3, which is indistinguishable from that of modern seawater. The external precision estimate for all Ca isotopic data obtained during this work is based on multiple analyses of this standard. Results of this analysis are presented in Tables A1.7 and A1.8 and in Fig. A1.6. In Table A1.7, mass spectrometry data for the Tridacna standard have been corrected for the effects of mass fractionation using various fractionation laws (see Appendix A2.6 for a listing of the computer program used for this analysis). Ca isotope ratios have

Table A1.8 Calcium isotopic results obtained for the Tridacna calcium isotopic standard, obtained during the 5 month period of this study.

Run No.	Date of analysis	$^{43}Ca/^{44}Ca \pm 2\sigma_{mean}$ [a]		$^{40}Ca/^{42}Ca \pm 2\sigma_{mean}$ [a]		blocks	ε_{Ca} [b]	$\pm 2\sigma_{mean}$
1.	7 April, 1987	0.064860	±8	151.068	±7	(25)	-0.66	±0.46
2.	"	0.064855	±10	151.077	±9	(17)	-0.07	±0.59
3.	8 April, 1987	0.064857	±3	151.099	±3	(20)	+1.39	±0.20
4.	"	0.064850	±4	151.088	±5	(15)	+0.66	±0.33
5.	9 April, 1987	0.064861	±5	151.058	±5	(14)	-1.32	±0.33
6.	28 April, 1987	0.064848	±6	151.079	±6	(14)	+0.07	±0.40
7.	29 April, 1987	0.064855	±6	151.092	±9	(8)	+0.93	±0.59
8.	"	0.064854	±11	151.074	±8	(9)	-0.26	±0.53
9.	"	0.064849	±6	151.064	±5	(16)	-0.93	±0.33
10.	25 May, 1987	0.064849	±4	151.067	±5	(10)	-0.73	±0.33
11.	27 May, 1987	0.064831	±14	151.115	±21	(10)	+2.45	±1.39
12.	11 August, 1987	0.064868	±8	151.103	±6	(18)	+1.65	±0.43
mean & 2σ external precision		0.064853	±17	151.079	±28		-0.066	±1.9

[a] Ratios normalised to $^{42}Ca/^{44}Ca = 0.31221$, using the linear mass fractionation law. Errors quoted refer to within-run precision at the 95% confidence level. All analyses have been given equal weighting. Because of its larger within-run uncertainty, the $^{40}Ca/^{42}Ca$ analysis of run 11 has not been included in the calculation of the external precision.

[b] $\varepsilon_{Ca} = [(^{40}Ca/^{42}Ca_{sample} - 151.078)/151.078] \times 10^4$.

been re-calculated from the raw data for each block, which consists of the means of 10 individual scans, excluding 2σ outliers. The "empirical" law uses a calculated best-fit value for γ which gives the minimum external precision for runs 1 to 9 of the Tridacna standard. The results given in Table A1.7 demonstrate that application of the power fractionation law results in an external agreement between runs ~4 times less precise than that obtained using the exponential, empirical and linear laws, which give similar external precision levels. However, for some individual mass spectrometry runs (such as runs 5 & 6), the power law provides at least as good a fit as the other laws. Variation in linear-law-corrected $^{40}Ca/^{42}Ca$ ratios with variation in raw $^{42}Ca/^{44}Ca$ for some of the Tridacna runs is shown in Fig. A1.6. The linear law correction removes all systematic variation in corrected $^{40}Ca/^{42}Ca$ ratios with time or with raw $^{42}Ca/^{44}Ca$, suggesting that this law adequately corrects for the effects of mass fractionation. The corrected $^{40}Ca/^{42}Ca$ ratios for run 4 (see Fig. A1.4h) show a small systematic increase with time but this drift is well within the precision of the $^{40}Ca/^{42}Ca$ measurements.

The results obtained for the Tridacna standard throughout the course of this study (Table A1.8) indicate an external precision of 0.018% (i.e. ±0.028) at the 95% confidence level for measurements of the $^{40}Ca/^{42}Ca$ ratio, using the linear mass fractionation correction. Many of the samples examined during this study were analysed in duplicate. Two-way analysis of variance of 30 duplicated $^{40}Ca/^{42}Ca$ analyses of these samples (see Appendix A2.7 for details of this analysis) indicates an experimental error of ±0.034 at the 95% confidence level. The external precision error is therefore ~4 times the typical internal (within-run) precision error. This difference is not unreasonable for data obtained by multiple collection. The main causes of this difference are attributable to a combination of factors, such as;

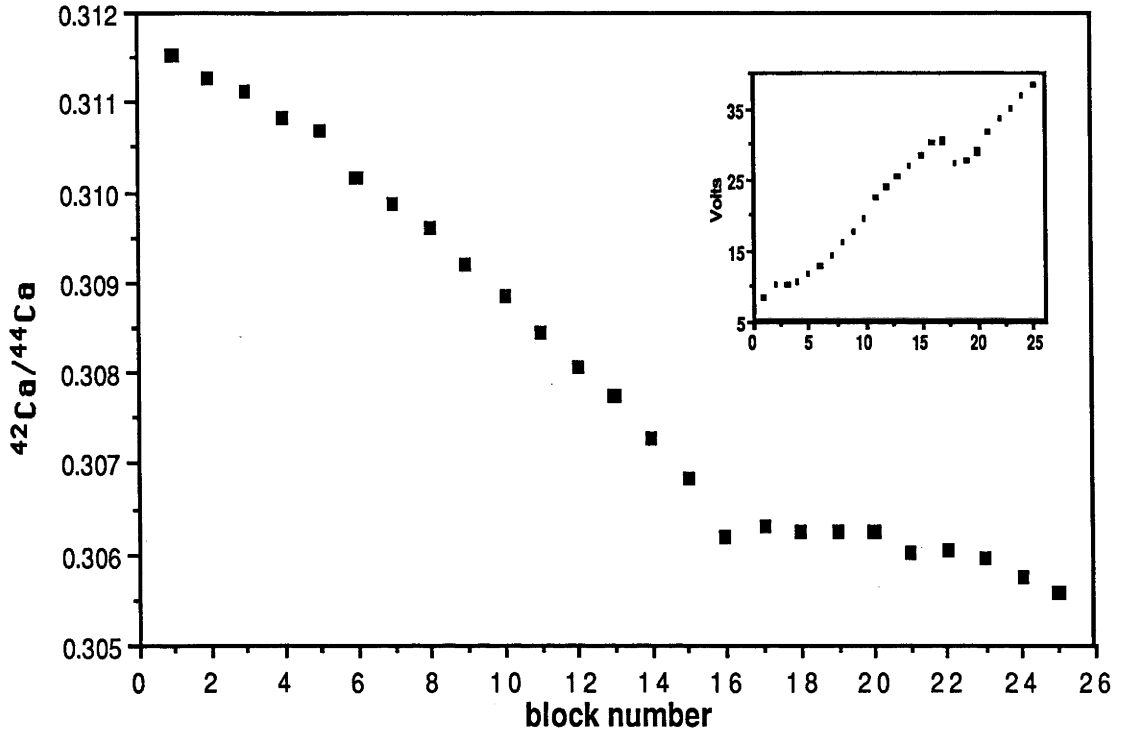

a).

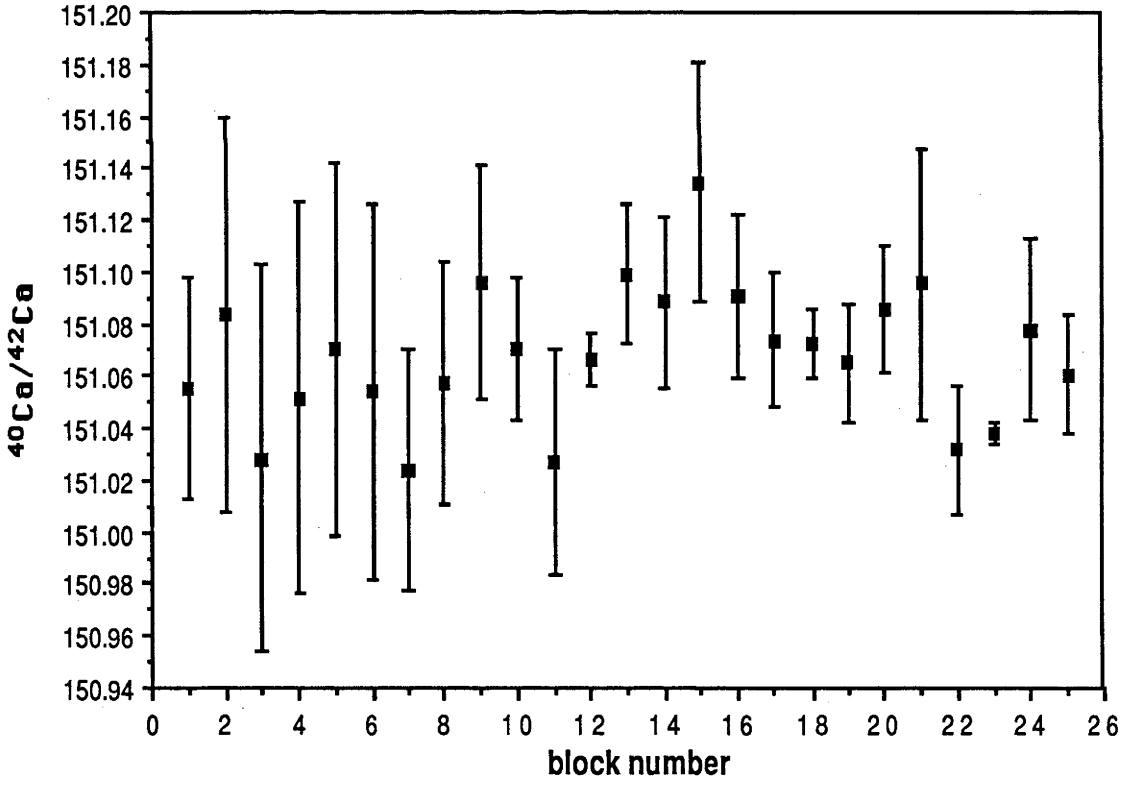

b).

Fig. A1.6 a). Variation in the raw $^{42}Ca/^{44}Ca$ ratio measured during run 1 of the Tridacna standard. Each point represents the mean value, excluding 2σ outliers, of 10 scans. The inset shows the intensity of ^{40}Ca in volts, measured on the 10^{11} Ω resistor. b). Fractionation-corrected $^{40}Ca/^{42}Ca$ for each block of 10 scans (with 1σ error-bars).

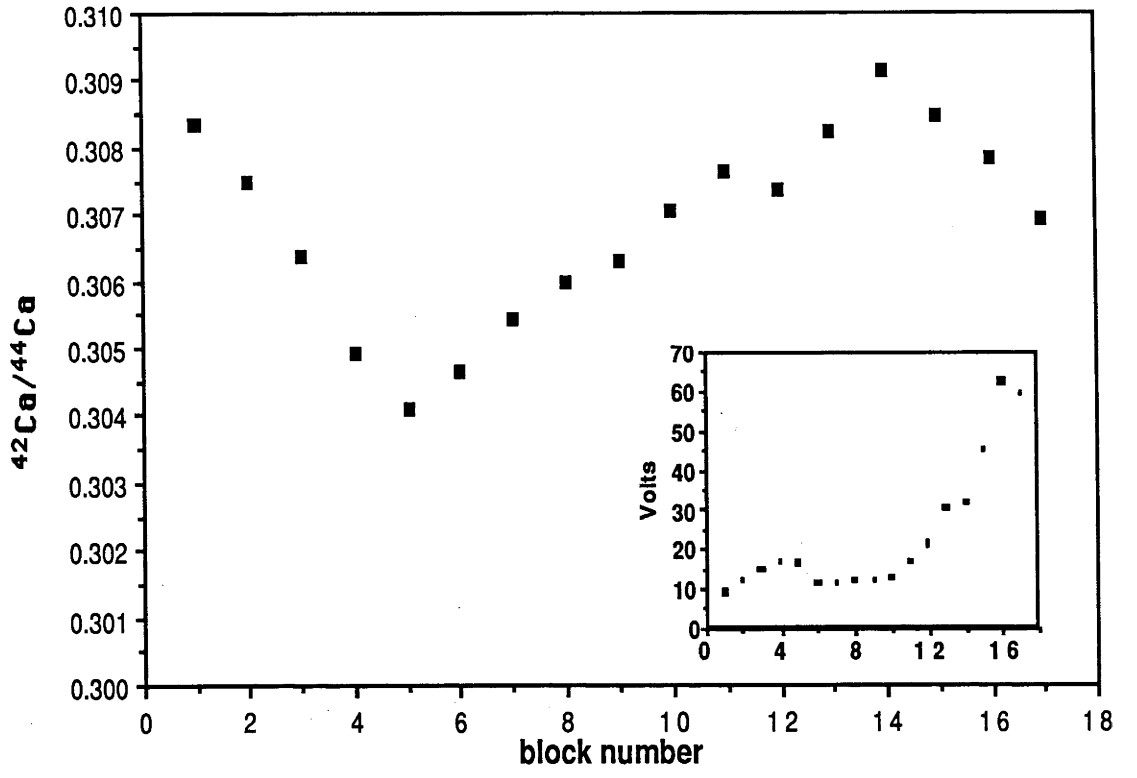

c).

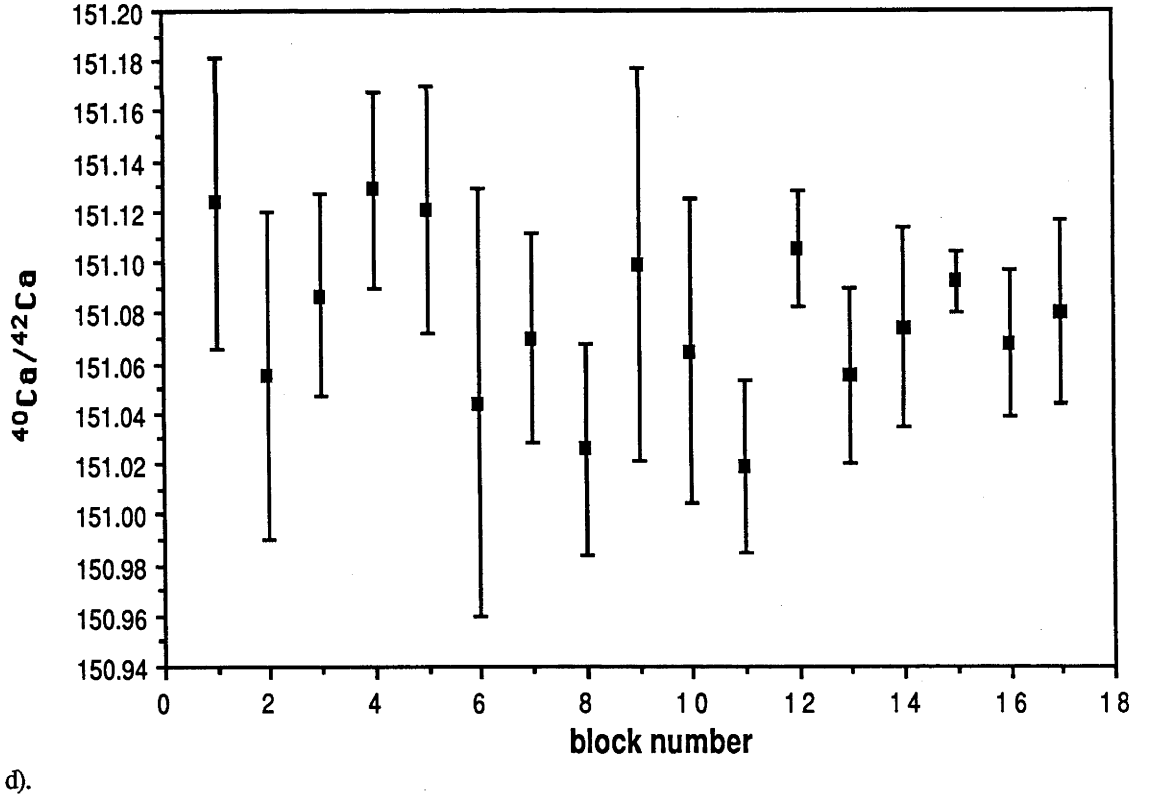

d).

Fig. A1.6 c). Variation in the raw $^{42}Ca/^{44}Ca$ ratio measured during run 2 of the Tridacna standard. Each point represents the mean value, excluding 2σ outliers, of 10 scans. d). Fractionation-corrected $^{40}Ca/^{42}Ca$ for each block of 10 scans (with 1σ error-bars).

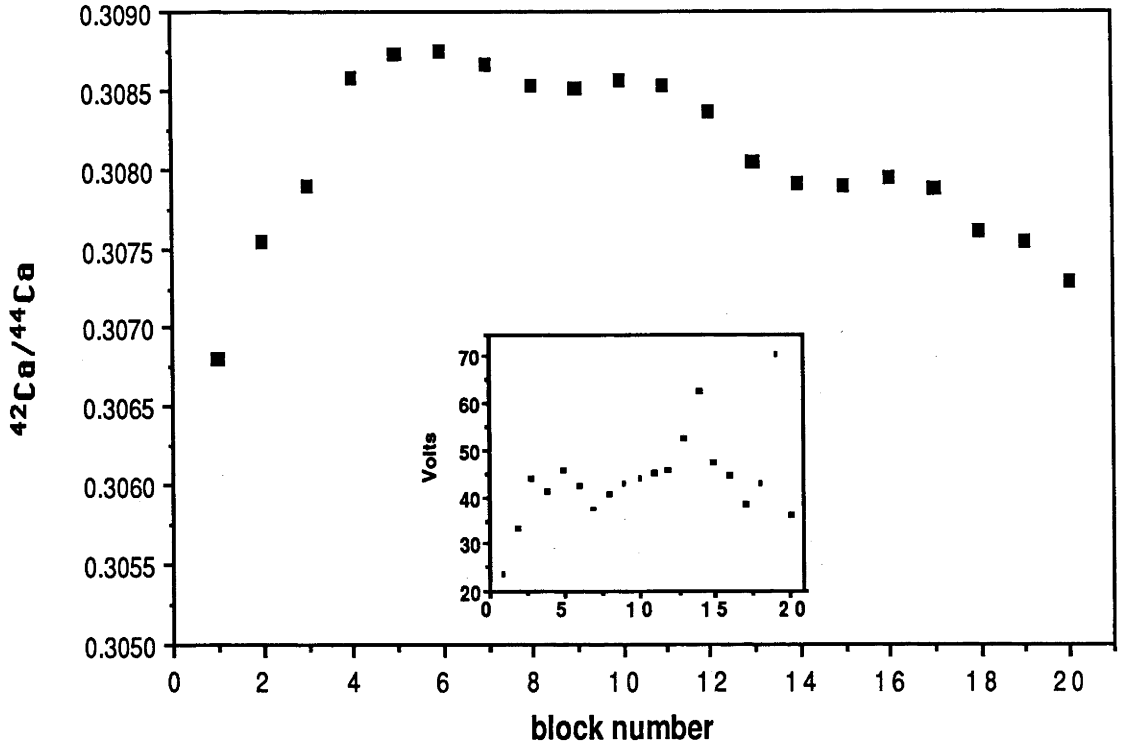

e).

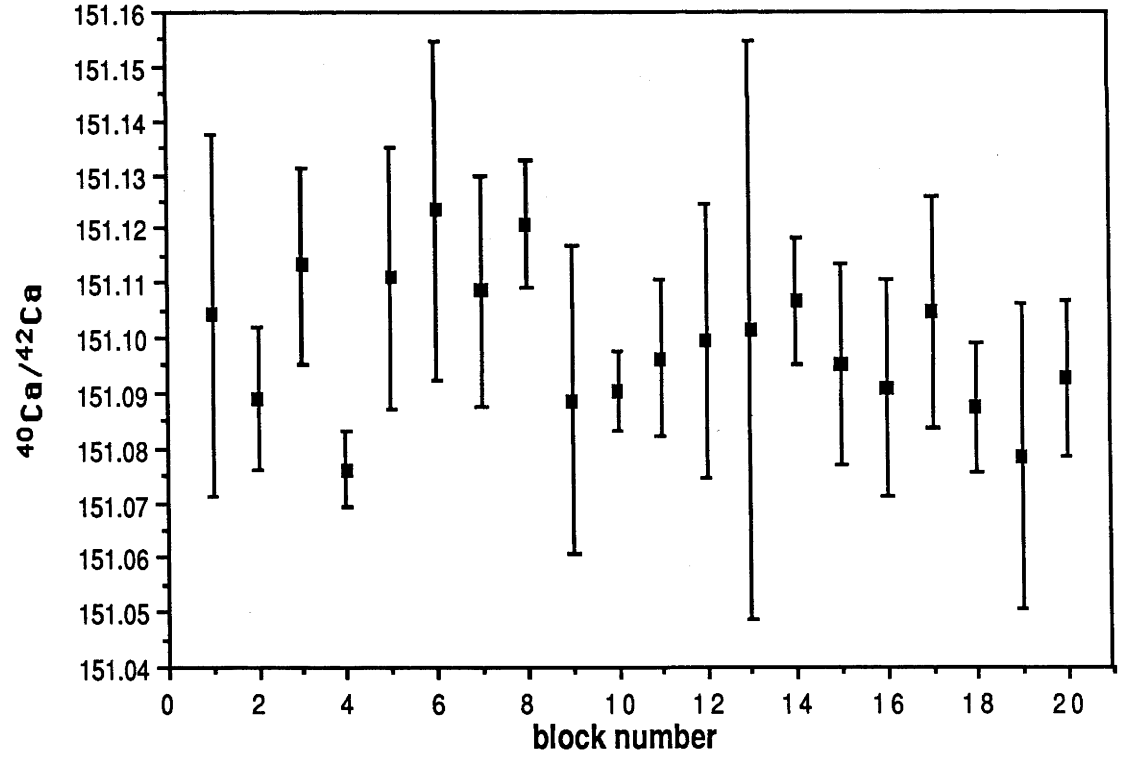

f).

Fig. A1.6 e). Variation in the raw $^{42}Ca/^{44}Ca$ ratio measured during run 3 of the Tridacna standard. Each point represents the mean value, excluding 2σ outliers, of 10 scans. f). Fractionation-corrected $^{40}Ca/^{42}Ca$ for each block of 10 scans (with 1σ error-bars).

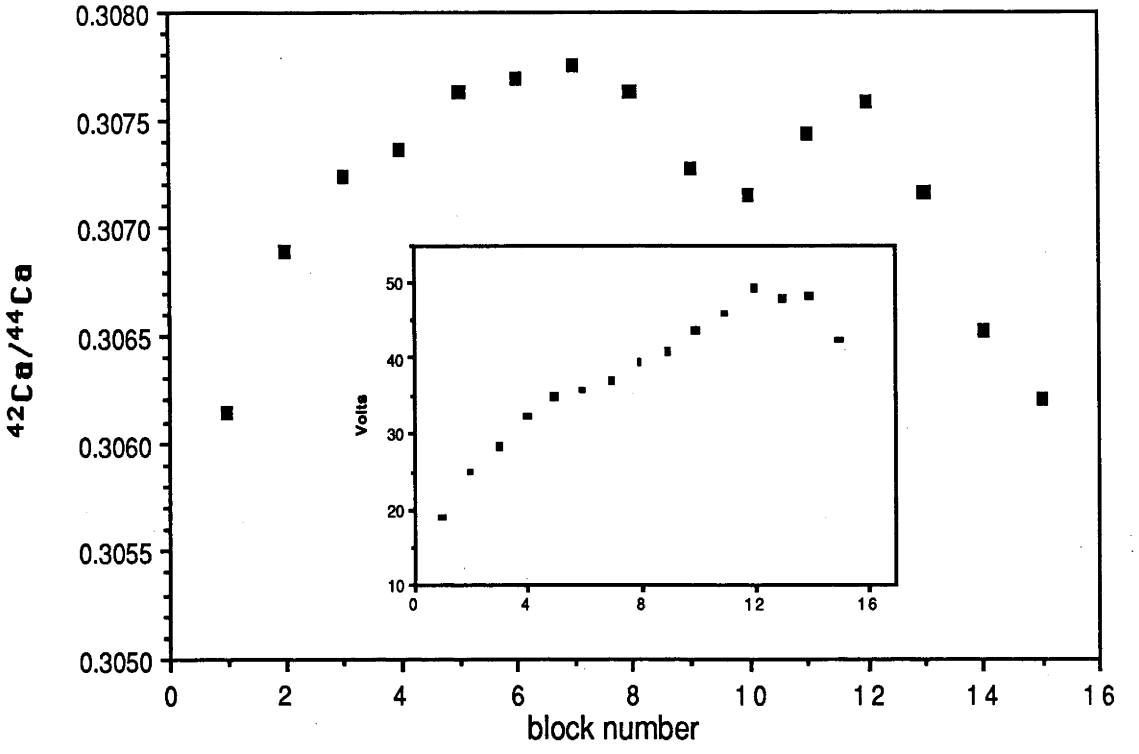

g).

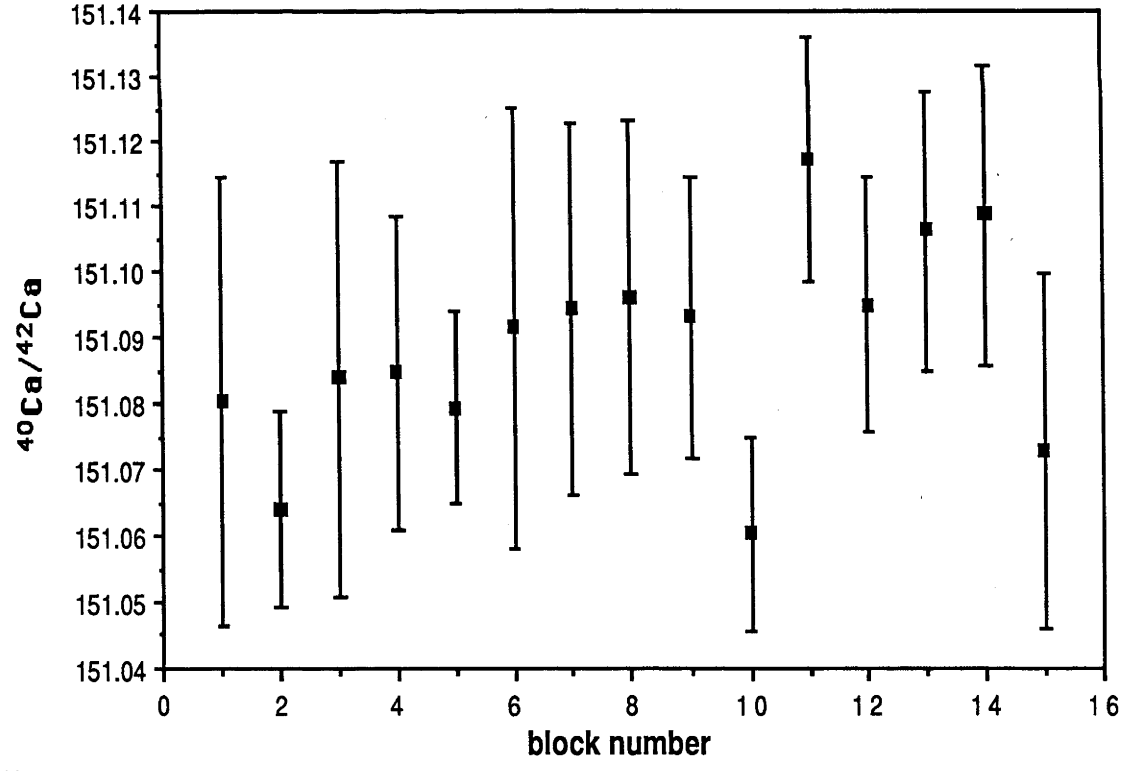

h).

Fig. A1.6 g). Variation in the raw $^{42}Ca/^{44}Ca$ ratio measured during run 4 of the Tridacna standard. Each point represents the mean value, excluding 2σ outliers, of 10 scans. h). Fractionation-corrected $^{40}Ca/^{42}Ca$ for each block of 10 scans (with 1σ error-bars).

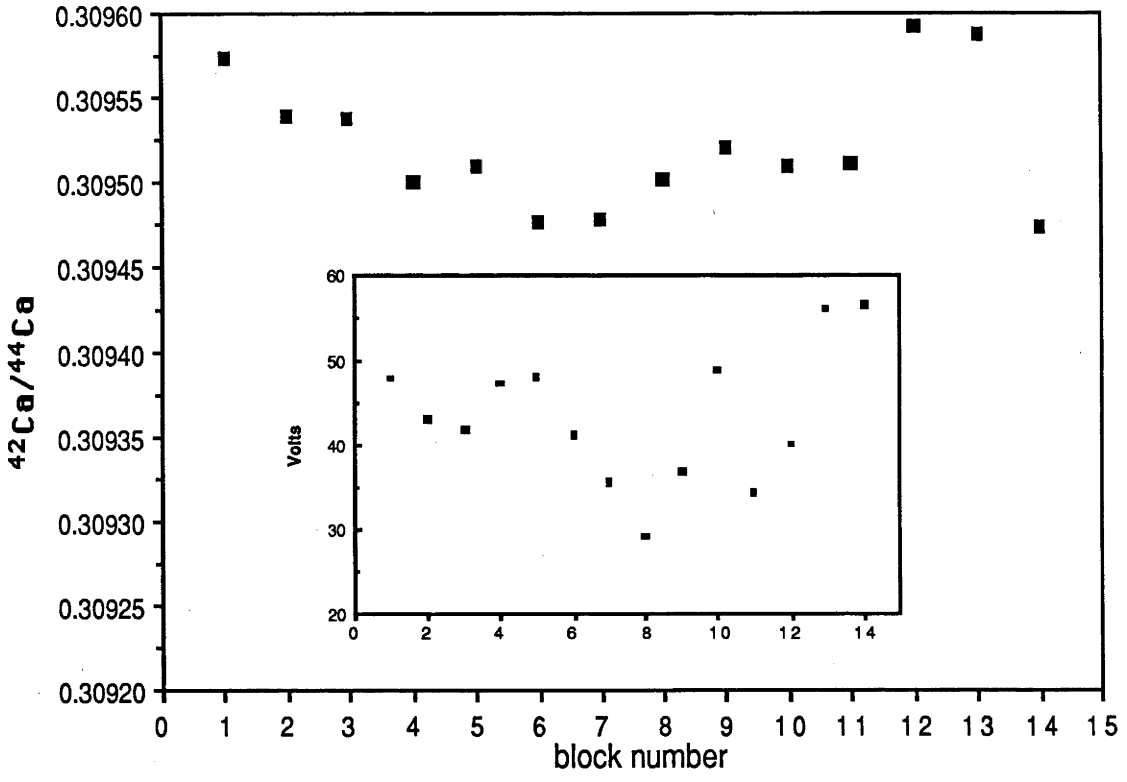

i).

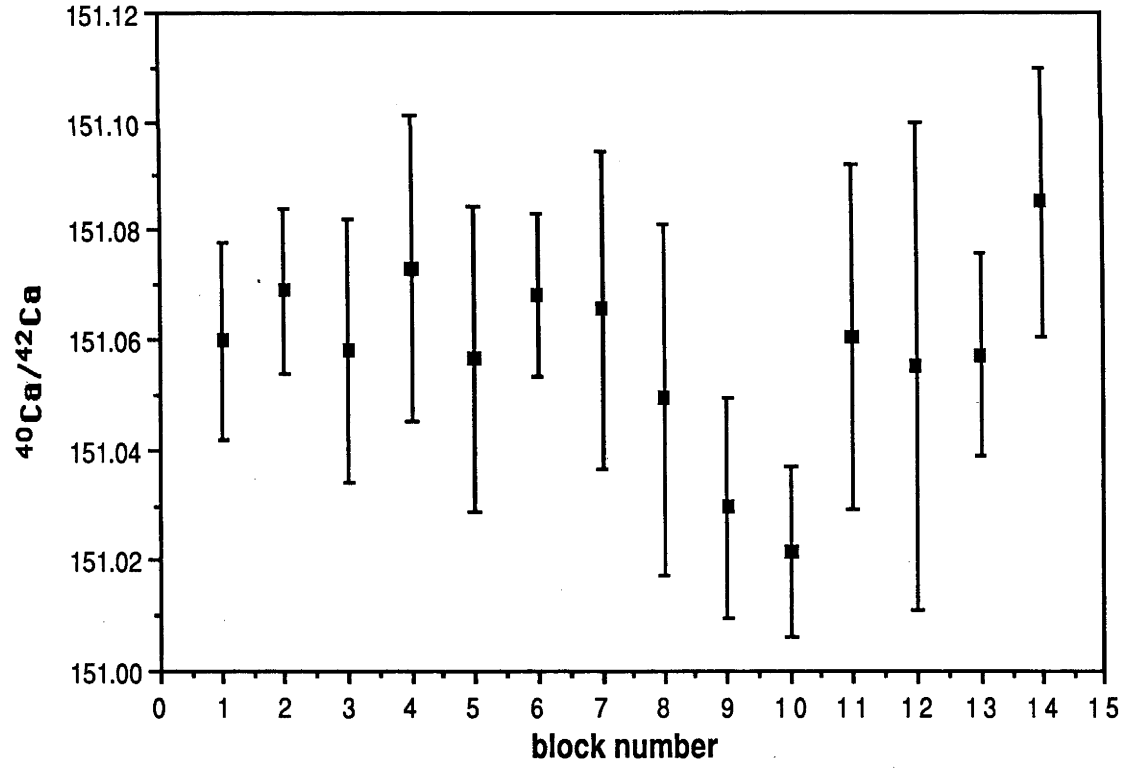

j).

Fig. A1.4 i). Variation in the raw $^{42}Ca/^{44}Ca$ ratio measured during run 5 of the Tridacna standard. Each point represents the mean value, excluding 2σ outliers, of 10 scans. j). Fractionation-corrected $^{40}Ca/^{42}Ca$ for each block of 10 scans (with 1σ error-bars).

1. Error in the fractionation correction caused by variability in the rate of change of mass fractionation. This error arises because the $^{42}Ca/^{44}Ca$ ratio is not measured simultaneously with the $^{40}Ca/^{44}Ca$ to which the correction is applied. There is an 8 second delay between measurement of these ratios during each scan.

2. Non-linearity in the current measurement systems.

3. Drift (especially long-term drift, occurring over a period of months) in the cup calibration electronics.

The external precision error estimate based on the Tridacna standard results uses analyses obtained over the entire 5 month period of this study and therefore provides a reliable estimate of the precision level applicable for comparison of all Ca analyses given here. However, duplicate analyses obtained for groups of data collected over shorter periods of a few days indicate an external precision which is substantially better than that which is applicable to the entire $^{40}Ca/^{42}Ca$ data pool.

APPENDIX 2. Computer Programs

A2.1 Three-stage Pb evolution program

Given a zero-age Pb isotopic composition, the following Pascal program defines its locus of evolution with time, assuming an U/Pb evolution involving 3 stages. Although this version of the program prints out values for μ_2 and μ_3 for different values of t_1 and t_2, the times at which the U/Pb fractionation occurs, the program can be readily modified to output a graph of μ_2 and μ_3 values for various values of t_1 and t_2 (see Fig. 3.7). The first evolution stage (i.e. during which the Pb evolves within the Earth's mantle) can be modelled using either a constant μ or the Cumming and Richards (1975) best-fit model based on the ore Pb (orogene) growth curve.

```
program three_stage_modelling;
 const
  lamda1 = 1.55125E-10;
  lamda2 = 9.8485E-10;
  Pb64initial = 9.307;
  Pb74initial = 10.294;
  U0 = 10.751;
  econst = 0.05E-9;
 var
  printer : text;
  answer : integer;
  A, B, C, D, T, T164, T174, U1, U2, U3, U264 : longreal;
  T264, T274, T364, T374, Meas64, Meas74 : longreal;
  time1, time2, decrement1, decrement2 : longreal;
begin
 decrement2 := -0.2;
 T := 4.57E+9;
 time1 := 4.5;
 rewrite(printer, 'printer:');
 write('single stage (0) or Cumming and Richards (1) growth curve?:');
 readln(answer);
 write('Enter Pb composition to be modelled (206/204,207/204):');
 readln(Meas64, Meas74);
 write('enter decrement steps (byrs):');
 readln(decrement1);
 repeat
  time1 := time1 - decrement1;
  if answer = 0 then
   begin
    if (U1 <= 0) or (U1 > 100) then
    begin
    write('enter 235U/204Pb:');
    readln(U1);
    end;
    T164 := Pb64initial + U1 * (exp(lamda1 * T) - exp(lamda1 * time1 * 1E+9));
    T174 := Pb74initial + (U1 / 137.88) * (exp(lamda2 * T) - exp(lamda2 * time1 * 1E+9));
   end;
  if answer = 1 then
   begin
    T := 4.509E+9;
    U1 := U0 * (1 - econst * time1 * 10E-9);
    T164 := Pb64initial + U0 * (exp(lamda1 * T) * (1 - econst * (T - (1 / lamda1))) - exp(lamda1 * time1
* 1E+9) * (1 - econst * (time1 * 1E+9 - (1 / lamda1))));
    T174 := Pb74initial + (U0 / 137.88) * (exp(lamda2 * T) * (1 - econst * (T - (1 / lamda1))) -
```

```
exp(lamda1 * time1 * 1E+9) * (1 - econst * (time1 * 1E+9 - (1 / lamda2))));
  end;
 time2 := time1;
 repeat
  time2 := time2 + decrement2;
  A := (exp(lamda1 * time2 * 1E+9) - 1) / (exp(lamda1 * time1 * 1E+9) - exp(lamda1 * time2 * 1E+9));
  B := (Meas64 - T164) / (exp(lamda1 * time1 * 1E+9) - exp(lamda1 * time2 * 1E+9));
  C := (exp(lamda2 * time2 * 1E+9) - 1) / (exp(lamda2 * time1 * 1E+9) - exp(lamda2 * time2 * 1E+9));
  D := 137.88 * (Meas74 - T174) / (exp(lamda2 * time1 * 1E+9) - exp(lamda2 * time2 * 1E+9));
  U3 := (D - B) / (C - A);
  U264 := (Meas64 - T164 - U3 * (exp(lamda1 * time2 * 1E+9) - 1)) / (exp(lamda1 * time1 * 1E+9) -
exp(lamda1 * time2 * 1E+9));
  T264 := T164 + U264 * (exp(lamda1 * time1 * 1E+9) - exp(lamda1 * time2 * 1E+9));
  T274 := T174 + (U264 / 137.88) * (exp(lamda2 * time1 * 1E+9) - exp(lamda2 * time2 * 1E+9));
  T364 := T264 + U3 * (exp(lamda1 * time2 * 1E+9) - 1);
  T374 := T274 + (U3 / 137.88) * (exp(lamda2 * time2 * 1E+9) - 1);
  writeln(printer, time1 : 8 : 2, U1 : 8 : 3, T164 : 8 : 3, T174 : 8 : 3, time2 : 8 : 2, U264 : 8 : 3, T264 :
8 : 3, T274 : 8 : 3, U3 : 8 : 3, T364 : 8 : 3, T374 : 8 : 3);
 until time2 + decrement2 <= 0;
until time1 <= 0;
end.
```

A2.2 Analysis of initial Sr and Nd isotopic composition variation

Because of the similar geochemical behavior of Sr and Nd, variation in $^{87}Sr/^{86}Sr$ and $^{143}Nd/^{144}Nd$ is often strongly correlated. The following Pascal program examines Rb-Sr and Sm-Nd data for possible correlated variation in the initial Sr and Nd isotopic compositions. The measured Sr and Nd isotopic compositions are corrected for radiogenic decay of the radioactive parent for various ages. The age-corrected Sr-Nd array is examined, as a function of time, for fit to a line or point using an unweighted mean square of deviates and for linearity using the correlation co-efficient (see Chapter 4 for application). Although it is advisable to give all points equal weighting, the program will allow points to be weighted in inverse proportionality to the square of their assigned error if required.

```
program Sr_Nd_Regression (input, output);
 const
  max = 30;
  LamdaSr = 1.420e-11;
  LamdaNd = 6.54e-12;
 type
  index = 1..max;
  arraytype = array[index] of real;
 var
  printer : text;
  subscript, subscript2, n, coun : integer;
  Age, Agestep, oldest, youngest : integer;
  SM1, SM2, SM3, SM4, D, cprop, Slope, SUMS, tot, Yintercept, MSWD : longreal;
  sumX, sumY, sumofcrossproduct, r, sumsqX, sumsqY : longreal;
  Xvalue, Yvalue, Yerror, W, RbSr, SrSr, SmNd, NdNd : arraytype;
  answer : char;
begin
 rewrite(printer, 'printer:');
 writeln('Enter range of ages (in myrs) of interest');
 write('oldest?: ');
 readln(oldest);
 write('youngest?: ');
 readln(youngest);
 writeln(' ');
 write('Enter the age decrement step sizes (in myrs) :  ');
 writeln(' ');
 readln(Agestep);
 Age := oldest + Agestep;
 writeln('Now enter the data (terminate data entry with zeros) :  ');
 writeln;
 subscript := 0;
 repeat
  subscript := subscript + 1;
  write(subscript : 2, ' 87Rb/86Sr,87Sr/86Sr,147Sm/144Nd, 143Nd/144Nd, error:  ');
  readln(RbSr[subscript], SrSr[subscript], SmNd[subscript], NdNd[subscript],Yerror[subscript]);
 until (RbSr[subscript] = 0) and (SrSr[subscript] = 0);
 writeln('  Age     Slope     Intercept      MSWD    Corr Co-eff');
 repeat
  Age := Age - Agestep;
 writeln(printer, 'corrected for ', Age : 4, 'myrs ');
  subscript2 := 0;
  repeat
   subscript2 := subscript2 + 1;
   Xvalue[subscript2] := NdNd[subscript2] - SmNd[subscript2] * (exp(Age * 1e+6 * LamdaNd) - 1);
   Yvalue[subscript2] := SrSr[subscript2] - RbSr[subscript2] * (exp(Age * 1e+6 * LamdaSr) - 1);
  until subscript2 = subscript - 1;
```

```
cprop := 0;
tot := 0;
SM1 := 0;
SM2 := 0;
SM3 := 0;
SM4 := 0;
D := 0;
Slope := 0;
SUMS := 0;
MSWD := 0;
Yintercept := 0;
SumX := 0;
SumY := 0;
SumsqX := 0;
SumsqY := 0;
Sumofcrossproduct := 0;
r := 0;
for n := 1 to subscript - 1 do
 tot := tot + 1 / (Yerror[n] * Yerror[n]);
cprop := 1 / tot;
for n := 1 to subscript - 1 do
 W[n] := cprop / (Yerror[n] * Yerror[n]);
writeln(printer, '      X value      Y value  Y error    Weighting   147Sm/144Nd  87Rb/86Sr');
for n := 1 to subscript - 1 do
 begin
  SM1 := SM1 + W[n] * Xvalue[n] * Xvalue[n];
  SM2 := SM2 + W[n] * Xvalue[n];
  SM3 := SM3 + W[n] * Xvalue[n] * Yvalue[n];
  SM4 := SM4 + W[n] * Yvalue[n];
  writeln(printer, n : 5, ' ', Xvalue[n] : 10 : 5, ' ', Yvalue[n] : 8 : 5, ' ', Yerror[n] : 8 : 5, '  ', W[n] :
10 : 4, '  ', SmNd[n] : 10 : 5, ' ', RbSr[n] : 10 : 5);
  sumX := sumX + Xvalue[n];
  sumY := sumY + Yvalue[n];
  sumsqX := sumsqX + sqr(Xvalue[n]);
  sumsqY := sumsqY + sqr(Yvalue[n]);
  sumofcrossproduct := sumofcrossproduct + Xvalue[n] * Yvalue[n];
 end;
r := (sumofcrossproduct - (sumX * sumY / (subscript - 1))) / sqrt(((sumsqX - (sqr(sumX) / (subscript -
1)))) * (sumsqY - (sqr(sumY) / (subscript - 1))));
D := SM1 - SM2 * SM2;
Slope := (SM3 - SM2 * SM4) / D;
Yintercept := (SM1 * SM4 - SM2 * SM3) / D;
for n := 1 to subscript - 1 do
 SUMS := SUMS + (Yvalue[n] - (Yintercept + Slope * Xvalue[n])) * (Yvalue[n] - (Yintercept + Slope
* Xvalue[n])) / (Yerror[n] * Yerror[n]);
MSWD := SUMS / ((subscript - 1) - 2);
writeln('  ', Age : 4, ' ', Slope : 10 : 6, ' ', Yintercept : 10 : 6, ' ', MSWD : 12 : 6, ' ', r : 10 : 6);
writeln(printer, 'Slope of line is ', Slope : 10 : 6);
writeln(printer, 'Y intercept of line is ', Yintercept : 10 : 6);
writeln(printer, 'MSWD is ', MSWD : 10 : 6);
writeln(printer, 'Correlation co-efficient of line is ', r : 10 : 6);
writeln(printer, ' ');
until Age < youngest;
end.
```

A2.3 Analysis of geological scatter about a Pb-Pb isochron regression line

The following Pascal program examines Pb-Pb regression data for possible variation in the initial isotopic composition. The measured Pb isotopic compositions are corrected for radiogenic decay of uranium for various ages. The age-corrected Pb-Pb array is examined, as a function of time, for fit to a line or point using an unweighted mean square of deviates and for linearity using the correlation co-efficient. (Although it is advisable to give all points equal weighting, the program will allow points to be weighted in inverse proportionality to the square of their assigned error if necessary.) The slope of this secondary array may, in certain circumstances, indicate the age of an earlier event.

```
program Pb-Pb_Regression (input, output);
 const
  max = 30;
  Lamda238 = 0.155125e-9;
  Lamda235 = 0.98485e-9;
 type
  index = 1..max;
  arraytype = array[index] of real;
 var
  printer : text;
  subscript, subscript2, n, coun : integer;
  Age, Agestep, oldest, youngest : integer;
  SM1, SM2, SM3, SM4, D, cprop, Slope, SUMS, tot, Yintercept, MSWD : longreal;
  sumX, sumY, sumofcrossproduct, r, sumsqX, sumsqY : longreal;
  Xvalue, Yvalue, Yerror, W, UPb, Pb74, Pb64 : arraytype;
  answer : char;
begin
 rewrite(printer, 'printer:');
 writeln('Enter range of ages (in myrs) of interest');
 write('oldest?: ');
 readln(oldest);
 write('youngest?: ');
 readln(youngest);
 writeln(' ');
 write('Enter the age decrement step sizes (in myrs) :  ');
 writeln(' ');
 readln(Agestep);
 Age := oldest + Agestep;
 writeln('Now enter the data (terminate data entry with zeros) :  ');
 writeln;
 subscript := 0;
 repeat
  subscript := subscript + 1;
  write(subscript : 2, ' 206Pb/204Pb, 207Pb/204Pb, 238U/204Pb, error:  ');
  readln(Pb64[subscript], Pb74[subscript], UPb[subscript],Yerror[subscript]);
 until (UPb[subscript] = 0) and (Pb74[subscript] = 0);
 writeln('  Age     Slope     Intercept      MSWD    Corr Co-eff');
 repeat
  Age := Age - Agestep;
  writeln(printer, 'corrected for ', Age : 4, 'myrs ');
  subscript2 := 0;
  repeat
   subscript2 := subscript2 + 1;
   Xvalue[subscript2] := Pb64[subscript2] - UPb[subscript2] * (exp(Age * 1e+6 * Lamda238) - 1);
   Yvalue[subscript2] := Pb74[subscript2] - (UPb[subscript2] / 137.88) * (exp(Age * 1e+6 * Lamda235) -
1);
  until subscript2 = subscript - 1;
```

```
 cprop := 0;
 tot := 0;
 SM1 := 0;
 SM2 := 0;
 SM3 := 0;
 SM4 := 0;
 D := 0;
 Slope := 0;
 SUMS := 0;
 MSWD := 0;
 Yintercept := 0;
 SumX := 0;
 SumY := 0;
 SumsqX := 0;
 SumsqY := 0;
 Sumofcrossproduct := 0;
 r := 0;
 for n := 1 to subscript - 1 do
  tot := tot + 1 / (Yerror[n] * Yerror[n]);
 cprop := 1 / tot;
 for n := 1 to subscript - 1 do
  W[n] := cprop / (Yerror[n] * Yerror[n]);
 writeln(printer, '      X value      Y value  Y error    Weighting   238U/204Pb');
 for n := 1 to subscript - 1 do
  begin
   SM1 := SM1 + W[n] * Xvalue[n] * Xvalue[n];
   SM2 := SM2 + W[n] * Xvalue[n];
   SM3 := SM3 + W[n] * Xvalue[n] * Yvalue[n];
   SM4 := SM4 + W[n] * Yvalue[n];
 writeln(printer, n : 5, '  ', Xvalue[n] : 10 : 5, '  ', Yvalue[n] : 8 : 5, '  ', Yerror[n] : 8 : 5, '   ', W[n] : 10 :
4, '   ', UPb[n] : 10 : 5);
   sumX := sumX + Xvalue[n];
   sumY := sumY + Yvalue[n];
   sumsqX := sumsqX + sqr(Xvalue[n]);
   sumsqY := sumsqY + sqr(Yvalue[n]);
   sumofcrossproduct := sumofcrossproduct + Xvalue[n] * Yvalue[n];
  end;
 r := (sumofcrossproduct - (sumX * sumY / (subscript - 1))) / sqrt(((sumsqX - (sqr(sumX) / (subscript -
1)))) * (sumsqY - (sqr(sumY) / (subscript - 1))));
 D := SM1 - SM2 * SM2;
 Slope := (SM3 - SM2 * SM4) / D;
 Yintercept := (SM1 * SM4 - SM2 * SM3) / D;
 for n := 1 to subscript - 1 do
  SUMS := SUMS + (Yvalue[n] - (Yintercept + Slope * Xvalue[n])) * (Yvalue[n] - (Yintercept + Slope
* Xvalue[n])) / (Yerror[n] * Yerror[n]);
 MSWD := SUMS / ((subscript - 1) - 2);
 writeln('  ', Age : 4, '  ', Slope : 10 : 6, '  ', Yintercept : 10 : 6, '  ', MSWD : 12 : 6, '  ', r : 10 : 6);
 writeln(printer, 'Slope of line is ', Slope : 10 : 6);
 writeln(printer, 'Y intercept of line is ', Yintercept : 10 : 6);
 writeln(printer, 'MSWD is ', MSWD : 10 : 6);
 writeln(printer, 'Correlation co-efficient of line is ', r : 10 : 6);
 writeln(printer, ' ');
 until Age < youngest;
end.
```

A2.4 Partial melting and rare-earth element enrichment modelling program

The following Pascal program examines the effects on the La/Yb ratio resulting from varying degrees of modal, non-modal and fractional partial melting of sources with various modal mineralogies.

```
program melting;
 const
  maxphases = 20;
 var
  Kd, M, F : array[1..maxphases] of real;
  printer : text;
  count, count2, phases, num1, num2 : integer;
  ML, Me, C, C1, C2, C3, BULKD, D, P, start, finish, step, sum : longreal;
  answer : char;
begin
 rewrite(printer, 'printer:');
 repeat
  count := 0;
  writeln('Enter % range of melting of interest:-');
  write('start at? ');
  readln(start);
  write('finish at?');
  readln(finish);
  write('increments?');
  readln(step);
  writeln;
  start := start / 100;
  finish := finish / 100;
  step := step / 100;
  write('Enter number of source mineral phases :');
  readln(phases);
  sum := 0;
  repeat
   count := count + 1;
   write('Enter modal proportion (in %) of source phase', count : 2, ' : ');
   readln(M[count]);
   sum := sum + M[count];
   M[count] := M[count] / 100;
  until count = phases;
  if sum <> 100 then
   writeln('***** WARNING- sum <>100% *****');
  count := 0;
  writeln;
  repeat
   count := count + 1;
   write('Enter distribution co-efficient of source phase', count : 2, ': ');
   readln(Kd[count]);
  until count = phases;
  writeln;
  writeln('For non-modal melting, enter % fraction of liquid contributed to melt from phase:-');
  writeln;
  count := 0;
  sum := 0;
  repeat
   count := count + 1;
   write('Enter mass fraction (%) of phase', count : 2, ' in melt: ');
   readln(F[count]);
   sum := sum + F[count];
   F[count] := F[count] / 100;
  until count = phases;
```

```
 if sum <> 100 then
 writeln('***** WARNING- sum <>100% *****');
 writeln(printer);
 writeln(printer, '      ', phases : 2, ' phases, ');
 for count := 1 to phases do
  writeln(printer, '    Phase ', count : 2, ' modal prop ', M[count] * 100 : 5 : 3, '%, Kd ', Kd[count] : 5 :
3, ', melt contrib ', F[count] * 100 : 5 : 3, ' % ');
 writeln(printer);
 writeln(printer, '              modal      non-modal      non- modal ');
 writeln(printer, ' %melting    equilibrium   equilibrium              Nernst');
 writeln(printer, '              batch              fractional   BULK Dist (l/t).');
 ML := start - step;
 repeat
  ML := ML + step;
  BULKD := 0;
  P := 0;
  C := 0;
  D := 0;
  for count := 1 to phases do
   begin
   D := D + M[count] * Kd[count];
   P := P + F[count] * Kd[count];
   end;
  C1 := 1 / (ML + D * (1 - ML));
  C2 := 1 / (D + ML * (1 - P));
  C3 := (1 / ML) * (1 - exp(ln(1 - (ML * P) / D) / P));
 writeln(printer, ' ', ML * 100 : 5 : 3, '      ', C1 : 8 : 4, '      ', C2 : 8 : 4, '      ', C3 : 8 : 4, '
', D : 6 : 4);
 until ML > finish;
 write('continue? (y/n) :');
 readln(answer);
until answer <> 'y';
end.
```

A2.5 Ca fractionation-corrected spike unmixing program

The following Pascal program calculates calcium concentrations determined by the isotope dilution technique. The program corrects for mass fractionation by an iteration procedure, where this is possible. A ^{43}Ca-enriched Ca spike has been used during this study to determine the Ca analytical processing blank.

```
program CaSpike;
 label
  98, 999;
 const
  R4244SP = 0.163053;
  R4344SP = 11.48963;
  CONCSP = 0.0002358145;
  R4244SA = 0.31221;
  R4344SA = 0.06486;
  R4844SA = 0.088727;
  R4644SA = 0.001518;
  R4044SA = 47.153;
 var
  printer : text;
  iloop : integer;
  R4243SP, R4442SP, R4342SP : longreal;
  R44421, R43421, R42431, R42441, R43441 : longreal;
  R4442SA, R4243SA, R4342SA, R4443SA : longreal;
  R4442M, R4244M, R4342M, R4243M, R4344M : longreal;
  R4442, R4244, R4342, R4243, R4344 : longreal;
  D, DISC, WTSP, WTSA, CACONC, CACONCPPM : longreal;
  CA40, CA42, CA43, CA44, CA46, CA48 : longreal;
begin
 rewrite(printer, 'printer:');
 writeln(printer, ' ');
 writeln('enter measured 42/44 and 43/44 ratios;');
 readln(R4244M, R4344M);
 R4442M := 1 / R4244M;
 R44421 := R4442M;
 R43421 := R4344M / R4244M;
 R42431 := R4244M / R4344M;
 R43441 := R4344M;
 R42441 := R4244M;
 R4243M := R4244M / R4344M;
 R4342M := R4344M / R4244M;
 R4442SP := 1 / R4244SP;
 R4342SP := R4344SP / R4244SP;
 R4243SP := 1 / R4342SP;
 R4442SA := 1 / R4244SA;
 R4342SA := R4344SA / R4244SA;
 R4243SA := 1 / R4342SA;
 R4443SA := 1 / R4344SA;
 writeln('enter weight of spike;');
 readln(WTSP);
 writeln('enter weight of sample;');
 readln(WTSA);
 DISC := 1;
 writeln('    44/42S      D      44/42N   43/42N     DISC ');
 for iloop := 1 to 400 do
  begin
   R4442 := R4442M - (R4442SP - R4442M) * (R4342M - R4342SA) / (R4342SP - R4342M);
   if r4442 <= 0 then
```

```
  begin
  writeln('   ***** calculated 44/42 ratio < or = 0 *****');
  writeln('    mass fractionation correction not possible');
  R4442M := R44421;
  R4344 := R43441;
  R4342M := R43421;
  R4244 := 1 / R44421;
  R4243 := R42431;
  goto 98;
  end;
 D := sqrt((1 / 0.31221) / R4442);
 R4442M := R4442M * D * D;
 R4342M := R4342M * D;
 D := D - 1;
 DISC := DISC + D;
 writeln(iloop : 3, R4442 : 10 : 5, D : 13 : 7, R4442M : 10 : 5, R4342M : 10 : 5, DISC : 13 : 8);
 if ABS(D) < 0.0000001 then
 begin
 writeln(' ');
 writeln('convergence (i.e. ABS(D)<1E-7) after ', iloop : 2, ' iterations');
 writeln(' ');
 R4344 := R4344M / DISC;
 R4243 := 1 / R4342M;
 R4244 := 1 / R4442M;
98 :
 CA44 := CONCSP * R4443SA * (WTSP / WTSA) * (R4344 - R4344SP) / (R4344SA - R4344);
 CA42 := CA44 * R4244SA;
 CA40 := CA44 * R4044SA;
 CA43 := CA44 * R4344SA;
 CA46 := CA44 * R4644SA;
 CA48 := CA44 * R4844SA;
 CACONC := CA40 + CA42 + CA43 + CA44 + CA46 + CA48;
 writeln('   ratio    spike  measured corrected   sample');
 writeln('   44/42', R4442SP : 10 : 5, R44421 : 10 : 5, R4442M : 10 : 5, R4442SA : 10 : 5);
 writeln('   43/42', R4342SP : 10 : 5, R43421 : 10 : 5, R4342M : 10 : 5, R4342SA : 10 : 5);
 writeln('   42/43', R4243SP : 10 : 5, R42431 : 10 : 5, R4243 : 10 : 5, R4243SA : 10 : 5);
 writeln('   42/44', R4244SP : 10 : 5, R42441 : 10 : 5, R4244 : 10 : 5, R4244SA : 10 : 5);
 writeln('   43/44', R4344SP : 10 : 5, R43441 : 10 : 5, R4344 : 10 : 5, R4344SA : 10 : 5);
 writeln(' ');
 writeln('43 in spike (micromoles) ', CONCSP : 10 : 8);
 writeln('weight of spike      (g)', WTSP : 10 : 5);
 writeln('weight of sample     (g)', WTSA : 10 : 5);
 writeln(' ');
 writeln('conc. (micromoles)');
 writeln('40Ca        ', Ca40 : 14 : 5);
 writeln('42Ca        ', Ca42 : 14 : 5);
 writeln('43Ca        ', Ca43 : 14 : 5);
 writeln('44Ca        ', Ca44 : 14 : 5);
 writeln('46Ca        ', Ca46 : 14 : 5);
 writeln('48Ca        ', Ca48 : 14 : 5);
 writeln('total Ca    ', CACONC : 14 : 5, ' micromoles');
 CACONCPPM := CACONC * 40.078;
 writeln('     Ca     ', CACONCPPM : 14 : 5, ' ppm');
 goto 999;
 end;
end;
if iloop = 400 then
 writeln('  ****NO CONVERGENCE after 400 iterations**** ');
999 :
writeln(' ');
end.
```

A2.6 Ca mass fractionation correction using various fractionation laws

The following Pascal program corrects raw Ca isotopic data for mass fractionation using 4 fractionation laws- the linear, exponental, power and empirical laws. The empirical law uses a calculated exponent which gives a minimum external precision error for 9 mass spectrometry runs of the Tridacna standard. The program allows Ca ratio data to be stored in arrays on disk and for these files to be updated as new data is acquired.

```
program Ca_reduction;
 const
  max = 200;
  M40 = 39.9625907;
  M42 = 41.9586218;
  M43 = 42.9587704;
  M44 = 43.9554848;
  exponent = 1.054242;
 type
  index1 = 0..max;
  arraytype1 = array[index1] of longreal;
  datafile = file of longreal;
 var
  fileddata, filedata2 : datafile;
  answer, continue, dfile, datafilename1, datafilename2, addata : string;
  printer : text;
  subscript, counter, counter1, N : integer;
  Sum4042linear, Sum4042exponental, Sum4042power, Sum4042emp, r : longreal;
  MeanR4042linear, MeanR4042exponental, MeanR4042power, MeanR4042emp, p, a : longreal;
  sumlinresidual, sumexpresidual, sumpowerresidual, sumempresidual : longreal;
  Sumsq4042linear, Sumsq4042exponental, Sumsq4042power, Sumsq4042emp : longreal;
  Sqsum4042linear, Sqsum4042exponental, Sqsum4042power, Sqsum4042emp : longreal;
  linearerror, exponentalerror, powererror, emperror : longreal;
  SEmeanlinear, SEmeanexponental, SEmeanpower, SEmeanemp : longreal;
  linresidual, expresidual, powerresidual, empresidual : longreal;
  R4244, R4042, R4042linear, R4042exponental, R4042power, R4042emp : arraytype1;
begin
 rewrite(printer, 'printer:');
 continue := 'yes';
 subscript := 0;
 while (continue = 'yes') or (continue = 'Yes') do
  begin
   write('Add new data to an existing file or create new files (Yes/No): ');
   readln(addata);
   if (addata = 'yes') or (addata = 'Yes') then
    begin
    writeln('Input data, terminating with zeros');
    repeat
    subscript := subscript + 1;
    write('Enter analysis ', subscript : 3, ' 42/44 and 40/42: ');
    readln(R4244[subscript], R4042[subscript]);
    until (R4244[subscript] = 0) and (R4042[subscript] = 0);
    subscript := subscript - 1;
    write('Add entered data to an existing data file (Yes/No) :  ');
    readln(answer);
    if (answer = 'yes') or (answer = 'Yes') then
    begin
    write('Enter name of existing datafile to add new data to:');
    readln(dfile);
    open(fileddata, dfile);
```

```
for counter := 1 to subscript do
write(fileddata, R4244[counter], R4042[counter]);
close(fileddata);
writeln('Data now written to data file ', dfile);
end;
write('Create new datafile ? (Yes/No) :');
readln(answer);
if (answer = 'yes') or (answer = 'Yes') then
begin
write('Enter name of new datafile : ');
readln(dfile);
rewrite(fileddata, dfile);
for counter := 1 to subscript do
write(fileddata, R4244[counter], R4042[counter]);
close(fileddata);
writeln('Data now written to new data file : ', dfile);
end;
end;
write('Merge two existing data files to create new file? (Yes/No) :  ');
readln(answer);
if (answer = 'yes') or (answer = 'Yes') then
begin
subscript := 0;
writeln('Enter name of datafiles to be merged:');
write('First filename? :');
readln(dfile);
open(fileddata, dfile);
while not eof(fileddata) do
begin
subscript := subscript + 1;
read(fileddata, R4244[subscript], R4042[subscript]);
end;
close(fileddata);
write('Second filename? :');
readln(dfile);
open(fileddata, dfile);
while not eof(fileddata) do
begin
subscript := subscript + 1;
read(fileddata, R4244[subscript], R4042[subscript]);
end;
close(fileddata);
write('Enter name of new datafile : ');
readln(dfile);
rewrite(fileddata, dfile);
for counter := 1 to subscript do
write(fileddata, R4244[counter], R4042[counter]);
close(fileddata);
writeln('Data now written to new data file :', dfile);
end;
write('Print data from an existing data file (Yes/No)? : ');
readln(answer);
if (answer = 'yes') or (answer = 'Yes') then
begin
write('Enter data file name: ');
readln(dfile);
reset(fileddata, dfile);
subscript := 0;
while not eof(fileddata) do
begin
subscript := subscript + 1;
```

```
 read(fileddata, R4244[subscript], R4042[subscript]);
 writeln(printer, R4244[subscript] : 10 : 5, R4042[subscript] : 10 : 5);
 end;
 close(fileddata);
 writeln('  ', subscript : 3 : 2, ' analyses read from data file ', dfile);
 end;
subscript := 0;
write('Enter name of datafile for Ca data reduction : ');
readln(datafilename1);
open(fileddata, datafilename1);
while not eof(fileddata) do
 begin
 subscript := subscript + 1;
 read(fileddata, R4244[subscript], R4042[subscript]);
 end;
close(fileddata);
writeln(' ');
writeln('  ', subscript : 2, '  analyses read from datafile ');
linresidual := 0;
expresidual := 0;
powerresidual := 0;
Sum4042linear := 0;
Sum4042exponental := 0;
Sum4042power := 0;
Sum4042emp := 0;
Sumsq4042linear := 0;
Sumsq4042exponental := 0;
Sumsq4042power := 0;
Sumsq4042emp := 0;
Sqsum4042linear := 0;
Sqsum4042exponental := 0;
Sqsum4042power := 0;
Sqsum4042emp := 0;
sumlinresidual := 0;
sumexpresidual := 0;
sumpowerresidual := 0;
sumempresidual := 0;
linearerror := 0;
exponentalerror := 0;
powererror := 0;
emperror := 0;
writeln(' ');
for counter := 1 to subscript do
 begin
 R4042linear[counter] := 0;
 R4042exponental[counter] := 0;
 R4042power[counter] := 0;
 end;
 writeln(printer, ' Analysis  (42/44)raw  (40/42)raw  (40/42)linear (40/42)exp  (40/42)power
(40/42)emp');
 for counter := 1 to subscript do
 begin
 R4042linear[counter] := R4042[counter] * (1 + (0.31221 - R4244[counter]) / R4244[counter]);
 Sum4042linear := Sum4042linear + R4042linear[counter];
 Sumsq4042linear := Sumsq4042linear + sqr(R4042linear[counter]);
 p := ln(0.31221 / R4244[counter]) / ln(M44 / M42);
 R4042exponental[counter] := R4042[counter] * exp(p * ln(M42 / M40));
 Sum4042exponental := Sum4042exponental + R4042exponental[counter];
 Sumsq4042exponental := Sumsq4042exponental + sqr(R4042exponental[counter]);
 a := exp(ln(R4244[counter] / 0.31221) / (M42 - M44)) - 1;
 R4042power[counter] := R4042[counter] / (exp(ln(1 + a) * (M40 - M42)));
```

```
    Sum4042power := Sum4042power + R4042power[counter];
    Sumsq4042power := Sumsq4042power + sqr(R4042power[counter]);
    R4042emp[counter] := R4042[counter] * exp(exponent * ln(0.31221 / R4244[counter]));
    Sum4042emp := Sum4042emp + R4042emp[counter];
    Sumsq4042emp := Sumsq4042emp + sqr(R4042emp[counter]);
    writeln(printer, '    ', counter : 3, R4244[counter] : 13 : 6, R4042[counter] : 13 : 6,
R4042linear[counter] : 13 : 6, R4042exponental[counter] : 13 : 6, R4042power[counter] : 13 : 6,
R4042emp[counter] : 13 : 6);
    end;
   MeanR4042linear := sum4042linear / subscript;
   MeanR4042exponental := Sum4042exponental / subscript;
   MeanR4042power := Sum4042power / subscript;
   MeanR4042emp := Sum4042emp / subscript;
   MeanR4042power : 13 : 6, MeanR4042emp : 13 : 6);
   writeln;
   writeln(printer, 'For ', subscript : 3, ' analyses');
   writeln;
   writeln(printer, '          linear    exponential    power    empirical');
   writeln(printer, ' Means and 1 sigma errors : ');
   writeln(printer, '      ', MeanR4042linear : 13 : 6, MeanR4042exponental : 13 : 6,
   Sqsum4042linear := sqr(Sum4042linear) / subscript;
   Sqsum4042exponental := sqr(Sum4042exponental) / subscript;
   Sqsum4042power := sqr(Sum4042power) / subscript;
   Sqsum4042emp := sqr(Sum4042emp) / subscript;
   linearerror := sqrt(abs(sumsq4042linear - sqsum4042linear));
   exponentalerror := sqrt(abs(sumsq4042exponental - sqsum4042exponental));
   powererror := sqrt(abs(sumsq4042power - sqsum4042power));
   emperror := sqrt(abs(sumsq4042emp - sqsum4042emp));
   writeln(printer, '+/-    ', linearerror : 13 : 6, exponentalerror : 13 : 6, powererror : 13 : 6, emperror : 13
: 6);
   SEmeanlinear := 2 * linearerror / (sqrt(subscript));
   SEmeanexponental := 2 * exponentalerror / (sqrt(subscript));
   SEmeanpower := 2 * powererror / (sqrt(subscript));
   SEmeanemp := 2 * emperror / (sqrt(subscript));
   writeln;
   writeln(printer, ' 2 x sigma of mean (n =', subscript : 3, ')');
   writeln(printer, '+/-    ', SEmeanlinear : 13 : 6, SEmeanexponental : 13 : 6, SEmeanpower : 13 : 6,
 SEmeanemp : 13 : 6);
   writeln(printer, ' residuals;');
   writeln(printer, '          linear    exponential    power    empirical');
   for N := 1 to subscript do
    begin
    linresidual := MeanR4042linear - R4042linear[N];
    sumlinresidual := sumlinresidual + abs(linresidual);
    expresidual := MeanR4042exponental - R4042exponental[N];
    empresidual := MeanR4042emp - R4042emp[N];
    sumexpresidual := sumexpresidual + abs(expresidual);
    powerresidual := MeanR4042power - R4042power[N];
    sumpowerresidual := sumpowerresidual + abs(powerresidual);
    sumempresidual := sumempresidual + abs(empresidual);
    writeln(printer, N : 3, '    ', linresidual : 13 : 6, expresidual : 13 : 6, powerresidual : 13 : 6,
 empresidual : 13 : 6);
    end;
   writeln;
   writeln(printer, 'Sum of residuals');
   writeln(printer, '      ', sumlinresidual : 13 : 6, sumexpresidual : 13 : 6, sumpowerresidual : 13 : 6,
 sumempresidual : 13 : 6);
   write('continue? (Yes/No):  ');
   readln(continue);
  end;
 end.
```

A2.7 Mass spectrometry external analytical precision analysis

The following Pascal program uses a two-way analysis of variance technique to compare duplicate analyses of mass spectrometry runs, in order to determine the external analytical precision. The program allows data to be stored in arrays on disk and for these data files to be updated as new data is acquired. The listing given below is of the program used to analyse duplicate Pb isotope analyses of samples analysed during the course of this thesis; a similar algorithm was used to analyse duplicate Ca isotope results.

```
program Pb_run_statistics;
 const
  max = 100;
 type
  index1 = 0..max;
  index2 = 0..2;
  arraytype1 = array[index1, index2] of longreal;
  arraytype2 = array[index2] of longreal;
  datafile = file of real;
 var
  fileddata : datafile;
  answer, continue, dfile : string;
  printer : text;
  subscript, counter1, counter2, duplicatenumber : integer;
  sum, mean, sumsq, squarsum, dupsquared, sigma, delta, experror, expsigma, sqrtexperror : arraytype2;
  sumofcrossproduct1, sumofcrossproduct2, sumofcrossproduct3 : longreal;
  r1, r2, r3 : longreal;
  sumaverage1, sumaverage2, sumaverage3 : longreal;
  sumsqaverage1, sumsqaverage2, sumsqaverage3 : longreal;
  Analysis1, Analysis2, average : arraytype1;
begin
 rewrite(printer, 'printer:');
 continue := 'yes';
 while (continue = 'yes') or (continue = 'Yes ') do
  begin
   subscript := 0;
   write('read from an existing datafile? (Yes/No):  ');
   readln(answer);
   if (answer = 'yes') or (answer = 'Yes') then
    begin
    write('Enter name of data file');
    read (dfile);
    while not eof(fileddata) do
    begin
    subscript := subscript + 1;
    read(fileddata, Analysis1[subscript, 0], Analysis1[subscript, 1], Analysis1[subscript, 2]);
    read(fileddata, Analysis2[subscript, 0], Analysis2[subscript, 1], Analysis2[subscript, 2]);
    if (Analysis2[subscript, 0] <> 0) and (Analysis2[subscript, 1] <> 0) and (Analysis2[subscript, 2] <> 0)
then
    duplicatenumber := duplicatenumber + 1;
    end;
    close(fileddata);
    writeln(Subscript : 3 : 2, ' duplicates read from datafile');
    end;
   write('Enter more new data? (Yes/No):  ');
   readln(answer);
   if (answer = 'yes') or (answer = 'Yes') then
    begin
    writeln('Input data, terminating with zeros');
    repeat
```

```
  subscript := subscript + 1;
  write('Enter 6/4, 7/4 and 8/4 of analysis', subscript : 3 : 2, ':          ');
  readln(Analysis1[subscript, 0], Analysis1[subscript, 1], Analysis1[subscript, 2]);
  write('Enter 6/4, 7/4 and 8/4 of duplicate analysis', subscript : 3 : 2, ': ');
  readln(Analysis2[subscript, 0], Analysis2[subscript, 1], Analysis2[subscript, 2]);
  if (Analysis2[subscript, 0] <> 0) and (Analysis2[subscript, 1] <> 0) and (Analysis2[subscript, 2] <> 0)
then
  duplicatenumber := duplicatenumber + 1;
  writeln(' ');
  until (Analysis1[subscript, 0] = 0) and (Analysis1[subscript, 1] = 0) and (Analysis1[subscript, 2] = 0);
  subscript := subscript - 1;
  write('store entered data (Yes/No): ');
  readln(answer);
  if (answer = 'yes') or (answer = 'Yes') then
  begin
  write('add entered data to an existing datafile (Yes/No) or create new file?: ');
  readln(answer);
  if (answer = 'yes') or (answer = 'Yes') then
  open(fileddata, 'dfile')
  else
  rewrite(fileddata, 'dfile');
  for counter2 := 1 to subscript do
  begin
  write(fileddata, Analysis1[counter2, 0], Analysis1[counter2, 1], Analysis1[counter2, 2]);
  write(fileddata, Analysis2[counter2, 0], Analysis2[counter2, 1], Analysis2[counter2, 2]);
  end;
  close(fileddata);
  writeln('data now written to datafile');
  end;
  end;
  writeln(printer, ' ');
  writeln(printer, '        ratios     206/204   207/204   208/204');
  for counter1 := 0 to 2 do
  begin
  for counter2 := 1 to subscript do
  begin
  if (Analysis2[counter2, 0] <> 0) and (Analysis2[counter2, 1] <> 0) and (Analysis2[counter2, 2] <> 0)
then
  begin
  Average[counter2, counter1] := (Analysis1[counter2, counter1] + Analysis2[counter2, counter1]) / 2;
  sum[counter1] := sum[counter1] + Analysis1[counter2, counter1] + Analysis2[counter2, counter1];
  sumsq[counter1] := sumsq[counter1] + sqr(Analysis1[counter2, counter1]) + sqr(Analysis2[counter2,
counter1]);
  dupsquared[counter1] := dupsquared[counter1] + sqr(Analysis1[counter2, counter1] +
Analysis2[counter2, counter1]) / 2;
  end
  else
  Average[counter2, counter1] := Analysis1[counter2, counter1];
  end;
  end;
  for counter2 := 1 to subscript do
  begin
  writeln(printer, counter2 : 3, '      Analysis 1', Analysis1[counter2, 0] : 10 : 3, Analysis1[counter2, 1]
: 10 : 3, Analysis1[counter2, 2] : 10 : 3);
  if (Analysis2[counter2, 0] <> 0) and (Analysis2[counter2, 1] <> 0) and (Analysis2[counter2, 2] <> 0)
then
  begin
  sumaverage1 := sumaverage1 + Average[counter2, 0];
  sumaverage2 := sumaverage2 + Average[counter2, 1];
  sumaverage3 := sumaverage3 + Average[counter2, 2];
  sumsqaverage1 := sumsqaverage1 + sqr(Average[counter2, 0]);
```

```
  sumsqaverage1 := sumsqaverage1 + sqr(Average[counter2, 0]);
  sumsqaverage2 := sumsqaverage2 + sqr(Average[counter2, 1]);
  sumsqaverage3 := sumsqaverage3 + sqr(Average[counter2, 2]);
  sumofcrossproduct1 := sumofcrossproduct1 + Average[counter2, 0] * Average[counter2, 1];
  sumofcrossproduct2 := sumofcrossproduct2 + Average[counter2, 0] * Average[counter2, 2];
  sumofcrossproduct3 := sumofcrossproduct3 + Average[counter2, 1] * Average[counter2, 2];
  writeln(printer, '        Analysis 2', Analysis2[counter2, 0] : 10 : 3, Analysis2[counter2, 1] : 10 : 3,
Analysis1[counter2, 2] : 10 : 3);
  end;
  writeln(printer, ' ');
  end;
 r1 := (sumofcrossproduct1 - (sumaverage1 * sumaverage2 / duplicatenumber)) / sqrt(((sumsqaverage1 -
(sqr(sumaverage1) / duplicatenumber))) * (sumsqaverage2 - (sqr(sumaverage2) / duplicatenumber)));
 r2 := (sumofcrossproduct2 - (sumaverage1 * sumaverage3 / duplicatenumber)) / sqrt(((sumsqaverage1 -
(sqr(sumaverage1) / duplicatenumber))) * (sumsqaverage3 - (sqr(sumaverage3) / duplicatenumber)));
 r3 := (sumofcrossproduct3 - (sumaverage2 * sumaverage3 / duplicatenumber)) / sqrt(((sumsqaverage2 -
(sqr(sumaverage2) / duplicatenumber))) * (sumsqaverage3 - (sqr(sumaverage3) / duplicatenumber)));
 writeln(printer, 'For ', duplicatenumber : 2, ' duplicated ratios: ');
 writeln(printer, ' ');
 writeln(printer, 'sum of all duplicated ratios is                    ', sum[0] : 12 : 3, sum[1] : 12 : 3,
sum[2] : 12 : 3);
 for counter1 := 0 to 2 do
  begin
  mean[counter1] := sum[counter1] / (2 * (duplicatenumber));
  squarsum[counter1] := sqr(sum[counter1]) / (2 * (duplicatenumber));
  sigma[counter1] := sqrt(abs(sumsq[counter1] - squarsum[counter1]));
  delta[counter1] := sqrt(abs(sigma[counter1] * sigma[counter1] / (duplicatenumber - 1)));
  expsigma[counter1] := sqrt(abs(sumsq[counter1] - dupsquared[counter1]));
  experror[counter1] := sqr(expsigma[counter1]) / (duplicatenumber - 1);
  sqrtexperror[counter1] := sqrt(experror[counter1]);
  end;
 writeln(printer, 'mean of all duplicated ratios is                  ', mean[0] : 12 : 4, mean[1] : 12 : 4,
mean[2] : 12 : 4);
 writeln(printer, 'sum of squares of all duplicated ratios is        ', sumsq[0] : 12 : 4, sumsq[1] : 12 :
4, sumsq[2] : 12 : 4);
 writeln(printer, 'sum of (duplicates squared)/2 is                  ', dupsquared[0] : 12 : 4,
dupsquared[1] : 12 : 4, dupsquared[2] : 12 : 4);
 writeln(printer, 'sum of duplicates squared/number of ratios is     ', squarsum[0] : 12 : 4,
squarsum[1] : 12 : 4, squarsum[2] : 12 : 4);
 writeln(printer, 'geological error- sigma of all duplicated ratios is  ', sigma[0] : 12 : 4, sigma[1] : 12
: 4, sigma[2] : 12 : 4);
 writeln(printer, 'sigma squared/', (duplicatenumber - 1) : 2, ' degrees of freedom is          ',
delta[0] : 12 : 4, delta[1] : 12 : 4, delta[2] : 12 : 4);
 writeln(printer, 'experimental error- sigma of duplicated dataset is   ', expsigma[0] : 12 : 4,
expsigma[1] : 12 : 4, expsigma[2] : 12 : 4);
 writeln(printer, 'sigma squared/', (duplicatenumber - 1) : 2, ' degrees of freedom is          ',
experror[0] : 12 : 7, experror[1] : 12 : 7, experror[2] : 12 : 7);
 writeln(printer, 'one sigma experimental error is                   ', sqrtexperror[0] : 12 : 4,
sqrtexperror[1] : 12 : 4, sqrtexperror[2] : 12 : 4);
 writeln(printer, 'Correlation coefficient between (averaged duplicates of) 6/4 and 7/4 is ', r1 : 10 : 7);
 writeln(printer, 'Correlation coefficient between (averaged duplicates of) 6/4 and 8/4 is ', r2 : 10 : 7);
 writeln(printer, 'Correlation coefficient between (averaged duplicates of) 7/4 and 8/4 is ', r3 : 10 : 7);
 write('continue? (Yes/No): ');
 readln(continue);
end;
```

APPENDIX 3. Sample identification

thesis designation	A.N.U. designation	locality	rock-type	references
New South Wales, Australia				
GA-3470	GA-3470	Begargo Hill	leucitite	Cundari (1973),
GA-3471	GA-3471	Begargo Hill	"	Nelson *et al.* (1986a)
GA-3472	GA-3472	Bygalore	"	
GA-3473	GA-3473	Bygalore	"	
GA-3474	GA-3474	Gorman Hills	"	
GA-3475	GA-3475	Tullibigeal	"	
GA-3476	GA-3476	Condobolin	"	
GA-3478	GA-3478	L. Cargellico	"	
GA-3479	GA-3479	El Capitan	"	
GA-3480	GA-3480	Burgooney	"	
GA-3481	GA-3481	Flagstaff	"	
70-139	70-139	Harden	analcimite	
Victoria, Australia				
E7980	87-231	Cosgrove	leucitite	Birch (1978),
				Nelson *et al.* (1986a)
Queensland, Australia				
HH-321	87-232	Inglewood	analcimite	Wilkinson (1977),
				Nelson *et al.* (1986a)
Kimberley region, Western Australia				
WAK-2L	87-245	Mt North	leucite lamproite	McCulloch *et al.* (1983),
WAK-6L	87-246	Oscar Plug	"	Jaques *et al.* (1984a, 1986a),
WAK-10L	87-247	Mt Percy	"	Nelson *et al.* (1986a)
WAK-11L	87-248	Noonkanbah	leucite lamproite	
WAK-14L	87-249	Fishery Hill	leucite lamproite	
WAK-25L	87-250	Walgidee Hill	"	
WAK-30L	87-251	"	"	
WAK-15K	87-252	Ellendale	olivine lamproite	
WAK-16K	87-253	"	"	
WAK-17L	87-254	"	leucite lamproite	
WAK-20K	87-255	"	olivine lamproite	
WAK-21K	87-256	"	"	
WAK-27L	87-257	"	leucite lamproite	
Mordor Complex, Northern Territory				
(Mordor samples are located within the rock collection of the Bureau of Mineral Resources, Canberra)				
3434			phlog. lherzolite	Langworthy and Black (1978)
3435			phlog. lherzolite	
3438			phlog. hy. shonkinite	
3441			phlog. lherzolite	
3446			phlog. shonkinite	
3450			phlog. werhlite	
3452			phlog. werhlite	
4142			syenite	
4202			melamonzonite	
4213			monzonite	
4578			shonkinite	
Ullung-do Island, Sea of Japan				
Ull-1	87-243		leucitite	Nelson *et al.* (1986a)
Fiji				
AJCF2	87-244		ankaramite	

thesis designation	A.N.U. designation	locality	rock-type	references
Gaussberg, Antarctica				
82-24	82-24		crustal xenolith	Collerson and McCulloch (1983),
82-27	82-27		leucitite	Nelson *et al.* (1986a)
82-30	82-30		leucitite	
Prince Charles Mountains, MacRobertson Land, Antarctica				
7328-1594	87-260	Manning Massif	leucite tristanite	Sheraton and England (1980),
6928-0225	87-261	Fox Ridge	alkali basalt	Sheraton (1983),
7328-1545	87-262	Mt Bayliss	alkali melasyenite	Nelson and McCulloch (1987)
Enderby Land, Antarctica				
7728-3439D	87-263	Priestley Peak	alkali melasyenite	Sheraton and England (1980), Nelson and McCulloch (1987)
Queen Mary Land, Antarctica				
7728-4730	87-264	Bunger Hills	trachybasalt	Sheraton (1980), Nelson and McCulloch (1987)
southwest Greenland				
5903	87-265	Sarfartûp nunâ	kimberlite	Smith (1979), Scott (1981)
5907	87-266	"	"	
5932	87-267	"	"	
5508	87-268	Umanarssuk	"	
5973	87-269	Manitsorssuaq	"	
5611	87-270	Sagdlerssuaq	lamproite	
5652		"	"	
5622	87-272	"	"	
5634	87-273	"	"	
5672	87-274	"	lamprophyre	
Roman Co-magmatic Region, Italy				
Ven-1	87-233	San Venanzo	leucite melilitite	
Cup-10	87-234	Cupaello	"	
southeastern Spain				
SP-034	87-235	Aljorra	lamproite	Venturelli *et al.* (1984),
SP-039	87-236	Zeneta	"	Nelson *et al.* (1986a)
SP-044	87-237	Fortuna	"	
SP-049	87-238	Fortuna	"	
SP-055	87-239	Jumilla	"	
SP-067	87-240	Cancarix	"	
SP-077	87-241	Calasparra	"	
SP-081	87-242	Puebla de Mula	"	
Leucite Hills, U.S.A.				
LH-4	87-258	Wyoming	wyomingite	Nelson and McCulloch (1987)
LH-7	87-259	"	"	
Carbonatites				
7821-0009	87-276	Walloway, SA	carbonatite	Stracke *et al.* (1979),
7521-0081	87-277	"	carb. kimberlite	Ferguson and Sheraton (1979)
7521-0090	87-278	Terowie, SA	kimberlite	"
MW-1	87-279	Mt Weld, WA	carbonatite	Willett *et al.* (1986)
MW-2	87-280	"	"	"
MC-1	86-137	Magnet Cove, USA	"	Nelson *et al.* (1987)
K-1	84-326	Kaiserstuhl, FRG	phonolite	"
K-2	84-327	"	carbonatite	"
K-3	84-328	"	"	"

thesis designation	A.N.U. designation	locality	rock-type	references
Carbonatites (cont.)				
K-5	84-329	Kaiserstuhl, FRG	lava clast	Nelson *et al.* (1987)
K-6	84-330	"	phonolite	"
NBS-18		Fen, Norway	carbonatite	"
5961	5961	Brasil	carbonatite	"
5963	5963	"	"	"
(the following sample is located within the rock collection of the Bureau of Mineral Resources, Canberra)				
7590-2015		Northern Territory	carbonatite	Black and Gulson (1978)
(the following carbonatite samples are from the collection of the Department of Geology, A.N.U.)				
6336	6336	Napak, Uganda	"	Nelson *et al.* (1987)
6330	6330	Tororo, Uganda	"	"
6335	6335	Sukulu, Uganda	"	"
3432	3432	Kangank., Malawi	"	"
7122	7122	Nachendaz.,Tanzania	"	"
33174	33174	Goudini, Sth Africa	"	"
33176	33176	"	"	"
Jugiong kimberlitic intrusions				
(Jugiong samples are located within the rock collection of the Bureau of Mineral Resources, Canberra)				
0041 Int#1		Jugiong, NSW	kimberlitic intrus.	Ferguson and Sheraton (1979),
0067A Int#4		"	kimberlitic autolith	Stracke *et al.* (1979),
0067B Int#4		"	"	Ferguson *et al.* (1979)
0047 Int#2		"	lapillus	
Tridacna calcium isotope standard				
81-732	81-732	Fantome Island, Queensland	aragonite, internal layers of *Tridacna Gigas*	
Mid-Atlantic ridge basalt calcium isotope reference				
(this sample is from the private collection of S.R. Taylor)				
529-4		Famous area	basalt	Langmuir *et al.* (1977)
Island-arc lavas and trough sediments				
(the following samples are from the private collection of M.T. McCulloch)				
MK-17		Aleutian arc	basalt	McCulloch and Perfit (1981)
MK4-33		"	"	"
MK-3A		"	andesite	"
B5328		Banda arc	basalt	McCulloch *et al.* (1982)
B5561		"	dacite	"
B5128		"	rhyolite	"
SS4		"	sediment	"
Gypsums				
(the following samples were collected by, and are from the private collection of, A.R. Chivas)				
LF-82/3		L. Frome, S.A.	gypsum	
GY-207		L. Gilmor, W.A.	"	
GY-185		L. Yarra Yarra, W.A.	"	
GY-165		L. Moore, W.A.	"	
GY-127		L. Brown, W.A.	"	
Archaean sediments				
(the following samples are from the private collection of M.T. McCulloch)				
AUS-52		Mt Narryer, W.A.	pelite	
AUS-75		"	"	
AUS-81		"	calc-silicate	

APPENDIX 4. Publications arising from this research

Nd-Sr ISOTOPE RATIOS IN ULTRAPOTASSIC ROCKS FROM S.E. AUSTRALIA AND THEIR IMPLICATIONS FROM THE SUBCONTINENTAL LITHOSPHERE

D. R. Nelson[1] M.T. McCulloch[1] and A. L. Jaques[2]

[1]Res. School of Earth Sci., Aust. Nat. Univ., Canberra
[2]Bureau of Mineral Resources, Canberra

Popular models of mantle structure assume that while the differentiation of the continental crust has resulted in an upper mantle depleted in LIL- and LRE- elements, the lower mantle has remained largely undifferentiated, with primitive Sm/Nd, Rb/Sr and U/Pb(?). However, a number of recent studies of rock types believed to be derived from deep (i.e., >100 km) subcontinental sources, such as kimberlites and related ultrapotassic rocks (e.g., Vollmer and Norry, 1983; Collerson and McCulloch, 1983; McCulloch et al, 1983) indicate long histories of LIL- and LRE- enrichment. In an attempt to assess the isotopic character of the deep subcontinental mantle beneath eastern Australia, we have analysed Cainozoic olivine leucitites from central New South Wales for Nd and Sr isotopic compositions.

The lavas are characterized by high Ti, K, P, Cr, Ni and Mg/(Mg + Fe) (Cundari, 1973) and have steep LREE-enriched REE patterns (Nd ~ 200x chondrites). Although the possibility of contamination by crustal rocks prior to or during emplacement must be considered, the high contents of REE and Sr make the Nd and Sr isotopic character relatively insensitive to crustal contamination. Sr and Nd isotopic compositions are quite uniform, ranging from 0.7050 to 0.7055 and ϵ_{Nd} -1.2 to -2.5 respectively, and plot within the mantle array slightly below Bulk Earth on the ϵ_{Nd} versus ϵ_{Sr} diagram. Sr_{UR} and Nd_{CHUR} model ages are <200 Ma, while using depleted mantle parameters gives model ages of ~700 Ma.

Several interpretations of our results are possible, the simplest being that the New South Wales olivine leucitites were derived from primitive undifferentiated mantle and were generated shortly (i.e., <200 Ma) before their emplacement. However, the bulk chemistry of the most primitive leucitites (Mg/(Mg + Fe) ≥70, Ni ≥400 ppm) shows significant enrichment in 'incompatible elements' (K, Rb, Sr, Ba, Ti, Zr) except for Na suggesting derivation from a non-chondritic source. Alternatively, the agreement between Nd and Sr depleted mantle model ages may be indicative of their derivation from depleted mantle, requiring the enrichment event to have occurred up to 700 Ma prior to emplacement. A third alternative is that the Nd and Sr isotopic compositions result from the mixing of depleted and enriched mantle components as has been suggested for the lamproitic rocks from the Fitzroy area, Western Australia (McCulloch et al, 1983). However, the uniformity of the isotopic characteristics does not appear to favour this hypothesis. We are presently analysing representatives of the suite for Pb isotopic composition in an attempt to distinguish between these alternatives.

Our results contrast with those obtained for the Cainozoic alkali basalts of southeastern Australia (McDonough and McCulloch, this meeting) which appear to be derived from shallower, more depleted (less radiogenic Sr for equivalent ϵ_{Nd}) mantle sources. The overlap of the isotopic compositions of the New South Wales leucitites with ocean islands data suggests that the deep (>100 km) subcontinental and oceanic lithospheres may have had similar histories.

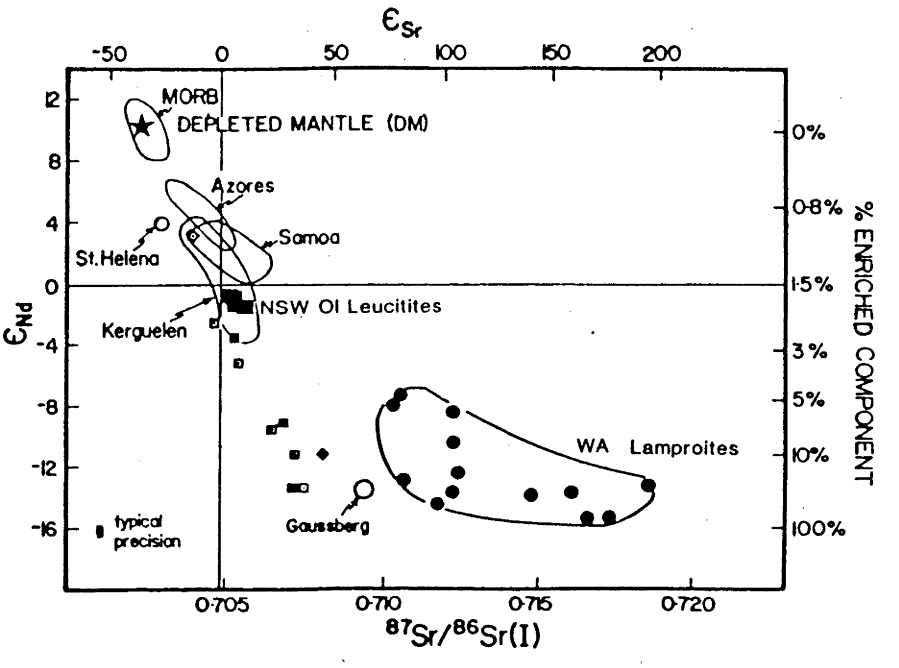

Figure 1: ε_{Nd} - $^{87}Sr/^{86}Sr$ of the NSW leucitites (■), compared with those of ocean islands, MORB, Gaussberg, (⊡) diopsides from kimberlite nodules, (◈) South African kimberlites and (●) West Kimberley lamproites (Data sources as in McCulloch et al, 1983).

References

Collerson, K.D. and McCulloch, M.T., 1983, Proc. 4th Symp. Antarctic Earth Sci.

Cundari, A., 1973, J. Geol. Soc. Aust. 20(4):465-492.

McCulloch, M.T., Jaques, A.L., Nelson, D.R. and Lewis, J.D., 1983, Nature 302:400-403.

Vollmer, R. and Norry, M.J., 1983, Earth Planet. Sci. Lett. 64:374-386.

CARBONATITES AND OCEAN ISLANDS: RELATED MAGMATIC PRODUCTS?

D.R. NELSON, M.T. McCULLOCH and A.R. CHIVAS
Research School of Earth Sciences, The Australian National University, Canberra, A.C.T., 2601.

Geochemical and Sr, Nd, Pb, O and C isotopic data are reported for carbonatites from Australia, Uganda, Malawi, South Africa, Kaiserstuhl in Germany and Fen in Norway. Samples range in age from Proterozoic to Tertiary and possess initial $^{87}Sr/^{86}Sr$ isotopic compositions between 0.7025 and 0.7036 and ε_{Nd} values of from -0.4 to +3.8. On a Nd-Sr isotope diagram, most samples plot below and to the unradiogenic Sr side of the oceanic mantle array. Initial Pb isotopic compositions are radiogenic, with $^{206}Pb/^{204}Pb$ from 19.21 to 21.15 and $^{207}Pb/^{204}Pb$ from 15.60 to 15.86, and generally lie within the field of St Helena-Austral type ocean islands. These data indicate that the sources of carbonatites have had time-integrated LREE-depletion, low Rb/Sr and high U/Pb. $\delta^{18}O$ compositions range from +5.5 to +17.4 permil with the higher $\delta^{18}O$ values found in the volcanic complexes, suggesting the involvement of secondary alteration processes. $\delta^{13}C$ ranges from -0.5 to -6.6 permil (vs PDB) with samples having near-primary $\delta^{18}O$ (between +5.5 and +8 permil) possessing $\delta^{13}C$ between -2.9 and -6.6 permil.

The isotopic similarities between carbonatites and the St Helena-Austral group of ocean islands suggest a common origin for their magma sources. By inference, the isotopic characteristics of carbonatites are not strongly influenced by interactions with the continental crust or subcontinental lithosphere. These results also suggest that carbonate or CO_2-rich phases may play an important rôle in generating the low Rb/Sr and Pb/U ratios characteristic of the St Helena type OIB source.

TERRA Cognita **6** (1986), 201-202.

ULTRAPOTASSIC MAGMAS: END-PRODUCTS OF SUBDUCTION AND MANTLE RECYLING OF SEDIMENTS?

D.R. Nelson, M.T. McCulloch and A.E. Ringwood

Research School of Earth Sciences, Australian National University, Canberra, 2601.

Isotopic studies indicate that some examples of potassic magmatism are derived from ancient, highly enriched (radiogenic $^{87}Sr/^{86}Sr$, unradiogenic $^{143}Nd/^{144}Nd$) sources, and in an attempt to investigate the origins of these enriched components, we have undertaken a comparative Sr, Nd and Pb isotopic and geochemical examination of potassic magmatism from a number of localities. Diamond-bearing lamproites from Western Australia, leucitites from Gaussberg, high-K alkaline dykes from MacRobertson Land, Enderby Land and Queen Mary Land regions of east Antarctica and madupites, wyomingites and orendites from Leucite Hills, Wyoming, have remarkably similar geochemical characteristics (Fig. 1). All have high Ni and Cr contents and high Mg numbers (each locality averaging Mg/(Mg+total Fe)>0.65 with the exception of Manning Massif, Mt Bayliss and Bunger Hills samples, which have Mg numbers of 0.58, 0.58 and 0.50 respectively) as well as high to extreme abundances of K_2O, TiO_2, F, Cl, SO_2, H_2O, P_2O_5, Ba, LREE, high K_2O/Na_2O, Fe^{3+}/Fe^{2+}, Th/U, La/Nb and Ba/La ratios, low K/Rb and K/Ba ratios and relatively low abundances of Al_2O_3, CaO and Na_2O. On a Sr-Nd isotope diagram (Fig. 2), these magmas lie within the "enriched" quadrant, indicating that their sources have had long histories (>1 byrs) of high Rb/Sr and low Sm/Nd (ie; LREE enrichment). Pb isotopic compositions (Fig. 3) indicate multistage histories of U/Pb fractionation, requiring an earlier high U/Pb stage to generate the high $^{207}Pb/^{204}Pb$, followed by a low U/Pb stage during which the evolution of $^{206}Pb/^{204}Pb$ is retarded.

There are a number of possible mechanisms which could account for these unusual chemical and isotopic properties, the most obvious of which is crustal contamination. However, the extremely high concentrations of Sr, Pb and the REE make these magmas insensitive to bulk contamination processes, requiring the assimilation of substantial amounts of crustal material to account for their isotopic compositions. Because of their extreme degree of LREE-enrichment, bulk assimilation of felsic granulite within the lower continental crust will effectively dilute the incompatible element contents of the magmas and should therefore produce a positive correlation between Nd concentration and εNd. In the case of the Western Australian lamproites, a correlation in the opposite sense was noted by McCulloch et al (1983). Crustal assimilation via specialised mechanisms, such as selective volatile transfer or zone refining, is conceivable but is unable to account for the high Mg numbers and Ni and Cr contents or the presence of mantle xenoliths (and in one case, diamonds). Furthermore, the remarkable similarities of unusual geochemical and isotopic compositions of these magmas from diverse localities are unlikely to be the result of random crustal contamination processes but instead, suggest their derivation by a common mechanism.

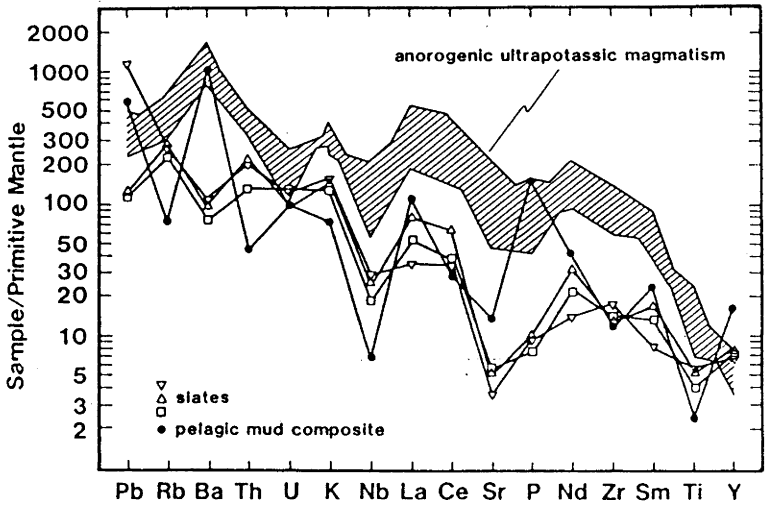

Figure 1. Trace element patterns, normalised to estimated primitive mantle abundances, of average potassic magmas (hatched) from Western Australia (McCulloch et al 1983, Nelson et al 1986, Jaques et al 1984, Nixon et al 1984), Priestley Peak and Gaussberg, Antarctica (Sheraton and England 1980, Sheraton 1983, Collerson and McCulloch 1983, Sheraton and Cundari 1980) and Leucite Hills (orendites and wyomingites, from Kuehner et al 1981, Vollmer et al 1984; Th and U data not available) compared with some examples of modern sediments (from Thompson et al 1984).

Petrogenetic models involving small degrees of partial melting of a lherzolitic or harzburgitic mantle source which has been variably "metasomatised" by an incompatible element rich component have been advocated by a number of workers (eg; Jaques et al 1984, Vollmer et al 1984). For example, enrichment events within the subcontinental lithosphere or upper mantle may result in crystallisation of phlogopite and LIL-rich titanates which are later reactivated to produce isotopically evolved ultrapotassic magmatism (cf. Jaques et al 1986). However, these models frequently fail to address the crucial question of the ultimate source of these metasomatic components. Furthermore, the unusual multistage histories of U/Pb fractionation indicated by the Pb isotopic compositions of these magmas, particularly the earlier high U/Pb stage, are not readily explained by models which favour the generation of these "metasomatic" components entirely within the upper mantle or subcontinental lithosphere.

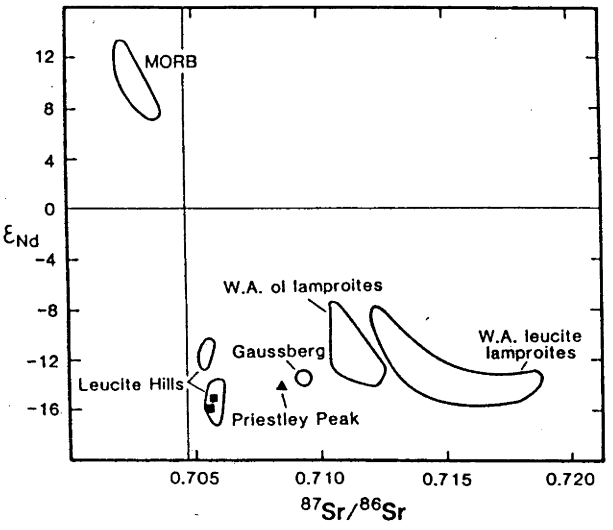

Figure 2. Initial Sr-Nd isotope diagram showing fields for Western Australian lamproites (McCulloch et al 1983), Leucite Hills (Vollmer et al 1984 and analyses of two wyomingites from this study), Gaussberg (Collerson and McCulloch 1983) and the Priestley Peak melasyenite at its emplacement age of 482 myrs (initial Sr and age data from Black and James 1983). Initial εNd values for Manning Massif tristanite (emplacement age; 50 myrs, from Sheraton 1983), Mt Bayliss alkali melasyenite (414 myrs old) and Bunger Hills trachybasalt dyke (Cambrian or younger) are -9.3, -12.3 and <-16.3 respectively. Initial Sr not determined for these samples. Field of mid-ocean ridge basalts shown for comparison.

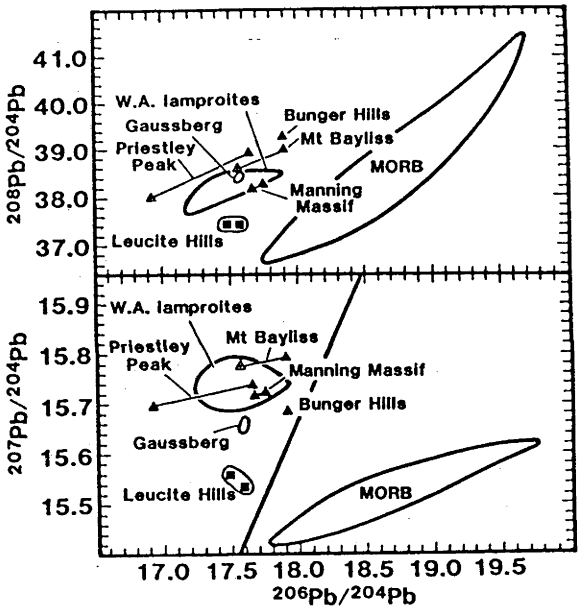

Figure 3. Pb-Pb isotope diagram showing compositions of Western Australian lamproites and Gaussberg leucities (from Nelson et al 1986), Leucite Hills and Antarctic dykes (Δ = measured, Δ = age corrected). Field of mid-ocean ridge basalts for comparison. Corrections to $^{206}Pb/^{204}Pb$ for decay since emplacement are small for the 50 myr old Manning Massif tristanite and because of its low U/Pb, to the Mt Bayliss alkali melasyenite dyke but are considerably larger for the Priestley Peak melasyenite. Age corrections to the measured $^{207}Pb/^{204}Pb$ ratios are within analytical error for the Manning Massif and Mt Bayliss samples. The exact emplacement age of the Bunger Hills trachybasalt dyke is uncertain but is believed to be Cambrian or younger. Its high measured $^{207}Pb/^{204}Pb$ requires a long history (>1 byrs) of high U/Pb and is a feature that predates emplacement. The general features of the Nd and Pb isotopic compositions of the Antarctic dykes are independent of any uncertainty introduced by the age corrections and are similar to those of lamproites from Western Australia and leucitites from Gaussberg.

We propose that the geochemical and isotopic characteristics of these and possibly other examples of continental potassic magmatism are due predominantly to the involvement of a sedimentary component, and that these magmas represent mixtures of mantle and the fusion products of ancient sediments which have been subducted into the mantle (to depths within the field of diamond stability) and stored for long time periods within the subcontinental lithosphere. A number of other studies (see, for example, Nelson et al 1986 and references cited therein) have argued for the involvement of more recently subducted sediments in the generation of highly potassic magmatism from Italy and Spain, whilst the arclike Ba/La, Ba/Nb and La/Nb ratios of some examples of continental potassic magmatism has been previously pointed out by Thompson et al (1984) and Varne (1985). The high abundances of F, Cl, P_2O_5, SO_2 and H_20, high K/Ba and low K/Rb ratios of these examples of continental potassic magmatism, their highly oxidised nature (evidenced by their high Fe^{3+}/Fe^{2+}) and their radiogenic Sr and unradiogenic Nd are readily explained by the involvement of a sedimentary component. By analogy with modern sediments, ancient oceanic sediments will probably have possessed high $^{206}Pb/^{204}Pb$ and $^{207}Pb/^{204}Pb$ due to the contribution of radiogenic Pb from the upper continental crust. Although the U/Pb ratio of modern pelagic oceanic sediments is variable, it is frequently low, and may have been generally lower during the Archean when the lower degree of oxidation of the Earth's atmosphere would favour the less soluble U^{4+} ion over U^{6+}. Ancient sediments therefore probably possessed low U/Pb ratios and the isotopic evolution of Pb would have been severely retarded following its erosion from the continents and deposition in the ocean basins. Hence, the unradiogenic $^{206}Pb/^{204}Pb$ of continental ultrapotassic magmas may be an indication of the time elapsed during sedimentation and storage within the mantle or subcontinental lithosphere, whereas the variation in $^{207}Pb/^{204}Pb$ may reflect the nature and age of the continental provenance.

The presence of diamonds in the Western Australian lamproites provides further support for the involvement of sediment recycling processes, as an extremely wide range of $\partial^{13}C$ values (including values as low as -34 per mil) have been documented by carbon isotopic studies of diamonds from kimberlites and lamproites (see Ozima et al 1985 and references therein), consistent with an origin of some diamonds from sedimentary sources of carbon. A wide range of $^3He/^4He$ ratios were also recently reported by Ozima et al (1985) for diamonds. These authors interpreted the high $^3He/^4He$ ratios of some South African examples as indicating that these diamonds had remained closed systems for almost the age of the Earth. However, an alternative interpretation is offered by the recently confirmed high $^3He/^4He$ ratios of modern ocean sediments (Ozima et al 1984) and manganese nodules (Sano et al 1985), believed to be carried by interplanetary dust particles. Furthermore, a common mineral assemblage of diamond inclusions, olivine + knorringite-rich garnet + enstatite, has been attributed to recrystallisation of the residue of olivine + chrome spinel + enstatite cumulates within oceanic crust following its hydrothermal alteration and partial melting during subduction into the mantle (Ringwood 1977). These data argue for the involvement of components derived from both subducted sediments and oceanic crust in the formation of diamonds.

Although these examples of continental potassic magmatism are not obviously associated with any known modern or past subduction zones, their unusual multistage Pb isotopic compositions require a significant time period (probably much greater than 1 byrs) to have elapsed between the fractionation events lowering the U/Pb ratio (ie; erosion and sedimentation at the Earth's surface) and subsequent potassic magmatism. As these suites all intrude old Archaean or Proterozoic cratons, their sources are probably stored for long periods within the subcontinental lithosphere. The existence of substantial reservoirs of low U/Pb, enriched mantle components within the subcontinental lithosphere may also account for the generally radiogenic Pb of the MORB and ocean island source reservoirs.

REFERENCES

BLACK L.P. and JAMES P.R. (1983) Geological history of the Archaean Napier Complex of Enderby Land. In Oliver R.L., James P.R. and Jago J.B. eds, **Proceedings of the 4th International Symposium on Antarctic Earth Science**, pp. 11-15.

COLLERSON K.D. and McCULLOCH M.T. (1983) Nd and Sr isotope geochemistry of leucite-bearing lavas from Gaussberg, East Antarctica. In Oliver R.L., James P.R. and Jago J.B. eds, **Proceedings of the 4th International Symposium on Antarctic Earth Science**, pp. 676-680.

JAQUES A.L., LEWIS J.D., SMITH C.B., GREGORY G.P., FERGUSON J., CHAPPELL B.W. and McCULLOCH M.T. (1984) The diamond-bearing ultrapotassic (lamproitic) rocks of the west Kimberley region, Western Australia. In Kornprobst J. ed, **Kimberlites and Related Rocks** Vol. 2A, pp. 225-254. Elsevier, Amsterdam.

JAQUES A.L., CHAPPELL B.W., SUN S.-S., LEWIS J.D. and SMITH C.B. (1986) The west Kimberley lamproites: intraplate volcanism of extreme character. (Abstr.) **International Volcanological Congress**, New Zealand. p171.

KUENHER S.M., EDGAR A.D. and ARIMA M. (1981) Petrogenesis of the ultrapotassic rocks from the Leucite Hills, Wyoming. **American Mineralogist 66**, 663-677.

McCULLOCH M.T., JAQUES A.L., NELSON D.R. and LEWIS J.D. (1983) Nd and Sr isotopes in kimberlites and lamproites from Western Australia: an enriched mantle origin. **Nature 302**, 400-403.

NELSON D.R., McCULLOCH M.T. and SUN S.-S. (1986) The origins of ultrapotassic rocks as inferred from Sr, Nd and Pb isotopes. **Geochimica et Cosmochimica Acta 50**, 231-245.

NIXON P.H., THIRWALL M.F., BUCKLEY F. and DAVIES C.J. (1984) Spanish and Western Australian lamproites: aspects of whole rock geochemistry. In Kornprobst J. ed, **Kimberlites and Related Rocks** Vol. 2A, pp. 285-296. Elsevier, Amsterdam.

OZIMA M., TAKAYANAGI M., ZASHU S. and AMARI S. (1984) High $^3He/^4He$ ratio in ocean sediments. **Nature 311**, 448-450.

OZIMA M., ZASHU S., MATTEY D.P. and PILLINGER C.T. (1985) Helium, Argon and Carbon isotopic compositions in diamonds and their implications in mantle evolution. **Geochemical Journal 1**, 127-134.

RINGWOOD A.E. (1977) Synthesis of pyrope-knorringite solid solution series. **Earth and Planetary Science Letters 36**, 443-448.

SANO Y., TOYODA K. and WAKITA H. (1984) $^3He/^4He$ ratios of modern marine ferromanganese nodules. **Nature 317**, 520-522.

SHERATON J.W. (1983) Geochemistry of mafic igneous rocks of the northern Prince Charles Mountains, Antarctica. **Journal of the Geological Society of Australia 30**, 295-304.

SHERATON J.W. and CUNDARI A. (1980) Leucitites from Gaussberg, Antarctica. **Contributions to Mineralogy and Petrology 71**, 417-427.

SHERATON J.W. and ENGLAND R.N. (1980) Highly potassic mafic dykes from Antarctica. **Journal of the Geological Society of Australia 27**, 1-18.

THOMPSON R.N., MORRISON M.A., HENDRY G.L. and PARRY S.J. (1984) An assessment of the relative roles of crust andmantle in magma genesis: an elemental approach. **Philosophical Transactions of the Royal Society of London A310**, 549-590.

VARNE R. (1985) Ancient subcontinental mantle: A source for K-rich orogenic volcanics. **Geology 13**, 405-408.

VOLLMER R., OGDEN P., SCHILLING J.-G., KINGSLEY R.H. and WAGGONER D.G. (1984) Nd and Sr isotopes in ultrapotassic volcanic rocks from the Leucite Hills, Wyoming. **Contributions to Mineralogy and Petrology 87**, 359-386.

Geochimica et Cosmochimica Acta Vol. 50, pp. 231–245
© Pergamon Press Ltd. 1986. Printed in U.S.A.

0016-7037/86/$3.00 + .00

The origins of ultrapotassic rocks as inferred from Sr, Nd and Pb isotopes

DAVID R. NELSON†, MALCOLM T. MCCULLOCH† and SHEN-SU SUN*

†Research School of Earth Sciences, Australian National University, GPO Box 4, Canberra, ACT, 2601
*Division of Petrology and Geochemistry, Bureau of Mineral Resources, GPO Box 378, Canberra, ACT, 2601

(*Received March* 7, 1985; *accepted in revised form November* 4, 1985)

Abstract—Pb, Nd and Sr isotopic compositions are reported for ultrapotassic rocks from a variety of tectonic settings. Olivine leucitites located within the Palaeozoic Lachlan Fold Belt of southeastern Australia have a range in initial $^{87}Sr/^{86}Sr$ of from 0.7042 to 0.7056, ϵ_{Nd} values of +1.5 to −4.1 and $^{207}Pb/^{204}Pb$ of 15.55 to 15.60. These isotopic characteristics overlap with those of contemporaneous alkali basalts and suggest derivation of the leucitites from sources which have been variably contaminated by either the hotspot which initiated volcanism or during earlier enrichment events. Lamproites from the West Kimberley region of Western Australia and leucitites from Gaussberg intrude stabilised Precambrian continental crust and have low $^{206}Pb/^{204}Pb$ (<17.86 and <17.60 respectively) and high $^{207}Pb/^{204}Pb$ (>15.69 and >15.65). Pb isotope correlations displayed by the Western Australian lamproites are consistent with the mixing of an ancient (>2.1 byr old) high $^{207}Pb/^{204}Pb$, low $^{206}Pb/^{204}Pb$ component with more typical mantle Pb. These ancient components probably evolved within the subcontinental lithosphere. Lamproites from southeastern Spain, which have geochemical features (*i.e.* negative Ti- and Nb-anomalies) suggesting a subduction-related origin, possess isotopic compositions ($^{87}Sr/^{86}Sr$ = 0.7173 to 0.7207, $^{206}Pb/^{204}Pb$ = 18.66 to 18.81, $^{207}Pb/^{204}Pb$ = 15.67 to 15.74 and ϵ_{Nd} = −11.2 to −12.6) and isotope correlations consistent with contamination of their sources by a component resembling modern oceanic sediments. This component is isotopically similar to that previously identified in the potassic rocks of Italy. A leucitite from a back-arc setting in the Sea of Japan has Pb isotopic composition similar to some ocean islands such as Kerguelen. The available isotopic data from this and other studies implicate enrichment processes frequently involving ancient, isotopically evolved components in the generation of continental potassic magmatism. These components are probably polygenetic with possible sources including subducted sediments, "megaliths" of recycled crust or the subcontinental lithosphere.

INTRODUCTION

A VARIETY OF mechanisms have been proposed to explain the unusual and diverse chemistry of representatives of the ultrapotassic rock suite, yet no single mechanism has so far proved entirely satisfactory. Although many examples of ultrapotassic volcanism possess geochemical features consistent with a mantle origin, it is also apparent that the characteristic feature of ultrapotassic rocks, their high K/Na ratios, is unlikely to result from the direct partial melting of unmodified or 'primitive' mantle peridotite. Experimental work (*e.g.*, EGGLER, 1978; WENDLANDT, 1984; FOLEY *et al.*, 1986) has demonstrated that melts of peridotite formed in the presence of CO_2 at pressures ≈27 kb would be carbonatitic, while the presence of H_2O or F may enhance the stability of phlogopite. These studies suggest that small degrees of partial melting of phlogopite-bearing peridotite at depths below the level of amphibole stability and in the presence of CO_2 might produce a high K_2O liquid with high Mg/Ca. The prerequisite modification (*i.e.* by the addition of volatiles) of the mantle sources of ultrapotassic rocks has commonly been attributed to metasomatic processes, often considered to be associated with either intraplate rifting or subduction (*e.g.* CUNDARI, 1979; EDGAR, 1980).

A number of recent studies of ultrapotassic rocks (VOLLMER and NORRY, 1983; MCCULLOCH *et al.*, 1983; COLLERSON and MCCULLOCH, 1983; VOLLMER *et al.*, 1984; FRASER *et al.*, 1985) have found Sr and Nd isotopic compositions indicating long histories of high Rb/Sr and Nd/Sm. As the generally very high abundances of trace elements (including Sr, Nd and Pb) of ultrapotassic lavas make them insensitive to bulk crustal contamination processes, these isotopic signatures have been interpreted as indicating derivation from ancient incompatible element enriched mantle. For example, diamond-bearing lamproites from Western Australia have Sr and Nd isotopic compositions indicating enrichment in Rb/Sr and Nd/Sm for at least ≈1 byrs (MCCULLOCH *et al.*, 1983), yet their major and trace element geochemistry argues against substantial assimilation or anatexis of continental crust. Most occurrences of highly potassic volcanism with these unusual isotopic features are found in old continental regions, suggesting that enriched components may exist within some regions of subcontinental lithosphere. The discovery of isotopic compositions indicating ancient enrichment in sub-calcic garnet inclusions in diamonds from African kimberlites led RICHARDSON *et al.* (1984) to propose that a harzburgitic subcontinental lithosphere, stabilised to depths within the diamond stability field since the Archaean, is the source of diamonds and by implication, diamond-bearing kimberlites and lamproites themselves. The low velocity zone, defined by the attenuation of s-wave velocity and where the geothermal gradient approaches or intersects the melting curve, may contain small amounts of melt which are likely to be highly enriched in incompatible elements (*e.g.* GREEN, 1976). Cooling of the lithosphere may result in the incorporation of such incompatible element enriched material within

the base of the subcontinental lithosphere, allowing its long term storage and eventually producing isotopically evolved, "enriched" mantle.

Several authors (CHASE, 1981; HOFMANN and WHITE, 1982; RINGWOOD, 1982) have suggested that ancient mantle enrichments such as those identified by isotopic studies of some ocean island basalts may be the result of the recycling of oceanic crust and sediments into the mantle *via* subduction. Highly incompatible element enriched partial melts of the subducted "megalith" generated as it attains thermal equilibrium with the surrounding mantle are envisaged to rise as magma diapirs, contaminating the overlying mantle and producing the alkali basaltic volcanism of ocean islands (RINGWOOD, 1982). Such plumes could conceivably also be the sources of ultrapotassic magmas, providing an explanation for the radiogenic Sr and Pb and unradiogenic Nd isotopic signatures found in some ultrapotassic suites.

Apart from models invoking origins from mantle reservoirs enriched in incompatible elements, it is also apparent from isotopic studies that members of the ultrapotassic suite may be derived from primitive or even originally incompatible element depleted mantle. As ultrapotassic magmas are believed to originate from considerable depths (as evidenced by the presence of diamonds in lamproites from Western Australia), they provide a direct means of sampling the deep subcontinental lithosphere. The origins of enriched mantle components are of particular interest because of their implications for both the Earth's trace element and isotopic budget and recent proposals of crustal recycling *via* subduction. In the following study, we present isotopic analyses of ultrapotassic rocks from a variety of tectonic settings in an attempt to investigate these models.

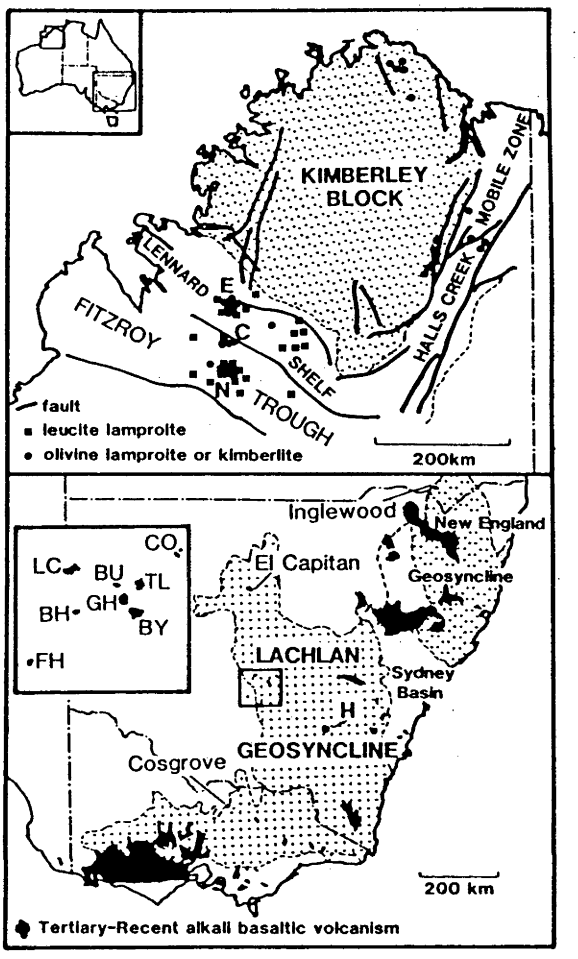

FIG. 1. Generalised geology of the Kimberley region (upper diagram), northwest Australia, showing localities of the Ellendale (E), Calwynyardah (C) and Noonkanbah (N) fields, and the distribution of leucitite volcanism in southeast Australia (lower diagram) relative to Tertiary-Recent alkali basaltic volcanism. H—Harden analcimite (Early Jurassic age). Inset: BH—Begargo Hill, BU—Burgooney, BY—Bygalore, CO—Condobolin, FH—Flagstaff Hill, GH—Gorman Hill, LC—Lake Cargellico, TL—Tullibigeal.

SAMPLES

Samples have been selected from a variety of tectonic settings, including both relatively young fold-belt terrains and stable cratons. The southeast Australian olivine leucitites occur as minor flow remnants along a north–south trending line extending from central New South Wales to Cosgrove in Victoria (Fig. 1). The geochemistry and mineralogy of the New South Wales occurrences have been described by CUNDARI (1973) and the Cosgrove occurrence by BIRCH (1978). The leucitites are located within the Lachlan Fold Belt, which consists of Palaeozoic geosynclinal sediments and granites and is possibly underlain by Precambrian basement. Leucitite outcrop distribution was noted by CUNDARI (1973) to conform to regional north–south structural trends, characterised by block-faulting and regional uplift. Potassic volcanism is temporally and spatially closely associated with alkali basalts, which several studies (*e.g.* WASS and ROGERS, 1980; O'REILLY and GRIFFIN, 1984) have shown to have been derived from metasomatised mantle. WELLMAN and MCDOUGALL (1974) demonstrated a prominent southward temporal migration of Cainozoic igneous activity, a feature also displayed by the leucitites, and attributed it to the northward migration of the eastern part of the Australian continent over several hotspots. SUTHERLAND (1983) proposed that the southerly migration of volcanism may have been related to movement of the continent over former sites of sea-floor spreading.

A vitrophyric analcimite occurrence at Inglewood in southeastern Queensland (see Fig. 1) was described by WILKINSON (1977), who considered the analcime to be an alteration product of leucite. The analcimite is believed to be of Cainozoic age (probably Late Oligocene-Early Miocene) and is possibly related to the extensive Cainozoic alkali basaltic volcanism of southeastern Queensland.

The Harden olivine analcimite, located ≈200 km southeast of the New South Wales leucitite occurrences (see Fig. 1), is of Early Jurassic age (WELLMAN *et al.*, 1970). Major and trace element analyses reported by CUNDARI (1973; analysis HAR II) suggest affinities with nepheline-bearing mid-Mesozoic intrusions and minor flows which occur throughout the southeastern highlands region of New South Wales.

The location, geochemistry and mineralogy of the ultrapotassic rocks from southeastern Spain is given in VENTURELLI *et al.* (1984). The tectonic evolution of the region is controversial, but most models invoke recent subduction processes. ARANA and VEGAS (1974) proposed that the increasing K content of calc-alkaline volcanism from south to north indicates that a northward-dipping subduction zone was active during the Lower Miocene. The ultrapotassic rocks were re-

garded as the most northerly and therefore deepest expression of arc volcanism resulting from the subduction of the African plate under the Iberian plate. A possible association between potassic volcanism and post-Nappe block faulting during the Pliocene was suggested by NIXON *et al.* (1984).

Ullung-do (Utsuryoto) Island is located in the western part of the Sea of Japan, 130 km off the eastern coast of Korea. Petrological studies by TSUBOI (1920) recognised several stages of volcanism, commencing with predominantly basaltic volcanism followed by trachytic and phonolitic flows and pyroclastics. Leucite-bearing lavas were described from an intracaldera dome at Arpong Hill, and were interpreted by TSUBOI (1920) to be the products of the final stage of volcanism on the island.

The early Miocene Western Australian lamproites consist of some ≈100 bodies intruding the Precambrian to Mesozoic rocks of the King Leopold Mobile Zone, the Lennard Shelf and the Fitzroy Trough, immediately south of the southwestern margin of the Precambrian Kimberley Block (ATKINSON *et al.*, 1984, see Fig. 1). Many of the intrusions are localised along deep west northwest-trending tensional faults and fractures with long histories of activity. Details of the geochemistry and mineralogy of the lamproites can be found in JAQUES *et al.* (1984a). The samples analysed for Pb isotopic composition in this study are the same as those analysed by MCCULLOCH *et al.* (1983) for Nd and Sr isotopic composition.

Gaussberg is an isolated volcano located on the eastern margin of the Antarctic continent. Gaussberg leucitites are characterised by extreme K_2O (up to 12 wt%) and incompatible element contents, high TiO_2 (averaging 3.4 wt%) and Mg/(Mg + Fe) values ≈0.70 (SHERATON and CUNDARI, 1980). Attempts have been made to relate Gaussberg volcanism to hotspot activity (DUNCAN, 1981) but, as emphasised by SHERATON and CUNDARI (1980), there is no evidence relating the volcanism to any other area of Cainozoic volcanic activity. Isotopic analyses of granitic crustal xenoliths indicate their derivation from early Proterozoic or late Archaean crust (COLLERSON and MCCULLOCH, 1983), suggesting that Gaussberg is sited on stable continental basement.

The trace element geochemistry of the suites investigated in this study is summarised and compared to average kimberlite values in Fig. 2. Complete trace element data are not available for the southeast Australian suite or Ullung-do Island leucitites. The available data indicate that New South Wales leucitites have overall abundances of the highly incompatible elements Pb, Rb and Ba (average 90, 230 and 260 times primitive mantle values, respectively) intermediate between average kimberlite values and those of Spanish and Western Australian lamproites and Gaussberg leucitites. Noteworthy is the remarkable similarity in the trace element characteristics of leucitites from Gaussberg and those of the Western Australian lamproites. Isotopic studies of Gaussberg (COLLERSON and MCCULLOCH, 1983) and of the Western Australian lamproites (MCCULLOCH *et al.*, 1983) indicates that the suites also have similar Nd and Sr isotopic character. The patterns display extremely high abundances of all trace elements with pronounced positive barium spikes. The patterns of the Spanish lamproites are characterised by similar overall abundances but with negative anomalies of niobium and titanium—features commonly observed in island arc lavas. NIXON *et al.* (1984) contrasted the chemistry of the Western Australian and Spanish lamproites, noting the higher K_2O/Al_2O_3, TiO_2 and incompatible elements Ba, Sr, and Nb of the Western Australian lavas. The Spanish lavas also have lower abundances of the LREE, negative Eu anomalies and higher abundances of the HREE, leading NIXON *et al.* (1984) to propose that they were derived from shallower depths than the Western Australian suite.

ANALYTICAL PROCEDURE

Approximately 500 mg of sample chips or powder was dissolved using hydrofluoric and perchloric acids in teflon bombs at 200°C for at least 48 hours. The resulting solution was

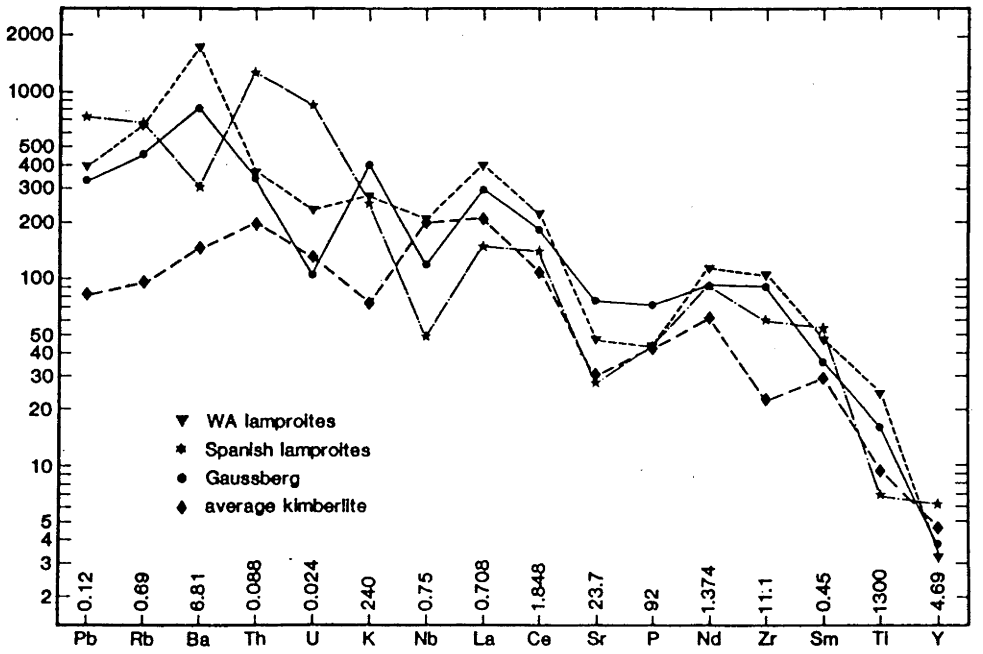

FIG. 2. Averaged trace element abundances in lamproites from Western Australia and SE Spain and leucitites from Gaussberg, normalised to estimated primitive mantle abundances (shown in ppm). Normalised trace element abundances in "average" kimberlite shown for comparison. Data sources: Spanish lamproites, VENTURELLI *et al.* (1984), NIXON *et al.* (1984), this study; Western Australian lamproites, JAQUES *et al.* (1984a), MCCULLOCH *et al.* (1983), this study; Gaussberg leucitites, SHERATON and CUNDARI (1980), COLLERSON and MCCULLOCH (1983); "average" kimberlite, WEDEPOHL and MURAMATSU (1979).

converted to chloride form using hydrochloric acid and split into 3 aliquots, one of which was spiked with both mixed ^{85}Rb-^{84}Sr and ^{147}Sm-^{150}Nd spikes, the second with ^{235}U-^{208}Pb spike and the third aliquot used for Pb isotopic composition. The remaining procedure for Rb-Sr and Sm-Nd analysis follows that of McCULLOCH and CHAPPELL (1982). Mineral separates were leached in 6 N HCl for 10 minutes to remove surface contamination. Pb was isolated from the spiked and unspiked aliquots by 2 passes through 2 gm Dowex-1 anion exchange columns using HBr-HCl for the first pass and HCl only for the second pass. About one microgram of Pb was then loaded onto an outgassed single rhenium filament and analysed using the silica-gel/phosphoric acid technique. A correction factor, determined by comparison of multiple analyses of NBS-982 with the corrected values of CATANZARO *et al.* (1968), was applied to the raw measurements to correct for mass fractionation. The correction factor averaged 0.15% mu^{-1}. The total processing blank was <10 ng for whole-rock samples and ≈3 ng for mineral separates and is insignificant for all samples analysed. As analytical precision for each run was typically better than ±0.008 ($2\sigma_{mean}$) for $^{207}Pb/^{204}Pb$, the main source of analytical error is due to variable mass fractionation. In order to obtain a meaningful estimate of the total error, 30 of the total of 40 Pb analyses listed in Table 2 were performed in duplicate. For duplicated analyses, quoted ratios refer to means of both analyses. Two way analysis of variance indicates that duplicate analyses of samples agree within the following errors at the 1σ level; $^{206}Pb/^{204}Pb$ error ±0.011, $^{207}Pb/^{204}Pb$ error ±0.014, $^{208}Pb/^{204}Pb$ error ±0.033. The values obtained for NBS-981 common Pb standard during this study (average of 7 analyses, error $2\sigma_{mean}$) are $^{206}Pb/^{204}Pb$ = 16.927 ± 0.009, $^{207}Pb/^{204}Pb$ = 15.486 ± 0.013, $^{208}Pb/^{204}Pb$ = 36.668 ± 0.044.

RESULTS

SE Australian leucitites

The results of Rb/Sr, Sm/Nd and U/Pb concentration and isotopic analysis are presented in Tables 1 and 2 and compared with other relevant data in Figs. 3, 4 and 5. K/Ar dating of the suite gave ages ranging from 10–16 myrs for the New South Wales representatives and 6 myrs for the Cosgrove occurrence (WELLMAN *et al.*, 1970; WELLMAN, 1974; SUTHERLAND, 1983). Where necessary, quoted ages have been recalculated using the constants of STEIGER and JAGER, 1977. The correction for radiogenic decay since emplacement is within or just outside analytical uncertainty for Sr and Nd isotope systems and for most of the Pb analyses. Nd/Sm ranges from 5.4 to 7.1 (chondritic ≈ 3), indicating that the leucitites are highly LREE-enriched. Nd and Sr isotopic compositions lie within the mantle array (Fig. 3), extending from the "depleted" quadrant for the most southerly occurrence, the Cosgrove leucitite (ϵ_{Nd} = +1.5, $^{87}Sr/^{86}Sr$ = 0.7042), into the "enriched" quadrant for the most northerly New South Wales occurrence at El Capitan (ϵ_{Nd} = −4.1, $^{87}Sr/^{86}Sr$ = 0.7057). As thorium concentrations were not determined for the southeast Australian rocks, the small age corrections to $^{208}Pb/^{204}Pb$ were made assuming Th/U = 4. The Condobolin leucitite (GA-3476) has high U/Pb and the age correction to $^{206}Pb/^{204}Pb$ and $^{208}Pb/^{204}Pb$ is significant compared to the analytical error. Age corrected Pb isotopic compositions show little variation, with the exception of the Cosgrove sample which has significantly lower $^{207}Pb/^{204}Pb$ than the other members of the suite, and El Capitan which has slightly lower $^{206}Pb/^{204}Pb$. The Pb isotopic compositions of the New South Wales leucitites are characterised by relatively high $^{207}Pb/^{204}Pb$ and $^{208}Pb/^{204}Pb$ compared to those of MORB but are similar to those determined by COOPER and GREEN (1969) for contemporaneous Tertiary-Recent continental alkali basalts from western Victoria.

The Cosgrove leucitite is chemically and petrographically distinct from the New South Wales leucitites, being poorer in olivine and leucite and richer in clinopyroxene (BIRCH, 1978), reflected in its lower Mg, K, Rb, Ni, and higher in Ca, Fe, Na, and possibly Ti contents and lower LREE/HREE. These features imply derivation of the Cosgrove leucitite from a more depleted source than the New South Wales leucitites, consistent with the isotopic data (*i.e.* the lower $^{207}Pb/^{204}Pb$ and $^{87}Sr/^{86}Sr$ and higher $^{143}Nd/^{144}Nd$ of the Cosgrove leucitite). The Cosgrove leucitite has Pb, Sr and Nd isotope compositions within the range determined for the southeast Australian Tertiary-

TABLE 1. Strontium and Neodymium Isotopic Data

Sample	Rb	Sr	Sm	Nd	$^{87}Rb/^{86}Sr$	$^{87}Sr/^{86}Sr$[1]	$^{87}Sr/^{86}Sr(I)$[2]	$^{147}Sm/^{144}Nd$	$^{143}Nd/^{144}Nd$[3]	ϵ_{Nd}
	ppm									
NEW SOUTH WALES										
GA-3470 Begargo Hill	179	2065	14.5	88.9	0.250	0.70562±4	0.70557	0.0989	0.51182±2	-0.3
GA-3471 Begargo Hill	78.9	1251	14.1	86.6	0.182	0.70514±3	0.70511	0.0983	0.51180±1	-0.7
GA-3472 Bygalore	159	1779	24.6	159.0	0.258	0.70523±6	0.70519	0.0938	0.51177±2	-1.3
GA-3473 Bygalore	128	1577	20.0	124.9	0.234	0.70522±4	0.70518	0.0973	0.51181±3	-0.6
GA-3474 Gorman Hills	147	1396	20.7	135.1	0.305	0.70502±4	0.70496	0.0937	0.51181±2	-0.4
GA-3475 Tullibigeal	173	1353	18.9	119.1	0.369	0.70554±5	0.70548	0.0962	0.51178±3	-1.1
GA-3476 Condobolin	135	1494	14.9	93.0	0.260	0.70506±6	0.70501	0.0967	0.51185±3	+0.3
GA-3478 L. Cargelligo	143	1670	17.3	107.1	0.248	0.70525±4	0.70520	0.0979	0.51181±2	-0.5
GA-3480 Burgooney	105	1323	14.6	88.6	0.229	0.70513±4	0.70508	0.0998	0.51184±1	+0.1
GA-3481 Flagstaff	185	1265	15.1	92.7	0.423	0.70522±4	0.70515	0.0986	0.51178±2	-1.2
GA-3479 El Capitan	265	972	16.7	118.3	0.596	0.70572±4	0.70561	0.0851	0.51163±2	-4.1
VICTORIA										
E7980 Cosgrove	76	1230	13.9	75.2	0.179	0.70422±3	0.70420	0.1117	0.51192±2	+1.5
QUEENSLAND										
MH-321 Inglewood	56.1	1492	15.9	90.9	0.109	0.70518±5	0.70515	0.1057	0.51177±2	-1.2
NEW SOUTH WALES JURASSIC										
70-139 Harden	96	816	9.27	49.3	0.423	0.70522±4	0.70403	0.1139	0.51185±2	+0.3
SPANISH LAMPROITES										
SP-034 Aljorra	176	547	19.1	100.7	0.931	0.72083±6	0.72073	0.1148	0.51126±2	-11.2
SP-039 Zeneta	173	555	18.7	90.0	0.903	0.72069±4	0.72060	0.1257	0.51119±2	-12.6
SP-044 Fortuna	29.9	558	21.7	108.1	0.155	0.71798±3	0.71796	0.1211	0.51125±2	-11.4
SP-049 Fortuna	306	539	23.4	120.5	1.647	0.71809±3	0.71792	0.1175	0.51126±2	-11.2
SP-055 Jumilla	232	816	28.0	148.1	0.822	0.71688±5	0.71680	0.1142	0.51122±2	-12.1
SP-067 Cancarix	241	902	30.2	160.4	0.774	0.71750±5	0.71742	0.1138	0.51125±2	-11.5
SP-077 Calasparra	266	584	30.7	161.3	1.317	0.72074±6	0.72061	0.1151	0.51124±3	-11.7
SP-081 Puebla de Mula	413	991	22.8	107.7	1.205	0.71745±5	0.71733	0.1279	0.51124±2	-11.6

[1] All errors quoted refer to within run precision at the $2\sigma_{mean}$ level. Uncertainty in $^{87}Rb/^{86}Sr$ is 0.25% (1σ), in $^{147}Sm/^{144}Nd$, 0.1% (2σ).

[2] Initial Sr calculated using the (recalculated) K/Ar ages of Wellman et al (1970), Wellman (1974) and Sutherland (1983) for southeast Australian samples, 22 myrs for Inglewood and 7 myrs for Spanish suite. Age correction to Nd isotopic compositions is within analytical error for all samples except Harden (see text).

[3] Nd isotopic ratios normalised using $^{146}Nd/^{144}Nd$-0.636151. The value obtained for BCR-1 standard is 0.511833±20. NBS-987 standard value is 0.71022±4, E & A standard carbonate value is 0.70800±3.

TABLE 2. Uranium, Thorium, Lead Concentration and Pb Isotopic Data

Sample	U[1]	Th	Pb	$^{238}U/^{204}Pb$	$^{206}Pb/^{204}Pb$[2]	$^{207}Pb/^{204}Pb$	$^{208}Pb/^{204}Pb$
	ppm						
NEW SOUTH WALES							
GA-3470 Begargo Hill	-	-	-	-	18.235	15.595	38.644
GA-3471 Begargo Hill	-	-	-	-	18.217	15.621	38.333
GA-3472 Bygalore	2.43	-	9.64	18.4	18.223 (18.19)[3]	15.618	38.202 (38.16)[3]
GA-3473 Bygalore	2.42	-	11.33	15.4	18.245 (18.21)	15.603	38.135 (38.09)
GA-3474 Gorman Hills	2.43	-	11.05	15.7	18.121 (18.09)	15.606	38.346 (38.30)
GA-3475 Tullibigeal	2.46	-	12.33	14.4	18.074 (18.05)	15.623	38.295 (38.27)
GA-3476 Cohdobolin	2.72	-	2.2	89.9	18.430 (18.25)	15.593	38.532 (38.30)
GA-3478 L. Cargellico	-	-	-	21.5	18.308 (18.27)	15.617	38.270
GA-3480 Burgooney	-	-	-	-	18.236	15.584	38.408
GA-3481 Flagstaff	-	-	-	-	18.172	15.595	38.193
GA-3479 El Capitan	2.14	-	9.32	16.6	17.877 (17.84)	15.593	38.125 (38.07)
VICTORIA							
E7980 Cosgrove	-	-	-	-	18.350	15.553	38.345
QUEENSLAND							
HH-321 Inglewood	3.19	-	6.92	34.5	19.156 (19.04)	15.637	39.522 (39.37)
NEW SOUTH WALES JURASSIC							
70-139 Harden	-	-	-	-	19.075	15.579	38.445
SPANISH LAMPROITES							
SP-034 Aljorra	-	-	89.4	-	18.659	15.675	39.025
SP-039 Zeneta	-	(85)	-	-	18.755	15.706	39.064
SP-044 Fortuna	21.9	-	105	15.4	18.793 (18.78)	15.739	39.198 (39.18)
SP-049 Fortuna	20.3	(89)	64.4	23.4	18.759 (18.73)	15.688	39.067 (39.03)
SP-055 Jumilla	15.4	(105)	67.0	17.1	18.802 (18.78)	15.718	39.146 (39.10)
SP-067 Cancarix	15.9	(128)	117	10.0	18.788 (18.78)	15.702	39.084 (39.05)
SP-077 Calasparra	-	(112)	-	-	18.815	15.712	39.066
SP-081 Puebla de Mula	29.0	(123)	74.8	28.7	18.809 (18.78)	15.715	39.065 (39.02)
ULLUNG-DO ISLAND							
5th stage leucitite					18.005	15.505	38.654
WESTERN AUSTRALIAN LAMPROITES							
WAK-2L Mt North	(7)	(54)	64.6	(7.8)	17.440 (17.42)	15.773	38.414 (38.35)
WAK-6L Oscar Plug	(8)	(21)	(46)	(12.5)	17.538 (17.50)	15.687	38.043 (38.01)
WAK-10L Mt Percy	(8)	(68)	104	(5.5)	17.324 (17.31)	15.733	38.194 (38.15)
phlogopite	-	-	-	-	17.342	15.736	38.167
WAK-11L Noonkanbah	-	-	(37)	-	17.448	15.724	38.079
WAK-13L 'P' Hill cpx	-	-	-	-	17.352	15.729	37.919
WAK-14L Fishery Hill	(1)	(21)	(51)	(1.4)	17.239 (17.23)	15.716	37.797 (37.77)
WAK-25L Walgidee Hill	(3)	(25)	(46)	(4.7)	17.414 (17.40)	15.729	38.096 (38.06)
WAK-30L Walgidee Hill	(2)	(30)	(23)	(6.2)	17.485 (17.46)	15.694	38.046 (37.95)
WAK-15K Ellendale	(<1)	(59)	(32)	(<2.2)	17.594 (17.59)	15.764	38.466 (38.33)
WAK-16K Ellendale	3.23	(18)	(22)	(6.6)	17.882 (17.86)	15.741	38.593 (38.53)
WAK-17L Ellendale	2.10	(14)	(50)	(7.2)	17.287 (17.26)	15.758	38.140 (38.12)
WAK-20K Ellendale	(4)	(60)	(47)	(6.1)	17.454 (17.43)	15.705	38.300 (38.21)
WAK-21K Ellendale	(2)	(63)	(53)	(2.7)	17.473 (17.46)	15.730	38.369 (38.28)
WAK-27L Ellendale	(2)	(31)	41.3	(3.5)	17.508 (17.50)	15.796	38.572 (38.52)
GAUSSBERG							
82-24 crustal xenolith	-	-	-	-	18.083	15.721	41.384
82-27 leucitite	-	-	-	-	17.602	15.674	38.478
82-30 leucitite	-	-	-	-	17.588	15.649	38.402

[1] U and Pb concentrations determined by isotope dilution mass spectrometry; values in brackets determined by XRF analysis; Thorium for Spanish lavas from Venturelli et al (1984).

[2] Errors (based on two way analysis of variance of duplicate analyses) at the 1σ level; $^{206}Pb/^{204}Pb$ ± 0.011, $^{207}Pb/^{204}Pb$ ± 0.014, $^{208}Pb/^{204}Pb$ ± 0.033. The values obtained for NBS-981 during this study (average of 7 analyses) are; $^{206}Pb/^{204}Pb$=16.926±0.009, $^{207}Pb/^{204}Pb$=15.486±0.013, $^{208}Pb/^{204}Pb$=36.668±0.044.

[3] Corrected for ^{238}U and ^{232}Th decay since emplacement, using ages from references cited in Table 1 and 20 myrs for Western Australian lamproites. Where Th data is not available, the correction has been made assuming Th/U=4. The age correction to $^{207}Pb/^{204}Pb$ is insignificant compared to the analytical error for all samples except the Harden Analcimite.

Recent Newer alkali basalts (COOPER and GREEN, 1969; MCDONOUGH *et al.*, 1985).

Although the exact age of emplacement of the Inglewood analcimite is not known, an age of 22 myrs has been assumed, based on K/Ar studies of nearby volcanism with which the Inglewood leucitite is associated (WELLMAN and MCDOUGALL, 1974). Despite some uncertainty in the exact age of volcanism, the age corrections to the measured Nd, Sr and Pb isotopic ratios are within or close to the analytical error. Initial Sr and Nd isotope ratios overlap with those of the New South Wales olivine leucitites, but the analcimite has slightly higher initial $^{207}Pb/^{204}Pb$ and substantially higher initial $^{206}Pb/^{204}Pb$. The combined isotope data therefore indicate that the Inglewood analcimite and the New South Wales suite were derived from isotopically similar sources, but with the Inglewood analcimite source having higher recent U/Pb.

After correction for age of emplacement (determined by WELLMAN *et al.*, 1970, as 198 ± 3 myrs) Nd and Sr isotopic data indicate that the Harden analcimite was derived from a depleted source with ϵ_{Nd} = +2.4 and $^{87}Sr/^{86}Sr(I)$ = 0.7042. Uranium and thorium abundances have not been determined so it is not possible to correct precisely for their radioactive decay since emplacement. Assuming reasonable values for μ ($^{238}U/^{204}Pb$) of 20 and Th/U of 4 results in age-corrected $^{206}Pb/^{204}Pb$ of 18.45, $^{207}Pb/^{204}Pb$ of 15.55 and $^{208}Pb/^{204}Pb$ of 37.65. Although $^{206}Pb/^{204}Pb$ and $^{208}Pb/^{204}Pb$ estimated in this way is subject to considerable uncertainty, the correction to $^{207}Pb/^{204}Pb$ is small (−0.03). The Pb isotopic data therefore indicate that the source of the Harden analcimite had $^{207}Pb/^{204}Pb$ lower than that of the New South Wales olivine leucitite suite but comparable to that of the Cosgrove olivine leucitite.

Spanish lamproites

Whole-rock and mineral K/Ar data on several of the Spanish ultrapotassic rocks indicates ages of ≈6–8 myrs (BELLON and LETOUSEY, 1977; NOBEL *et al.*, 1981). The high Rb/Sr ratios require small but significant age corrections to be applied to the Sr isotopic data. Initial Sr isotopic compositions show a wide range and are highly radiogenic (0.717–0.720), similar to the values reported by POWELL and BELL (1970) for samples from Jumilla. Nd/Sm varies from 4.8 to 5.2, suggesting mod-

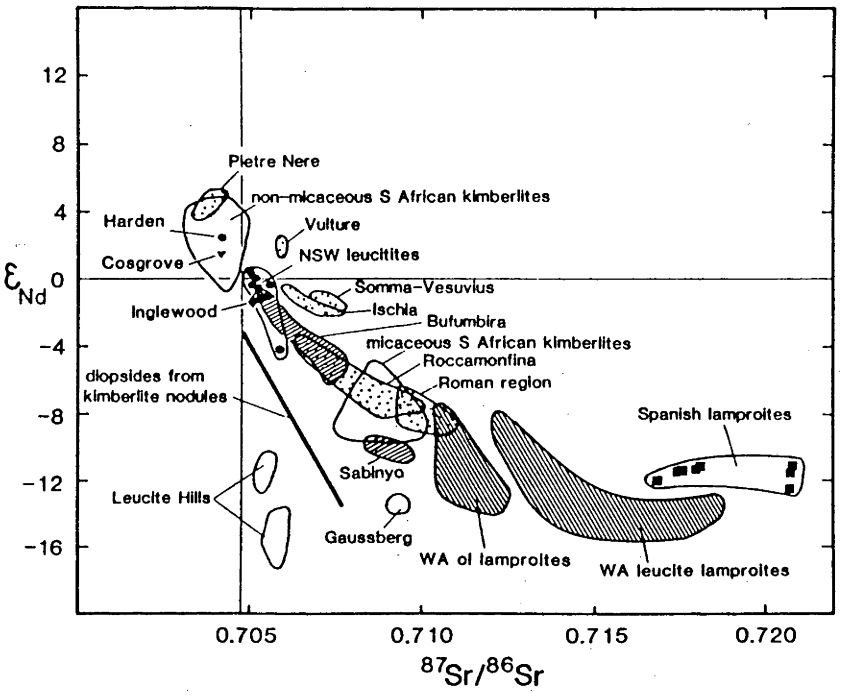

FIG. 3. Nd-Sr isotope initial ratio correlations of southeast Australian leucitites and Spanish lamproites compared to ultrapotassic and selected kimberlite suites from other localities. Many localities display a negative correlation between Sr and Nd isotopes consistent with mixing between two isotopically distinct components. Additional data sources: HAWKESWORTH and VOLLMER (1979), MENZIES and MURTHY (1980), COLLERSON and MCCULLOCH (1983), MCCULLOCH *et al.* (1983), SMITH (1983), VOLLMER and NORRY (1983), VOLLMER *et al.* (1984).

erate LREE-enrichment. Nd isotopic compositions are unradiogenic and fall within the narrow range of ϵ_{Nd} of from −11.2 to −12.6, indicating that the sources of these rocks have had long-term LREE-enrichment (>1 byrs). These isotopic features are like those of the Western Australian lamproites (MCCULLOCH *et al.*, 1983) and the micaceous South African kimberlites (SMITH, 1983; see Fig. 3). The measured Pb isotopic compositions are within the range $^{206}Pb/^{204}Pb$ of 18.66 to 18.81, $^{207}Pb/^{204}Pb$ of 15.67 to 15.74 and $^{208}Pb/^{204}Pb$ of 39.0 to 39.2. Of present-day reservoirs, the Pb isotopic compositions of the Spanish ultrapotassic rocks most closely resemble that of pelagic oceanic sediments (*e.g.* SUN, 1980).

Ullung-do Island leucitite

The Ullung-do Island leucitite has $^{206}Pb/^{204}Pb$ within the range observed for MORB (Fig. 4), but has slightly higher $^{207}Pb/^{204}Pb$ and significantly higher $^{208}Pb/^{204}Pb$ than is found in MORB, plotting within the Kerguelen field. The high $^{208}Pb/^{204}Pb$ suggests a mantle source resembling that of ocean islands rather than that of MORB. Several other Pb isotopic studies of alkali basalts from the southwestern Japan region (KURASAWA, 1968; TATSUMOTO and KNIGHT, 1969; ALLÈGRE *et al.*, 1979) have found Pb isotopic compositions comparable to some ocean islands. The relatively unradiogenic $^{207}Pb/^{204}Pb$ of the leucitite implies that its source was not substantially contaminated by Pb derived from subducted sediments.

Western Australian lamproites

The correction for radiogenic decay since emplacement of the Fitzroy lamproites during the Early Miocene (WELLMAN, 1973; JAQUES *et al.*, 1984b) is small for $^{206}Pb/^{204}Pb$ (≈ -0.04 for the highest U/Pb sample analysed, WAK-6L) and insignificant for the other Pb isotope ratios. The lamproites have relatively low $^{206}Pb/^{204}Pb$ of from 17.24 to 17.88, extremely high and variable $^{207}Pb/^{204}Pb$ values ranging from 15.69 to 15.80 and $^{208}Pb/^{204}Pb$ of 37.80 to 38.59. Acid washed clinopyroxene separated from the 'P' Hill lamproitic intrusion (WAK-13L) has Pb isotopic composition within the range displayed by the Western Australian lamproitic suite. In addition, acid-washed phlogopite separated from the Mt. Percy lamproite (WAK-10L) has Pb isotopic composition within analytical error of the host lava. These mineral isotope data indicate that the unusual Pb isotopic compositions of the Western Australian lamproites represent magmatic compositions and are unlikely to have been significantly affected by post-emplacement alteration. A distinctive feature of the Pb compositions is their unusual position to the left of the zero age geochron (Fig. 4).

Gaussberg leucitites

Fission track data and geomorphological studies suggest that Gaussberg volcanism is of Late Pleistocene-Recent age (SHERATON and CUNDARI, 1980) so corrections to the Pb isotopic data for age of emplacement are unnecessary. Leucitites from Gaussberg have similar Pb isotopic signatures to those displayed by the Western Australian lamproites, but with slightly lower $^{207}Pb/^{204}Pb$ (Fig. 4). Nd and Sr isotopic characteristics (COLLERSON and MCCULLOCH, 1985) of Gaussberg leucitites are also similar to those of the Western Australian suite except for the slightly lower $^{87}Sr/^{86}Sr$ (0.7097, compared to 0.710–0.720; MCCULLOCH *et al.*, 1983). A crustal xenolith (82-24) has Pb isotopic composition distinct from the host leucitite, with significantly higher $^{208}Pb/^{204}Pb$. The very high $^{208}Pb/^{204}Pb$ of the xenolith indicates that it is unlikely that the Pb isotopic compositions of the leucitites have been substantially modified by assimilation of crustal material like that of the xenolith.

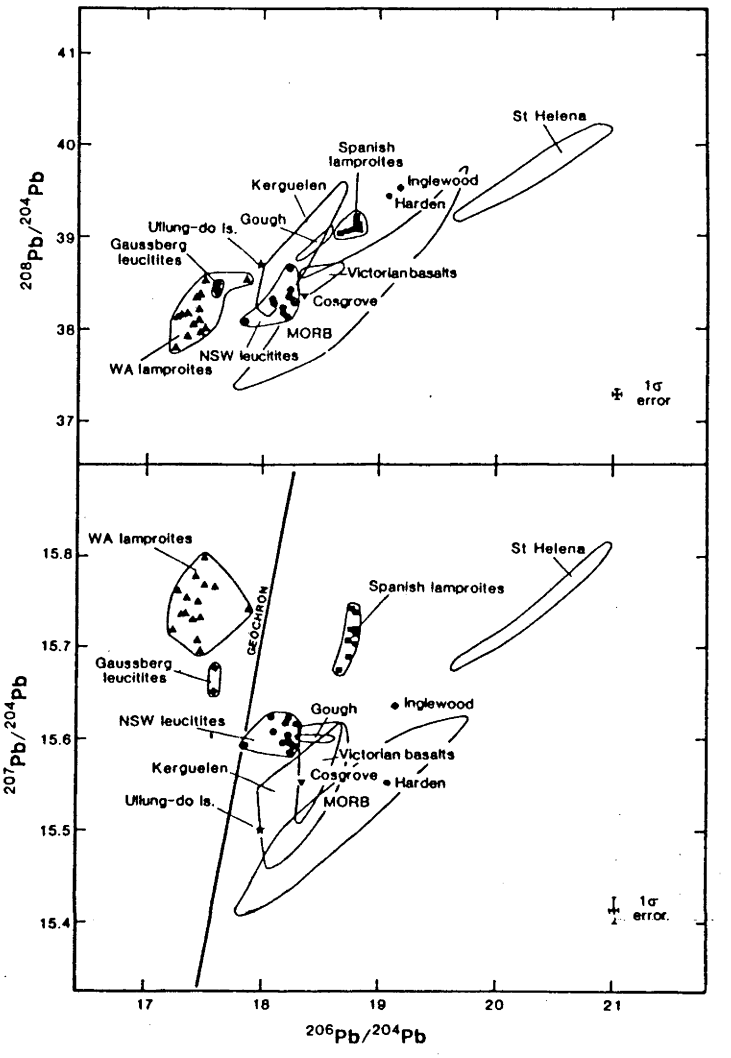

FIG. 4. Pb-Pb isotope variation of southeast Australian, Ullung-do Island and Gaussberg leucitites and Western Australian and Spanish lamproites compared to MORB (from DUPRÉ and ALLÈGRE, 1980; COHEN and O'NIONS, 1982a), Victorian Newer basalts (COOPER and GREEN, 1969; MCDONOUGH *et al.*, 1985), Kerguelen (DOSSO *et al.*, 1979) and some other ocean islands (SUN, 1980; COHEN and O'NIONS, 1982b).

DISCUSSION

S.E. Australian leucitites

Although the evolved isotopic characteristics of the New South Wales leucitites may be attributed to contamination by continental crust, there is no compelling evidence for the assimilation of crustal material in the major and trace element characteristics of the lavas. The suite has high Ni (average ≈375 ppm), Cr (≈400 ppm), MgO (12.4 wt%), Mg/(Mg + Fe^{2+}) (excluding some of the fractionated Begargo Hill samples, averaging ≈0.71 recalculated assuming $Fe^{3+}/(Fe^{2+} + Fe^{3+})$ = 0.15), combined with low SiO_2 (44.3 wt%) and Al_2O_3 (8.7 wt%) (CUNDARI, 1973), consistent with their derivation from the mantle. In addition, while the El Capitan leucitite (GA-3479) has the most radiogenic Sr and least radiogenic Nd and is therefore the most likely candidate to have been contaminated by continental crust, there is no evidence of this in its major and trace element chemistry. TAYLOR *et al.* (1984) analysed the same samples used in this study for $^{18}O/^{16}O$, and found that the whole-rock and leucite phases are enriched in ^{18}O but that the clinopyroxenes have $\delta^{18}O$ of ≈ +6.5, considered to represent primary magmatic values. They attributed the high ^{18}O of the leucites to interaction with late-stage K-rich magmatic fluid with high $\delta^{18}O$ (≈ +8), although they did not discount the possibility of the involvement of small amounts of meteoric water which had isotopically equilibrated with magmatic fluid. The primary $\delta^{18}O$ values estimated from the clinopyroxenes are similar to the values of alkali basalts and argue against the assimilation of upper crustal material. It is unlikely that the possible involvement of small amounts of meteoric water could have significantly affected the Sr, Nd and Pb isotopic compositions.

The variation in isotopic characteristics of the New

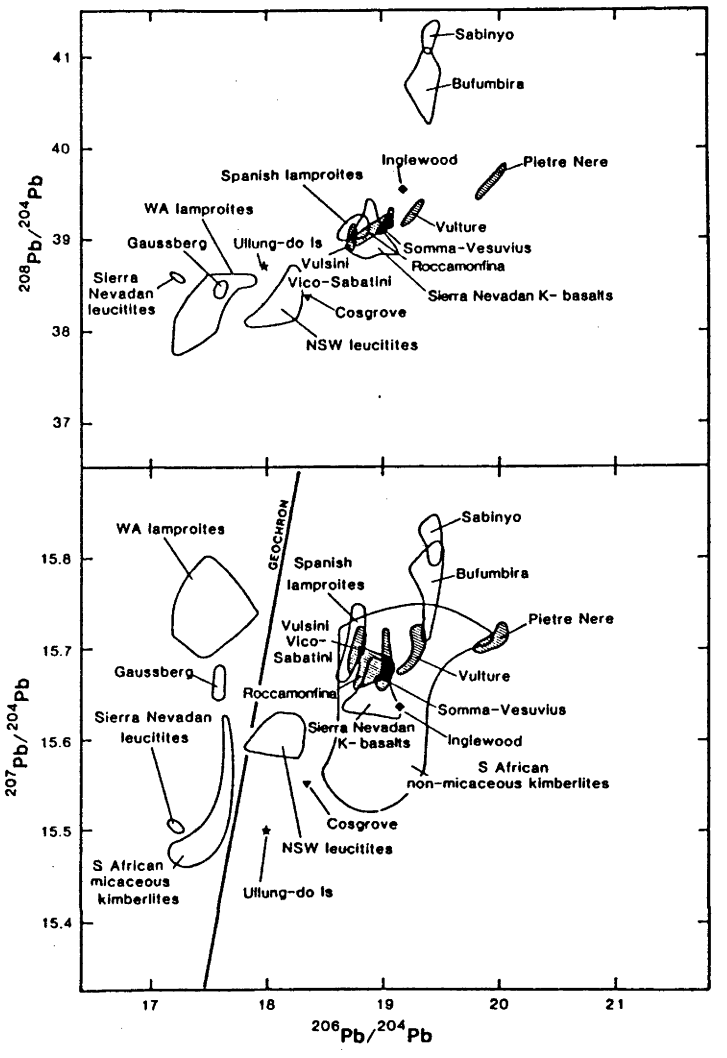

FIG. 5. Pb-Pb isotope characteristics of ultrapotassic rocks. A notable feature is the generally high and variable $^{207}Pb/^{204}Pb$ accompanied by comparatively unradiogenic $^{206}Pb/^{204}Pb$ of many examples compared to those of MORB and ocean islands. Additional data sources: VOLLMER (1976, 1977); VOLLMER and HAWKESWORTH (1980); VAN KOOTEN (1981); SMITH (1983); VOLLMER and NORRY (1983).

South Wales leucitites may therefore be the result of either: a) contamination of their sources by a component having radiogenic $^{87}Sr/^{86}Sr$, unradiogenic ϵ_{Nd} and $^{207}Pb/^{204}Pb \geq 15.6$; or b) derivation from variably enriched mantle sources which have evolved the observed isotopic compositions since the enrichment events. The latter alternative is considered less likely as a period of at least $\approx$300 myrs is required to produce the observed range in Nd isotopic compositions of 4 ϵ units from closed system decay within source regions which have undergone varying degrees of incompatible element enrichment (*i.e.* increase in Nd/Sm and Rb/Sr accompanied by a decrease in U/Pb), assuming a source Sm/Nd like that of the leucitites themselves. As the source Sm/Nd is likely to be considerably higher than that of the leucitite melt, this time estimate is probably greatly underestimated. The El Capitan leucitite has the highest measured Rb/Sr and Nd/Sm ratios and significantly more radiogenic Sr and less radiogenic Nd compared to the other New South Wales leucitites, consistent with greater contribution of an incompatible element enriched, high $^{87}Sr/^{86}Sr$, low ϵ_{Nd} component to its source, but also has identical $^{207}Pb/^{204}Pb$ to the other New South Wales leucitite occurrences. This suggests that either the Pb isotopic compositions of the leucitites are dominated by that of the added component, or that the added component and the invaded mantle had similar $^{207}Pb/^{204}Pb$. The less radiogenic $^{206}Pb/^{204}Pb$ of the El Capitan leucitite compared to the other New South Wales occurrences may be due to some variation in the timing or degree of enrichment in the leucitite sources, or may indicate differences in the $^{206}Pb/^{204}Pb$ of the added components involved at El Capitan and the other occurrences.

The geochemical and isotopic data are therefore consistent with the derivation of the New South Wales leucitites from mantle which has been contaminated by a component with $^{87}Sr/^{86}Sr \geq 0.7057$, $\epsilon_{Nd} \leq -4$ and

$^{207}Pb/^{204}Pb \approx 15.6$. Compared to the Tertiary-Recent Victorian Newer alkali basalts (McDONOUGH *et al.*, 1985), the Cosgrove leucitite has similar Sr, Nd and Pb isotopic compositions whereas the New South Wales leucitites have higher $^{87}Sr/^{86}Sr$ and lower $^{143}Nd/^{144}Nd$, forming an extension of the array displayed by the Newer basalts into the enriched quadrant on the $^{87}Sr/^{86}Sr$-$^{143}Nd/^{144}Nd$ diagram. The New South Wales leucitites have similar $^{207}Pb/^{204}Pb$ and $^{208}Pb/^{204}Pb$ but have lower $^{206}Pb/^{204}Pb$ than the Newer basalts (COOPER and GREEN, 1969; Fig. 4). Although these features may simply reflect regional isotopic heterogeneity within the subcontinental lithosphere beneath southeastern Australia, they may also be interpreted as mixing trends, with the addition of a component having isotopic characteristics like those of the New South Wales leucitites to the sources of the Newer basalts responsible for their isotopic variation. WELLMAN and McDOUGALL (1974) and SUTHERLAND (1983) showed that the locations and eruption ages of the southeast Australian leucitites and Newer basalts are consistent with the initiation of volcanism by the passage of the Australian continent over a hotspot. As the isotope variation found in the Newer basalts was attributed by McDONOUGH *et al.* (1985) to mixing between a component derived from the hotspot plume component and the subcontinental lithosphere, it is conceivable that the hotspot plume represents the enriched, low $^{206}Pb/^{204}Pb$ end-member component. Further Pb isotope analyses of the Newer basalts are required in order to assess this possibility.

A number of studies of Cainozoic alkali basaltic volcanism and incorporated xenoliths from the eastern margin of New South Wales (*e.g.* KESSON, 1973; WASS and ROGERS, 1980; O'REILLY and GRIFFIN, 1984) have argued that the mantle from which the products of volcanism were derived was chemically and isotopically heterogeneous. The widespread occurrence of amphibole ± mica ± apatite-bearing mantle xenoliths has been interpreted as evidence for the operation of metasomatic processes in the source regions of the host lavas. O'REILLY and GRIFFIN (1984) found a range of Sr isotope compositions of from 0.7031 to 0.7054 for New South Wales alkali basalts, and attributed the isotope variation to the metasomatic addition of varying amounts of radiogenic Sr to their sources. Much of the New South Wales alkali basaltic volcanism considered by O'REILLY and GRIFFIN (1984) and others to be derived from metasomatised subcontinental lithosphere predates, and is therefore unrelated to, the passage of the hotspot responsible for the leucitite volcanism. Although leucitite volcanism was probably activated by the hotspot, metasomatism of the leucitite sources may have been related to that of the sources of the New South Wales alkali basalts and may have occurred prior to the passage of the hotspot.

Spanish lamproites

The large range in $^{207}Pb/^{204}Pb$ displayed by the Spanish lamproites is notable, especially as it is accompanied by a relatively limited range in $^{206}Pb/^{204}Pb$ (Fig. 4). Such a correlation is unlikely to have resulted directly from closed system decay of uranium, as the range in $^{207}Pb/^{204}Pb$ requires the existence of long term variation in U/Pb, which would result in large variation in $^{206}Pb/^{204}Pb$. The correlation is most readily explained by the mixing of highly radiogenic Pb with that of a source with low $^{207}Pb/^{204}Pb$, such as the depleted mantle source of MORB. An origin of the Spanish suite involving mixing is consistent with trace element relations (VENTURELLI *et al.*, 1984).

Comparison between Pb and Sr isotopes of ultrapotassic rocks from this and other studies are displayed in Fig. 6. Lavas from Spain and Western Australia resemble those from the Virungan volcanic field described by VOLLMER and NORRY (1983) in possessing large ranges in Sr isotopic compositions but limited variation in Pb compositions, particularly $^{206}Pb/^{204}Pb$, and very high $^{207}Pb/^{204}Pb$. An interesting aspect of the Spanish lamproite isotopic data is that it lies on an extension of the Sr-Pb isotopic correlations displayed by ultrapotassic rocks from Italy (Fig. 6). The Pb isotopic compositions of the Spanish lavas are identical to those of the Vico-Vulsini-Sabatini region, which has among the most radiogenic Sr and unradiogenic Nd of the Italian lavas (*i.e.* most like the Spanish lamproites). This may indicate that the metasomatic component invoked to explain the isotopic correlations of lavas from the southern region of Italy (HAWKESWORTH and VOLLMER, 1979) is similar to that identified in the Spanish lamproites. This component has the Sr, Nd and Pb isotopic characteristics of continental crust or sediments derived from continental crust.

Ullung-do Island leucitite

NAKAMURA *et al.* (1985) found that the island arc character, indicated by enrichment in K, Ba, Sr and Rb and depletion of Ta and Ti, of alkali basalts across the Japanese island arc to Korea and Eastern China becomes progressively weaker, and that the trace element patterns of islands from the Sea of Japan show no evidence of the influence of subduction processes. The relatively unradiogenic Pb isotopic composition of the Ullung-do Island leucitite limits the possible involvement of subducted oceanic crust and sediments as a source of their high potassium, as has been proposed to explain the well-documented relationship between potassium and depth to Benioff zone evident in some island arcs (*cf.* DICKINSON and HATHERTON, 1967). Geochemical and isotopic studies of lavas from the west Sunda arc, Indonesia, (WHITFORD, 1975; WHITFORD *et al.*, 1981) demonstrated that although tholeiitic and calc-alkaline lavas display evidence of contamination by a component derived from subducted lithosphere, the leucite-bearing lavas of Mt. Muriah, situated ≈300 km above the Benioff zone, manifest least evidence of such contamination. However, leucite-normative lavas from the east Sunda arc region have radiogenic Sr compared to calc-alkaline lavas from the same region (WHITFORD *et al.*, 1978),

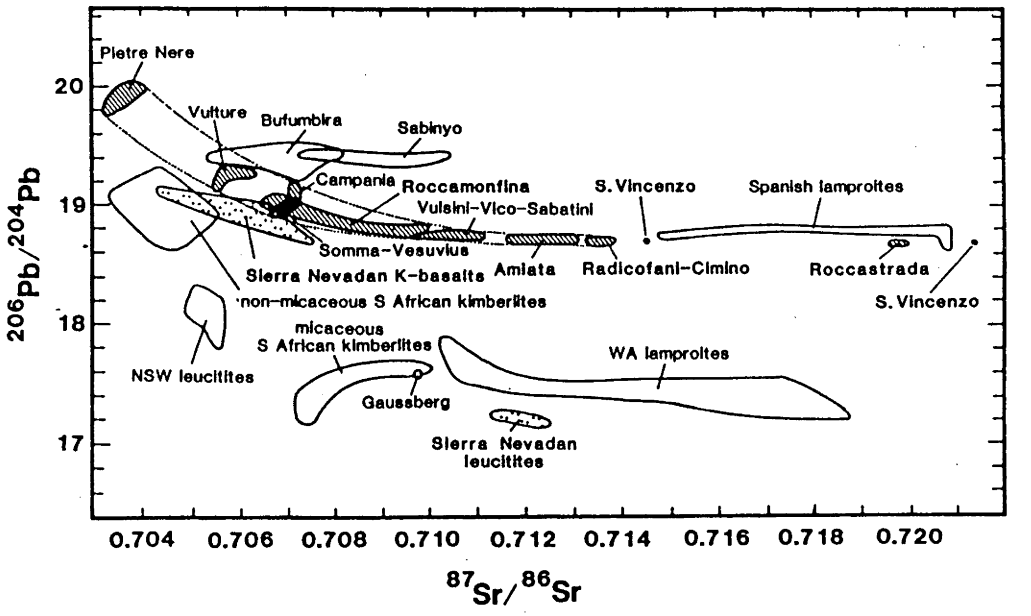

FIG. 6. Fields of initial isotopic compositions of $^{206}Pb/^{204}Pb$ against $^{87}Sr/^{86}Sr$ for ultrapotassic suites and some kimberlites. In many cases the range of $^{87}Sr/^{86}Sr$ is large while $^{206}Pb/^{204}Pb$ variation is limited, suggesting that one component has dominated the Pb isotope character. As the field for the Italian lavas extends towards that of the Spanish lamproites (also the case for $^{207}Pb/^{204}Pb$ and $^{208}Pb/^{204}Pb$ *vs.* $^{87}Sr/^{86}Sr$), the metasomatic components in both cases may be the same. Additional data sources as in Figs. 3 and 5.

suggesting that they may have been more strongly contaminated by a component derived from the subducted slab. It is therefore evident that the direct chemical influence of the subducted lithosphere on leucite-bearing lavas located in or near subduction zones, such as those of Ullung-do Island and the west and east Sunda arcs, varies considerably.

In contrast with most continental potassic volcanism, leucitites from island arcs frequently have low TiO_2, Nb and Zr, characteristics in common with arc volcanism. Although the source of the potassium in high-K island arc volcanism is controversial, a number of studies (*e.g.* NICHOLLS and WHITFORD, 1978; FODEN and VARNE, 1980) favour the derivation of high-K arc lavas from mantle which has been modified by the addition of a LIL-rich component to their source regions. It seems likely that melts or fluids derived from the subducted slab are involved, but that in some cases these may not be isotopically distinguishable from the invaded mantle. LLOYD and BAILEY (1975) attributed the scarcity of highly potassic volcanism in oceanic settings to the effects of generally steeper geotherms in ocean basins compared to the continental geotherm, reducing the depths to which phlogopite persists without amphibole also being stable.

Western Australian lamproites and Gaussberg leucitites

The distinctive Pb isotopic signature of the Western Australian lamproites and Gaussberg leucitites is indicative of an extremely ancient component which had high U/Pb early in its history, followed by a lowering of U/Pb more recently, relative to the observed array displayed by oceanic islands and MORB. This is in contrast to the sources of most MORB and many ocean islands, which have undergone (either progressively or episodically) an increase in their U/Pb ratios. As with the Spanish suite, the Western Australian lamproites display little variation in $^{206}Pb/^{204}Pb$ for the correspondingly large variation in $^{207}Pb/^{204}Pb$. MCCULLOCH *et al.* (1983) modelled the correlation between Nd and Sr isotopes displayed by the Western Australian lamproites by mixing of enriched and depleted components. This is consistent with the Pb isotope variation, which is most readily explained by mixing. However, rather than trending towards the present-day MORB field on the $^{206}Pb/^{204}Pb$-$^{207}Pb/^{204}Pb$ diagram (Fig. 4) as in the case of the Spanish lamproites, the Western Australian lamproite array (excluding WAK-16L) appears to extend to more primitive $^{206}Pb/^{204}Pb$ values. The array may result from the mixing, at some time in the past, of a high $^{207}Pb/^{204}Pb$ component with a MORB component (*i.e.*, when the MORB reservoir had $^{207}Pb/^{204}Pb \approx 15.5$ like the present-day value but $^{206}Pb/^{204}Pb$ less than ≈ 17.00). A primitive or (more probably) depleted mantle component which dominates the major elements can account for the high MgO, Ni, Cr and low Al, Ca and Na contents, while a "metasomatic" component enriched in incompatible elements and which dominates the isotopic characteristics can account for the trace element contents (JAQUES *et al.*, 1984a). If produced at depth, the metasomatic component may pass through isotopically different regions of the mantle and subcontinental lithosphere, resulting in the observed isotopic correlations.

Origins of the high $^{207}Pb/^{204}Pb$, low $^{206}Pb/^{204}Pb$ component

That ultrapotassic rocks from Gaussberg and Western Australia possess similar unusual isotopic compositions is strong evidence for their generation by a common process. Although their Sr, Nd and $^{207}Pb/^{204}Pb$ isotopic characteristics are more like those of the upper continental crust, many aspects of their major and trace element characteristics, such as their high Mg/(Mg + Fe) and Ni and Cr contents, and in the case of the Western Australian lamproites, the presence of mantle xenocrysts and diamonds, are more consistent with a mantle origin. In the following modelling of the isotope data, some general inferences about the long term histories of the sources of the Western Australian lavas are made.

The unusual Pb isotopic compositions of the Western Australian and Gaussberg leucitites require an evolution involving at least two stages. A general model of the evolution of their Pb is shown in Fig. 7. Modelling of the high $^{207}Pb/^{204}Pb$, low $^{206}Pb/^{204}Pb$ component recognised in the Western Australian lamproites allows the ranges of possible values of μ_1 and μ_2 and minimum age for t_1, the time of differentiation of the component from the mantle, to be determined. Figure 7 shows, for selected values of t_1, the range of possible values for μ_1 and μ_2 plotted against t_2, the time at which the U/Pb ratio was lowered. The modelling uses the Pb composition of the Western Australian lamproite having the highest $^{207}Pb/^{204}Pb$ and relatively low $^{206}Pb/^{204}Pb$ (WAK-27L), regarded as the least contaminated by Pb from other sources. In the case of an evolution involving two stages (where $t_1 = t_0$), the range of possible values for μ_1 and μ_2 is given by the $t_1 = 4.5$ byr curves. For decreasing values of t_2, μ_1 approaches 8.6 while μ_2 approaches zero, until at $t_2 \approx 0.5$ byrs, μ_2 becomes negative and it is not possible to generate the measured Pb composition of WAK-27L. Because a two stage model requires the existence of an extremely ancient, moderately high U/Pb reservoir, perhaps the only instance where a two stage model could be applied is when the first stage reservoir is known to be very ancient sialic crust.

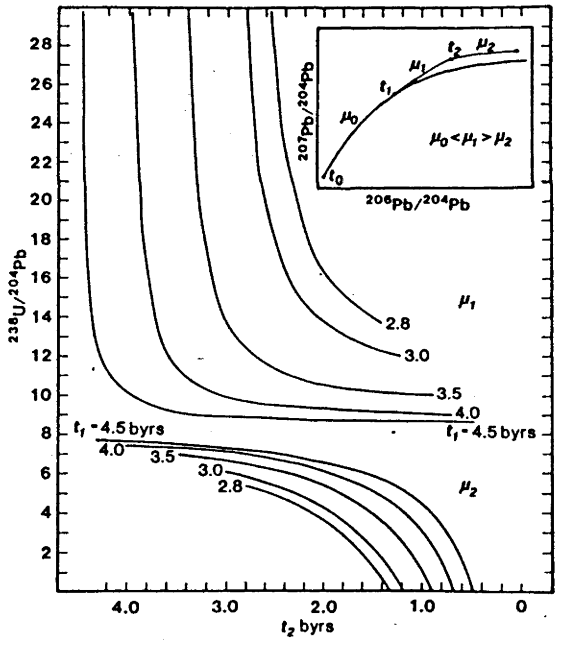

FIG. 7. Three stage evolution of the sources of Pb in the Western Australian lamproites. At time t_1, the components differentiate from the mantle reservoir with higher $^{238}U/^{204}Pb$ (μ_1) and at time t_2 an event lowers the U/Pb (μ_2) of the components. The initial Pb compositions at t_0 are those of Canyon Diablo troilite (TATSUMOTO, 1973). A mantle reservoir μ_0 of 8.0 and the end Pb isotopic composition of WAK-27L have been used. Solutions are given for μ_1 (upper curves) and μ_2 (lower curves) for selected values of t_1 (in byrs), plotted against t_2 on the lower axis, for two and three stage models. The $t_1 = 4.5$ byr curves give the range of possible values of μ_1 and μ_2 for a model involving only two stages. For a three stage model, younger values of t_1 require higher values of μ_1 and lower values of μ_2 until at $t_1 \approx 2.1$ byrs, values of μ_2 become negative.

A more general and geologically plausible three stage model differs from the two stage case in having an earlier period prior to the high U/Pb stage during which the Pb evolves in the "normal" mantle reservoir with $\mu_0 \approx 8.0$. It can be seen from Fig. 7 that younger values of t_1 require higher μ_1 and lower μ_2, until at $t_1 \approx 2.1$ byrs $\mu_2 < 0$ and it becomes impossible to produce the Pb isotopic composition of WAK-27L. A first stage $\mu_0 = 8.0$ has been used, based on ore Pb isotope data from Archaean greenstone belts (TILTON, 1983; RODDICK, 1984; DUPRÉ *et al.*, 1984; BREVART *et al.*, 1986) although the three stage modelling is not particularly sensitive to the value of μ_0. For example, no solutions are possible for $t_1 < 2.1$ byrs using the CUMMING and RICHARDS (1975) Model 3 growth curve based on conformable ores, which is considered to provide a reasonable upper limit of the value of time integrated μ_0 evolution for the mantle (as ores are likely to contain some Pb derived from the crust), while using values of $\mu_0 < 8.0$ will tend to increase the minimum allowable values of t_1.

The three stage modelling establishes that the Pb component identified in the Western Australian lamproites cannot have differentiated from primitive mantle at times less than 2.1 byrs ago. From Fig. 7 it is apparent that for older values of t_1, lower and more geologically reasonable values of μ_1 are possible. Younger values of t_1 require higher values for μ_1 or longer periods between the events t_1 and t_2.

Additional information about the source history of the Western Australian lamproites is provided by their Nd isotopic systematics. For example, ZINDLER *et al.* (1984) estimated that during low degrees of modal melting ($\approx$ <1%) of a garnet lherzolite source, the Sm/Nd ratio of the melt will be at least one half that of the source. The measured Sm/Nd values of the Western Australian lamproites are relatively constant at $\approx$0.11 (MCCULLOCH *et al.*, 1983), implying a source Sm/Nd of at least 0.22. A minimum period of 2.1 byrs is re-

quired for a source with Sm/Nd ratio equal to or greater than this value to evolve the Nd isotopic compositions observed in the Western Australian lamproites from an initially depleted mantle source. As the Pb isotope data indicates a more complex history, probably involving at least two stages, the calculated Nd depleted mantle model source ages should be regarded as an estimate of the minimum age of first differentiation of the lamproite sources from primitive mantle (*cf.* MCCULLOCH *et al.*, 1983). The minimum estimate of $\approx$2.1 byrs for the differentiation event is in accord with the value determined from the Pb systematics.

Implications for the origins of the ultrapotassic suite

The remarkable diversity of isotopic characteristics displayed by representatives of the ultrapotassic suite is apparent from Figs. 3 and 5. However, the available geochemical and isotopic data taken from this and other earlier studies favour the generation of many examples of continental potassic volcanism by the invasion of regions of the subcontinental mantle by an isotopically foreign incompatible element enriched "metasomatic" component. In many cases these components possess high $^{207}Pb/^{204}Pb$, radiogenic Sr and unradiogenic Nd relative to MORB, indicating that the sources of these components have had long and complex histories. The trace element and isotopic identity of the resulting melts is strongly influenced by that of the added component, resulting in isotope/isotope and isotope/abundance relations indicative of mixing. Examples include the Spanish and Western Australian lamproites and probably the New South Wales leucitites. In view of their remarkable geochemical and isotopic similarity with Western Australian lamproites, leucitites from Gaussberg may also have been generated by a similar process. The isotopic characteristics of the Virungan lavas (VOLLMER and NORRY, 1983) are also consistent with the addition to their sources of a similar radiogenic $^{207}Pb/^{204}Pb$ and $^{87}Sr/^{86}Sr$, unradiogenic $^{143}Nd/^{144}Nd$ component, but the sources of the Virungan lavas may have evolved variable $^{87}Sr/^{86}Sr$ since the mixing event. There is no consensus about the origins of the Italian potassic lavas, although $^{18}O/^{16}O$, Nd, Sr and Pb isotopic studies (*e.g.* TAYLOR and TURI, 1976; HAWKESWORTH and VOLLMER, 1979; VOLLMER and HAWKESWORTH, 1980; HOLM and MUNKSGAARD, 1982 and others) favour the involvement of crustal material, either by assimilation within high level magma chambers or by metasomatism of the sources of the magmas by subducted sediments.

The metasomatic components of many potassic occurrences possess high $^{207}Pb/^{204}Pb$, radiogenic Sr and unradiogenic Nd, limiting the sources of these components to only a few geological reservoirs;

1. *Old subcontinental lithosphere*—the Western Australian, Gaussberg, Leucite Hills and Virungan suites are situated on stable, thick Precambrian basement which may have had the specific long-term history required. A major difficulty is that many ultrapotassic suites are generated at great depths; within the diamond stability field in the case of the Western Australian lamproites. The depths to which the continental lithosphere extends beneath old continents is unknown but if, as speculated by RICHARDSON *et al.* (1984), it is in some circumstances stable to depths within the diamond stability field, then the subcontinental lithosphere could be an important reservoir for the storage of ancient, isotopically evolved components. Spanish lamproites have geochemical features which suggest that they were generated at shallower depths than the Western Australian lamproites (NIXON *et al.*, 1984) but are located on relatively young Proterozoic basement which may not have had sufficient prior history to have evolved the isotopic characteristics required.

2. *Subducted sediments*: The findings of this study are consistent with the recent proposal of THOMPSON *et al.* (1984) that some potassic volcanism is derived from subducted sediments. In particular, the trace element characteristics of the Spanish lavas resemble those of arc lavas and isotopic compositions overlap with those of modern sediments. Although Western Australian, Gaussberg and Virungan ultrapotassic volcanism cannot be obviously related to any modern subduction zone, the antiquity of the source enrichments indicated by the isotopic data suggest that subduction processes cannot be discounted. Isotopic modelling and further discussion of the possible involvement of subducted sediments in the genesis of ultrapotassic magmatism will be published at a later date.

3. *Subducted "megaliths"*: Oceanic crust and sediments subducted into the mantle and having residence times of $\approx$1 byrs (HOFMANN and WHITE, 1982; RINGWOOD, 1982). Partial melting of the megalith may cause incompatible element enriched diapirs to rise upward, contaminating the overlying regions of the mantle and eventually manifesting as hotspots in oceanic regions or, in the continental environment, as alkaline volcanism. The involvement of sedimentary material or the long timescales involved during storage of the megalith in the mantle could result in isotopic characteristics indicative of long term incompatible element enrichment. While many ocean islands bear little isotopic resemblance to continental potassic volcanism, lavas from Kerguelen and Society islands have Sr and Nd isotopic compositions extending into the "enriched" quadrant on the Sr-Nd isotope diagram and have generally higher $^{207}Pb/^{204}Pb$ than MORB (WHITE, 1985). These isotope characteristics are similar to those of the New South Wales leucitites, which may also be products of hotspot volcanism.

It is probable that no single origin is responsible for all of the various ancient components identified in representatives of the ultrapotassic suite. That most isotopically evolved potassic volcanism (*e.g.* Western Australian, Gaussberg, Virungan, Leucite Hills, mi-

caceous South African) is confined to old cratons is strong indirect evidence that the continental lithosphere acts as a site of long term storage of enriched mantle components. In a discussion of models of subcontinental lithospheric growth, BROOKS *et al.* (1976) suggested that mantle plumes rising beneath continents may underplate the subcontinental lithosphere and are later reactivated, appearing as isotopically evolved continental alkaline magmatism. Differences in the time elapsed between underplating and reactivation events might then explain the range in isotopic characteristics observed in continental alkaline lavas. Alternatively, mantle plumes may be responsible for the reactivation of pre-existing enriched subcontinental lithosphere. In this case, the age of the subcontinental lithosphere will determine the isotopic character of subsequent volcanism.

The Sr, Nd and Pb isotopic characteristics of Gaussberg leucitites and Western Australian lamproites are unlike any previously identified, lying off the mantle plane of ZINDLER *et al.* (1982). Their high $^{207}Pb/^{204}Pb$ and low $^{206}Pb/^{204}Pb$ contrasts with the Pb isotopic compositions found in ocean islands, which define a linear array of positive slope extending from the unradiogenic Pb field of MORB to the high $^{207}Pb/^{204}Pb$ and $^{206}Pb/^{204}Pb$ of St. Helena and Tubuai. The ocean island array lies to the right of the geochron (on which all present-day single stage Pb should lie, assuming an initial Pb isotopic composition like that of Canyon Diablo troilite lead), indicating that the sources of ocean islands have undergone an increase in U/Pb within the last $\approx$2.5 byrs or less. The geochemical history of the metasomatic components of Gaussberg leucitites and Western Australian lamproites inferred from their Pb isotopic characteristics differs from that inferred for ocean islands because of the ancient fractionation events which lowered U/Pb. Although the position of MORB and ocean island Pb to the right of the geochron has been attributed to the progressive loss of Pb from the mantle to the Earth's core, the existence within the subcontinental lithosphere of substantial reservoirs of low $^{206}Pb/^{204}Pb$ components with moderate to high $^{207}Pb/^{204}Pb$ like those identified in this study may also explain the position of the ocean island array relative to the geochron, as such low U/Pb reservoirs can also compensate for the general increase of U/Pb in the sources of ocean islands.

Acknowledgements—We have benefitted from discussions with and the constructive comments of Prof. A. E. Ringwood, A. L. Jaques (B.M.R.), W. F. McDonough, W. Compston, J. R. Richards and P. D. Kinny (RSES). Excellent reviews by J.-G. Schilling, R. Vollmer and an anonymous reviewer are gratefully acknowledged. B. Chappell and A. L. Jaques generously provided some of the WA lamproite U, Th and Pb concentration data. We would also like to thank C.R.A. Exploration Pty Ltd, A. J. Crawford (Univ. of Tasmania), J. D. Lewis (G.S.W.A.), E. Nakamura (Univ. of Toronto), K. D. Collerson (Univ. of Regina), A. Cundari (Univ. of Melbourne), H. D. Hensel (A.N.U.) and L. Sutherland (Aust. Museum) for provision of samples. S.-S. Sun publishes with the permission of the Director, B.M.R. This work was supported by a Commonwealth Government Research Scholarship to D. R. Nelson.

Editorial handling: J. D. Macdougall

REFERENCES

ALLÈGRE C. J., RICHARD P., TREUIL M. and JORON J. L. (1979) Neodymium-strontium-lead isotopes and magmatophile elements (Zr, Hf, Ta, Th, U, Ba, Cs, Rb) in east–west Japan traverse. Consequences for island arc magmatism. (abstr.) *EOS, Trans. Amer. Geophys. Union* **60**, 413–414.

ARANA V. and VEGAS R. (1974) Plate tectonics and volcanism in the Gibraltar arc. *Tectonophysics* **24**, 197–212.

ATKINSON W. J., HUGHES F. E. and SMITH C. B. (1984) A review of the kimberlitic rocks of Western Australia. In *Kimberlites and Related Rocks* (ed. J. KRONPROBST), pp. 195–224.

BELLON H. and LETOUSEY J. (1977) *Volcanism Related to Plate-Tectonics in the Western and Eastern Mediterranean Basins.* pp. 165–184. Technip, Paris.

BIRCH W. D. (1978) Mineralogy and geochemistry of the leucitite at Cosgrove, Victoria. *J. Geol. Soc. Aust.* **25(7)**, 369–385.

BREVART O., DUPRÉ B. and ALLÈGRE C. J. (1986) Lead-lead age of komatiitic lavas and sulphides from Barberton, Munro Township and Cape Smith, and the mantle growth curve. *Earth Planet. Sci. Lett.* (in press).

BROOKS C., JAMES D. E. and HART S. R. (1976) Ancient lithosphere: Its role in young continental volcanism. *Science* **193**, 1086–1094.

CATANZARO E. J., MURPHY T. J., SHIELDS W. R. and GARNER E. L. (1968) Absolute isotopic abundance ratios of common, equal atom, and radiogenic lead isotopic standards. *J. Res. Nat. Bur. Stand. (U.S.)* **72A**, 261–267.

CHASE C. G. (1981) Oceanic island Pb: Two stage histories and mantle evolution. *Earth Planet. Sci. Lett.* **52**, 277–284.

COHEN R. S. and O'NIONS R. K. (1982a) The lead, neodymium and strontium isotopic structure of ocean ridge basalts. *J. Petrol.* **23**, 299–324.

COHEN R. S. and O'NIONS R. K. (1982b) Identification of recycled continental material from Sr, Nd and Pb isotope investigations. *Earth Planet. Sci. Lett.* **61**, 73–84.

COLLERSON K. D. and MCCULLOCH M. T. (1983) Nd and Sr isotope geochemistry of leucite-bearing lavas from Gaussberg, East Antarctica. *Proc. 4th Symp. Antarctic Earth Sci.*, 676–680.

COOPER J. A. and GREEN D. H. (1969) Lead isotope measurements on lherzolite inclusions and host basanites from western Victoria, Australia. *Earth Planet. Sci. Lett.* **6**, 69–76.

CUMMING G. L. and RICHARDS J. R. (1975) Ore lead isotope ratios in a continuously changing Earth. *Earth Planet. Sci. Lett.* **28**, 155–171.

CUNDARI A. (1973) Petrology of the leucite-bearing lavas in New South Wales. *J. Geol. Soc. Aust.* **20(4)**, 465–492.

CUNDARI A. (1979) Petrogenesis of leucite-bearing lavas in the Roman volcanic region, Italy. The Sabatini lavas. *Contrib. Mineral. Petrol.* **70**, 9–21.

DICKINSON W. R. and HATHERTON T. (1967) Andesitic volcanism and seismicity around the Pacific. *Science* **157**, 801–803.

DOSSO L., VIDAL P., CANTAGREL J. M., LAMEYRE J. and MAROT S. Z. (1979) "Kerguelen: continental fragment or ocean island?": Petrology and isotopic geochemistry evidence. *Earth Planet. Sci. Lett.* **43**, 44–60.

DUNCAN R. A. (1981) Hotspots in the southern oceans—an absolute frame of reference for motion of the Gondwana continents. *Tectonophysics* **74**, 29–42.

DUPRÉ B. and ALLÈGRE C. J. (1980) Pb-Sr-Nd isotopic correlation and chemistry of North Atlantic mantle. *Nature* **286**, 17–22.

DUPRÉ B., CHAUVEL C. and ARNDT N. T. (1984) Pb and Nd isotopic study of two Archean komatiitic flows from Alexo, Ontario. *Geochim. Cosmochim. Acta* **48**, 1965–1972.

EDGAR A. D. (1980) Role of subduction in the genesis of leucite-bearing rocks: Discussion. *Contrib. Mineral. Petrol.* **73**, 429–431.

EGGLER D. H. (1978) The effect of CO_2 upon partial melting of peridotite in the system Na_2O-CaO-Al_2O_3-MgO-SiO_2-CO_2 to 34 Kb, with an analysis of melting in a peridotite-H_2O-CO_2 system. *Amer. J. Sci.* **278**, 305–343.

FODEN J. D. and VARNE R. (1980) The petrology and tectonic setting of Quarternary-Recent volcanic centres of Lombok and Sumbawa, Sunda arc. *Chem. Geol.* **30**, 201–226.

FOLEY S. F., TAYLOR W. R. and GREEN D. H. (in press) The effects of fluorine on phase relationships in the system $KAlSiO_4$-$MgSiO_4$-SiO_2 with application to the genesis of ultrapotassic rocks. *Contrib. Mineral. Petrol.* (in press).

FRASER K. J., HAWKESWORTH C. J., ERLANK A. J. and MITCHELL R. H. (1985) Sr, Nd and Pb isotope and minor element geochemistry of lamproites and kimberlites. (abstr.) *Terra Cognita* **5**(2–3), 275.

GREEN D. H. (1976) Experimental petrology in Australia—a review. *Earth Sci. Rev.* **12**, 99–138.

HAWKESWORTH C. J. and VOLLMER R. (1979) Crustal contamination versus enriched mantle: $^{143}Nd/^{144}Nd$ and $^{87}Sr/^{86}Sr$ evidence from the Italian volcanics. *Contrib. Mineral. Petrol.* **69**, 151–165.

HOFMANN A. W. and WHITE W. M. (1982) Mantle plumes from ancient oceanic crust. *Earth Planet. Sci. Lett.* **57**, 421–436.

HOLM P. M. and MUNKSGAARD N. C. (1982) Evidence for mantle metasomatism: an oxygen and strontium isotope study of the Vulsinian District, Central Italy. *Earth Planet. Sci. Lett.* **60**, 376–388.

JAQUES A. L., LEWIS J. D., SMITH C. B., GREGORY G. P., FERGUSON J., CHAPPELL B. W. and MCCULLOCH M. T. (1984a) The diamond-bearing ultrapotassic (lamproitic) rocks of the West Kimberley region, Western Australia. In *Kimberlites and Related Rocks* (ed. J. KRONPROBST), pp. 225–254.

JAQUES A. L., WEBB A. W., FANNING C. M., BLACK L. P., PIDGEON R. T., FERGUSON J., SMITH C. B. and GREGORY G. P. (1984b) The age of the diamond-bearing pipes and associated leucite lamproites of the West Kimberley region, Western Australia. *B.M.R. J. Geol. Geophys.* **9**, 1–7.

KESSON S. E. (1973) The primary geochemistry of the Monaro alkaline volcanics, southeastern Australia—Evidence for upper mantle heterogeneity. *Contrib. Mineral. Petrol.* **42**, 93–108.

KURASAWA H. (1968) Isotopic composition of lead and concentrations of uranium, thorium, and lead in volcanic rocks from Dogo and the Oki Islands, Japan. *Geochem. J.* **2**, 11–28.

LLOYD F. E. and BAILEY D. K. (1975) Light element metasomatism of the continental mantle: the evidence and the consequences. *Phys. Chem. Earth* **9**, 389–416.

MCCULLOCH M. T. and CHAPPELL B. W. (1982) Nd isotopic characteristics of S- and I-type granites. *Earth Planet. Sci. Lett.* **58**, 51–64.

MCCULLOCH M. T., JAQUES A. L., NELSON D. R. and LEWIS J. D. (1983) Nd and Sr isotopes in kimberlites and lamproites from Western Australia: an enriched mantle origin. *Nature* **302**, 400–403.

MCDONOUGH W. F., MCCULLOCH M. T. and SUN S.-S. (1985) Isotopic and geochemical systematics in Tertiary-Recent basalts from southeastern Australia and implications for the evolution of the sub-continental lithosphere. *Geochim. Cosmochim. Acta* **49**, 2051–2068.

MENZIES M. A. and MURTHY R. (1980) Enriched mantle: Nd and Sr isotopes in diopsides from kimberlite nodules. *Nature* **283**, 634–636.

NAKAMURA E., CAMPBELL I. H. and SUN S.-S. (1985) The influence of subduction processes on the geochemistry of Japanese alkaline basalts. *Nature* **316**, 55–58.

NICHOLLS I. A. and WHITFORD D. J. (1978) Geochemical zonation in the Sunda volcanic arc, and the origin of K-rich lavas. *Bull. Aust. Soc. Explor. Geophys.* **9**, 93–98.

NIXON P. H., THIRWALL M. F., BUCKLEY F. and DAVIES C. J. (1984) Spanish and Western Australian lamproites: aspects of whole rock geochemistry. In *Kimberlites and Related Rocks* (ed. J. KRONPROBST), pp. 285–296.

NOBEL F. A., ANDRIESSEN P. A. M., HEBEDA E. H., PRIEM H. N. A. and RONDEEL H. E. (1981) Isotopic dating of the post-alpine Neogene volcanism in the Betic Cordilleras, southern Spain. *Geol. Mijnb.* **60**, 209–214.

O'REILLY S. Y. and GRIFFIN W. L. (1984) Sr isotopic heterogeneity in primitive basaltic rocks, southeastern Australia: correlation with mantle metasomatism. *Contrib. Mineral. Petrol.* **87**, 220–230.

POWELL J. L. and BELL K. (1970) Strontium isotopic studies of alkalic rocks. Localities from Australia, Spain, and the western United States. *Contrib. Mineral. Petrol.* **27**, 1–10.

RICHARDSON S. H., GURNEY J. J., ERLANK A. L. and HARRIS J. W. (1984) Origin of diamonds in old enriched mantle. *Nature* **310**, 198–202.

RINGWOOD A. E. (1982) Phase transformations and differentiation in subducted lithosphere: implications for mantle dynamics, basalt petrogenesis and crustal evolution. *J. Geol.* **90**, 611–643.

RODDICK J. C. (1984) Emplacement and metamorphism of Archaean mafic volcanics at Kambalda, Western Australia—geochemical and isotopic constraints. *Geochim. Cosmochim. Acta* **48**, 1305–1318.

SHERATON J. W. and CUNDARI A. (1980) Leucitites from Gaussberg, Antarctica. *Contrib. Mineral. Petrol.* **71**, 417–427.

SMITH C. B. (1983) Pb, Sr and Nd isotopic evidence for sources of southern African Cretaceous Kimberlites. *Nature* **304**, 51–54.

STEIGER R. H. and JAGER E. (1977) Subcommission on geochronology: convention on the use of decay constants in geo- and cosmochronology. *Earth Planet. Sci. Lett.* **36**, 359–362.

SUN S.-S. (1980) Lead isotopic study of young volcanics from mid-ocean ridges, ocean islands and island arcs. *Phil. Trans. Roy. Soc. London* A **297**, 409–445.

SUTHERLAND F. L. (1983) Timing, trace and origin of basaltic migration in eastern Australia. *Nature* **305**, 123–126.

TATSUMOTO M. (1973) Time differences in the formation of meteorites as determined from the ratio of lead-207 to lead-206. *Science* **180**, 1279–1283.

TATSUMOTO M. and KNIGHT R. J. (1969) Isotopic composition of lead in volcanic rocks from central Honshu- with regard to basalt petrogenesis. *Geochem. J.* **3**, 53–86.

TAYLOR H. P. and TURI B. (1976) High ^{18}O igneous rocks from the Tuscan magmatic Province, Italy. *Contrib. Mineral. Petrol.* **55**, 33–54.

TAYLOR H. P., TURI B. and CUNDARI A. (1984) $^{18}O/^{16}O$ and chemical relationships in K-rich volcanic rocks from Australia, East Africa, Antarctica, and San Venanzo-Cupaello, Italy. *Earth Planet. Sci. Lett.* **69**, 263–276.

THOMPSON R. N., MORRISON M. A., HENDRY G. L. and PARRY S. J. (1984) An assessment of the relative roles of crust and mantle in magma genesis: an elemental approach. *Phil. Trans. Roy. Soc. London* A **310**, 549–590.

TILTON G. R. (1983) Evolution of depleted mantle: the lead perspective. *Geochim. Cosmochim. Acta* **47**, 1191–1197.

TSUBOI S. (1920) On a leucite rock vulsinite vicoite from Utsuryoto Island in the sea of Japan. *Geol. Soc. Japan* **27**, 91–103.

VAN KOOTEN G. K. (1981) Pb and Sr systematics of ultrapotassic and basaltic rocks from central Sierra Nevada, California. *Contrib. Mineral. Petrol.* **76**, 378–385.

VENTURELLI G., CAPEDRI S., DI BATTISTINI G., CRAWFORD

A., KOGARKO L. N. and CELESTINI S. (1984) The ultrapotassic rocks of southeastern Spain. *Lithos* **7**, 37–54.

VOLLMER R. (1976) Rb-Sr and U-Th-Pb systematics of alkaline rocks: the alkaline rocks of Italy. *Geochim. Cosmochim. Acta* **40**, 283–295.

VOLLMER R. (1977) Isotopic evidence for genetic relations between acid and alkaline rocks in Italy. *Contrib. Mineral. Petrol.* **60**, 109–118.

VOLLMER R. and HAWKESWORTH C. J. (1980) Lead isotopic composition of the potassic rocks from Roccamonfina (South Italy) *Earth Planet. Sci. Lett.* **47**, 91–101.

VOLLMER R. and NORRY M. T. (1983) Possible origin of K-rich volcanic rocks from Virunga, East Africa, by metasomatism of continental crustal material: Pb, Nd and Sr isotopic evidence. *Earth Planet. Sci. Lett.* **64**, 374–386.

VOLLMER R., OGDEN P., SCHILLING J.-G., KINGSLEY R. H. and WAGGONER D. G. (1984) Nd and Sr isotopes in ultrapotassic volcanic rocks from the Leucite Hills, Wyoming. *Contrib. Mineral. Petrol.* **87**, 359–368.

WASS S. Y. and ROGERS N. W. (1980) Mantle metasomatism—precursor to continental alkaline volcanism. *Geochim. Cosmochim. Acta* **44**, 1811–1823.

WEDEPOHL K. H. and MURAMATSU Y. (1979) The chemical composition of kimberlites compared with the average composition of three basaltic magma types. In *Kimberlites, Diatremes and Diamonds* (eds. BOYD F. R. and MEYER H. O. A.), pp. 300–312. A.G.U. Washington.

WELLMAN P. (1973) Early Miocene potassium-argon age for the Fitzroy Lamproites of Western Australia. *J. Geol. Soc. Aust.* **19**, 471–474.

WELLMAN P. (1974) Potassium-argon ages on the Cainozoic volcanic rocks of Eastern Victoria. *J. Geol. Soc. Aust.* **21**, 359–376.

WELLMAN P. and MCDOUGALL I. (1974) Cainozoic igneous activity in eastern Australia. *Tectonophys.* **23**, 49–65.

WELLMAN P., CUNDARI A. and MCDOUGALL I. (1970) Potassium-argon ages for leucite-bearing rocks from New South Wales, Australia. *J. Proc. Roy. Soc. N.S.W.* **103**, 103–107.

WENDLANDT R. F. (1984) An experimental and theoretical analysis of partial melting in the system $KAlSiO_4$-CaO-MgO-SiO_2-CO_2 and applications to the genesis of potassic magmas, carbonatites and kimberlites. In *Kimberlites and Related Rocks* (ed. J. KRONPROBST), pp. 359–369.

WHITE W. M. (1985) Sources of oceanic basalts: radiogenic isotopic evidence. *Geology* **13**, 115–118.

WHITFORD D. J. (1975) Strontium isotopic studies of the volcanic rocks of the Sunda arc, Indonesia, and their petrogenetic implications. *Geochim. Cosmochim. Acta* **39**, 1287–1302.

WHITFORD D. J., FODEN J. D. and VARNE R. (1978) Sr isotope geochemistry of calc-alkaline and alkaline lavas from the Sunda arc in Lombok and Sumbawa, Indonesia. *Carnegie Inst. Wash. Yearb.* **77**, 613–620.

WHITFORD D. J., WHITE W. M. and JEZEK P. A. (1981) Neodymium isotopic composition of Quarternary island arc lavas from Indonesia. *Geochim. Cosmochim. Acta* **45**, 989–995.

WILKINSON J. F. K. (1977) Analcime phenocrysts in a vitrophyric analcimite—primary or secondary? *Contrib. Mineral. Petrol.* **64**, 1–10.

ZINDLER A., JAGOUTZ E. and GOLDSTEIN S. (1982) Nd, Sr and Pb isotopic systematics in a three-component mantle: a new perspective. *Nature* **298**, 519–523.

ZINDLER A., STAUDIGEL H. and BATIZA R. (1984) Isotope and trace element geochemistry of young Pacific seamounts: implications for scale of upper mantle heterogeneity. *Earth Planet. Sci. Lett.* **70**, 175–195.

Reprinted from Nature, Vol. 322, No. 6079, pp. 534-538, 7 August 1986

Plume versus lithospheric sources for melts at Ua Pou, Marquesas Islands

R. A. Duncan*‡, M. T. McCulloch*, H. G. Barsczus† & D. R. Nelson*

* Research School of Earth Sciences, The Australian National University, Canberra, ACT 2601, Australia
† ORSTOM, Centre de Papeete Tahiti, French Polynesia, and Géologique et Géophysique du CCNRS, USTL, Montpellier, France
§ Permanent address: College of Oceanography, Oregon State University, Corvallis, Oregon 97331, USA

The remarkable distinction between the compositions of ocean island basalts (OIBs) and mid-ocean ridge basalts (MORBs) provides an important constraint on models of mantle composition and structure[1-3]. Previous studies of OIBs[4-8], however, have emphasized regional isotopic variations, often relying on a small number of samples from many separate volcanoes. Although this type of sampling has now established the basic range of isotopic variations, with the notable exception of the Hawaiian Islands[6,9,10], there is little information on either spatial or temporal variations within a single volcano. Here we report isotopic (Sr, Nd and Pb) and K–Ar age measurements for tholeiites, alkali basalts and differentiated rocks from the island of Ua Pou. In this island volcanism spanned the interval from 5.6 to 1.8 Myr, with the ratio of highly to moderately incompatible trace elements increasing with time; however, in contrast to Hawaii, $^{87}Sr/^{86}Sr$ and $^{207}Pb/^{204}Pb$ increased while $^{143}Nd/^{144}Nd$ decreased from the tholeiitic to alkalic magmas. The total variation in isotopic composition within this single island is nearly as great as within the entire French Polynesian region[8,11,12], and argues against systematic geographical correlations[13].

The island of Ua Pou, at 9°24′ S, 140°04′ W, is one of a chain of more than 20 volcanic islands and seamounts which constitute the Marquesas archipelago in the south-central Pacific Basin (Fig. 1). These volcanoes are linearly arrayed in a WNW–ESE direction, sub-parallel with other young intra-plate Pacific island chains. This characteristic geometry and the reported southeasterly progression in volcano ages[14,15], from 6.3 to 1.4 Myr, has linked Marquesan volcanism to a hotspot origin.

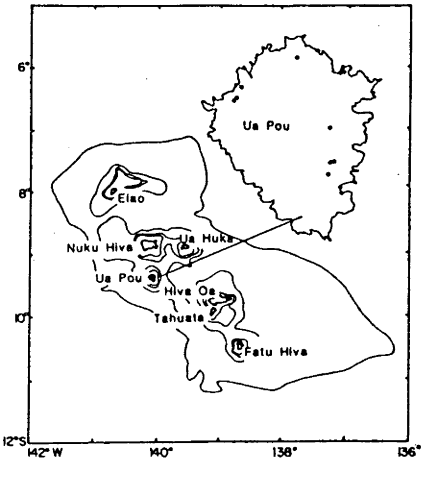

Fig. 1 Map of the Marquesas Islands, an age-progressive volcanic lineament in the south-central Pacific basin, showing the island of Ua Pou. Solid circles (on the enlarged map of the island) mark the location of samples (tholeiites, alkali basalts and differentiates) analysed in the present study.

The abyssal (>4,000 m) ocean floor on which these islands were constructed formed at the Galapagos Rise (ancestral East Pacific Rise) between 50 and 60 Myr (ref. 16).

Ua Pou hosts a particularly wide range of rock compositions, from tholeiitic to alkalic basalts; the latter have undergone low-pressure fractionation towards trachytic and phonolitic rocks[17,18]. Although tholeiites are the main rock type in the Hawaiian islands[19], they have not been reported elsewhere in the French Polynesian region; their occurrence in the initial stage of volcanism at Ua Pou suggests that tholeiitic eruptions may occur throughout this region, but may be almost totally confined to submarine portions of the volcanoes.

We report here age determinations for rocks from Ua Pou. Previous age studies[14] on other islands from the Marquesas chain have documented an age progression in volcanism from north-west to south-east at a rate of ~10.4 cm yr^{-1} (ref. 9). From this regular age distribution along the lineament, the expected age range at Ua Pou is 4.0–2.7 Myr. Re-examination[20] of the published age data showed that at the islands of Nuku Hiva and Hiva Oa dated rocks defined two age groups separated by about the same timespan, 0.6 Myr. Furthermore, at each island the older group was predominantly olivine tholeiite while the younger group was alkali basalt. To investigate this apparent petrogenetic evolution at individual Marquesan volcanoes, additional sampling was undertaken by one of us (H.G.B.).

Ua Pou does not exhibit the central collapsed caldera commonly seen at other Marquesas Islands; instead, the island's centre is a complex zone of high-level intrusions of trachytic and phonolitic rocks which have obscured the early shield structure of the volcano. Shield lavas outcrop around the perimeter of the island, in stream valleys, in road cuts and along wave-cut cliffs. The samples analysed in this study are well distributed, coming from the northwestern, northern and eastern sides of the island (Fig. 1).

Initial studies[18] of trace element compositions of tholeiites and alkali basalts collected from Ua Pou revealed striking differences in the inferred source compositions for the two groups. Rocks which plot as tholeiites in a standard alkalis versus silica diagram predate the alkali basalt assemblage. The tholeiitic phase of volcanism (5.6–4.5 Myr) is separated from the alkali basalt eruptions (2.9–2.7 Myr) and subsequent flows and intrusions of liquids evolved by high-level fractional crystallization (2.5–1.8 Myr). The entire age range of subaerial volcanism at Ua Pou is ~3.8 Myr (Table 1). The apparent 1.6-Myr hiatus between the tholeiitic and alkalic stages of volcanism could be the result of incomplete sampling and may be reduced by future geochronological studies on well-mapped sections. The progression from tholeiitic to alkalic volcanism at Ua Pou and its likelihood at the neighbouring islands of Nuku Hiva and Hiva Oa[20] is reminiscent of the volcanic evolution of the Hawaiian Islands[19]. In the Marquesas Islands, however, no very undersaturated, post-erosional eruptions have followed the alkali basalt stage. It is probable, therefore, that each of the Marquesas islands evolved through a common sequence. Initially, eruptions may have been a mixture of tholeiitic and alkalic compositions, as seen at Macdonald[21] seamount at the southeastern end of the Austral Islands, and Loihi seamount[22] in the Hawaiian Islands. Tholeiitic compositions dominated the early shield-building phase, which at Ua Pou barely reached sea level. This was followed by eruptions of alkali basalt and, later, highly evolved rocks. It is not yet known whether the change from tholeiites to alkali basalts occurred as a gradual transition or as a sharp compositional break after a significant hiatus in volcanic activity.

Major and trace element concentrations for Ua Pou rocks have been reported elsewhere[17,18]. Liotard *et al.*[18] identified tholeiitic rocks at many of the Marquesas Islands and, in particular, quartz-normative tholeiites at Ua Pou, in addition to the earlier described alkali basalts. The tholeiites and alkali basalts cannot be related to one another by either variable partial melting from a common source or fractional crystallization from a parental melt, because of many clear differences in their trace

2

Table 1 Sr, Nd and Pb isotopic compositions and K-Ar ages for volcanic rocks from Ua Pou, Marquesas Islands

Samples	Rock type	K (%)	Rb (p.p.m.)	Sr (p.p.m.)	Sm (p.p.m.)	Nd (p.p.m.)	$^{87}Sr/^{86}Sr$	$^{143}Nd/^{144}Nd$	ε_{Nd}	$^{206}Pb/^{204}Pb$	$^{207}Pb/^{204}Pb$	$^{208}Pb/^{204}Pb$	K-Ar age (Myr) $\pm 1\sigma$
UAP-011	Tholeiite	0.554	15	548	10.3	43.3	0.70289 ± 2	0.512070 ± 12	+4.6	19.50	15.54	39.15	4.46 ± 0.07
UAP-017	Tholeiite	0.204	3	434	10.0	40.3	0.70294 ± 4	0.512118 ± 16	+5.5	19.39	15.54	38.99	4.51 ± 0.14
UAP-024	Tholeiite	0.651	11	610	13.0	57.6	0.70318 ± 5	0.512084 ± 24	+4.8	19.45	15.55	39.01	5.61 ± 0.06
UAP-001	Alkali basalt	0.871	41	985	11.4	71.4	0.70500 ± 5	0.511944 ± 27	+2.1				2.75 ± 0.03
UAP-002	Alkali basalt	0.554	76	904	11.8	62.4	0.70497 ± 5						2.78 ± 0.03
UAP-003	Alkali basalt	0.855	40	972	11.3	61.5	0.70482 ± 5						2.70 ± 0.06
UAP-010	Alkali basalt	1.039	145	1,235	13.3	76.0	0.70509 ± 5	0.511867 ± 14	+0.6	19.18	15.65	39.31	2.70 ± 0.04
UAP-026	Alkali basalt	0.524	84	910	11.5	60.7	0.70497 ± 5	0.511876 ± 20	+0.8	19.14	15.64	39.20	2.88 ± 0.08
UAP-012	Tephrite	2.640	116	1,373	15.3	84.6	0.70515 ± 5	0.511918 ± 10	+1.6				2.24 ± 0.05
UAP-015	Hawaiite	2.643	241	1,358	7.9	48.6	0.70481 ± 5	0.511907 ± 12	+1.4	19.36	15.65	39.35	1.78 ± 0.03
UAP-025	Mugearite	4.276	72	1,282	13.0	52.2	0.70531 ± 6	0.511891 ± 25	+1.1				2.49 ± 0.03
UAP-004	Trachyte						0.70508 ± 5						
UAP-019	Phonolite	5.693	240	146	15.3	108.0	0.70497 ± 4	0.511917 ± 22	+1.6				2.42 ± 0.04
UAP-037	Phonolite	5.887	235	136	6.9	52.8	0.70474 ± 5						2.42 ± 0.03

$^{87}Sr/^{86}Sr$ and $^{143}Nd/^{144}Nd$ ratios are normalized to $^{86}Sr/^{88}Sr = 0.1194$ and $^{146}Nd/^{142}Nd = 0.636151$, K-Ar ages were calculated using the following decay and abundance constants: $\lambda_\varepsilon = 0.581 \times 10^{-10}$ yr^{-1}; $\lambda_\beta = 4.963 \times 10^{-10}$ yr^{-1}; $^{40}K/K = 1.167 \times 10^{-4}$ mol mol^{-1} respectively. For the standard NBS 987, $^{87}Sr/^{86}Sr = 0.71023$ and for BCR-1 $^{143}Nd/^{144}Nd = 0.511833$. Rb, Sr, Sm and Nd concentrations are from ref. 18.

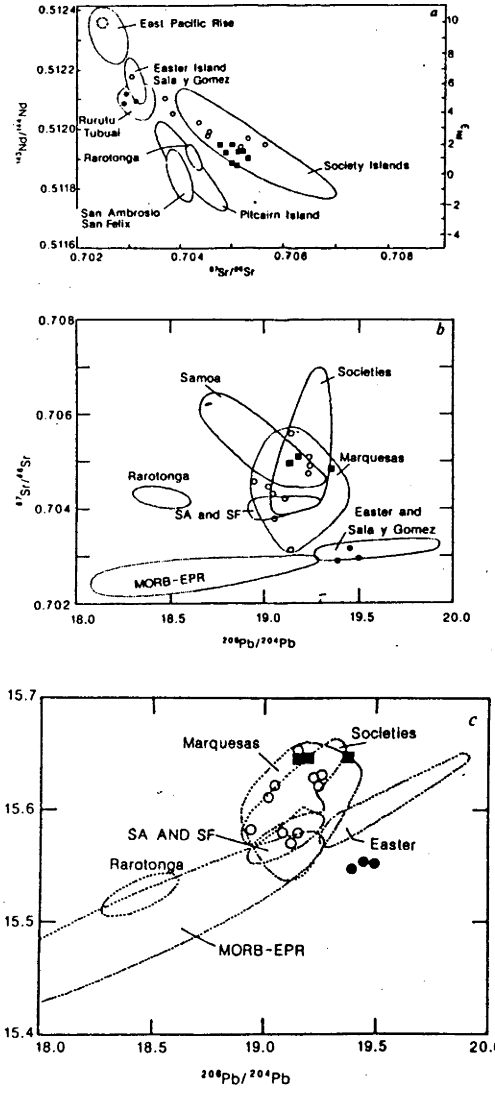

element patterns. Both groups are enriched in light rare earth elements, relative to MORBs, but whereas the alkali basalts exhibit uniformly steep patterns, the tholeiitic samples show much flatter profiles between La and Sm. The tholeiite trace element patterns are similar in shape to those for Hawaiian tholeiites[23,24], with normalized La ≃ normalized Ce, but abundances are higher in Ua Pou tholeiites. Tholeiites and alkali basalts at Ua Pou can also be distinguished by Zr/Nb (11.3 versus 4.8, average values, respectively), La/Nb (0.85 versus 0.98) and La/Ce (0.37 versus 0.51). In addition, on a spidergram diagram the tholeiites show significant depletions of Ba, Rb, Th, K and Sr relative to La.

To characterize further the two magma types present at Ua Pou, we have measured Sr, Nd and Pb isotopic compositions (Table 1). Previous isotopic studies of Marquesas Islands rocks[11,12,25] have not recognized the importance of the tholeiites, nor have they examined the compositional variation with age at a single island. Our results are in excellent agreement with the isotopic analyses of alkali basalts from Ua Pou reported by Vidal *et al.*[12]. The data were obtained using separation techniques and mass spectrometric analysis, as described in refs 26 (Sr and Nd) and 27 (Pb). Measured Sr, Nd and Pb isotopic ratios are generally within the analytical uncertainty of initial ratios because of the young age of the samples. Corrections to $^{87}Sr/^{86}Sr$ were applied only to the high Rb/Sr phonolite samples. Our results are plotted on three diagrams: $^{143}Nd/^{144}Nd$ against $^{87}Sr/^{86}Sr$ (Fig. 2*a*), $^{87}Sr/^{86}Sr$ against $^{206}Pb/^{204}Pb$ (Fig. 2*b*), and $^{207}Pb/^{204}Pb$ against $^{206}Pb/^{204}Pb$ (Fig. 2*c*).

Tholeiites are distinguishable from alkali basalts and differentiated rocks using each of the three isotopic systems. The strontium composition of the tholeiites is among the least radiogenic reported from oceanic islands, while the alkali basalt $^{87}Sr/^{86}Sr$ values fall in the middle of the range for other Marquesas and Society Islands[8,11,12]. The corresponding $^{143}Nd/^{144}Nd$ values are also distinctive ($\varepsilon_{Nd} = 4.6$–5.5 for tholeiites verus 0.6–2.1 for alkali basalts) and, together with the Sr data, form an array parallel to the Society Islands compositions but oblique to the mantle array[5–8]. The extreme isotopic heterogeneity of the French Polynesian region has been noted, but at Ua Pou, as recognized for Nuku Hiva by Vidal *et al.*[12],

Fig. 2 Isotopic compositions of lavas from Ua Pou compared with those for other basaltic rocks from the south-central Pacific basin. *a*, $^{143}Nd/^{144}Nd$ versus $^{87}Sr/^{86}Sr$; *b*, $^{87}Sr/^{86}Sr$ verus $^{206}Pb/^{204}Pb$; *c*, $^{207}Pb/^{204}Pb$ versus $^{206}Pb/^{204}Pb$. Fields of data are from ref. 25 for islands and East Pacific Rise, except Rurutu and Pitcairn Islands[30]. Solid circles and squares are tholeiites and alkali basalts, respectively, from Ua Pou. Open circles are other analysed samples from the Marquesas Islands[12]. SA, San Ambrosio; SF, San Felix; EPR, East Pacific Rise.

nearly the entire range of variability exists on the scale of a single island. At Ua Pou the tholeiitic magmas have low $^{87}Sr/^{86}Sr$ ratios and moderate $^{143}Nd/^{144}Nd$ ratios, indicative of a mantle source with low time-integrated Rb/Sr and a (chondrite-normalized) Nd/Sm < 1. The later alkali basalt magmas have high $^{87}Sr/^{86}Sr$ and low $^{143}Nd/^{144}Nd$, which would derive from a less depleted mantle source. This contrasts with the Hawaiian Islands volcanism, where the tholeiites have higher $^{87}Sr/^{86}Sr$ and lower ϵ_{Nd} values than the alkali basalts and post-erosional lavas[9,10].

The Pb compositions of the two magma types are equally distinct, as seen in the $^{207}Pb/^{204}Pb$ versus $^{206}Pb/^{204}Pb$ diagram (Fig. 2c). The tholeiites are most similar to rocks from Easter and Sala y Gomez Islands near the East Pacific Rise[25], whereas the alkali basalts lie in the field of other reported Pb isotopic analyses from the Society and Marquesas Islands[12,25]. The Pb isotopic compositions of the Ua Pou tholeiites are not as extreme as those of rocks from Tubuai[12] (Austral Islands) which exhibit similar low $^{87}Sr/^{86}Sr$ and moderate ϵ_{Nd}. They are similar, however, to analysed rocks from Rimatara[28] and Rurutu[29], neighbouring volcanoes in the Austral Islands.

There has been much recent interest in the geographical distribution of isotopic compositions at oceanic islands, culminating in the Dupal anomaly proposal[13], which postulates a region of higher $^{87}Sr/^{86}Sr$, $^{207}Pb/^{204}Pb$ and $^{208}Pb/^{204}Pb$, circling the globe at ~30° S. The new isotopic data for Ua Pou presented here do not, however, support this view. The Marquesas Islands lie within the proposed Dupal anomaly belt, but only the alkali basalts have the appropriate radiogenic compositions. Apparently both Dupal and non-Dupal mantle reservoirs have been tapped at Ua Pou. The same sequence might also be seen at other French Polynesian islands, if the suspected early tholeiite phase of volcanism could be sampled. Hence, the regional significance of the Dupal anomaly, at least in this area, is questionable (see also refs 8, 26, 30).

It is evident from trace element and isotopic compositions that the tholeiites and alkali basalts at Ua Pou cannot be related by variable degrees of partial melting or crystal fractionation of primary melts from a common mantle or lithospheric source. Thus at least two, and probably three distinct source end-member compositions have contributed to volcanism at this island. In addition, the alkali basalts postdate the tholeiites in a clear age progression implying that the chemically distinct sources were tapped at different times. This suggests that the sources are not ubiquitous and continuously available for melting, but are likely to be physically separate. We will consider two possibilities for the spatial distribution of these source components: first, partial melting of both the mantle plume and the overlying lithosphere, and second, melting of the plume alone. In the first case the lithospheric mantle and plume have differing isotopic compositions and are the sources for the tholeiitic and alkali basalts respectively; in the second, both the alkalic and tholeiitic melts are derived from the plume, implying an isotopically heterogeneous plume.

The lower oceanic lithosphere probably consists of an unmelted mix of enriched mantle blobs and depleted asthenosphere which could possess considerable isotopic heterogeneity[26,31-33] (Fig. 3a). Samples from the East Pacific Rise exhibit a rather small range of $^{87}Sr/^{86}Sr$ and ϵ_{Nd} compositions (Fig. 2a), but are quite variable in $^{206}Pb/^{204}Pb$ composition[25,33] (Fig. 2b). Variation in these MORB compositions can be explained by mixing melts from depleted upper mantle with those from a small proportion of enriched mantle of the Rurutu/Tubuai type (low $^{87}Sr/^{86}Sr$, moderate ϵ_{Nd}, high $^{206}Pb/^{204}Pb$). Interestingly, rocks from Easter and Sala y Gomez Islands have compositions at the high-$^{206}Pb/^{204}Pb$ end of this trend[25] (Fig. 2b). Mantle upwelling in this region of the East Pacific Rise may be a major source for the enriched mantle blobs which became incorporated into the lower oceanic lithosphere by thickening of the plate during cooling away from the spreading centre.

At Ua Pou we propose that such heterogeneous oceanic lithosphere of 50–60 Myr age approached and crossed the Marquesas hotspot (Fig. 3a). Melts and heat from the mantle plume entered the lower lithosphere, where wall rock reached temperatures sufficient to melt. The plume and lithosphere melts could then mix to produce the magmas seen at the island. The trace element and isotopic compositions of the mixed magmas would vary depending on the degree of melting of each source and the proportions of melt contributed. At Ua Pou the isotopic composition of the early tholeiitic phase lies on a mixing line between MORB and Rurutu/Tubuai compositions, and reflects the proposed composition of the lower oceanic lithosphere beneath the island. Hence, in this model, melting of the lower lithosphere was significant and dominates the composition of tholeiitic magmas.

As the volcano migrated away from the hotspot, temperatures at the base of the lithosphere decreased. Smaller degrees of melting (of alkali basalt character) developed in the margin of

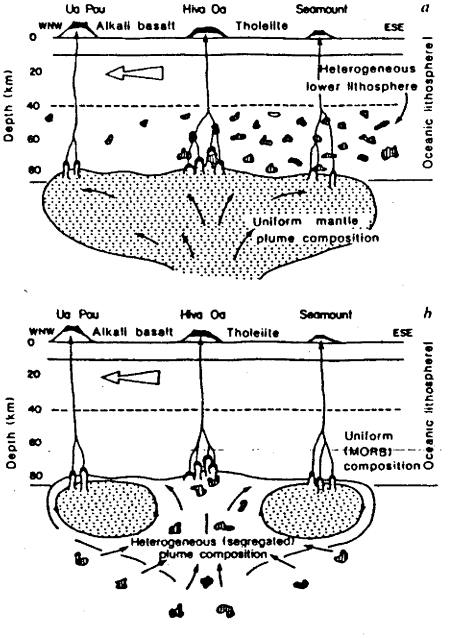

Fig. 3 Two models for the isotopically distinct magmas at Ua Pou, illustrated by vertical cross-sections along the line of the Marquesas Islands. Both models show volcanic activity at ~2.5 Myr, when alkali basalts erupted onto an older tholeiite shield at Ua Pou, concurrently with tholeiitic basalts at Hiva Oa and, possibly, with the initial seamount basalts beneath Fatu Hiva. *a*, Heterogeneous lower lithosphere. The plume (~400 km diameter) has a uniform, undepleted isotopic composition and is crossed by a Pacific plate composed of an upper section of uniform, MORB-like isotopic composition formed at the East Pacific Rise and an isotopically heterogeneous lower lithosphere accreted to the plate as it cooled away from the spreading ridge. Tholeiitic melts are formed over the centre of the plume as melts from the plume mix with melts from the lower-lithosphere wall rock. Alkali basalt melts erupt from the margin of the plume, where temperatures are cooler, and pass through previously heated lithosphere without significant contamination. *b*, Heterogeneous plume. The lithosphere has a uniform, MORB-like isotopic composition throughout and passes over a plume which has developed large-scale chemical heterogeneities by entraining depleted upper mantle material during its diapiric rise[34]. The original plume material concentrates in a torus around the plume margin (shaded), while entrained material flows into the centre[35]. Hence tholeiitic melts from the plume centre are MORB-like in isotopic character, whereas alkali basalt melts from the margin are more like the original plume. The lower lithosphere may melt but the isotopic differences in erupted magmas are controlled by heterogeneities in the plume.

the plume (Fig. 3*a*). These melts passed through the same column of oceanic lithosphere which had earlier yielded its low-temperature melting fraction; hence, the wall rock was much more refractory and less assimilation occurred at this stage, so that the alkali basalt compositions essentially reflect the isotopic composition of the plume. Contemporaneous with this phase of Ua Pou volcanism was tholeiitic, shield-building volcanism at Hiva Oa, the next major volcano upstream, and perhaps the seamount phase at Fatu Hiva, another 100 km to the south-east. From this model we would expect the same correlation of trace element and isotopic composition with time to emerge at other Marquesas islands.

An analogous model for the origin of Hawaiian tholeiitic and alkali basalts has been proposed by Chen and Frey[9]. At Hawaii, however, there is an inverse correlation between $^{87}Sr/^{86}Sr$ and abundances of incompatible elements; that is, the tholeiitic phase is dominated by the composition of melts from the plume, whereas the alkali basalts are thought to reflect the composition of the lower lithosphere. This relationship is thought to result from small degrees of melting of the lower lithosphere and variable proportions of mixing with plume-derived melts[9]. Although lithosphere melting occurs during the tholeiitic phase, the volume of melts from the plume is sufficiently high that these determine the composition of Hawaiian tholeiites. During the formation of alkali basalt melts, however, very small (<1%) degrees of melting of the wall rock produce high concentrations of trace elements which dominate the composition of small-volume plume melts. Thus the isotopic composition of the Hawaiian alkali basalts reflects that of the lower lithosphere.

The source end-members for melting and magma mixing are different for the two island chains. At Ua Pou the enriched mantle, or plume composition, has $^{87}Sr/^{86}Sr > 0.7053$ and $\varepsilon_{Nd} < 0.5$ and lies to the right of the Sr–Nd mantle array. This may be similar to, but possibly not so extreme as, the plume component for Society Islands alkali basalt magmas[1,12]. The lower lithosphere beneath Hawaii, as reflected by the isotopic composition of the alkali basalts[9], does not appear to contain the Rurutu/Tubuai component seen in the Ua Pou tholeiites. This model therefore requires that the oceanic lithosphere of the Pacific plate has accreted mantle blobs of different isotopic character.

An alternative explanation for the isotopically distinct phases of tholeiitic and alkalic volcanism at Ua Pou is that heterogeneities occur within the plume or diapir itself. These heterogeneities may be either a consequence of initial heterogeneities in the plume source, or result from the incorporation of asthenospheric mantle material into the diapir during its ascent. Recent experimental and theoretical studies[34,35] have demonstrated that thermally activated diapirs will entrain a significant quantity of surrounding mantle material during their ascent. This is illustrated in Fig. 3*b*, where the central portion of the diapir consists of entrained depleted upper mantle (MORB-like plus mantle blobs), while the original plume material is contained in an outer torus. Tholeiitic melts are generated over the centre of the plume while smaller-volume alkali basaltic melts form over the perimeter. If isotopic heterogeneities are distributed uniformly through the diapir, then isotopically distinct magmas could be formed by variable degrees of partial melting. Larger degrees of melting (tholeiite) would tend to homogenize the variable composition of the diapir, whereas smaller degrees of melting (alkali basalt) would emphasize the composition of incompatible-element rich segregations[31,32].

We thank W. F. McDonough for technical assistance and thoughtful discussions, and W. M. White for data in advance of publication. We also thank Y. and J. Hituputoka and J.-L. and C. Candelot for their assistance during fieldwork on Ua Pou. R.A.D. acknowledges the support of NSF and H.G.B. the support of ORSTOM.

Received 17 October 1985; accepted 9 April 1986.

1. White, W. M. & Hofman, A. W. *Nature* **296**, 821–825 (1982).
2. Davies, G. F. *Nature* **290**, 208–213 (1981).
3. Ringwood, A. E. *J. Geol.* **90**, 611–643 (1982).
4. *Basaltic Volcanism on the Terrestrial Planets* (eds Kaula, W. M. *et al.*) 161–192 (Pergamon, New York, 1981).
5. DePaolo, D. J. & Wasserburg, G. J. *Geophys. Res. Lett.* **3**, 743–746 (1976).
6. O'Nions, R. K., Hamilton, P. J. & Evensen, N. M. *Earth planet. Sci. Lett.* **34**, 13–22 (1977).
7. Richard, P., Shimizu, N. & Allègre, C. J. *Earth planet. Sci. Lett.* **31**, 269–278 (1976).
8. White, W. M. *Geology* **13**, 115–118 (1985).
9. Chen, C.-Y. & Frey, F. A. *Nature* **302**, 785–789 (1983).
10. Stille, P., Unruh, D. M. & Tatsumoto, M. *Nature* **304**, 25–29 (1983).
11. Duncan, R. A. & Compston, W. *Geology* **4**, 728–732 (1976).
12. Vidal, Ph., Chauvel, C. & Brousse, R. *Nature* **307**, 536–538 (1984).
13. Hart, S. R. *Nature* **309**, 753–757 (1984).
14. Duncan, R. A. & McDougall, I. *Earth planet. Sci. Lett.* **21**, 414–420 (1974).
15. Brousse, R. & Bellon, H. *C. r. hebd. Séanc. Acad. Sci., Paris* **278**, 827–830 (1974).
16. Epp, D. *J. geophys. Res.* **89**, 11273–11286 (1984).
17. Bishop, A. C. & Woolley, A. R. *Contr. Miner. Petrol.* **39**, 309–326 (1973).
18. Liotard, J. M., Barsczus, H. G., Dupuy, C. & Dostal, J. *Contr. Miner. Petrol.* **92**, 260–268 (1986).
19. Macdonald, G. A. & Katsura, T. *J. Petrol.* **5**, 82–133 (1964).
20. Barsczus, H. G. *Notes Doc. (Géophys.) ORSTROMA Papeete* **1981**, 1–22 (1981).
21. Barsczus, H. G & Liotard, J. M. *C.r. hebd. Séanc. Acad. Sci., Paris* **300**, 915–918 (1985).
22. Frey, F. A. & Clague, D. A. *Earth planet. Sci. Lett.* **66**, 337–355 (1983).
23. Leeman, W. P., Budahn, J. R., Gerlach, D. C., Smith, D. R. & Powell, B. N. *Am. J. Sci.* **280A**, 794–819 (1980).
24. Wright, T. L. *J. geophys. Res.* **89**, 3233–3252 (1984).
25. White, W. M. *EOS* **66**, 408 (1985).
26. McDonough, W. F., McCulloch, M. T. & Sun, S.-S. *Geochim. cosmochim. Acta* **49**, 2051–2068 (1985).
27. Nelson, D. R., McCulloch, M. T. & Sun, S.-S. *Geochim. cosmochim. Acta* **50**, 231–246 (1986).
28. Tatsumoto, M., Unruh, D. M., Stille, P. & Fujimaki, H. *Proc. 27th int. Geol. Congr.* **11**, 485–501 (1984).
29. Palacz, Z. & Saunders, A. D. *Abstr. int. Volcanol. Congr.* Feb., 194 (1986).
30. McDonough, W. F. *et al. Abstr. int. Volcanol. Congr.* Feb., 180 (1986).
31. Zindler, A., Staudigel, H. & Batiza, R. *Earth planet. Sci. Lett.* **70**, 175–195 (1984).
32. Staudigel, H. *et al. Earth planet. Sci. Lett.* **69**, 13–29 (1984).
33. Hamelin, B., Dupré, B. & Allègre, C. J. *Earth planet. Sci. Lett.* **67**, 340–350 (1984).
34. Griffiths, R. W. *Earth planet. Sci. Lett.* (submitted).
35. Griffiths, R. W. *Phys. Earth planet. Inter.* (submitted).

Printed in Great Britain by Turnergraphic Limited, Basingstoke, Hampshire

Geochemical and isotopic systematics in carbonatites and implications for the evolution of ocean-island sources

D.R. Nelson[1], A.R. Chivas[1], B.W. Chappell[2] and M.T. McCulloch[1]

[1] Research School of Earth Sciences, Australian National University, Canberra, A.C.T., 2601.

[2]Department of Geology, Australian National University, Canberra, A.C.T., 2601.

Abstract- Geochemical and Sr, Nd, Pb, O and C isotopic data are reported for 13 carbonatites from Africa, Australia, Brazil, Europe and the United States. The carbonatites possess generally high Ba, Th, LREE, Sr and low Cs, Rb, K and HREE abundances. Some examples have low Ti, Nb, Ta, P, Zr, Hf and U concentrations which are consistent with variable fractionation of sphene, apatite, perovskite, monazite or zircon. The samples range in age from Proterozoic to Tertiary and possess a range of initial Sr isotopic compositions between 0.7020 and 0.7054, initial ε_{Nd} values of -0.4 to +3.8 and (with the exception of the Brazilian Jacupiranga carbonatite) generally radiogenic initial Pb isotopic compositions. $\delta^{18}O_{SMOW}$ compositions of the intrusive carbonatites range from +5.5 to +12.4 ‰. Higher $\delta^{18}O_{SMOW}$ values of +14 and +17 ‰ are found in the volcanically-emplaced Proterozoic Goudini complex of South Africa, suggesting the involvement of secondary alteration processes. $\delta^{13}C_{PDB}$ ranges from -0.5 to -6.6 ‰ with samples having near-primary $\delta^{18}O_{SMOW}$ (between +5.5 and +8 ‰) possessing $\delta^{13}C_{PDB}$ between -2.9 to -6.6 ‰. On the initial Sr-Nd isotope diagram, most carbonatites plot below the mantle array and below or within the field characteristic of many ocean-island basalts. The Pb isotopic compositions of carbonatites generally lie along the array defined by oceanic basalts. The characteristics of carbonatites from a number of continents and their isotopic similarity to some ocean-island basalts favour an asthenospheric mantle "plume" origin. This conclusion suggests that some ocean-island alkali basalts may have been derived from trace-element-depleted mantle sources which have been re-fertilised by low-viscosity, trace-element-rich carbonatitic melts. The common close spatial and temporal association and the overlap in trace-element geochemistry and isotopic characteristics of Group 1 (basaltic) kimberlites and carbonatites argues strongly for a genetic relationship. Although secondary differentiation processes such as late-stage melt/vapour fractionation may play some role, the extreme LREE-enrichment typical of carbonatites requires their derivation by small degrees of melting ($<\approx 1\%$) from a garnet-rich eclogitic source. This source may originally have been CO_2- and volatile-rich subducted oceanic lithosphere.

INTRODUCTION

CARBONATITES are magmatic, carbonate-rich (>50 wt%) rocks characterised by high abundances of Sr, Ba, P and the light rare-earth elements. Examples have been reported from both continental settings, commonly associated with nephelinitic or kimberlitic igneous provinces, and more recently from oceanic settings, such as the Cape Verde and Canary Islands (ALLEGRE *et al.*, 1971; SILVA *et al.*, 1981; BARRERA *et al.*, 1981) and the Solomon Islands (NIXON and BOYD, 1979). Despite the interest these unusual rocks have attracted, their origin remains a perplexing petrogenetic problem. Earlier models favouring the syntexis of limestone are untenable in the light of subsequent isotopic studies. Other proposals have invoked such mechanisms as Na-rich carbonate/silicate liquid immiscibility (demonstrated experimentally by HAMILTON *et al.* 1979), fractional crystallisation from an alkaline silicate parent magma or extreme alkali metasomatism of silicate rocks during the differentiation of an intrusive ultrabasic magma. More recently, experimental evidence favours a primary igneous origin for carbonatitic magmas, emphasising the important role of CO_2 in their genesis. CO_2 is a major component in volcanic glasses and is probably contained in minor carbonate phases such as dolomite or magnesite in the upper mantle (BREY *et al.*, 1983). Experimental studies (e.g. WYLLIE and HUANG, 1976; WENDLANDT, 1984) indicate that, due to a rapid increase in the solubility of CO_2 and a concomittant lowering of the solidus temperature at pressures ≈25-30 kbar, partial melts of carbonate-bearing peridotite at these pressures will be carbonate-rich. Carbonatite magmas may therefore be produced by small degrees of partial melting of carbonated peridotite at depths greater than ≈80 km, followed by the separation of a carbonatitic liquid by immiscibility processes.

Radiogenic isotope studies (e.g. BELL *et al.*, 1973; LANCELOT and ALLEGRE, 1974; BASU and TATSUMOTO, 1980; BELL *et al.*, 1982; BARREIRO, 1983; RODEN *et al.*, 1985; GRÜNENFELDER *et al.*, 1986) indicate that most carbonatites examined so far have generally similar isotopic characteristics, with unradiogenic initial $^{87}Sr/^{86}Sr$ (≈0.703), slightly positive ε_{Nd} and radiogenic initial Pb compared to those of MORB, and isotopically resemble the alkali basalts from many ocean islands. As the isotopic characteristics of ocean-island basalts have been interpreted as evidence that they are derived from subducted oceanic lithosphere (CHASE, 1981; HOFMANN and WHITE, 1982), a similar origin is also suggested for carbonatites. Alternatively, BELL *et al.* (1982) and BELL and BLENKINSOP (1986, 1987a) have argued that Canadian carbonatites are derived from a depleted upper mantle reservoir which has remained coupled to the Canadian continental crust since the late Archaean. BARREIRO (1983) also proposed a similar model for carbonatites from Westland, New Zealand, involving crystallisation at depth of a LREE- and carbonate-rich magma originally derived from a depleted mantle source. At some later time, during which the evolution of its Nd isotopic composition had been retarded, this magma was re-activated, resulting in carbonatitic magmatism having only slightly positive ε_{Nd}. CO_2-dominated "metasomatic" processes have also been implicated in the generation of continental alkaline volcanism. For example, NORRY *et al.* (1980) reported Sr-, Nd- and Pb- isotope compositions similar to those of carbonatites and ocean islands for alkali basalts, basanites, nephelinites and phonolites from the Kenya rift. These authors argued for the operation of CO_2-metasomatism of the sources of these magmas in order to account for their silica-undersaturation and unusual trace-element chemistry. Information concerning the relative mobility of trace elements in carbonate fluids provided by the characterisation of the trace-element features

of carbonatites may be of value in understanding these processes.

In this study, trace-element and isotopic data are reported for carbonatites of a variety of localities and ages. Although it is recognised that many carbonatite complexes have had complicated histories of differentiation and intrusion, the approach adopted here is to compare broad geochemical and isotopic features of many different complexes in order to identify possible common processes which may be responsible for the generation of carbonatite magmas. The data obtained are used to characterise the sources of carbonatites, to evaluate the hypotheses advanced for carbonatite origin and to assess the importance of CO_2-rich "metasomatic" processes within the mantle.

SAMPLES

African carbonatites

Six African carbonatite localities, ranging in age from mid-Proterozoic to Tertiary, have been sampled. The youngest carbonatite locality examined, from the Napak alkaline complex in eastern Uganda, consists of both intrusive and extrusive alkaline rocks surrounding a central core of carbonatite (Lokupoi carbonatite) which have intruded Precambrian granitic gneiss. The petrology and geochemistry of the complex has been investigated by KING (1965) and KING and SUTHERLAND (1966). The carbonatite sample obtained for this study (#6336) consists of a flow-banded fine-grained calcite-carbonatite (alvikite, following the terminology of STRECKEISEN, 1979) containing rare phenocrysts of phlogopite, minor rutile and magnetite. A mid- to late-Tertiary emplacement age is indicated by lower Miocene mammalian fauna in sediments interbedded with the volcanics and from K-Ar studies (BAKER *et al.*, 1971). The Sukulu and nearby Tororo carbonatites, situated about 150 km south of Napak, are believed to be of similar age. Their petrology, geochemistry and field relationships have been summarised by KING and SUTHERLAND (1966) and HEINRICH (1966). The Sukulu sample examined here (#6335) is a melanite-bearing calcite-dolomite carbonatite and the Tororo sample (#6330) is a scapolite-bearing alvikite containing minor melanite. Details of the geology and geochemistry of the Kangankunde carbonatite, Malawi, can be found in GARSON (1966). An early Cretaceous K-Ar age of 126 Ma was reported for this carbonatite by SNELLING (1965). The specimen from the Kangankunde complex used in this study (#3432) is a coarse monazite-scapolite dolomite carbonatite (beforsite). The Nachendazwaya carbonatite, located in Tanzania near the border with Malawi, is believed to be genetically related to the Ilomba Hill carbonatite complex (GITTINS, 1966), 2 km further south in Malawi, which has been dated by the U-Pb zircon method at 655 Ma (SNELLING *et al.*, 1964). A similar K-Ar age of 680 Ma has been reported for phlogopite from metasomatised country rock adjacent to the Nkombwa carbonatite ≈75 km to the southwest in Zambia (SNELLING, 1965). The Nachendazwaya carbonatite specimen (#7122) is an apatite-biotite-magnetite sövite (coarse-grained calcite carbonatite) having rare phenocrysts of blue-green amphibole and trace amounts of rutile. The age of the Goudini carbonatite, South Africa, is uncertain, but has been tentatively correlated with magmatic activity associated with the Pienaars River Alkaline Complex which dates from 1430 to 1300 Ma ago (HARMER, 1986). Goudini specimen #33174 consists of ocelli of coarse calcite up to several millimeters in diameter with radial aggregates of green amphibole (probably riebeckite), scapolite, magnetite, nepheline, goethite and opaques

in a carbonate matrix and #33176 is a fine grained apatite-bearing calcite-dolomite carbonatite with minor sodic amphibole (riebeckite), albitised plagioclaise, white mica (possibly fuchsite) and chlorite.

Australian carbonatites

The Jurassic Walloway carbonatite occurs as a ≈10 km long, 100 to 800 m wide diapir associated with a suite of contemporaneous carbonate-rich ultrabasic lamprophyric and kimberlitic intrusions located in the Flinders Ranges region of South Australia (TUCKER and COLLERSON, 1972; STRACKE *et al.*, 1979). The mineralogy and chemistry of both the Walloway carbonatites and the nearby kimberlitic intrusions at Terowie and Orroroo have been described by FERGUSON and SHERATON (1979) and SCOTT-SMITH *et al.* (1984). The Walloway carbonatite specimen examined here (#7821-0009) is a coarse-textured calcite carbonatite (sövite) containing minor phlogopite (commonly rimmed by sodic amphibole), nepheline, sodic amphibole and opaques. The Mudtank carbonatite complex, located on the deep-seated Woolanga Lineament 50 km east-northeast of Alice Springs in central Australia, consists of 4 separate lenses of crystalline, micaceous and feldspathic carbonate rocks and has been reliably dated by both U-Pb zircon and Rb-Sr whole-rock techniques at 732 ±5 Ma and 735 ±75 Ma respectively (BLACK and GULSON, 1978). Further details of the geology and geochemistry can be found in BLACK and GULSON (1978) and references therein. Mudtank sample #7590-2015 is a coarse apatite-bearing dolomite carbonatite (beforsite). The Mt Weld carbonatite, located within the Eastern Goldfields province of the Yilgarn Block, Western Australia, is a ≈4 km diameter circular intrusion which has been dated by both K-Ar and Rb-Sr techniques at ≈2040 Ma (reported in WILLETT *et al.*, 1986). Its emplacement is believed to be tectonically related to the long-active deep-seated Laverton tectonic zone. Two samples of coarse calcite carbonatite (sövite) containing phenocrysts of apatite, magnetite and biotite (#MW-1 and #MW-2) were obtained for this study.

Jacupiranga carbonatite

The Jacupiranga alkalic complex is an oval-shaped plug of ≈65 km^2 area consisting of a central body of carbonatite surrounded by jacupirangites, pyroxenites, ijolites and syenites, that have intruded the Precambrian schists and granodiorite of southwest São Paulo, Brazil. The age of intrusion is well constrained by both K-Ar (AMARAL, 1978) and Rb-Sr (RODEN *et al.*, 1985) methods at 131 ±3 Ma, contemporaneous with both the flood basaltic volcanism of Parana to the west and the opening of the South Atlantic Ocean. RODEN *et al.* (1985) reported a range in initial $^{87}Sr/^{86}Sr$ and ε_{Nd} values of 0.7051 to 0.7053 and +0.1 to +1.6 respectively from the 5 distinct intrusions which comprise the central body of the Jacuparinga alkalic complex and attributed the range in initial isotopic compositions to crustal contamination. Both Jacupiranga samples examined here (#5961 and #5963) are magnetite- phlogopite-bearing sövites.

Kaiserstuhl and Fen carbonatites

The Kaiserstuhl is situated in the Upper Rhine Graben ≈15 km from Freiburg im Breisgau, Germany. Carbonatitic, phonolitic and other alkalic intrusives form the core of the complex, which is rimmed by pyroclastic deposits. Kaiserstuhl carbonatite sample #K-3 consists of coarse calcite with minor biotite,

melanite and apatite. K-Ar dating indicates emplacement ages of 16-18 Ma (in WIMMENAUER, 1966). The Fen carbonatite, Norway, has been the subject of extensive study (e.g. BARTH and RAMBERG, 1966; MITCHELL and CROCKET, 1970; GRIFFIN and TAYLOR, 1975) and has been dated by several independent techniques at ≈550 Ma old. Specimen #NBS-18 consists of carbonate from the Fen carbonatite prepared for use as a stable-isotope standard (FRIEDMAN *et al.*, 1982).

Magnet Cove carbonatite

The Magnet Cove carbonatite complex, Arkansas, is a ≈6 km^2 oval body that has intruded Palaeozoic shales and sandstones and consists of ijolite and carbonatite intrusions surrounded by ring dykes of phonolite, melteigite, jacupirangite and nepheline syenite (ERICKSON and BLADE, 1963). ZARTMAN *et al.* (1967) obtained K-Ar and mica Rb-Sr ages of 97 Ma indicating emplacement of the complex during the late Cretaceous. Specimen #MC-1 consists of coarse (≈1 cm^3) rhombs of transparent calcite.

ANALYTICAL PROCEDURES

Major-element analyses were obtained by X-ray fluorescence spectrometry on fused glass discs using an automated Siemens SRS300 spectrometer located in the ANU Department of Geology, following the procedure of NORRISH and HUTTON (1969). Abundances of the trace elements Ni, Cu, Zn, Rb, Sr, Y, Zr, Nb and Pb were determined by X-ray fluorescence on pressed powder pellets using a Phillips PW1400 spectrometer, following the method of NORRISH and CHAPPELL (1967). The other trace-element abundances were obtained on ≈300 mg of powdered sample by instrumental neutron activation analysis using an internal synthetic kimberlite standard included in each batch. All trace-element analyses given here represent averages of at least two determinations.

Samples for isotopic analysis were sawn into ≈3 cm^3 cubes, scrubbed thoroughly and then washed in an ultrasonic bath in ultrapure H_2O and acetone. The cubes were then coarsely crushed in a stainless steel mortar and small rock chips with fresh fracture surfaces were hand-picked and used for isotopic analysis. About 1-3 g of carbonatite chips were initially treated with 6N HCl in teflon beakers until all carbonate was decomposed, the solution then evaporated and the residue dissolved using a mixture of HF-$HClO_4$. The resulting solution was then re-dissolved in 1N HCl and split into two aliquots, one of which was spiked with mixed ^{235}U-^{208}Pb spike and the other used for Pb isotopic composition. Rb-Sr and Sm-Nd concentration and isotopic analyses were undertaken on ≈70 mg of sample chips using mixed ^{85}Rb-^{84}Sr and ^{147}Sm-^{150}Nd spikes. Samples were dissolved in HF-$HClO_4$ in teflon pressure capsules at 200 °C or in teflon beakers for at least 48 hrs. The remaining procedures for Rb-Sr, Sm-Nd and U-Pb concentration and isotopic analysis have been described elsewhere (McCULLOCH and CHAPPELL, 1982; NELSON *et al.*, 1986). All Pb isotopic composition analyses were performed in duplicate or triplicate and the analytical error, based on two-way analysis of variance of replicate analyses, is < ±0.1% at the 1σ level. The total procedural blanks were ≈1 ng for Sr, <1 ng for Nd and <5 ng for Pb and were insignificant for all analyses.

Carbonates for $\delta^{13}C$ and $\delta^{18}O$ analysis were reacted in duplicate with 100% H_3PO_4 at 25 °C for 1 day (calcite samples) and 3 days (dolomitic/ankeritic samples) and analysed on a highly modified MS-12

triple-collector mass spectrometer (overall precision ±0.1‰). $\delta^{18}O$ values were calculated using 1000lnα values for acid-liberated CO_2 of 10.20 for calcite and 11.03 for dolomite/ankerite. $\delta^{13}C$ and $\delta^{18}O$ values are expressed as per mil differences relative to the PDB and SMOW standards. $\delta^{18}O_{SMOW}$ and $\delta^{13}C_{PDB}$ (‰) values for NBS-18 and NBS-19 standards of +7.20, -5.00 and +28.65, +1.95 respectively, are obtained in our laboratory.

CO_2 contents (Table 1) of calcitic samples were measured by manometry of the CO_2 evolved at 25 °C. After collection of the CO_2 evolved at 25 °C from ankeritic samples, the phosphoric acid was boiled vigorously for ten minutes and the additional CO_2 released measured manometrically to provide a total CO_2 content. Due to the small sample weight (20 mg) and inhomogeneity of the samples, reproducibility of the manometric yields is only ±3%. This uncertainty is largely responsible for some of the poorer major-element sums (Table 1).

RESULTS

Major- and trace-element analysis

Geochemical data are tabulated in Table 1 and presented diagramatically in Figs. 1 and 2. In Fig. 1, the concentrations of trace elements have been normalised to estimated primitive mantle abundances (from McDONOUGH *et al.*, 1985 and NELSON *et al.*, 1986) and plotted in order of increasing compatibility in peridotitic mantle of garnet lherzolite mineralogy. Also shown for comparison are trace-element patterns for ocean-island basalts (CHEN and FREY, 1983; THOMPSON *et al.*, 1984; PALACZ and SAUNDERS, 1986). General features of the geochemistry of carbonatites apparent from Table 1 and Fig. 1 are; a) the typically high abundances of Ba, Th, LREE, Sr, variable abundances of Nb, Ta, P and low Cs, Rb, K, Ti and HREE abundances of most examples; b) with the notable exception of Goudini and Walloway carbonatites, most examples possess large negative Zr and Hf concentration anomalies. These negative Zr and Hf anomalies are generally accompanied by large negative U anomalies and (with some exceptions) high Th/U ratios. The South African Goudini and South Australian Walloway carbonatites possess higher SiO_2, Cr, Sc, Ni, Co, Rb, Zr and Hf than the other low-SiO_2, U- and Zr- anomalous carbonatites.

Rare-earth element concentrations normalised to chondritic values are plotted in Fig. 2. The rare-earth element patterns for two secondary vein carbonate samples of sedimentary origin are also shown for comparison. All carbonatites have steep LREE-enriched patterns with low HREE abundances. Slight decoupling of the LREE from the HREE is apparent in a few of the patterns, especially those of Nachendazwaya, Mudtank and Jacupiranga (#5963) examples for which the slopes of the patterns are steepest between Sm and Tb. Some of the carbonatites (e.g. Kaiserstuhl #K-3 and Magnet Cove #MC-1) have patterns with steep LREE but relatively flat HREE. The Goudini carbonatite #33176 pattern possesses a positive slope between Nd and Eu. Small positive Eu anomalies are evident in Kaiserstuhl (#K-3) and Magnet Cove (#MC-1) carbonatite patterns and in the Terowie kimberlite (#0090) pattern.

Rb-Sr and Sm-Nd isotope analysis

Sr and Nd isotopic analyses are presented in Table 2 and are compared with available data for

carbonatites from other studies and with the fields of modern ocean-island basalts, MORB and non-micaceous (Group 1) South African kimberlites on an initial Sr-Nd isotope diagram in Fig. 3. As most of the carbonatites have very low Rb contents and high abundances of Sr, corrections to the measured $^{87}Sr/^{86}Sr$ for ^{87}Rb decay since emplacement are small and insensitive to possible errors in the emplacement ages. In order to minimise the possibility of contamination during rock crushing, isotopic analysis was performed on small hand-picked chips, which are not likely to be geochemically representative of the larger hand-specimen. This has resulted in some discrepancies between the concentrations of Rb, Sr, Sm, Nd, U and Pb determined by isotope dilution and those determined by XRF/INAA. However, there is generally good agreement between the Rb/Sr, Sm/Nd and U/Pb ratios determined by these methods.

Sr and Nd isotopic compositions of Tororo, Sukulu, Kaiserstuhl, Fen, Magnet Cove and Jacupiranga carbonatites from this study generally agree within analytical error with the results obtained in previous studies of these complexes (e.g. BELL and POWELL, 1970; MITCHELL and CROCKET, 1970; RODEN *et al.*, 1985; BELL and BLENKINSOP, 1987b; TILTON *et al.*, 1987). DERRY and JACOBSEN (1986) reported a wide range of ε_{Nd} values of from +3.1 to +7.7 for the intrusive rocks of the Fen Complex, confirming that some carbonatite complexes display considerable isotopic heterogeneity, possibly as a result of late-stage hydrothermal processes. Nevertheless, it is apparent from Fig. 3 that most carbonatites fall within a restricted range of initial $^{87}Sr/^{86}Sr$ of between 0.7025 to 0.7036 and have initial ε_{Nd} between 0 and +4. The Walloway carbonatite and the associated carbonated micaceous kimberlite have initial Nd isotopic compositions within this range but have more radiogenic initial $^{87}Sr/^{86}Sr$ of 0.7049 and 0.7054 respectively. Although STRACKE *et al.* (1979) obtained a phlogopite- whole-rock two-point Rb-Sr isochron for the Terowie kimberlitic intrusion, a sufficiently precise initial $^{87}Sr/^{86}Sr$ could not be determined. The Jacupiranga carbonatite also possesses significantly more radiogenic Sr than the other carbonatites despite having ε_{Nd} values (-0.4 and +0.5) which are only slightly lower than the range of isotopic compositions of most of the other examples. The younger African (i.e. Sukulu, Tororo, Lokupoi and Kangankunde) and Westland carbonatites fall below the mantle array and below the fields of St Helena, Austral, Comoros and Ascension ocean-island basalts on the initial Sr-Nd isotope diagram (Fig. 3). The older occurrences, such as the Proterozoic Mt Weld and Goudini carbonatites, the Late Precambrian Mudtank and Nachendazwaya carbonatites and the Cambrian Fen carbonatite, have generally less radiogenic initial $^{87}Sr/^{86}Sr$ and similar ε_{Nd} values compared to those of younger carbonatites. Phonolites associated with the Kaiserstuhl carbonatite occurrences have ε_{Nd} within analytical error of the carbonatites but have slightly more radiogenic initial $^{87}Sr/^{86}Sr$.

As with many ocean-island and continental alkali basalts, the Nd isotopic characteristics of most of the carbonatites examined in this study indicate their derivation from sources with time-integrated near-chondritic LREE/HREE or slight LREE depletion, despite the LREE-enrichment evident in the magmas themselves. The initial Sr and Nd isotopic characteristics of carbonatites of various ages from throughout the world therefore indicate derivation from sources which have had generally similar long-term evolutionary histories.

U-Pb isotope analysis

Whole-rock U and Pb concentration and Pb isotopic composition analyses are given in Table 3. The carbonatites possess an extremely wide range of U and Pb concentrations and U/Pb ratios. Corrections to the Pb isotope ratios for post-emplacement radiogenic decay of U and Th are significant for Mudtank, Walloway, Nachendazwaya and Goudini samples and the age-corrected Pb isotopic compositions will be reliable only if there has been no mobility of U, Th or Pb since their emplacement. Age corrections to the remaining examples are relatively small due to either the younger emplacement ages, lower U/Pb ratios or a combination of these factors. For example, the Cambrian Fen carbonatite requires a correction of -0.33 (or 1.6%) to the $^{206}Pb/^{204}Pb$ and the correction to $^{207}Pb/^{204}Pb$ is within the analytical uncertainty. Due to possible error in the Th/Pb correction assumptions (age corrections have been applied using thorium abundances calculated from the INAA-determined Th/U ratio and the isotope dilution uranium abundances), a much larger uncertainty applies to the calculated initial $^{208}Pb/^{204}Pb$ ratios. Despite the wide variation in U/Pb, most of the carbonatites have radiogenic Pb isotopic compositions (Fig. 4) and plot along the Pb-Pb array determined for MORB and ocean-island basalts. Kaiserstuhl samples overlap the field of the Society group of ocean islands, whereas the younger African carbonatites have considerably more radiogenic Pb values which extend beyond the St Helena field. Similar radiogenic Pb compositions were found in Ugandan carbonatites (including samples from Napak, Sukulu and Tororo) by LANCELOT and ALLEGRE (1974). Radiogenic initial Pb compositions have also been reported by GRÜNENFELDER *et al.* (1986) for the Cretaceous Oka carbonatite from Quebec and by WILLIAMS *et al.* (1986) for the Oldoinyo Lengai carbonatite. The Cambrian Fen carbonatite has an initial Pb isotopic composition similar to that of some Ugandan carbonatites.

The Jacupiranga carbonatite is exceptional in having unradiogenic initial Pb and lies to the unradiogenic side of the modern geochron, although it still plots along an extension of the Pb-Pb array of modern oceanic basalts. RODEN *et al.* (1985) demonstrated that the Jacupiranga carbonatite is isotopically heterogeneous, with later intrusions possessing slightly more radiogenic initial Sr isotopic compositions, and argued that the Sr and Nd isotopic composition of the Jacupiranga carbonatite has been modified by crustal assimilation. If the Pb isotopic composition of the Jacupiranga intrusion has also been modified by crustal assimilation, its unradiogenic Pb isotopic compositions suggest that this assimilation probably occurred within the lower crust, as the lower crust is generally believed to be depleted in U and to possess unradiogenic Pb. The stable-isotope characteristics of the Jacupiranga carbonatite (see below) have apparently not been effected by assimilation of the extensive amounts of crustal material required to modify the Sr isotopic composition.

The large difference in both the Sm/Nd and U/Pb ratios of the two Goudini samples enables determination of the age of emplacement. Regression of the Goudini analyses gives an Sm-Nd age of 1190 ±80 Ma and a similar but imprecise Pb-Pb age of 1110 ±300 Ma (1σ errors given on ages). These emplacement ages are similar to those determined for a variety of alkaline rocks and kimberlites from the region (HARMER, 1986). The two Mt Weld Pb analyses yield a Pb-Pb age of 2090 ±10 Ma, within error of the K-Ar age of 2064 ±40 Ma but statistically significantly older than the Rb-Sr age of 2020 ±17 Ma (WILLETT *et al.*, 1986).

O and C isotope analysis

$^{18}O/^{16}O$ and $^{13}C/^{12}C$ results are given in Table 3 and shown graphically in Fig 5. The carbon and oxygen isotopic compositions of Kaiserstuhl, Tororo and Sukulu carbonatites from this study fall within the ranges determined for these localities by previous studies (GONFIANTINI and TONGIORGI, 1964; DEINES and GOLD, 1973; see Fig. 5). The results of PINEAU *et al.* (1973) and this study indicate similar carbon but slightly heavier oxygen isotopic compositions for the Lokupoi carbonatite compared to those of the other Ugandan carbonatites. The Cretaceous Kangankunde carbonatite has a carbon isotopic composition within the range of $\delta^{13}C$ obtained by SUWA *et al.* (1975) (averaging -3.4 ‰ using only those samples with $\delta^{18}O$ between +6 and +8 ‰) for the Mbeya carbonatite of similar age (SNELLING, 1965) located near the southwest border of Tanzania, whereas the late Precambrian Nachendazwaya example, situated near the Mbeya carbonatite, has slightly lighter carbon. Our results support the assertion of DEINES and GOLD (1973) of regional variation in the carbon isotopic compositions of carbonatites from East Africa, with the inter-rift region surrounding Lakes Victoria, Malawi and Chilwa (where Tororo, Sukulu, Lokupoi, Kangankunde and Nachendazwaya carbonatites are located) characterised by higher ^{13}C contents (between -2.4 and -4.4 ‰) compared to their results for carbonatites located within the East and West African Rifts (-5.8 to -7.9 ‰).

The Goudini complex consists predominantly of ejected tuffaceous material and breccia (VERWOERD, 1966). DEINES and GOLD (1973) have observed that volcanically emplaced carbonatites generally display greater carbon and (especially) oxygen isotopic variability than plutonic carbonatites and attributed this to the greater opportunities available for isotopic exchange during emplacement of the volcanic carbonatites. The heavy carbon and oxygen compositions of the Goudini samples compared with results obtained from other localities probably reflect greater loss of isotopically light carbon and oxygen during their emplacement and substantial post-emplacement isotopic exchange of these samples with their surroundings.

Carbon- and oxygen- isotope analyses for the Mudtank carbonatite from this study are significantly heavier than those reported by WILSON (1979). Correction of WILSON'S (1979) results to account for recent re-calibration of the C.S.I.R.O. internal standard (for $\delta^{13}C_{PDB}$, from -12.8 to -13.3 ‰ and for $\delta^{18}O_{PDB}$, from -5.6 to -5.3 ‰) indicates $\delta^{13}C_{PDB}$ and $\delta^{18}O_{SMOW}$ values of -4.8 and +7.2 ‰ respectively, compared to our results of -3.6 and +7.5. The slight discrepancy between these two data sets may indicate some carbon- and oxygen- isotope heterogeneity in this intrusion.

Many of our carbonatite samples have oxygen- isotope compositions outside the range of +6 to +8 ‰ vs SMOW, considered by DEINES and GOLD (1973) to represent the range of values expected for primary carbonatites. However, there is compelling evidence from the large amount of ^{13}C data on carbonatites for the existence of considerable isotopic heterogeneity which is difficult to attribute entirely to secondary processes. Although the regional ^{13}C compositions displayed by the African rift carbonatites noted by DEINES and GOLD (1973) may be due to subtle regional differences, either in the style of emplacement or in the basement rocks through which the carbonatites intrude, these differences may also indicate that the sources of carbonatites are isotopically heterogeneous. If this is the case for ^{13}C, it is probable also for ^{18}O. Distinguishing between the effects of primary and secondary variation in oxygen (and to a lesser extent, carbon) isotopic compositions is, however, likely to prove difficult even

with detailed sampling of each locality.

A recent study of carbon isotopic compositions in mid-ocean ridge basalts by DES MARAIS and MOORE (1984) has found $\delta^{13}C$ values between -5 and -7 ‰. KYSER *et al.* (1982) reported a range of $\delta^{18}O$ for mantle-derived basic lavas between +4.9 to +8.3 ‰, with most mid-ocean ridge and alkali basalts having values between +5.0 and +6.2 ‰. If these compositions are typical of mantle values, they indicate that most carbonatites have similar or slightly heavier $\delta^{13}C$ and $\delta^{18}O$ values compared to mantle values. Two exceptions, both of which have considerably lighter $\delta^{13}C$ values, are the modern Oldoinyo Lengai carbonatite volcano (SUWA *et al.*, 1975), whose lavas are deliquescent and readily exchange carbon and oxygen with the atmosphere, and the recently discovered carbonatites from the Murun alkalic block, Aldan (PLYUSNIN *et al.*, 1984).

DISCUSSION

Geochemical characteristics of carbonatites and associated magmatism

Although magmas parental to carbonatites are probably generated by extremely low degrees of partial melting of a carbonated peridotitic or eclogitic source and are therefore likely to have high abundances of incompatible trace elements, the trace-element characteristics of carbonatites are anticipated to be strongly influenced by the operation of complex secondary processes such as extensive differentiation, liquid immiscibility or volatile transport. The pronounced negative anomalies of U, Zr, Hf Nb, Ta and Ti displayed by some carbonatites in Fig. 1 may be attributed entirely to late-stage fractional crystallisation processes, including removal of sphene, apatite, perovskite, monazite or zircon. However, abundances of Ba, P and Sr are in most cases not anomalous compared with the degree of enrichment displayed by the light and middle REE which have similar incompatibility. Apart from negative anomalies for K, the Walloway and Goudini carbonatites have relatively smooth trace-element abundance patterns (Fig. 1) suggesting that they have not undergone extensive modification by secondary processes. Negative K anomalies are also common in the trace-element patterns of ocean-island basalts (see Fig. 1) and may be characteristic of ocean-island sources. The Walloway and Goudini carbonatites have similar HREE abundances but have significantly higher SiO_2, Cr, Sc, Ni and Co concentrations compared to the other examples, consistent with the suggestion that they have undergone substantially less differentiation.

As the Nd isotopic compositions of carbonatites indicate that they are derived from sources having time-integrated near-chondritic LREE/HREE or slight LREE-depletions, generation of the extreme LREE/HREE of carbonatites requires either an unusual source mineralogy, specialised conditions during melt generation and extraction processes or the operation of suitable secondary differentiation processes. WENDLANDT and HARRISON (1979) demonstrated that the HREE are preferentially partitioned into the carbonate melt during carbonate/silicate immiscibility. Carbonatites typically have low abundances of the HREE, suggesting that immiscibility processes are not responsible for the REE fractionation. These authors have also shown that the LREE are fractionated into any CO_2-vapour phase present relative to silicate or carbonate melts, especially at low pressures. Transport of the LREE in a vapour phase may therefore contribute to the extreme LREE-enrichment of carbonatites. However, many carbonatites possess enrichments in the elements Ba, Sr and P similar to that of the REE (evident from the relatively

flat normalised patterns of these elements in Fig. 1). This is unlikely to be due to melt/vapour enrichment processes but instead, suggests that the enrichment is due to partial melting processes. Using the distribution coefficients of WOOD (1979), calculations indicate that modal, non-modal or fractional partial melting of garnet lherzolite or eclogite like those found as xenoliths in kimberlite pipes is incapable of producing the extreme La/Yb ratios found in some kimberlites and carbonatites. McKENZIE (1985) has suggested that because of the extremely low viscosity of carbonate melts, segregation of very small melt fractions (as low as 0.1%) on geologically reasonable timescales may be possible. Extreme fractionation of La from Yb can occur in low melt fractions (<≈1%) generated from eclogitic sources with relatively high modal abundances of garnet (i.e. Gnt_{80}:Cpx_{20}). Under these circumstances, the extreme LREE-enrichment and low HREE abundances of carbonatites may be a primary magmatic feature and may not require the operation of secondary processes. This general conclusion is probably still valid for melts generated at high pressures even though it is possible that distribution co-efficients determined from rocks of low-pressure origin are not applicable at very high pressures or for highly volatile-rich melts. At depths greater than ≈350 km, subducted basaltic oceanic crust is believed to transform to garnet-rich eclogitic assemblages (RINGWOOD, 1982) and may therefore provide a suitable source material for carbonatite and kimberlite melt generation.

Small Eu- and Ce- anomalies have been observed in the rare-earth patterns of some carbonatites (e.g. WIMMENAUER, 1966; LOUBET *et al.*, 1972; EBY, 1975; MÖLLER *et al.*, 1980). EBY (1975) demonstrated that many different mineral phases of the Oka carbonatite possess positive or negative Eu-anomalies even though the whole-rocks from which these phases were separated lack Eu-anomalies. Both the Eu- and Ce-anomalies are therefore probably strongly influenced by competition for the REE between minerals and/or a volatile phase during late-stage crystallisation. LOUBET *et al.* (1972) found a correlation between the magnitude of the negative Ce anomaly and $\delta^{18}O$ in Ugandan carbonatites and attributed this to increasing oxidation during carbonatite differentiation. This correlation might also be caused by melt/CO_2-rich vapour fractionation or by secondary alteration processes. The slight decoupling of LREE and HREE apparent in rare-earth element patterns of some differentiated carbonatites might reflect preferential substitution of the LREE and HREE into different mineral lattice sites during crystallisation (for example, the LREE in calcite Ca lattice sites or in monazite etc. and the HREE in zircon or in dolomite Mg and Fe sites) or may be due to vapour/melt fractionation processes.

Isotopic characteristics of carbonatites and associated magmatism

From the results of this and earlier studies, it is apparent that carbonatites comprise an isotopically relatively homogeneous group of magmas possessing a restricted range of radiogenic and (when the effects of secondary alteration processes are taken into account) stable isotope characteristics. Most young carbonatites have initial $^{87}Sr/^{86}Sr$ ≈0.703. Similar initial $^{87}Sr/^{86}Sr$ ratios have been reported by BELL and POWELL (1970) and BELL *et al.* (1982) for Cambrian and mid- to late- Proterozoic examples from Ontario, Canada. However, a few carbonatites, such as the Na-rich carbonatite from the active Oldoinyo Lengai volcano in Tanzania (BELL *et al.* 1973) and carbonatites from India and Pakistan (DEANS and POWELL, 1968) have considerably more radiogenic initial $^{87}Sr/^{86}Sr$ ratios. The Oldoinyo Lengai carbonatite has Nd (ε_{Nd} of ≈0; DePAOLO, 1978; BELL and BLENKINSOP 1987b) and Pb isotopic

compositions ($^{206}Pb/^{204}Pb$ of 19.19, $^{207}Pb/^{204}Pb$ of 15.55 and $^{208}Pb/^{204}Pb$ of 39.14, given in WILLIAMS *et al.* 1986) similar to those of other carbonatites, although a wide range of $^{87}Sr/^{86}Sr$ ratios have been reported (POWELL, 1966; BELL *et al.*, 1973; DePAOLO, 1978; BELL and BLENKINSOP 1987b). POWELL (1965) noted that vein carbonatites commonly possess more radiogenic Sr isotopic compositions compared to central intrusive complex examples. Because of their extreme concentrations of Sr, POWELL (1965) argued against crustal contamination, but instead proposed that vein carbonatites were genetically unrelated to central intrusive complex carbonatites. The Walloway carbonatite is a vein carbonatite and although it possesses significantly more radiogenic Sr than the central intrusive complex carbonatites examined in this study, it has similar Nd and Pb isotopic compositions, suggesting that a genetic relationship does exist in this case. Involvement of late-stage fluids during emplacement of the Walloway carbonatite, suggested by petrographic features such as the rimming of mica phenocrysts by sodic amphibole, may have resulted in isotopic exchange of Sr with the country rock and may account for the more radiogenic Sr isotopic composition of this intrusion.

All Nd isotopic compositions so far reported for mid-Proterozoic to Recent carbonatites indicate time-integrated near-chondritic or depleted LREE/HREE histories, with most having ε_{Nd} values between 0 and +5. For example, BELL and BLENKINSOP (1987a) reported initial ε_{Nd} values between 0 to +5 for twelve Canadian carbonatites ranging in age from 1900 to 110 Ma. Similar ε_{Nd} values to those reported by BELL and BLENKINSOP (1987a) were presented by KWON and TILTON (1986) for the early Proterozoic Cargill and Borden carbonatites from Ontario. BASU and TATSUMOTO (1980) measured ε_{Nd} values of +3.3 and +5.3 (after correction for instrumental bias) for the Palaeozoic McClure Mountains and Mesozoic Magnet Cove carbonatites respectively, whereas SUN *et al.* (1986) found an initial $^{87}Sr/^{86}Sr$ of 0.703 and ε_{Nd} of +2.0 ±0.4 for the late Proterozoic Cummins Range carbonatite of Western Australia. MIDENDE *et al.* (1986) have reported similar initial $^{87}Sr/^{86}Sr$ and ε_{Nd} values for 3 carbonatites, of late Precambrian to Cretaceous age, from the western branch of the African rift. COHEN *et al.* (1984) also found similar isotopic characteristics ($^{87}Sr/^{86}Sr$ of 0.7035, ε_{Nd} of +1.8, $^{206}Pb/^{204}Pb$ of 20.60, $^{207}Pb/^{204}Pb$ of 15.77 and $^{208}Pb/^{204}Pb$ of 40.30) in an ankaramite from the Recent Lashaine carbonatite vent, Tanzania. An initial ε_{Nd} of ≈0 has also been determined for the late Archaean Siilinjarvi carbonatite, eastern Finland (A.R. BASU, personal communication). Furthermore, initial ε_{Nd} values of ≈+3.5 and $^{87}Sr/^{86}Sr$ of 0.7046 have been measured in alnöites from Malaita in the Solomon Islands (BASU and TATSUMOTO, 1980; BIELSKI-ZYSKIND *et al.*, 1984). The Malaita alnöite was suggested by ALLEN and DEANS (1965) to be genetically related to carbonatite, a suggestion later supported by NIXON *et al.* (1980). However, the early Proterozoic Phalaborwa Complex, South Africa, is exceptional in having highly negative initial ε_{Nd} (ALLSOPP and ERIKSSON, 1986). The Phalaborwa complex consists of a carbonatite core and closely associated alkali-rich dykes emplaced during many intrusive events and possesses considerable Sr and Nd isotopic diversity which is believed to be a primary feature of the magmatism (ALLSOPP and ERIKSSON, 1986).

BELL and BLENKINSOP (1986, 1987a) suggested that a correlation exists between the ages of Canadian carbonatites and their initial Sr and Nd isotopic compositions and argued that most Canadian carbonatites were derived from a common trace-element-depleted mantle source which had remained coupled to the Canadian Shield. However, this correlation is not confined only to carbonatites found

within the Canadian shield but (when allowance is made for the influence of crustal contamination) is a global phenomenon (Fig. 6) and therefore does not provide support for a subcontinental lithospheric origin for carbonatites. Furthermore, this correlation does not necessarily require all carbonatites to be derived from a single common reservoir. As the correlation holds for carbonatites from a number of separate continents, it probably reflects ageing, at a similar rate, of a number of spatially discontinuous but isotopically similar reservoirs within the Earth. Moreover, the correlation strongly suggests that similar processes have been responsible for generating the sources of carbonatites worldwide. BARREIRO (1983) proposed a 2-stage mechanism involving freezing at depth and later re-activation of a carbonate-rich melt originally derived from depleted mantle to produce the Westland dyke swarm, New Zealand. However, as the Nd isotopic compositions of carbonatites produced by this mechanism are a function of the time elapsed between crystallisation and re-activation, the Nd isotopic consistency which is observed in carbonatites worldwide argues against the operation of this mechanism.

The possible role of CO_2 in the generation of highly alkaline continental magmatism is suggested by the close association between carbonatitic, nephelinitic and phonolitic magmatism in many alkaline complexes. Phonolites associated with the Kaiserstuhl carbonatite occurrences have ε_{Nd} within analytical error of the carbonatites but have slightly higher initial $^{87}Sr/^{86}Sr$. Other studies (for example, MITCHELL and CROCKET, 1970; BELL and POWELL, 1970; BELL *et al.*, 1973; BARREIRO, 1983; ALLSOPP and ERIKSSON, 1986) have also found a considerable range of Sr isotopic compositions for alkaline (potassic and nephelinitic) and carbonatite magmas from the same intrusive complex, with the alkaline silicate magmas commonly (but not universally) possessing the more radiogenic initial Sr isotopic compositions. In some cases, this isotopic variation may result from interaction of the alkaline silicate magmas with the wall rocks, as these magmas have considerably lower Sr contents compared to carbonatite magmas and are therefore more sensitive to contamination processes. Although carbonatites may have differentiated from an alkaline silicate parent, the lower $^{87}Sr/^{86}Sr$ of some carbonatites compared to the alkaline silicate magmas with which they are associated rules out the possibility that the carbonatite differentiated within a closed system from the alkaline silicate magmas in these complexes. Instead, the Sr isotopic variability suggests that in these complexes, the associated silicic magmas may not be directly genetically related to the carbonatites, but may have been generated during the passage of a CO_2-rich magma through the upper mantle and crust, as this is likely to induce melting in the surrounding mantle and crust wall rocks.

Possible relationships between carbonatites, kimberlites and ocean islands

The similar Sr, Nd and Pb isotopic characteristics of most carbonatites and some ocean-island basalts suggest a common origin for these otherwise apparently unrelated magma groups. As carbonatites have extreme abundances of incompatible elements, it is conceivable that some ocean-island basalts represent mixtures between a carbonatitic component and (for example) a component derived from a depleted mantle reservoir. On the initial Sr-Nd isotope diagram (Fig. 3), many young carbonatites lie below the mantle array with the fields for many ocean-island basalts positioned between the field of young carbonatites and that of MORB, consistent with this suggestion. The same applies for the Pb isotope characteristics (Fig. 4); many young carbonatites possess initial Pb isotopic compositions which lie along the array of

ocean-island basalts. The isotopic similarities between ocean-island basalts and carbonatites raises the possibility that the sources of some ocean-island basalts consist of trace-element-depleted mantle, such as that from which MORB is derived, which has been re-fertilised by incompatible-element-rich, low-viscosity carbonate melts. Alternatively, the isotopic similarities may indicate that carbonatites and ocean-island basalts are derived from sources which have had similar long-term isotopic histories but with the obvious chemical differences controlled by differences in other variables, such as degree of partial melting, depth of generation or CO_2 content in the sources. Although melts generated from peridotite following addition of a component with trace-element characteristics like that of carbonatite would be expected to inherit the large anomalies evident in the trace-element patterns of some carbonatites, as discussed earlier, these anomalies are probably due to high-level, late-stage differentiation processes. If carbonatitic magmas have relatively smooth normalised trace-element patterns prior to the extensive operation of differentiation processes (as is suggested by the trace-element patterns of the Walloway and Goudini carbonatites), evidence of fertilisation of the sources of ocean-island alkali basalts by these carbonatitic components would not be readily detectable. Such trace-element fertilisation of the source regions of alkali basalts alleviates the need for the low degrees of partial melting which the high abundances of incompatible trace elements of alkali basalts were thought to require.

If CO_2-rich components are involved in the generation of the alkali basalts of ocean islands, it might be anticipated that carbonatites would be common on ocean islands. As pointed out by SILVA *et al.* (1981) and LE BAS (1984), when only plutonic rocks are considered, rocks belonging to the carbonatite-ijolite association are volumetrically relatively abundant on ocean islands. Moreover, the plutonic basement rocks of ocean islands are rarely exposed unless the island is subjected to uplift and extensive erosion, as in the case of the Cape Verde Islands. In addition, CO_2-rich magmas intruding continental regions must pass through a considerable thickness of crust, during which the magma can unmix into carbonate and silicic components. By contrast, introduction of a CO_2-rich component to mantle peridotite in the hotter oceanic environment (and probably also in regions of thin, young continental crust) is likely to cause large-scale melting at shallow depths. Under these conditions, segregation of carbonatitic magma may be more difficult and alkali basaltic volcanism would be expected to predominate. Furthermore, experimental studies (*cf.* WENDLANDT, 1984 and references therein) have shown that the major-element characteristics of any partial melt generated from carbonated peridotite depends strongly on the solubility of CO_2 in the melt which in turn varies with depth of melt generation. At pressures less than ≈25 kbar, the solubility of CO_2 in the melt is generally low and the melt becomes progressively less silica-undersaturated with decreasing pressure (WYLLIE and HUANG, 1975). Partial melting of carbonated peridotite at depths less than ≈70 km may produce a melt resembling the alkali basalts of some ocean islands. At pressures approaching 25 kbar, the melts may resemble kimberlite magmas. At pressures greater than 25 kbar, partial melting of peridotite in the presence of CO_2 will produce carbonate-rich magmas (WYLLIE and HUANG, 1975; HOLLOWAY *et al.*, 1977). Depth of magma generation therefore strongly influences the major-element chemistry of magmas derived from peridotite in the presence of CO_2. As the depth of magma generation is likely to be influenced by both geothermal gradient and crustal thickness, kimberlitic and carbonatitic rocks are likely to be more common in stabilised, thickened cratons and might be expected to be less common in the oceanic

environment. It is noteworthy that the oceanic island of Malaita, Solomon Islands, from which alnöites have been reported (NIXON and BOYD, 1979), lies along the southern margin of the Ontong Java Plateau, which consists of thickened (up to 40 km) crust (KROENKE, 1972).

The importance of CO_2 in the generation of kimberlites is well established (e.g. SPERA and BERGMAN, 1980). For example, BAILEY (1984) demonstrated a correlation between CaO and CO_2 in kimberlites and suggested that a $CaCO_3$ component is involved in their generation. The "alleged" close association between kimberlitic and carbonatitic magmatism is controversial (see GASPAR and WYLLIE, 1984) but the recent recognition of two genetically distinct groups of kimberlites (SMITH, 1983) may help to clarify possible relationships between kimberlites and carbonatites. South African Group 1 (non-micaceous) kimberlites have Sr, Nd, Pb and $\delta^{13}C$ isotopic compositions closely resembling those of carbonatites. SMITH (1983) has also noted the isotopic similarities between Group 1 kimberlites and ocean islands. A close spatial and temporal relationship exists between kimberlitic and carbonatitic rocks at both the Walloway/Terowie region, South Australia and in Pretoria, South Africa. Although many of the kimberlitic intrusives at Walloway are evolved and contain generally lower trace-element contents than typical kimberlite (FERGUSON and SHERATON, 1979), diamond-bearing intrusions of the same age have been identified in the Walloway region and one has been classified as hypabyssal, calcite-phlogopite-kimberlite (SCOTT-SMITH *et al.*, 1984). The Walloway carbonated kimberlite and Terowie kimberlitic intrusion have similar slightly positive ε_{Nd}, like that of the Walloway carbonatite, suggesting a genetic relationship. The emplacement age of the Goudini carbonatite is within error of that of the Premier kimberlite pipe, and "carbonatites" at Premier have initial $^{87}Sr/^{86}Sr$ of 0.7028 (POWELL, 1966; WELKE *et al.*, 1974) and ε_{Nd} (BASU and TATSUMOTO, 1980) identical to that of the Goudini carbonatite. Although the Goudini and Walloway carbonatites are isotopically similar to other carbonatites, these two carbonatites lack the distinctive negative U and Hf anomalies found in all of the other carbonatites examined. As discussed earlier, these anomalies are probably due to crystallisation of phases such as monazite or zircon. The high SiO_2 contents and lower degree of trace-element enrichment of the Walloway and Goudini carbonatites compared to the other carbonatites indicates incomplete segregation of carbonate and silicate phases. If, as the evidence presented here suggests, kimberlites and carbonatites are genetically related, these two carbonatites may be transitional between kimberlite and more differentiated carbonatite.

Evolution of the sources of carbonatites

Many carbonatites possess isotopic characteristics indicating that their sources have long histories of high U/Pb, low Rb/Sr and LREE-depletion. HOFMANN and WHITE (1982) have attributed similar isotopic characteristics found in ocean-island basalts to their derivation from subducted oceanic lithosphere which has been enriched in uranium during hydrothermal circulation or low-temperature alteration and stored for ≈1-2 Ga in the mantle. Subducted altered basaltic crust is also likely to be CO_2- and volatile-rich, offering an excellent source material for carbonatite generation. At depth, subducted basalt converts to eclogite, which TREIMANN and ESSENE (1983) have advanced as a possible source for Na-rich carbonatites (with the jadeitic pyroxene component of eclogite providing a source of Na). Derivation from a garnet-rich eclogitic source can also explain the extreme LREE-enrichment typical of

carbonatites. The relatively unradiogenic initial Sr and slightly radiogenic initial Nd of carbonatites is also compatible in general terms with an origin from ancient low Rb/Sr, slightly LREE-depleted, altered basaltic crust. If this is the case, the difference in the Pb isotopic characteristics of young carbonatites and the MORB depleted mantle reservoir from which their subducted basaltic sources may have been derived indicates a recycling rate similar to that inferred for ocean-island sources (CHASE, 1981) of the order of ≈1.5 Ga. Although the correlations between initial $^{87}Sr/^{86}Sr$, ε_{Nd} and emplacement age of Fig. 6 require a relatively rapid and steady recycling rate, a rate of this order is probably rapid enough to generate such a trend.

A number of $\delta^{13}C$ and $\delta^{18}O$ studies of carbonatites have been undertaken in an attempt to determine values characteristic of the mantle. These studies found a considerable range of $\delta^{13}C$ and $\delta^{18}O$ compositions which overlap with those more recently determined for mid-ocean ridge basalts. Although these $\delta^{13}C$ and $\delta^{18}O$ compositions have been interpreted as representing primitive mantle values, the radiogenic Pb isotope characteristics of carbonatites are not compatible with a primitive mantle origin. Furthermore, if carbonatites are derived from subducted lithosphere which has been subjected to degassing, low-temperature alteration and/or hydrothermal processes, significant shifts in $\delta^{13}C$ and $\delta^{18}O$ from mantle values are probable. Because of the low concentrations of magmatic carbon in tholeiitic basalt, the $\delta^{13}C$ composition of altered MORB will be strongly influenced by that of the contaminants. Phanerozoic pelagic carbonates and secondary carbonates in weathered and hydrothermally altered basalt generally have $\delta^{13}C_{PDB}$ values of ≈ 0 to +2 ‰ (DEGENS, 1969; ANDERSON and LAWRENCE, 1976; McKENZIE, 1980). Measurements of the oxygen isotopic compositions of altered oceanic tholeiites (for example, GREGORY and TAYLOR, 1981) have generally found both ^{18}O enrichments, attributed to low-temperature hydrothermal exchange, and depletions, probably due to high-temperature exchange, with $\delta^{18}O_{SMOW}$ values typically ranging from +4 to +12 ‰. The $\delta^{13}C$ and $\delta^{18}O$ values of carbonatites fall within the range of altered and unaltered sea-floor tholeiite and it is therefore conceivable that the shifts towards higher $\delta^{13}C$ and $\delta^{18}O$ values, relative to those of MORB, found in many carbonatites are due to exchange of the carbon and oxygen of the oceanic lithospheric sources of carbonatites with seawater, prior to their subduction. Because of the generally low Rb, Sr and REE concentrations of secondary carbonate compared to oceanic tholeiites (*cf.* McCULLOCH *et al.*, 1981), the Sr and Nd isotopic evolution of oceanic crust may not be significantly effected by the addition of secondary carbonate during low-temperature alteration processes, although some shifts towards more radiogenic $^{87}Sr/^{86}Sr$ might be anticipated due to Sr exchange with seawater. The generally radiogenic Pb isotopic compositions of many carbonatites may be attributable to uptake of uranium from seawater by basalt during low-temperature alteration, as was advanced by HOFMANN and WHITE (1982).

The geochemical and stable and radiogenic isotopic characteristics of carbonatites are therefore consistent with their generation from subducted oceanic lithospheric sources. That similar isotopic features are found in some late Archaean alkaline and carbonatite complexes, such as the Siilinjarvi Carbonatite Complex of eastern Finland and in the Poohbah Lake complex from the Superior Province of the Canadian Shield, suggests that subduction and recycling processes have operated since at least the late Archaean. Future detailed studies of carbonatite complexes of different ages may enable the geochemical and isotopic evolution of ocean-island sources throughout the Earth's differentiation history to be

determined.

Acknowledgements- We are grateful to J. Ferguson (Greater Pacific Investments), R.K. Duncan (C.S.B.P. and Farmers Ltd.), I. McDougall (R.S.E.S.) and L.P. Black (B.M.R.) for provision of samples, H. Hensel (Geology Dept., A.N.U.) for assistance with the petrography, and R. Hill (R.S.E.S.), S. Kesson (R.S.E.S.), K. Bell (Carleton University, Ottawa), W.F. McDonough (R.S.E.S.), S.-S. Sun (R.S.E.S.) and J.W. Bristow (De Beers Consolidated Mines Ltd.) for useful discussions. The manuscript also benefitted from constructive reviews by A.R. Basu (Rochester, New York), W.M. White (Cornell, New York) and an anonymous reviewer. Technical assistance was provided by J. Cali (XRD), E. Webber (INAA) and J. Cowley (stable-isotope preparation).

REFERENCES

ALLEGRE C.J., PINEAU F., BERNAT M. and JAVOY M. (1971) Geochemical evidence for the occurrence of carbonatites on the Cape Verde and Canary Islands. *Nature* **233**, 103.

ALLEN J.B. and DEANS T. (1965) Ultrabasic eruptives with alnöitic-kimberlitic affinities from Malaita, Solomon Islands. *Mineral. Mag.* **34**, 16-34.

ALLSOPP H.L. and ERIKSSON S.C. (1986) The Phalaborwa complex; isotopic evidence for ancient lithospheric enrichment. (abstr.) Joint Ann. Meeting, G.A.C.-M.A.C., Carleton University, Ottawa, 40.

AMARAL G. (1978) Potassium-argon studies on the Jacupiranga alkaline district, State of São Paulo, Brazil. In *Proc. First Int. Symp. Carbonatites.* Brasilia, Departmento Nacional da Producao Mineral, 297-302.

ANDERSON T.F. and LAWRENCE J.R. (1976) Stable isotope investigations of sediments, basalts and authigenic phases from Leg 35 cores. In *Init. Reps. DSDP* **35**, 497-505. U.S. Govt. Printing Office, Washington, D.C.

BAKER B.H., WILLIAMS L.A.J., MILLER J.A. and FITCH F.J. (1971) Sequence and geochronology of the Kenya rift volcanics. *Tectonophys.* **11**, 191-215.

BAILEY D.K. (1984) Kimberlite: the mantle sample formed by ultrametasomatism. In *Kimberlites. I: Kimberlites and Related Rocks.* (ed. J. Kornprobst). pp. 323-357. Elsevier, Amsterdam.

BARREIRO B. (1983) An isotopic study of the Westland dyke swarm, South Island, New Zealand. *Carnegie Inst. Wash. Yearb.* **82**, 471-475.

BARRERA J.L., FERNANDEZ SANTIN S., FUSTER J.M. and IBARROLA E. (1981) Ijolitas-sienitas-carbonatitas de los macizos del norte del complejo plutonico basal de Fuerteventura (Islas Canarias). *Bol. Geol. Min.* (Madrid) **92**, 309-321.

BARTH T.F.W. and RAMBERG I. (1966) The Fen complex. In *Carbonatites.* (eds. O.F. Tuttle and J. Gittins), pp. 225-257. Interscience, New York.

BASU A.R. and TATSUMOTO M. (1980) Nd-isotopes in selected mantle-derived rocks and minerals and their implications for mantle evolution. *Contrib. Mineral. Petrol.* **75**, 43-54.

BELL K. and POWELL J.L. (1970) Strontium isotopic studies of alkalic rocks: the alkalic complexes of eastern Uganda. *Bull. Geol. Soc. Amer.* **81**, 3481-3490.

BELL K. and BLENKINSOP J. (1986) Carbonatites and the subcontinental mantle. (abstr.) Joint Ann. Meeting, G.A.C.-M.A.C., Carleton University, Ottawa. p44.

BELL K. and BLENKINSOP J. (1987a) Archean depleted mantle- evidence from Nd and Sr initial isotopic ratios of carbonatites. *Geochim. Cosmochim. Acta* **51**, 291-298.

BELL K. and BLENKINSOP J. (1987b) Nd and Sr isotopic compositions of East African carbonatites: implications for mantle heterogeneity. *Geology* **15**, 99-102.

BELL K., DAWSON J.B. and FARQUHAR R.M. (1973) Strontium isotope studies of alkalic rocks: the active carbonatite volcano Oldoinyo Lengai, Tanzania. *Bull. Geol. Soc. Amer.* **84**, 1019-1030.

BELL K., BLENKINSOP J., COLE T.J.S. and MENAGH D.P. (1982) Evidence from Sr isotopes for long-lived heterogeneities in the upper mantle. *Nature* **298**, 251-253.

BIELSKI-ZYSKIND M., WASSERBURG G.J. and NIXON P.J. (1984) Sm-Nd and Rb-Sr systematics in volcanics and ultramafic xenoliths from Malaita, Solomon Islands, and the nature of the Ontong Java Plateau. *J. Geophys. Res.* **89**, 2415-2424.

BLACK L.P. and GULSON B.L. (1978) The age of the Mud Tank carbonatite, Strangways Range, Northern Territory. *B.M.R. J. Geol. Geophys.* **3**, 227-232.

BLATTNER P. and COOPER A.F. (1974) Carbon and oxygen isotopic composition of carbonatite dikes and metamorphic country rock of the Haast Schist terrain, New Zealand. *Contrib. Mineral. Petrol.* **4**, 17-27.

BREY G., BRICE W.R., ELLIS D.J., GREEN D.H., HARRIS K.L. and RYABCHIKOV I.D. (1983) Pyroxene-carbonate reactions in the upper mantle. *Earth Planet. Sci. Lett.* **62**, 63-74.

CHASE C.G. (1981) Oceanic island Pb: Two stage histories and mantle evolution. *Earth Planet. Sci. Lett.* **52**, 277-284.

CHEN C.-Y. and FREY F.A. (1983) Origin of Hawaiian tholeite and alkali basalt. *Nature* **302**, 785-789.

COHEN R.S. and O'NIONS R.K. (1982a) The lead, neodymium and strontium isotopic structure of ocean ridge basalts. *J. Petrol.* **23**, 299-324.

COHEN R.S. and O'NIONS R.K. (1982b) Identification of recycled continental material in the mantle from Sr, Nd and Pb isotope investigations. *Earth Planet. Sci. Lett.* **61**, 73-84.

COHEN R.S., O'NIONS R.K. and DAWSON J.B. (1984) Isotope geochemistry of xenoliths from East Africa: implications for development of mantle reservoirs and their interaction. *Earth Planet. Sci. Lett.* **68**, 209-220.

DEANS T. and POWELL J.L. (1968) Trace elements and strontium isotopes in carbonatites, fluorites and limestones from India and Pakistan. *Nature* **218**, 750-752.

DEGENS E.T. (1969) Biogeochemistry of stable isotopes. In *Organic Geochemistry.* (ed. G. Eglinton and M.T.J. Murphy), pp. 304-329. Springer Verlag, New York.

DEINES P. and GOLD D.P. (1973) The isotopic composition of carbonatite and kimberlite carbonates and their bearing on the isotopic composition of deep-seated carbon. *Geochim. Cosmochim. Acta* **37**, 1709-1733.

DePAOLO D.J. (1978) Nd and Sr isotope systematics of young continental igneous rocks. 4th Int. Isotope Conference, Geochronology, Cosmochronology, Isotope Geology. *U.S. Geol. Surv. Open-File Rep.* **78-701**, 91-93.

DERRY L.A. and JACOBSEN S.B. (1986) Nd and Sr isotopic measurements from the Fen Complex, south Norway. (Abstr.) *Eos* **67**, 1265.

DES MARAIS D.J. and MOORE J.G. (1984) Carbon and its isotopes in mid-oceanic basaltic glasses. *Earth Planet. Sci. Lett.* **69**, 43-57.

DUPRÉ B. and ALLEGRE C.J. (1980) Pb-Sr-Nd isotopic correlation and chemistry of North Atlantic mantle. *Nature* **286**, 17-22.

EBY G.N. (1975) Abundance and distribution of the rare earth elements and yttrium in the rocks and minerals of the Oka carbonatite complex, Quebec. *Geochim. Cosmochim. Acta* **39**, 597-620.

ERICKSON R.L. and BLADE L.V. (1963) Geochemistry and petrology of the alkalic igneous complex at Magnet Cove, Arkansas. *U.S. Geol. Surv. Prof. Paper* 425.

FERGUSON J. and SHERATON J.W. (1979) Petrogenesis of kimberlitic rocks and associated xenoliths of southeastern Australia. In *Kimberlites, Diatremes and Diamonds; their Geology, Petrology, and Geochemistry.* (eds. F.R. Boyd and H.O.A. Meyer), pp. 140-161. Amer. Geophys. Union Monogr., Washington.

FRIEDMAN I., O'NEIL J. and CEBULA G. (1982) Two new carbonate stable-isotope standards. *Geostandards Newsletter* **6**, 11-12.

GARSON M.S. (1966) Carbonatites in southern Malawi. In *Carbonatites*. (eds. O.F. Tuttle and J.Gittins), pp. 33-71. Interscience, New York.

GASPAR J.C. and WYLLIE P.J. (1984) The alleged kimberlite-carbonatite relationship: evidence from illmenite and spinel from Premier and Wesselton Mines and the Benfontein Sill, South Africa. *Contrib. Mineral. Petrol.* **85**, 133-140.

GITTINS J. (1966) Summaries and bibliographies of carbonatite complexes. In *Carbonatites*. (eds. O.F. Tuttle and J.Gittins), pp. 417-540. Interscience, New York.

GONFIANTINI R. and TONGIORGI E. (1964) La composition isotopique des carbonatites du Kaiserstuhl. In *Report E.U.R. 1827 d.e.f. of the European Atomic Energy Commission.* (ed. L.V. Wambecke) 193-199.

GREGORY R.T. and TAYLOR H.P. Jr. (1981) An oxygen profile in a section of Cretaceous oceanic crust, Samail Ophiolite, Oman: evidence for $\delta^{18}O$ buffering of the oceans by deep (>5 km) seawater-hydrothermal circulation at mid-ocean ridges. *J. Geophys. Res.* **86**, 2737-2755.

GRIFFIN W.L. and TAYLOR P.N. (1975) The Fen damkjernite: petrology of a "central complex kimberlite". In *Physics and Chemistry of the Earth.* (eds. L.H. Ahrens, F. Press, S.K. Runcorn and H.C. Urey) Vol. 9, pp. 163-177.

GRÜNENFELDER M.H., TILTON G.R., BELL K. and BLENKINSOP J. (1986) Lead and strontium isotope relationships in the Oka carbonatite complex, Quebec. *Geochim. Cosmochim. Acta* **50**, 461-468.

HAMILTON D.L., FREESTONE I.C., DAWSON J.B. and DONALDSON C.H. (1979) Origin of carbonatites by liquid immiscibility. *Nature* **279**, 52-54.

HARMER R.E. (1986) Rb-Sr isotopic study of units of the Pienaars River Alkaline Complex, north of Pretoria, South Africa. *Trans. Geol. Soc. S. Africa* **88**, 215-223.

HEINRICH E.W. (1966) *The Geology of Carbonatites.* Rand McNally, Chicago, 555p.

HOFMANN A.W. and WHITE W.M. (1982) Mantle plumes from ancient oceanic crust. *Earth Planet. Sci. Lett.* **57**, 421-436.

HOLLOWAY J.R., MYSEN B.O. and EGGLER D.H. (1977) The solubility of CO_2 in liquids on the join CaO-MgO-SiO_2-CO_2. *Carnegie Inst. Wash. Yearb.* **75**, 626-631.

KING B.C. (1965) Petrogenesis of the alkaline igneous rock suites of the volcanic and intrusive centres of eastern Uganda. *J. Petrol.* **6**, 67-100.

KING B.C. and SUTHERLAND D.S. (1966) The carbonatite complexes of eastern Uganda. In *Carbonatites.* (eds. O.F. Tuttle and J.Gittins), pp. 73-126. Interscience, New York.

KROENKE L.W. (1972) Geology of the Ontong Java Plateau. *Hawaiian Inst. Geophysics Report, HIG-72-5*, Univ. of Hawaii, 19p.

KWON S.T. and TILTON G.R. (1986) Comparative isotopic studies of Cargill and Borden carbonatite complexes from the Kapuskasing gravity high zone, Ontario. (abstr.) Joint Ann. Meeting, G.A.C.-M.A.C., Carleton University, Ottawa, 92.

KYSER T.K., O'NEIL J.R. and CARMICHAEL I.S.E. (1982) Genetic relations among basic lavas and ultramafic nodules: evidence from oxygen isotope compositions. *Contrib. Mineral. Petrol.* **81**, 88-102.

LANCELOT J.R. and ALLEGRE C.J. (1974) Origin of carbonatitic magma in the light of the Pb-U-Th isotope system. *Earth Planet. Sci. Lett.* **22**, 233-238.

LE BAS M.J. (1984) Oceanic Carbonatites. In *Kimberlites. I: Kimberlites and Related Rocks.* (ed. J. Kornprobst), pp. 169-178. Elsevier, Amsterdam.

LOUBET M., BERNAT M., JAVOY M. and ALLEGRE C.J. (1972) Rare earth contents in carbonatites. *Earth Planet. Sci. Lett.* **14**, 226-232.

McCULLOCH M.T. and CHAPPELL B.W. (1982) Nd isotopic characteristics of S- and I- type granites. *Earth Planet. Sci. Lett.* **58**, 51-64.

McCULLOCH M.T., GREGORY R.T., WASSERBURG G.J. and TAYLOR H.P. Jr. (1981) Sm-Nd, Rb-Sr, and $^{18}O/^{16}O$ systematics in an oceanic crustal section: evidence from the Samail Ophiolite. *J. Geophys. Res.* **86**, 2721-2735.

McDONOUGH W.F., McCULLOCH M.T. and SUN S.-S. (1985) Isotopic and geochemical systematics in Tertiary-Recent basalts from southeastern Australia and implications for the evolution of the sub-continental lithosphere. *Geochim. Cosmochim. Acta* **49**, 2051-2067.

McKENZIE D. (1985) The extraction of magma from the crust and mantle. *Earth Planet. Sci. Lett.* **74**, 81-91.

McKENZIE J. (1980) Stable isotope study of carbonate minerals from the basalt flows on Suiko Seamount: D.S.D.P. Leg 55 Hole 433C. In *Init. Reps DSDP* **55**, 653-657. U.S. Govt. Printing Office, Washington, D.C.

MIDENDE G., DEMAIFFE D., WEIS D. and MENNESSIER J.P. (1986) Sr, Nd and Pb isotope evidence for the origin of carbonatites from the western branch of the African Rift (abstr.) *Eos* **67**, 1267.

MITCHELL R.H. and CROCKET J.H. (1970) Isotopic composition of strontium in rocks of the Fen Alkaline Complex, south Norway. *J. Petrol.* **13**, 83-97.

MÖLLER P., MORTEANI G. and SCHLEY F. (1980) Discussion of REE distribution of carbonatites and alkalic rocks. *Lithos* **13**, 171-179.

NELSON D.R., McCULLOCH M.T. and SUN S.-S. (1986) The origins of ultrapotassic rocks as inferred from Sr, Nd and Pb isotopes. *Geochim. Cosmochim. Acta* **50**, 231-245.

NIELSEN T.F.D. and BUCHART B. (1985) Sr-C-O isotopes in nephelinitic rocks and carbonatites, Gardiner Complex, Tertiary of east Greenland. *Chem. Geol.* **53**, 207-217.

NIXON P.H. and BOYD F.R. (1979) Garnet-bearing lherzolites and discrete nodule suites from the Malaita alnöite, Solomon Islands, SW Pacific, and their bearing on oceanic mantle composition and geotherm. In *The Mantle Sample.* (eds. F.R. Boyd and H.O.A. Meyer), pp 400-423. Amer. Geophys. Union Monogr., Washington.

NIXON P.H., MITCHELL R.H. and ROGERS N.W. (1980) Petrogenesis of alnöitic rocks from Malaita, Solomon Islands, Melanesia. *Mineral. Mag.* **43**, 587-596.

NORRISH K. and CHAPPELL B.W. (1967) X-ray fluorescence spectrography. In *Physical Methods in Determinative Mineralogy.* (ed. J. Zussman), pp. 161-214. Academic Press, Oxford.

NORRISH K. and HUTTON J.T. (1969) An accurate X-ray spectrographic method for the analysis of a wide range of geological samples. *Geochim. Cosmochim. Acta* **33**, 6091-6101.

NORRY M.J., TRUCKLE P.H., LIPPARD S.J., HAWKESWORTH C.J., WEAVER S.D. and MARRINER G.F. (1980) Isotopic and trace element evidence from lavas, bearing on mantle heterogeneity beneath Kenya. *Phil. Trans. Roy. Soc. London* **A 297**, 259-271.

O'NIONS R.K., HAMILTON P.J. and EVENSEN N.M. (1977) Variations in $^{143}Nd/^{144}Nd$ and $^{87}Sr/^{86}Sr$ ratios in oceanic basalts. *Earth Planet. Sci. Lett.* **34**, 13-22.

PALACZ Z.A. and SAUNDERS A.D. (1986) Coupled trace element and isotope enrichment in the Cook-Austral-Samoa islands, southwest Pacific. *Earth Planet. Sci. Lett.* **79**, 270-280.

PINEAU F., JAVOY M. and ALLEGRE C.J. (1973) Étude systématique des isotopes de l'oxygène, du carbone et du strontium dans les carbonatites. *Geochim. Cosmochim. Acta* **37**, 2363-2377.

PLYUSNIN G.S., VOROB'YEV I. and PERMINOV A.V. (1984) Isotopic composition ($\delta^{18}O$, $\delta^{13}C$) of carbonatites in the Murun alkalic rock block. *Doklady Academii Nauk. SSSR* **275**, 999-1003.

POWELL J.L. (1965) Low abundance of Sr^{87} in Ontario carbonatites. *Amer. Mineral.* **50**, 1075-1079.

POWELL J.L. (1966) Isotopic composition of strontium in carbonatites and kimberlites. *Mineral. Soc. India, IMA volume*, 58-66.

RINGWOOD A.E. (1982) Phase transformations and differentiation in subducted lithosphere: implications for mantle dynamics, basalt petrogenesis, and crustal evolution. *J. Geol.* **90**, 611-643.

RODEN M.F., MURTHY R.V. and GASPAR J.C. (1985) Sr and Nd isotopic composition of the Jacupiranga carbonatite. *J. Geol.* **93**, 212-220.

SCOTT-SMITH B.H., DANCHIN R.V., HARRIS J.W. and STRACKE K.J. (1984) Kimberlites near Orroroo, South Australia. In *Kimberlites. I: Kimberlites and Related Rocks.* (ed. J. Kornprobst), pp. 121-142. Elsevier, Amsterdam.

SILVA L.C., LE BAS M.J. and ROBERTSON A.H.F. (1981) An oceanic carbonatite volcano on Santiago, Cape Verde Islands. *Nature* **294**, 644-645.

SMITH C.B. (1983) Pb, Sr and Nd isotopic evidence for sources of southern African Cretaceous kimberlite. *Nature* **304**, 51-54.

SNELLING N.J. (1965) Age determinations on three African carbonatites. *Nature* **205**, 491.

SNELLING N.J., HAMILTON E.I., DRYSALL A.R. and STILLMAN C.J. (1964) A review of age determinations from northern Rhodesia. *Econ. Geol.* **59**, 961-981.

SPERA F.J. and BERGMAN S.C. (1980) Carbon dioxide in igneous petrogenesis: 1. Aspects of the dissolution of CO_2 in silicate liquids. *Contrib. Mineral. Petrol.* **74**, 55-66.

STEIGER R.H. and JÄGER E. (1977) Subcommission on geochronology: convention on the use of decay constants in geo- and cosmochronology. *Earth Planet. Sci. Lett.* **36**, 359-362.

STRACKE K.J., FERGUSON J. and BLACK L.P. (1979) Structural setting of kimberlites in south-eastern Australia. In *Kimberlites, Diatremes and Diamonds: their Geology, Petrology, and Geochemistry.* (eds. F.R. Boyd and H.O.A. Meyer), pp. 71-91. Amer. Geophys. Union Monogr., Washington.

STRECKEISEN A. (1979) Classification and nomenclature of volcanic rocks, lamprophyres, carbonatites, and melilitic rocks: Recommendations and suggestions of the IUGS Subcommission on the Systematics of Igneous Rocks. *Geology* **7**, 331-335.

SUN S.-S. (1980) Lead isotopic study of young volcanics from mid-ocean ridges, ocean islands and island arcs. *Phil. Trans. Roy. Soc. London* **A 297**, 409-445.

SUN S.-S., JAQUES A.L. and McCULLOCH M.T. (1986) Isotopic evolution of the Kimberley Block, Western Australia (extended abstr.) 4th Int. Kimberlite Conf., Perth. *Geol. Soc. Aust. Abstr. Series* **16**, 346-348.

SUWA K., OANA S., WADA H. and SUSUMU O. (1975) Isotope geochemistry and petrology of African carbonatites. In *Physics and Chemistry of the Earth.* (eds. L.H. Ahrens, F. Press, S.K. Runcorn and H.C. Urey) Vol. 9, pp. 735-745.

TAYLOR S.R. and GORTON M.P. (1977) Geochemical application of Spark Source Mass Spectrometry - III. Element sensitivity, precision, accuracy. *Geochim. Cosmochim. Acta* **41**, 491-510.

THOMPSON R.N., MORRISON M.A., HENDRY G.L., and PARRY S.J. (1984) An assessment of the relative roles of crust and mantle in magma genesis: an elemental approach. *Phil. Trans. Roy. Soc. London* **A 310**, 549-590.

TILTON G.R., KWON S.T. and FROST D.M. (1987) Isotopic relationships in Arkansas Cretaceous alkalic complexes. *Geol. Soc. Amer. Spec. Paper* **215.**

TREIMANN A.H. and ESSENE E.J. (1983) Mantle eclogite and carbonate as sources of sodic carbonatites and alkalic magmas. *Nature* **302**, 700-703.

TUCKER D.H. and COLLERSON K.D. (1972) Lamprophyric intrusions of probable carbonatitic affinity from South Australia. *J. Geol. Soc. Aust.* **19**, 387-391.

VERWOERD W.J. (1966) South African carbonatites and their probable mode of origin. *Annale, Univ. Stellenbosch* **41** (serie A), number 2.

VIDAL P., CHAUVEL C. and BROUSSE R. (1984) Large mantle heterogeneity beneath French Polynesia. *Nature* **307**, 536-538.

WELKE H.J., ALLSOPP H.L. and HARRIS J.W. (1974) Measurements of K, Rb, U, Sr and Pb in diamonds containing inclusions. *Nature* **252**, 35-37.

WENDLANDT R.F. (1984) An experimental and theoretical analysis of partial melting in the system $KAlSiO_4$-CaO-MgO-SiO_2-CO_2 and applications to the genesis of potassic magmas, carbonatites and kimberlites. In *Kimberlites. I: Kimberlites and Related Rocks.* (ed. J. Kornprobst), pp. 359-369. Elsevier, Amsterdam.

WENDLANDT R.F. and HARRISON W.J. (1979) Rare earth partitioning between immiscible carbonate and silicate liquids and CO_2 vapour: results and implications for the formation of light rare earth-enriched rocks. *Contrib. Mineral. Petrol.* **69**, 409-419.

WHITE W.M. and HOFMANN A.W. (1982) Sr and Nd isotope geochemistry of oceanic basalts and mantle evolution. *Nature* **296**, 821-825.

WILLETT G.C., DUNCAN R.K. and RANKIN R.A. (1986) Geology and economic evaluation of the Mt Weld carbonatite, Laverton, Western Australia (extended abstr.) 4th Int. Kimberlite Conf., Perth. *Geol. Soc. Aust. Abstr. Series* **16**, 97-99.

WILLIAMS R.W., GILL J.B. and BRULAND K.W. (1986) Ra-Th disequilibria systematics: Timescale of carbonatite magma formation at Oldoinyo Lengai volcano, Tanzania. *Geochim. Cosmochim. Acta* **50**, 1249-1259.

WILSON A.F. (1979) Contrast in the isotopic composition of oxygen and carbon between the Mud Tank Carbonatite and the marbles in the granulite terrane of the Strangways Range, central Australia. *J. Geol. Soc. Aust.* **26**, 39-44.

WIMMENAUER W. (1966) The eruptive rocks and carbonatites of the Kaiserstuhl, Germany. In *Carbonatites.* (eds. O.F. Tuttle and J. Gittins), pp. 183-204. Interscience, New York.

WOOD D.A. (1979) Dynamic partial melting: its application to the petrogenesis of basalts erupted in Iceland, the Faeroe Islands, the Isle of Skye (Scotland) and the Troodos Massif (Cyprus). *Geochim. Cosmochim. Acta* **43**, 1031-1046.

WYLLIE P.J. and HUANG W.-L. (1975) Peridotite, kimberlite, and carbonatite explained in the system $CaO-MgO-SiO_2-CO_2$. *Geology* **3**, 621-624.

WYLLIE P.J. and HUANG W.-L. (1976) Influence of mantle CO_2 in the generation of carbonatites and kimberlites. *Nature* **257**, 297-299.

ZARTMAN R.E., BROCK M.R., HEYL A.V. and THOMAS H.H. (1967) K-Ar and Rb-Sr ages from some alkalic intrusive rocks from central and eastern United States. *Amer. J. Sci.* **265**, 848-870.

Figure Captions

FIGURE 1. Trace-element abundances normalised to estimated primitive mantle abundances (from McDONOUGH *et al.*, 1985 and NELSON *et al.*, 1986) for carbonatites and a phonolite from Kaiserstuhl. Two groups are distinguishable; those possessing pronounced negative Zr and Hf anomalies typically accompanied by negative U anomalies and a second group (comprising the Walloway and Goudini carbonatites) which lack these features and generally possess relatively smooth trace-element patterns but with negative K anomalies. The latter group also have higher abundances of SiO_2 and the transition elements. Also shown for comparison is the field of trace-element patterns for some ocean-island basalts (from CHEN and FREY, 1983; THOMPSON *et al.*, 1984 and PALACZ and SAUNDERS, 1986).

FIGURE 2. Chondrite-normalised rare-earth element patterns for carbonatites and the Kaiserstuhl phonolite. Chondrite values are those of TAYLOR and GORTON (1977). Thr rare-earth element patterns for two secondary (sedimentary origin) carbonate veins (from the Walloway region, South Australia) are also shown for comparison.

FIGURE 3. Initial ε_{Nd} versus initial $^{87}Sr/^{86}Sr$ for carbonatites compared to the fields for MORB, Group 1 (basaltic) South African kimberlites and alkali basalts from the St Helena isotopic type of ocean island (comprising St Helena, Ascension, Comoros and Austral ocean islands). The carbonatites have been separated into four age groups. Mixtures of a component isotopically resembling young carbonatite and the depleted MORB mantle reservoir could generate the isotopic characteristics of some ocean-island basalts. Additional data sources; RODEN *et al.* (1985); BARREIRO (1983); SMITH (1983); VIDAL *et al.* (1984); WHITE and HOFMANN (1982); O'NIONS *et al.* (1977); DUPRÉ and ALLEGRE (1980); COHEN and O'NIONS (1982a, b).

FIGURE 4. a) $^{206}Pb/^{204}Pb$ versus $^{207}Pb/^{204}Pb$ and b) $^{206}Pb/^{204}Pb$ versus $^{208}Pb/^{204}Pb$ for carbonatites compared to the field of mid-ocean ridge basalts and ocean-island basalts (dots). Some of the samples in Table 3 require relatively large age corrections, so only samples for which initial Pb compositions can be confidently determined are shown. In general, carbonatites have Pb isotopic compositions which fall along the array defined by MORB and ocean-island basalts. Data sources as in Fig. 3 and LANCELOT and ALLEGRE (1974); SUN (1980); GRÜNENFELDER *et al.* (1986), WILLIAMS *et al.* (1986) and TILTON *et al.* (1987).

FIGURE 5. Oxygen- and carbon- isotope compositions of carbonatites compared to the inferred mantle field (determined from isotopic studies of MORB, from DES MARAIS and MOORE, 1984 and KYSER *et al.*, 1982) and to the field of sedimentary carbonate. Additional data from DEINES and GOLD (1973) and BLATTNER and COOPER (1974). The isotopically heavy oxygen and carbon of the volcanically-emplaced Goudini carbonatite may result from greater degree of isotopic exchange during its emplacement compared to intrusively-emplaced carbonatites. The trend toward isotopically heavier carbon and oxygen compared to inferred mantle compositions may be attributable to crustal interaction during

emplacement, Rayleigh fractionation processes (ie; preferential loss of the lighter isotopes in volatile phases) or may reflect differences within the source regions of carbonatites.

FIGURE 6. a) Initial Sr, and b) Initial Nd isotopic composition versus age of emplacement for carbonatites worldwide. When the possible effects of crustal contamination are considered, there is a general trend to higher initial $^{87}Sr/^{86}Sr$ and ε_{Nd} for younger carbonatites. Analytical error limits are shown; no account has been made for error in the age determinations. Although this trend is relatively well-defined for the well-characterised Canadian carbonatites (see BELL and BLENKINSOP, 1987a), it is not confined to any one continent but is a global feature. Additional data sources; BELL and POWELL (1970); WELKE *et al.*, (1974); BLACK and GULSON (1978); STRACKE *et al.*, (1979); BASU and TATSUMOTO (1980); BARREIRO (1983); NIELSEN and BUCHARDT (1985); GRÜNENFELDER *et al.*, (1986); BELL and BLENKINSOP (1987a,b).

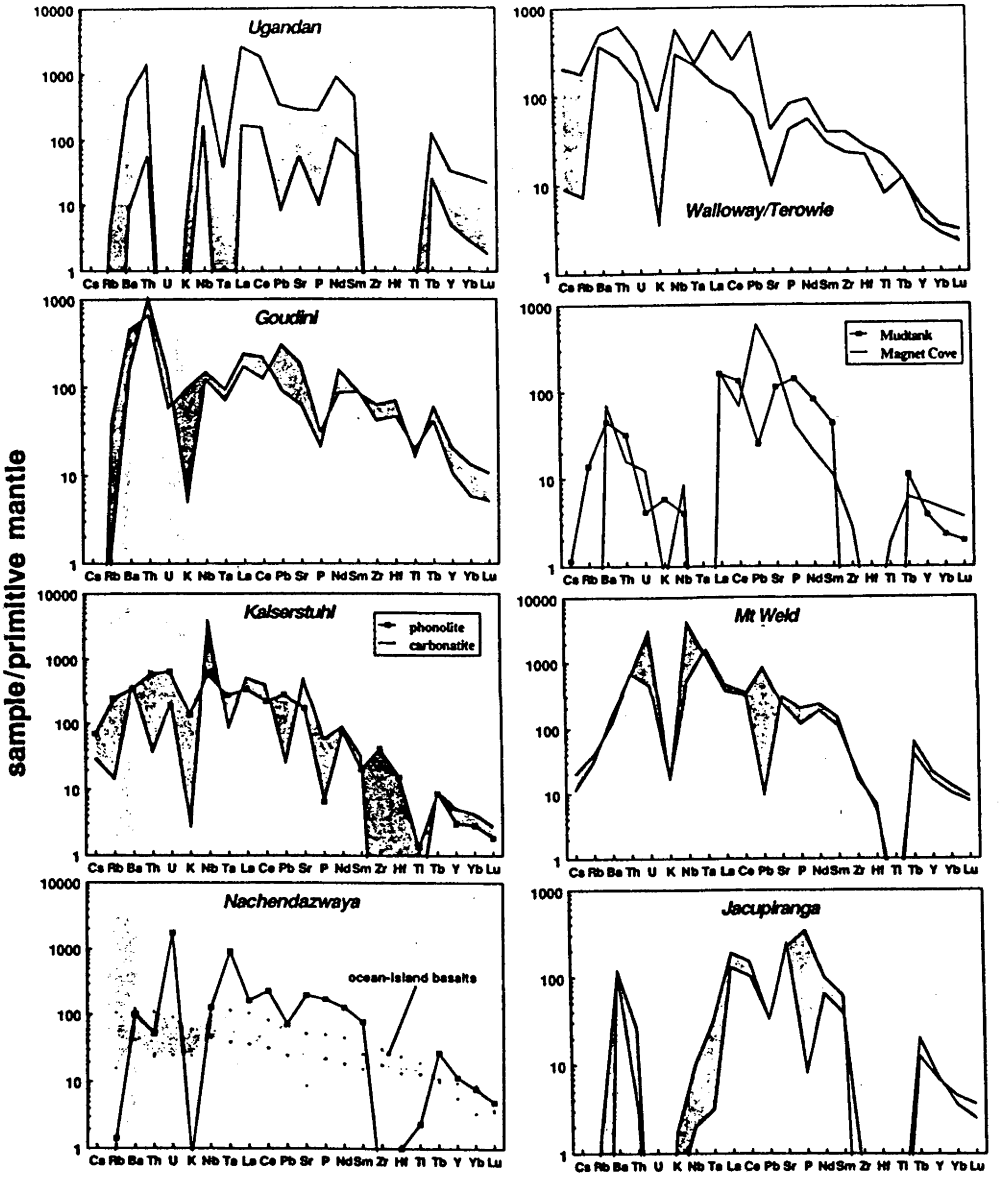
sample/primitive mantle
Ugandan
Walloway/Terowie
Goudini
Mudtank
Magnet Cove
Kalserstuhl
phonolite
carbonatite
Mt Weld
Nachendazwaya
ocean-island basalts
Jacupiranga
Cs Rb Ba Th U K Nb Ta La Ce Pb Sr P Nd Sm Zr Hf Ti Tb Y Yb Lu

Fig. 1.

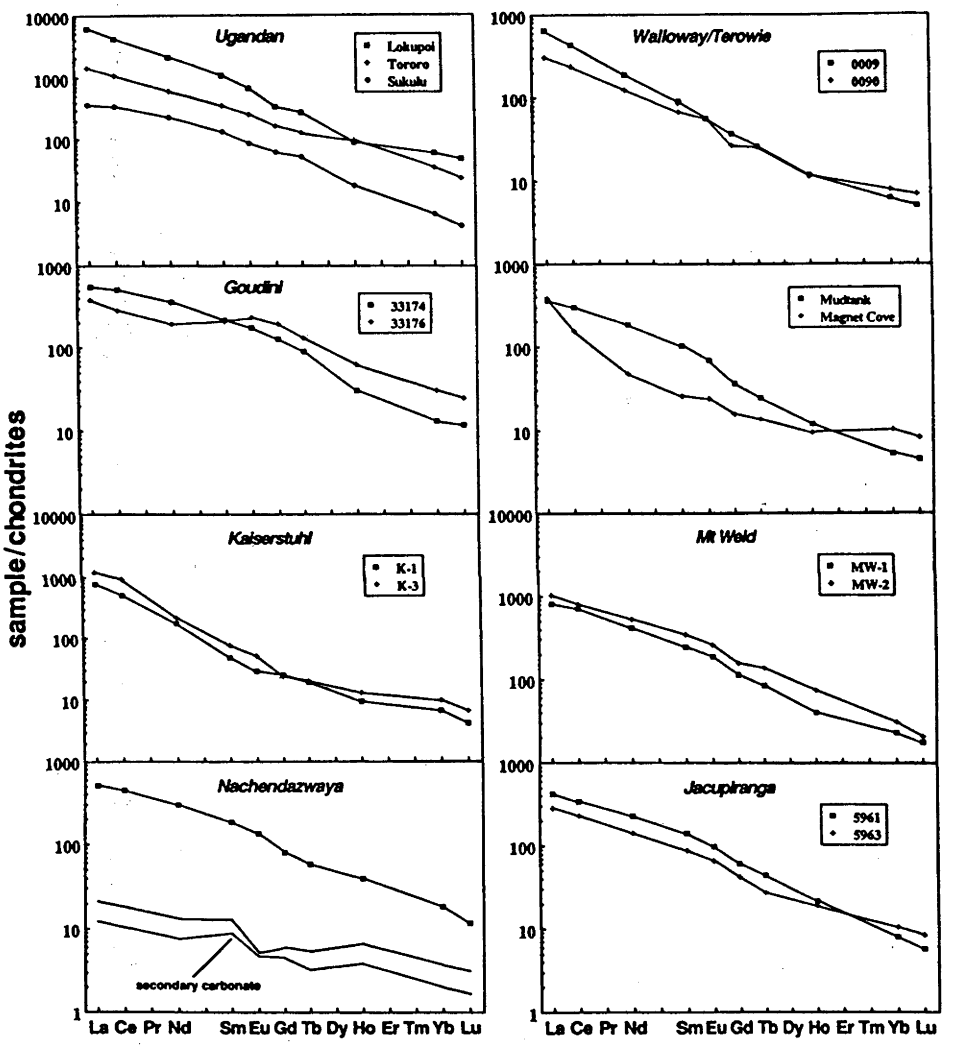
Ugandan
Lokupoi
Tororo
Sukulu
Walloway/Terowie
0009
0090
Goudlini
33174
33176
Mudtank
Magnet Cove
Kaiserstuhl
K-1
K-3
Mt Weld
MW-1
MW-2
Nachendazwaya
secondary carbonate
Jacupiranga
5961
5963
sample/chondrites
La Ce Pr Nd Sm Eu Gd Tb Dy Ho Er Tm Yb Lu

Fig. 2.

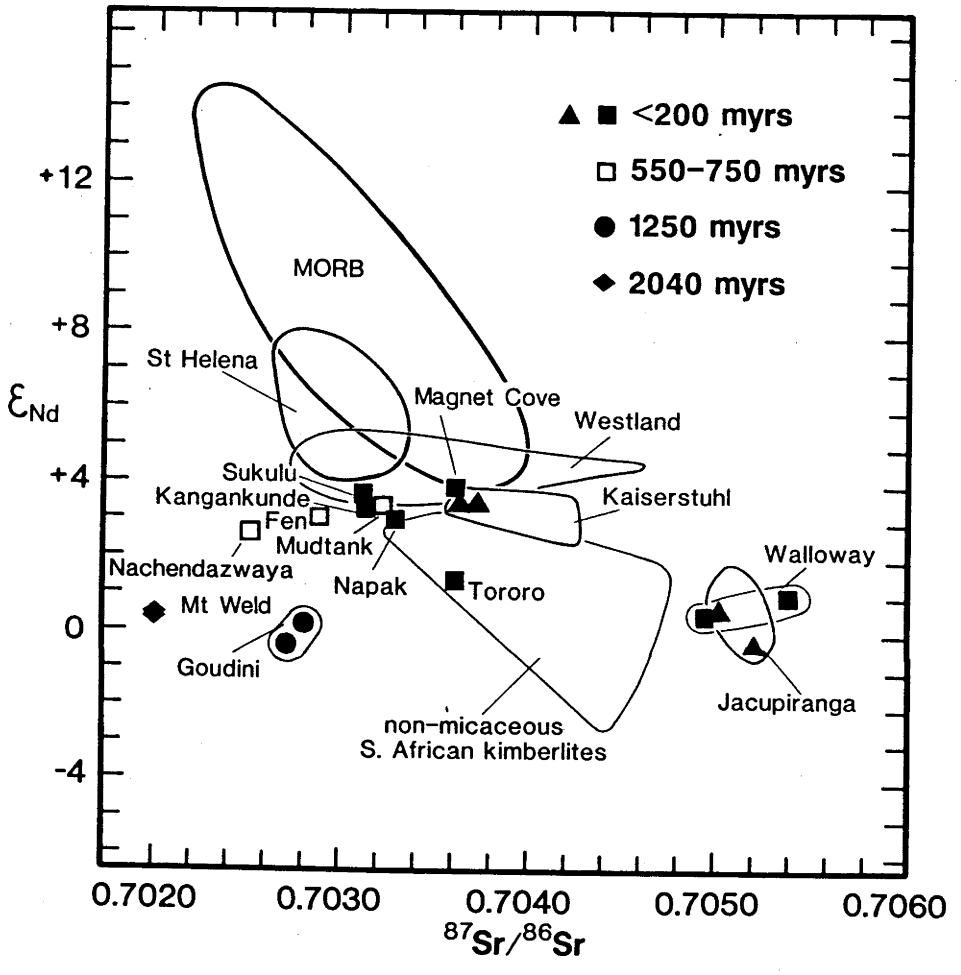
▲ ■ <200 myrs
□ 550–750 myrs
● 1250 myrs
◆ 2040 myrs
MORB
St Helena
Magnet Cove
Westland
Sukulu
Kangankunde
Fen
Kaiserstuhl
Mudtank
Nachendazwaya
Napak
Tororo
Walloway
Mt Weld
Goudini
Jacupiranga
non-micaceous
S. African kimberlites
+12
+8
+4
0
-4
εNd
0.7020
0.7030
0.7040
0.7050
0.7060
87Sr/86Sr

Fig. 3.

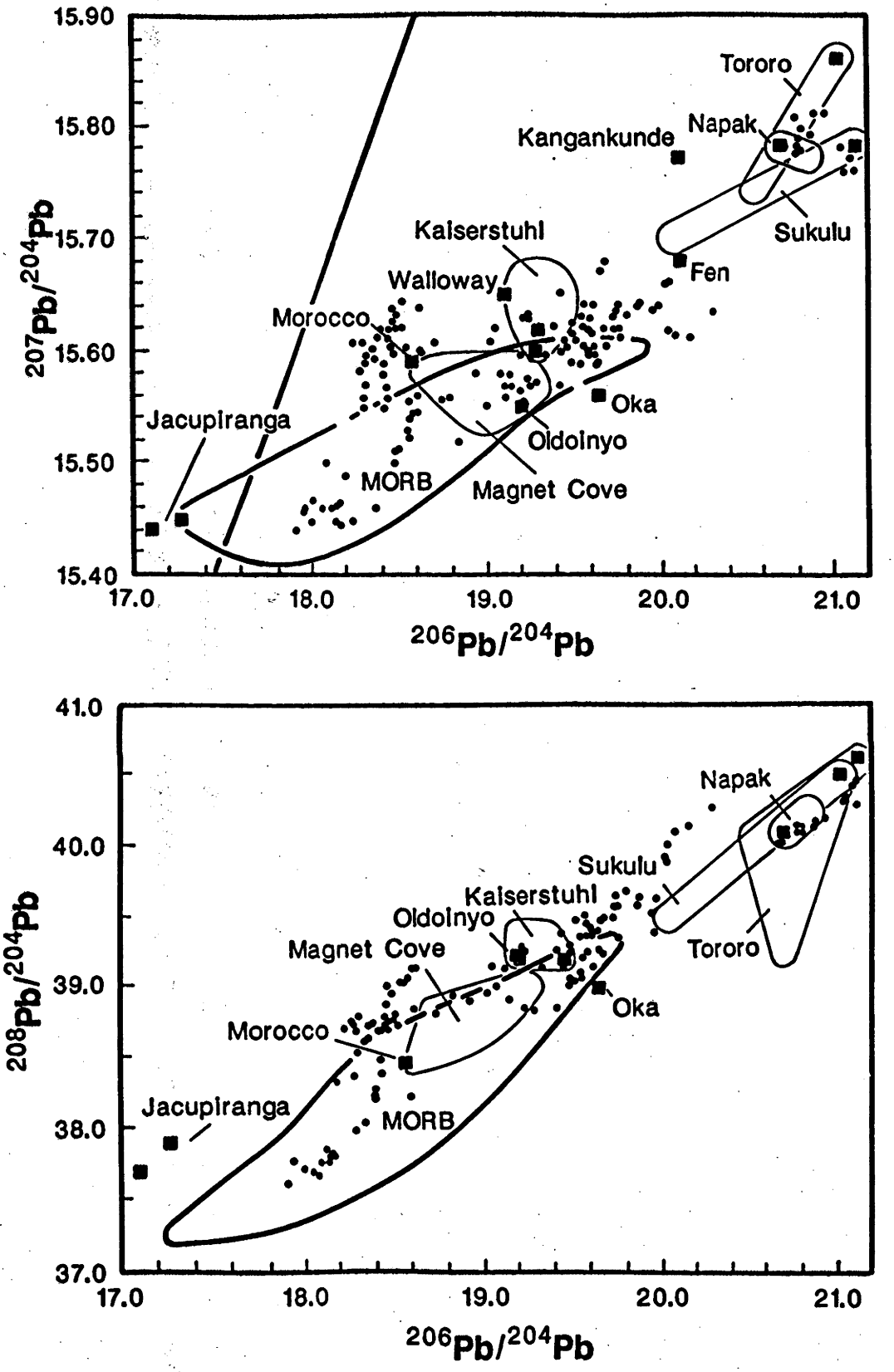
15.90
15.80
15.70
15.60
15.50
15.40
17.0
18.0
19.0
20.0
21.0
207Pb/204Pb
206Pb/204Pb
Tororo
Napak
Kangankunde
Sukulu
Kaiserstuhl
Fen
Walloway
Morocco
Oka
Jacupiranga
Oldoinyo
MORB
Magnet Cove
41.0
40.0
39.0
38.0
37.0
17.0
18.0
19.0
20.0
21.0
208Pb/204Pb
206Pb/204Pb
Napak
Sukulu
Kaiserstuhl
Oldoinyo
Magnet Cove
Tororo
Oka
Morocco
Jacupiranga
MORB

Fig. 4.

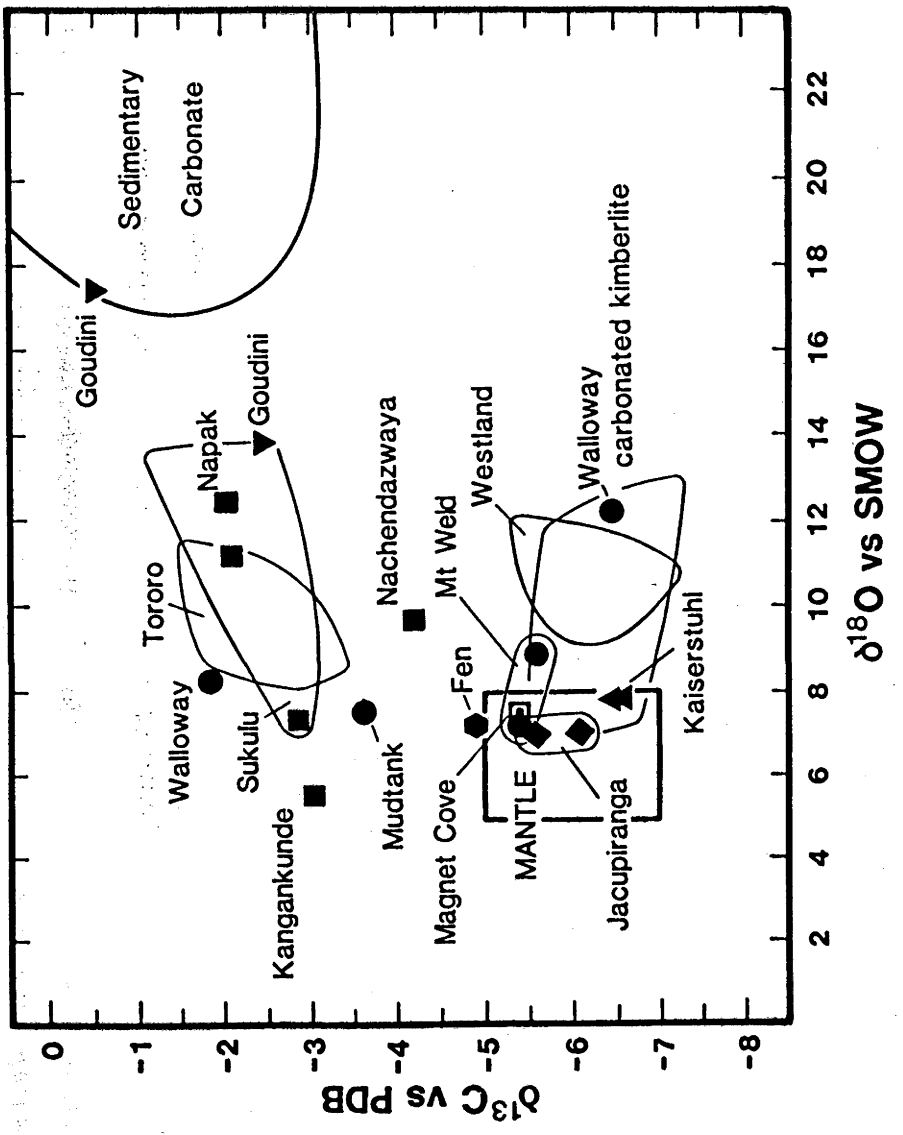
Sedimentary
Carbonate
Goudini
Goudini
Napak
Tororo
Walloway
Sukulu
Kangankunde
Nachendazwaya
Mudtank
Mt Weld
Westland
Fen
Magnet Cove
MANTLE
Walloway
carbonated kimberlite
Kaiserstuhl
Jacupiranga
δ13C vs PDB
δ18O vs SMOW
0
-1
-2
-3
-4
-5
-6
-7
-8
2
4
6
8
10
12
14
16
18
20
22

Fig. 5.

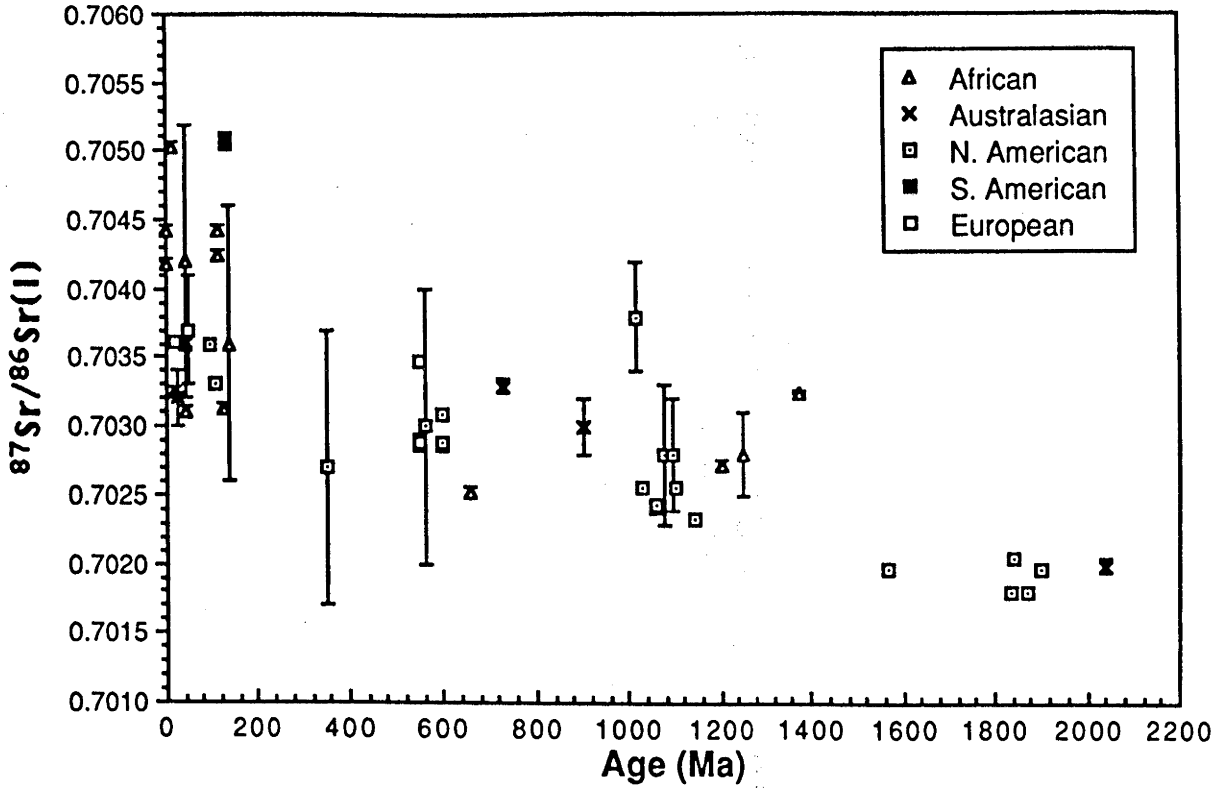
0.7060
0.7055
0.7050
0.7045
0.7040
0.7035
0.7030
0.7025
0.7020
0.7015
0.7010
$^{87}Sr/^{86}Sr(I)$
0
200
400
600
800
1000
1200
1400
1600
1800
2000
2200
Age (Ma)
African
Australasian
N. American
S. American
European

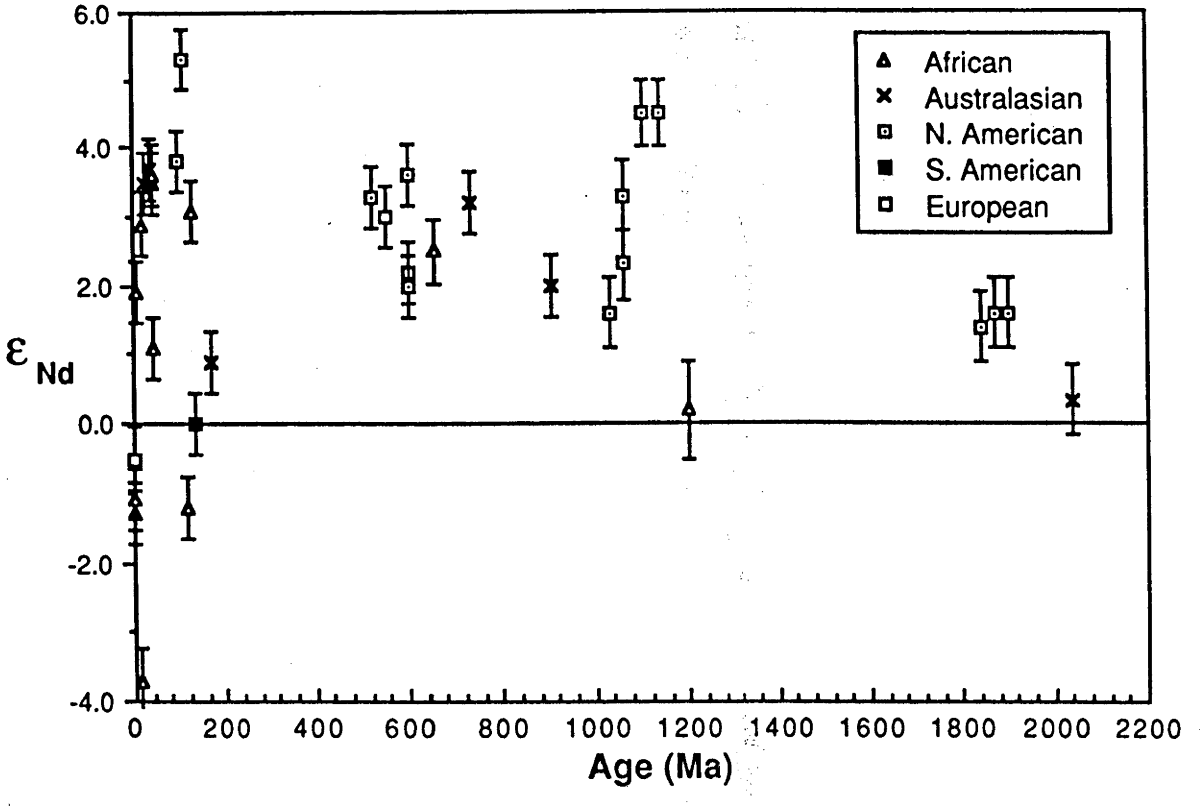
6.0
4.0
2.0
0.0
-2.0
-4.0
ε_{Nd}
0
200
400
600
800
1000
1200
1400
1600
1800
2000
2200
Age (Ma)
African
Australasian
N. American
S. American
European

Fig.6.

Table 1. Major- and trace- element analyses of carbonatites and associated rocks.

location	Lokupoi	Tororo	Sukulu	Kangankunde	Nachendaz.	Goudini	Goudini	Walloway	Walloway†	Terowie	Mudtank	Mt Weld	Mt Weld	Jacupiranga	Jacupiranga	Kaiserstuhl	Kaiserstuhl	Magnet Cove
sample	6336	6330	6335	3432	7122	33174	33176	0009	0081	0090	2015	MW-1	MW-2	5961	5963	K-3	K-1	MC-1
rock-type	carbonatite	alvikite	carbonatite	carbonatite	sövite	carbonatite	carbonatite	sövite	carb. kimb.	kimberlite	sövite	sövite	sövite	carbonatite	carbonatite	carbonatite	phonolite	sövite
main carbonate	calcite	calcite	dolomite	dolomite	calcite	ankeritic dolomite	ankeritic dolomite	calcite	calcite		dolomite	calcite	calcite	calcite	calcite	calcite		calcite
SiO_2	0.82	1.06	0.02	1.17	1.27	25.12	15.90	7.69	21.99	36.39	0.85	2.25	2.84	0.24	0.40	1.64	48.91	0.23
TiO_2	0.08	-	-	-	0.50	4.36	3.49	1.64	1.83	4.48	-	0.04	0.01	0.04	0.01	0.04	0.30	0.04
Al_2O_3*	0.19	0.02	0.01	0.17	0.35	3.23	2.83	3.02	3.40	6.62	0.25	0.12	0.23	0.17	0.05	0.44	18.20	0.05
Fe_2O_3	1.99	2.26	1.62	1.73	7.79	14.95	12.93	7.49	10.39	14.45	7.12	9.20	2.51	2.38	0.98	1.09	3.88	0.08
MnO	0.46	0.55	0.39	0.56	0.29	0.20	0.32	0.13	0.22	0.17	0.33	0.22	0.16	0.08	0.11	0.17	0.26	0.11
MgO	1.30	1.42	16.90	3.92	3.42	6.49	8.92	4.97	22.23	17.16	15.02	2.30	2.21	1.95	4.39	0.96	0.32	0.14
CaO	55.40	54.70	36.21	6.83	49.48	15.94	21.24	41.88	17.03	2.52	33.37	45.86	50.37	52.26	50.64	55.23	7.83	56.38
Na_2O	0.10	0.09	0.06	0.21	0.13	3.08	3.15	0.12	0.03	0.49	0.03	0.47	0.51	0.27	0.21	0.05	7.60	0.24
K_2O	0.13	0.01	0.01	-	0.02	2.83	0.14	0.74	0.10	2.02	0.17	0.47	0.47	0.05	0.01	0.08	4.19	0.02
P_2O_5	0.21	2.37	5.86	3.77	3.60	0.44	0.68	0.85	1.72	1.26	2.99	2.43	4.18	7.16	0.17	1.26	0.14	0.88
S	0.06	0.11	0.03	0.40	-	0.17	0.03	0.02	-	0.01	-	0.20	0.26	0.16	0.41	0.03	0.13	0.02
CO_2	43.9	39.4	34.8	21.9	36.9	19.1	30.2	34.5	11.2	nd	40.6	32.2	36.4	34.5	41.9	38.5	nd	nd
SUM	104.64	101.97	95.91		103.75	95.91	99.83	99.28			100.72	95.75	100.15	99.28	99.28	99.49		
Cr	-	-	-	-	2.7	665	364	810		1080	2.4	-	-	-	-	0.3	1.6	-
Sc	19	0.26	5.7	1.86	5.44	38	19	30	23	34	15.2	8.1	5.2	10.7	10.4	0.09	0.32	0.25
Ni	2	<1	<1	16	<1	232	425	155	523	745	3	<1	3	2	1	2	2	<1
Co	6	-	3	-	11	30	84	28		82	18	4.6	11	12	27	0.2	4	0.10
Cu	<1	2	<1	148	1	134	82	28	65	nd	2	nd	nd	5	7	12	11	nd
Zn	20	31	15	159	25	163	137	35	100	107	28	25	20	7	2	30	236	5
Cs	-	-	-	-	-	-	-	0.31		7.1	0.04	0.69	0.4	-	-	1.02	2.42	-
Ba	2450	2970	56	18900	690	3140	1100	2340	3000	3440	310	800	1100	820	720	2660	2430	470
Rb	3	<0.5	<0.5	<0.5	1	26.5	1	28.5	5	126	9.5	28.0	20.5	1.0	<0.5	10.0	170	<0.5
Sr	1250	6930	2760	280000	4430	1490	4360	980	1700	225	2690	5600	7010	5290	5880	11850	4100	5290
Pb	41	7	<1	99	9	11	37	7		63	3	106	110	4	4	3	34	70
Y	143	159	23	27	55	46	98	18	25	21	18	73	97	34	32	24	14	25
Th	126	35	4.8	164	4.7	57	93	39	54	23.6	2.8	60	56	2.3	0.25	3.3	52.4	1.4
U	-	-	-	-	42	1.4	3.6	6.5		3.4	0.1	10.5	76	-	-	4.9	15.3	0.3
Zr	<1	<1	<1	12930	2	459	715	244	430	330	<1	227	184	<1	5	<1	470	31
Hf	-	0.16	0.14	1.0	0.36	16.8	25.4	7.5		9.7	-	1.9	2.41	-	0.26	0.12	5.55	0.04
Nb	1030	116	390	123	97	113	91	265	418	220	3.0	3140	398	7.5	1.5	3010	426	6.5
Ta	-	-	2.1	-	49.7	5.2	3.8	12.8		11.8	-	66	86	1.7	0.17	4.7	15.5	-
Mo	-	-	-	-	11	18	-	-		-	-	-	18	-	-	4	10	-
Sb	0.4	0.07	-	0.4	-	5.0	1.7	0.6		-	0.2	0.12	-	-	-	0.06	0.56	0.04
Au	-	-	-	-	0.01	-	-	-		-	-	-	0.25	-	0.05	-	0.01	-
La	1890	446	115	25700	162	174	121	203	392	97	113	256	328	134	90	373	245	120
Ce	3370	865	277	23000	365	416	233	351	472	192	248	577	665	282	188	743	413	125
Nd	1260	362	138	11000	178	217	118	115		74	112	252	322	136	86	127	102	29
Sm	205	69	25.7	1030	36.2	42.1	39.8	17.4		12.9	19.8	47	66	27.4	16.7	14.7	9.4	5.0
Eu	49	18.6	6.4	153	9.8	12.6	17.1	4.07		4.07	5.04	13.5	18.6	7.0	4.7	3.7	2.12	1.72
Gd	87	43.1	16.7	224	21.3	33	51	9.5		6.9	9.6	29	40	15.7	10.9	6.1	6.5	4.0
Tb	13.6	6.4	2.62	nd	2.91	4.4	6.5	1.26		1.24	1.21	4.1	6.7	2.16	1.33	1.02	0.95	0.66
Ho	6.7	7.1	1.33	nd	2.86	2.2	4.6	0.86		0.81	0.88	2.9	5.4	1.57	1.36	0.95	0.69	0.69
Yb	13.0	7.5	1.35	nd	3.79	2.7	6.4	1.29		1.64	1.09	4.7	6.4	1.68	2.16	2.02	1.35	2.1
Lu	1.63	0.79	0.137	<1	0.373	0.38	0.79	0.16		0.22	0.144	0.56	0.67	0.186	0.27	0.21	0.134	0.268

* All Fe calculated as Fe_2O_3. (-) not detected, (nd) not determined.

† Walloway carbonated kimberlite (#0081) analysis from FERGUSON and SHERATON (1979).

Table 2. Sr and Nd isotopic results for carbonatites and associated rocks.

	Sample	Rb	Sr	Sm	Nd	$^{87}Rb/^{86}Sr$	$^{87}Sr/^{86}Sr$ meas	$^{87}Sr/^{86}Sr$ initial	$^{147}Sm/^{144}Nd$	$^{143}Nd/^{144}Nd^{\dagger}$	$\varepsilon_{Nd}(0)^{\#}$	ε_{Nd}
		ppm										
Australia												
Strangways Range, Northern Territory (732 ±5 Ma; Black and Gulson 1978)												
2015	Mudtank carb.	9.97	2731	18.23	116.3	0.0105	0.70329±5	0.7032	0.0948	0.51151±2	-6.5	+3.2
Walloway/Terowie, South Australia (160 - 180 Ma; Stracke *et al.*, 1979)												
0009	carbonatite	2.91	999.4	16.61	126.8	0.0084	0.70547±4	0.7054	0.0792	0.51175±2	-1.6	+0.9
0081	carb. kimb.	4.66	1463	17.54	129.2	0.0092	0.70490±4	0.7049	0.0821	0.51172±2	-2.3	+0.2
0090	kimberlite	130	461.6	9.54	58.32	0.8170	0.7085*		0.0989	0.51192±3	+1.7	+3.8
Mt Weld, Western Australia (2060 Ma; Willett *et al.*, 1986, this study)												
MW-1	carbonatite	23.2	6033	40.88	244.5	0.0111	0.70235±5	0.7020	0.1011	0.51057±2	-24.8	+0.3
MW-2	carbonatite	18.6	7410	50.61	297.7	0.0072	0.70220±6	0.7020	0.1028	0.51060±2	-24.2	+0.4
Magnet Cove, Arkansas (97 Ma; Zartman *et al.*, 1967)												
MC-1	carbonatite	5.38	5597	5.35	33.53	0.0028	0.70360±4	0.7036	0.0965	0.51197±2	+2.6	+3.8
Kaiserstuhl, Germany (16 - 18 Ma; Wimmenauer 1966)												
K-2	carbonatite	12.6	17989	11.63	108.5	0.0020	0.70362±4	0.7036	0.0648	0.51199±2	+3.0	+3.2
K-3	carbonatite	10.6	15012	14.07	131.5	0.0020	0.70368±4	0.7037	0.0647	0.51201±2	+3.4	+3.6
K-1	phonolite	157	4281	8.39	87.26	0.1057	0.70406±3	0.7040	0.0581	0.51196±2	+2.4	+2.7
K-6	phonolite	200	1435	6.75	60.74	0.2995	0.70423±3	0.7042	0.0673	0.51196±2	+2.3	+2.6
K-5	lava clast	165	991	8.56	49.01	0.4823	0.70434±6	0.7042	0.1056	0.51199±2	+2.9	+3.2
Fen, Norway (≈550 Ma; see Mitchell and Crocket 1970)												
NBS-18	carbonatite	0.26	6457	22.82	127.3	0.0001	0.70289±6	0.7029	0.1085	0.51167±2	-3.3	+3.0
Jacupiranga, Brazil (130 Ma; Amaral 1978, Roden *et al.*, 1985)												
5961	carbonatite	1.53	5370	26.30	152.5	0.0008	0.70507±6	0.7050	0.1043	0.51178±4	-1.1	+0.5
5963	carbonatite	0.27	6161	15.79	88.27	0.0001	0.70525±6	0.7052	0.1082	0.51174±4	-1.9	-0.4
Uganda (17 - 22 Ma; Baker *et al.*, 1971)												
6336	Napak carb.	0.930	1226	197.2	1453	0.0022	0.70325±3	0.7032	0.0821	0.51197±2	+2.7	+2.9
	(25 - 55 Ma; Baker *et al.*, 1971)											
6330	Tororo carb.	0.056	7100	60.31	354.2	-	0.70360±3	0.7036	0.1030	0.51187±2	+0.7	+1.1
6335	Sukulu carb.	0.063	2783	16.83	101.1	-	0.70311±4	0.7031	0.1007	0.51199±2	+3.1	+3.5
Kangankunde, Malawi (126 ±6 Ma; Snelling 1965)												
3432	carbonatite	0.013	>20000	720	8620	-	0.70313±4	0.7031	0.0505	0.51187±3	+0.8	+3.1
Nachendazwaya, Tanzania (≈655 Ma; Snelling *et al.*, 1964)												
7122	carbonatite	0.48	3754	24.03	130.0	0.0004	0.70251±4	0.7025	0.1118	0.51160±2	-4.6	+2.5
Goudini, South Africa (≈1.2 Ga; Verwoerd 1966, Harmer 1986, this study)												
33174	carbonatite	32.1	1637	34.98	187.4	0.0565	0.70389±4	0.7029	0.1129	0.51116±2	-13.2	+0.2
33176	carbonatite	1.18	3705	30.32	94.06	0.0009	0.70272±4	0.7027	0.1949	0.51180±2	-0.6	-0.4

† Nd isotopic ratios normalised using $^{146}Nd/^{142}Nd = 0.636151$. BCR-1 standard measured in this laboratory is 0.511833±20. NBS-987 $^{87}Sr/^{86}Sr$ is measured at 0.71022±4, E & A standard carbonate is 0.70800±3. All errors quoted refer to within-run precision at the 95% confidence level.

\# Epsilon notation calculated using $^{143}Nd/^{144}Nd_{CHUR} = 0.511836$, $^{147}Sm/^{144}Nd_{CHUR} = 0.1967$. Decay constants used are those recommended by Steiger and Jager (1977) and $\lambda_{Sm} = 6.54 \times 10^{-12}$ yr^{-1}.

* Rb-Sr concentration and isotope data from Stracke *et al.* (1979).

Table 3. Pb, O and C isotopic analyses of carbonatites and some associated rocks.

Sample		U	Pb	$^{238}U/^{204}Pb$	$^{206}Pb/^{204}Pb$*		$^{207}Pb/^{204}Pb$		$^{208}Pb/^{204}Pb$		$\delta^{18}O_{SMOW}$	$\delta^{13}C_{PDB}$
		– ppm –			meas	initial			meas	initial		
		meas	initial†									
Australia												
Strangways Range, Northern Territory												
2015	Mudtank carb.	0.391	3.12	9.20	18.538	17.38	15.589	15.52	38.840	-	+7.5	-3.6
Walloway/Terowie, South Australia												
0009	carbonatite	7.08	5.81	98.4	21.743	19.11	15.784	15.65	42.814	-	+8.3	-1.8
0081	carb. kimb.	7.71									+12.2	-6.5
0090	kimberlite	4.42	12.17	27.5	19.547	18.84	15.642	15.61	40.008	-	-	-
Mt Weld, Western Australia												
MW-1	carbonatite	-	24.5		50.476	-	19.484	-	264.72	-	+8.9	-5.6
MW-2	carbonatite	-	25.6		244.09	-	44.56	-	71.20	-	+7.2	-5.4
Magnet Cove, Arkansas												
MC-1	carbonatite	-	-	-	-		-		-		+7.5	-5.4
Kaiserstuhl, Germany												
K-2	carbonatite	2.38	3.73	47.7	19.357	19.23	15.604	15.60	39.288	39.1	+7.8	-6.5
					19.334	19.21	15.626	15.62	39.351	39.2		
K-3	carbonatite	5.70	3.57	119	19.487	19.17	15.601	15.59	39.263	39.3	+7.8	-6.6
K-1	phonolite	19.07	35.05	40.9	19.490	19.38	15.673	15.67	39.493	39.4	-	-
K-6	phonolite	2.52	30.43	6.19	19.197	19.18	15.673	15.67	39.468	39.4	-	-
K-5	lava clast	2.26	3.91	43.3	19.573	19.46	15.646	15.64	39.357	39.2	-	-
Fen, Norway												
NBS-18	carbonatite	0.282	5.84	3.73	20.442	20.11	15.701	15.68	40.696	-	+7.2	-5.0
Jacupiranga, Brazil												
5961	carbonatite	0.013	4.58	0.20	17.273	17.27	15.457	15.45	37.970	37.9	+7.1	-6.1
5963	carbonatite	0.237	9.13	1.84	17.140	17.10	15.445	15.44	37.800	37.7	+7.3	-5.6
Uganda												
6336	Napak carb.	0.566	40.52	1.08	20.719	20.71	15.780	15.78	40.379	40.1	+12.4	-2.0
6330	Tororo carb.	0.350	6.34	4.33	21.068	21.04	15.865	15.86	41.112	40.5	+11.1	-2.1
6335	Sukulu carb.	0.027	1.06	1.97	21.154	21.14	15.781	15.78	40.646	40.6	+7.3	-2.9
Kangankunde, Malawi												
3432	carbonatite	0.077	89.3	0.065	20.115	20.11	15.772	15.77	39.660	-	+5.5	-3.0
Nachendazwaya, Tanzania												
7122	carbonatite	4.11	6.82	63.6	48.804	42.00	17.847	17.43	38.545	-	+9.6	-4.2
Goudini, South Africa												
33174	carbonatite	2.29	12.28	17.9	22.005	18.17	15.856	15.54	57.940	-	+17.4	-0.5
33176	carbonatite	2.03	36.7	4.43	18.409	17.46	15.580	15.50	45.681	-	+13.8	-2.4

* Analyses of NBS-981 common-Pb standard gave $^{206}Pb/^{204}Pb$ =16.927±0.009, $^{207}Pb/^{204}Pb$ =15.486±0.013, $^{208}Pb/^{204}Pb$ = 36.668±0.044 (2σ errors).

† Corrections to $^{208}Pb/^{204}Pb$ made using Th/U ratio determined by INAA.

Enriched mantle components and mantle recycling of sediments

Running title: Enriched mantle and sediment recycling

David R. Nelson and Malcolm T. McCulloch

Research School of Earth Sciences,
Australian National University,
GPO Box 4, Canberra, ACT, Australia, 2601

Aust. J. Earth Sci. Special Publication,
4th International Kimberlite Conference

Author responsible for proofs: D.R. Nelson

ABSTRACT

Many examples of highly potassic continental magmatism derived from enriched (radiogenic $^{87}Sr/^{86}Sr$, unradiogenic $^{143}Nd/^{144}Nd$) mantle sources also have unusual Pb isotopic compositions with unradiogenic $^{206}Pb/^{204}Pb$. Here we propose that the geochemical and isotopic characteristics of these magmas are consistent with the involvement of a low U/Pb crustal component, and that their mantle sources have been contaminated by sediments which were subducted into the mantle and stored for long periods within the subcontinental lithosphere. The increase in U/Pb of MORB and ocean-island reservoirs with time, as indicated by their position to the right of the geochron on the $^{206}Pb/^{204}Pb$-$^{207}Pb/^{204}Pb$ diagram, can be accounted for by the existence of substantial reservoirs of these low U/Pb components within the subcontinental lithosphere.

Key words: potassic magmatism, enriched mantle, sediment subduction, subcontinental lithosphere, Sr, Nd and Pb isotopes.

INTRODUCTION

Despite a long history of investigation (see Gupta and Yagi 1980, for a review), the petrogenesis of the ultrapotassic suite has remained enigmatic. A number of recent isotopic studies (for example, McCulloch *et al.* 1983; Collerson and McCulloch 1983; Vollmer and Norry 1983; Vollmer *et al.* 1984; Fraser *et al.* 1985; Nelson *et al.* 1986) have found that, in contrast to other mantle-derived magmas such as mid-ocean-ridge and ocean-island basalts, many examples of potassic magmatism possess highly radiogenic Sr and unradiogenic Nd isotopic compositions. Although these isotopic characteristics may have been acquired by extensive assimilation of continental crust, these studies have generally argued against the operation of crustal contamination processes in favour of an "enriched mantle" origin. The high Mg numbers and Ni and Cr contents of these magmas and the presence of mantle xenoliths (and in one case, diamonds) are cited in support of this. Furthermore, the extremely high contents of most trace-elements, including Sr and the REE, of these magmas make them insensitive to bulk contamination processes, requiring the assimilation of substantial amounts of crustal material to modify their Sr and Nd isotopic characteristics. As geochemical and isotope correlations indicative of mixing are evident in many potassic suites (for example, in the Italian, Spanish and Western Australian examples), most recently advanced petrogenetic models (e.g. McCulloch *et al.* 1983; Jaques *et al.* 1984; Vollmer *et al.* 1984) invoke partial melting of a lherzolitic or harzburgitic mantle source which has been variably contaminated by an incompatible-element- rich "metasomatic" component. However, the question of the ultimate sources of these "metasomatic" components, which presumably confer the enriched mantle isotopic character to the sources of potassic magmas, is rarely addressed and remains problematic.

Based on geochemical similarities with modern arc lavas, many recent studies (e.g. Thompson 1977; Edgar 1980; Civetta *et al.* 1981; Venturelli *et al.* 1984; Peccerillo *et al.* 1984; Peccerillo 1985; Rogers *et al.* 1985; Nelson *et al.* 1986) have argued for the involvement of subduction processes in the genesis of potassic volcanics of Italy and southeastern Spain. Trace-element characteristics of the Spanish lavas, such as their high Ba concentrations, low K/Rb, high Ba/La and REE patterns with negative Eu-anomalies (Venturelli *et al.* 1984; Nixon *et al.* 1984) are consistent with contamination of their

mantle source by a component resembling modern sediments. Isotopic analysis indicates that the Spanish lavas possess Sr, Nd and Pb isotope ratios similar to those of modern sediments and, although possibly complicated by extensive high level crustal contamination in the more differentiated magmas (e.g. Turi and Taylor 1976), the involvement of a similar crustal component can also account for the isotopic and trace-element features of the Italian potassic suite (see discussion in Nelson *et al.* 1986). However, many other occurrences of potassic magmatism are confined to old stable cratonic regions and are not obviously associated with modern subduction zones (for example, Gaussberg, Western Australian, Leucite Hills, Sierra Nevadan and Virungan high-K lavas). In this study, new isotopic data for potassic magmas from east Antarctica and the Leucite Hills, Wyoming, are presented and the geochemical and isotopic features of these and other examples of continental potassic magmatism compared. A model is proposed in which the mantle sources of at least some examples of continental potassic magmas have also been contaminated by crustal components. As these magmas originate from great depths (i.e. within the field of diamond stability in the case of the Western Australian lamproites), we will argue here that these crustal contaminants were derived from marine sediments which have been subducted into the mantle and stored for long time periods within the subcontinental lithosphere. This interpretation reconciles the mantle characteristics of continental potassic magmatism, such as their high Mg numbers and transition element concentrations, with apparent crustal features such as their incompatible-element patterns and Sr, Nd and Pb isotope characteristics. Furthermore, the complex multistage U/Pb fractionation histories indicated by the unusual Pb isotopic compositions of these magmas are not readily explained by models advocating their generation entirely within the upper mantle or subcontinental lithosphere, but are consistent with our interpretation.

CHEMICAL AND ISOTOPIC CHARACTERISTICS OF CONTINENTAL POTASSIC MAGMATISM

Averaged element abundance patterns for potassic magmas from 4 separate localities, normalised to estimated primitive mantle abundances (from McDonough *et al.* 1985 and Nelson *et al.* 1986), are shown in Fig. 1. Diamond-bearing lamproites from Western Australia, leucitites from Gaussberg, high-K alkaline dykes from MacRobertson Land, Enderby Land and Queen Mary Land regions of east Antarctica and madupites, wyomingites and orendites from Leucite Hills, Wyoming, have remarkably similar geochemical characteristics. All are characterised by high Mg numbers (each locality averaging Mg(Mg+total Fe)>0.65 with the exception of Manning Massif, Mt Bayliss and Bunger Hills samples, which have Mg numbers of 0.58, 0.58 and 0.50 respectively) and high Ni and Cr contents, as well as high to extreme abundances of K_2O, TiO_2, P_2O_5, SO_2, H_2O, F, Cl, Ba, LREE, high K_2O/Na_2O and Fe^{3+}/Fe^{2+}, and relatively low abundances of Al_2O_3, CaO and Na_2O. The ratios of highly incompatible elements of these magmas more closely resemble those of subduction-related magmas and pelagic sediments than those of anorogenic mantle-derived rocks. The arc-like Ba/La and Ba/Nb ratios of some examples of high-K magmas have been previously noted by Thompson *et al.* (1984) and Varne (1985). For example, the Western Australian lamproites possess high Th/U (averaging 5.8) and Ba/La ratios (36.6) and low K/Rb (146) and K/Ba ratios (6.07, average of 20 analyses by Jaques *et al.* 1984). Although these ratios may be affected by extensive fractionation of some mineral phases, such as leucite

and phlogopite, there is no correlation between Ba/La and K/Ba ratios and differentiation parameters such as wt% MgO. Th/U and K/Rb ratios are respectively positively and negatively correlated with wt% MgO (i.e. olivine lamproites have generally higher Th/U and lower K/Rb ratios than leucite lamproites) indicating that although these ratios may have been influenced by differentiation processes, the high Th/U and low K/Rb are not due to crystal fractionation. The Western Australian lamproite values compare with ranges for pelagic sediments of 4.7 to 7.5 for Th/U (Elderfield *et al.* 1981; Thomson *et al.* 1984; White *et al.* 1985; considerably lower Th/U values, <0.1, may be typical of metalliferous sediments such as those examined by Veeh 1981), 7.2 to 47 for Ba/La (White *et al.* 1985, and average of 35 Walvis Ridge sediments analysed by Liu and Schmitt 1984), 240 for K/Rb (estimated by Kay 1980, and average value for 35 Walvis Ridge sediments from Liu and Schmitt 1984) and 8.6 to 9.9 for K/Ba (Kay 1980; Liu and Schmitt 1984). By contrast, ocean-island alkali basalts typically possess Th/U between 3.7 and 4.3 (compilation by Galer and O'Nions 1985), Ba/La of 5 to 13, K/Rb of 370 to 900 and K/Ba between 12 and 40 (from compilation by Morris and Hart 1983).

The results of Sr, Nd and Pb isotopic analysis of alkaline dykes from east Antarctica and of potassic volcanics from Leucite Hills, Wyoming, are given in Table 1. Detailed descriptions of the Antarctic dykes, including their geology, ages, petrology and major- and trace-element geochemistry, were presented by Sheraton and England (1980) and Sheraton (1983). The Priestley Peak melasyenite dyke has high Mg/(Mg+total Fe) of 0.71 and high Ni (298 ppm) and Cr (348 ppm) contents and may represent a near-primary magma. The exact emplacement age of the trachybasalt from Bunger Hills, Queen Mary Land, is unknown but is probably younger than Cambrian. Age-corrected Nd isotopic compositions of the Antarctic samples are all highly unradiogenic, with initial ε_{Nd} values ranging from -9 to <-16. The Antarctic samples have high concentrations of both U and Pb (Table 1) and, with the exception of the Mt Bayliss dyke, have U/Pb ratios close to those estimated for the MORB mantle source from Pb isotopic studies of MORB. Corrections to $^{206}Pb/^{204}Pb$ for radiogenic decay of ^{238}U since emplacement are small for the 50 Ma old Manning Massif tristanite and (because of its low U/Pb) the Mt Bayliss dyke but are considerably larger for the Priestley Peak melasyenite. Age corrections to the measured $^{207}Pb/^{204}Pb$ ratios are within analytical error for the Manning Massif and Mt Bayliss samples. The Manning Massif, Mt Bayliss and Priestley Peak samples have unusually high initial $^{207}Pb/^{204}Pb$ ratios combined with relatively low initial $^{206}Pb/^{204}Pb$ (see Fig. 2). Although its exact emplacement age is uncertain, the Bunger Hills trachybasalt also has high measured $^{207}Pb/^{204}Pb$ and low $^{206}Pb/^{204}Pb$, requiring a multistage history of U/Pb variation with a relatively recent $^{238}U/^{204}Pb$ considerably less than 8. The measured $^{238}U/^{204}Pb$ of 8.24 is too high to be the cause of the retarded evolution of the $^{206}Pb/^{204}Pb$ ratio. Furthermore, as the high measured $^{207}Pb/^{204}Pb$ requires a long history (>1 Ga) of high U/Pb prior to the low U/Pb stage, the high $^{207}Pb/^{204}Pb$ of the Bunger Hills dyke is a feature that predates the time of its emplacement. The unusual Pb and Nd isotopic characteristics of the Antarctic samples, the general features of which are independent of any uncertainty introduced by the age corrections, are similar to those of lamproites from Western Australia (McCulloch *et al.* 1983; Fraser *et al.* 1985; Nelson *et al.* 1986) and leucitites from Gaussberg (Collerson and McCulloch 1983; Nelson *et al.* 1986).

In thin section, the Leucite Hills samples consist of phenocrysts of phlogopite in a fine glassy groundmass and are therefore classified, following Kuehner *et al.* (1981), as wyomingites. Sr and Nd

isotopic compositions (Table 1) plot within the fields previously determined for wyomingites by Vollmer *et al.* (1984) (see Fig. 3) and interpreted by them to indicate derivation from enriched mantle sources. Compared to other examples of potassic continental magmatism considered to be derived from enriched mantle sources, Leucite Hills potassic lavas have similar unradiogenic $^{143}Nd/^{144}Nd$ but have less radiogenic $^{87}Sr/^{86}Sr$ (Fig. 3). The Sr isotopic differences displayed by these potassic suites may be due to differences in the Sr isotopic compositions of the "metasomatic" contaminants involved, to the existence of different long-term Rb/Sr ratios within the "metasomatised" source regions of the magmas and/or to differences in the time elapsed between enrichment and emplacement events. Our Pb results for Leucite Hills wyomingites are slightly more radiogenic than those reported for wyomingites by Salters and Barton (1985) but are comparable to their results for madupites. The wyomingites have unradiogenic $^{206}Pb/^{204}Pb$ and relatively radiogenic $^{207}Pb/^{204}Pb$ ratios (Fig. 2) and plot to the left of the geochron. Their $^{208}Pb/^{204}Pb$ is particularly low compared to other examples of potassic magmatism, indicating a long time-integrated history of low Th/U. The isotopic characteristics of Leucite Hills potassic volcanics indicate a generally similar long-term history of Sm/Nd and U/Pb but generally lower Rb/Sr compared to other examples of potassic magmatism from Antarctica, Western Australia and Gaussberg.

The incompatible-element characteristics, radiogenic $^{87}Sr/^{86}Sr$ and $^{207}Pb/^{204}Pb$ and unradiogenic $^{143}Nd/^{144}Nd$ of these examples of potassic magmatism may be attributed to the involvement of crustal contaminants. However, as discussed briefly earlier, these magmas are insensitive to crustal contamination processes because of their extremely high concentrations of trace-elements, including Sr, Pb and the REE. Geochemical considerations exclude their contamination by bulk assimilation processes because of the substantial amounts of crustal material required to modify their isotopic compositions. For example, because of the extreme degree of LREE-enrichment of these magmas, bulk assimilation of felsic granulite within the lower continental crust will effectively dilute their incompatible-element contents and should therefore produce a positive correlation between Nd concentration and ε_{Nd}. In the case of the Western Australian lamproites, a correlation in the opposite sense was noted by McCulloch *et al.* (1983). Although selective contamination processes (for example, by highly LREE-enriched phases such as monazite or allanite) could account for this correlation, there is no evidence in the trace-element patterns (i.e. large positive Th or P_2O_5 spikes) of the assimilation of such phases, nor can they explain the Sr or Pb isotopic characteristics of these magmas. Crustal contamination via specialised mechanisms, such as volatile transfer or zone refining, is unable to account for the high Mg numbers and Ni and Cr contents or the presence of mantle xenoliths (and in one case, diamonds). An alternative interpretation which may account for the unusual geochemical properties of these magmas (i.e. their generally high MgO, Ni, Cr and low Al, Ca and Na contents combined with their apparently "crustal" incompatible-element ratios and isotopic compositions) is that they were derived from relatively depleted (lherzolitic or harzburgitic) mantle sources which have been contaminated by incompatible-element-rich "metasomatic" components derived from subducted sediments.

The Pb isotope compositions of these examples of potassic magmatism indicate a history of U/Pb variation involving at least two stages; an earlier high U/Pb stage is required to generate the high $^{207}Pb/^{204}Pb$ while there is still sufficient of the parent ^{235}U, followed by a low U/Pb stage to retard the increase in $^{206}Pb/^{204}Pb$ by the decay of the parent ^{238}U (see Fig. 4). Long histories are required to

generate these unusual Pb isotopic compositions. For example, modelling of the Pb isotopic compositions of the Western Australian lamproites (Nelson *et al.* 1986) indicates that their Pb cannot have differentiated from the mantle later than ≈2.1 Ga ago, and is probably much older. The Pb isotope ratios of these potassic magmas are unlike those of modern marine sediments, due to the histories of more recent low U/Pb. Because of the similar chemical behavior of uranium and lead during igneous processes, the dramatic fractionation events lowering the U/Pb ratios in the sources of these potassic magmas are considered unlikely to have been the result of magmatic fractionation/differentiation processes. However, an effective means of fractionating uranium from lead is by either weathering, sedimentation or hydrothermal processes at the Earth's surface, due to the greater insolubility of U^{4+} in aqueous systems under reducing conditions.

To investigate the possible involvement of sediments in the generation of potassic magmatism in more detail, further discussion of some aspects of the geochemical and isotopic properties of marine sediments is warranted.

THE CHEMISTRY OF MARINE SEDIMENTS

The isotopic characteristics of modern marine sediments vary with provenance, with most of the observed variation attributable to mixing in varying proportions of material derived from the upper continental crust (a continental detrital component) with that derived from the mantle (consisting of a hydrothermal component principally derived from oceanic spreading centers and a terrigenous component derived from young arcs). The proportion of each component derived from these sources varies depending on the element, with a large proportion of the Sr and most of the Nd found in oceanic sediments and manganese nodules derived from continental sources (Dasch *et al.* 1971; Addy 1979; Elderfield *et al.* 1981; Goldstein and O'Nions 1981). Most studies of oceanic sedimentary Pb have found relatively uniform Pb isotopic compositions with high $^{207}Pb/^{204}Pb$ and moderate $^{206}Pb/^{204}Pb$ (Chow and Patterson 1962; Dasch *et al.* 1971; Reynolds and Dasch 1971; Church 1973; Meijer 1976; Unruh and Tatsumoto 1976; Sun 1980; White *et al.* 1985) consistent with a predominantly upper continental derivation, although a study of metalliferous sediments from the Nazca plate (Dasch 1981) found Pb isotopic compositions resembling those of mid-ocean-ridge basalts, indicating that sediments located near oceanic spreading centers may contain a considerable proportion of mantle-derived Pb. The similar $^{206}Pb/^{204}Pb$ ratio of the MORB and continent-derived components results in relatively limited variation in the observed $^{206}Pb/^{204}Pb$ ratio of modern sediments, whereas considerable variation is observed in $^{207}Pb/^{204}Pb$ due to the much higher $^{207}Pb/^{204}Pb$ of continental detritus relative to MORB.

If time-scales of mantle recycling of $\approx 10^8$-10^9 years apply, possible differences in the geochemistry of Archaean and Proterozoic sediments compared to their modern counterparts and the effects of radiogenic decay during storage in the mantle must also be considered. As there are no modern equivalents to the extensive banded iron formations and chert sediments of the Archaean and early Proterozoic, sedimentation processes operating during the Archaean may have differed from those operating today. Geochemical (e.g. Taylor and McLennan 1981; McLennan 1982; McLennan and Taylor 1983; McLennan *et al.* 1984) and Nd isotopic studies (e.g. McCulloch and Wasserburg 1978; Hamilton *et al.* 1983; Miller and O'Nions 1985) suggest that Archaean clastic and chemical sediments were typically less LREE-enriched and isotopically

less evolved than modern sediments. These features are believed to reflect the more mafic character of the Archaean continental crust from which the sediments were derived. Sr isotopic studies of chemical sediments (e.g. Veizer and Compston 1976) have found that many Archaean carbonates have $^{87}Sr/^{86}Sr$ values similar to that of the contemporaneous mantle, with a significant increase in $^{87}Sr/^{86}Sr$ occurring toward the end of the Archaean. The low $^{87}Sr/^{86}Sr$ of many Archaean carbonates was attributed by Veizer *et al.* (1982) to extensive interaction of Archaean seawater and ocean-floor basalts, possibly as a consequence of a higher Archaean geothermal gradient. It is likely that the Pb isotopic compositions of Archaean marine sediments were also influenced to some extent by this process. Continental crust was already well-differentiated by the late Archaean, however, and provided a source of radiogenic Sr and Pb to the marine environment. Oceanic sediments during the geologic past therefore probably possessed Pb isotopic compositions which varied with provenance from contemporaneous mantle to upper crustal values. The Sm/Nd ratio of modern oceanic pelagic sediments are generally similar to those estimated for the upper continental crust, implying that this ratio is not substantially fractionated by erosion and sedimentation processes. The Rb/Sr ratio is dependent on the clay/carbonate content and is more variable. However, the available data (Chow and Patterson 1962; Church 1973; Calvert 1976; Chester and Ashton 1976; Unruh and Tatsumoto 1976; White *et al.* 1985) suggests that the U/Pb ratio of modern pelagic oceanic sediments is extremely variable and is commonly low, and may have been generally lower during the Archaean when the lower degree of oxidation of the Earth's atmosphere would favour the less soluble U^{4+} ion over U^{6+}. If sediment subduction has been an important process throughout the Earth's evolution, this has important implications for the global U/Pb and Th/U budget, as will be discussed later.

Since the late Archaean at least, the Nd isotopic composition and Sm/Nd ratio of oceanic sediments were therefore probably similar to those of the contemporaneous upper crust, whereas Sr and Pb isotopic compositions were influenced by a combination of contemporaneous mantle and upper crustal inputs. For oceanic sediments containing a significant proportion of continent-derived Pb, fractionation of the U/Pb ratio during sedimentation will retard further isotopic evolution of their already radiogenic upper crustal Pb (Fig. 4). Although processes acting during subduction (i.e. dehydration or partial melting) may modify the chemistry of subducted sediments, their effect on the Rb/Sr, Sm/Nd and U/Pb ratios of sediments is dependent on the element partitioning effects of the various mineral phases involved in the subduction zone and is largely unknown. If the extent of such modification is not too severe, the Nd isotopic characteristics of subducted oceanic sediments following their storage within the mantle will evolve roughly parallel to the upper continental crust (i.e. towards highly unradiogenic Nd), due to the similarity of the Sm/Nd ratio of oceanic sediments and the upper continental crust. However, if extensive partial melting of the sediments occurs within the subduction zone, an increase in the Sm/Nd ratio of the residue is likely. The effect of this on the Nd isotopic evolution of the sediments is not quantifiable and depends on the extent of Sm/Nd fractionation. If the Sm/Nd ratio of the sediments following the extraction of a melt remains less than chondritic (i.e. they are still LREE-enriched) their Nd isotopic composition will remain unradiogenic, whereas if the sediments become LREE-depleted, they will evolve more radiogenic Nd during the period of their storage within the mantle or the subcontinental lithosphere. The subducted sediments, or possibly a melt derived from both subducted oceanic crust and sediments, may become

incorporated into the subcontinental lithosphere during or after periods of active subduction along the cratonic margin. At some later stage this modified lithosphere is reactivated, generating potassic magmatism derived from so-called "enriched mantle" sources.

SEDIMENT SUBDUCTION AND POTASSIC MAGMATISM

Although the effects of partial melting and mixing with the mantle must be considered, many aspects of the geochemistry of these examples of continental potassic magmatism are consistent with the involvement of a sedimentary component. High Ba contents and Ba/La and low K/Rb are features which have been attributed to the involvement of sediment components in studies of island arc lavas (e.g. Kay 1980; McCulloch and Perfit 1980). The generally high Th/U ratios may reflect the low U abundances in the sedimentary source or may have been compounded by preferential loss of U relative to Th from the subducted slab in exsolved fluids during dehydration (Newman *et al.* 1984). The highly variable oxidation state of this group of potassic magmas (Foley 1985), their high abundances of P_2O_5 (≤3.3 wt%) and of volatiles such as F (≤1.0 wt%), Cl (≤0.1 wt%) and H_2O (>6 wt%) (Sheraton and Cundari 1980; Sheraton and England 1980; Kuehner *et al.* 1981; Jaques *et al.* 1984), their variable but generally radiogenic Sr and their unradiogenic Nd are all readily explained by the involvement of sedimentary components. As the isotopic evolution of Pb in sediments may be severely retarded following its erosion from the continents and deposition in the ocean basins, the unradiogenic $^{206}Pb/^{204}Pb$ of these magmas may be an indication of the time elapsed during sedimentation and storage within the convecting mantle or subcontinental lithosphere, whereas variation in the $^{207}Pb/^{204}Pb$ may reflect the nature and age of the continental provenance.

The presence of diamonds in the Western Australian lamproites provides further support for the involvement of recycling processes, as an extremely wide range of $\delta^{13}C$ values (including values as low as -34 ‰ vs PDB) have been documented by carbon isotopic studies of diamonds from kimberlites and lamproites (Sobolev *et al.* 1979; Milledge *et al.* 1983; Swart *et al.* 1983; Ozima *et al.* 1985; Jaques *et al.* 1986) consistent with an origin of some diamonds from sedimentary sources of carbon. A wide range of $^3He/^4He$ ratios were also recently reported by Ozima *et al.* (1985) for diamonds. These authors interpreted the high $^3He/^4He$ ratios of some diamonds as indicating that they had remained closed systems for almost the age of the Earth. However, an alternative interpretation is offered by the recently confirmed high $^3He/^4He$ ratios of some ocean sediments (Ozima *et al.* 1984) and manganese nodules (Sano *et al.* 1985), believed to be carried by interplanetary dust particles (Amari and Ozima 1985). Furthermore, a common mineral assemblage of diamond inclusions, olivine + knorringite-rich garnet + enstatite, has been attributed to recrystallisation of olivine + chrome spinel + enstatite cumulates within oceanic crust following its hydrothermal alteration and partial melting during subduction into the mantle (Ringwood 1977). These data argue for the involvement of components derived from both subducted sediments and oceanic crust in the formation of diamonds.

Although these examples of continental potassic magmatism are not obviously associated with any known modern or past subduction zones, their unusual multistage Pb isotopic compositions indicate that a significant time period has elapsed between the event lowering the U/Pb ratio (i.e. sediment formation) and subsequent potassic magmatism. It is therefore not surprising that they are commonly not associated

with the operation of modern subduction processes. That most are found intruding Archaean or early Proterozoic cratons provides indirect evidence that the sources of these examples of continental potassic magmatism are stored within the subcontinental lithosphere. Evidence for the operation of subduction during the Proterozoic has been presented for Antarctica by Craddock (1975) and the western American continent by Lipman *et al.* (1972).

Based on geochemical and Sr and Nd isotopic similarities between the Kimberley lamproites and orogenic lavas of the Sunda and Banda arcs to the north of the Kimberley craton, Varne (1985) proposed that arc volcanoes which have erupted K-rich lavas were tapping subcontinental mantle similar to that from which the Kimberley lamproites were derived. Differences between the Pb isotopic compositions of the arc rocks (White *et al.* 1983) and the lamproites (Fraser *et al.* 1985; Nelson *et al.* 1986) are not consistent with the direct involvement of the Kimberley lamproite source in the generation of the arc lavas. However, an alternative explanation for the isotopic characteristics of the Sunda arc lavas is that recently subducted sediments are involved in their genesis, as was suggested by White *et al.* (1983). We favour this latter explanation and interpret the geochemical similarities of the Western Australian lamproites and high-K arc lavas noted by Varne (1985) as providing further supporting evidence of the involvement of a subducted sedimentary component in the genesis of the Western Australian lamproites. The Pb isotopic differences are due to the involvement of comparatively younger, recently subducted sediments in the case of the arc lavas and, in the case of the lamproites, to the involvement of ancient subducted sediment components which have been stored for long periods within the subcontinental lithosphere of the Kimberley craton.

SEDIMENT RECYCLING AND MANTLE EVOLUTION

Unless subducted sedimentary components are well mixed with the mantle, the overall effect of the incorporation of high Th/U, low U/Pb sediments within the subcontinental lithosphere is a redistribution of Th, U and Pb within the continental crust and subcontinental lithosphere and its direct effect on the isotopic evolution of the Earth's mantle may not even be detectable. However, the position of MORB, ocean-island and upper continental crust Pb to the right of the geochron indicates that their sources have undergone either progressive or episodic enrichment in U relative to Pb, requiring the existence of a compensating reservoir from which U has been donated. This compensating reservoir should possess relatively unradiogenic Pb and lie to the left of the geochron. Although the Earth's core (Allègre *et al.* 1982) and the lower continental crust (O'Nions *et al.* 1979) have been advanced as possible reservoirs in which this missing unradiogenic Pb is stored, due to the operation of sediment subduction processes, the subcontinental lithosphere may also have acquired these characteristics. The existence of substantial reservoirs of low U/Pb, enriched mantle components within the subcontinental lithosphere can therefore compensate for the generally radiogenic Pb of the MORB and ocean-island source reservoirs.

ACKNOWLEDGEMENTS

We are particularly indebted to Prof. A.E. Ringwood (RSES) for his encouragement, interest and contribution during many stimulating discussions. J.W. Sheraton (B.M.R., Canberra), S.C. Bergman (Arco Resources, Texas, U.S.A) and A.L. Jaques (B.M.R., Canberra) generously provided samples. Critical reviews by C.J. Hawkesworth (Open Univ., U.K.), J.W. Bristow (De Beers Consolidated Mines Ltd., South Africa), S.M. McLennan (RSES), R. Hill (RSES), S.-S. Sun (B.M.R., Canberra), D.H. Green (Univ. of Tasmania) and the reviewers greatly improved the manuscript.

REFERENCES

ADDY S.K. 1979. Rare earth element patterns in manganese nodules and micronodules from northwest Atlantic. **Geochimica et Cosmochimica Acta** 43, 1105-1115.

ALLEGRE C.J., BEN OTHMAN D., POLVE M. and RICHARD P. 1979. The Nd-Sr isotopic correlation in mantle materials and geodynamic consequences. **Physics of the Earth and Planetary Interiors** 19, 293-306.

ALLEGRE C.J., DUPRE B. and BREVART O. 1982. Chemical aspects of the formation of the core. **Philosophical Transactions of the Royal Society of London A** 306, 49-59.

AMARI S. and OZIMA M. 1985. Search for the origin of exotic helium in deep-sea sediments. **Nature** 317, 520-522.

BLACK L.P. and JAMES P.R. 1983. Geological history of the Archaean Napier Complex of Enderby Land. In Oliver R.L., James P.R. and Jago J.B. eds, **Proceedings of the 4th International Symposium on Antarctic Earth Science,** pp11-15. Australian Academy of Science, Canberra.

CALVERT S.E. 1976. The mineralogy and geochemistry of near-shore sediments. In Riley J.P. and Chester R. eds, **Chemical Oceanography,** Vol. 6, pp. 187-280. 2nd edition. Academic Press, London.

CHESTER R. and ASHTON S.R. 1976. The geochemistry of deep sea sediments. In Riley J.P. and Chester R. eds, **Chemical Oceanography,** Vol. 6, pp. 281-390. 2nd edition. Academic Press, London.

CHOW T.J. and PATTERSON C.C. 1962. The occurrence and significance of Pb isotopes in pelagic sediments. **Geochimica et Cosmochimica Acta** 26, 263-308.

CHURCH S.E. 1973. Limits of sediment involvement in the genesis of orogenic volcanic rocks. **Contributions to Mineralogy and Petrology** 39, 17-32.

CIVETTA L., INNOCENTI F., MANETTI P., PECCERILLO A. and POLI G. 1981. Geochemical characteristics of potassic volcanics from Mts. Ernici (southern Latium, Italy). **Contributions to Mineralogy and Petrology** 78, 37-47.

COHEN R.S. and O'NIONS R.K. 1982. The lead, neodymium and strontium isotopic structure of ocean ridge basalts. **Journal of Petrology** 23, 299-324.

COLLERSON K.D. and McCULLOCH M.T. 1983. Nd and Sr isotope geochemistry of leucite-bearing lavas from Gaussberg, east Antarctica. In Oliver R.L., James P.R. and Jago J.B. eds, **Proceedings of the 4th International Symposium on Antarctic Earth Science,** pp. 676-680. Australian Academy of Science, Canberra.

CRADDOCK C. 1975. Tectonic evolution of the Pacific margin of Gondwanaland. In Campbell K.S.W. ed, **Gondwana Geology,** pp. 609-618. Australian National University Press, Canberra.

DASCH E.J. 1981. Lead isotopic composition of metalliferous sediments from the Nazca plate. **Geological Society of America Memoir** 154, 199-209.

DASCH E.J., DYMOND J. and HEATH G.R. 1971. Isotopic analysis of metalliferous sediments from the East Pacific Rise. **Earth and Planetary Science Letters** 13, 175-180.

DUPRE B. and ALLEGRE C.J. 1980. Pb-Sr-Nd isotopic correlation and chemistry of North Atlantic mantle. **Nature** 286, 17-22.

EDGAR A.D. 1980. Role of subduction in the genesis of leucite-bearing rocks: Discussion. **Contributions to Mineralogy and Petrology** 73, 429-431.

ELDERFIELD H., HAWKESWORTH C.J., GREAVES M.J. and CALVERT S.E. 1981. Rare earth element geochemistry of oceanic ferromanganese nodules and associated sediments. **Geochimica et Cosmochimica Acta** 45, 513-528.

FOLEY S.F. 1985. The oxidation state of lamproitic magmas. **Tschermaks Mineralogische und Petrographische Mitteilungen** 34, 217-238.

FRASER K.J., HAWKESWORTH C.J., ERLANK A.J., MITCHELL R.H. and SCOTT-SMITH B.H. 1985. Sr, Nd and Pb isotope and minor element geochemistry of lamproites and kimberlites. **Earth and Planetary Science Letters** 76, 57-70.

GALER S.J.G. and O'NIONS R.K. 1985. Residence time of thorium, uranium and lead in the mantle with implications for mantle convection. **Nature** 316, 778-782.

GOLDSTEIN S.L. and O'NIONS R.K. 1981. Nd and Sr isotopic relationships in pelagic clays and ferromanganese deposits. **Nature** 292, 324-327.

GUPTA A.K. and YAGI K. 1980. **Petrology and genesis of leucite-bearing rocks.** Springer-Verlag, Berlin, Heidelberg, NewYork. 252pp.

HAMILTON P.J., O'NIONS R.K., BRIDGWATER D. and NUTMAN A. 1983. Sm-Nd studies of Archaean metasediments and metavolcanics from West Greenland and their implications for the Earth's early history. **Earth and Planetary Science Letters** 62, 263-272.

JAQUES A.L., LEWIS J.D., SMITH C.B., GREGORY G.P., FERGUSON J., CHAPPELL B.W. and McCULLOCH M.T. 1984. The diamond-bearing ultrapotassic (lamproitic) rocks of the West Kimberley region, Western Australia. In Kornprobst J. ed, **Kimberlites I: Kimberlites and Related Rocks,** pp. 225-254. Elsevier, Amsterdam.

JAQUES A.L., SHERATON J.W., HALL A.E., SMITH C.B., SUN S.-S., DREW R. and FOUDOULIS C. 1986. Composition of crystalline inclusions and C-isotopic composition of Argyle and Ellendale diamonds. (Extended Abstr.) 4th International Kimberlite Conference, Perth. **Geological Society of Australia Abstracts** 16, 426-428.

KAY R.W. 1980. Volcanic arc magmas: implication of a melting-mixing model for element recycling in the crust-upper mantle system. **Journal of Geology** 88, 497-522.

KUEHNER S.M., EDGAR A.D. and ARIMA M. 1981. Petrogenesis of the ultrapotassic rocks from the Leucite Hills, Wyoming. **American Mineralogist** 66, 663-677.

LIPMAN P.W., PROTSKA H.J. and CHRISTIANSEN R.L. 1972. Cenozoic volcanism and plate tectonic evolution of the western United States. **Philosophical Transactions of the Royal Society of London A** 271, 217-248.

LIU Y.-G. and SCHMITT R.A. 1984. Chemical profiles in sediment and basalt samples from Deep Sea Drilling Project leg 74, Hole 525A, Walvis Ridge. In Moore T.C., Jr., Rabinowitz P.D. and others, eds, **Initial Reports of the Deep Sea Drilling Project,** Vol. 74, pp. 713-730. U.S. Govt. Printing Office, Washington.

McCULLOCH M.T., JAQUES A.L., NELSON D.R. and LEWIS J.D. 1983. Nd and Sr isotopes in kimberlites and lamproites from Western Australia: an enriched mantle origin. **Nature** 302, 400-403.

McCULLOCH M.T. and PERFIT M.R. 1980. $^{143}Nd/^{144}Nd$, $^{87}Sr/^{86}Sr$ and trace-element constraints on the petrogenesis of Aleutian island arc magmas. **Earth and Planetary Science Letters** 56, 167-179.

McCULLOCH M.T. and WASSERBURG G.J. 1978. Sm-Nd and Rb-Sr chronology of continental crust formation. **Science** 200, 1003-1011.

McDONOUGH W.F., McCULLOCH M.T. and SUN S.-S. 1985. Isotopic and geochemical systematics in Tertiary-Recent basalts from southeastern Australia and implications for the evolution of the sub-continental lithosphere. **Geochimica et Cosmochimica Acta** 49, 2051-2068.

McLENNAN S.M. 1982. On the geochemical evolution of sedimentary rocks. **Chemical Geology** 37, 335-350.

McLENNAN S.M. and TAYLOR S.R. 1983. Geochemical evolution of Archaean shales from South Africa. 1. The Swaziland and Pongola Supergroups. **Precambrian Research** 22, 93-124.

McLENNAN S.M., TAYLOR S.R. and McGREGOR V.R. 1984. Geochemistry of Archaean rocks from West Greenland. **Geochimica et Cosmochimica Acta** 48, 1-13.

MEIJER A. 1976. Pb and Sr isotopic data bearing on the origin of volcanic rocks from the Marianas island arc system. **Geological Society of America Bulletin** 87, 1358-1369.

MILLEDGE H.J., MENDELSSOHN M.J., SEAL M., ROUSE J.E., SWART P.K. and PILLINGER C.T. 1983. Carbon isotopic variations in spectral type 2 diamonds. **Nature** 303, 791-792.

MILLER R.G. and O'NIONS R.K. 1985. Source of Precambrian chemical and clastic sediments. **Nature** 314, 325-330.

MORRIS J.D. and HART S.R. 1983. Isotopic and incompatible element constraints on the genesis of island arc volcanics from Cold Bay and Amak Island, Aleutians, and implications for mantle structure. **Geochimica et Cosmochimica Acta** 47, 2015-2030.

NELSON D.R., McCULLOCH M.T. and SUN S.-S. 1986. The origins of utrapotassic rocks as inferred from Sr, Nd and Pb isotopes. **Geochimica et Cosmochimica Acta** 50, 231-245.

NEWMAN S., MacDOUGALL J.D. and FINKEL R.C. 1984. ^{230}Th-^{232}U disequilibrium in island arcs: evidence from the Aleutians and the Marianas. **Nature** 308, 268-270.

NIXON P.H., THIRWALL M.F., BUCKLEY F. and DAVIES C.J. 1984. Spanish and Western Australian lamproites: aspects of whole rock geochemistry. In Kornprobst J. ed, **Kimberlites I: Kimberlites and Related Rocks,** pp. 285-296. Elsevier, Amsterdam.

O'NIONS R.K., EVENSEN N.M. and HAMILTON P.J. 1979. Geochemical modelling of mantle differentiation and crustal growth. **Journal of Geophysical Research** 84, 6091-6101.

OZIMA M., TAKAYANAGI, M., ZASHU S. and AMARI S. 1984. High $^{3}He/^{4}He$ ratio in ocean sediments. **Nature** 311, 448-450.

OZIMA M., ZASHU S., MATTEY D.P. and PILLINGER C.T. 1985. Helium, argon and carbon isotopic compositions in diamonds and their implications in mantle evolution. **Geochemical Journal** 19, 127-134.

PECCERILLO A. 1985. Roman comagmatic province (central Italy): evidence for subduction-related magma genesis. **Geology** 13, 103-106.

PECCERILLO A., POLI G. and TOLOMEO L. 1984. Genesis, evolution and tectonic significance of K-rich volcanics from the Alban Hills (Roman comagmatic region) as inferred from trace-element chemistry. **Contributions to Mineralogy and Petrology** 86, 230-240.

REYNOLDS P.H. and DASCH E.J. 1971. Lead isotopes in marine manganese nodules and the ore-growth curve. **Journal of Geophysical Research** 76, 5124-5129.

RINGWOOD A.E. 1977. Synthesis of pyrope-knorringite solid solution series. **Earth and Planetary Science Letters** 36, 443-448.

ROGERS N.W., HAWKESWORTH C.J., PARKER R.J. and MARSH J.S. 1985. The geochemistry of potassic lavas from Vulsini, central Italy and implications for mantle enrichment processes beneath the Roman region. **Contributions to Mineralogy and Petrology** 90, 244-257.

SALTERS V.J.M. and BARTON M. 1985. The geochemistry of ultrapotassic lavas from the Leucite Hills, Wyoming. (Abstr.) **Eos** 66(46), 1109.

SANO Y., TOYODA K. and WAKITA H. 1985. $^{3}He/^{4}He$ ratios of modern marine ferromanganese nodules. **Nature** 317, 518-520.

SHERATON J.W. 1983. Geochemistry of mafic igneous rocks of the northern Prince Charles Mountains, Antarctica. **Journal of the Geological Society of Australia** 30, 295-304.

SHERATON J.W. and CUNDARI A. 1980. Leucitites from Gaussberg, Antarctica. **Contributions to Mineralogy and Petrology** 71, 417-427.

SHERATON J.W. and ENGLAND R.N. 1980. Highly potassic mafic dykes from Antarctica. **Journal of the Geological Society of Australia** 27, 1-18.

SOBOLEV N.V., GALIMOV E.M., IVANOVSKAYA N.N. and YEFIMOVA E.S. 1979. The carbon isotopic composition of diamonds containing crystalline inclusions. **Doklady Akademii Nauk SSSR** 249, 1217-1220.

SUN S-S. 1980. Lead isotopic study of young volcanics from mid-ocean ridges, ocean islands and island arcs. **Philosophical Transactions of the Royal Society of London A** 297, 409-445.

SWART P.K., PILLINGER C.T., MILLEDGE H.J. and SEAL M. 1983. Carbon isotopic variation within individual diamonds. **Nature** 303, 793-795.

TAYLOR S.R. and McLENNAN S.M. 1981. The composition and evolution of the continental crust: rare earth element evidence from sedimentary rocks. **Philosophical Transactions of the Royal Society of London A** 301, 381-399.

THOMPSON R.N. 1977. Primary basalts and magma genesis. III. Alban Hills, Roman comagmatic province, central Italy. **Contributions to Mineralogy and Petrology** 60, 91-108.

THOMPSON R.N., MORRISON M.A., HENDRY G.L. and PARRY S.J. 1984. An assessment of the relative roles of crust and mantle in magma genesis: an elemental approach. **Philosophical Transactions of the Royal Society of London A** 310, 549-590.

THOMSON J., CARPENTER M.S.N., COLLEY S., WILSON T.R.S., ELDERFIELD H. and KENNEDY H. 1984. Metal accumulation rates in northwest Atlantic pelagic sediments. **Geochimica et Cosmochimica Acta** 48, 1935-1948.

TURI B. and TAYLOR H.P. 1976. Oxygen isotope studies of potassic volcanic rocks of the Roman province, central Italy. **Contributions to Mineralogy and Petrology** 55, 1-31.

UNRUH D.M. and TATSUMOTO M. 1976. Lead isotopic compositions and uranium, thorium and lead concentrations in sediments and basalts from the Nazca Plate. In Yeats R.S., Hart S.R. and others, eds, **Initial Reports of the Deep Sea Drilling Project,** Vol. 34, pp. 341-347. U.S. Govt. Printing Office, Washington.

VARNE R. 1985. Ancient subcontinental mantle: a source for K-rich orogenic volcanics. **Geology** 13, 405-408.

VEEH H.H. 1981. Uranium and thorium isotopic investigations in metalliferous sediments of the northwestern Nazca plate. **Geological Society of America Memoir** 154, 251-267.

VEIZER J. and COMPSTON W. 1976. $^{87}Sr/^{86}Sr$ in Precambrian carbonates as an index of crustal evolution. **Geochimica et Cosmochimica Acta** 40, 905-914.

VEIZER J., COMPSTON W., HOEFS J. and NIELSEN H. 1982. Mantle buffering of the early oceans. **Naturwissenschaften** 69, 173-180.

VENTURELLI G., CAPEDRI S., DI BATTISTINI G., CRAWFORD A., KOGARKO L.N. and CELESTINI S. 1984. The ultrapotassic rocks of southeastern Spain. **Lithos** 7, 37-54.

VOLLMER R. and NORRY M.T. 1983. Possible origin of K-rich volcanic rocks from Virunga, East Africa, by metasomatism of continental crustal material: Pb, Nd and Sr isotopic evidence. **Earth and Planetary Science Letters** 64, 374-386.

VOLLMER R., OGDEN P., SCHILLING J.-G., KINGSLEY R.H and WAGGONER D.G. 1984. Nd and Sr isotopes in ultrapotassic volcanic rocks from the Leucite Hills, Wyoming. **Contributions to Mineralogy and Petrology** 87, 359-368.

WHITE W.M., DUPRE B. and VIDAL P. 1985. Isotope and trace-element chemistry of sediments from the Barbados Ridge-Demerara Plain region, Atlantic Ocean. **Geochimica et Cosmochimica Acta** 49, 1875-1886.

WHITE W.M. and HOFMANN A. W. 1982. Sr and Nd isotope geochemistry of oceanic basalts and mantle evolution. **Nature** 296, 821-825.

WHITE W.M., JENNER G., DUPRE B., FODEN J. and VARNE R. 1983. Pb isotope geochemistry of the Lesser Antilles and Sunda (Indonesia) island arcs. (Abstr.) **Eos** 64(18), 333-334.

FIGURE CAPTIONS

Figure 1. Trace-element abundances (in order of increasing compatibility in garnet peridotite) normalised to the abundances estimated for primitive mantle (from McDonough *et al.* 1985 and Nelson *et al.* 1986) of potassic magmas from Western Australia (McCulloch *et al.* 1983; Jaques *et al.* 1984; Nixon *et al.* 1984; Nelson *et al.* 1986), Antarctica (Sheraton and England 1980; Sheraton and Cundari 1980; Sheraton 1983; Collerson and McCulloch 1983) and Leucite Hills (Kuehner *et al.* 1981; Vollmer *et al.* 1984). Th and U abundances for Leucite Hills examples not available. The field of normalised trace-elements (hatched) for 4 sediments (3 slates and 1 pelagic mud composite) from Thompson *et al.* (1984) also shown for comparison.

Figure 2. Pb-Pb isotope diagram showing compositions of Western Australian lamproites and Gaussberg leucites (Nelson *et al.* 1986), Leucite Hills and Antarctic dykes (Δ =measured, Δ =age corrected compared to the field for mid-ocean-ridge basalts (Dupré and Allègre 1980; Cohen and O'Nions 1982).

Figure 3. Initial Sr-Nd isotope diagram showing fields for Western Australian lamproites (McCulloch *et al.* 1983), Leucite Hills high-K volcanics (Vollmer *et al.* 1984 and this study), Gaussberg leucitites (Collerson and McCulloch 1983) and the Priestley Peak melasyenite at its emplacement age of 482 myrs. Mid-ocean-ridge basalt field from Allègre *et al.* (1979) and White and Hofmann (1982).

Figure 4. Proposed mechanism to explain the Pb isotopic evolutionary history of this group of potassic magmas. As an example, a possible Pb evolution trajectory for Ellendale lamproite WAK-27L (analysis from Nelson *et al.* 1986) is shown. At time t_1 (3.0 Ga), Pb is extracted from the mantle during a crust forming event and evolves for some period in the high U/Pb upper crust. For the example shown, μ ($^{238}U/^{204}Pb$) is 13.75 for 1.0 Ga. At t_2 (2.0 Ga), this upper crustal Pb is eroded from the continent and deposited in the low μ marine environment. These sediments are then subducted into the mantle and stored in the subcontinental lithosphere. For the example shown, μ is 4.25 during this ≈2.0 Ga period.

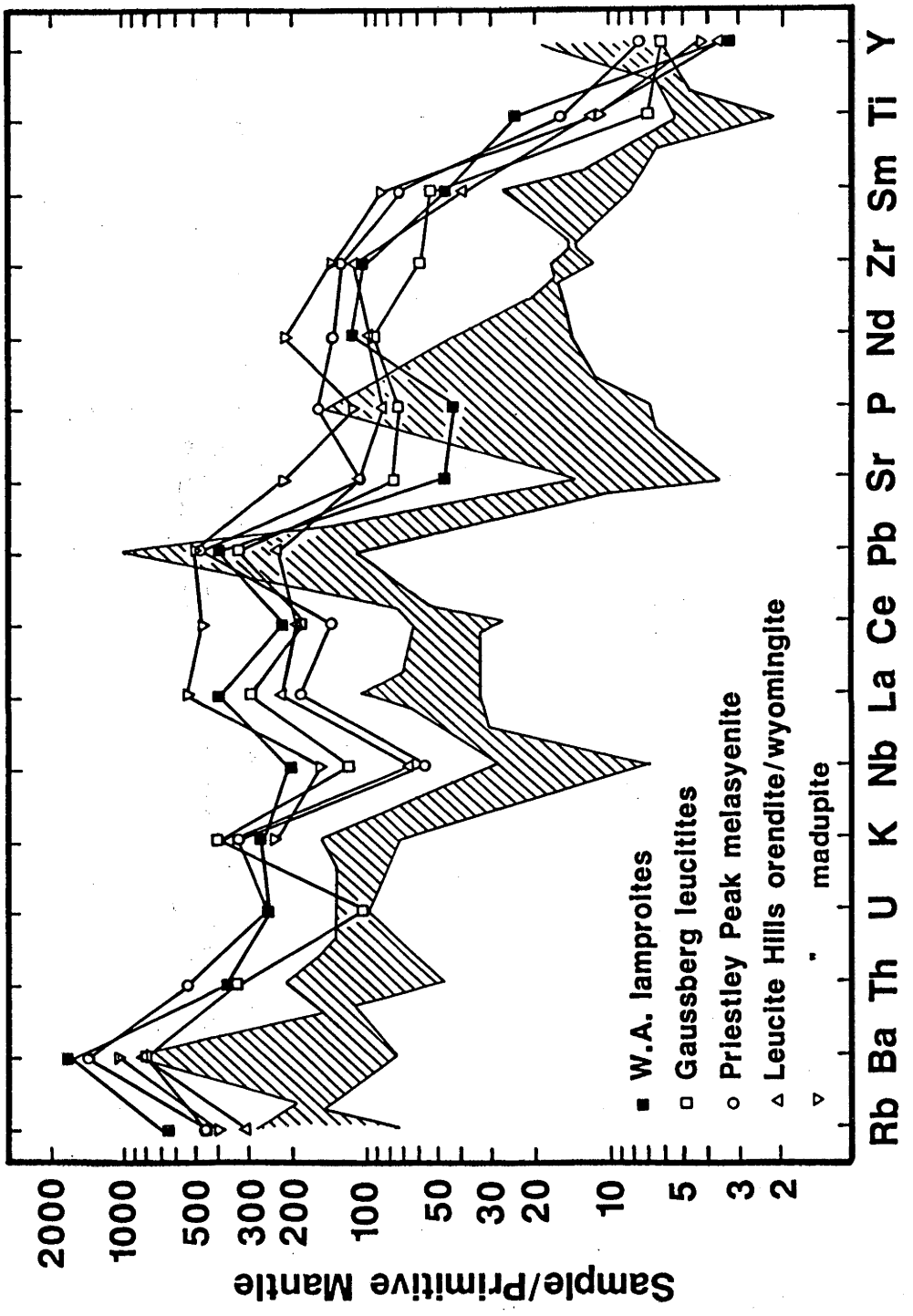
Sample/Primitive Mantle
2000
1000
500
300
200
100
50
30
20
10
5
3
2
Rb Ba Th U K Nb La Ce Pb Sr P Nd Zr Sm Ti Y
W.A. lamproites
Gaussberg leucitites
Priestley Peak melasyenite
Leucite Hills orendite/wyomingite
" madupite

Fig. 1.

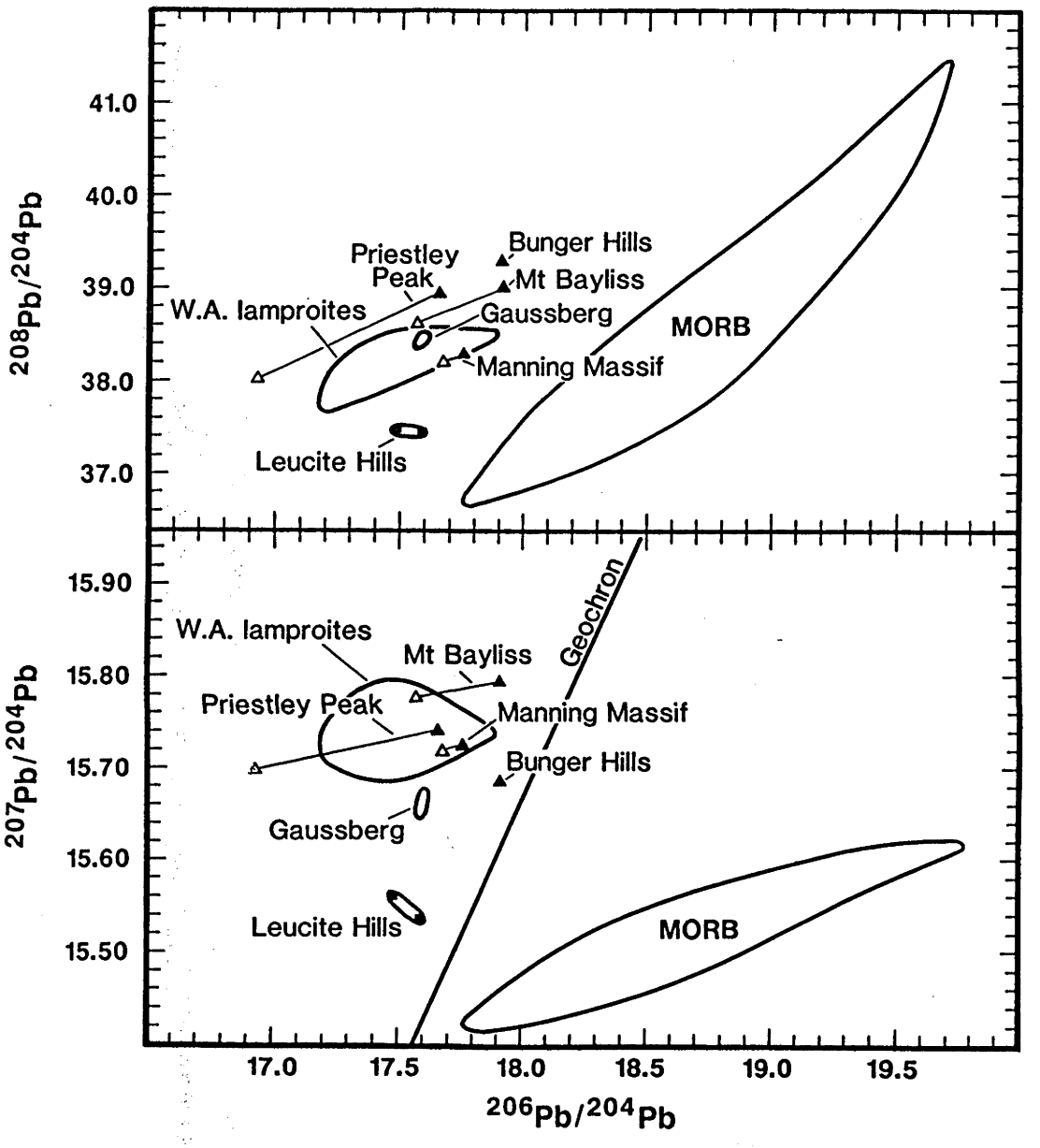
41.0
40.0
39.0
38.0
37.0
$^{208}Pb/^{204}Pb$
Priestley Peak
Bunger Hills
Mt Bayliss
W.A. lamproites
Gaussberg
MORB
Manning Massif
Leucite Hills
15.90
15.80
15.70
15.60
15.50
$^{207}Pb/^{204}Pb$
W.A. lamproites
Mt Bayliss
Geochron
Priestley Peak
Manning Massif
Bunger Hills
Gaussberg
Leucite Hills
MORB
17.0
17.5
18.0
18.5
19.0
19.5
$^{206}Pb/^{204}Pb$

Fig. 2.

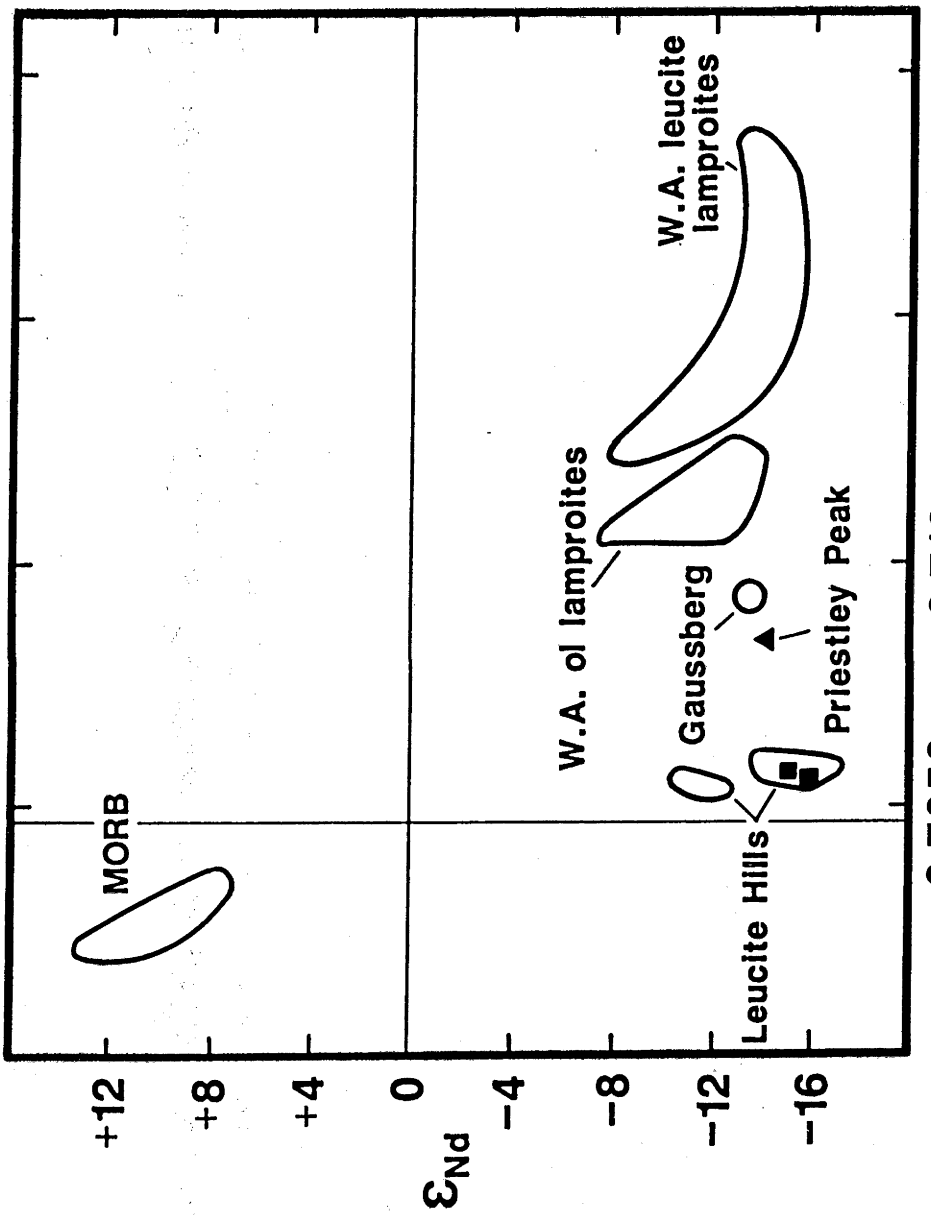
MORB
W.A. ol lamproites
W.A. leucite lamproites
Gaussberg
Priestley Peak
Leucite Hills
+12
+8
+4
0
-4
-8
-12
-16
ε_{Nd}
0.7050
0.710
0.7150
0.720
$^{87}Sr/^{86}Sr$

Fig. 3.

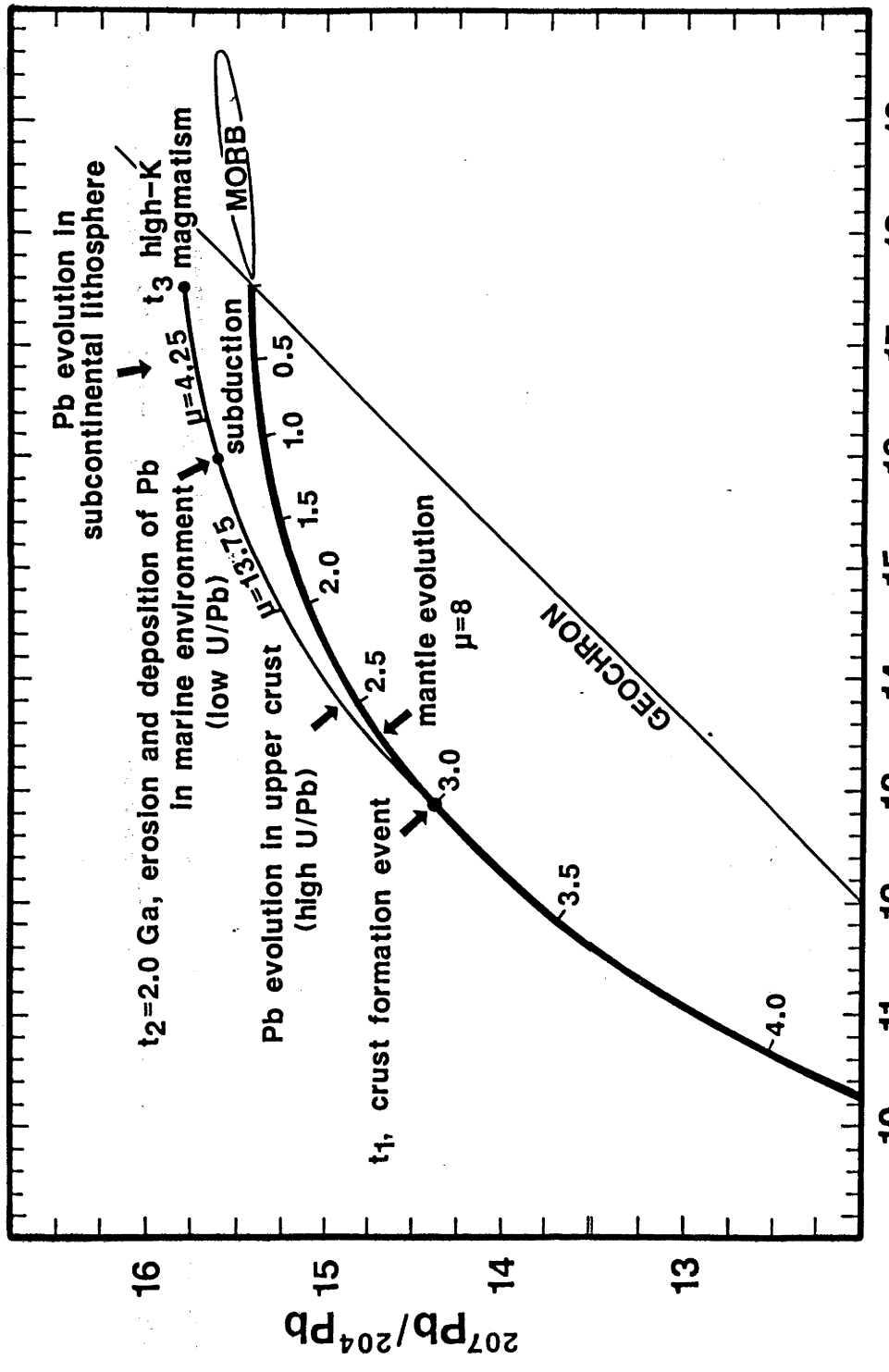
Pb evolution in
subcontinental lithosphere
t_2=2.0 Ga, erosion and deposition of Pb
in marine environment
(low U/Pb)
t_3 high-K
magmatism
μ=4.25
subduction
MORB
Pb evolution in upper crust
(high U/Pb)
μ=13.75
t_1, crust formation event
mantle evolution
μ=8
GEOCHRON
0.5
1.0
1.5
2.0
2.5
3.0
3.5
4.0
$^{207}Pb/^{204}Pb$
$^{206}Pb/^{204}Pb$
13
14
15
16
10
11
12
13
14
15
16
17
18
19

Fig. 4.

Table 1. Ages and Sr, Pb and Nd isotopic data for Antarctic dykes and Leucite Hills volcanics.

Sample	Rb	Sr	U	Pb	Sm	Nd	$^{87}Rb/^{86}Sr$	$^{87}Sr/^{86}Sr$	$^{238}U/^{204}Pb$	$^{206}Pb/^{204}Pb$	$^{207}Pb/^{204}Pb$	$^{208}Pb/^{204}Pb$	$^{147}Sm/^{144}Nd$	$^{143}Nd/^{144}Nd$	εNd(0)	εNd
Prince Charles Mountains, MacRobertson Land																
Manning Massif leucite tristanite (K/Ar age 50±2myrs)																
7328-1594	-	-	4.14	36.45	9.35	64.28	-	-	8.20	17.749 (17.68)[1]	15.729 (15.72)	38.296 (38.21)	0.0879	0.51132±2	-10.0	-9.
Mt Bayliss alkali melasyenite (K/Ar age 414±10 myrs)																
7328-1545	-	-	1.89	28.46	2.93	20.94		-	4.87	17.904 (17.58)	15.799 (15.78)	39.016 (38.61)	0.0847	0.51092±2	-18.0	-12.
Enderby Land																
Priestley Peak alkali melasyenite (Rb/Sr age 482±3 myrs)																
7728-3439D	293.3	2514	7.90	61.56	32.45	189.4	-	0.70852±7[2]	9.34	17.646 (16.92)	15.742 (15.70)	38.909 (38.00)	0.1036	0.51081±3	-20.0	-14.
Queen Mary Land																
Bunger Hills trachybasalt (probably Cambrian or younger)																
7728-4730	-	-	11.35	101.1	20.03	131.5	-		8.24	17.904	15.689	39.276	0.0921	0.51062±2	-23.7	←16
Leucite Hills, Wyoming (Pleistocene)																
Wyomingites																
LH-4	263	2137	-	-	15.79	124.0	0.3557	0.70593±4	-	17.596[3]	15.535	37.441	0.0770	0.51107±2	-14.9	-14
LH-7	296	3022	-	-	20.69	157.1	0.2833	0.70564±5	-	17.494	15.556	37.500	0.0796	0.51103±2	-15.8	-15
								0.70558±5[3]		17.47[3]	15.56	37.46				

[1] Analytical procedures described in *Nelson et al. (1986)*. All concentrations obtained by isotope dilution. Nd isotope ratios normalised to $^{146}Nd/^{142}Nd=0.636151$. εNd(I) and Pb isotope ratios in brackets are age corrected using the cited ages (from *Black & James 1983 and Sheraton 1983.*) Age corrected $^{208}Pb/^{204}Pb$ ratios calculated assuming Th/U =4.

[2] Rb & Sr data, including $^{87}Sr/^{86}Sr(I)$ (obtained by internal isochron) from *Black & James 1983.*

[3] Isotope analysis performed on acid-leached chips.